Strain partitioning in transpression zones: examples from the lapetus suture zone in Britain and Ireland

Clegg, Phillip

STRAIN PARTITIONING IN TRANSPRESSION ZONES: EXAMPLES FROM THE IAPETUS SUTURE ZONE IN BRITAIN AND IRELAND.

by

Phillip Clegg

A thesis submitted in partial fulfilment of the degree of Doctor of Philosophy at the Department of Geological Sciences, University of Durham.
2002.

To Helen

Helen and Moss
Calf Sound Isle of Man

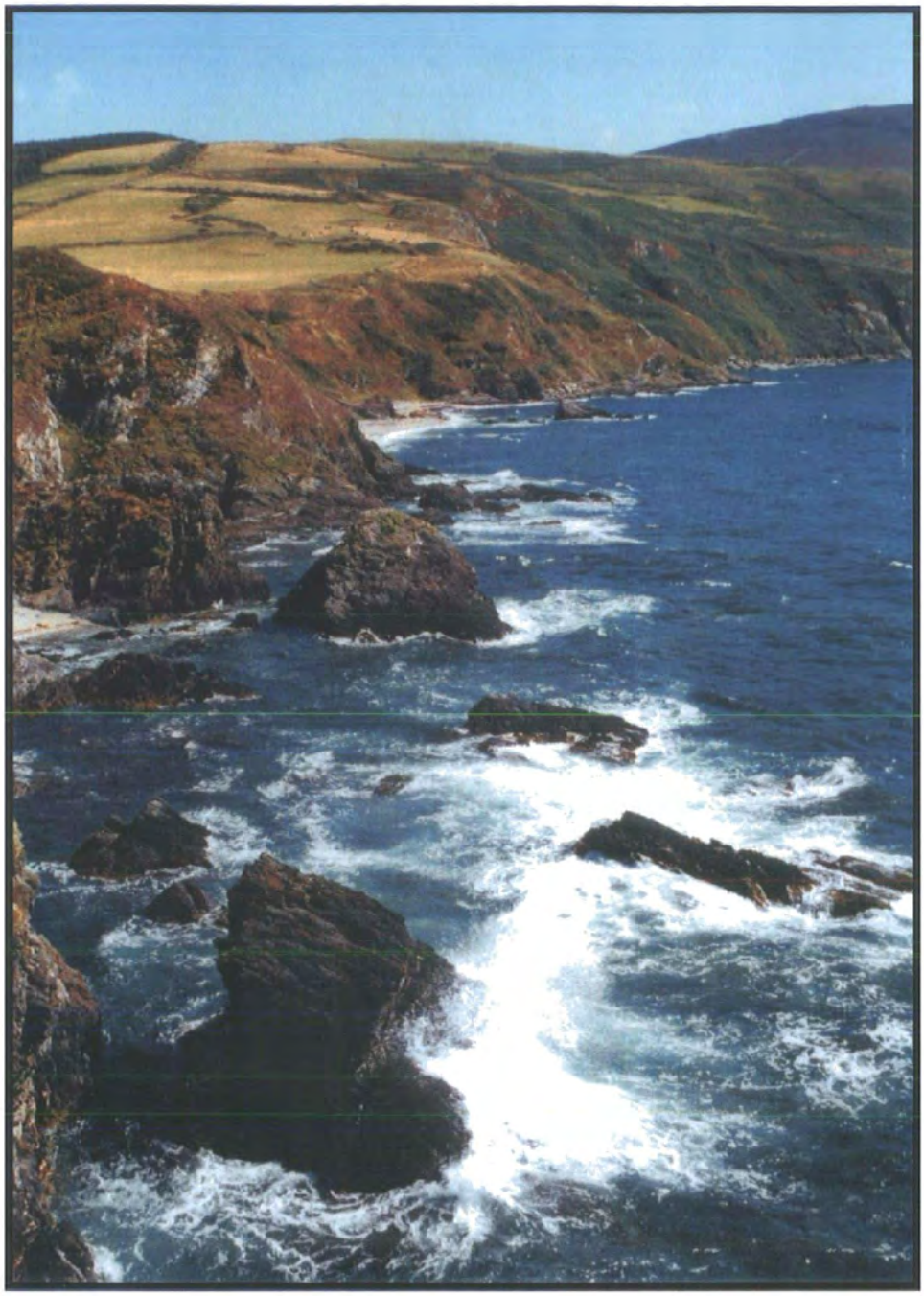

Frontispiece
'The West Coast, Isle of Man'
(July 1999)

Copyright

ABSTRACT

Kinematic partitioning in transpression zones is well documented and leads to the development of discrete domains of contraction- and wrench-dominated deformation. Although widely reported there are few detailed descriptions of such partitioning in ancient transpression zones.

The Iapetus Suture Zone comprises a broad band of Lower Palaeozoic rocks that were deformed within a sinistral transpression zone immediately prior to or during the Acadian phase of the Caledonian Orogeny. Excellent coastal exposure of these rocks in SE Ireland, the Isle of Man and SE Scotland allow detailed comparative studies of the deformational patterns and processes within an ancient transpression zone to be made.

All three areas preserve a highly heterogeneous assemblage of contemporaneous structures, including folds, interlinked strike-slip detachment faults and a regional cleavage that locally transects in a clockwise sense. Geometrically and kinematically different assemblages of these structures define a series of fault bounded, structural domains that are interpreted to result from the kinematic partitioning of a regional triclinic transpressional deformation. This interpretation lends support to assertions that many transpression zones are triclinic in nature. However, the geometric and kinematic patterns in the different domains suggest a strain model where the triclinic transpressional strain is partitioned into monoclinic end-members (dip-slip non-coaxial contraction and strike-slip simple shear) rather than into domains of pure shear and oblique simple shear. Clockwise transected cleavage, sinistral strike-slip faulting and zones of sideways and downwards facing sinistrally verging folds have been used to infer sinistral transpressive strain. This project suggests that such features are particularly obvious in regions where significant amounts of partitioning have occurred. The nature and distribution of strain partitioning appears to be controlled by the presence of mechanical heterogeneities on regional and local scales, e.g. the proximity to weak tract-bounding faults and the presence of lithologically controlled regions of high pore fluid pressures, respectively.

How the Isle of Man was formed

Although modern geologists may tell us otherwise, the Isle of Man was *not* fashioned by geological processes, but by the hand of the giant Finn McCool.

Legend tells that Finn McCool, giant, Ulster warrior and the king of Ireland's armies, could pick thorns out of his heels while running and was capable of amazing feats of strength.

During a battle with the Scottish giant and arch enemy Benandonner, Finn took a clod of earth and flung it at his fleeing enemy. The clod fell into the Irish Sea and turned into the Isle of Man. The hole it left filled with water and became Lough Neagh.

Acknowledgements

Although the credit for any project of this nature is given to the author, there are however, a multitude of people who have had a part in making this project possible. Within the limited space available here it is not possible to list everybody, so I apologise now if you're are not mentioned by name. However, several people have played key roles during my project and I wish to thank them for all their help, advice and support.

First and foremost, thanks must go to Bob Holdsworth, my supervisor. Not only was he responsible, as one of my undergraduate lecturers, for getting me interested in the 'black art' of structural geology, but as my PhD supervisor helped me to begin to unravel some of its secrets. During my field work he has endured storms at Eyemouth, driving rain in SE Ireland and rotting seaweed on the Isle of Man. Despite all this, he has still managed to impart both knowledge and enthusiasm even when I was lacking in both. His constant encouragement and cajoling kept me going during some difficult times while writing up. Many thanks Bob.

I must also thank Enrico Tavarnelli, for his boundless enthusiasm and help at Eyemouth, and also for leaving his boots outside when he stayed with us. Additional thanks go to Ken McCaffrey and Richard Jones. Nigel Woodcock's extensive knowledge of the geology and stratigraphy of Isle of Man was invaluable, as was his advice and discussions on various aspects of Manx geology during his visit. Continuing the Isle of Man theme, a big thank you to Dave Quirk and Dave Burnett for their help and advice on the geology of the island, to Peter and Phillippa Davey and Fenella Bazin of the Centre for Manx Studies for providing accommodation, advice and support during my field work on the Isle of Man. A special mention must go to Tim 'Safeways Savers' Crumplin, who was also an inmate of the Manx Studies Centre and not only had an eye for a bargain but was a good mate. Thanks also to: Juan Watterson for his hospitality and boating skills; Charles Guard of the Manx Heritage Trust for aerial photographs and Dave Kelly at the D.O.L.G.E. for providing maps. In Ireland, I'd like to thank John Morris and Brian McConnell of the Irish Geological Survey for their sound advice and for providing base maps.

In the department at Durham, special thanks must go to Dave Schofield, who knows just about everything- from building Roman Ballista to ordering maps and memoirs. To my fellow postgrads, thanks to Ade, Rich, and in particular Lee, Janine and Helen who kept me sane (most of the time).

As a self funding postgraduate student money was always an issue, so I'd like to thank the John Ray Trust and the Annie Greenly Fund of the Geological Society for helping fund my fieldwork.

Finally to my family; I would like to thank Irene for all her help over the past 4 years, my mum and dad for helping when and however they could and, in particular my dad for acting as field assistant and pack horse. The most important thank you of all must go to my wife Helen, who has had to endure my long absences, a lack of holidays, and my ceaseless ramblings on all things geological. She believed that I could even when I didn't and, without her support none of this would have been possible. A final special thanks to Moss who looked after Helen for me.

Contents

Chapter 1

Transpressional Tectonics and Structural Definitions

1.1 Transpression

1.1.1 Introduction

The term transpression was first employed by Harland (1971) to describe the deformation produced by the oblique closure of lithospheric plates. Although largely conceptual, Harland defined transpression in terms of the stress regime operating in a zone of oblique convergence. Implicit within this definition was the association between transpression and oblique plate collision. He further suggested that transpression should be a relatively common mode of deformation stating that: '*...any orogenic belt with a curvature greater than a great circle and forming between two plates must undergo a degree of transpression*'.

However, transpression is not the sole preserve of lithospheric plate tectonics and it can be seen to operate within a number of different settings and at a variety of scales. Within tectonic plates, strain is often focused into narrow fault or shear zones that bound blocks of relatively undeformed material at several scales. Block convergence slip vectors are rarely orthogonal to the deformation zones; so at some time during their histories the bounding deformation zones will have experienced oblique relative motions (Dewey *et al.*1998).

The complex strain patterns encountered in natural examples, makes the evaluation of stress directions problematical. Harland's original definition and concept of transpression was therefore redefined by Sanderson & Marchini (1984) as '*...a wrench or transcurrent shear accompanied by horizontal shortening across, and vertical lengthening along, the shear plane*'. This rather specific model was more generally defined by Dewey *et al.* (1998) as '*...a strike-slip deformation that deviates from simple shear by a component of shortening orthogonal to the deforming zone*'. These definitions describe the strain state within a transpressional environment and are non-specific to any one tectonic setting.

1.1.2 Modelling transpressional strains

Present studies have modelled transpression using either finite or incremental

strain. These have been shown to be effective starting points in analysing complex three-dimensional deformation zones (Dewey *et al.* 1998; Jiang *et al.* 2001).

Finite strain

Sanderson & Marchini (1984) imposed a number of mathematically convenient boundary conditions as a means of modelling finite bulk strains within transpression zones. In their model they considered a constant volume homogenous deformation within a vertical zone that was basally and laterally confined (Fig. 1.1). In order to maintain constant volume, the component of horizontal shortening is exactly compensated by vertical extension of the zone. By separating the deformation into its pure shear and simple shear components, Sanderson & Marchini (1984) were able to define the resulting finite strain in terms of two factors α (pure shear) and γ (simple shear). Using the deformation matrix **D** (equation 1), they were able to model the kinematics of transpressional strain.

$$\mathbf{D} = \begin{bmatrix} 1 & \gamma & 0 \\ 0 & 1 & 0 \\ 0 & 0 & 1 \end{bmatrix} \begin{bmatrix} 1 & 0 & 0 \\ 0 & \alpha^{-1} & 0 \\ 0 & 0 & 0 \end{bmatrix} = \begin{bmatrix} 1 & \alpha^{-1}\gamma & 0 \\ 0 & \alpha^{-1} & 0 \\ 0 & 0 & \alpha \end{bmatrix} \quad \text{(equation 1)}$$

By changing the values of the parameters α^{-1} and γ, (see Table 1.1 for definitions) it is possible to evaluate, the effects of varying the amounts of shortening and shear strain on the bulk finite strain. Thus, this method can be used as a predictive tool in determining the orientation of lines and planes for a given finite strain ellipsoid (see Sanderson & Marchini 1984 for methodology).

Fossen & Tikoff (1993) and Tikoff & Fossen (1993) showed the limitations of the factorisation scheme employed by Sanderson & Marchini (1984). The deformation matrix developed by Fossen & Tikoff (1993) and Tikoff & Fossen (1993) proposed a more rigorous model, defining transpression as the consequence of simultaneous rather than sequential simple and pure shears (equation 2).

$$\mathbf{D} = \begin{bmatrix} k & \Gamma \\ 0 & 1/k \end{bmatrix} = \begin{bmatrix} k & \dfrac{\gamma\,(k - 1/k)}{2 \ln k} \\ 0 & 1/k \end{bmatrix} \quad \text{(equation 2)}$$

Any combination of these two simultaneous strains gives rise to a unique state of

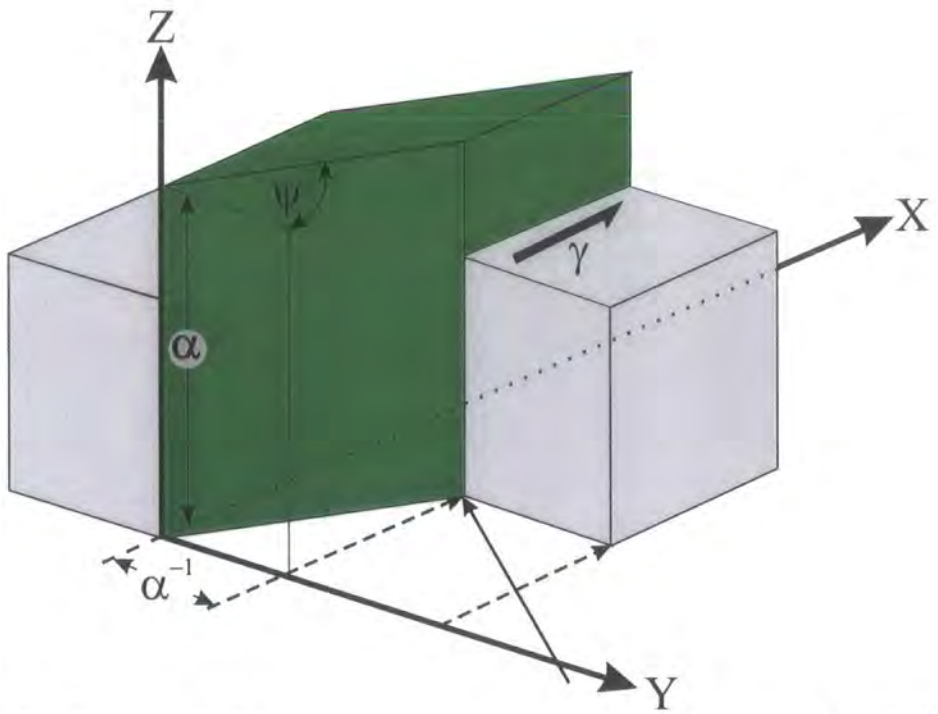

Figure 1.1. Geometry of homogenous transpression. Deformation of unit cube, with shortening parallel to Y-axis and shearing parallel to X-axis. Volume is conserved by extension in the Z-axis. α^{-1} = shortening across the zone; α = vertical extension of zone; ψ = angular shear & γ = shear strain parallel to zone margin (= tan ψ) (after Sanderson & Marchini 1984).

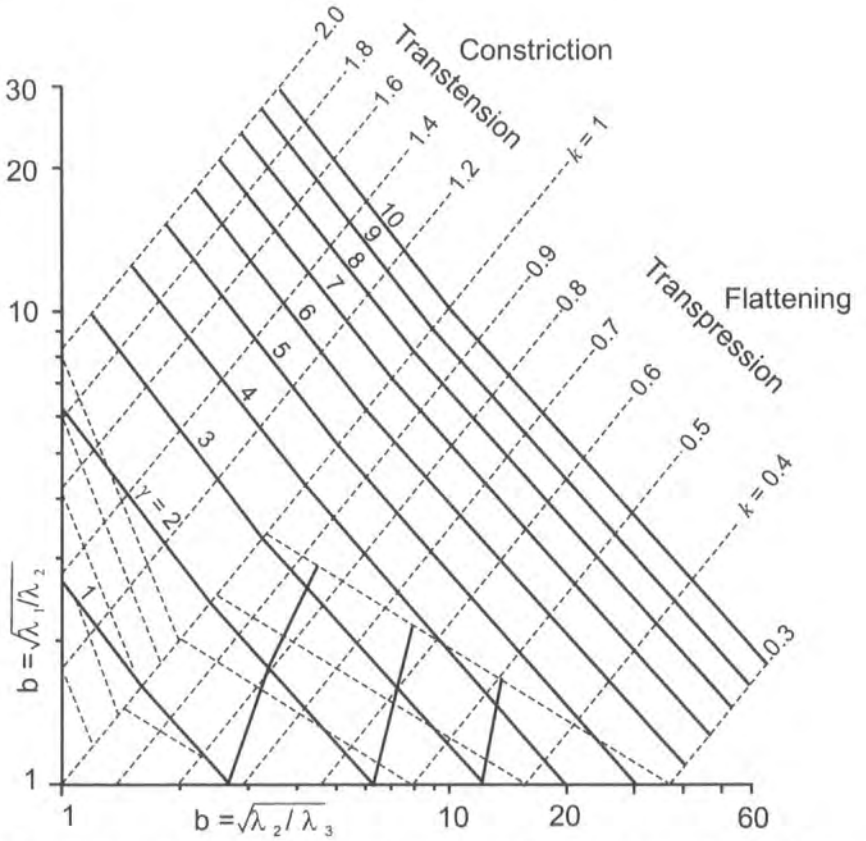

Figure 1.2. Logarithmic Flinn diagram contoured for various values of γ (simple shear, solid lines) and k (pure shear, dashed lines) values assuming constant volume (Fossen and Tikoff 1993).

strain (see Fossen & Tikoff 1993 and Tikoff & Fossen 1993 for methodology). The resulting shape of the strain ellipsoid can be illustrated on a contoured, logarithmic Flinn diagram (Fig. 1.2). This clearly shows that transpressional deformations give rise to flattening strain ($0<k<1$), while transtensional deformations give rise to constrictional strain ($1<k<\infty$). This corroborated the work of Sanderson and Marchini (1984) who predicted S(L)-fabrics in transpression zones and L(S)-fabrics in transtension zones.

Mathematical notation	Description
α	Vertical stretch of deformation zone (Sanderson & Marchini, 1984) **or** Angle between the plate margin (or deformation zone boundary) and the plate motion vector (Tikoff & Teyssier, 1994)
α^{-1}	Shortening across the deforming zone (strictly it is the ratio of the deformed to the original width of the zone) (Sanderson & Marchini, 1984)
γ	Shear strain parallel to the zone boundary (= tan Ψ)
Ψ	Angular shear strain
λ_1, λ_2 & λ_3	Maximum, intermediate and minimum axes of the finite strain ellipsoid, respectively
s_1, s_2 & s_3	Maximum, intermediate and minimum axes of the incremental strain ellipsoid, respectively
θ	Angle between the *XY*-plane of principal strain and the zone margin (Sanderson & Marchini 1984) **or** Angle between plate margin and s_3 (Fossen & Tikoff, 1993)
W_k	The kinematic vorticity number
k	Horizontal pure shear component, perpendicular to the shear plane
Γ	Effective shear strain

Table 1.1 Terms and abbreviations used in text

Incremental (or Instantaneous, or Infinitesimal) strain

Teyssier *et al.* (1995) suggested that because most geological and geophysical measurements within active tectonic settings are based on small strains, incremental

strain is a more suitable quantity to model transpression rather than either finite strain or stress. The incremental strain axes ($s_1 > s_2 > s_3$; after Tikoff & Teyssier 1994) can be inversely correlated with stresses (s_1, s_2, s_3 correlate with σ_3, σ_2, σ_1; Weijermars 1991) assuming steady-state deformation and rheology (Teyssier *et al.* 1995).

Switching of finite strain axes

An interesting feature of transpressional and transtensional deformation is the varying orientation of the principal axes (X > Y > Z) of the finite strain ellipsoid. This feature was noted by Sanderson and Marchini (1984) where they showed that one principal strain axis is always vertical. For simple shear ($\alpha^{-1} = 1$) this is the Y-axis. For $\alpha^{-1} < 1$ (transpression) the vertical axis may be X or Y, therefore the XY-plane (= cleavage) is always vertical, lying at an angle θ to the zone boundary, whilst associated stretching lineations may be vertical or horizontal (Fig. 1.3). For $\alpha^{-1} > 1$ (transtension), either Z or Y may be vertical. So the cleavage can be vertical or horizontal, whilst the associated stretching lineation will always be horizontal.

Fossen and Tikoff (1993) expanded this idea, defining two styles of transpression based on the orientation of the incremental stretching axes. They called these *wrench-dominated* and *pure shear-dominated* (Fig. 1.4). In pure shear-dominated transpression, s_1 is vertical, while s_2 and s_3 lie in the horizontal plane and are oblique to the shear (XZ) plane. At the outset, the finite strain ellipsoid starts parallel to the incremental strain, however, as deformation progresses, λ_2 and λ_3 rotate progressively to become parallel and perpendicular, respectively to the shear plane at infinite strain. This rotation is due purely to the non-coaxial component of the deformation. In contrast, during wrench-dominated transpression s_1 and s_3 lie in the horizontal plane and oblique to the shear plane, while s_2 is vertical. Initially λ_1 and λ_3 are horizontal and λ_2 is vertical. However, as strain increases, λ_1 switches with λ_2 and becomes vertical (Fossen & Tikoff 1993; Tikoff & Greene 1997; Tikoff & Teyssier 1994; Teyssier *et al.* 1995). This highlights the complex nature of fabric orientation within transpression (and transtension) zones and the need to distinguish between pure- and wrench-dominated transpression (transtension) in field based kinematic analysis. Using the kinematic vorticity number (W_k) as a measure of non-coaxiality Fossen and Tikoff (1993) were able to quantitatively distinguish between wrench- and pure shear-dominated transpression. The kinematic vorticity number simply describes the non-linear ratio of the pure and simple shear components of the deformation. They were able to determine

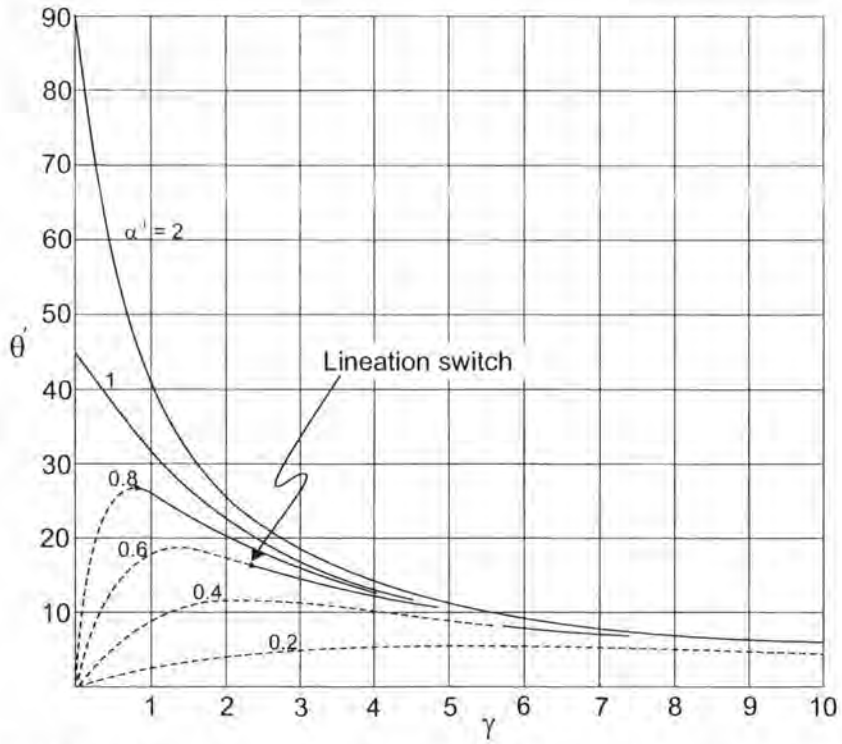

Figure 1.3. Plot of orientation of long axis of strain ellipse in horizontal plane (θ') for transpression. Continuous lines indicate X-axis horizontal, dashed lines indicate X-axis vertical (Sanderson and Marchini 1984).

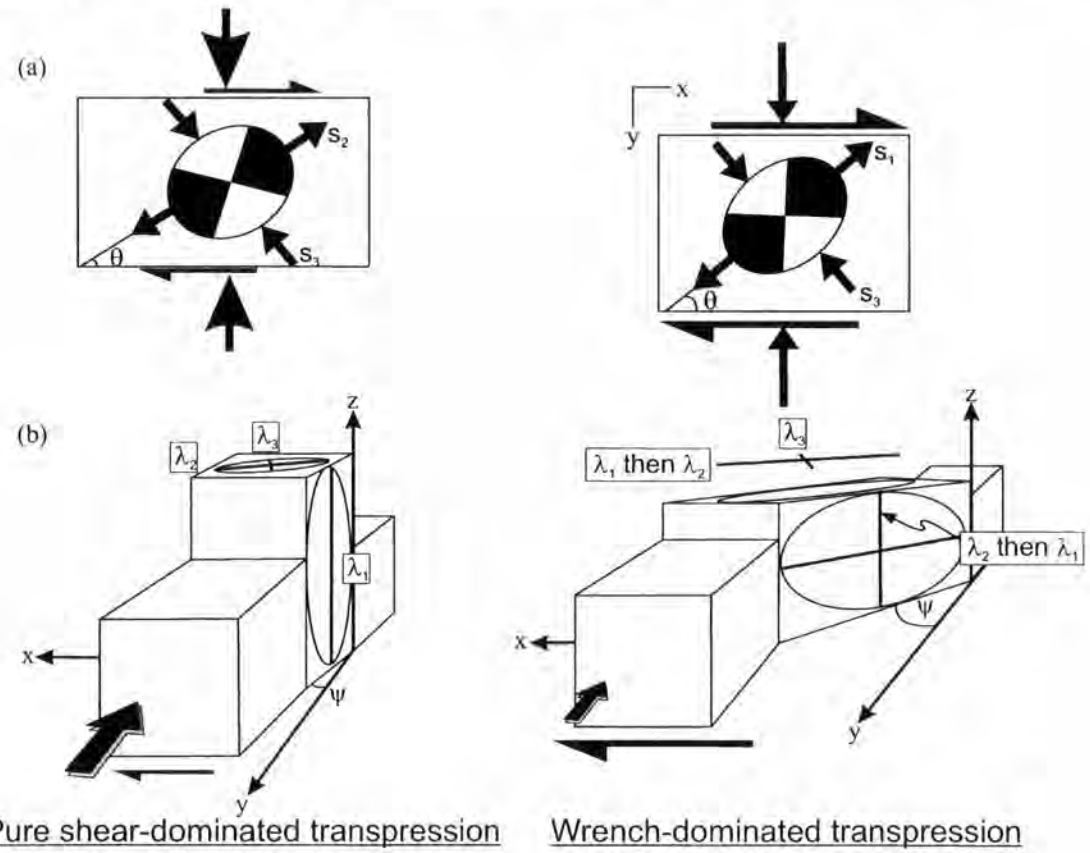

Figure 1.4 (a) Plan view of pure shear- and wrench-dominated transpressions distinguished by the orientation of the incremental strain axes (s_1 - s_3). **(b)** block diagrams illustrating difference in the shape and orientation of the finite strain ellipsoid resulting from pure shear- and wrench-dominated transpressions (after Tikoff & Teyssier 1994).

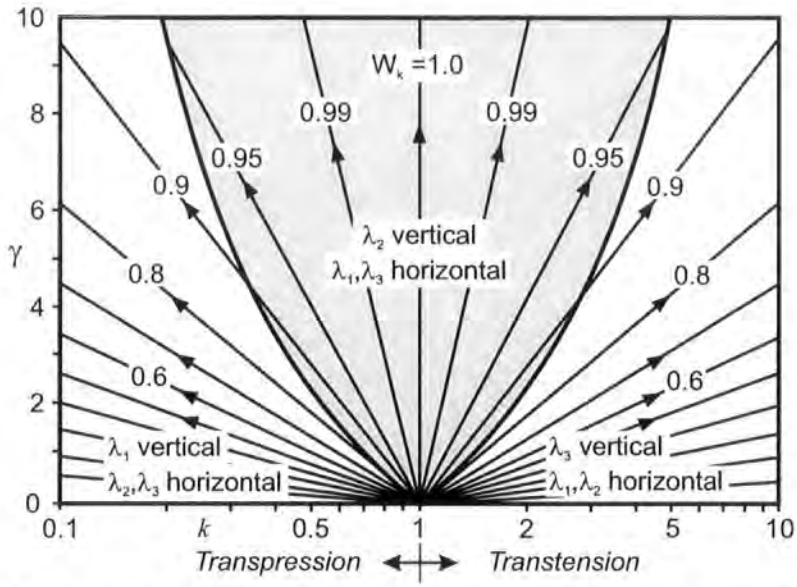

Figure 1.5. Orientation of the finite strain ellipse for transpression-transtension. Note change in the vertical principal strain axis for progressive deformations with $W_k > 0.81$. k = pure shear. W_k 1.0 = simple shear, $W_k = 0$ pure shear. (from Fossen and Tikoff 1993).

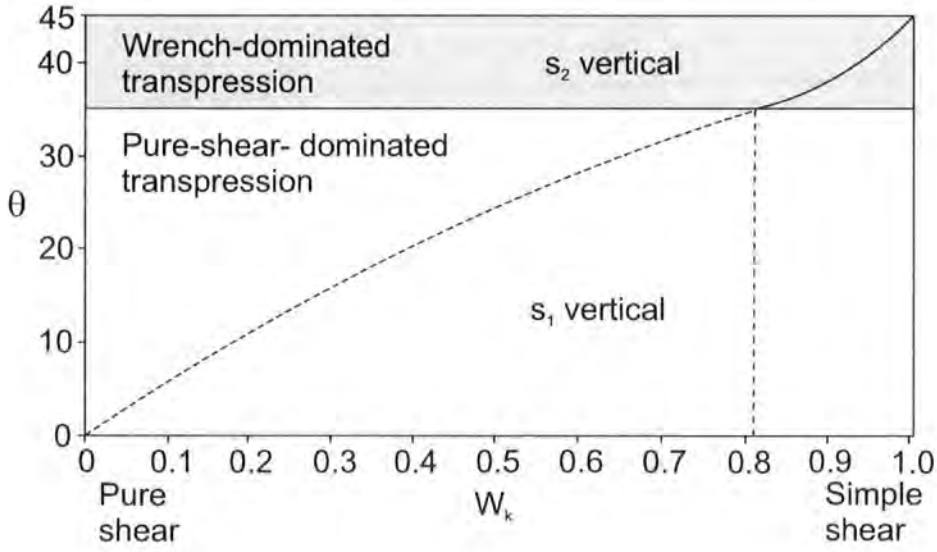

Figure 1.6. Relationship between W_k and the angle θ, showing the transition from pure shear- to wrench-dominated transpression at $w_{cck} = 0.81$ and $\theta = 35^\circ$ (Tikoff & Teyssier 1994).

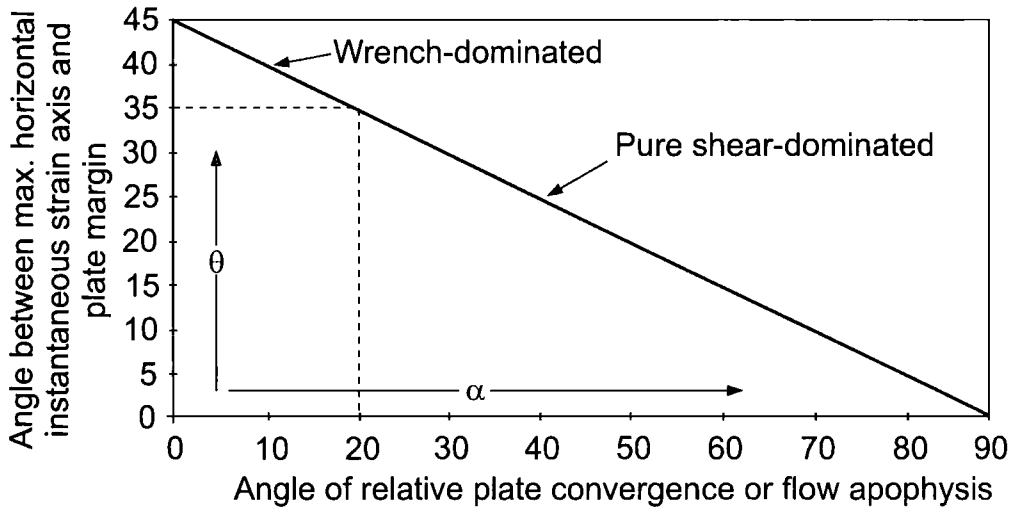

Figure 1.7. Relationship between angle of plate convergence (α) and the angle θ, showing the transition between wrench-dominated and pure shear-dominated transpression occurs at $\alpha = 20^{\circ}$ (Tikoff & Teyssier 1994).

the three-dimensional orientation of the finite strain ellipsoid by mapping various combinations of pure shear and simple shear components (Fig. 1.5), and demonstrated that λ_1 switches with λ_2 at wk = 0.81. This represents the transition from pure shear- to wrench-dominated transpression. The angle θ between the minimum incremental strain axis s_3 and the transpression zone boundary corresponds to a unique value of W_k (Fig 1.6). Wrench-dominated transpression is defined when $1 > W_k > 0.81$ and $35^\circ < \theta < 45^\circ$, while for pure shear-dominated transpression $0.81 \geq W_k > 0$ (Fossen & Tikoff 1993). They also derived a linear relationship between the angle of plate convergence (their α parameter) and θ which predicts that the transition between pure shear- and wrench-dominated transpression occurs at an angle of convergence of 20° (Fig. 1.7, Fossen & Tikoff 1993).

Towards more realistic models of transpression

The models of transpression proposed by Sanderson and Marchini (1984) and Tikoff and Fossen (1993) are highly simplified and the boundary conditions they employed are not wholly representative of natural transpression zones. However, by varying each of the boundary conditions of the basic model it is possible to develop models that are geologically more realistic (Fig 1.8). These allow for factors such as: volume change (Fig. 1.8(a), Fossen & Tikoff 1993), lateral stretch (Fig. 1.8(b), Dias & Ribeiro 1994; Jones *et al.* 1997), the displacement of bounding blocks vertically and laterally by oblique simple shear (Fig. 1.8(c), Robin & Cruden 1994; Jones & Holdsworth 1998; Lin *et al.* 1998) and zones of inclined transpression (Fig. 1.8(d), Jones *et al.* 2001). Despite their increasing realism, all these homogenous strain models possess a number of limitations and are idealised in comparison to the strain patterns occurring in natural shear zones. In particular, two important limitations of models shown in Fig. 1.8(a)-(d) are:

1. The zone boundaries must allow frictionless slip at the boundary of the deforming zone to allow it to extrude while simultaneously permitting the transmission of horizontal simple shear strain, an unlikely scenario in real transpression zones (Dewey *et al.*1998).
2. These models can only accommodate a finite amount of shortening across the deformation zone before the zone boundaries meet and no further transpressive strain can be accommodated (Dutton 1997) i.e. the deformation zone has a fixed volume.

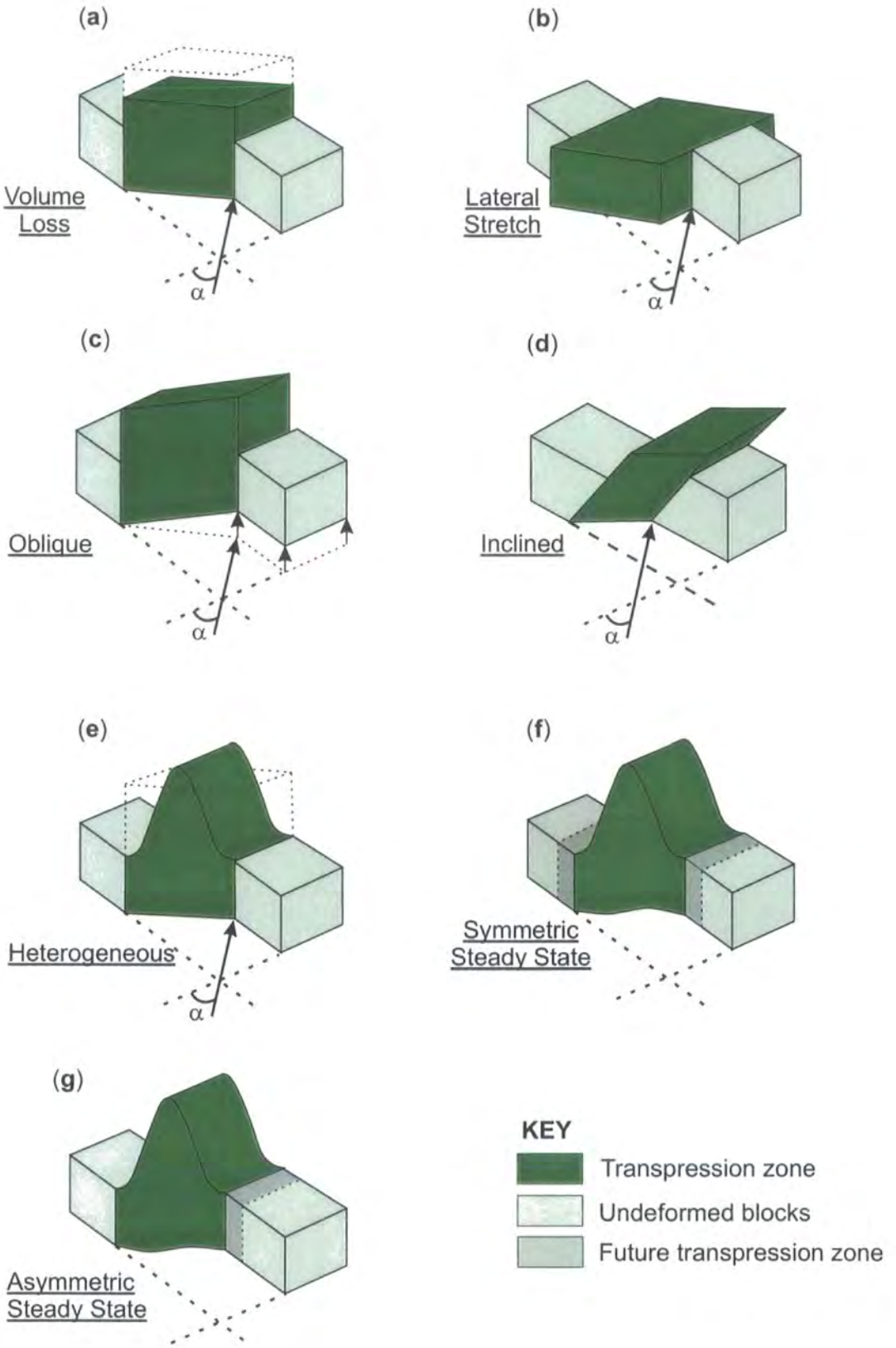

Figure 1.8. Examples of transpressional strain models. See text for details. α is the angle of convergence. (Note that the arrows and angle α are omitted in (**f**) and (**g**) for simplicity; modified from Dewey *et al.* 1998).

Robin and Cruden (1994) overcame the boundary slip problem by using continuum mechanics to model heterogeneous transpression (Fig. 1.8(e)). This model displays a strain gradient from zero slip at the boundary walls to maximum vertical extension at the centre of the zone. Dutton (1997) modelled 'steady-state' transpression where the width of the deformation zone was maintained by the addition of new material from the zone boundaries (Fig. 1.8(f)). This model was further modified to include asymmetrical 'steady state' transpression (Fig. 1.8(g)). The latter two models yield constant strain rates, an important consideration when attempting to correlate flow parameters such as vorticity with finite strains, as this will only be valid if the deformation is steady state (Dewey *et al.* 1998). Despite the increasing realism of these models they are extremely complex and don't easily allow generalisations to be made regarding finite strains. Therefore, Dewey *et al.* (1998) suggest that their use in the analysis of most naturally deformed rocks may be limited.

In the more straightforward models for transpression and transtension (e.g. Fig. 1.8(a)-(c), Sanderson & Marchini 1984; Fossen & Tikoff 1993; Dias & Ribeiro 1994; Jones *et al.* 1997), one of the principal axes of finite strain remains fixed as deformation progresses, and due to the non-coaxial wrench simple-shear component the other two rotate in the plane normal to the fixed axis (see earlier). This produces strains that, in common with simple shear, have a monoclinic symmetry. In contrast, more complex models requiring an oblique simple shear component (e.g. Fig. 1.8(d)-(g), Robin & Cruden 1994, Lin *et al.* 1998, Jones & Holdsworth, Dutton 1997) generally have a triclinic symmetry in which all three axes of finite strain rotate relative to a fixed external reference frame (Fig. 1.9, Lin *et al.* 1998, 1999). The fabric patterns of triclinic transpression/transtension zones are significantly different from those of monoclinic zones. In contrast to the 'switch' in lineation orientation observed in monoclinic transpression, those in triclinic transpression zones may vary continuously from down-dip to subhorizontal (Fig. 1.10), and are dependant upon transpression obliquity (ϕ), γ/ε_b ratio and intensity of strain (Fig. 1.9, Lin *et al.* 1998, 1999).

1.1.3 Kinematic partitioning within transpression zones

Kinematic partitioning of strain into its strike-slip (simple shear) and contractional (pure shear) components is a widely recognised feature of regional transpression and shear zones (e.g. Woodcock *et al.* 1988; Oldow *et al.* 1990; Holdsworth & Strachan 1991; Tikoff & Teyssier 1994; Jones & Tanner 1995; Teyssier

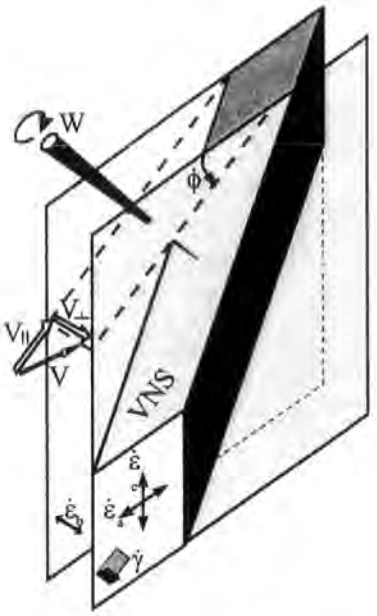

Figure 1.9. Homogeneous oblique transpression ($0°<\phi<90°$), with a general triclinic movement picture. The velocity **V** is oblique to the shear zone boundary and is resolved into a boundary-normal component $\mathbf{V}_{\perp}$, leading to thinning or thickening of the zone ($\dot{\varepsilon}_b$), and a boundary-parallel component $\mathbf{V}_{\parallel}$, leading to simple shear $\dot{\gamma}$. Biaxial stretching of the boundaries is given by $\dot{\varepsilon}_a$ and $\dot{\varepsilon}_c$, which are here assumed to be horizontal and down-dip respectively. The angle between the shear direction (**V** or $\dot{\gamma}$) and the strike of the zone ϕ is the transpression obliquity. **W** = vorticity and **VNS** = vorticity-normal section (the section parallel to the shear direction and perpendicular to the shear zone boundary) (from Lin *et al.* 1999).

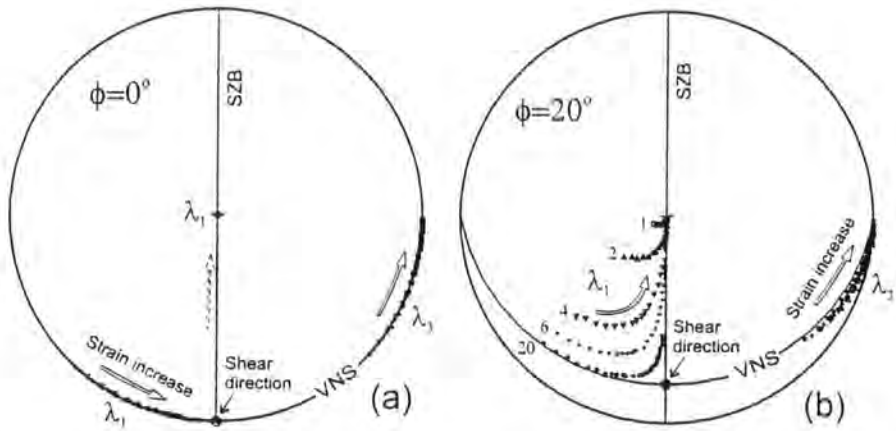

Figure 1.10. Equal-area lower hemisphere projection showing variation and evolution with time of lineations subparallel to λ_1 and poles to foliations subparallel to λ_3 in an isochoric transpression zone with constant strike length. **(a)** Transcurrent transpression ($\phi = 0°$) with monoclinic symmetry. **(b)** Oblique transpression ($\phi = 20°$) with triclinic symmetry. Nos. 1, 2, 4, 6, & 20 are values of γ/ε_b. White arrows indicate evolution with time (increasing finite strain) for differet values of γ/ε_b. Dashed white arrow in **(a)** indicates the 'switch' in orientation of lineation from horizontal to down-dip. VNS = vorticity-normal section, SZB = shear zone boundary (from Lin *et al.* 1999).

et al. 1995; Curtis 1998; Tavarnelli 1998). Woodcock *et al.* (1988) define strain or kinematic partitioning as '*...resulting from the resolution of the oblique relative plate motion vector into its two constituent components of displacement, perpendicular to, and parallel to, the plate margin'*. In particular, the strike-slip component is often partially or wholly partitioned into narrow, discrete zones dominated by monoclinic strike-slip simple shear, which delineate broader zones of distributed largely coaxial pure shear deformation ('slip partitioning' as defined by Lin *et al.* (1999), Fig. 1.11(a)). In the case of triclinic transpression zones Lin *et al.* (1998) suggest that the bulk triclinic strain is partitioned into zones of monoclinic oblique-slip simple shear and largely coaxial pure shear ('deformation path' partitioning as defined by Lin *et al.* (1999)). However, the assertion that transpression and transtension zones are generally triclinic because of oblique simple shear boundary conditions (Lin *et al.* 1998) remains to be proven from detailed field evidence (Dewey *et al.* 1999). Strains in many zones of oblique convergence and divergence are partitioned into orogen-parallel strike-slip or dip-slip faults/shear zones respectively, bounding less deformed crustal blocks in which the deformation is one of orthogonal convergence or divergence (Dewey *et al.* 1999). Molnar (1992) has provided the best rationale to date to explain plate boundary-scale partitioning. He suggests that, in a strong and ductile continental upper mantle, principal stresses and strain rates, generated by a viscous continuum should be parallel to or perpendicular to the Earth's surface. Therefore, oblique-slip faults should not be stable and slip partitioning onto orogen parallel strike-slip or dip-slip faults should be the norm (Dewey *et al.* 1998).

Partitioning of strain may also be facilitated by the presence of pre-existing zones of weakness or weak lithological or rheological boundaries in the crust (Zoback *et al.* 1987; Holdsworth & Strachan 1991; Jones & Tanner 1995; Curtis 1998; Tavarnelli 1998; Tavarnelli & Holdsworth 1999). Tikoff & Teyssier (1994), using a plastic rheological model suggest that it is the relative angle of convergence that controls the effectiveness of partitioning rather than pre-existing weaknesses in the crust (Tikoff & Teyssier 1994; Teyssier *et al.* 1995). They argue that it is the mismatch between the incremental and finite strain axes that is responsible for strain partitioning. Initial faults within a homogenous transpression zone are controlled by the orientation of the incremental strain, and once formed are likely to be preferentially reactivated. Within wrench-dominated transpression zones, s_1 and s_3 are horizontal and therefore strike-slip faults will develop first. During pure shear-dominated transpression s_1 and s_3 lie in a

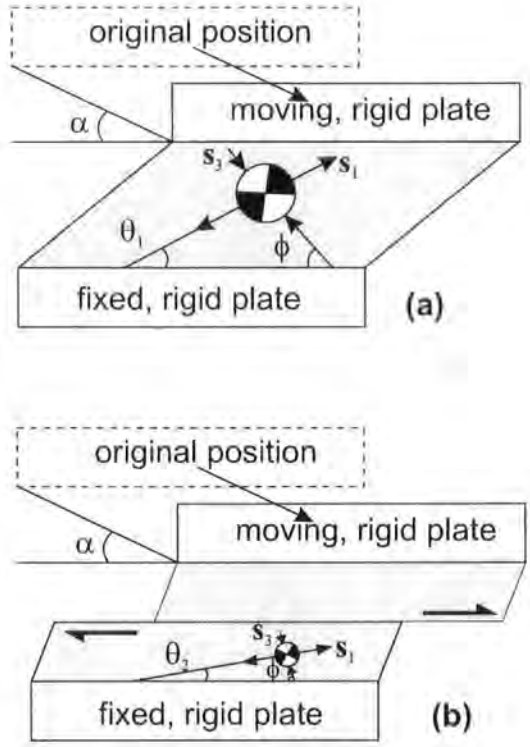

Figure 1.11. Schematic diagram of two plates converging at an angle α, and the resulting transpressional plate boundary characterised by **(a)** homogeneous and **(b)** partitioned displacement. If partitioning occurs, the angle θ_2 is always smaller than θ_1: i.e. the deforming zone contains a larger component of pure shear compared to the non-partitioned case (after Tikoff & Teyssier 1994; Teyssier *et al.* 1995).

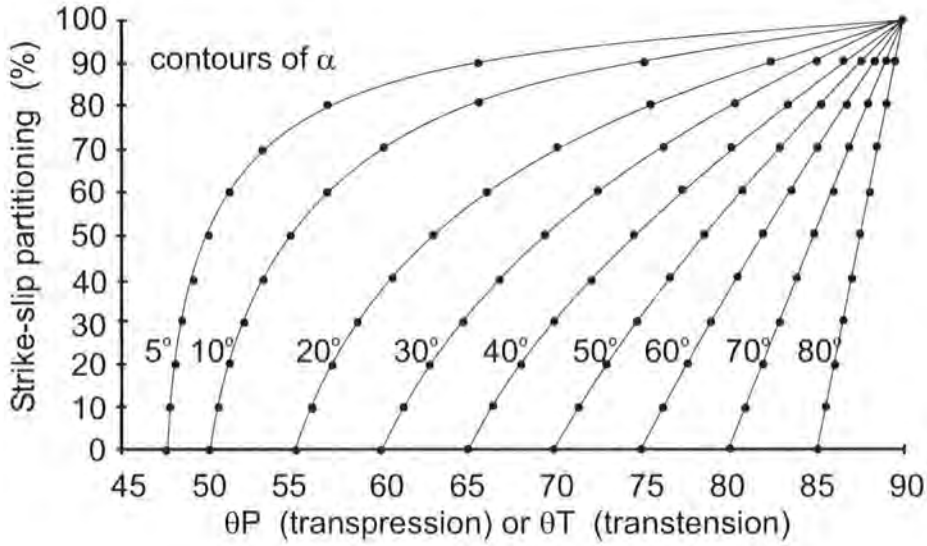

Figure 1.12. Relationship between angle of plate convergence (α), orientation of minimum incremental shortening axis in horizontal plane for transpression (θ), and degree of strike-slip partitioning (after Teyssier *et al.*1995).

vertical plane and reverse faults will develop first. However, because reverse faults are not suitably orientated to accommodate the strike-slip movement imposed by transpressional boundary conditions, strike-slip faults form in response to the finite strain (Tikoff & Teyssier 1994). Importantly, for any angle of convergence, an increase in the degree of strike-slip partitioning along faults results in increased contraction (pure shear) in the adjacent wall rocks. As a consequence of this, s_3 becomes increasingly perpendicular to the plate boundary with increasing partitioning of the strike-slip component (Teyssier *et al.* 1995) (Fig 1.11(b)). Using the orientations of the relative plate motion vectors and the maximum incremental shortening direction (s_3), Tikoff and Teyssier (1994) modelled strain partitioning in transpression zones and provided a means of approximating the degree of strike-slip partitioning likely to occur (Fig. 1.12). Whilst, the model of strain partitioning presented by Tikoff and Teyssier (1994) does not rely on pre-existing weaknesses within the deforming zone, natural examples of deformation zones are rarely homogeneous. Therefore, the effects of pre-existing anisotropies and rheological variations may be profound and should be taken into consideration, especially where the angle of convergence is known to have been at a high angle to the zone boundary.

By modelling a variety of bulk rheologies for accretionary-prisms, (thrust wedges) Platt (1993) showed how the nature and degree of partitioning was influenced by the geometry and mechanical properties of the wedge. In a linear viscous model strain is partitioned continuously, from orthogonal near the toe of the wedge to a rapidly increasing strike-slip component near the back-stop. A plastic rheology however, demonstrated a strong dependence upon the angle of convergence; at high angles, there is little or no partitioning, whereas at low angles, there is a strong partitioning into thrust and strike-slip components (Platt 1993).

Two broad forms of strain partitioning are recognised based on the spatial and chronological relationship between the margin-parallel and margin-normal displacements. These are:

a) Spatial strain partitioning and

b) Temporal strain partitioning.

These two styles of partitioning form the end members of a continuum that exists within natural examples of transpression zones. However, it is useful to define them separately.

Spatial strain partitioning

Curtis (1993) defined spatial strain partitioning as occurring when '*...the resolved components of the oblique relative motion vector are manifest as synchronous, spatially distinct domains of deformation*'. Important in this definition is the contemporaneous development of contraction-dominated (e.g. folds and reverse faults) and wrench- dominated (e.g. strike-slip faults and ductile shear zones) structures (Fig. 1.13). Examples of this type of partitioning have been documented by a number of authors (e.g. Fitch 1972; Holdsworth & Strachan 1991; Strachan *et al.* 1992; Jones & Tanner 1995; Goodwin & Williams 1996; Curtis 1998; Tavarnelli 1998; Holdsworth *et al.* 2002).

Temporal strain partitioning

'*Temporal strain partitioning describes the change in deformational style from one resolved component of the oblique relative motion vector to the other, with respect to time*' (Curtis 1993). Both Sanderson and Marchini (1984) and Tikoff and Teyssier (1994) note that during transpressional deformation, the X-axis of the finite strain ellipsoid switches from vertical to horizontal or vice-versa at high values of shear strain (γ) (Figs. 1.4 & 1.5). Therefore, there may be a progressive overprinting of structures that develop during the early stages of progressive transpressional deformation by those forming at a later stage. Holdsworth and Pinheiro (2000) suggest that temporal partitioning of the contraction- and wrench-dominated phases during transpression may lead to the complex fold patterns observed in the Carajás fault zone in Brazil. Changes in the relative motion vector or changes in the value of α^{-1} will lead to a change in the incremental strain, and thus, lead to temporal strain partitioning. It could be argued however, that temporal partitioning is, in reality, simply changes in spatial partitioning with time.

1.1.4 Folding and cleavage patterns in transpressive regimes

Transpression and associated én echelon folding

There is a well-documented geometrical relationship between the initial orientation of fold axes and the fault zone margins within transcurrent simple shear zones (Moody & Hill 1956; Ramsay 1980). In simple shear, the incremental minimum stretch lies at an angle of 45° to the zone boundary, and hence, folds would tend to

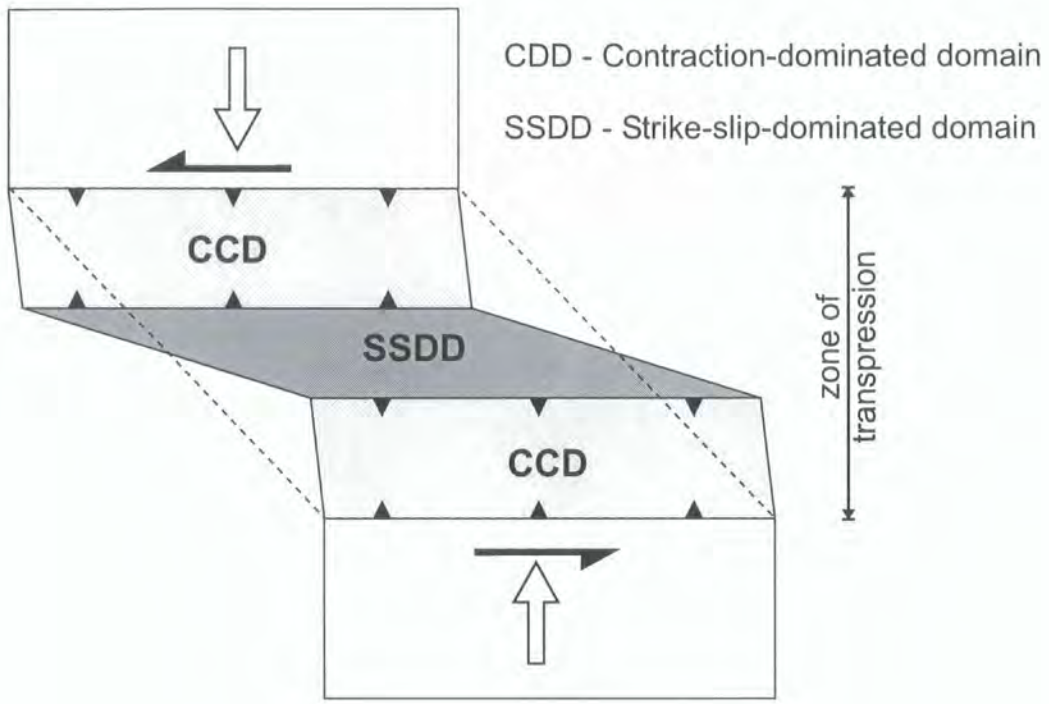

Figure 1.13. Spatial strain partitioning, where the pure shear and simple shear components of the transpressive deformation are expressed as separate, synchronous, distinct domains of contraction-dominated and strike-slip-dominated deformation respectively.

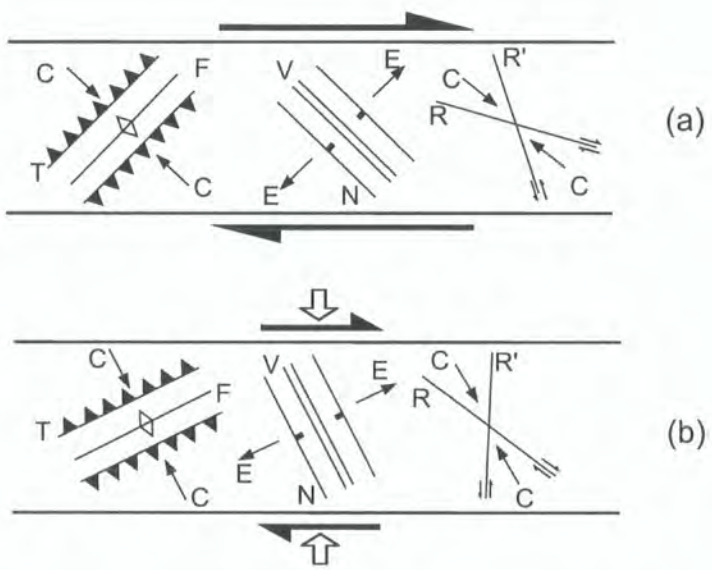

Figure 1.14. Diagrams to illustrate the orientations of folds and fractures in simple shear zones **(a)** and transpression zones **(b)**. C - compression axis (s1); E - extension axis (s3); N - normal faults; T - thrusts; R, R' - Riedel shears or wrench faults; V - veins, dykes or extension fractures; F - fold axes. (redrawn from Sanderson & Marchini 1984).

initiate normal to this direction (Fig. 1.14(a)). Subsequent rotation of the fold axis towards the shear plane as the strain increases modifies this relationship so that the fold axis lies at an angle of $< 45^{\circ}$ to the zone margins. However, in many examples of *én echelon* folding (e.g. Moody & Hill 1956; Moody 1973; Harding 1973, 1974; Wilcox *et al.* 1973), the fold axes lie at angles much less than 45° and if a strike-slip model is applied the required shear strains are much greater than those actually observed. A shear strain ($\gamma > 2$) is required to reduce the fold axis from 45° to 22.5°, implying shortening of c. 60% (Sanderson & Marchini 1984). During transpression fold axes initiate at angles $< 45^{\circ}$ (Fig. 1.14(b)). Figure 1.15 shows the angle of fold axis initiation for different values of incremental strain during simple transpression. Modelling the progressive deformation of folds within a monoclinic transpressive regime, Sanderson and Marchini (1984) showed that early folds passively rotate and tighten, while new folds initiate at a fixed angle to the zone boundary. This results in a pattern of folding where early formed folds lie at low angles to the zone boundary, while later minor folds formed on their shallow dipping limbs or hinge zones lie at higher angles to the zone boundary.

Making some important modifications to the model of Sanderson and Marchini (1984), Fossen and Tikoff (1993) showed that horizontal material lines (for example fold axes, lineations) remain horizontal during transpression/transtension but rotate at different rates, and to different points during deformation. A horizontal line that is initially perpendicular to the shear direction rotates in a similar manner under simple shear and transpression. However, other horizontal lines with different orientations will rotate more slowly with transpression than simple shearing. During transtension, all horizontal lines rotate more slowly than with simple shearing, and the lines rotate towards a horizontal asymptotic line which makes an angle of ϕ with the X-axis (Fig. 1.16). The value of ϕ is dependant upon W_k ($W_k = 1$ for simple shear and $W_k = 0$ for pure shear). In Figure 1.16, the value of $\phi = 24^{\circ}$ and $W_k = 0.75$ (Fossen & Tikoff 1993). More significant still is the observation that all inclined material lines rotate more slowly during transpression/transtension than during simple shear. For transtension, the lines rotate to an angle ϕ with the X-axis, whereas for transpression the inclined lines begin to rotate away from the horizontal to the vertical at some point (Fig 1.16). This change in rotation direction only occurs when λ_1 is vertical.

These observations demonstrate that fold hinges and other material lines that behave in a passive manner can never become parallel to the shear direction in

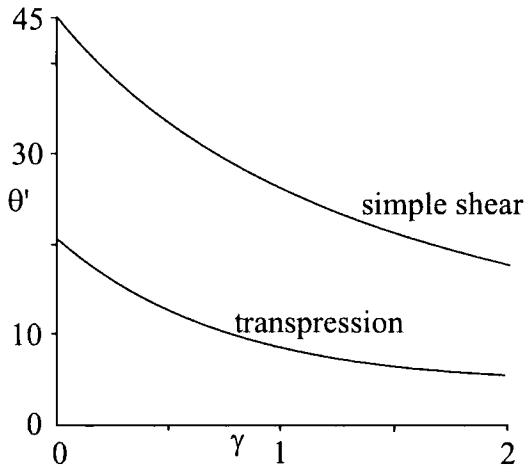

Figure 1.15. Angle of initiation (θ') and subsequent rotation of folds during progressive simple shear (upper curve) and transpression (lower curve). The plate convergence angle is 45° (after Soper 1986).

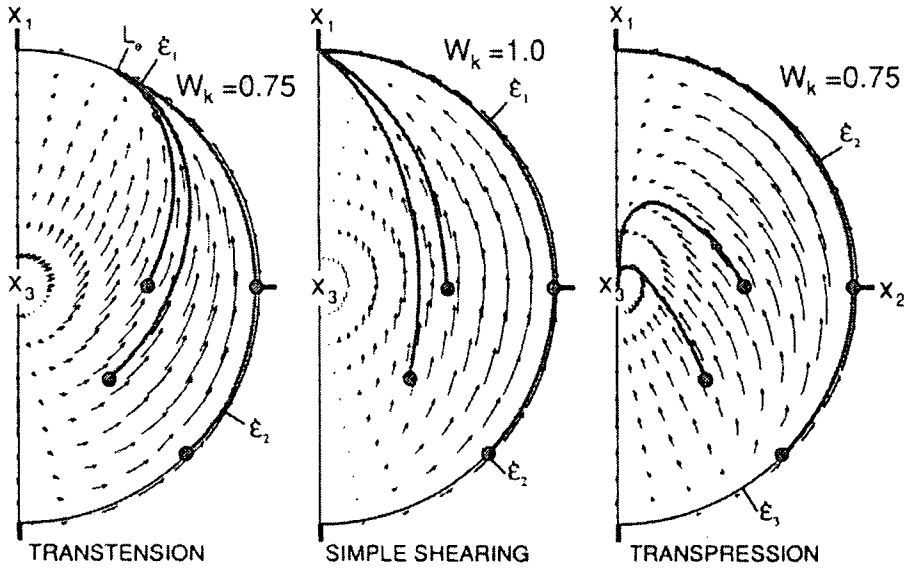

Figure 1.16. Stereographic illustration of the progressive rotation of passive line markers for transpression/transtension (Wk = 0.75) and simple shearing (wrenching). Arrows indicate the result of simple shear strains of 0.25 combined simultaneously with k = 1.1165456 (transpression), k-1= 1.1165456 (transtension), and k = 1 (simple shear) to perform the rotations. The length of the arrows therefore, indicate the rates of rotation in the different fields of the stereograms (after Fossen & Tikoff 1993).

transtension and only if they originate as perfectly horizontal lines during transpression (Fossen & Tikoff 1993).

Cleavage transected folds

'*Transected folds have contemporaneous cleavage that is not parallel to their axial surface, but cuts through the axial surface and both limbs with the same sense*' (Borradaile 1978). Powell (1974) defined them as '*...folds in which a cleavage surface can be traced from one limb across the axial plane surface, to the other limb*' In the field, they are commonly recognised by the divergence of the cleavage-bedding intersection lineations on the opposite limbs of the fold (Johnson 1991). The more usual relationship between folds and their contemporaneous cleavage is that cleavage closely approximates the orientation of the axial surface. Therefore, cleavage-bedding intersection lineations are parallel to the fold axis in all parts of the fold. This angular relationship between folds and cleavage is commonly utilised by field geologists to assist in the location and orientation of large-scale antiforms and synforms. However, in transected folds, both the direction and the amount of plunge of the lineations may change across the axial plane (Fig. 1.17, Pratt & Fitches 1993).

Two angular components are required to describe the three-dimensional relationship between the fold axis, axial plane and planar cleavage (Fig. 1.17):
Δ = the dihedral angle, the minimum angle between the cleavage and the fold axis (measured in the plane that contains the fold axis and the pole to cleavage).
d = the angle between the axial plane and the cleavage in the plane of the fold profile (Borradaile 1978).

In modelling transpression, neither Sanderson and Marchini (1984) nor Fossen and Tikoff (1993) made any association between transpression and folds transected by cleavage. However, transected folds are commonly interpreted in terms of transpression. The resulting combination of pure shear and simple shear during transpression results in a progressive rotation of the principal strain axes. Therefore, any delay between the initiation of folds and the development of cleavage will result in cleavages that are non-axial planar (Pratt & Fitches 1993). Over recent years, a number of authors have closely linked sinistral transpression with the development of clockwise-transected cleavage (e.g. Soper & Hutton 1984; Murphy 1985; Soper 1986; Woodcock *et al.* 1988; Pratt & Fitches 1993). Clockwise-transected folds are thought to develop during sinistral transpression because most folds initiate prior to the pressure

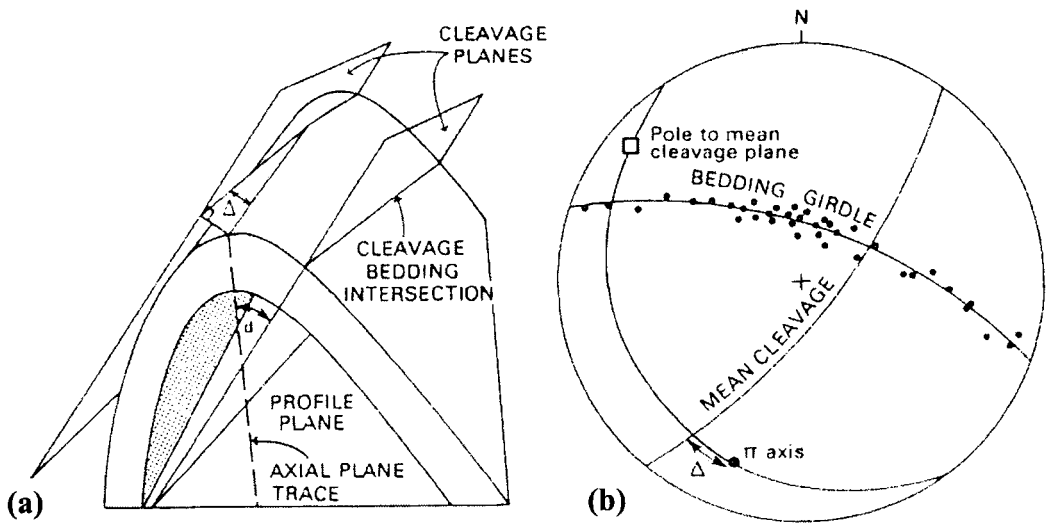

Figure 1.17. **(a)** Diagram of transected fold showing Δ and *d* transection angles. Note that cleavage-bedding intersections plunge in opposite directions on the two fold limbs. **(b)** Stereogram demonstrating Δ angle (after Pratt & Fitches 1993).

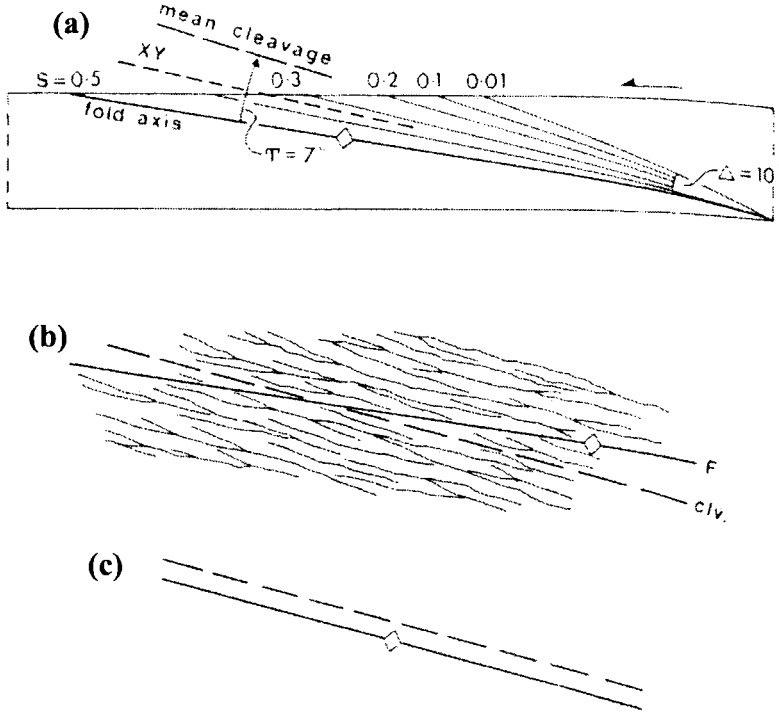

Figure 1.18. Cleavage dispersion and transection in sinistral simple transpression. **(a)** fold is generated during the first deformation increment and rotates passively. Cleavage develops parallel to XY incremental after 10% shortening, continues to develop through successive strain increments and rotates passively. **(b)** Dispersion and clockwise transection geometry produced by model (a). **(c)** Axial planar cleavage produced when buckling takes place half-way through the period of cleavage formation (after Soper 1986).

solution stage of cleavage development. This is particularly true of rigid layers within ductile envelops, which begin to buckle after very little layer parallel shortening and well before cleavage development (Pratt & Fitches 1993). Soper (1986) provided a persuasive rationale for the link between sinistral transpression and clockwise transected cleavage. He suggested that the domainal anastomosing cleavage common to many lithologies within the British Caledonides, was the result of the incremental development of a pressure solution cleavage. During sinistral transpression, early cleavage traces are passively rotated with a sinistral sense, with later increments being superimposed in a clockwise sense. Soper (1986) used this model to account for both the anastomosing style of cleavage and transection angles (Δ) up to 10° (Fig. 1.18). In his model, Soper (1986) followed Sanderson and Marchini (1984) in considering fold hinges to be markers of small incremental strain that passively rotate with further increments of strain. Therefore, the fold hinge doesn't remain parallel with the XY-plane during transpression. However, arguing against this, Treagus & Treagus (1992) suggest that no fold would be visible after a small strain increment, and that folds will develop progressively with accumulating finite strain. They further suggest that, only after considerable layer parallel shortening (c.50%) would fold hinges become fixed by considerable curvature and thereafter passively rotate as a material marker to lie slightly closer to the zone margin than the XY trace. This mechanism cannot account for folds cross-cut by cleavage by as much as 10° (Treagus & Treagus 1992). Countering the argument put forward by Treagus and Treagus (1992), Pratt and Fitches (1993) cite examples from the Lower Palaeozoic Welsh Basin that indicates that folds here were established after small values of shortening (c.5-25%). They propose that the layers began to buckle into long wavelength folds after only minor amounts of layer-parallel shortening and long before the onset of pressure solution cleavage. Subsequent passive rotation of the folds led to the large transection angles observed.

The above models assume that prior to deformation the bedding was horizontal. However, this may not always be the case. Treagus and Treagus (1992) argue that it is highly unlikely that rock layers would be deformed in exact layer-parallel compression/extension. They were able to demonstrate a variety of transection relationships, controlled by the obliquity of strike to the zone margin by modelling the deformation of inclined layers. They considered two cases of inclined layers during sinistral transpression. Case 1 are layers parallel to the converging plate margin, with varying initial dips. Case 2 are layers oblique in strike and dip.

In the first case, the XY-plane trace (cleavage) is anticlockwise of the fold axis. This is opposite to the relationship commonly associated with sinistral transpression. As the dip of the layer increases so does the transection angle (Fig. 1.19(a)). In the second case, inclined layers, which strike oblique to the plate margin, show a wide range of discordance angles and trends between expected fold axes and the XY-plane (Fig. 1.19 (b)). The sense of layer strike to the XY-plane is critical, and divides fields of anticlockwise, axial planar and clockwise cross-cutting relationships (Fig. 1.19(c); Treagus & Treagus 1992).

As yet, a general mechanism for cleavage transected folding is still not available, and the phenomenon may indeed be polygenetic. However, the sense of cleavage transection alone should not be used as evidence for the sense of shear in transpression zones. Further supporting kinematic data should be sought to substantiate interpretations based on transection sense. That said, the wide spread nature and consistency of the sense of cleavage transection within the Lower Palaeozoic British Caledonides is often cited as compelling evidence for its use for determining the sense of shear in transpression zones (e.g. Soper 1986; Treagus & Treagus 1992; Pratt & Fitches 1993).

1.1.5 Characteristics of transpression zones: a summary

a) Transpression is a three-dimensional non-coaxial strain that can be resolved into a combination of strike-slip or oblique-slip simple shear and pure shear (Dewey *et al.* 1998; Lin *et al.* 1998).
b) The simple and pure shear components probably act simultaneously.
c) Strains are normally flattening or oblate ($k < 1$).
d) Cleavages are sub-vertical with variably orientated stretching lineations.
e) Compressional structures e.g. folds and thrusts initiate at angles <45°to the zone margin.
f) Extensional structures, e.g. normal faults, veins and dykes, initiate at angles >45° to the zone margin.
g) The pure shear and simple shear components of the deformation may be partitioned into separate contraction-dominated and wrench-dominated domains.
h) The complex deformation patterns formed during transpression may be incorrectly interpreted as being the consequence of polyphase deformational events.

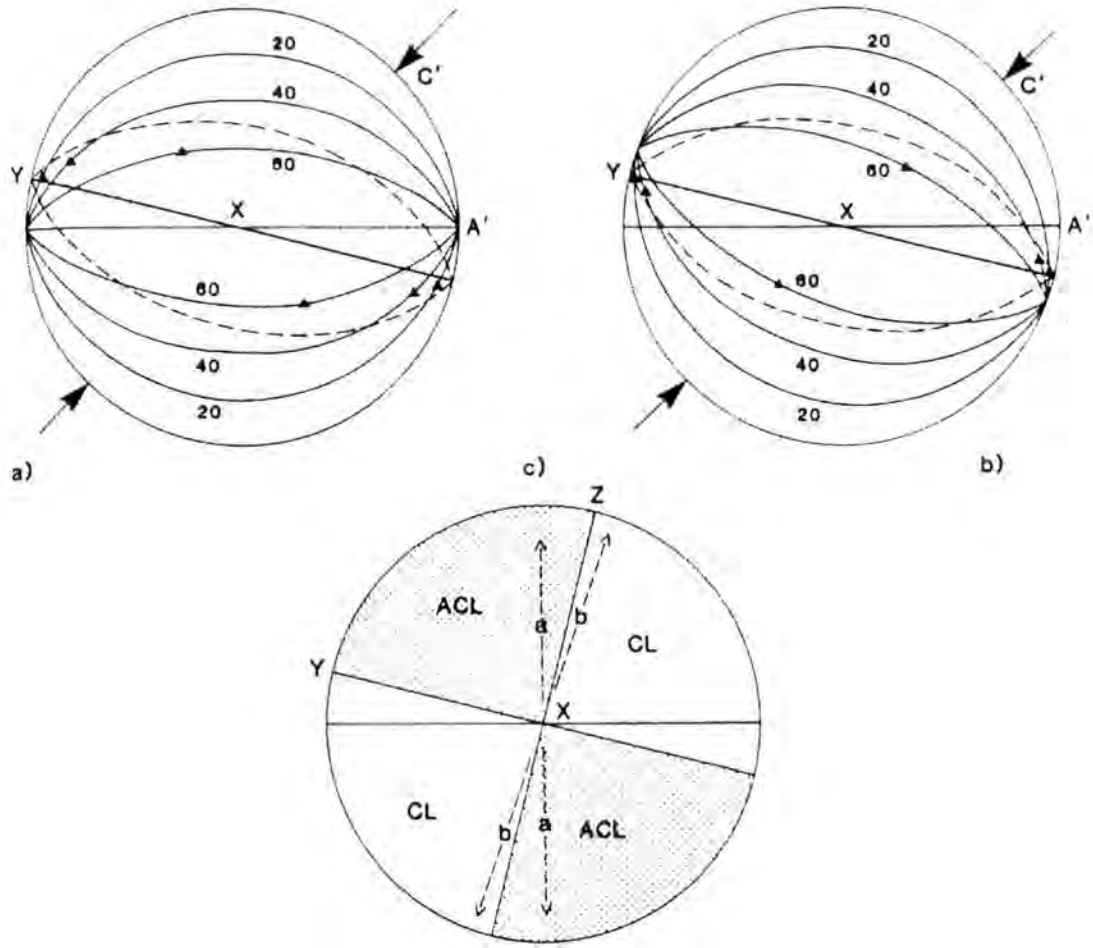

Figure 1.19. The effect of inclined and oblique layering on cleavage transection, with respect to a sinistral transpressive deformation. Transpression vector is bold arrow, transpression zone margin (A') east-west. Solid line XY-plane, broken curves circular sections. (a) Planes striking parallel to zone margin, dips 20°, 40° and 60°. Fold axes (solid dots) are cut anticlockwise by the XY-plane. (b) Planes striking 20° to the zone margin, otherwise as (a). Fold axes are transected clockwise. (c) Fields for which bedding poles would have anticlockwise transection of fold axes by XY-plane (ACL shaded), and clockwise (CL, blank) positions for examples in (a) and (b) indicated by broken lines, labelled a and b (after Treagus & Treagus 1992).

1.1.6 Curvilinear fold hinges in transpression zones

Many folds display fold hinge geometries that are significantly curvilinear, sometimes referred to as 'whaleback folding' (Fig. 1.20(a)). This may be a consequence of the mode of fold initiation (Dubey & Cobbold 1977), and/or be due to fold initiation in inclined layers oblique to all three finite strain axes (Treagus & Treagus 1981). Using empirical modelling of flexural slip folds, Dubey and Cobbold (1977) showed that non-cylindrical folds were the result of folds initiating as non-cylindrical deflections, fold amplification being more rapid than hinge lengthening and fold interference. Treagus and Treagus (1981) describe a mechanism whereby two sets of orthogonal fold axes can develop simultaneously when the three-dimensional relationship between bedding and the principal axes of finite strain is markedly non-parallel. Holdsworth and Pinheiro (2000) also suggest that folds with curvilinear hinges may be the result of locally constrictional strains during transpression or a consequence of highly localised Type 1 interference of Ramsay (1967) due to temporal strain partitioning. In the latter case, folds formed during the contraction-dominated phase of transpression are subsequently overprinted during the wrench-dominated phase.

Generally, in contractional or thrusting regimes non-cylindrical folds are upward facing (Fig. 1.20(a)). However, in strike-slip or wrench-dominated transpression zones, the fold hinge may pass through the vertical to face sideways and then downwards (Fig. 1.20(b)). Such folds have been documented by a number of authors (e.g. Dearman *et al.* 1962; Simpson 1965; Brenchley & Treagus 1970; Holdsworth 1989; Holdsworth & Pinheiro 2000). At higher strains these folds should grade into sheath folds like those formed in highly deformed belts of ductile deformation (Carreras *et al* 1977; Holdsworth 1994; Alsop & Holdsworth 1999).

1.2 Vergence

1.2.1 Introduction

Introduced by Stille (1924) the concept of vergence has been extensively used by geologists, although its precise meaning has been much debated (e.g. Roberts 1974; Bell 1981). Stille's use of the word 'vergenz' described the directional sense of overturning of minor folds and the up-dip direction of planar fabrics. The implication was that 'vergenz' was the product of kinematic overthrusting. This has led to a number of differing definitions of the term and, therefore, a degree of confusion amongst

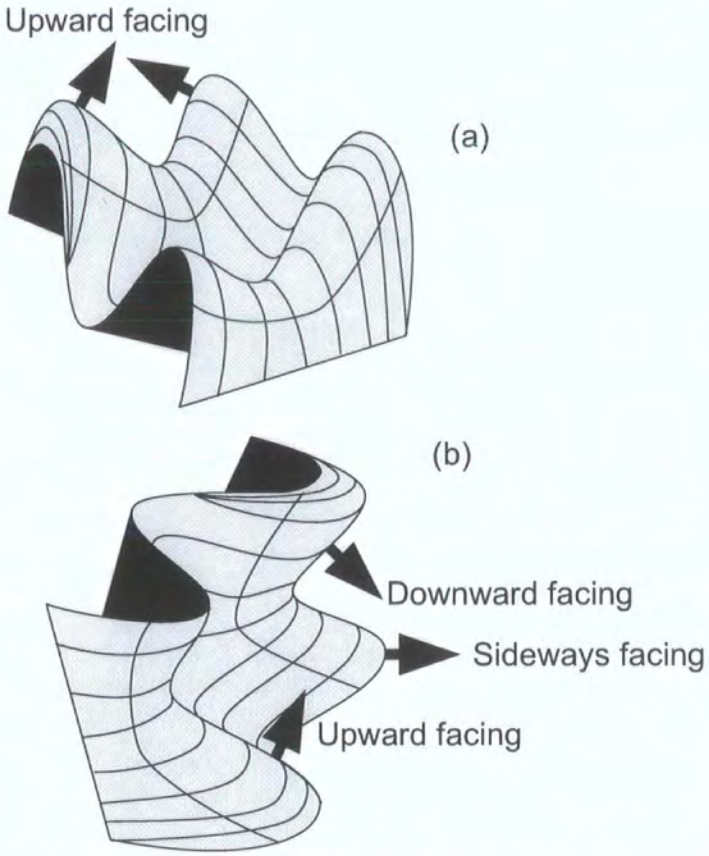

Figure 1.20. Diagram of non-cylindrical folds **(a)** upward facing 'whale back' folds **(b)** Upward, sideways and downward facing curvilinear folds..

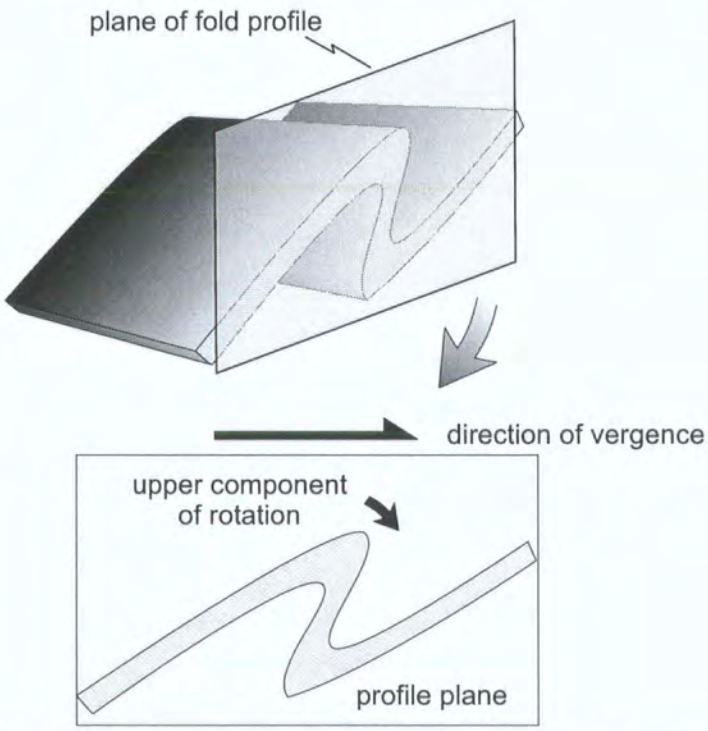

Figure 1.21. Definition of fold vergence (see text for details) (redrawn from Bell 1981).

geologists. In particular, the American usage of the term is synonymous with facing (e.g. Gary *et al.* 1972). Bell (1981) in keeping with modern usage defines vergence only in terms of geometrical relationships, thus avoiding any directional implications or association with facing. Two types of vergence are recognised.

1.2.2 Fold vergence

The principal use of minor fold vergence is in the location of larger fold hinges. Geometrically, asymmetric folds can be considered to have short limbs which have been rotated from a position now preserved by the longer limb (Bell 1981). Roberts (1974) defined asymmetric fold vergence '*...as the horizontal direction, within the plane of the fold profile, towards which the upper component of rotation is directed*' (Fig. 1.21). This definition using the azimuth of fold vergence is preferable to the use of 'S' (sinistral) and 'Z' (dextral) prefixes, as it is independent of fold plunge variations. However, the use of 'S' and 'Z' vergence remains in use and is perfectly acceptable provided that it is described as viewed down the plunge of the fold axes. Where the profile plane of the fold is horizontal (i.e. vertical fold plunge) then no unique direction of fold vergence exists since the upper component of rotation cannot be recognised (Fig. 1.22). In such cases, the term sinistral or dextral vergence is applied (Bell 1981).

1.2.3 Cleavage vergence

The concept of vergence can also be extended to describe cleavage-bedding relationships where bedding is not folded (Roberts 1974). Although Roberts did not provide a definition of cleavage vergence, (Bell 1981) defined it as '*...the horizontal direction within the plane normal to the fabric intersection lineation, towards which a younger fabric needs to be rotated* (through the acute angle) *so that it becomes parallel to the older fabric*' (Fig. 1.23). The earlier fabric may commonly be bedding, but if vergence of a later cleavage is being considered, it must be related to the immediately previous fabric. Cleavage vergence, like fold vergence may be used to locate major fold axes (Bell 1981).

The concepts of fold and cleavage vergence are distinct from, and should not be confused with, the concepts of fold and cleavage facing, although the two are often used in conjunction when describing folded terrains.

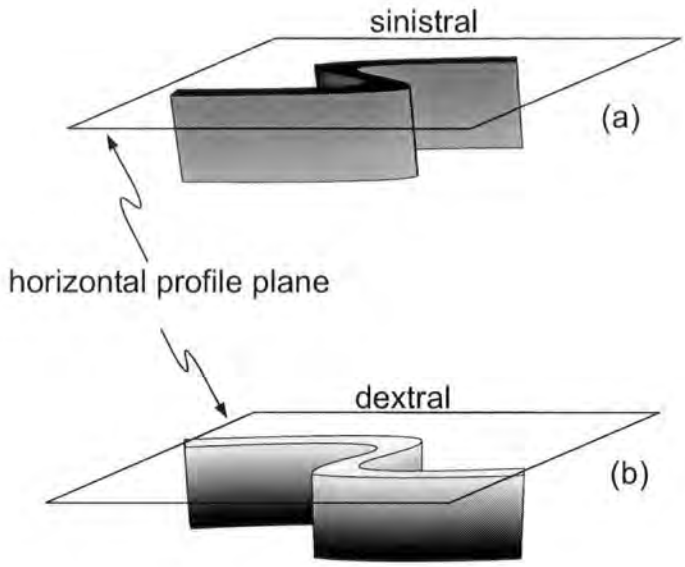

Figure 1.22. Folds that plunge vertically have either sinistral **(a)** or dextral **(b)** vergence (redrawn from Bell 1981).

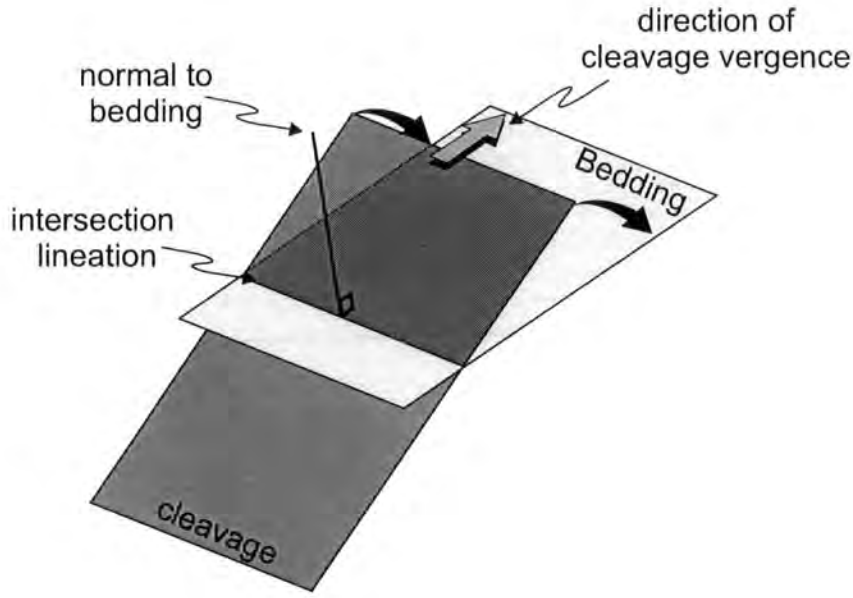

Figure 1.23. Definition of cleavage vergence (see text for details) (Bell 1991).

1.3 Facing

Significant advances have been made in the field of structural geology by the use of sedimentary structures as a means of identifying primary younging in rocks that have undergone complex tectonism and metamorphism (Holdsworth 1988). The term facing was first employed by Shackelton (1957) while describing folds and cleavage from the Highland Border. He defined fold facing (Fig. 1.24) as '*...the direction, normal to the fold axis, along the fold axial plane, and towards the younger beds*'. This coincides with the direction the beds face at the fold hinge. He also defined cleavage facing (Fig. 1.25) as '*...the direction normal to the bedding plane intersection, along the cleavage plane, and towards the younger beds*'. Although originally applied to areas which display folds and cleavage, Lisle (1985) extended its use to include faults and defined fault facing as '*...the direction normal to the bedding plane intersection, along the fault plane and towards the younger beds*'.

Holdsworth (1988) noted, that in common with any linear feature, facing possesses both and inclination and azimuth. However, because it is a polar, rather than an axial lineation, a horizontal reference plane is used and the terms upward-, downward- and neutral facing are used to qualify the facing azimuth. Holdsworth (1988) provided a simple construction (Fig 1.26) for the stereographic analysis of facing that enabled the facing data to be analysed in a quantitative manner (see Holdsworth 1988 for methodology). This technique can be applied to a wide variety of geological problems where way up criteria are available and facing is an important factor e.g. areas of refolding and areas of sheath folding (Holdsworth 1988; Alsop & Holdsworth 1999).

1.4 Kinematic indicators

1.4.1 Introduction

A range of minor structures can be employed as kinematic indicators to determine the sense of movement across faults and shear zones, particularly when the sense of slip cannot be determined by offset geological structures. Two categories can be defined, dependent upon whether they are associated with brittle or ductile deformation. When determining the sense of movement it is important to ensure that structures are viewed in the correct orientation. Firstly, lineations that parallel the

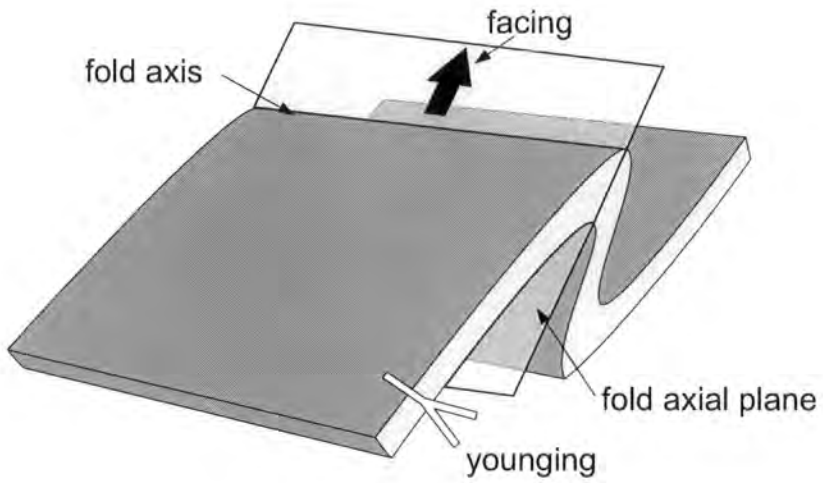

Figure 1.24. Definition of fold facing (see text for details).

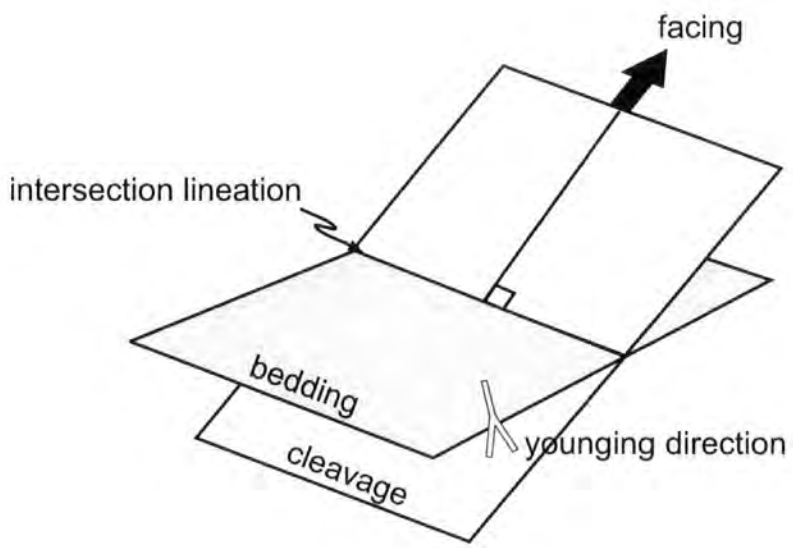

Figure 1.25. Definition of cleavage facing (see text for details).

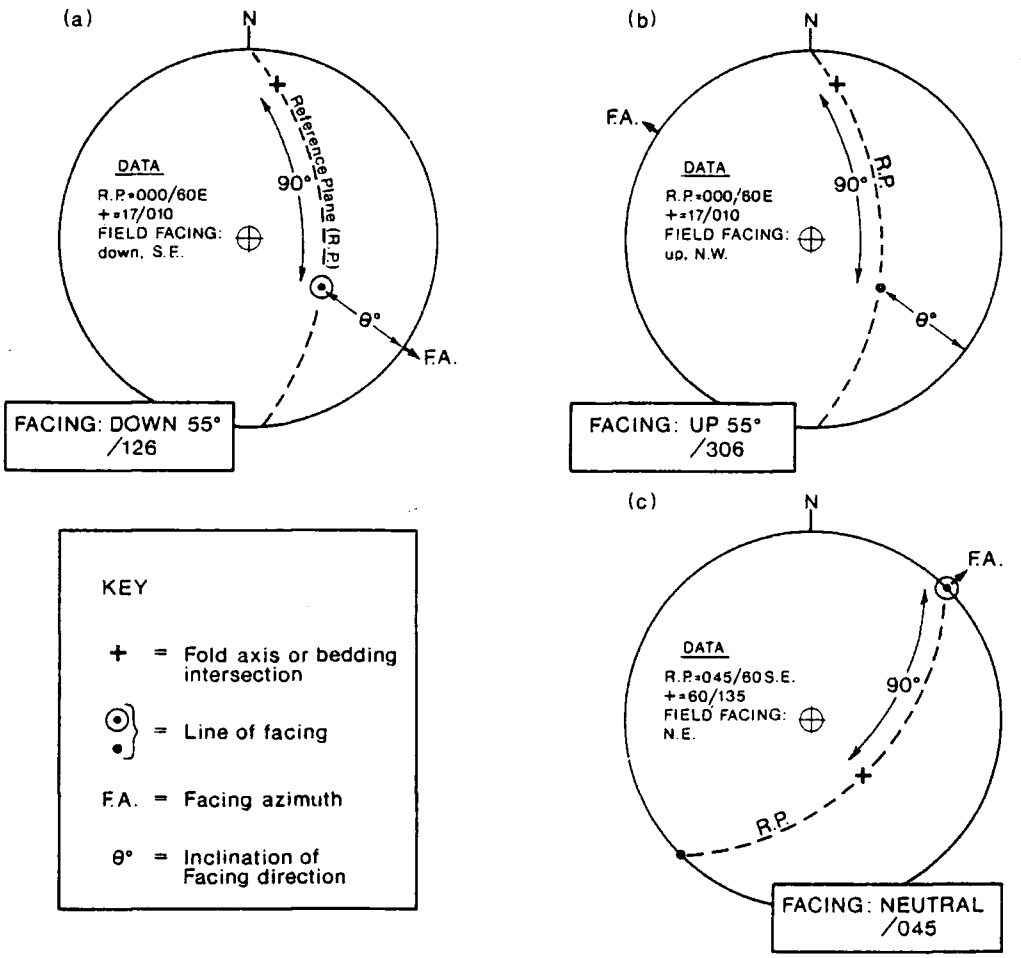

Figure 1.26. Stereographic projections showing examples of how to determine facing directions. The line of facing lies within the reference plane at 90° to the fold axis or bedding intersection. The appropriate line of facing intersection is selected on the basis of field data, and the azimuth and inclination of facing are 'read-off' in the normal manner. **(a)** Downward-facing. **(b)** Upward-facing. **(c)** Neutral-facing. Solid circles and circle with dot symbol denote upward- and downward-facing lines respectively. The arrow outside the primitive shows the facing azimuth (from Holdsworth 1988).

motion vector, must be identified. Common lineations include brittle fault striae, slicken fibres and ductile mineral stretching lineations. Once such lineations are identified, any shear sense indicator should be viewed in the plane parallel to the lineation and orthogonal to the shear plane. Wherever possible a number of different shear sense criteria should be used in conjunction to determine the sense of shear.

1.4.2. Brittle shear sense indicators

In the absence of geological offsets to determine the relative sense of fault movement, the study of minor structures associated with slickensides and slicken fibres, along with the presence of secondary structures associated with faults and the adjacent wallrock can be used to infer the relative sense of movement on brittle faults.

1.4.2.1. Slickenside striations

Several types of lineations present on fault surfaces and associated with fault movement can be identified. Their morphologies and causes can be varied but are usually dependent on lithology. Figure 1.27 illustrates several types of slickenside lineations and their sense of movement interpretation.

i) Striations

Striations occur when fragments of rock or mineral grains scratch grooves in the fault surface (Fig. 1.27(a)). The end of the resultant striae or plough mark points towards the movement of the missing fault-wall (Petit 1987). These features have also been called prod marks (Tjia 1971) and tool marks (Hancock 1985). All these can be integrated into the more general case of asperity ploughing (Means 1987) where the grooves are the product of resistant protuberances or asperities on one or other of the fault surfaces.

ii) Crystallisation linked to irregularities on the fault surface

Irregularities, in the form of steps, generally form perpendicular to the striation on the fault surface. The risers to these steps face in the direction of the missing block (Fig. 1.27(b)). The voids created by these accretion steps can be filled by fibrous quartz or calcite (in the case of limestones) during slow dilation of the voids, or blocky euhedral calcite when the voids open rapidly such as during a microseismic event (Petit 1987). The fibres produced on fault planes during shearing may show curved

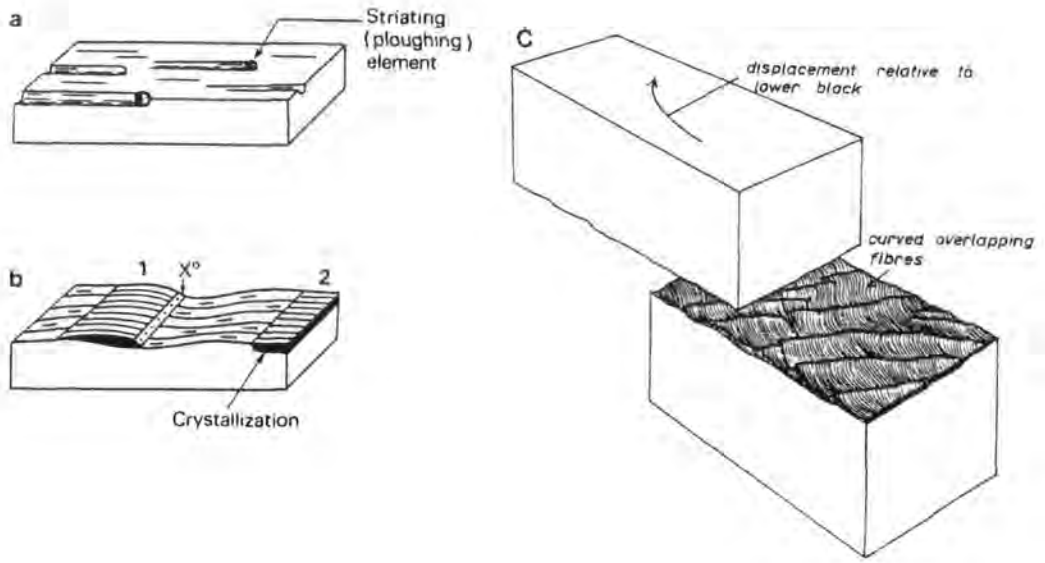

Figure 1.27. Slickenside striations. **(a)** Striations (grooves) produced due to fragments of rock or mineral grains on the fault surface. **(b)** Crystalisation on the lee side of irregularities on the fault surface forming overlapping sheets of fibrous mineralisation. **(c)** Sheets of curved fibrous mineralisation caused by changes in the displacement vector during faulting. (from Ramsay & Huber 1983 and Petit 1987).

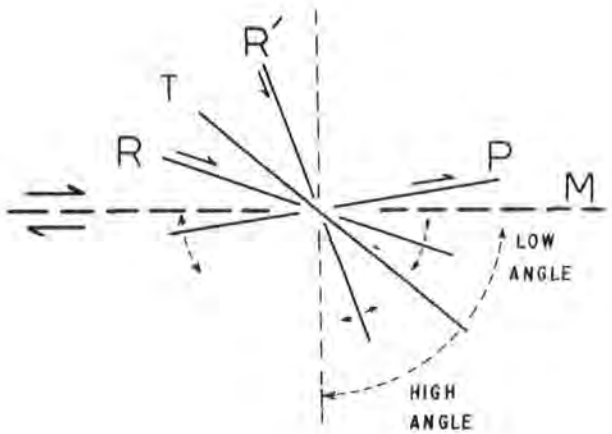

Figure 1.28. Sense of shear criteria based on the angular relationship between repetitive fractures and the main fault/shear plane (from Petit 1987).

geometries, reflecting the change in direction of the displacement vector as the shear progresses (Fig. 1.27(c) Ramsay & Huber 1983).

1.4.2.2. Shear sense structures involving secondary fractures

A common feature observed along fault planes are the presence of sets of repeated, secondary brittle fractures. These are asymmetrically orientated at an angle to the mean shear plane and may be used to determine the overall sense of shear. Figure 1.28 illustrates the angular relationship that these sets of fractures possess with respect to the mean fault plane. The nomenclature adopted here is that of Petit (1987) and is based mainly on Riedel-type experimental terminology.

Three types of fractures can be identified:

a) T-fractures: These are tensional fractures and are therefore unstriated. They can make an angle of 30° to about 90° to the mean shear plane, and may be open or mineralised. When viewed on the fault plane they may be straight or crescentic. The horns of the crescents point in the direction of the missing block (Petit 1987).

b) R-fractures: Two types of extensional R (or Riedel) fractures may be present. R-fractures form at low angles (10°-20°) to the mean fault plane and are synthetic to the main fault. R'-fractures form at high angles (70°-90°) to the mean fault plane and are antithetic (Twiss & Moores 1992).

c) P-fractures: These form in response to contraction and are synthetic to the main fault, forming at low angles (10°-20°) to the mean fault plane (Twiss & Moores 1992).

1.4.3. Ductile Shear Criteria

In its simplest form, a shear zone can be considered as a zone of highly strained rock between approximately planar and parallel-sided boundaries. The rocks outside the boundaries remain unaffected by the shear deformation (Ramsay & Graham 1970; Ramsay 1980). Where the margins of the shear zone can be observed, the geometry of structures formed by the strain gradient can be used to define the sense of shear. For example, the sigmoidal form of schistosity, orientation of folded and boudinaged competent layers, fracture openings and the geometry of *én-echelon* vein arrays.

However, many shear zones are very wide, and the margins may not be exposed and offset markers may be absent. In such cases, the use of small-scale asymmetric structures to deduce the sense of shear is necessary (Simpson & Schmid 1983). These are formed during non-coaxial strain and comprise a number of structures, microstructures and fabrics that have an asymmetry reflecting the sense of vorticity within the shear zone.

Following the review of Hanmer and Passchier (1991) four main groups of ductile (to brittle-ductile) kinematic indicators are cited:

- Shape fabrics
- Porphyroclast systems
- Veins
- Folds

1.4.3.1. Shape fabrics

Shape fabrics include the rotation and deflection of pre-existing foliations, C/S fabrics and asymmetrical extensional shear bands (AESBs).

With progressive simple shear and increasing strain, schistosity within the shear zone is rotated from an initial angle of 45° to the zone boundary towards parallelism to the zone margin (Fig. 1.29, Ramsay & Graham 1970).

The standard work on C/S fabrics is that of Berthé *et al.* (1979). They observed two sets of planar anisotropies that they described as C- and S- surfaces, referring to 'cisaillement' (shear) and 'schistosité (schistosity, foliation) (Fig. 1.30). The C-planes are discrete shear zones, tens of centimetres in length and a millimetre or more in thickness. They tend to form in rocks where strain is heterogeneously distributed at the grain scale, initiating and remaining parallel to the main shear zone boundary with progressive deformation (Simpson & Schmid 1983). The S-planes are flattening fabrics that define sigmoidal microlithons between adjacent C-planes. S-planes are rotated into C-planes in the direction that reflects the sense of shear (Passchier & Trouw 1996).

One of the commonest shear sense indicators in anisotropic rocks are AESBs, (Fig. 1.31) also termed shear band foliations (White *et al.* 1980), C' (Berthé *et al.* 1979), or asymmetrical extensional crenulation cleavage (Platt & Vissers 1980). They consist of discrete shear zones or 'shear bands' oriented at about 15°- 25° to the bulk flow plane. Ideally, only one set of shear bands develops whose sense of slip is synthetic to the shear sense of the bulk flow plane. However, it is not uncommon for a conjugate, but

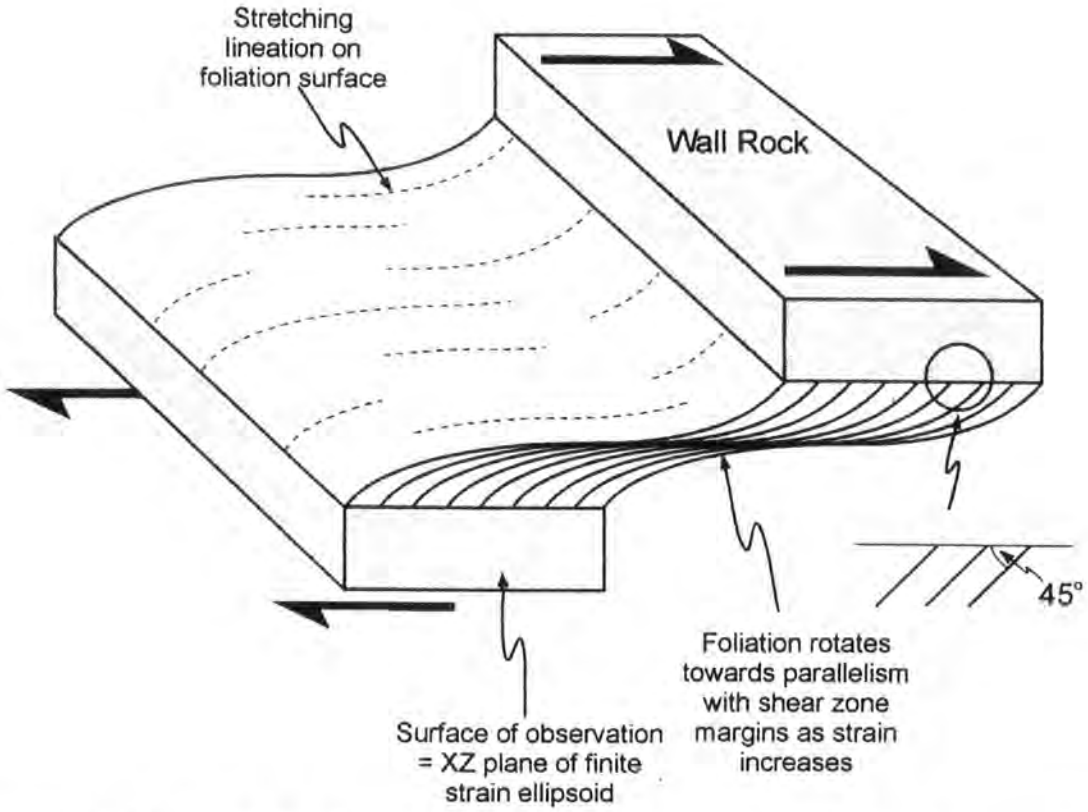

Figure 1.29. Idealised ductile shear zone, illustrating rotation of foliation from an initial angle of 45° towards parallelism with the zone margin with progressive simple shear and increasing strain. This also shows the correct plane in which to observe sense of shear criteria (after Hanmer & Passchier 1991).

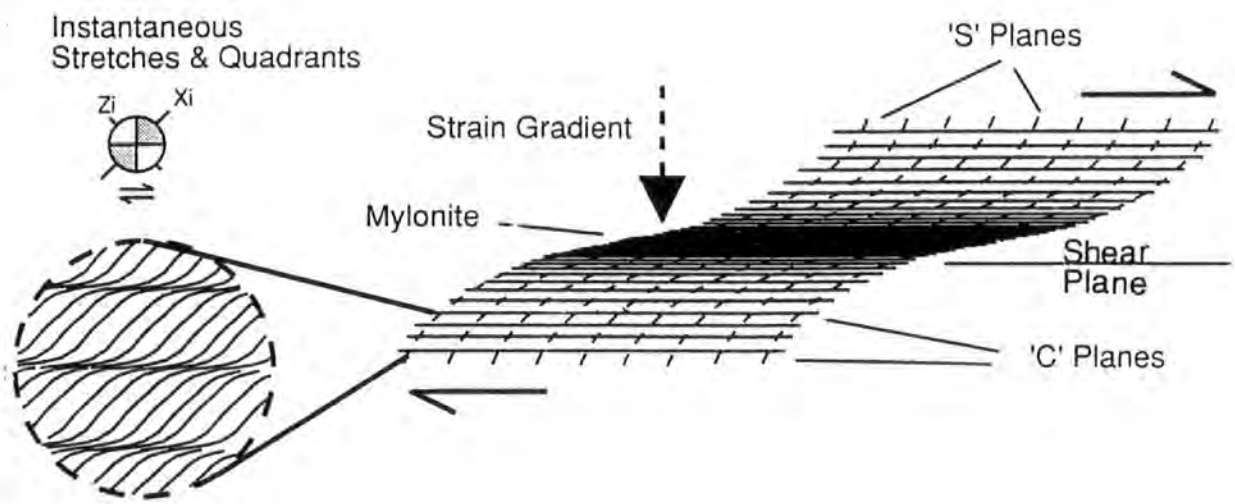

Figure 1.30. Cartoon illustrating the main characteristics of C/S fabrics (from Hanmer & Passchier 1991).

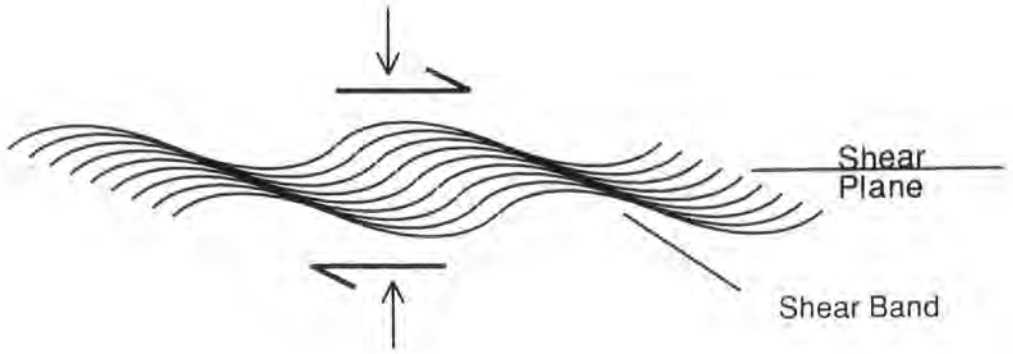

Figure 1.31. Asymmetrical extensional shear band fabric (AESB) (from Hanmer & Passchier 1991).

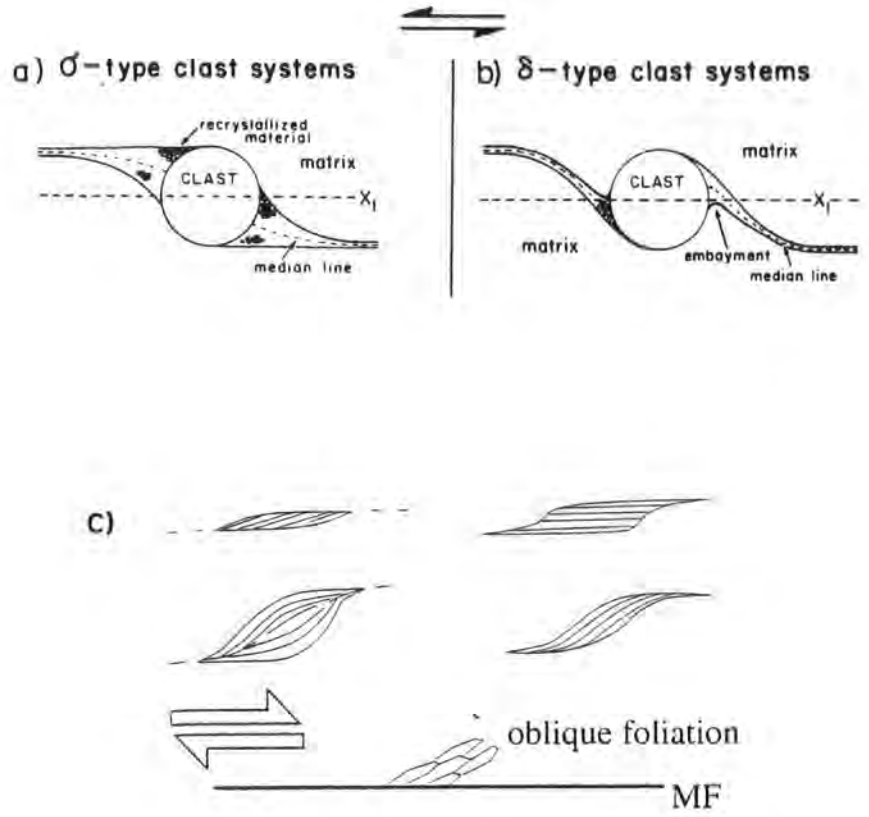

Figure 1.32. Schematic diagram showing **(a)** σ and **(b)** δ porphyroclasts. Both show a sinistral sense of vorticity. **(c)** Several common types of mica fish and their orientation relationship with the mylonitic foliation (MF) and an oblique foliation. All show a dextral sense of shear (after Passchier & Trouw 1996).

numerically subordinate set to form (Hanmer & Passchier 1991).

1.4.3.2. Porphyroclast systems

Many rocks in ductile shear zones contain rigid inclusions or porphyroclasts whose geometry is the result of non-coaxial deformation. Such structures may be used to determine the sense of shear. In many cases when viewed parallel to the rotation axis of the bulk flow, most porphyroclasts consist of a circular to elliptical monocrystalline core, attached to thin, often asymmetric, wing-like appendages similar in composition to the parent porphyroclast. Polymineralic inclusions are also possible, and their wings may consist of reaction products, deformed pressure shadows, or bands of matrix material entrained by the rotating inclusion, all of which extend along the foliation planes in the direction of shear (Hanmer & Passchier 1991). Two types of porphyroclast systems may be defined based on the relationship between their wings and a reference plane drawn through the centre of the inclusion and parallel to the foliation. These are termed σ- and δ-types (Fig. 1.32, Passchier & Simpson 1986). In σ-type porphyroclasts, the wings are wedge-shaped, extending from each side of the inclusion in the downstream direction of the relative shear in the matrix, and the wings do not cross the reference plane (Fig 1.32(a)). δ-type porphyroclasts have wings that are generally constant thickness and curve close to the inclusion so that their wings cross the reference plane (Fig 1.32(b)).

Related structures common in micaceous quartz mylonites and phyllonites are mica fish (Fig.1.32(c)). These are lozenge-shaped single crystals of mica, that lie with their long axis in the extensional quadrant of the deformation. Many mica fish have a monoclinic shape symmetry with one curved and one planar side that can be used as a sense of shear indicator (Passchier & Trouw 1996).

Domino type faulting of large crystals such as plagioclase has often been used to indicate sense of shear. However, a note of caution should be applied, it is possible to produce structures with identical geometries even though the bulk non-coaxial flow is in the opposite sense (Fig.1.33, Hanmer & Passchier 1991).

1.4.3.3. Veins

The sigmoidal shape of dilational veins is an excellent means of determining the orientation of the finite strain ellipsoid and its progressive rotation with respect to the instantaneous stretching axes of the flow. Hence, they can be used as shear sense

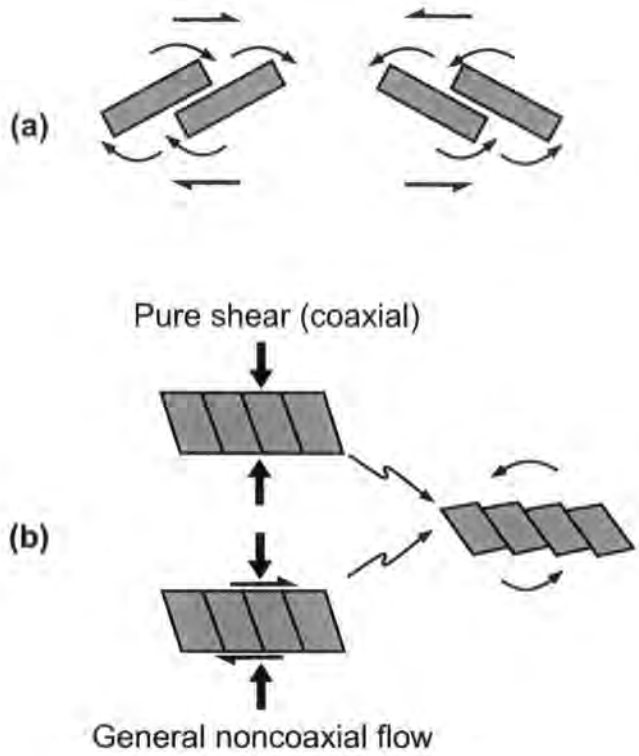

Figure 1.33. **(a)** Dextral or sinistral rotation of rigid inclusions can give rise to domino structures. **(b)** However, the geomtries illustrated in (a) could equally have resulted from clockwise or anticlockwise rotation. In either pure shear or a general noncoaxial flow the rotation of the dominos is a function of the angle the slip planes make with the maximum instananeous stretching axis of the coaxial component of the flow (i.e. the bulk flow plane) (from Hanmer & Passchier 1991).

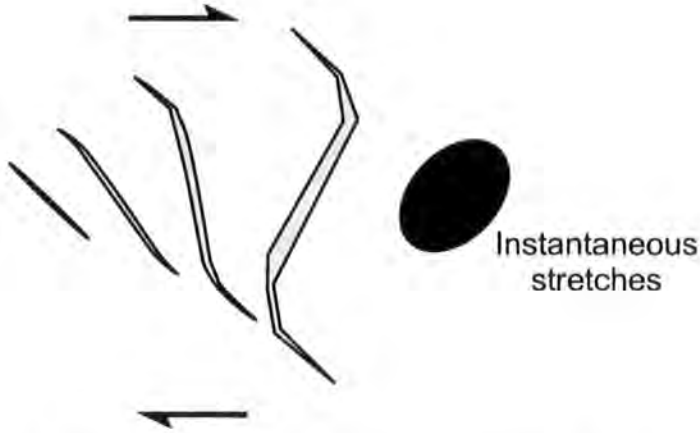

Figure 1.34. The sigmoidal form of *en echelon* tension gashes reflects the fact that the younger, narrower tips form as fractures initially orientated perpendicular to the maximum instantaneous stretching axis of the flow, while the older dilated central portion rotates with the same sense as the vorticity of the flow during progressive deformation (from Hanmer & Passchier 1991).

indicators (Fig 1.34, Hanmer & Passchier 1991).

1.4.3.4. Folds

The sense of overturning on minor folds can be used to determine shear sense (Fig 1.35). However, a note of caution. Fold vergence and the plunge of the fold hinge should be measured with respect to the stretching lineation. Any relationship where the fold hinge is not significantly normal to the stretching lineation will give unreliable results (Hanmer & Passchier 1991).

1.5 Aims of thesis and layout

The aim of this thesis is to document the geometric, kinematic and rheological evolution of transpression zones, and characterise the highly heterogeneous and geometrically complex systems of folds, faults and fabrics that developed during the Silurian and late (Acadian) phase of the Caledonian Orogeny. Field based studies were focused on three key localities close to the ancient oceanic suture zone of the Caledonian orogenic belt in Britain and Ireland which formed during left-lateral oblique collision. The following chapter summarises the evolution of the Iapetus Suture Zone and the Caledonian Orogen in the British Isles and Ireland. Subsequent chapters provide a brief synthesis of the regional geology and previous research for the three study areas, followed by a detailed account of the geometry and kinematics of the structures observed within each study area.

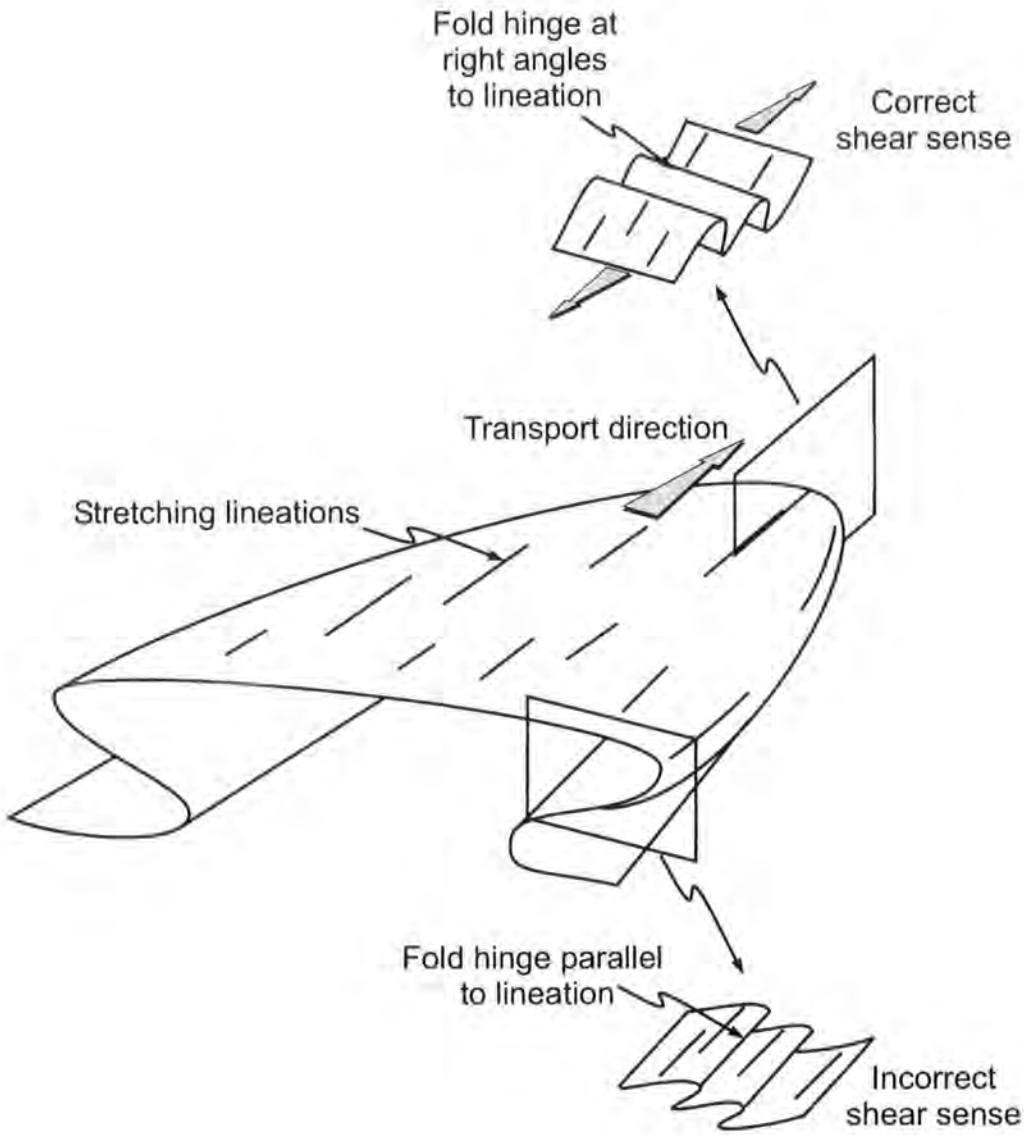

Figure 1.35. Sense of overturning on minor folds to measure shear sense. During ductile shear, fold hinges progressively rotate into parallelism with the transport direction with increasing strain. Therefore, only folds whose hinges are significantly normal to the stretching lineation should be used for determining shear sense.

Chapter 2

The Evolution of the Iapetus Suture Zone and Caledonian Orogen in Britain and Ireland

2.1 Introduction

The Lower Palaeozoic sequences of the Isle of Man and SE Ireland form part of a single terrane (the Leinster/Lakesman Terrane: Gibbons *et al.* 1985; Bluck *et al.* 1992) which is juxtaposed to the NW against another terrane comprising sequences of similar age, which crop out in southern Scotland and northern Ireland (the Southern Uplands/Longford-Down Terrane, Figs. 2.1, 2.2). Due to the well-documented separation of southern Britain (including the Isle of Man and SE Ireland) and northern Britain (including Scotland and northern Ireland) by the Iapetus Ocean, the geological histories of these two juxtaposed terranes were very different during the Ordovician and the early part of the Silurian (e.g. Wilson 1966; Dewey 1969; Phillips *et al.* 1979; McKerrow & Soper 1989). During the greater part of the Lower Palaeozoic, northern Britain was part of the southern margin of the continent of Laurentia, whilst southern Britain was part of the microcontinent of Eastern Avalonia (Fig. 2.3). Closure of the intervening Iapetus Ocean during the late Llandovery onwards, resulted in the gradual convergence of the geological histories of the northern and southern terranes, with a number of common geological characteristics developing. By the early Devonian, Laurentia and Eastern Avalonia had collided. The resulting tectonic boundary between the two margins of Laurentia and Avalonia is known as the Iapetus Suture, and it runs NE-SW across northern England and Ireland (Figs. 2.1, 2.2, Chadwick *et al.* 2001).

The study areas- Eyemouth (SE Scotland), the Isle of Man and Courtown (SE Ireland) straddle the Iapetus Suture, and provide excellent exposure of the limited outcrops of Lower Palaeozoic rocks deposited and deformed on the outboard margins of Laurentia (Eyemouth) and Avalonia (Isle of Man, Courtown). The suture zone- or a structure related to it may be exposed on the Isle of Man (Niarbyl Shear Zone) (Kimbell & Quirk 1999; Morris *et al.* 1999). These three areas therefore provide an excellent opportunity to study the structural assemblages that were produced during the sinistral oblique closure of the Iapetus Ocean and the final collision between Laurentia and Eastern Avalonia, culminating in the Acadian phase of the Caledonian Orogeny (see

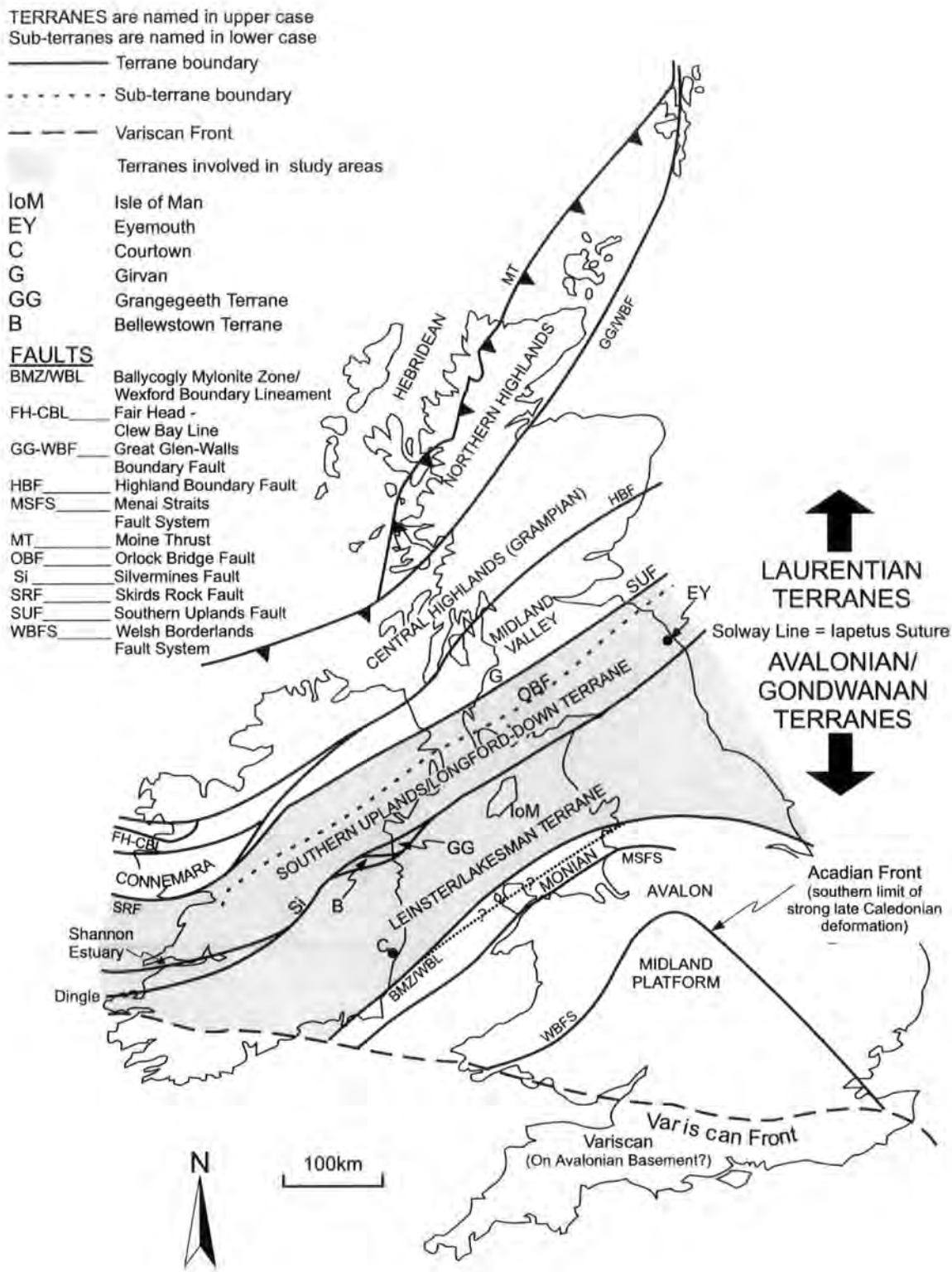

Figure 2.1. Simplified Palaeozoic terrane map of Britain and Ireland. The Southern Uplands/Longford-Down and Leinster/Lakesman terranes are shaded (after Holdsworth *et al.* 2000).

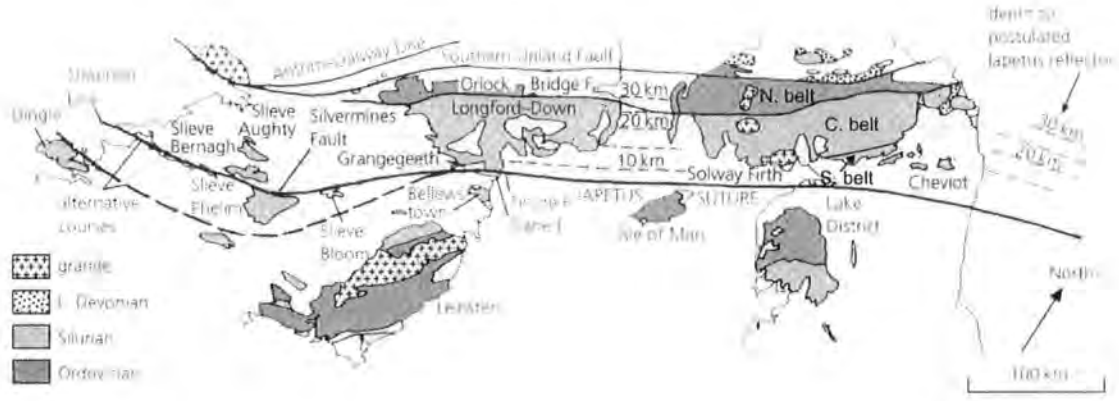

Figure 2.2. Map showing the course of the Iapetus Suture, and the location of Lower Palaeozoic rocks of the Southern Uplands/Longford-Down and Leinster/Lakesman terranes (from Soper *et al.* 1992a).

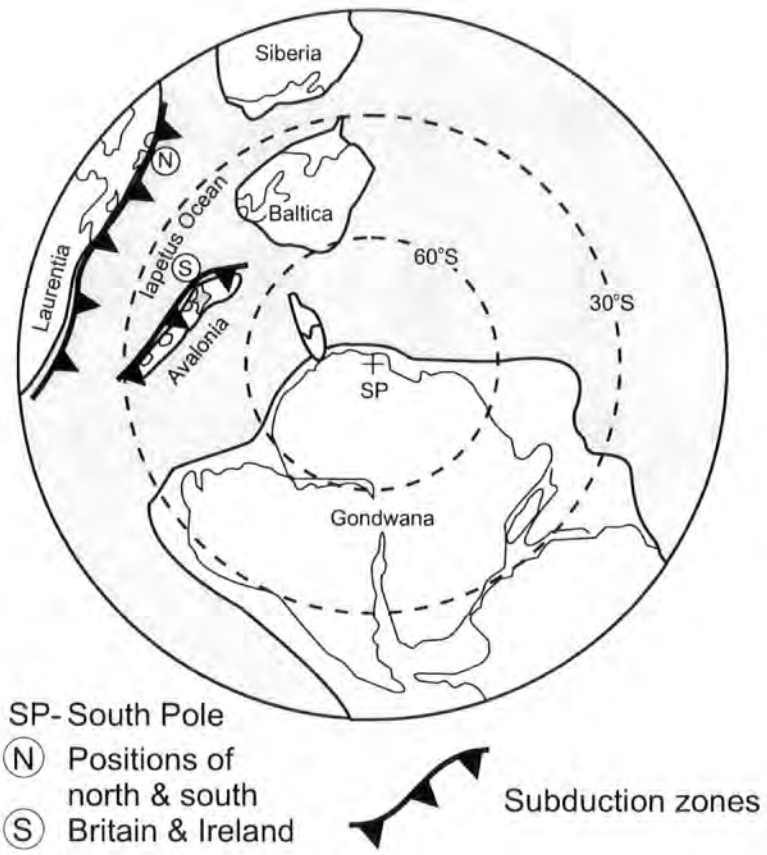

Figure 2.3. Global palaecontinental reconstruction for the Mid-Ordovician c. 470Ma. Note that not all continents are shown due to lack of data. Only selected subduction zones are shown (after Holdsworth *et al.* 2000).

below).

This chapter provides an overview of the Ordovician to Early Devonian tectonic evolution of the Southern Uplands/Longford-Down and Leinster/Lakesman terranes respectively, and relies substantially on the recent review articles in Woodcock & Strachan (2000).

2.2 The southern margin of the Laurentian continent

2.2.1 General structure

The Mid-Ordovician to Silurian rocks of the Southern Uplands Terrane of Scotland and their lateral equivalents in Ireland (Longford-Down Terrane, Figs. 2.1, 2.2) record the development of the southern margin of Laurentia. Due in part to substantial modification by major sinistral strike-slip faulting and thrusting during the final collision of Eastern Avalonia with Laurentia, controversy surrounds the tectonic and palaeogeographic settings of these sedimentary sequences (Strachan 2000).

The Southern Uplands/Longford-Down Terrane forms a broad NE-trending belt characterised by thick sequences of Ordovician and Silurian deep marine turbidites and early Ordovician (Arenig) volcanics (Stone 1996). Separated from the Midland Valley Terrane (Figs. 2.1, 2.2) by the Southern Uplands Fault and from the Leinster/Lakesman Terrane to the S by the Iapetus Suture, it is divided into three major fault-bounded tectono-stratigraphic units: the Northern, Central and Southern Belts (Fig. 2.4, Peach & Horne 1899). These units are further sub-divided into a series of smaller, highly elongate fault-bounded tracts (Murphy *et al.* 1991; Stone 1995; Strachan 2000 and references therein).

Comprising an early to late Ordovician succession of basal lavas, cherts and black shales overlain by clastic turbidites, the Northern Belt is bounded to the N by the Southern Uplands Fault and to the S by the Orlock Bridge Fault (Figs. 2.1, 2.2). The Central Belt is bounded to the N and S by the Orlock Bridge and Riccarton Faults respectively in Britain and by the Iapetus Suture in Ireland (Murphy *et al.* 1991; Strachan 2000, Figs 2.1, 2.2, 2.4). In the NW of the Central Belt the oldest sediments consists of minor, Ordovician graptolitic mudstones and carbonaceous shales of Caradoc-Ashgill age (Fig. 2.4), but the majority of the belt is formed by a thick sequence of Silurian sandstone greywackes and minor conglomerates (Strachan 2000). These are subdivided into the Gala and Hawick groups, which lie to the N and S of the

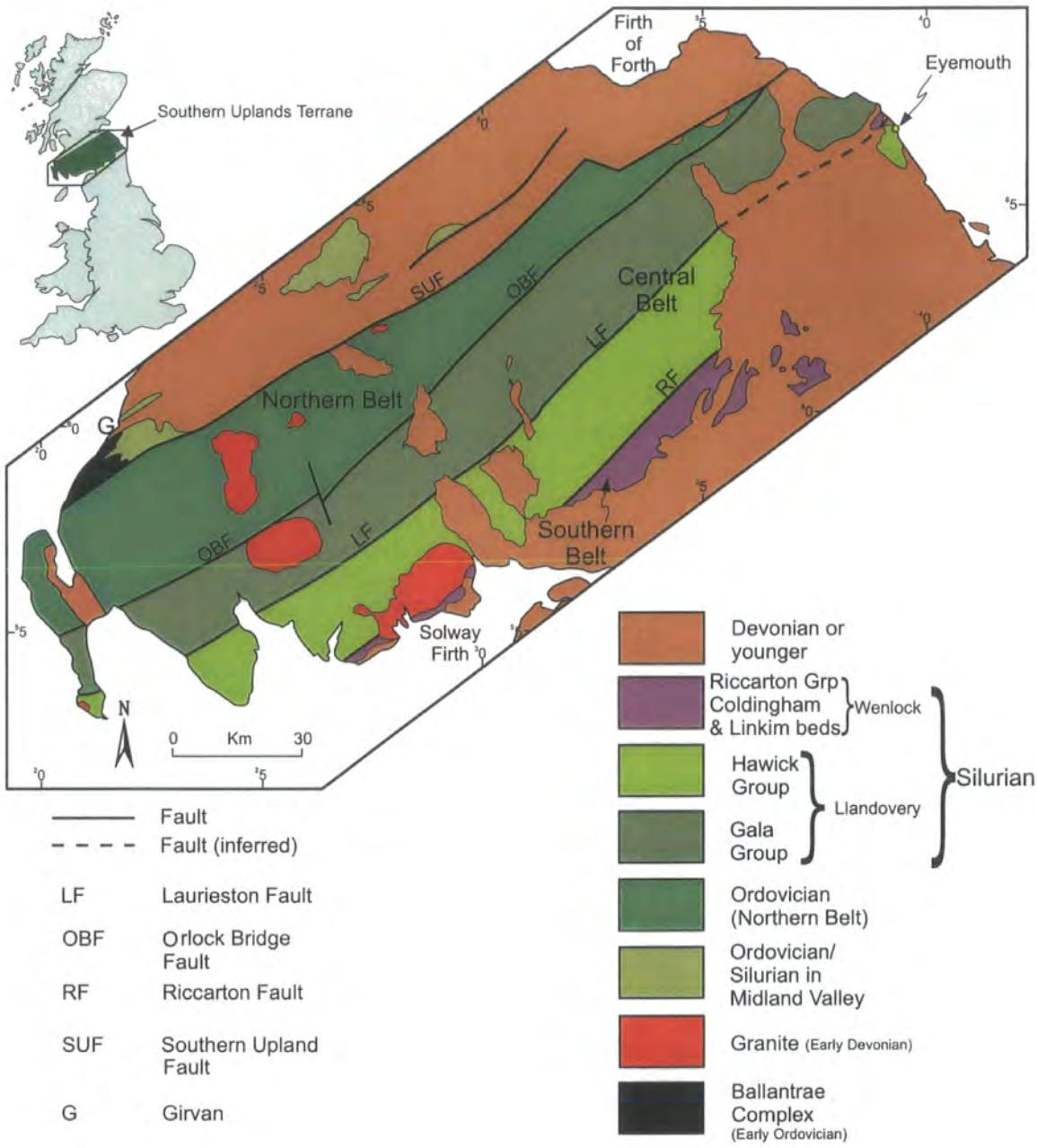

Figure 2.4. Regional map of the Southern Uplands Terrane showing the main tectono-stratigraphic units and Tract bounding faults. The likely correlation between the Berwickshire outcrops and the main outcrop to the SW is also shown. The Iapetus Suture lies just off the southern edge of the map (after Stone 1996; Treagus 1992).

Laurieston Fault, respectively (Fig. 2.4). The Southern Belt in Scotland lies to the S of the Riccarton Fault and is composed entirely of a 4km thick succession of Wenlock greywacke sandstones (Strachan 2000). There is no equivalent to the Southern Belt in Ireland (Murphy *et al.* 1991).

Although the structural evolution of the Southern Uplands Terrane has been studied in most detail in the Northern and Central Belts, a similar evolution is recorded throughout the terrane. The presence of slump sheets and slump folds suggests that the initial phases of deformation occurred while the sediments were still unconsolidated (Needham 1993; Treagus 1992; Strachan 2000). This was then followed by the main phase of deformation, which is associated with complex systems of top-to-the SE-thrusts and associated SE-vergent folds (Knipe & Needham 1986). Based on the low grade of metamorphism, (diagenetic to prehnite-pumpellyite facies) deformation is thought to have occurred at relatively shallow (10km) crustal depths (Oliver & Leggett 1980; Kemp *et al.* 1985). Deformation across the Southern Uplands/Longford-Down Terrane was diachronous, becoming progressively younger southwards (see section 3.2 for detailed explanation). In the Northern Belt, the main NE-SW trending cleavage is axial-planar to folds, indicating approximately orthogonal contractional deformation (Strachan 2000). By contrast in the southern part of the Central Belt, clockwise transection of the fold hinges by cleavage is widespread and is thought to indicate sinistral transpression (e.g. Sanderson *et al.* 1980; Stringer & Treagus 1980). In both the Northern and Central Belts, early thrusts were reactivated as sinistral strike-slip faults (e.g. Orlock Bridge Fault, Laurieston Fault, Moniaive Shear Zone).

2.2.2 Models of the Southern Uplands/Longford-Down Terrane

Several tectonic models have been proposed to explain the sedimentological and tectonic evolution of the Southern Uplands/Longford-Down Terrane. Any model proposed needs to be able to account for a number of particular features of the terrane. These include:

1. The dominance of deep marine, pelagic and submarine fan deposits.
2. Their location to the N of the Iapetus Suture and S of an active volcanic arc probably preserved at depth in the Midland Valley Terrane (Fig. 2.1).
3. The presence of elongate, reverse fault-bounded tracts, each with a different, detailed stratigraphy.
4. The seemingly paradoxical younging relationships, where, within tract younging is

predominately to the NW, whilst the tracts get progressively younger to the SE.

2.2.2.1 Accretionary prism model

Many of the features observed within the Southern Uplands are similar to those seen in the accretionary prisms associated with modern active margins (Fig. 2.5, McKerrow *et al.* 1977; Leggett *et al.* 1979; Leggett 1987). The sedimentary cover of the oceanic floor is generally not subducted but accumulates as thick piles of deformed sediment (accretionary prism) in the fore-arc region of convergent plate boundaries (Fig. 2.5, Sample & Moore 1987). Packets of sediment are scraped off the downgoing oceanic plate and are typically divided into a series of fault-bounded slices (Fig. 2.5). Initially the faults are low-angled thrusts, which, because of continuous underthrusting and build-up of the accretionary prism are progressively back-rotated into a steep orientation (Fig. 2.5, McKerrow *et al.* 1977). Within each slice, the sediments young towards the continent (i.e. in the case of the Southern Uplands to the NW, Fig. 2.6), whilst the slices forming the prism will young towards the ocean (i.e. SE in the Southern Uplands, Fig. 2.6). Thrusting is typically accompanied by widespread folding at all stages prior to, during and following lithification. Folding in the latter stage is accompanied by the development of cleavage and low-grade metamorphism within the thickening accretionary prism (Fig. 2.6). Using this analogy, the Southern Uplands was inferred to represent an accretionary prism developed on the active continental margin of Laurentia during the closure and northward subduction of the Iapetus Ocean (McKerrow *et al.* 1977; Leggett *et al.* 1979; Leggett 1987).

2.2.2.2 Back-arc basin model

Although the accretionary prism model elegantly explains the overall geological relationships within the Southern Uplands, many details remain difficult to reconcile (Stone 1996). A similar structural geometry could also form in a thrust belt, whether developed in a foreland basin, back-arc basin or accretionary prism. The provenance of volcaniclastic rich turbidites within the Northern Belt led some workers (e.g. Stone *et al.* 1987; Hutton & Murphy 1987; Morris 1987) to suggest that the sediments of the Northern Belt were deposited in a back-arc basin located to the N of a major volcanic arc lying above a northward dipping subduction zone (Fig. 2.7(a)). The composition of these turbidites suggests that any such arc was developed on a microcontinent (Strachan 2000) located at either the present day southern margin of the Northern Belt or within

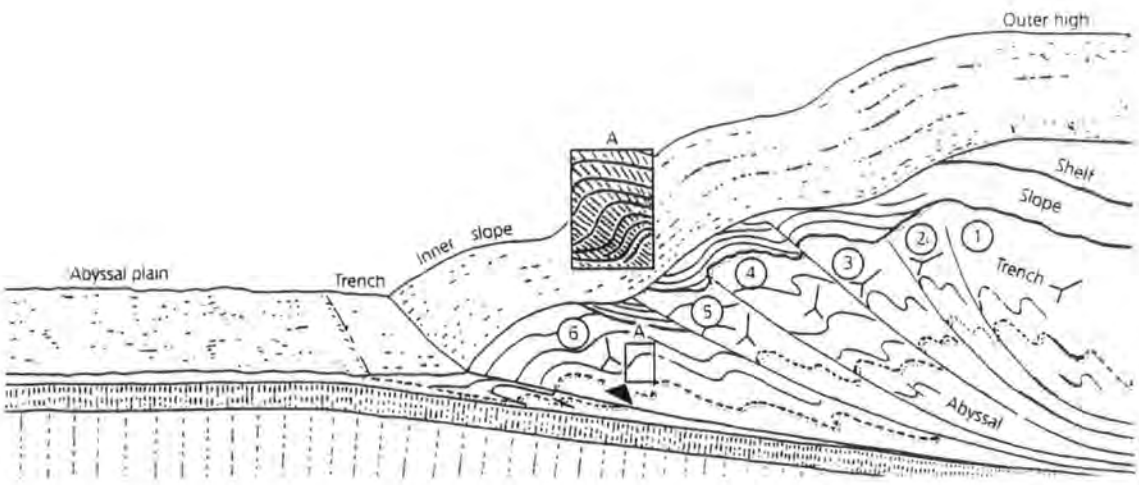

Figure 2.5. A model for the development of an accretionary prism at an oceanic trench. The fault-bounded packages of deformed sediments are accreted in the order 1-6. The faults originate as low-angled thrusts, which are passively rotated into a steep orientation as younger units are continually underthrust. Thrusting is accompanied by oceanward vergent folding and cleavage development (inset A). An overall upward younging direction is characteristic of each unit (after Anderton *et al.* 1979).

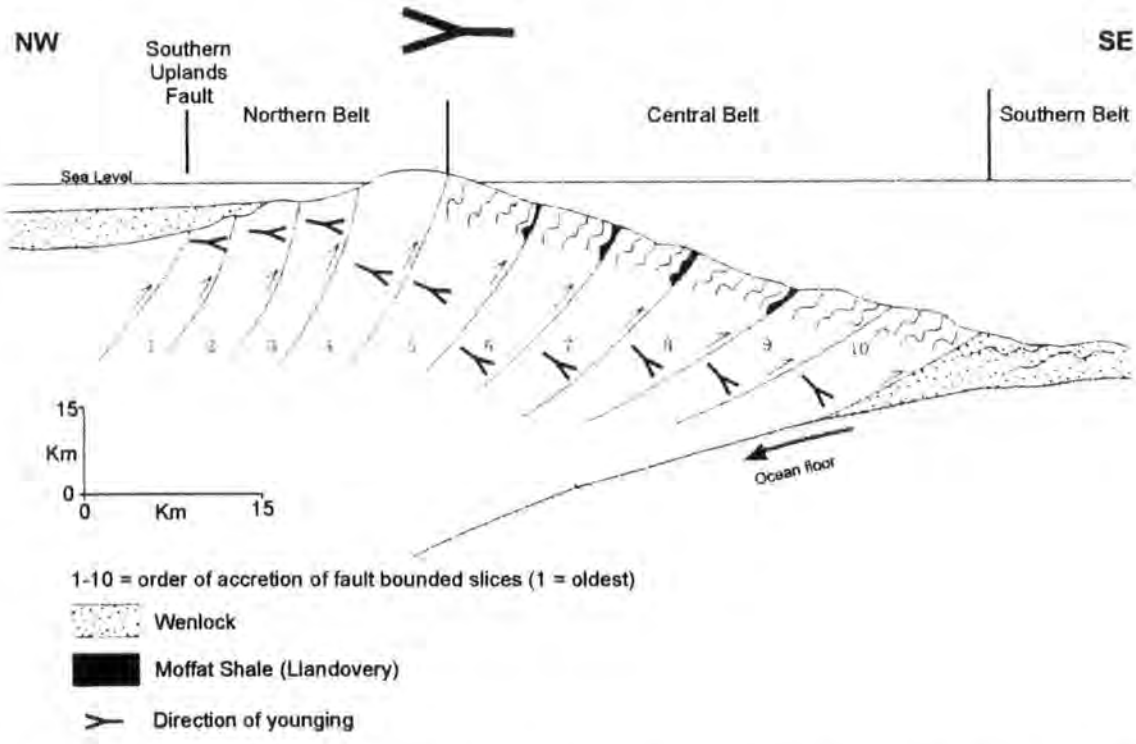

Figure 2.6. Reconstructed profile of the Southern Uplands accretionary prism in Wenlock times showing that younging within individual thrust slices (numbered 1-10) is to the NW, whilst overall the succesion youngs to the SE (after Leggett *et al.* 1979).

the Central Belt. There are various explanations to account for the subsequent removal of the arc from southern Scotland. Stone *et al.* (1987) argue that it is buried at depth as a result of thrusting that deformed and carried the sediments over the remnant arc (Fig. 2.7(b)). An alternative explanation is that the arc was removed by strike-slip faulting along the Orlock Bridge Fault (Figs. 2.1, 2.2, 2.4, Hutton & Murphy 1987). The Central and Southern belts are thought to represent recycled sediments derived from the rising thrust stack to the N which were progressively accreted into the thrust stack as it migrated southwards (Fig. 2.7(b), Strachan (2000) and references therein).

Proponents of the accretionary prism model provide several arguments against the back-arc model:

1. The southerly sourced volcaniclastic turbidites could have resulted from the erosion of seamounts on the oceanic plate rather than an outboard volcanic arc.
2. The southerly-derived palaeocurrents in the Northern Belt should not be taken as firm evidence for the location of the source area. Within modern trench systems, axial turbidite channels can meander considerably, and in certain circumstances they direct sediment towards the accretionary prism (Strachan 2000; Smith *et al.* 2001).
3. Isotopic ages for the southerly-derived volcanic detritus have so far only yielded latest Precambrian-early Cambrian ages. These are considerably older than any sediments within the Southern Uplands itself, appearing to rule out derivation from a contemporaneous arc (Kelly & Bluck 1989, 1990).
4. The modest volume of arc-derived volcanic detritus present in the Northern Belt is in stark contrast to the vast amounts seen in modern back-arc basins (Strachan 2000).
5. Given the buoyancy of the arc crust and its underlying continental basement it seems unlikely that this could be overthrust by the back-arc basin sediments. Furthermore no trace of an arc has been exposed by subsequent uplift and erosion (Strachan 2000)

2.2.2.3 Rifted continental margin model

A third model (Armstrong *et al.* 1996) considers the Northern Belt to have been deposited on rifted continental crust in a fore-arc basin (Fig. 2.8). This model argues for only minor displacements across the Southern Upland Fault on the basis that there are considerable sedimentological and faunal similarities linking the Mid- to Late-Ordovician successions of the Northern Belt and Girvan in the Midland Valley (Fig. 2.4,

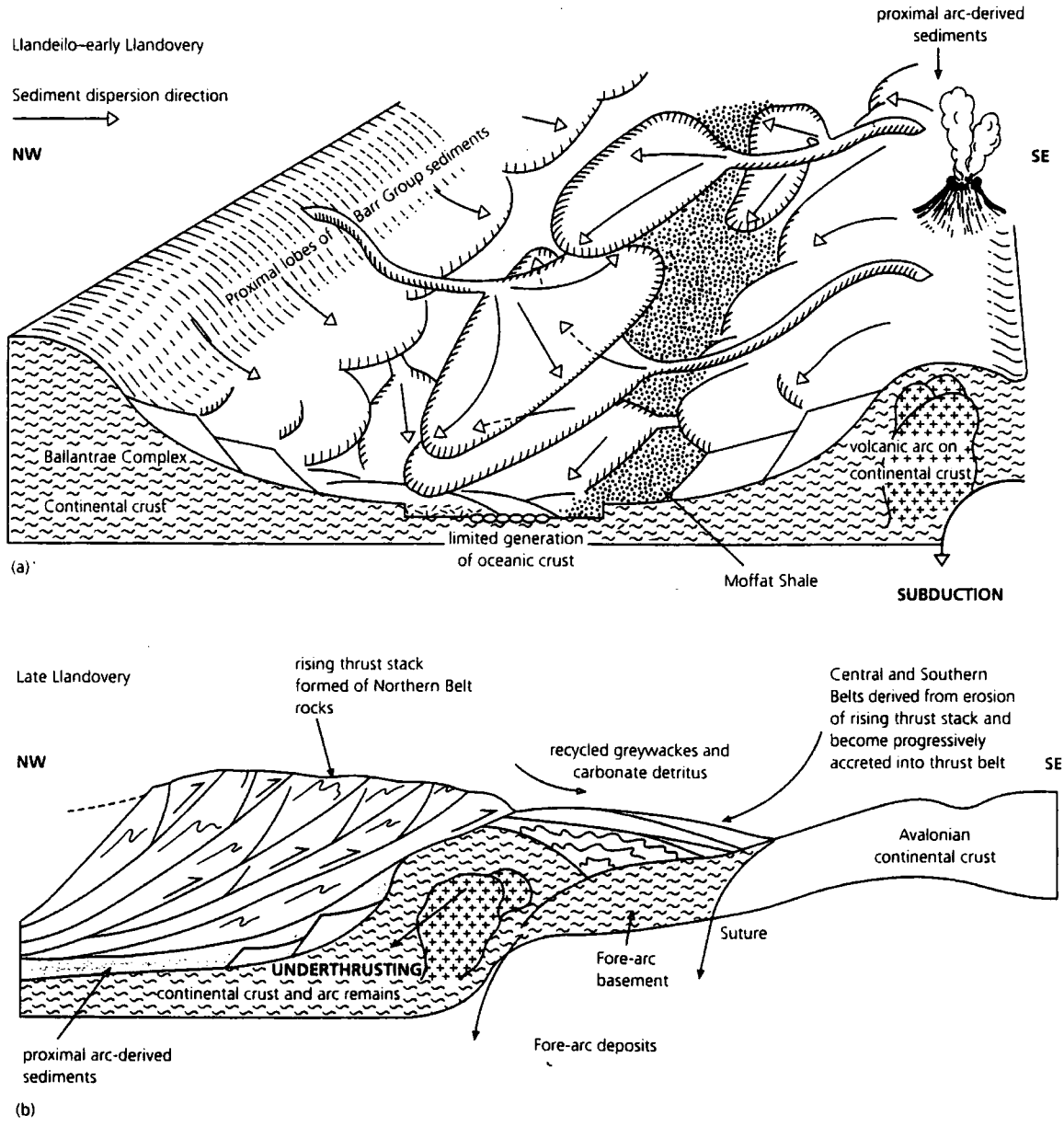

Figure 2.7. A back-arc interpretation for the Northern Belt of the Southern Uplands. **(a)** A volcanic arc on continental crust supplied sediment into a back-arc basin until Llandovery times. **(b)** Thrusting carried deformed sediments over the remnant arc (after Stone *et al.* 1987).

Armstrong *et al.* 1996). Together these successions could be viewed as recording progressive rifting of a continental margin and outbuilding of submarine fans onto a subsiding shelf (Fig. 2.8). This is further supported by the geochemical signature of the lower Caradoc basalt lavas within the Northern Belt. These show a closer affinity to those erupted into rifted continental crust rather than modern-day oceanic basalts (Armstrong *et al.* 1996). In addition, rare earth element (REE) signatures of Caradoc and Ashgill radiolarian cherts from the Northern Belt are comparable with those of more recent deposits from continental margin settings, rather than those characteristic of the open oceanic setting required by the accretionary prism model (Armstrong *et al.* 1999). Oblique collision of a fragment of rifted Avalonian continental crust with the margin of Laurentia during the latest Caradoc-Ashgill initiated southward directed thrusting in the Northern Belt. As the margin of Eastern Avalonia docked obliquely with Laurentia during the Late Llandovery, the Central and Southern belts formed as a southward propagating thrust duplex (Armstrong & Owen 2001).

2.2.3 Summary

The controversy surrounding the evolution of the Southern Uplands remains unresolved, with none of the above models fully reconciling all the sedimentological and structural features present in the Southern Uplands. From the viewpoint of the present thesis, the details of whether the Southern Uplands/Longford-Down Terrane is an accretionary prism, a back-arc basin, or a rifted continental margin are less important as the eventual geometry of a thrust imbricate zone is essentially the same. However, a general consensus has emerged indicating that an active volcanic arc (now missing) was located in the region of the Midland Valley (Figs. 2.1, 2.9(a)) and developed in response to NW directed subduction as indicated by the geometry of the Southern Uplands accretionary prism (Strachan 2000 and references therein). The present geological and geometrical relationship between the Southern Uplands and Midland Valley terranes suggests that there is a significant area of "lost" crust. In present day active margins, there is normally a gap between the arc and the trench of ca. 90km occupied by the fore-arc basin. It has been suggested that this "lost" section of crust is at present located at depth beneath the Southern Uplands accretionary prism which is thought to be allochthonous (Fig. 2.9(b), Strachan 2000 and references therein). Two lines of evidence support this interpretation. Firstly, a major S-dipping reflector beneath the Southern Uplands revealed by deep seismic profiling is interpreted as a major top-to-the

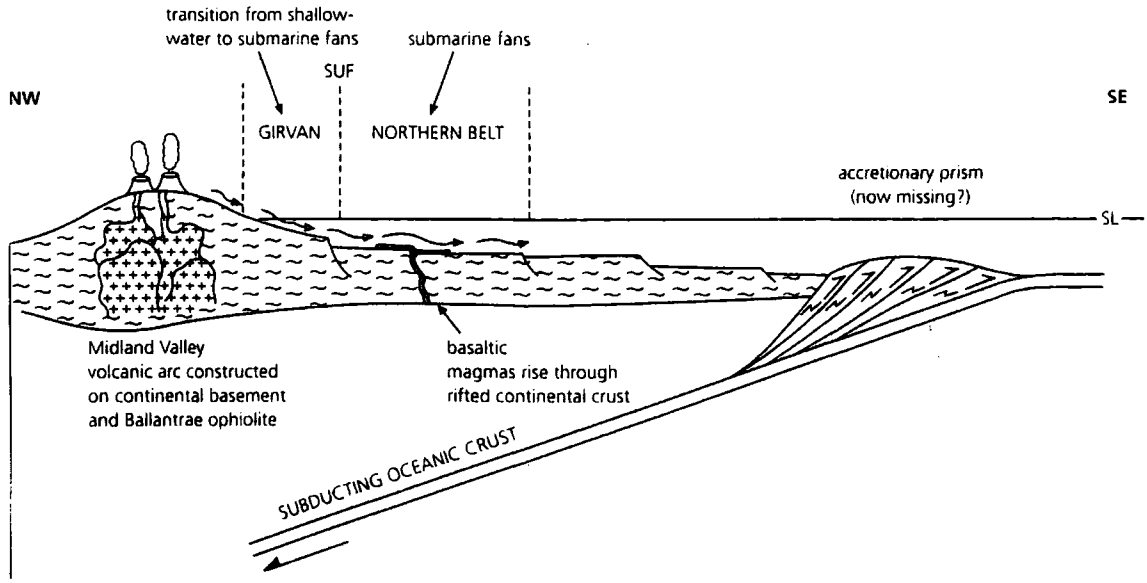

Figure 2.8. A fore-arc interpretation for the Northern Belt of the Southern Uplands (after Strachan 2000a).

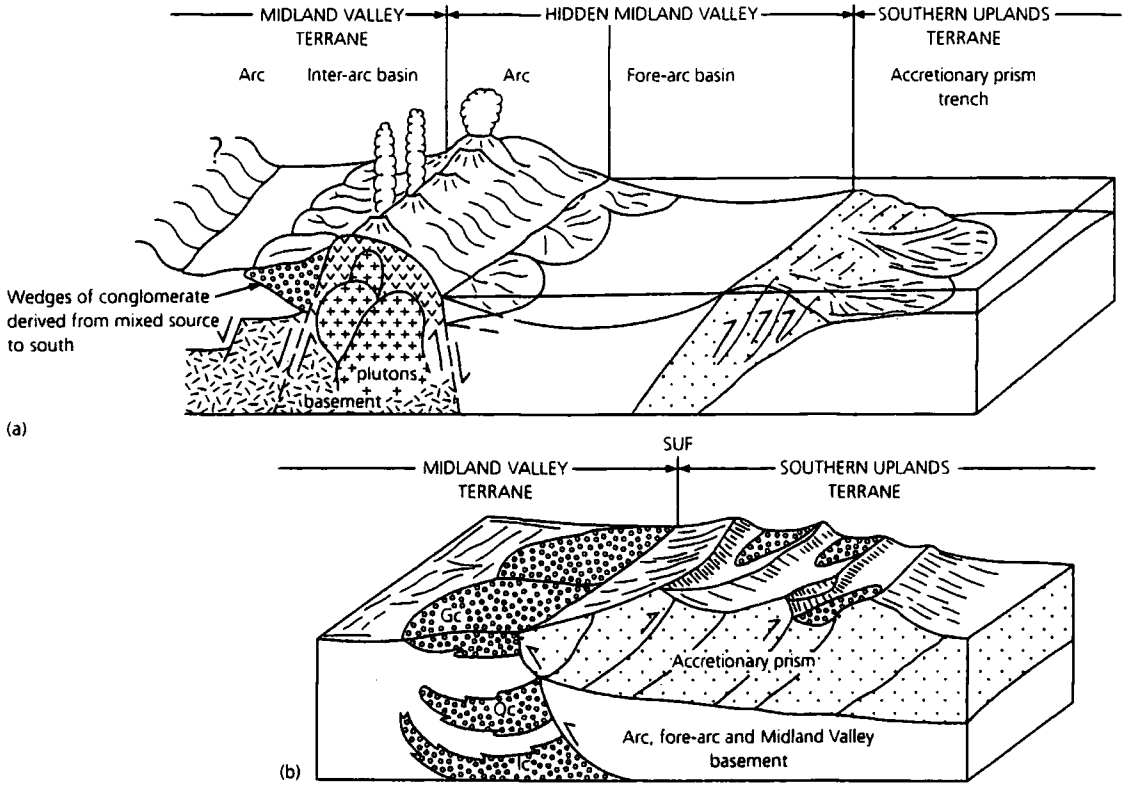

Figure 2.9. Tectonic reconstruction of the Midland Valley and Southern Uplands Terrane during Silurian times. **(a)** The relative postions of the volcanic arc, fore-arc basin and accretionary prism prior to top-to-the NW thrusting. **(b)** The present relationship across the Southern Upland Fault, with the accretionary prism overlying thrust the arc and fore-arc basin following NW-directed thrusting (after Bluck 1984).

NW thrust formed during the late Caledonian collision of Eastern Avalonia with Laurentia (Soper *et al.* 1992a) (see below). Secondly, granulite facies gneisses, derived presumably from an underlying continental basement have been found in Carboniferous volcanic vents in the Southern Uplands (Strachan 2000 and references therein). The late, low-angled top-to-the NW thrusts found within the Northern and Central belts are likely to be related to large-scale backthrusting of the Southern Uplands Terrane over the Midland Valley Terrane (Fig. 2.9(b)).

2.3 The northern margin of Eastern Avalonia

2.3.1 Introduction

Following its formation by the accretion of volcanic arcs and continental crust during the Neoprotozoic Cadomian Orogeny, the Gondwana margin that now forms England, Wales and SE Ireland remained relatively passive throughout the Cambrian and earliest Ordovician (Gibbons *et al.* 1994; Tietzsch-Tyler 1989, 1996). However, during the late Tremadoc, subduction of Iapetus Ocean beneath Gondwana resumed, producing the volcanic sequences preserved in Leinster and Wales (McConnell 2000). During the early to mid Ordovician (Arenig or Llanvirn), subduction-related rifting caused a fragment of crust (containing the present-day landmass of England, Wales and SE Ireland) to separate from the NW margin of the continental landmass of Gondwana (Fig. 2.3, Cocks & Fortey 1982). The resulting microcontinental fragment (Eastern Avalonia) moved northwards, progressively closing the intervening Iapetus Ocean. By the earliest Silurian, Eastern Avalonia had begun to impinge on the Laurentian margin to the N (Torsvik *et al.* 1996). The closure of the Iapetus Ocean involved oceanic subduction at both its Laurentian (see section 2.2) and Avalonian margins, with abundant igneous rocks characterising the subduction beneath Eastern Avalonia (McConnell 2000; Woodcock *et al* 1999a; Woodcock 2000a).

2.3.2 The lithological and structural evolution of Eastern Avalonia

Lying to the S of the Iapetus Suture, the former northern margin of the Eastern Avalonian microcontinent comprises the Leinster/Lakesman, Monian and Avalon terranes (Fig. 2.1). Each terrane contains thick deposits of Ordovician sedimentary and volcanic rocks of Arenig, Llanvirn or Caradoc age that outcrop in the Isle of Man, SE Ireland, Wales, the Welsh Borderland, and the Lake District, (Fig. 2.10, Woodcock

2000a). The palaeogeographical map of the Avalonian margin for the early Ordovician (Fig. 2.11) highlights the relationship between the depositional basins, volcanic centres, landmasses and the terrane boundaries. The Leinster and Lake District basins (including the Isle of Man) correspond to the Leinster/Lakesman Terrane (Figs. 2.1, 2.11). These are separated from the Irish Sea Platform (Monian Terrane) by the 'Wexford Boundary Lineament' (Gardiner 1975) which in turn is separated from the Welsh Basin (Avalon Terrane) by the Menai Straits Fault System (Figs. 2.1, 2.11, Woodcock & Strachan 2000).

The subduction-related history of Eastern Avalonia can be divided into four parts (Fig. 2.12):

1. Onset of arc volcanism during the late Tremadoc to early Arenig (Fig 2.12(a)).
2. Marginal basin development in Wales during the mid-Arenig to mid-Llanvirn (Fig. 2.12(b)).
3. The climax of arc volcanism during the late Llanvirn to early Caradoc (Fig. 2.12(c)).
4. Cessation of subduction and the shut down of arc volcanism during the mid-Caradoc (Fig. 2.12(d)).

2.3.2.1 Onset of arc volcanism

Iapetus Ocean lithosphere is thought to have subducted approximately southwards beneath Eastern Avalonia along a NE-trending trench, which is assumed to have lain close to the present trace of the Iapetus Suture (Fig. 2.11, Woodcock 2000a). Late Tremadoc volcanic centres in Wales (Kokelaar 1988) and SE Ireland (McConnell & Morris 1997) preserve evidence of the first arc volcanism above the subducting Iapetus crust (Figs. 2.11 2.12(a)). The contrast in arc-trench distances between the Welsh and Irish centres when compared with present-day subduction systems suggests that they may not now be in their original position. Several lines of evidence suggest that southward-directed subduction produced sinistral oblique movements across the NE-trending margin of Eastern Avalonia throughout the history of Ordovician volcanism. In particular, volcanism and later extrusive activity in N Wales were localised along N-S striking fractures and graben, suggesting E-W extension or transtension oblique to the trench (Woodcock 2000a). Late Tremadoc or earliest Arenig, sinistral strike-slip displacement along the Wexford Boundary Lineament may be a component of this oblique subduction (Max *et al.* 1990; Murphy *et al.* 1991). The magnitude of sinistral displacement along the Wexford Boundary Lineament may be

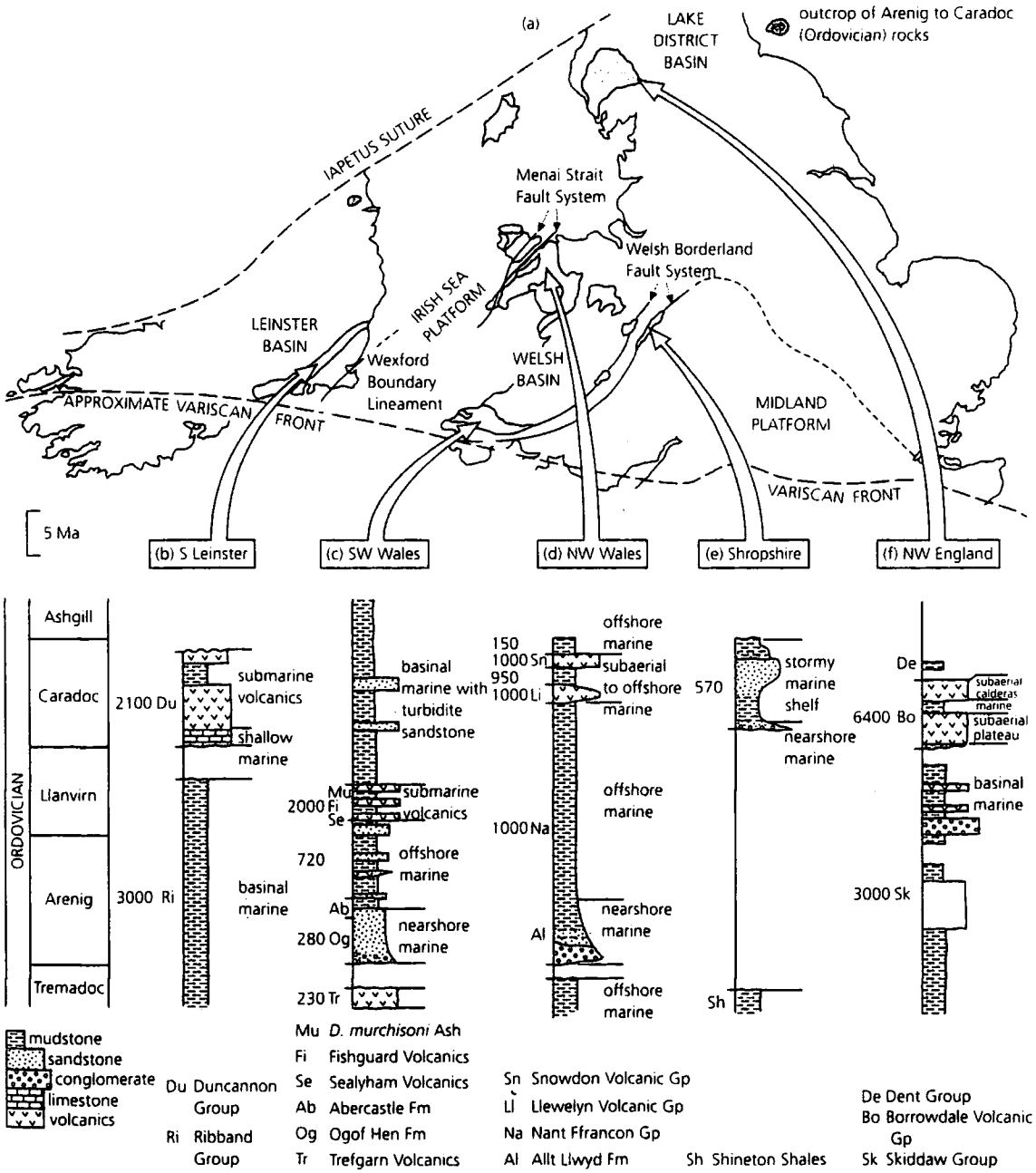

Figure 2.10. Map showing distribution of Ordovician (Arenig-Caradoc) sedimentary and volcanic rocks in southern Britain and Ireland with representative stratigraphic columns (from Woodcock 2000a).

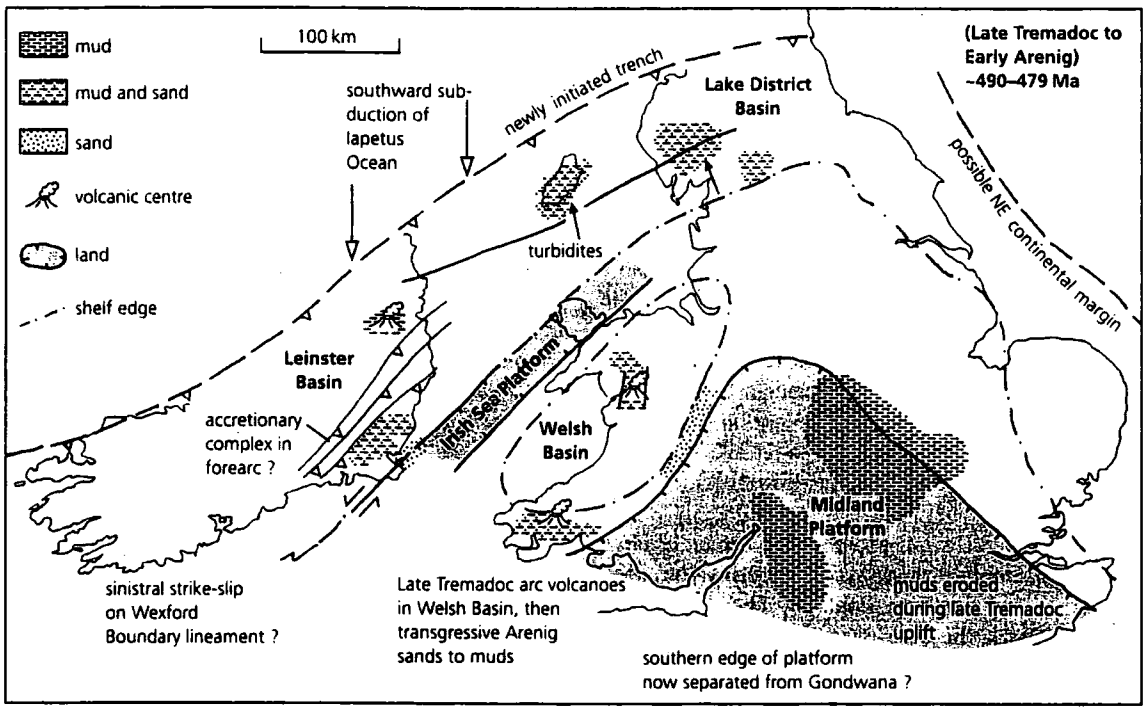

Figure 2.11. Palaeogeographic map of southern Britain and Ireland for late Tremadoc to Arenig times (from Woodcock 2000a).

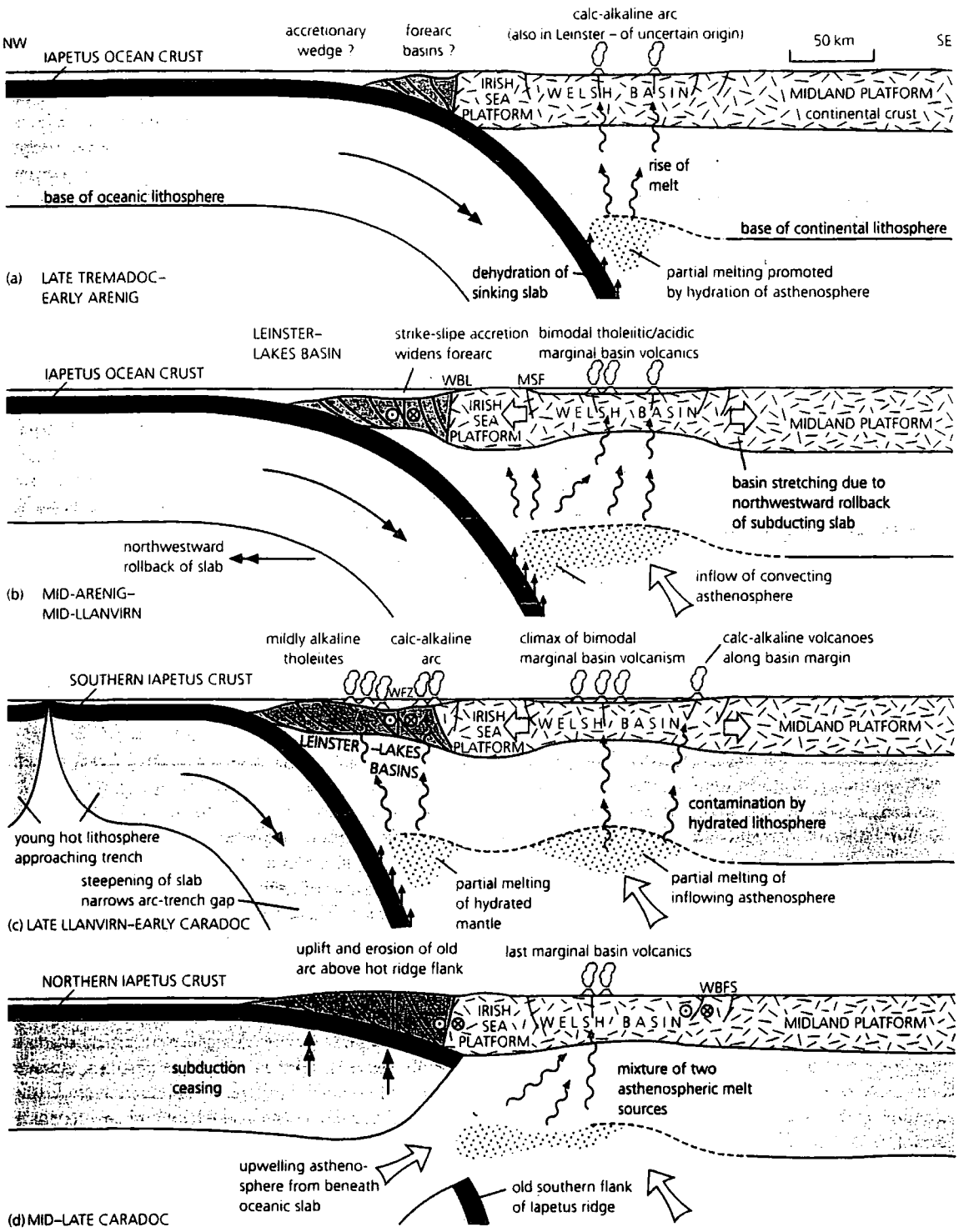

Figure 2.12. Lithospheric cross-sections through Ordovician time, showing the main centres of volcanism and the different modes of magma generation. WBL, Wexford Boundary Lineament; MSF, Menai Strait Fault; WFZ, Wicklow Fault Zone; WBFS, Welsh Borderland Fault System (from Woodcock 2000a).

substantial, and it has been suggested (e.g. Max *et al.* 1990; Murphy *et al.* 1991) that the terrane comprising the Leinster, Manx and Lake District successions may have been slid into place along such strike-slip faults during or after the first burst of arc volcanism (e.g. Max *et al.* 1990; Murphy *et al.* 1991; Tietzsch-Tyler 1989, 1996). Terrane accretion in this manner would help to explain the wide separation that apparently exists between the Welsh arc and the inferred location of the trench. Additional crustal shortening and strike-slip displacements during the Early Devonian Acadian Orogeny may also have contributed to the reorganisation of the Avalonian crust (Woodcock 2000a).

2.3.2.2 Marginal basin development

The first phase of arc volcanism was short-lived, (5-10Myr) and as the volcanic centres expired and subsided they were progressively buried by Arenig sediments. In Wales and the extreme SE of Ireland, these sediments record a deepening marine environment. To the NW of the Irish Sea Platform, the succession comprises deep marine mudstones and sandstone turbidites of the Skiddaw, Manx and Ribband groups of the Lake District, Isle of Man and Leinster respectively (McConnell *et al* 1999; Stone *et al.* 1999). The deep-water turbidites were supplied from the SE from the direction of the Irish Sea Platform (Cooper *et al.* 1995) and may represent sedimentation in the fore-arc of the subduction system. Within the Leinster Basin, (Fig. 2.11) Max *et al.* (1990) suggest that the presence of steep NW directed thrusts and the presence of diapiric melanges indicate that the Ribband Group may represent an accretionary complex within the fore-arc of the subduction system. There are no equivalent accretionary structures along strike to the NE of the Leinster Basin but late Ordovician strike-slip faulting could have removed any such complex (Max *et al.* 1990).

The early Arenig shutdown of volcanism was followed by a brief period of quiescence. However, by the late Arenig new volcanic centres were forming in Wales (Fig. 2.12(b)). These have bimodal basic/acid compositions and show a more tholeiitic geochemistry suggesting derivation from primitive asthenospheric mantle implying a marginal basin setting formed due to lithospheric stretching within or behind a volcanic arc (Kokelaar *et al.* 1984). Additional volcanic centres developed within the Welsh Basin and along its SE Margin during the Llanvirn (Fig. 2.12(b) & (c)). Deep-water sedimentation continued to the NW of the Irish Sea Platform through late Arenig and early Llanvirn time. Large, submarine slump sheets within the turbidite successions of

the Skiddaw and Manx groups preserve evidence of major instability on the margin of Avalonia during the late Arenig (Woodcock & Morris 1999). Within the Leinster Basin an analogous, but slightly later sequence of events are preserved in the Ribband Group. Here, deep marine sedimentation pre-dates a late Llanvirn unconformity before arc volcanism resumed in the Caradoc (McConnell 2000; Woodcock 2000a).

2.3.2.3 The climax of arc volcanism

Arc volcanism restarted during late Caradoc time in the Lake District Basin represented by the Eycott and Borrowdale Volcanic groups, and during the early Caradoc in the Leinster Basin with the Duncannon Group. Eruption was further outboard on the Avalonian margin and consisted of calc-alkaline volcanics formed in much greater volumes compared to the earlier episodes. The tectonic history of this fore-arc region probably varied both along- and across-strike. Variations in chemistry of the arc rocks suggest that the fore-arc was thinner in the NW than in the SE (Fig. 2.12(c), McConnell 2000; Woodcock 2000a). In SE Ireland, this change took place across the Wicklow Fault Zone, (Fig. 2.12(c)) and in the Lake District across the Causey Pike Fault. Both structures may have acted as major displacement zones during and after arc volcanism. Back-arc extension and volcanism continued in the Welsh Basin while the Lakes and Leinster arc was active, with large volumes of material being erupted during the Caradoc (Kokelaar 1988). This extensive volcanism appears to be absent from the Manx group of the Isle of Man. However, there is some suggestion that it may have accumulated, but has since been removed by erosion (Piper *et al.* 1999; Power and Crowley 1999; Woodcock *et al.* 1999a). The Poortown intrusive complex in the NW of the island comprises a series of basaltic sheets, probably sills, that have a compositional range from tholeiitic basalt to basaltic andesite, and a chemistry consistent with a volcanic arc setting (Power & Crowley 1999). The sills were intruded at a high level into probable upper Arenig rocks. Although the intrusive complex could be of any subsequent age, the possibility that it represents the substructure to a late Ordovician volcanic succession is supported by estimates of its palaeolatitude (Piper *et al.* 1999).

2.3.2.4 The cessation of subduction

Mid-way through the Caradoc, volcanism in both the volcanic arc of the Leinster and Lake District basins and the back-arc Welsh Basin waned dramatically, and the volcanic centres were covered by the sea (Woodcock 2000a). This transgression was accelerated by a late Caradoc eustatic rise in sea level. The reason for this sudden cessation of volcanic activity is uncertain. One explanation is that during the Mid-Caradoc, the Avalonian margin overran the spreading ridge in the Iapetus Ocean (Figs. 2.12(d), 2.13, Pickering & Smith 1995). The slab of southern Iapetus lithosphere then decoupled from that north of the ridge and descended into the asthenosphere (Fig. 2.12(d)). The leading edge of the northern Iapetus plate was too young and buoyant to be subducted so became lodged beneath the Avalonian lithosphere forming a slab window (Fig. 2.12(d), Woodcock 2000a). This had several important consequences:

- A change in magma chemistry occurred as the upwelling asthenosphere now rose through a widening window behind the subducting slab. This new source of magma is recorded geochemically in latest mid-Caradoc volcanics in the Welsh back-arc basin (Fig. 2.12(d)).
- Due to the obliquity between the Iapetus ridge and the overriding Avalonian margin, triple junctions would have migrated along the margin so that the end to volcanism was diachronous (Fig. 2.13). The apparently later end to arc volcanism in Ireland compared with the Lake District suggests a southward migration of the triple Junction.
- The plate boundary that formed in the wake of the triple junction, between the northern Iapetus plate and the continental margin probably had a strike-slip component. This may be recorded in a late Caradoc to early Llandovery phase of strike-slip faulting along the Welsh Borderland Fault System (Woodcock 1984).

By the Caradoc, palaeomagnetic and faunal evidence indicates that Eastern Avalonia was in close proximity to the continent of Baltica, and by the end of the Ordovician or the earliest Silurian the intervening Tornquist Sea had closed (Torsvik *et al.* 1993, 1996). The closure of the Tornquist Sea does not appear to have involved major crustal continent-continent collision, but was probably sufficiently dominated by strike-slip tectonics not to have left a strong orogenic imprint on Eastern Avalonia (Torsvik *et al.*1996).

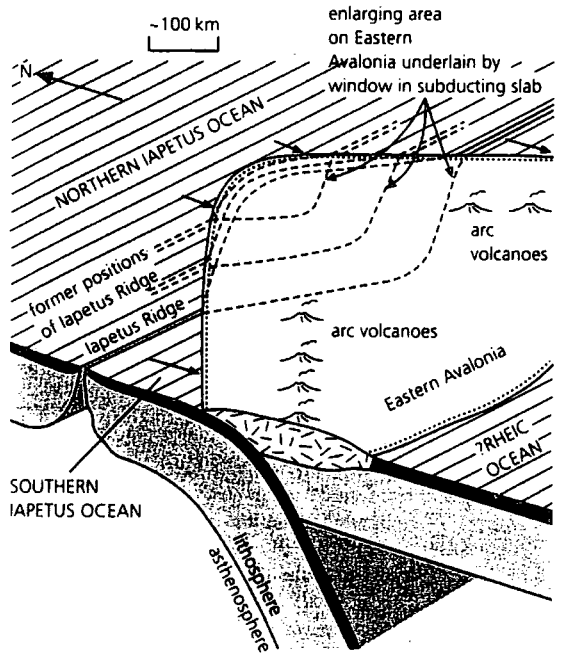

Figure 2.13. Schematic 3D representation of the interaction between the Iapetus ridge and the Avalonian subduction margin. showing the development of oblique-slip margins and a growing slab window (from Woodcock 2000a).

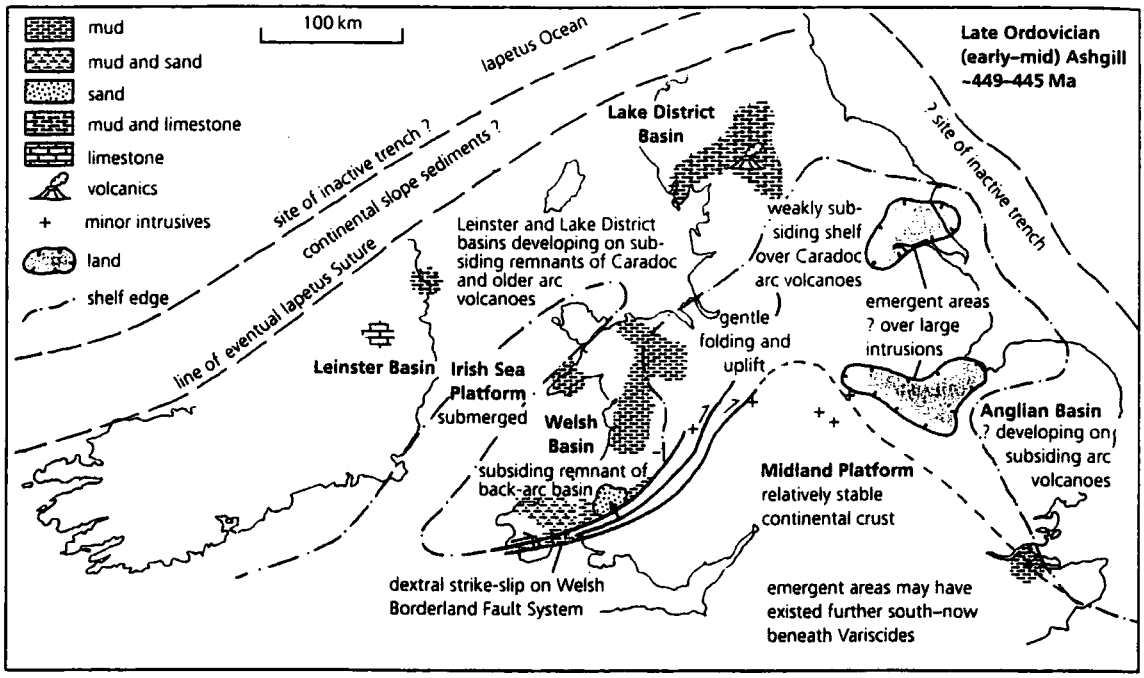

Figure 2.14. Palaeogeographic map of southern Britain and Ireland for late Caradoc to early Ashgill time (from Woodcock 2000b).

2.3.3 Late Ordovician and Silurian sedimentation and volcanism on the Avalonian margin

In general terms the sedimentary successions of the upper Ordovician (Ashgill) and Silurian are predominately marine and lack the thick volcanic accumulations that characterised most of the Ordovician (Fig. 2.14). This reflects the shut down of the subduction related volcanic centres of Leinster, Wales and the Lake District. Late Ordovician and Early Silurian (Llandovery) successions are predominately marine, although they host several unconformities, probably the result of gentle tectonic tilting and uplift, (Branney & Soper 1988), glacio-eustatic falls in sea level (Hambrey 1985) or the residual relief of the Ordovician volcanoes. Later in the Silurian, (Wenlock, Ludlow and Prídolí) the successions are more conformable, perhaps reflecting more stable sea levels and lack of contractional tectonics (Woodcock 2000b). All the successions show an upward transition from marine to paralic or non-marine sedimentation, which heralded the demise of the basinal areas as Eastern Avalonia collided with Laurentia.

Although much reduced in volume, when compared to that during the Caradoc, volcanic activity continued throughout the late Ordovician and Silurian. Late Ordovician volcanism occurred in areas that had previously hosted Caradoc and earlier centres, and is probably the result of late-stage eruption of magmas above the old, SW-dipping Iapetus subduction zone. The early Silurian volcanics, however, have a different distribution and geochemistry to those of the Caradoc and earlier centres. They occur in an E-W zone through the southern part of the Welsh Basin, and may reflect crustal extension along the southern flank of Eastern Avalonia (Woodcock 2000b).

2.3.4 Summary

For much of Ordovician time, the southern British Isles was part of the discrete microcontinent of Eastern Avalonia. The rocks of the Leinster/Lakesman, Monian and Avalon terranes record the events of arc volcanism, lithospheric rifting and fore-arc and back arc sedimentation throughout the subduction history of the Avalonian margin. The presence of an inferred Ordovician volcanic substructure within the Manx Group, but an absence of substantial extrusive volcanics suggests that here they were subsequently removed by erosion. Following the cessation of extensive subduction related volcanism, thermal subsidence and a eustatic rise in sea level led to a widespread

marine transgression. Minor volcanism persisted throughout the area, probably the result of late stage magmatic activity above the old subduction zone and crustal extension. Possible significant strike-slip displacements along terrane bounding faults such as the Wexford Boundary Lineament (Fig. 2.1) may have been responsible for rearranging the Ordovician and Early Silurian sedimentary and volcanic sequences into their present day geographical positions.

2.4 The closure of the Iapetus Ocean and the Caledonian Acadian Orogeny

2.4.1 Definition of the Caledonian and Acadian Orogenies

The Caledonian Orogen can be traced for approximately 7500km SW-NE, from SE USA through the British Isles to Scandinavia and Greenland (Fig 2.15, Treagus 1992). In the British Isles and Ireland, the orogen extends from NW Scotland to the Welsh Borders (Fig. 2.1). The NW boundary of the orogen is usually placed at the Moine Thrust Zone, (Fig. 2.1) whilst its opposing boundary lies along the Welsh Borderland Fault System (Fig. 2.1, Woodcock & Strachan 2000b). The 'Caledonian' Orogenic Belt has had a complex and protracted constructional history throughout the early Palaeozoic. There are many tectonic phases within the Caledonides that reflect distinct tectonic, metamorphic and igneous events, including subduction and obduction of Iapetus oceanic crust, collisions between volcanic arcs, mobile terranes and the adjacent continental margins of Laurentia, Avalonia and Baltica (McKerrow *et al.* 2000). Although many of these were local events within the orogen, several were intense or widespread enough to have their own names. Two of the most notable examples are the Grampian Orogeny on the Laurentian margin and the Cadomian Orogen on the Avalonian margin. It is useful therefore, to use the term 'Caledonian Orogeny' in a more specific and restricted sense to distinguish it from these earlier events. In this thesis, the Caledonian Orogeny concerns the events that resulted from the Silurian to Devonian collision of Laurentia and Eastern Avalonia and other former fragments of Gondwana (Woodcock & Strachan 2000b). Even using this more restricted definition, several distinct tectonic phases can be distinguished within the Caledonian Orogeny. One of these is the Acadian deformation, which produced the Early Devonian deformation within the 'slate belts' south of the Iapetus Suture. Textural evidence around the ca. 400-Ma Leinster and Shap Granites, in SE Ireland and the Lake District respectively, suggests that their intrusion overlapped the end of cleavage

formation in the country rocks, which is thereby dated as being late Early Devonian (Emsian) (Woodcock & Strachan 2000b).

2.4.2 The three plate model of closure

Early syntheses modelled the terminal collision phase as a two-plate configuration (e.g. Dewey 1969; Phillips *et al.* 1976), involving E-W closure between Laurentia and Baltica. This configuration, it was argued, was responsible for the N-S-striking Scandinavian and East Greenland Caledonides and dextral transpressive strain along the NE-SW orientated British sector of the Iapetus suture (Fig. 2.16). However, following subsequent work, (e.g. Dewey 1982; Soper & Hutton 1984; Soper 1988) a three-plate model became accepted. This postulated that, during the early Palaeozoic closure of the Iapetus Ocean, Britain lay close to a triple collisional junction between the two major continental masses of Laurentia and Baltica, and the microcontinental terrane of Eastern Avalonia (Fig. 2.17, Soper & Woodcock 1990). This new model for the terminal collisional phase of the closure of Iapetus was based on three important lines of evidence.

1. The presence of distinct Cambro-Ordovician shelf faunas on either side of the proposed suture line between the colliding continents.
2. The orogen, comprising the Appalachians, the North Atlantic Caledonides and the German-Polish zone has a Y-shaped configuration, marking the collisional sutures between three plates not two (Fig. 2.15)
3. Late Caledonian structures within the Highlands of Scotland and the slate belts of central Britain indicate sinistral, not dextral transpression (e.g. Soper 1988).

2.4.3 'Soft' docking of Eastern Avalonia with Laurentia and Acadian deformation

Estimates of the timing of impingement of Avalonia with the Laurentian margin vary according to the criteria used. However, the first clear signs of sedimentary links between the Southern Uplands and Avalonian terranes are seen in the late Llandovery and early Wenlock (e.g. Barnes *et al.* 1989; Lintern *et al.* 1992; Soper & Woodcock 1990). Based on sedimentary provenance and dispersal patterns, Soper & Woodcock (1990) proposed a model for the anticlockwise 'soft' docking of Eastern Avalonia against the Scottish margin of Laurentia (Fig. 2.18). This involved initial impingement at the western end of Eastern Avalonia in the early Silurian (Llandovery), and was followed by the progressive elimination of a wedge-shaped remnant of the Iapetus

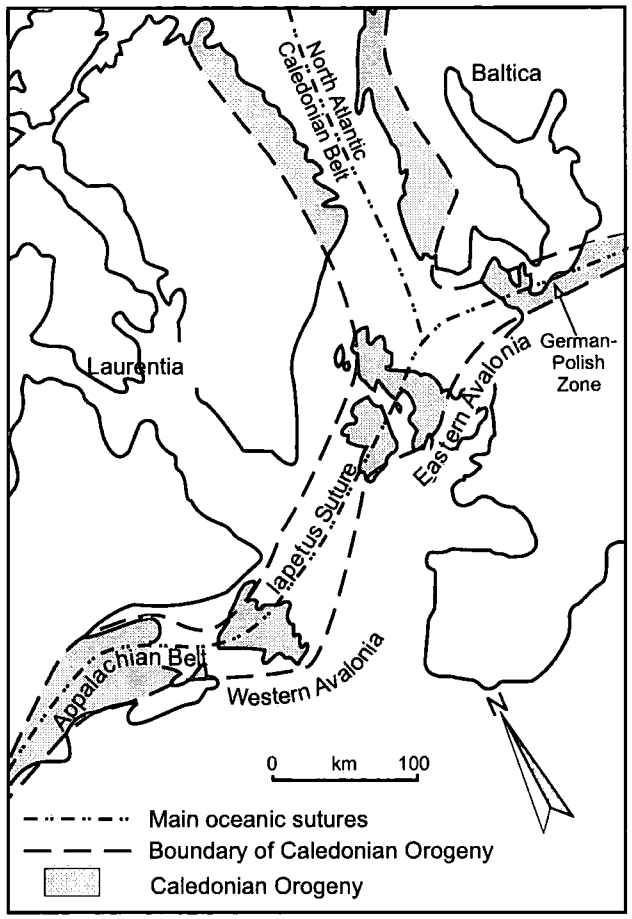

Figure 2.15. Map showing the palaeocontinental fragments around Britain and Ireland on a reconstruction before the opening of the Atlantic Ocean. Note also the Y-shaped geometry of the Caledonian Orogen and the position of the Iapetus suture in the British Isles and Ireland (based on Treagus 1992).

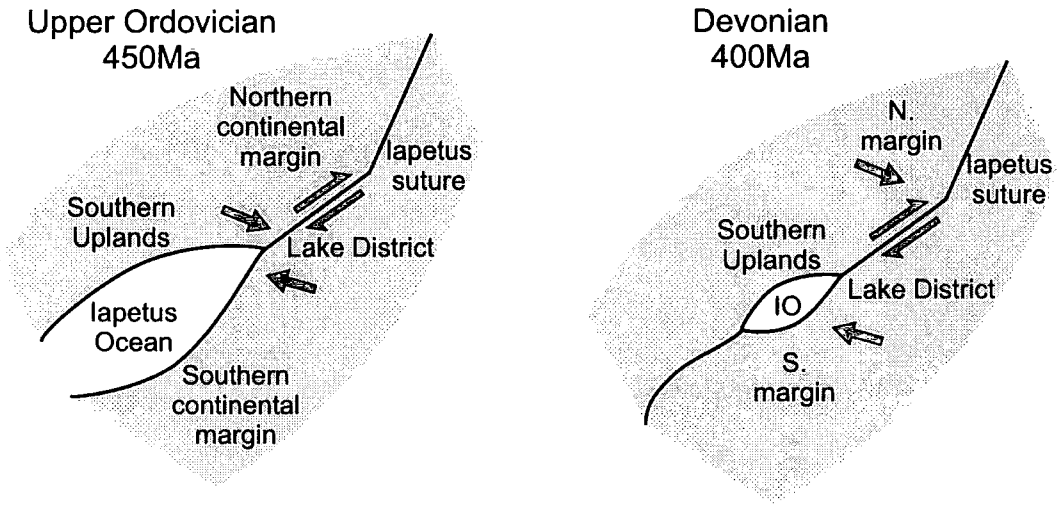

Figure 2.16. Cartoon showing the final closure of the Iapetus Ocean. Note the continental misfit and the dextral movement along the Iapetus suture (after Phillips *et al.* 1976).

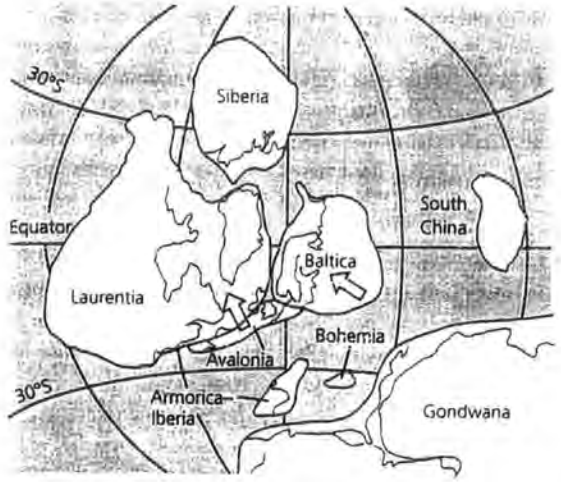

Figure 2.17. Palaeocontinental reconstruction for mid-Silurian(Wenlock) time, showing position of triple junction between Laurentia, Baltica and Eastern Avalonia. Arrows show direction of movement of Baltica and Eastern Avalonia up to this time (from Woodcock 2000b).

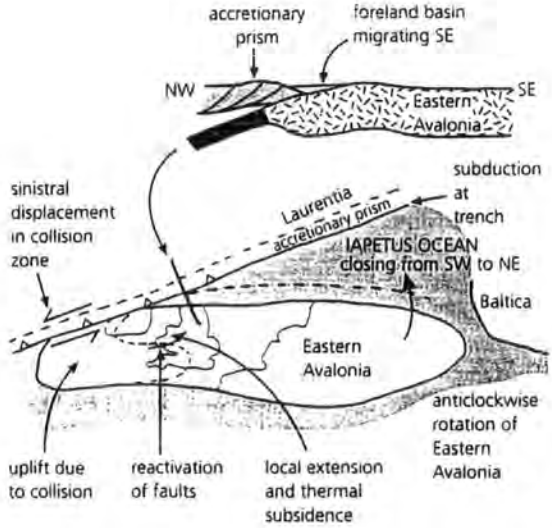

Figure 2.18. 'Soft' docking of Eastern Avalonia with Laurentia during the Wenlock. The remaining wedge-shaped fragment of the Iapetus Ocean closes from SW to NE as Eastern Avalonia rotates anticlockwise (from Woodcock 2000b).

Ocean. Based on studies in the Cordilleran terranes of western North America, anticlockwise rotation of Eastern Avalonia is inferred to have resulted from oblique sinistral convergence with the Laurentian margin (Soper *et al.* 1992a). There is no clear indication of a collisional event in the Southern Uplands sequences, although Rushton *et al.* (1996) suggest that an extended period of apparently conformable greywacke sedimentation, coincident with NW-vergent folds and back- and out-of-sequence thrusting in the hinterland indicates that the forward progress of the Southern Uplands accretionary thrust belt and the associated southward-propagating phase of folding and cleavage formation, may have been interrupted in the late Llandovery. This may reflect the initial blocking of the thrust belt at the very leading edge of Laurentia, by its first encounter with rifted Avalonian continental crust followed by the accommodation of the obstacle and the advancement of the thrust belt on to Avalonia (Barnes & Stone 1999). Another proposal is that the geometry of NW-vergent folds and thrusts is consistent with a short-lived phase of backthrusting that may have occurred due to changes in the rheology of the thrust wedge or its basal detachment (Barnes *et al.* 1987; Stone 1995). This phase of backthrusting in the Southern Uplands thrust wedge coincides with a change in the kinematic boundary conditions from a regime of orthogonal contraction to one of sinistral transpression in a southward-migrating deformation system (Holdsworth *et al.* 2002a). Since deformation in the Southern Uplands is strongly diachronous, the main phase of deformation (D1) becomes progressively younger to the S. This has important implications for the structural style observed across strike in the Southern Uplands. In the Northern Belt, D1 was overprinted by accommodation structures in the thrust hinterland (D2) and a phase of sinistral strike-slip deformation (D3). In the Southern Belt however, D1 and D3 were effectively occurring at the same time producing folds that plunge steeply and locally face downwards, and folds clockwise transected by cleavage (Barnes & Stone 1999).

As the accretionary prism on the leading edge of Laurentia overthrust onto Eastern Avalonia, a southward-migrating foreland basin was created on the Avalonian margin in the region corresponding to southern Ireland and NW England (Figs. 2.18, 2.19(a), Soper & Woodcock 1990). Evidence for the timing and NE progradation of closure is provided by the age of large-volume sand turbidites that first crossed the suture from Laurentia: in the Wenlock in Ireland and the Ludlow in NW England. This timing is consistent with the mid-Wenlock slowing in convergence, inferred from sedimentological evidence in the Southern Uplands (Kemp 1987) and the Lake District

(Kneller 1991). A unified sedimentary system was established across the suture in Britain by the Wenlock, with Scandinavia becoming an important sediment source (Soper *et al.* 1992a).

By the end of the Silurian (Pridoli), the wave of folding and cleavage formation to the N of the Iapetus Suture had propagated as far as the Lake District and Wales. Later, in the Early Devonian (Pragian, Emsian), the whole orogenic belt underwent sinistral strike-slip shear, possibly as a result of a collision between the Armorican continent and the southern edge of Eastern Avalonia. This resulted in widespread folding and formation of clockwise transecting cleavage in the Isle of Man, Leinster and the Lake District as the area underwent sinistral transpression (Fig. 2.1, Soper *et al.* 1992a). To the N of the Southern Uplands (Fig. 2.1), this phase of sinistral shear was expressed as major displacements along the Highland Boundary Fault, Southern Upland Fault, and Moniaive Shear Zone (Fig. 2.19(b)).

2.4.4 Structural comparison between Laurentia and Avalonia

The principal contrast which emerges in any structural comparison between the Southern Uplands and Leinster/Lakesman terranes is the marked difference in timing of penetrative ductile deformation (Barnes & Stone 1999). In the Southern Uplands, the main (D1) phase of deformation was systematically diachronous from the Late Ordovician in the N of the terrane to Wenlock in the S. In contrast the tectonic cleavage in the rocks of the Leinster/Lakesman Terrane is early Devonian (Acadian). The Leinster Granite (404±24Ma, Rb-Sr) was intruded during cleavage formation (Woodcock & Strachan 2000b). At this time only the D3 sinistral shear phase of deformation was operative in the Southern Uplands (Barnes & Stone 1999). The contrast between the largely pre-Wenlock tectonism in the Southern Uplands and the Early Devonian tectonic cleavage in the Leinster/Lakesman Terrane, is even more surprising considering that continental collision occurred between the two terranes during the middle-late Silurian (Soper *et al.* 1992a). This event appears to have left no orogenic imprint on either terrane, although crustal shortening did continue, as shown by the Windermere Supergroup foreland basin (Kneller *et al.* 1993). It is suggested (Barnes & Stone 1999) that a structural décollement may have separated the converging terranes to act as a barrier to the northward propagation of the Acadian deformation (Barnes & Stone 1999).

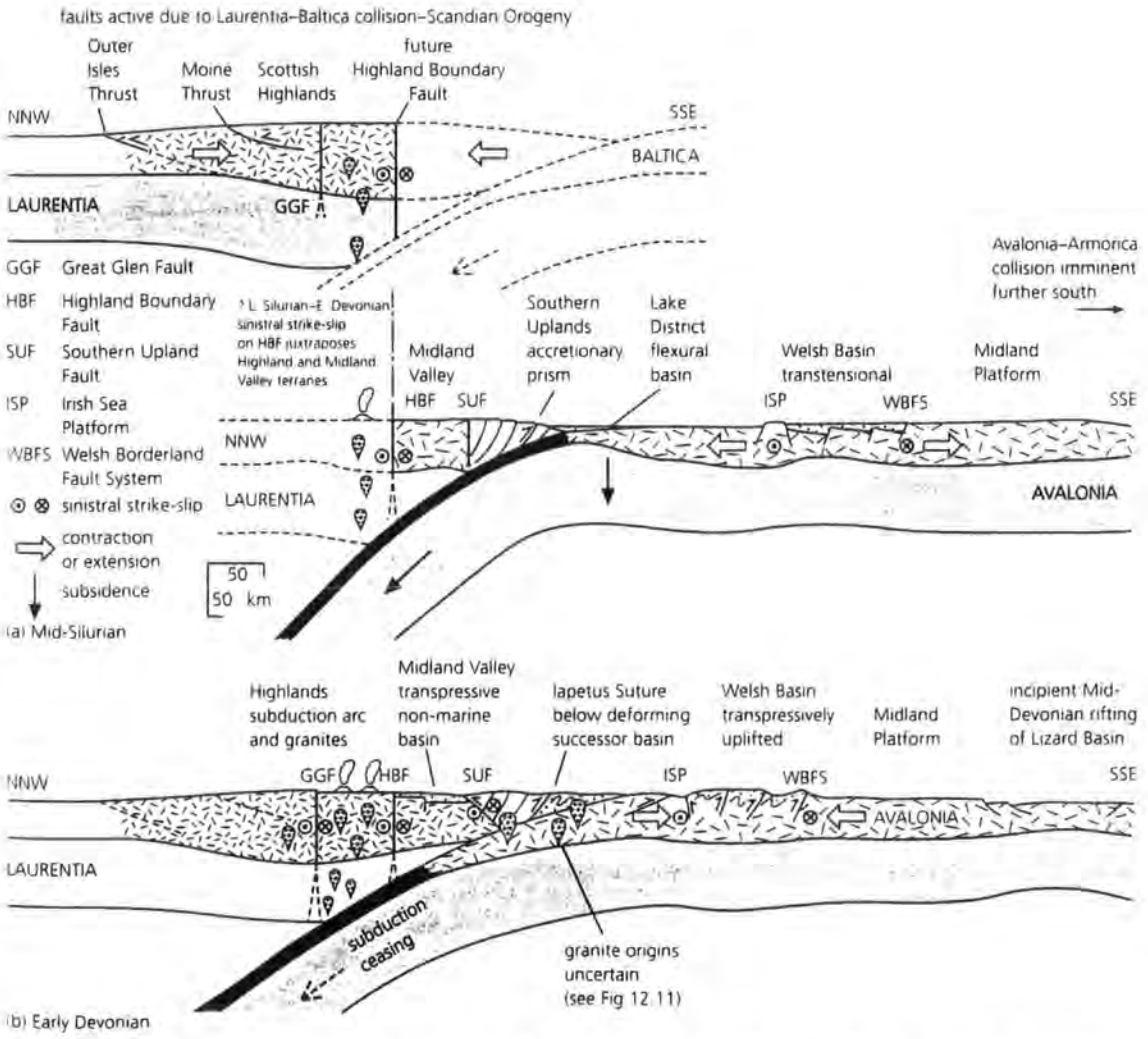

Figure 2.19. Schematic cross-sections through the Caledonian Orogen during **(a)** Mid-Silurian and **(b)** Early Devonian (from Woodcock & Strachan 2000b).

2.4.5 The Iapetus Suture

The suture between the former Laurentian and Eastern Avalonian continents can be justifiably regarded as the most important Caledonian structural feature within the British Isles and Ireland (Figs. 2.1, 2.2, Woodcock & Strachan 2000b). It can be traced from SW Ireland, running diagonally to the NE Irish coast, and then across the Irish Sea just N of the Isle of Man, to cross the W coast of England near to the Solway. From there it crosses northern England to emerge into the North Sea. Despite this bold delineation across the British Isles, the Iapetus Suture is the least well exposed of the Palaeozoic terrane boundaries. Along much of its length it is obscured by post Caledonian strata, and only in NE Ireland, the Isle of Man and SE Scotland do rocks of Ordovician or Silurian age outcrop at or near to the suture (Woodcock *et al.* 1999a). Consequently there is still some uncertainty about its exact surface trace.

In N England and S Scotland, the suture is constrained by faunal contrasts in Ordovician rocks, and is thought to lie between the Lake District and the Northern Belt of the Southern Uplands (Figs. 2.1, 2.2). Deep seismic surveys in the Irish Sea and North Sea are an additional guide to the position of the suture in this region (Brewer *et al.* 1983; Klemperer & Mathews 1987; Soper *et al.* 1992b). These show a prominent reflector (Fig. 2.20), separating southern crust containing reflectors from less reflective crust to the N. The seismic data show that the Iapetus suture is a northward-dipping plane, and that the Laurentian crust overthrusts the Avalonian crust. In the NW Isle of Man, Ordovician rocks of the Manx Group are overlain tectonically by mid-Silurian units that match those of similar age in the Southern Uplands. It may be that in this case the thrust contact represents a fault strand of the suture zone. Whether this is the case or not, seismic and aeromagnetic profiles across the Irish Sea and the Isle of Man (Fig. 2.21) show a series of low angled reflectors and a belt of short wavelength magnetic disturbances dipping to the NW corresponding to the Iapetus Suture (Hall *et al.* 1984; Kimbell & Quirk 1999). In Ireland, the Southern Uplands accretionary prism extends into the Longford-Down massif (Figs. 2.1, 2.2) and the suture is drawn between the Grangegeeth and Bellewstown inliers (Fig. 2.2), which show Laurentian and Avalonian faunal affinities respectively (Woodcock & Strachan 2000b). Through central Ireland the suture is usually taken along the Silvermines Fault (Fig. 2.1) to emerge along the line of the Shannon Estuary (Fig. 2.1), although seismic profiles (Klemperer 1989) to the west have imaged a dipping reflector just N of the Dingle Peninsular (Todd *et al.* 1991).

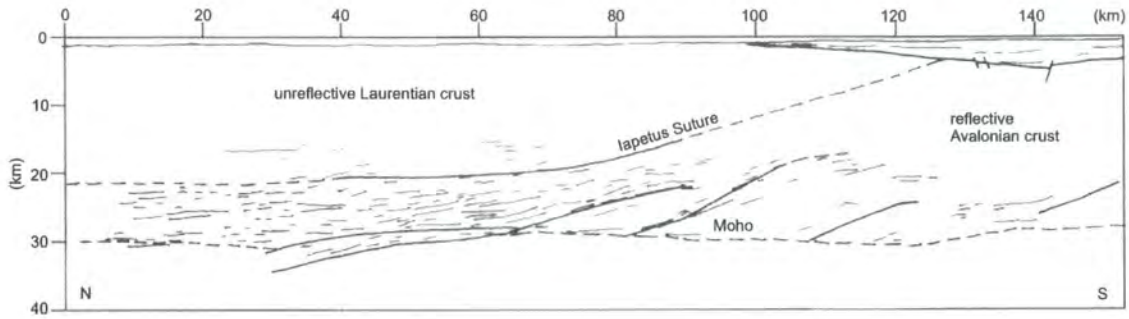

Figure 2.20. Interpreted line drawing of the main reflectors on the NEC seismic profile offshore SE Scotland (from Soper *et al.* 1992b).

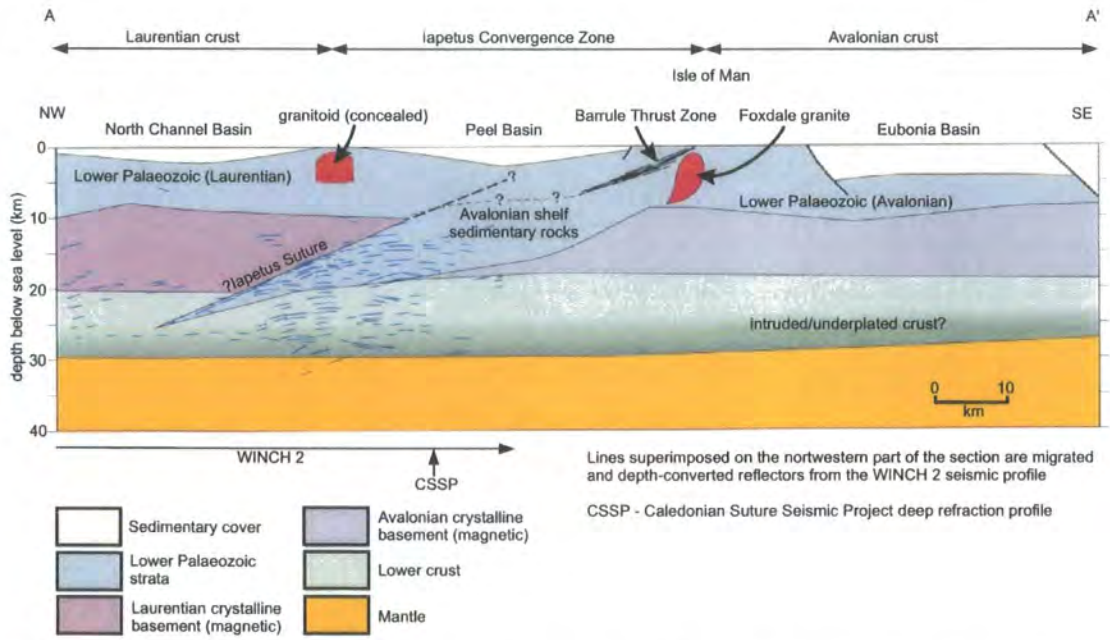

Figure 2.21. Crustal cross-section NW-SE across the Isle of Man showing the position of the Iapetus Suture and related structures. Based on WINCH 2 and CSSP seismic lines (from Chadwick *et al.* 2001)

2.4.6 Summary

The events leading up to and including the final collision between Laurentia and Avalonia are protracted and complex, involving episodes of subduction-related volcanism, crustal rifting, and strike-slip faulting at both margins of the Iapetus Ocean. Early ideas of a simple 'Caledonian Cycle' of sedimentation followed by deformation, metamorphism and igneous activity have proved too simplistic. The existence of a wide Ordovician ocean separating Laurentia and Avalonia implies that they had very different tectonic histories at least until the Silurian. Although only the two main continental landmasses of Laurentia and Eastern Avalonia are discussed in this chapter, it is important to note that these were only two of a collage of fragments that were converging in mid-Palaeozoic times. Both Baltica and Western Avalonia were also converging with Laurentia at this time, while further S, Armorica probably collided with the assembled northern continents during the Early Devonian, and Iberia with Armorica in the mid-Devonian (Woodcock & Strachan 2000b).

As discussed in the previous sections, the strain histories of the Southern Uplands and the Leinster/Lakesman terranes are very different and reflect different events during the closure of the Iapetus Ocean. However, the geometry, orientation and the style of deformation developed during these deformational events outlined above are remarkably similar (see chapter 6). This suggests that the orientation of the far-field stresses in the region remained relatively constant throughout the Silurian to Devonian, and that the deformation processes were similar in all three study areas.

Chapter 3

The Regional Geology of the Southern Uplands and the Structure and Kinematics of the Berwickshire Coast Between Eyemouth and Burnmouth

3.1 Introduction

Comprising part of the Caledonian Orogen, the Southern Uplands Terrane of Scotland (Fig. 3.1(a)) is thought to form a broad band of Palaeozoic transpressional deformation, created during the Palaeozoic, sinistral oblique closure of the Iapetus Ocean (Dewey & Shackelton 1984; Soper & Hutton 1984; Soper *et al.* 1992). Numerous structures, thought to be related to sinistral transpression, such as folds transected clockwise by their associated cleavage (e.g. Stringer & Treagus 1980; Anderson 1987) and major strike parallel sinistral faults (e.g. Orlock Bridge Fault, Anderson & Oliver 1986; Moniaive Shear Zone, Lintern *et al.* 1992; Phillips *et al.* 1995) have long been recognised within the Southern Uplands Terrane. Although much of the Southern Uplands Terrane has been widely studied, activity has generally been concentrated in the western coastal sections and inland. This chapter provides a synthesis of the regional geology of the Southern Uplands and goes on to present a brief history of previous work and a detailed account of folds and associated structures in a less well known area of deformed Silurian rocks exposed on the Berwickshire coast in SE Scotland (Fig. 3.1(b))

3.2 Regional setting

The Lower Palaeozoic rocks of the Southern Uplands are divided into a series of NE-SW trending, elongate, slices by major, steeply-dipping faults that predominately originated as low angled thrusts (Fig. 3.1(a), McKerrow *et al.* 1977). The individual slices have a limited stratigraphical range and are dominated by turbidite deposits of greywacke, siltstone and shale (Stone 1996). Throughout the Southern Uplands the greywacke turbidite beds are generally steeply inclined with a fairly uniform strike of about 060° (Stone 1996). Within the majority of thrust slices the younging direction is

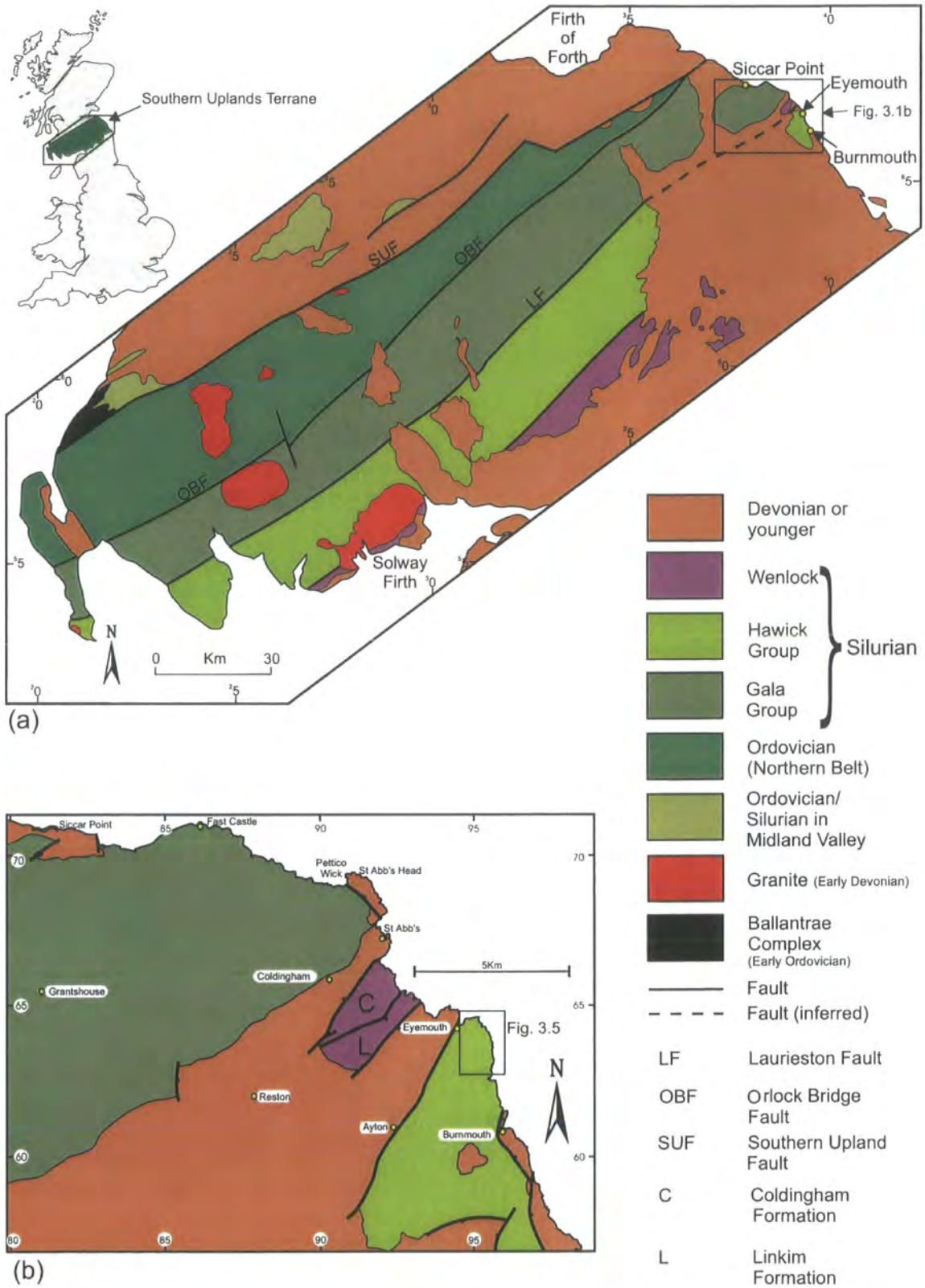

Figure 3.1(a). Regional map of the Southern Uplands Terrane showing the main tectono-stratigraphic units and Tract bounding faults. The likely correlation between the Berwickshire outcrops and the main outcrop to the SW is also shown. Box indicates the location of Fig. 3.1b (after Stone 1996; Treagus 1992). **(b)** Simplified sketch geological map of SE Scotland. Box indicates location of Fig. 3.5 (after BGS sheet 34, 1982).

to the NW, whilst, the regional younging of the strata within the Southern Uplands is to the SE. Thus, the Northern Belt of the Southern Uplands is exclusively composed of Ordovician rocks whilst the Central and Southern Belts predominately or exclusively comprise Silurian age strata (Figs. 3.1(a), 3.2, Peach & Horne 1899). This seemingly paradoxical relationship reflects the progressive stacking up of thrust sheets from NW to SE, with each newly accreted unit containing younger strata (McKerrow *et al.* 1977). Throughout the Southern Uplands, complex systems of mainly SE-verging folds and associated top-to-the-SE thrusts are recognised (e.g. Knipe & Needham 1986; Knipe *et al.* 1988). The development of this system of folds and imbricate thrusts was accompanied by regional low-grade metamorphism (diagenetic to prehnite-pumpellyite facies) (Oliver & Leggett 1980; Kemp *et al.* 1985). Therefore, they are thought to have formed at relatively shallow crustal depths (<10km).

Two regional tectonic models have been proposed to account for the structural and stratigraphical relationships seen within the Southern Uplands (see also section 2.2.2). Firstly, the accretionary prism hypothesis (McKerrow *et al.* 1977; Leggett *et al.* 1979; Leggett 1987), in which the greywackes are envisaged as being deposited in a deep ocean trench at the long-lived, active, northern continental margin of the Lower Palaeozoic Iapetus Ocean. As the oceanic plate was subducted northwestwards the sediments covering it were progressively scraped off as a series of underthrust, imbricated fault tracts. Back rotation of the thrust stack during subsequent accretion and the final closure of Iapetus in the late Silurian or early Devonian rotated the originally low-angled thrust sheets into their present day steeply orientation (McKerrow *et al.* 1977; Leggett *et al.* 1979; Leggett 1987). Although, this model elegantly explained many of the geological relationships seen within the Southern Uplands it failed to address a number of issues. In particular, palaeocurrent and compositional studies of sediments within the Northern Belt indicated two distinct source regions. One, a mature continental margin to the north and northeast and the other, an active volcanic island arc to the south and southwest. The palaeogeographical implications of this led to a second, alternative tectonic model, in which the region formed part of a back-arc to fore-arc basin thrust system related to early Silurian arc-continent collision (e.g. Stone *et al.* 1987; Hutton & Murphy 1987; Armstrong *et al.* 1996). Which ever of these hypotheses is preferred, the fundamental thrust geometry is the same. Importantly, in both models the thrust related deformation was diachronous across the region, becoming progressively younger towards the south, with those in the NW

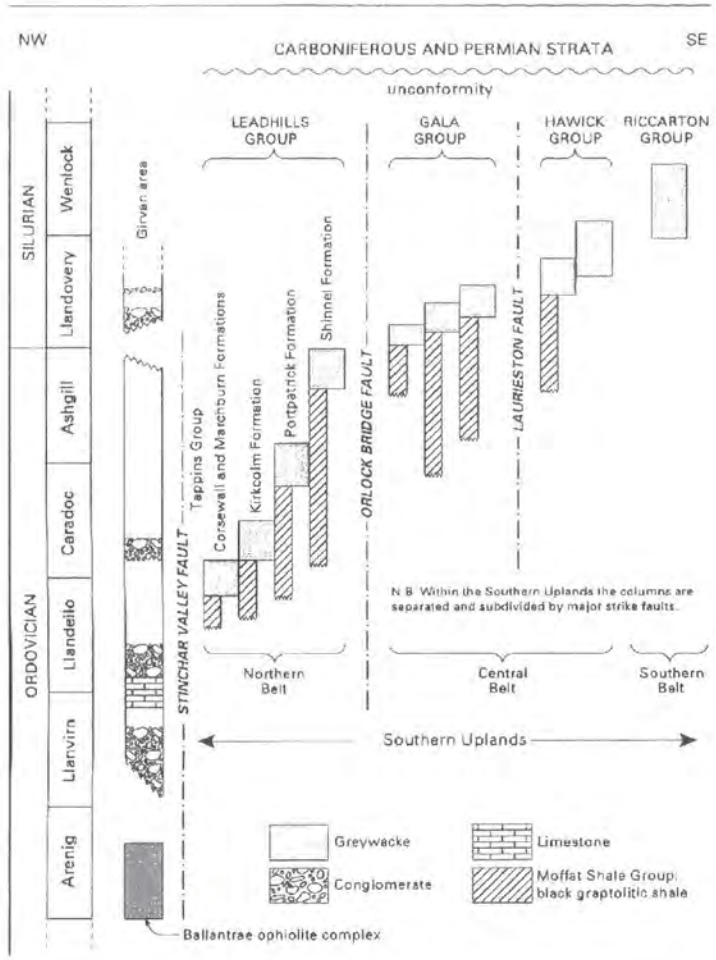

Figure 3.2. Schematic representation of stratigraphical relationships in SW Scotland (from Stone 1996).

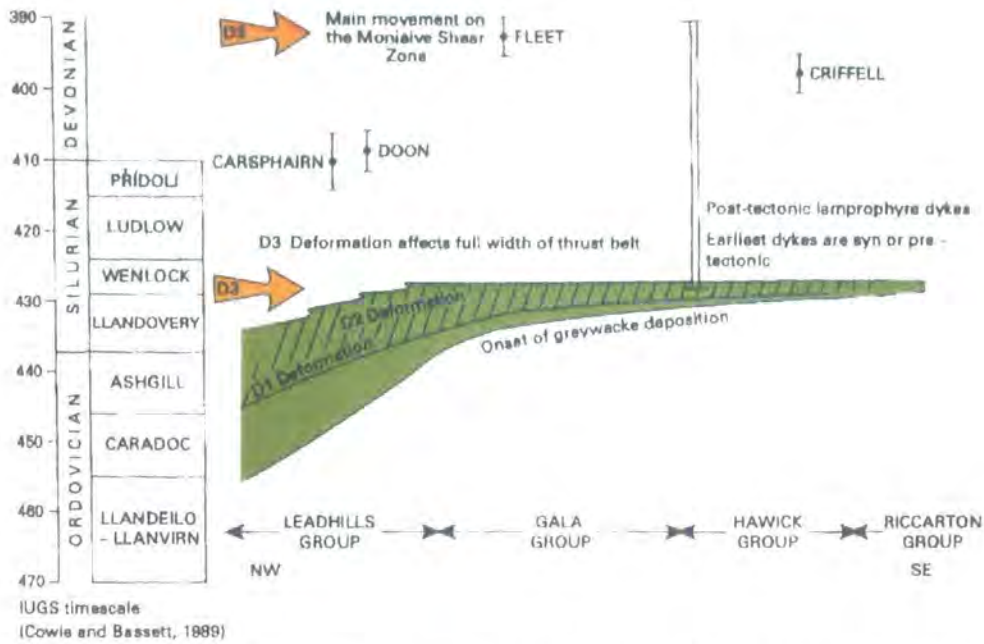

Figure 3.3. Timing of deformation within the Southern Uplands Terrane (after Stone 1996).

forming significantly earlier than those in the SE (Fig. 3.3). This is supported by biostratigraphic and radiometric data, which suggests that the onset of thrusting began by the Ashgill in the NW through to the Wenlock in the SE (Barnes *et al.* 1989). The first phase ('D1') of thrust related contractional deformation was accompanied by refolding ('D2') within the hinterland to accommodate the steepening of the thrust sheets. However, from the Llandovery onwards, in addition to the contractional deformation there was a component of regional sinistral shear ('D3'). In the northwestern parts of the region, the ('D1') and ('D2') structures are overprinted by sinistral faults and shear zones, often with associated steeply plunging late folds (F3) (Fig. 3.3; Barnes *et al.* 1989). As a consequence of the diachronous nature of the deformation, the sinistral shear becomes increasingly synchronous with accretion in the frontal parts of the thrust wedge (Hawick Group rocks and younger; Fig 3.1(a)). Therefore, the most southeasterly tracts of the Southern Uplands Terrane are often characterised by sinistral transpressional primary ('F1') fold belts with clockwise cleavage transection and local steeply-plunging axes with sinistral vergence (e.g. Stringer & Treagus 1980; Anderson 1987; Kemp 1987).

3.3 The Lower Palaeozoic rocks of the Berwickshire coast, south east Scotland

In SE Scotland, the mainly Silurian strata of the Southern Uplands Terrane form three separate outcrops all of which are exposed along the Berwickshire coast (Fig. 3.1(b); Greig 1988). The strata comprise an interbedded sequence of greywackes, siltstone and shales typical of turbidite deposits (Greig 1988). Although the Silurian outcrops are commonly bounded by steeply-dipping faults, unconformable relationships with the overlying Devonian and younger sediments and extrusive volcanics are locally preserved (e.g. Hutton's unconformity at Siccar Point; Fig. 3.1(b)).

The rocks exposed in the north of the region, from Siccar Point to Pettico Wick (Fig. 3.1(b)) are thought to be Llandovery in age (Gala Group), based on poorly preserved graptolites (Greig 1988). Exposed along the central coastal section, south of St. Abb's and north of Eyemouth (Fig. 3.1(b)) are the Coldingham and Linkim formations. These highly disrupted and deformed greywackes and shales were, based on their intense deformation, thought to be Ordovician (Geikie 1863). However, subsequently, the complex deformation has been shown to be most consistent with soft sediment deformation (Oliver *et al.* 1984) and the rocks are now thought to be of

Wenlock age, based on poorly preserved faunal and microfaunal evidence (Molyneux 1987). The significantly lower metamorphic grade of these rocks, compared to the Silurian rocks in adjacent coastal sections suggests that they may have formed in a very shallow part of the thrust wedge, where the effects of gravity driven, down-slope deformation were dominant (Oliver *et al.* 1984). The southernmost section, from Eyemouth to Burnmouth (Fig. 3.1(b)) comprises an apparently unfossiliferous sequence of turbidites that, on the basis of their similarity to Hawick Group rocks further to the SW, have been correlated with that group (Greig 1988). The strata comprise a thick succession of well-bedded, strongly folded, steeply-dipping turbidites. The predominance of thinner (<50cm) individual greywackes and a higher proportion of shales and mudstones suggested a more variable density of flows within the depositional environment than the turbidites in the northern section (Greig 1988).

3.3.1 Summary of the Fast Castle to Pettico Wick section

This section summarises the structure of the northern section between Fast Castle and Pettico Wick (Fig. 3.1(b)) and provides a comparison with the structure of the Eyemouth to Burnmouth section described in the following sections.

The almost completely exposed, 6km long coastal section between Fast Castle and Pettico Wick comprises a relatively simply, but highly folded, uniform sequence of turbidites, with an estimated total stratigraphic thickness of at least 1200m (Sheills & Dearman 1966; Greig 1988). Developed within the turbidites is a single set of open to tight folds with gentle, whaleback hinge geometries, that typically plunge shallowly to the NE or SW (Holdsworth *et al.* in 2002a). A weakly developed slaty to spaced-solution cleavage is present in many mudstone and siltstone horizons, and exhibits a largely axial planar or gently fanning relationship to the folds. All folds and associated cleavage face steeply up to the SW and NE. Folds in the WNW part of the section are more upright and symmetric, whilst those to the ESE are more asymmetric and overturned to the NW (Fig. 3.4(a), Sheills & Dearman 1966; Greig 1988; Holdsworth *et al.* 2002a). Faults, although widespread, are relatively minor structures in terms of displacement and are often associated with minor amounts of carbonate mineralisation. Conjugate NW- and SE-dipping thrust faults are common in some disrupted fold hinge regions (Greig 1988). Well-defined carbonate slicken fibres present on bedding-parallel shear surfaces are widespread in all fold limb regions and lie normal to the fold hinges. The sense of shear deduced from slickenfibre steps and offset markers are reversed on

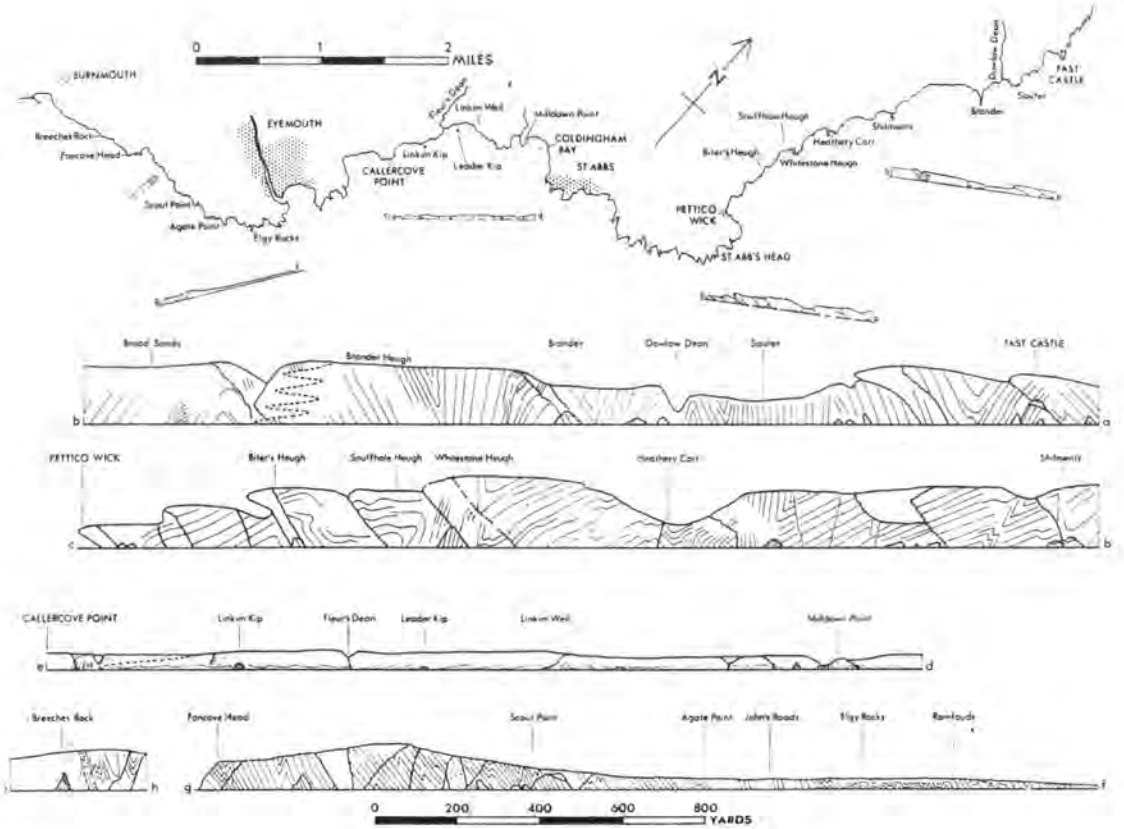

(a)

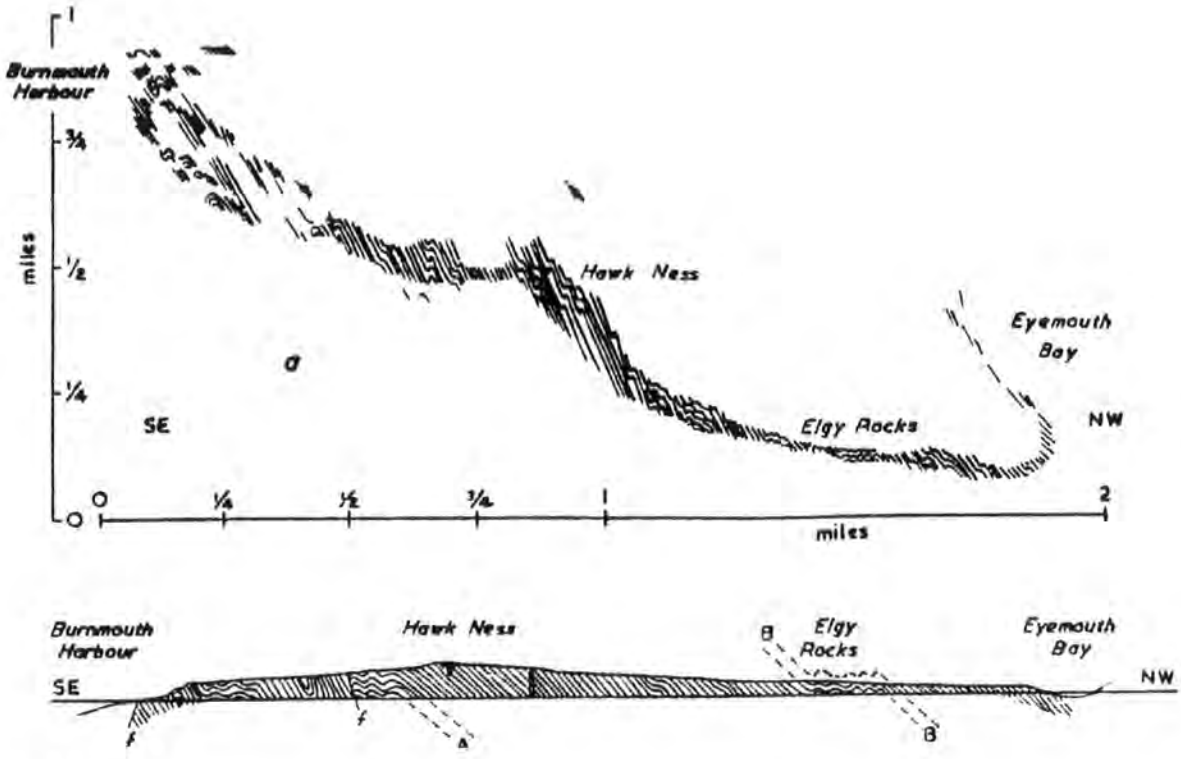

(b)

Figure 3.4. **(a)** Map and sketch cross-section of the Berwickshire coast between Fast Castle and Burnmouth (from Sheills & Dearman 1962). **(b)** Profile of observed structures as viewed from the NE and sketch cross-section (from MacKenzie 1956).

opposite fold limbs and are consistent with a flexural slip model (e.g. Ramsay & Huber 1987). The folded bedding is cross-cut by steeply-dipping, NNE-SSW sinistral and NW-SE dextral strike-slip faults that may form a conjugate set. The age of the faulting is uncertain and may be late Caledonian (Stone 1995) or be related to younger deformation episodes such as the Variscan inversion of the Northumberland Basin that lies to the south (e.g. Roper 1997). This relatively simple structure contrasts strongly with that described for the Eyemouth - Burnmouth section below.

3.4 The Eyemouth to Burnmouth coastal section

3.4.1 Previous studies

Early studies include those of Geikie (1863), MacKenzie (1956), Dearman *et al.* (1962) and Sheills & Dearman (1966). The first systematic account of the area was by Geikie (1863). In particular, he noted the steep north-westerly regional dip of the bedding and a number of distinctive zones of intense folding. Similarly, these features were noted by MacKenzie (1956) who, in addition, concluded that the general younging direction was to the NW. This observation cast doubt on the traditional interpretation of the regional structure as a series of overturned isoclinal folds repeating a thin group of strata (Dearman *et al.* 1962). Sheills and Dearman (1966) corroborated much of MacKenzie's work and provided a synthesis of the structures observed between Fast Castle and Burnmouth (Figs. 3.1(b), 3.4(a)).

A more detailed study of the coast between Dulse Craig and Agate Point (Fig. 3.5, grid refs. 948647 and 954642 respectively) was provided by Dearman *et al.* (1962). They identified three distinct structural units. A zone centred on Elgy Rocks (Figs. 3.4(b), 3.5, grid ref. 953645) dominated by 'box' type folds, with axial plunges consistently to the SW at angles between 20° – 45°. This zone is flanked to the north and south by NW-dipping homoclines. The monotonous structure of the homoclines is broken by smaller folds that have variable plunges to both the SW and the NE. In addition, they also noted the presence of a number of folds that possessed highly curvilinear fold axes such that the fold hinges pass through the vertical to produce folds that locally face downwards. The resultant structures exhibit rapid changes in fold plunge and are particularly well exposed at Agate Point and John's Roads (Figs. 3.5, 3.6(a), grid refs. 954642 and 953642 respectively). They suggested that these cross-folds were the product of refolding an original set of folds, in which the second folds

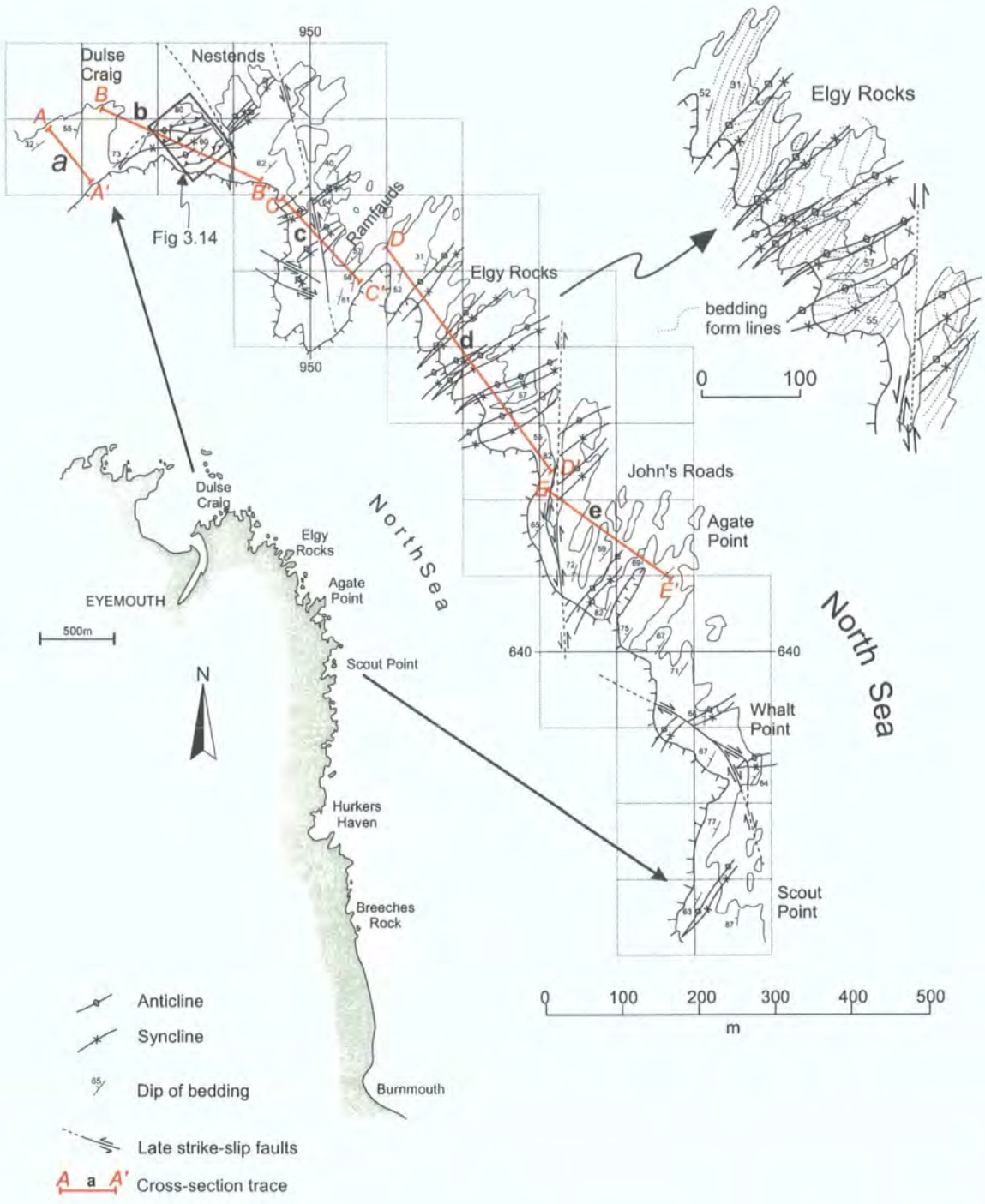

Figure 3.5. Simplified structural map of the northern part of the Eyemouth-Burnmouth section between Scout Point and Eyemouth Harbour. Inset to bottom left shows location of coastal section. Inset to top right shows a more detailed map of folded bedding around Elgy Rocks. Lines of sections shown in Figure 3.7 are shown in red on the main map, together with the location of the large scale map of Dulse Craig in Figure 3.14 (box) (adapted from Holdsworth *et al.* 2002b).

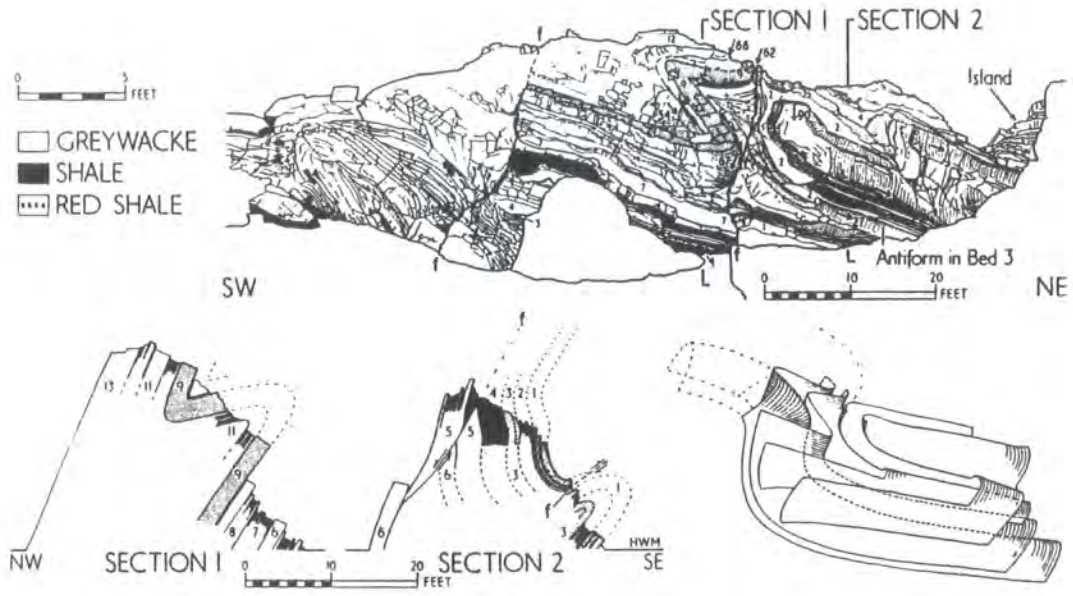

(a)

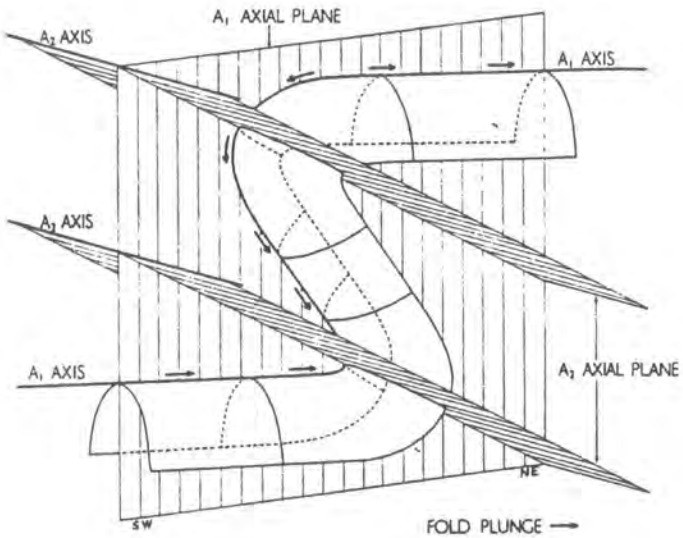

(b)

Figure 3.6 (a). Field sketches and 3-D interpretational diagram of fold structures observed at John's Roads by Dearman *et al.* (1962). **(b)** 3-D diagram to illustrate the geometry of cross-folds formed by refolding about A_2 axis (from Dearman *et al.* 1962)

share the same axial plane to the first folds (Fig. 3.6(b)). Dearman *et al.* (1962) provided a number of remarkably detailed sketch maps, field sketches and three-dimensional diagrams to illustrate their findings (e.g. Fig. 3.6(a)). They concluded that the original fold structures were formed during NW to SE directed primary compression and possess a Caledonoid trend. This was followed by a second phase of compression at right angles to the primary phase, which refolded the original folds about NW to SE axes. In addition, these authors suggested that the close relationship between the structures reflected successive fluctuations in the stress distribution during a single major phase of deformation. Hence, the various phases need not have been greatly separated in time, and may have been contemporaneous (Dearman *et al.* 1962). The following detailed study of the structure and kinematics of the Eyemouth to Burnmouth coast builds on the work of Dearman *et al.* (1962) in the light of advances in structural geology made in the past 40yrs. The section was initially remapped by Holdsworth, Tavarnelli and Pinheiro during 1997 – 99, with the present author carrying out more detailed structural measurements and observations during 2000 – 2001. This work is collectively published by Holdsworth *et al.* (2002).

3.4.2. Introduction

Eyemouth and Burnmouth lie in the southeastern corner of the Southern Uplands Terrane (Fig. 3.1(a) & (b)). The rocks are generally NW-younging, uniform turbidites and comprise an estimated total structural thickness of at least 2500 metres (Geikie 1864; MacKenzie 1956; Dearman et al. 1962; Sheills & Dearman 1966). They are almost continuously exposed along the NNW – SSE trending, 4km long coastline to the south of Eyemouth Harbour (Fig. 3.5). These rocks are typical turbidite sequences comprising units of greywacke sandstone, siltstone and shale interlayered on a metre to centimetre scale (Plate 3.1(a)). They contain abundant way up criteria, including graded bedding, cross-laminations, sole marks (mainly flutes and grooves) load casts and ripple marks (Plate 3.1(b) & (c), Greig 1988). This has enabled a detailed analysis of fold and cleavage facing patterns to be made in addition to a standard orientation analysis using stereographic projections. Cross-cutting and locally concordant minor intrusions of Devonian-age lamprophyre and porphyrite are locally abundant (e.g. around Breeches Rock) (Greig 1988). Much of the section is easily accessible, apart from parts of the steep cliffs between Scout Point and Breeches Rock (Fig. 3.5).

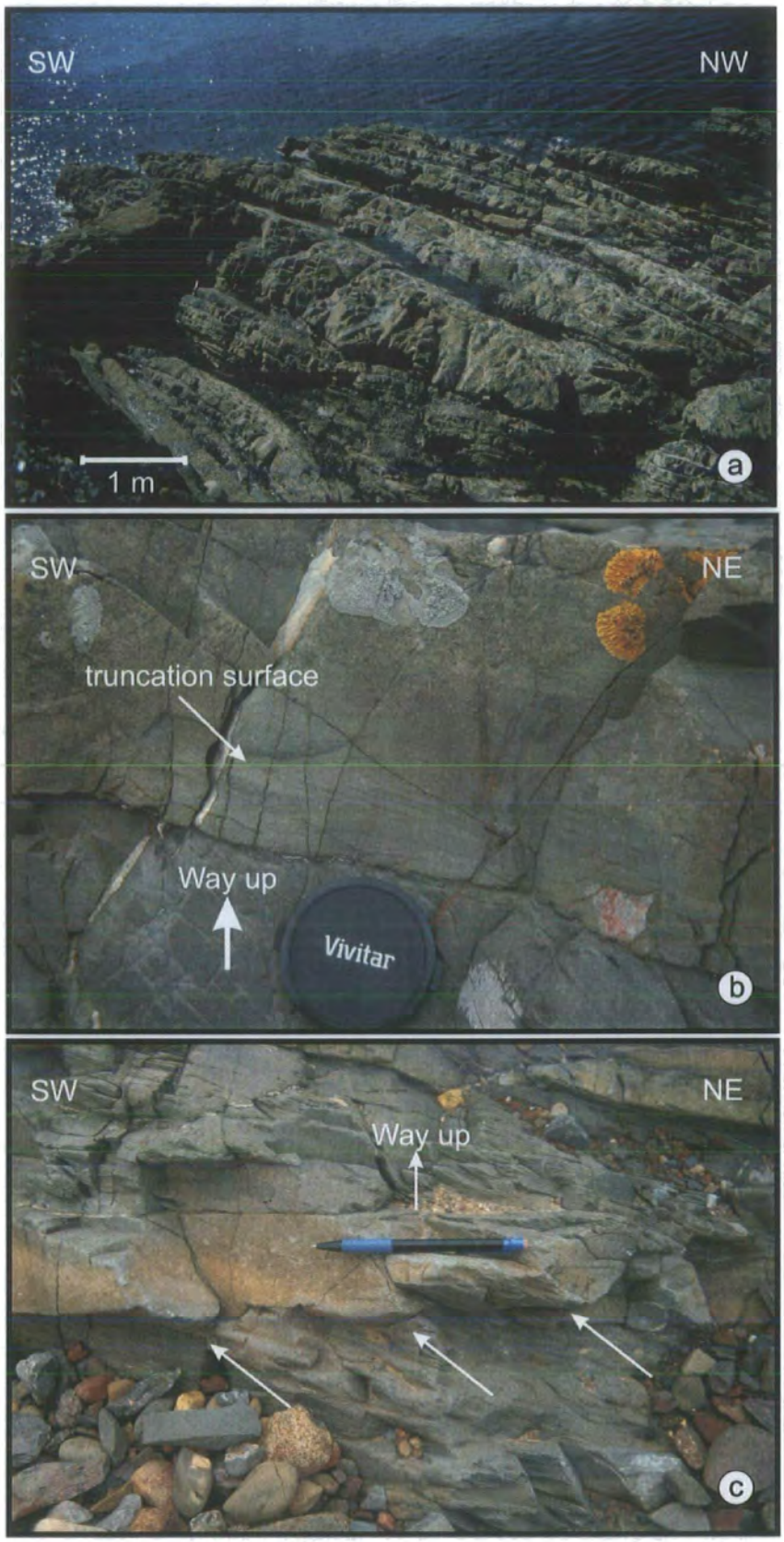

Plate 3.1. (a) North west dipping turbidite sequence consisting of greywacke sandstones, siltstones and shales. NW side of Eyemouth Harbour (Fig. 3.5, grid ref. 94526452) **(b)** Cross lamination in greywacke indicates way up (lens cap diameter is 55mm). **(c)** Sole structures (arrowed) on base of thin greywacke bed.

3.5 General structure

In general, the coastline between Eyemouth and Burnmouth exposes a homoclinal, NW-dipping and -younging sequence (Figs. 3.7, 3.8(i), c.f. Fig 3.6(a) & (b), Plate 3.2(a)). Regions of generally S-vergent folding occur locally, in particular near to the north of the section around Elgy Rocks (Figs. 3.5, 3.7, grid ref. 952645). Poles to bedding lie along a rather diffuse NE-dipping girdle that defines a shallowly SW-plunging β axis with a well-defined point maximum consistent with a moderately to steeply NW-dipping homoclinal bedding plane (Fig. 3.8(i)). Minor fold axes show a SW plunging maximum that corresponds broadly to the regional β axis, but these are distributed very significantly along a girdle lying sub-parallel to the mean fold axial plane (Fig. 3.8(ii)). This suggests that the fold hinges are significantly curvilinear. This is confirmed by field observations (see below). Mudstone and siltstone horizons contain a steeply dipping slaty to spaced solution cleavage (Plate 3.2(b)). Within sandstone units, this is only very weakly developed and then only in the finer grained units. No mineral lineations are visible in exposed cleavage surfaces. Cleavage-bedding intersection lineations and poles to cleavage planes are broadly consistent with the minor fold plunges and axial plane data, but both exhibit a small amount (ca. 8°) of *apparent* clockwise transection (Figs. 3.8(ii), 3.8(iii)). Fold and cleavage facing directions collectively exhibit approximately 270° of variation from sideways NE, through upwards to SW sideways and downwards (Figs. 3.9(i), 3.9(ii)).

Faults are widespread and are often associated with significant amounts of pale pink and white carbonate mineralisation (calcite, baryte). They include conjugate thrust faults in disrupted fold hinge regions (Plate 3.3(a)), bedding-parallel shears in fold limbs and interlinked networks of detachment faults lying at low-angles or sub-parallel to bedding (see below). The latter structures are abundant in some homoclinal regions, particularly in the north of the section around Dulse Craig (Fig. 3.5, grid ref. 948647). Carbonate slickenfibres along all of these shears and faults exhibit variable orientations and locally complex movements (Figs. 3.8(iv), 3.8(v)), but those lying at low angles to strike always display a sinistral sense of movement (Plate 3.3(b)). The subdivision between bedding-parallel shears (Fig. 3.8(iv)) and detachments (Fig. 3.8(v)) is to some extent arbitrary, since many detachments are bedding-parallel over many metres along-strike, particularly those developed in the long-limbs of the SE-verging folds. In this

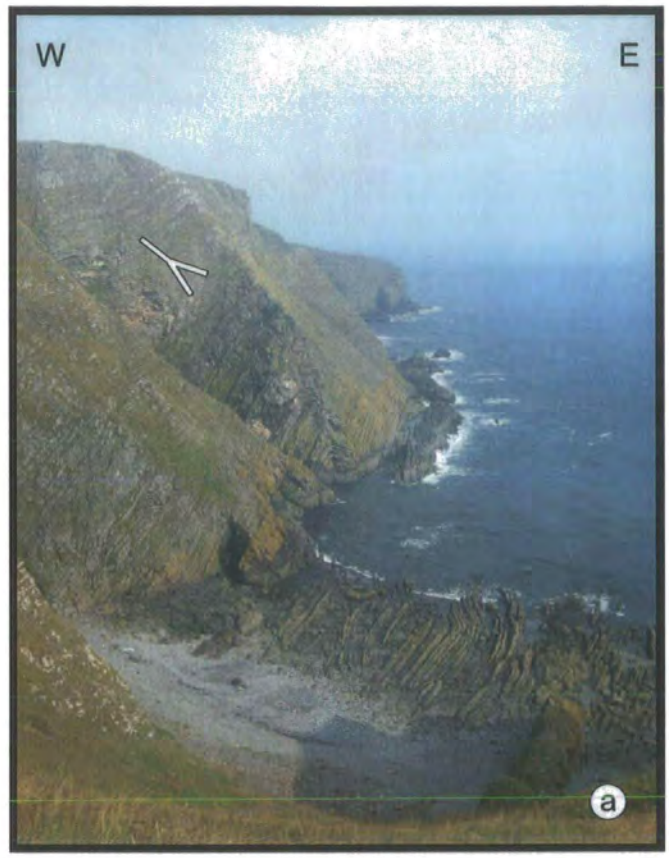

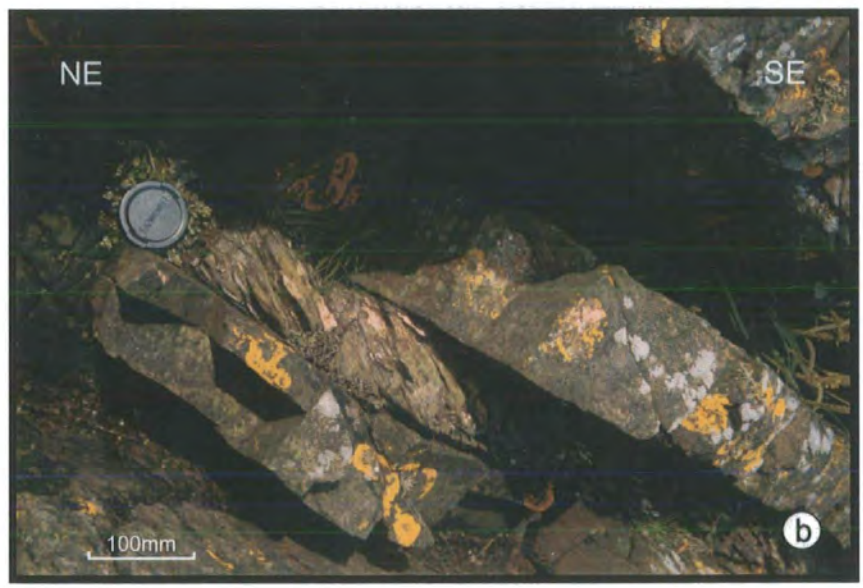

Plate 3.2. (a) View looking north from above Hurkers Haven (Fig. 3.5, grid ref. 954625). Note NW younging, largely NW-dipping homoclinal structure with S-vergent folds pair. **(b)** Clevage developed within siltstone unit bounded by thin sandstones. Cleavage is weak or absent within the sandstones. Near to Agate Point (Fig. 3.5, grid ref. 95396447). Lens cap is 55cm in diameter.

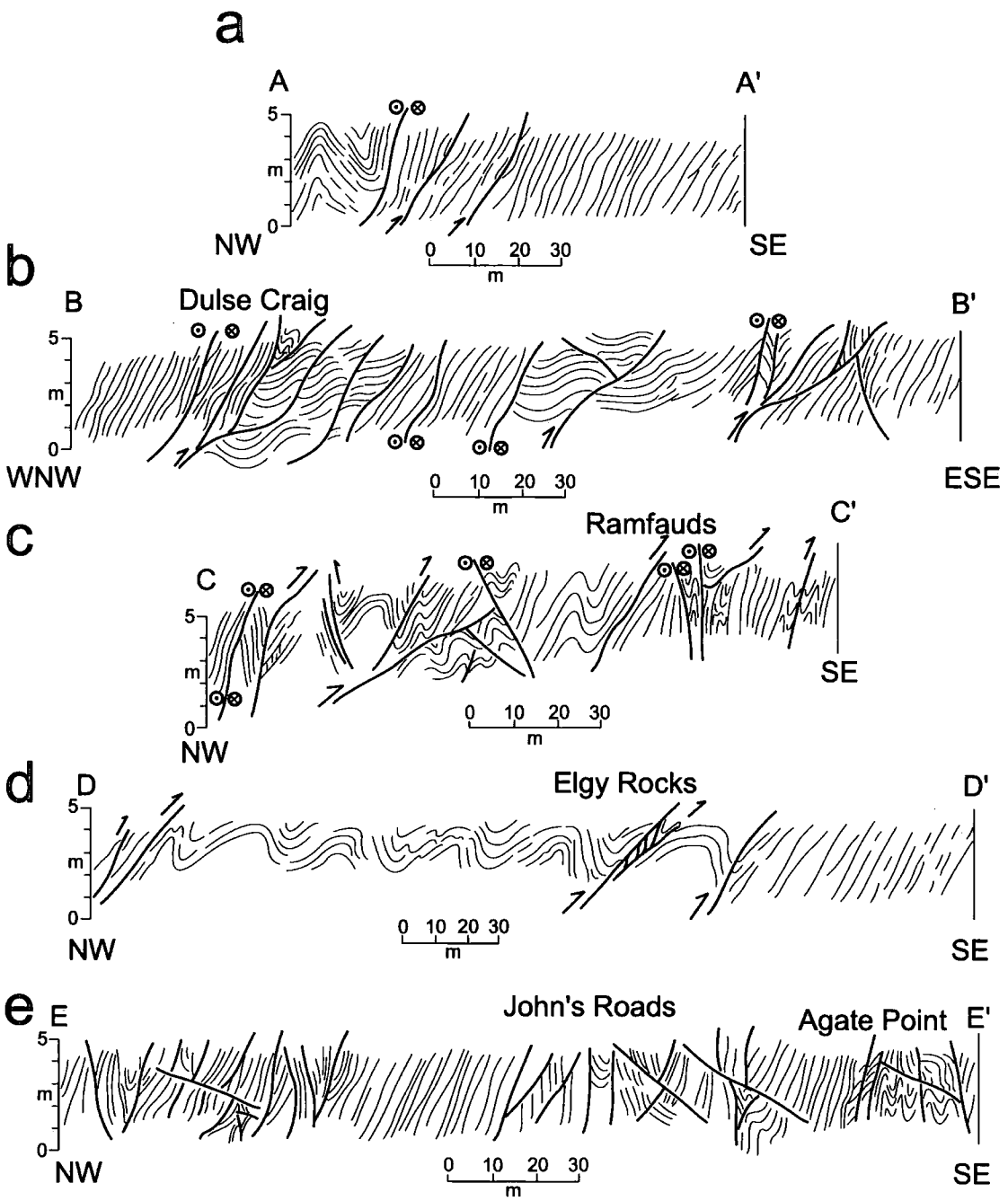

Figure 3.7. NW-SE sketch sections between Dulse Craig and Agate Point; lines of section indicated on Figure 3.5 (from Holdsworth *et al.* 2002b).

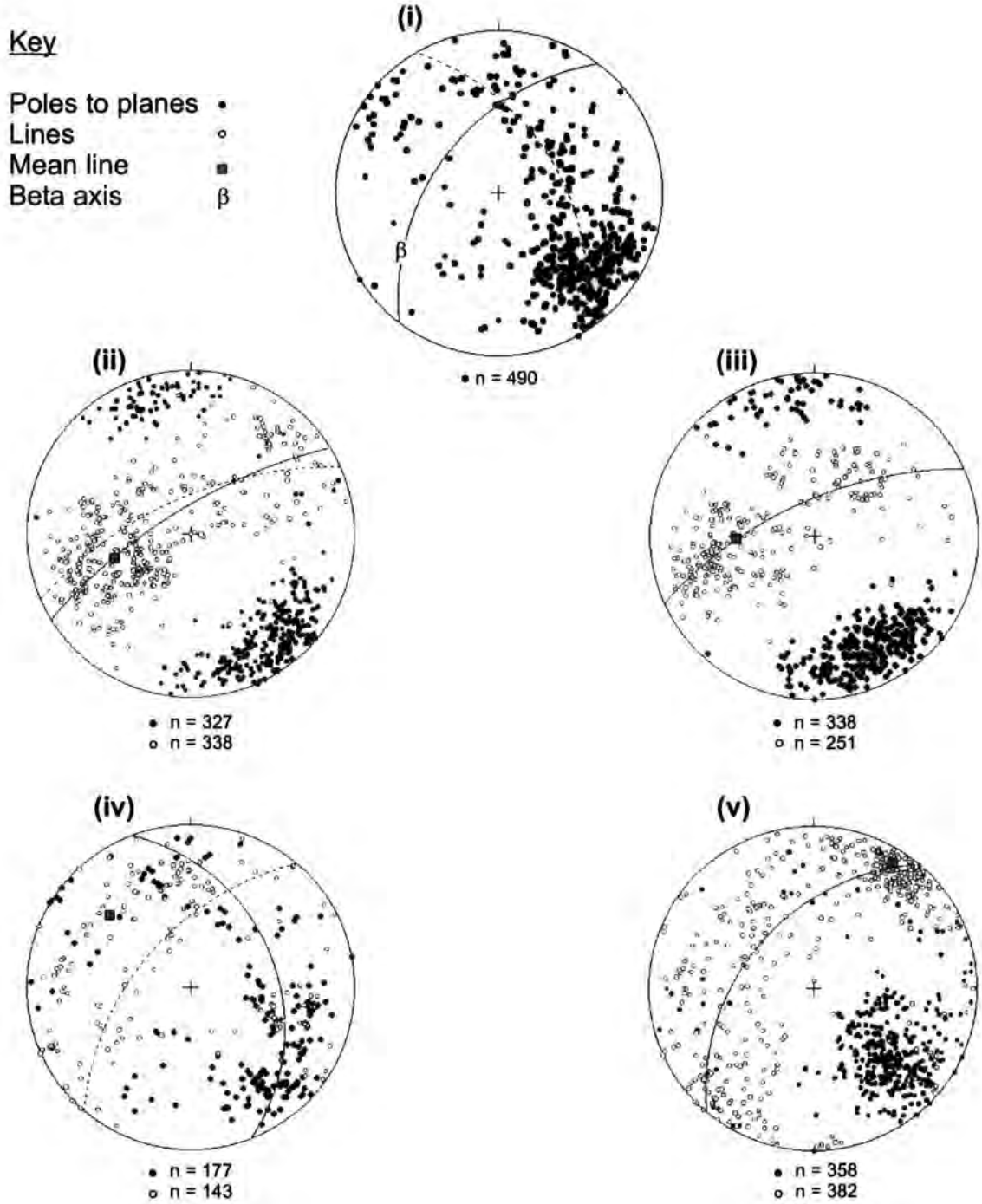

Figure 3.8. Stereoplots of structural data from the area between Eyemouth Harbour and Burnmouth **(i)** Poles to bedding, with best-fit great circle (dashed, 149/59NE), mean homoclinal bedding (solid, 038/60W) and regional β axis (29/237). **(ii)** Poles to fold axial planes and fold hinges, with mean fold hinge (50/252), axial plane (solid, 058/77NW) and cleavage plane (dashed, 066/72NW) shown. **(iii)** Poles to bedding-cleavage intersection lineations (BCIL), with mean BCIL (51/267) and cleavage plane (066/72N) shown. **(iv)** Poles to bedding-parallel shear planes and slickenfibre lineations, with best-fit great circle girdle (solid, 159/46ENE), mean plane (dashed, 040/64NW) and mean lineation (34/312) shown. **(v)** Poles to detachment faults and slickenfibre lineations, with mean fault plane (040/54NW) and lineation (10/032) shown.

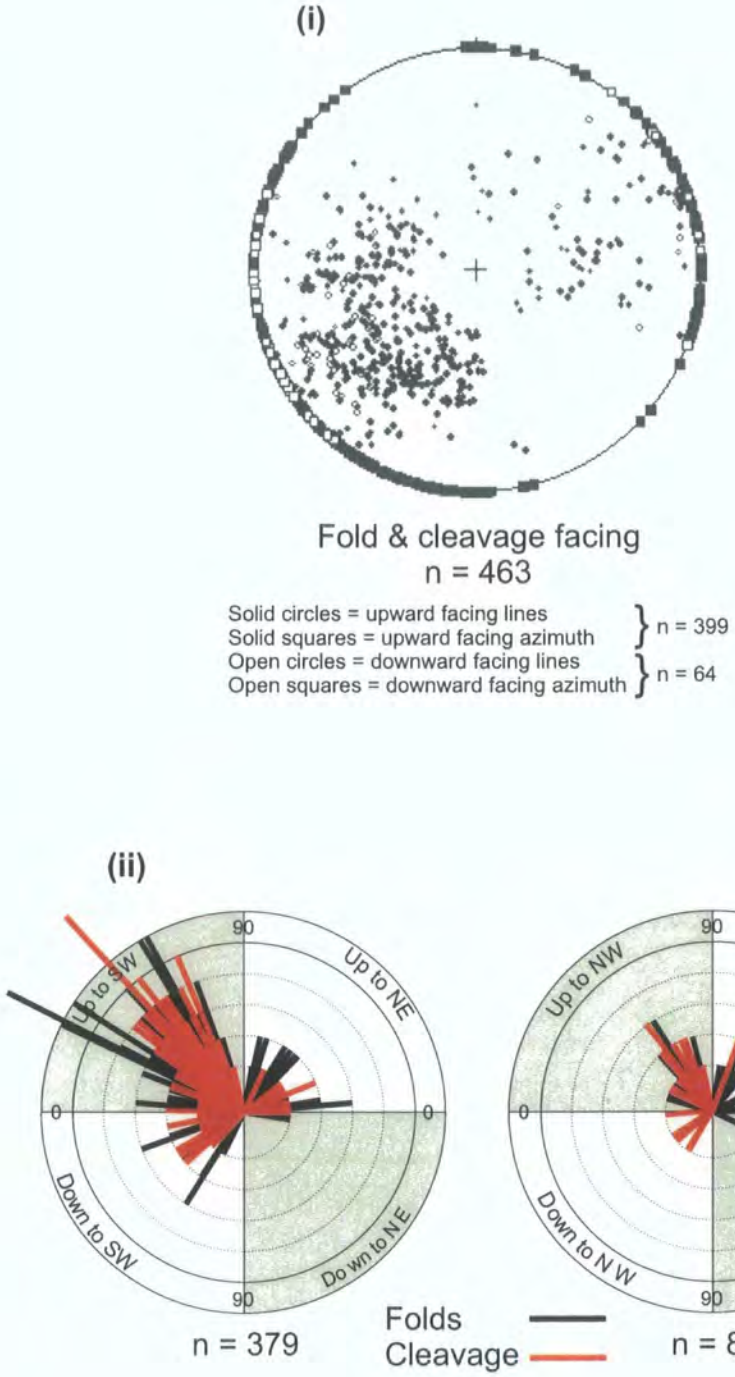

Figure 3.9. Facing data from the area between Eyemouth Harbour and Burnmouth. **(i)** Fold and cleavage facing lines and azimuths plotted using the construction method of Holdsworth (1988) (see section 1.3). **(ii)** Plots showing the pitch of fold and cleavage facing directions in planes parallel to the fold axial and cleavage planes in which they were measured.

Plate 3.3. (a) Fold hinge zone with top-to-SE thrust imbricate zone with top-to-NW minor, conjugate backthrusts (Elgy Rocks, Fig 3.5, grid ref. 95186439). Scale bar is 15cm. **(b)** Sub-horizontal carbonate slickenfibres on bedding parallel shear plane. Orientation of steps indicate a sinistral sense of movement (Dulse Craig, Fig. 3.5, grid ref. 94906465).

analysis, a bedding-parallel fault is classed as a 'detachment' only where it is seen to cross-cut due to the presence of a local ramp or where it is clearly linked to other cross-cutting detachments and associated structures (e.g. Plate 3.4(a)).

Folded bedding and detachments are cross-cut by steeply dipping, possibly conjugate strike-slip faults (Fig. 3.5). These are often associated with prominent zones of white carbonate-cemented breccia up to one metre wide and metre-scale brittle kink folds (e.g. immediately west of the N-S fault in John's Roads; Fig. 3.5, grid ref. 95306417, Plate 3.4(b)). Sinistral faults trend mainly N-S, whereas dextral faults trend NW-SE; collectively they appear to be consistent with NNW-SSE contraction. The age of this faulting is uncertain and, may be related to younger deformation episodes such as the Variscan inversion of the Northumberland basin to the south (e.g. Roper 1997).

Detailed mapping of the Eyemouth-Burnmouth section shows that the deformation is markedly heterogeneous on a mesoscale. This heterogeneity is particularly marked in the northern part of the coastal section between Scout Point and Eyemouth Harbour. There several distinct, often fault-bounded domains (labelled 1 to 4 in Fig. 3.10) exhibit very different assemblages of structures which nevertheless appear to be broadly contemporaneous and can be defined on the map scale. Running NE-SW, these domains (labelled 1 4) lie sub-parallel to the regional strike. The structures in each are now described separately.

3.6 Description of separate domains

3.6.1 Domain 1

Running from Burnmouth in the south to a narrow inlet immediately W of Whalt Point (Figs. 3.5, 3.10) this domain forms the southern two thirds of the section. As indicated by the well-defined point maximum of poles to bedding (Fig. 3.11a(i)), the sequence forms a steeply NW dipping and younging homocline. A series of metre to tens-of metre scale, S-verging fold pairs occur throughout the section (e.g. Plate 3.5(a), (b)) spreading a subordinate number of bedding poles along a girdle that indicates a moderately to steeply WSW-plunging β axis (Fig. 3.11a(i)). This corresponds well with the mean plunge of minor folds and cleavage-bedding intersection lineations (Fig. 3.11a(ii), (iii)) which mostly show only minor amounts of hinge line curvilinearity (30-40°).

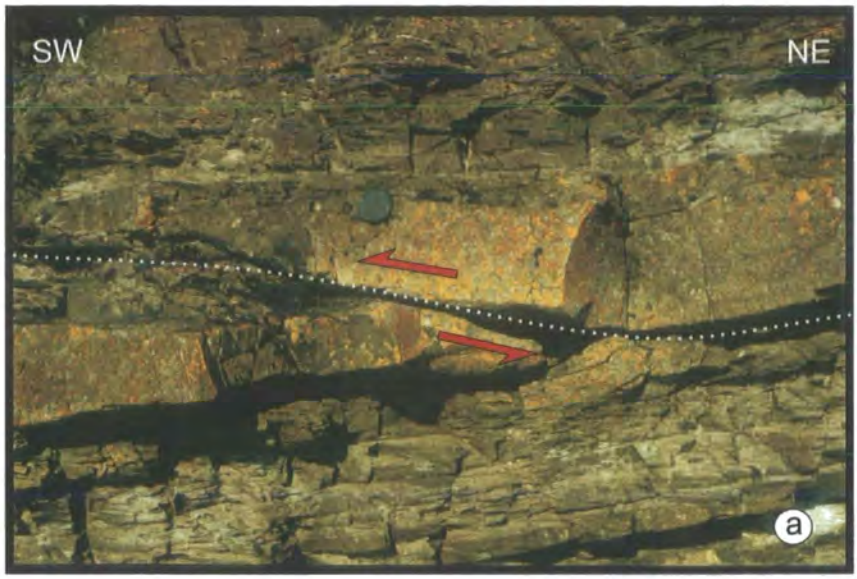

Plate 3.4. **(a)** Low angled, sinistral detachment fault/bedding parallel shear (marked). This is typical of the geometry of many detachments throughout the Eyemouth-Burnmouth section. Originating as bedding-parallel shear planes, they commonly locally cross-cut bedding as detachment faults and then become parallel to bedding once again. Dulse Craig (Fig. 3.5, grid ref. 94856665). **(b)** Metre-scale brittle kink folds related to steeply inclined, possibly conjugate strike-slip faults. Two N-S trending sinistral strike-slip faults are shown. Looking down and to the NE onto the foreshore north of John's Roads (Fig. 3.5, grid ref. 95306
415).

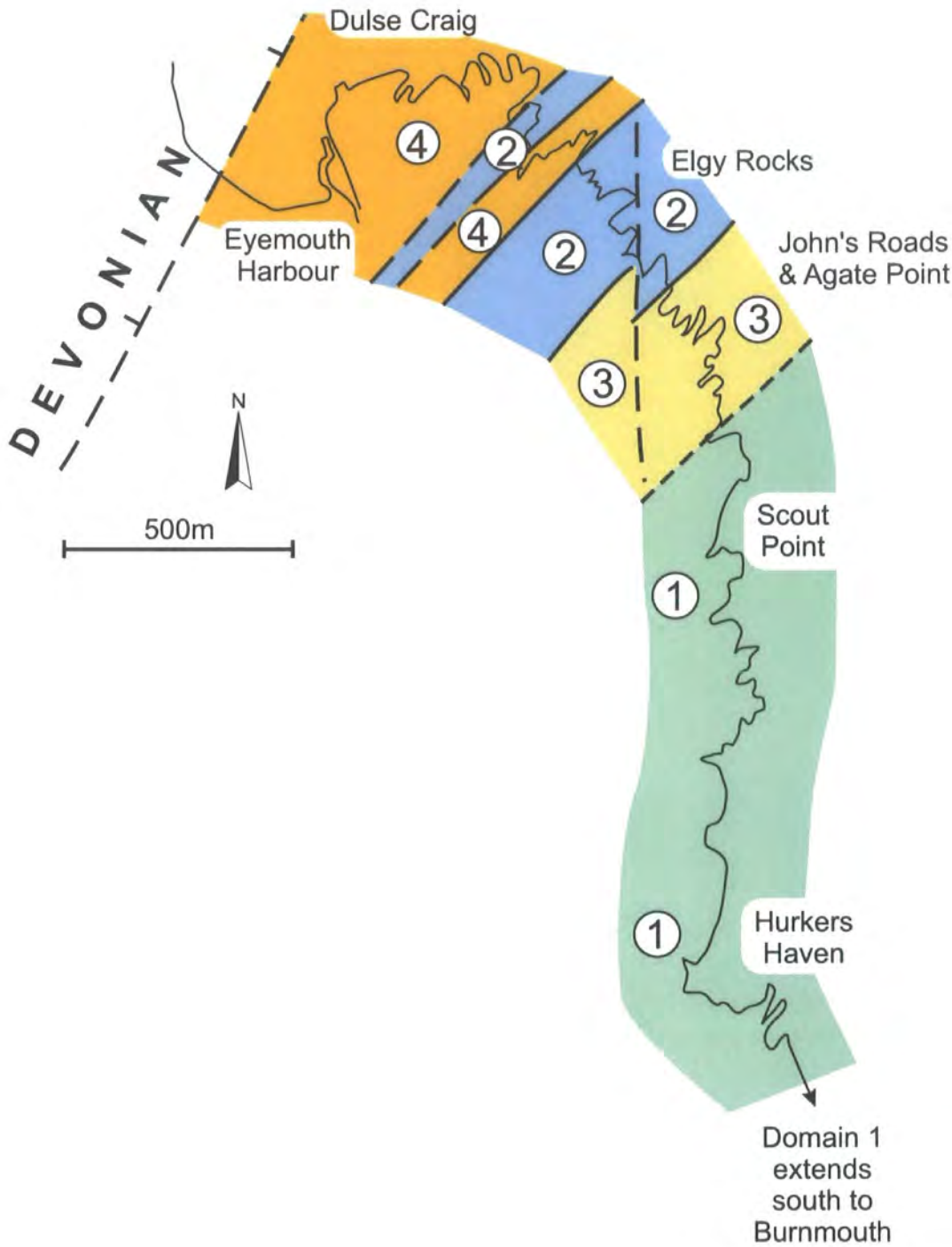

Figure 3.10. Map showing extent of structural domains, labled 1-4, between Eyemouth Harbour and Hurkers Haven. Domain 1 extends south to Burnmouth.

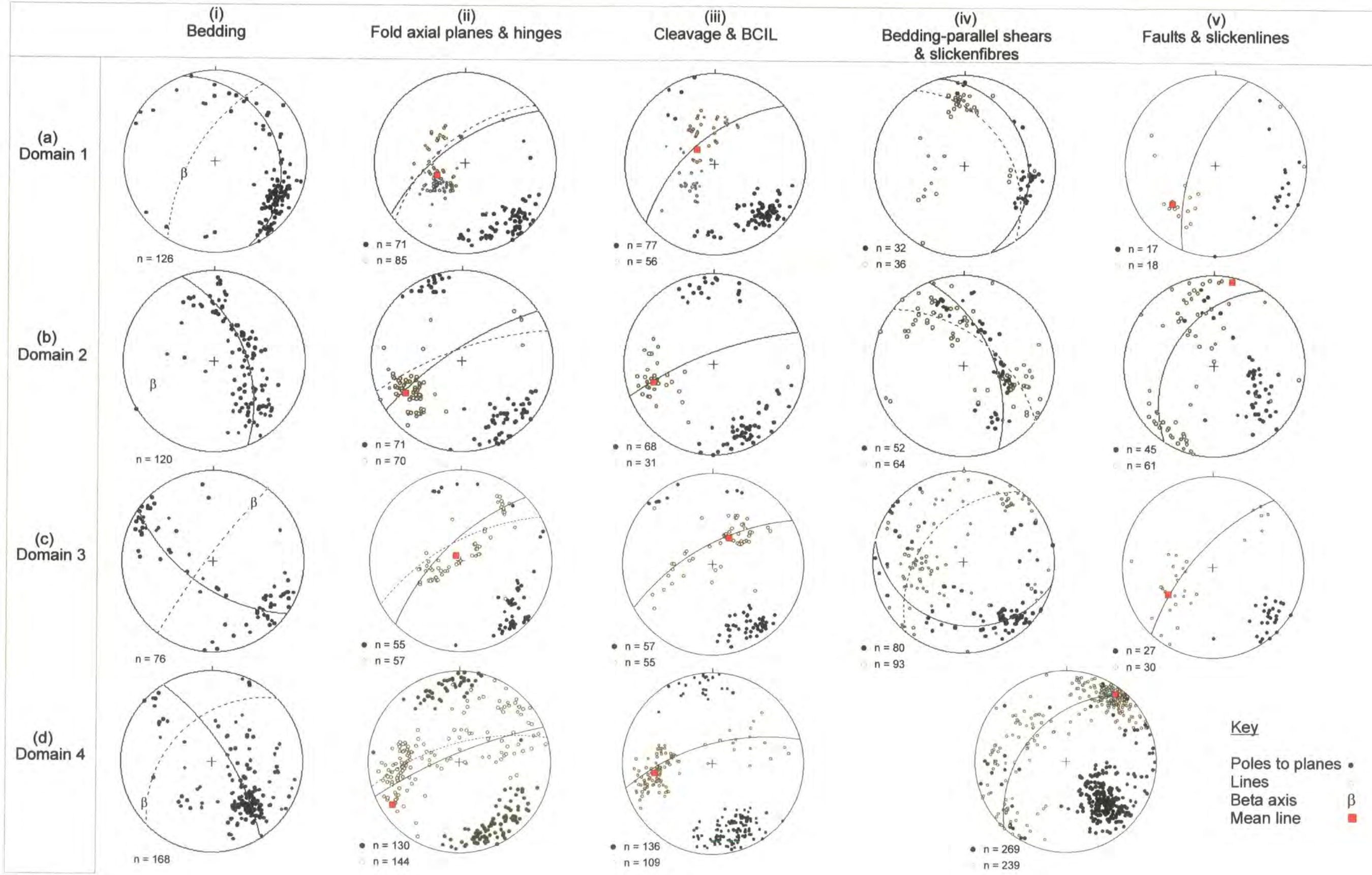

Figure 3.11. Stereoplots of structural orientation data from domains 1-4 (a-d respectively). In each case **(i)** Poles to bedding planes, **(ii)** Poles to fold axial planes and fold hinges, **(iii)** Poles to cleavage planes and BCIL, **(iv)** Poles to bedding parallel shear planes and slickenfibre lineations, **(v)** Poles to faults and slickenfibre lineations (see text for details).

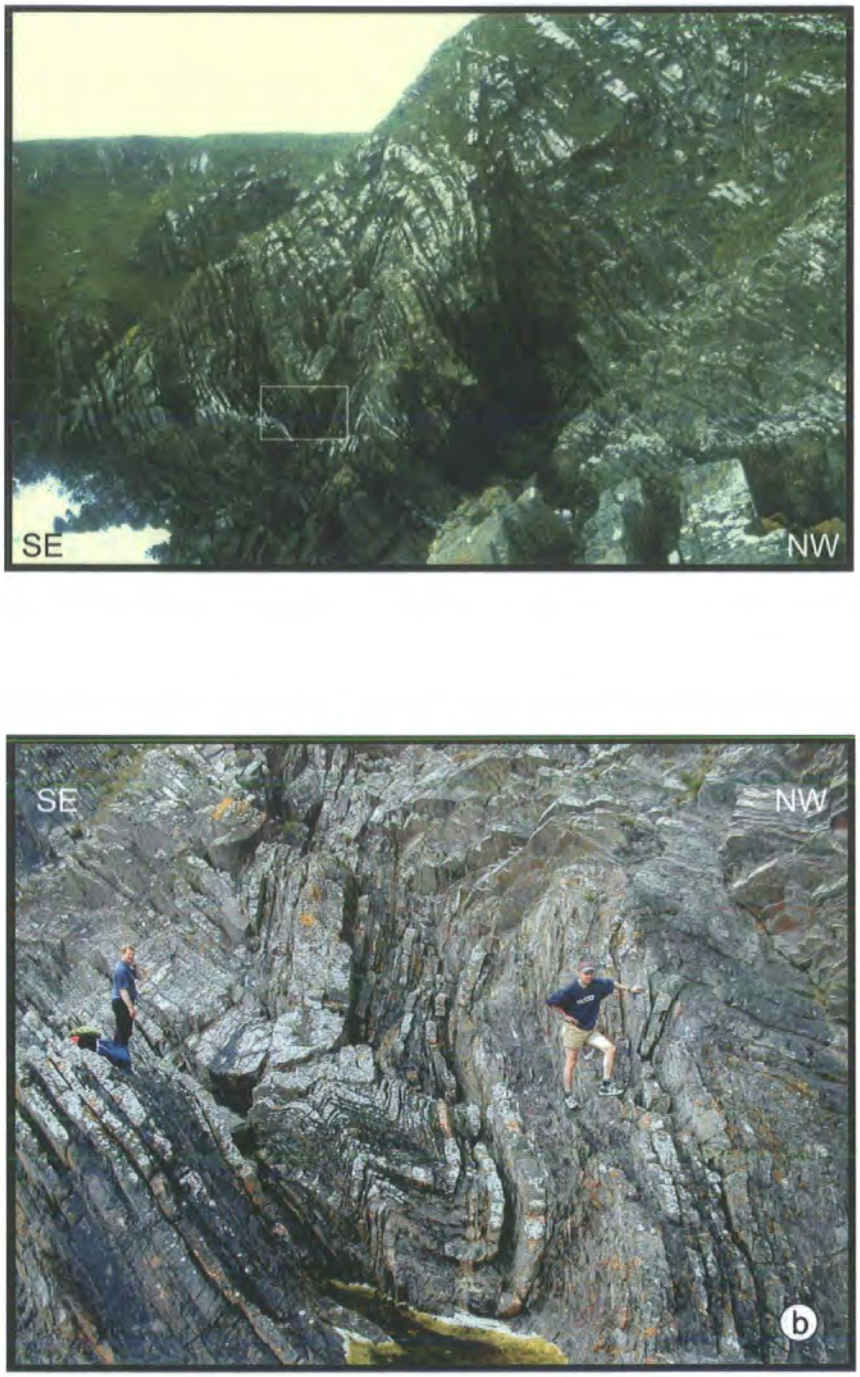

Plate 3.5.(a) Typical S-verging and upward facing fold pair in NW dipping homoclinal section. Domain 1 Scout Point (Fig. 3.5, grid ref. 955636) cliff is approximately 35m high. Box shows location of Plate 3.5(b). **(b)** Detail of fold shown in (a) above Scout Point (Fig. 3.5, grid ref. 95506365).

The stereonets, for cleavage and fold axial planes (Fig. 3.11a(ii) & (iii)) suggest that the mean cleavage plane lies slightly anticlockwise of the mean axial plane (ca. 5°), whilst the mean cleavage-bedding intersection lineation is clockwise of the mean fold plunge (Fig. 3.11a(ii), (iii)). However, these stereonet relationships may not be statistically significant and field observations suggest that everywhere in Domain 1 the cleavage and axial planes are essentially parallel. As would be expected given the predominance of south-verging S folds, both planes define moderately to steeply NW-dipping surfaces that lie clockwise of the mean homoclinal bedding orientation, (Fig. 3.11a(i)-(iii), Plate 3.5(a)). The folds and cleavage face mainly upwards and to the SW at low to moderate angles (Fig. 3.12(i), (ii)).

Poles to bedding-parallel shears cluster in two maxima corresponding to different limbs of the fold pairs, with shears in NW-dipping long-limbs dominant (Fig. 3.11a(iv)). Most slickenlines in short limbs plunge moderately to shallowly east, whilst a majority on long-limbs plunge shallowly north. These two sets lie on a moderately NE-dipping girdle that lies almost 20° anticlockwise of the girdle for poles to bedding-parallel shears. Thus many of the slickenlines lie at high angles, but not orthogonal to the regional β axis. Senses of shear determined from offsets of markers and slickenline steps observed in the field show that the senses of shear on opposite fold limbs are reversed, showing a pattern consistent with flexural slip folding, but with a significantly oblique component (Fig. 3.13(a), (b), Ramsay 1967). A subordinate number of bedding-parallel shears mainly on long limbs display lineations plunging moderately NW to SW (Fig. 3.11a(iv)), with the readings spread along a girdle sub-parallel to the mean detachment plane, with the SW plunging lineations lying close to the mean slickenline orientation on the detachment planes (Fig. 3.11a(v)). This suggests that either some detachments have been misidentified as bedding-parallel shears or that some interaction between these structures occurs. Multiple slickenline sets are locally present, but show no consistent overprinting relationships. The slickenline lineations developed on both the bedding parallel shears and detachments are mineralogically the same, which seems to suggest that all slickenline lineations are broadly contemporaneous.

Detachment faults are spatially associated with and cross-cut metre- to tens of metre-scale fold pairs at low angles. Poles to detachment faults form a point maximum defining a steeply NW-dipping plane sub-parallel to the homoclinal bedding/long limbs of the folds (compare stereoplots (i) (v), Fig. 3.11(a)). Most slickenline lineations

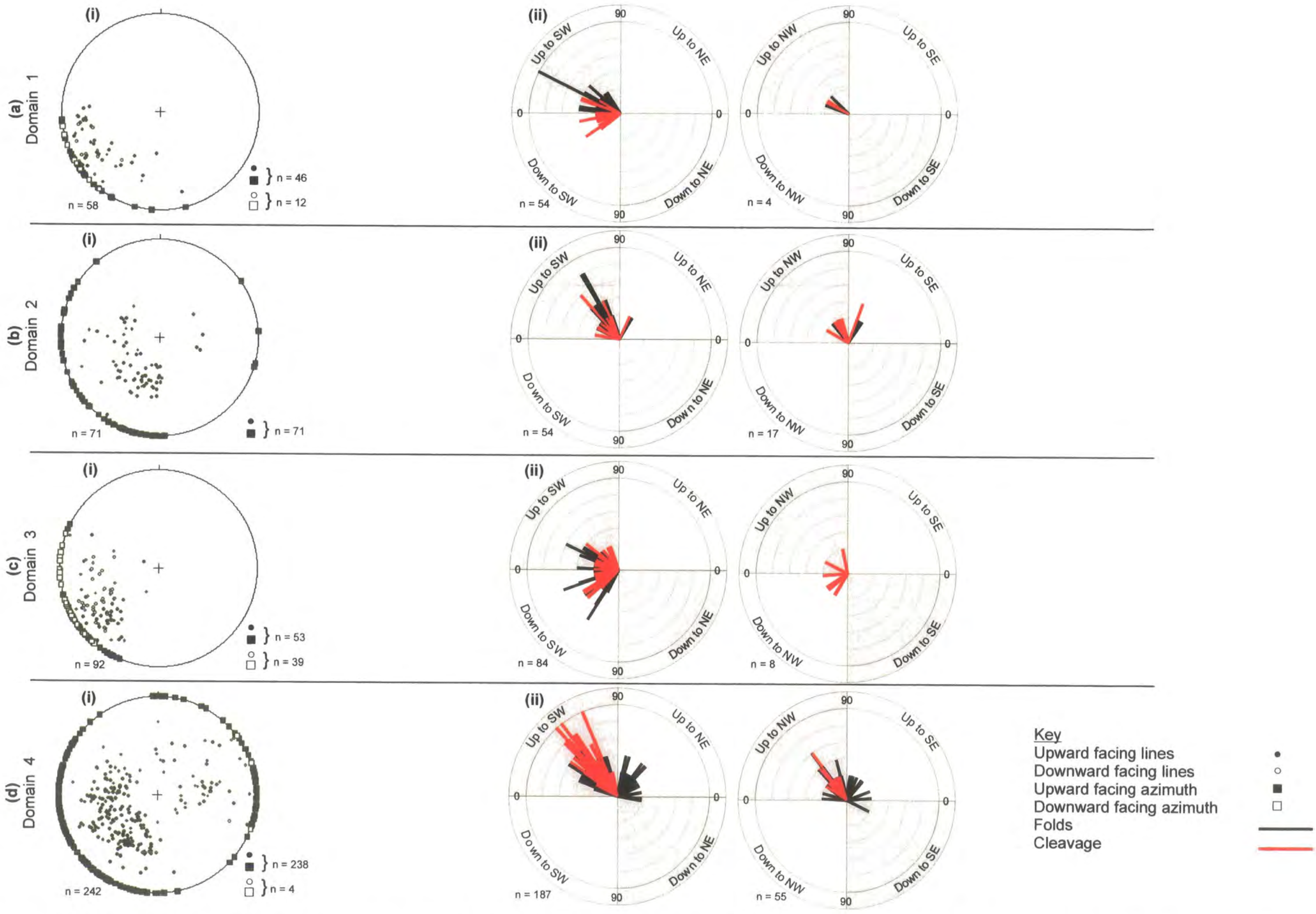

Figure 3.12. Facing data from the Eyemouth to Burnmouth area for domains 1-4 (a-d respectively). **(i)** Fold and cleavage facing lines and azimuths plotted using the construction method of Holdsworth (1988). **(ii)** Plots showing the pitch of fold and cleavage facing directions in planes parallel to the fold axial and cleavage planes in which they were measured.

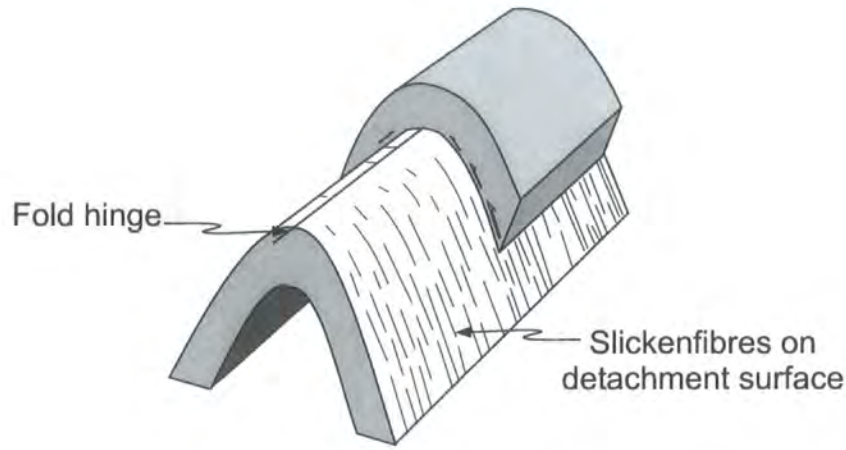

(a)

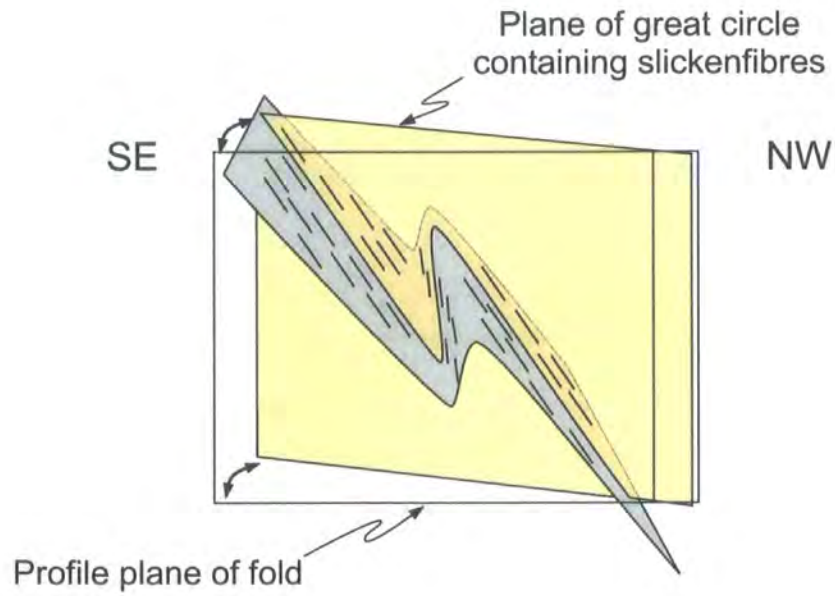

(b)

Figure 3.13. Relationship between bedding parallel detachments and slickenfibres in flexural slip folds. **(a)** Pattern of slicken fibres observed on bedding-parallel slip surfaces around simple flexural slip folds, where the contraction is normal to the fold hinge. Slickenfibres are perpendicular to the hinge (from Ramsay & Huber 1987). **(b)** Pattern of slickenfibres observed on asymmetric folds in domain 1. Note that the slickenfibres lie at an oblique angle to the fold hinge indicating oblique flexural slip.

plunge moderately to shallowly SW, with slickenline steps and offsets of markers indicating mainly sinistral and NW-side-down senses of shear in a present-day reference frame.

3.6.2 Domain 2

Domain 2 corresponds to two regions of highly folded strata located immediately to the N and S of Ramfauds (Fig. 3.5, grid ref. 951646) and includes the spectacularly exposed section around Elgy Rocks (Figs. 3.5, 3.10, grid ref. 95264, MacKenzie 1956; Sheills & Dearman 1966). The folds are generally upright to SE-overturned metre- to tens of metre-scale structures that generally verge to the SE (Figs 3.4, 3.7, Plate 3.6(a), (b)). Poles to bedding are evenly distributed along a girdle that defines a shallowly SW plunging β axis which lies sub-parallel to minor fold plunges (Fig. 3.11b(i)). The cleavage planes dip steeply NNW and the mean planes lie significantly clockwise of the mean fold axial plane (Fig. 3.11b(ii), (iii)). This confirms a slight clockwise sense of transection that is observed in the field in Domain 2. Cleavage-bedding intersection lineations are also significantly clockwise of minor fold plunges with both exhibiting relatively minor amounts of curvilinearity (Fig. 3.11b(ii) & (iii)). Cleavage and folds everywhere face steeply upwards mainly to the SW (Fig. 3.12b(i), (ii)).

Poles to bedding-parallel shears are evenly dispersed along a girdle almost exactly normal to the regional β axis for poles to bedding (Fig. 3.11b(iv)). Slickenlines fall on a well-defined girdle that strikes 30° anticlockwise of the poles to bedding-parallel faults girdle; this suggests that the slickenlines lie at high angles, but not orthogonal to the regional β axis. Offsets of markers and slickenline steps observed in the field show that the senses of shear on opposite fold limbs are reversed. This pattern is again consistent with flexural slip folding, but with a significantly oblique component. Cross-cutting detachment faults form conjugate sets of apparently top-to-the-SE 'thrusts' (dipping NW) and subordinate top-to-the-NW 'backthrusts' (dipping south) (Fig. 3.11b(v)) and are especially common in fold hinge zones (Plate 3.3(a)). The SE-plunging lineations on the south-dipping 'backthrusts' consistently indicate top-to-the-NW dextral reverse offsets of markers and slickenfibre steps. Pink carbonate slickenfibre lineations are complex, however, on the NW-dipping thrusts, with curvilinear and locally multiple overprinting sets of dip-slip, oblique-slip and strike-slip sets. Dip-slip movements are consistently contractional and strike-slip components are

Plate 3.6. Typical upward facing, upright folds from Domain 2. **(a)** Large fold pair to the north of Elgy Rocks (Fig. 3.5, grid ref. 95206440). **(b)** Elgy Rocks, large, slightly SE-verging fold (Fig. 3.5, grid ref. 95146415).

sinistral. In the absence of consistent overprinting relationships, it is suggested that these two movement components were broadly contemporaneous. The well-defined sinistral detachments seen in all the other domains are not present.

3.6.3 Domain 3

Domain 3 lies between Domains 1 and 2 (Figs. 3.5, 3.7, 3.10) and includes the John's Roads and Agate Point localities (grid refs. 953641 & 954641 respectively) described and discussed by Dearman et al (1962), Greig (1988) and Treagus (1992). The sequence here forms NE-SW-striking, subvertical NW-younging homocline indicated by the well-defined sub-horizontal point maximum of poles to bedding (Fig. 3.11c(i)). A series of metre-scale, variably plunging S fold pairs occur at John's Roads and Agate Point (Plate 3.7(a), Fig. 3.6(a)). Fold hinges and associated cleavage-bedding intersections are mostly moderately to steeply plunging (Fig. 3.11c(ii), (iii)), exhibiting up to 110° of curvilinearity in the fold axial plane, often over distances of a few metres (Plate 3.7(a), (b)). All folds consistently exhibit sinistral vergence (S shapes) viewed down plunge.

On the stereonet, the mean cleavage plane lies slightly clockwise of the mean axial plane, and cleavage-bedding intersection lineations are also significantly clockwise of minor fold plunges (Fig. 3.11c(ii), (iii)). In the field, however, both clockwise and anticlockwise transecting relationships are observed and in some localities (e.g. Agate Point) local fold hinges and cleavage-bedding intersections are markedly non-parallel. At present, it is unclear whether the apparent transection observed from the stereonet data results from the complexity of the curvilinear folds or is a real transecting relationship. Fold axial and cleavage planes dip steeply NW, lying clockwise of the mean homoclinal bedding orientation, as would be expected given the predominance of sinistrally verging fold pairs (Fig. 3.11c(i), (iii), Plate. 3.7(a)). Minor folds and cleavage exhibit generally SW facing directions, facing shallowly to moderately upwards where the folds plunge SW and shallowly to steeply downwards where the folds plunge NE (Fig. 3.12c(i), (ii)).

Poles to bedding-parallel shears display a complex pattern, with a diffuse point maximum defining a steeply NW-dipping plane sub-parallel to the homoclinal bedding (Fig. 3.11c(iv)). Such a scattered arrangement is perhaps not surprising given the complex and curvilinear nature of the minor folds in this domain. Carbonate slickenfibre lineations are also diffusely distributed with two point maxima plunging

Plate 3.7. (a) Sinistral verging, SW-facing fold pair with highly curvilinear hinges (arrows) in homoclinal NW-younging sequence in domain 3, John's Roads (Fig. 3.5, grid ref. 95356412) Where the folds plunge inland and SW (to the left) they are upward facing (note younging arrow). Where they plunge NE and out to sea (to the right) they face downwards (younging arrow). Fig. 3.6a shows an excellent series of drawings of the features in these exposures. X shows location of viewer in Plate 3.7b. Note sinistral detachment and later dip-slip fault.**(b)**View of same folds as in (a) viewed from position X looking inland and to the SW. Note the clear 'eye' structure where the fold hinges pass through the vertical (top right of centre) and the flute casts on the exposed base of the inverted sandstone unit in the core of the downward-facing synformal part of the fold lower down the exposure.

moderately SW and shallowly NE (Fig. 3.11c(iv)), crudely sub-parallel to the lineations on the detachment surfaces. Slickenfibres in these orientations predominantly exhibit offset markers and step-features indicating sinistral senses of movement. Again, this may indicate that some detachments have been misidentified as bedding-parallel shears or that some interaction between these structures occurs. Multiple slickenline sets are locally present, but show no consistent overprinting relationships.

Detachment faults are typically spatially associated with and cross-cut metre- to tens of metre-scale fold pairs at low angles. Poles to detachment faults form a point maximum defining a steeply NW-dipping plane sub-parallel to the homoclinal bedding/long limbs of the folds (Fig. 3.11c(v)). Slickenline lineations mainly plunge moderately to shallowly SW, with offsets of markers and slickenline steps indicating sinistral and mainly NW-side-down senses of shear.

3.6.4 Domain 4

Domain 4 occurs at the northernmost end of the section close to Eyemouth Harbour, and includes exposures in Ramfauds, Nestends and Dulse Craig (Figs. 3.5, 3.7, 3.10, 3.14, grid refs. 951645, 949647 & 948647 respectively). The sequence forms a moderately NW dipping and younging homocline indicated by the point maximum of poles to bedding (Fig. 3.11d(i)). A series of metre-scale, generally S-verging fold pairs occur throughout the section (Plate 3.8(a)) spreading a subordinate number of bedding poles along a poorly-defined girdle that indicates a shallowly WSW-plunging β axis (Fig. 3.11d(i)). This corresponds well with the mean plunge of minor folds and cleavage-bedding intersection lineations (Fig. 3.11d(ii), (iii)) which both locally show up to 180° of hinge line curvilinearity within the axial plane, often over a few tens of centimetres.

The mean cleavage plane and cleavage-bedding intersection lineation lies slightly clockwise of the mean axial plane and fold plunge, respectively (Fig. 3.11d(ii), (iii)). Clockwise-transected folds are seen in the field, for example around Dulse Craig (e.g. locality A on Fig. 3.14). Minor folds and cleavage exhibit mainly upward facing directions both to the SW and NE, with the former direction being slightly dominant; locally slightly downward facing examples occur in both directions (Fig. 3.9 (i), (ii)). Both axial and cleavage planes define moderately to steeply NW-dipping surfaces that dip more steeply and lie clockwise of the mean homoclinal bedding orientation, as would be expected given the predominance of SW-verging S folds (Fig. 3.11d(ii), (iii),

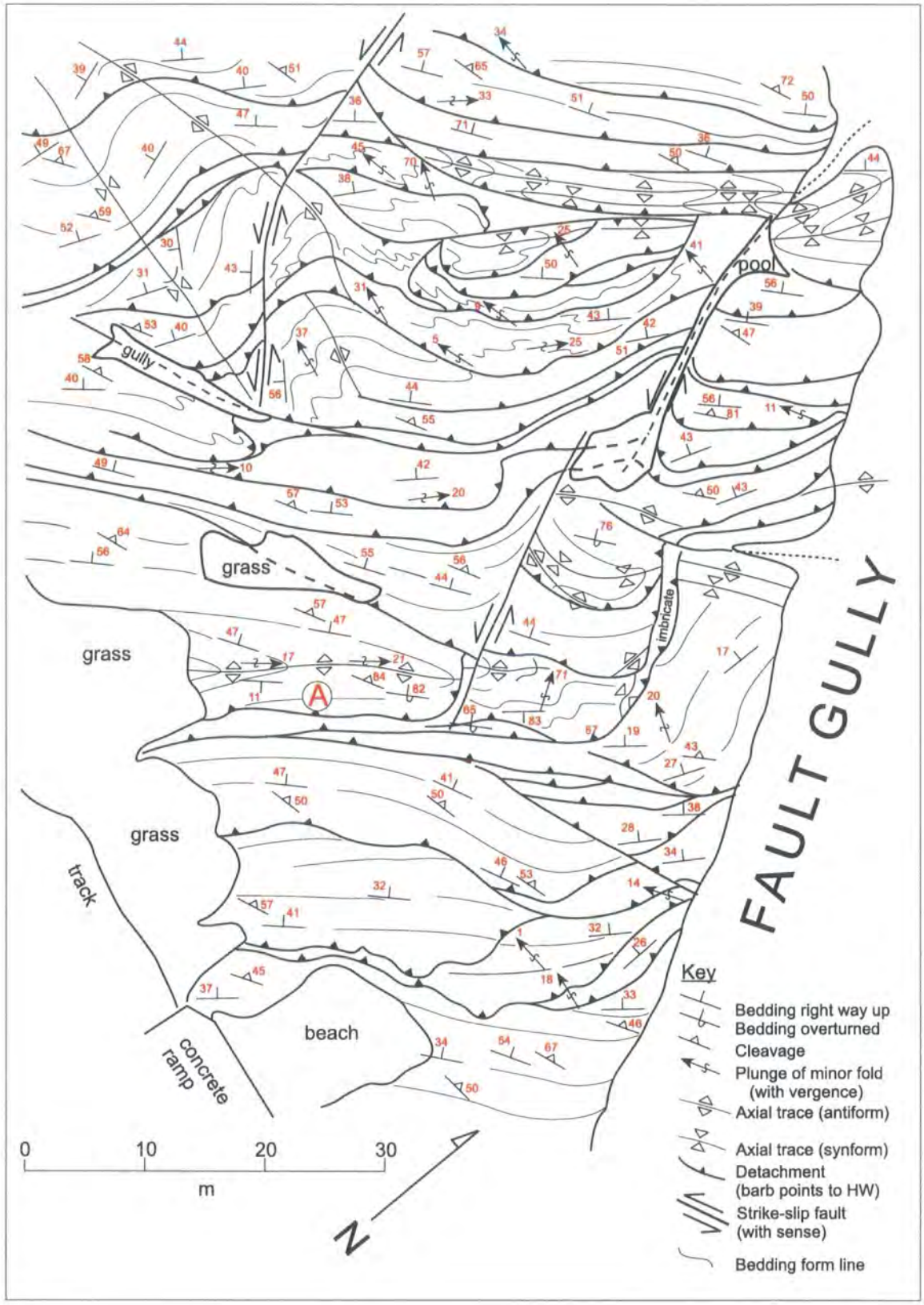

Figure 3.14. Detailed map of structures from part of the Dulse Craig area. Location shown in Fig. 3.5. A = location of example of markedly clockwise transecting cleavage. Reproduced with the permission of R.E. Holdsworth and E. Tavarnelli.

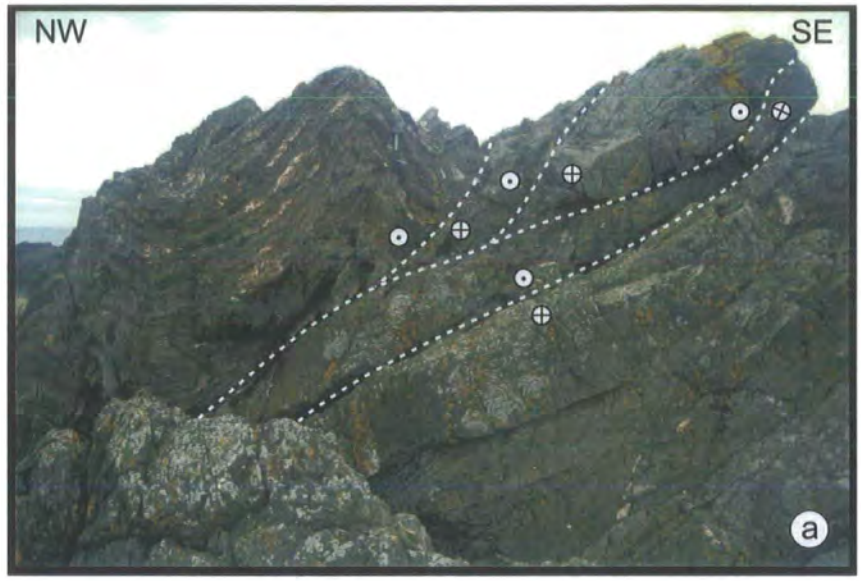

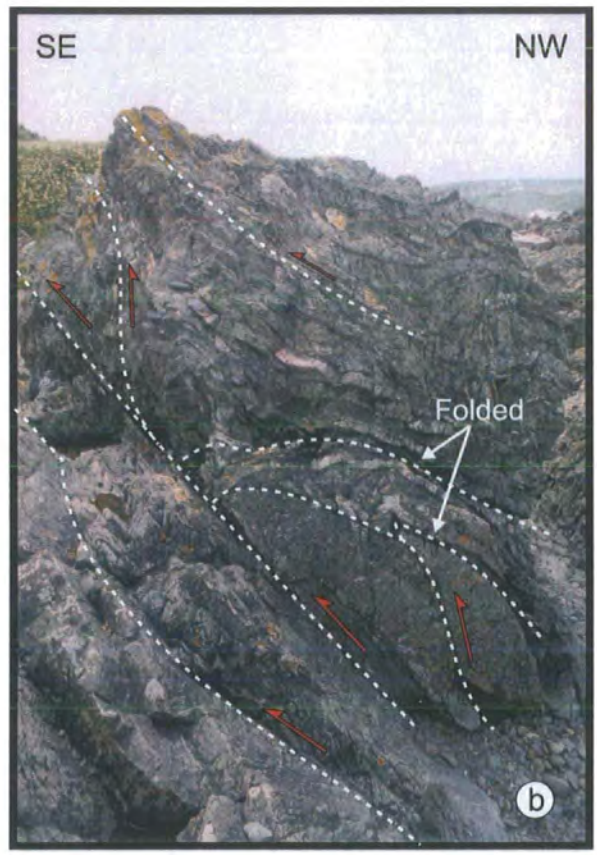

Plate 3.8. **(a)** SE-verging, upward facing folds and underlying sinistral detachment faults sub-parallel to bedding (marked). Dulse Craig (Figs. 3.5, 3.14, grid ref. 948264 65). **(b)** Imbricate of sinistral detachments (marked) and associated sinistrally-verging, SW-facing folds. Note also folded detachments (arrowed). Dulse Craig (Figs. 3.5, 3.14, grid ref. 94806462).

Plate. 3.8(b)).

Detachment faults, including both P-type and R-type shears (Fig. 3.14, Plates 3.8(a), (b), 3.9, 3.10(a), (b), 3.11(a), (b)) are one of the predominant structures in this domain and are closely associated with a series of metre-scale fold pairs. These define a complex interconnected network of bedding-parallel faults (e.g. Plates 3.8(a), (b), 3.9) and cross-cutting ramps that locally extend (R-type shears Plate 3.10(a), (b)) or shorten (P-type shears Plates 3.8(b), 3.10(a)) bedded units where they lie anticlockwise and clockwise of bedding, respectively, when viewed down-dip. Poles to detachment faults form a point maximum defining a moderately NW-dipping plane sub-parallel to the homoclinal bedding (Fig. 3.11d(iv)). Carbonate slickenline lineations fall into two distinct orientation groups. The dominant set lie sub-parallel to strike and uniformly exhibit sinistral senses of shear based on offsets of markers (Plates 3.3(a), 3.8(b), 3.10(a), (b), 3.11(a)), slickenfibre steps, the presence of local pull-apart features (Plate 3.11(b)) and by the asymmetric arrangement of contractional and extensional ramps (Plates 3.11(a), 3.10(a)) which clearly correspond to P-shears and R-shear features, respectively. The second, subordinate group of slickenlines plunge moderately NW (Fig. 3.11d(iv)), with slickenline steps and offsets of markers indicating mainly NW-side-down senses of shear in a present-day reference frame. Locally, both sets of slickenlines are present on single fault surfaces as overprinting sets, with no consistent relative age relationship, i.e. strike-slip fibres overprint dip-slip fibres and vice-versa. In other surfaces, the slickenfibres exhibit complex curvilinear patterns, with strike- and dip-parallel orientations forming end members (Plate 3.9). Based on these relationships, it is concluded that the two movement components are not only kinematically compatible (Fig. 3.15) but occurred at broadly the same time.

3.7 Summary, general interpretation and regional context

The main structural characteristics of domains 1-4 within the Eyemouth-Burnmouth section are summarised in Table 1 and Figure 3.16. All are significantly different in terms of the structural patterns preserved.

The Eyemouth-Burnmouth section (Fig. 3.5) contains a more complex assemblage of structures than has hitherto been described. Cleavage shows a clear clockwise transecting relationship in parts of the north of the section (e.g. A in Fig. 3.14). Folds are generally SE overturned but locally exhibit steep plunges and marked

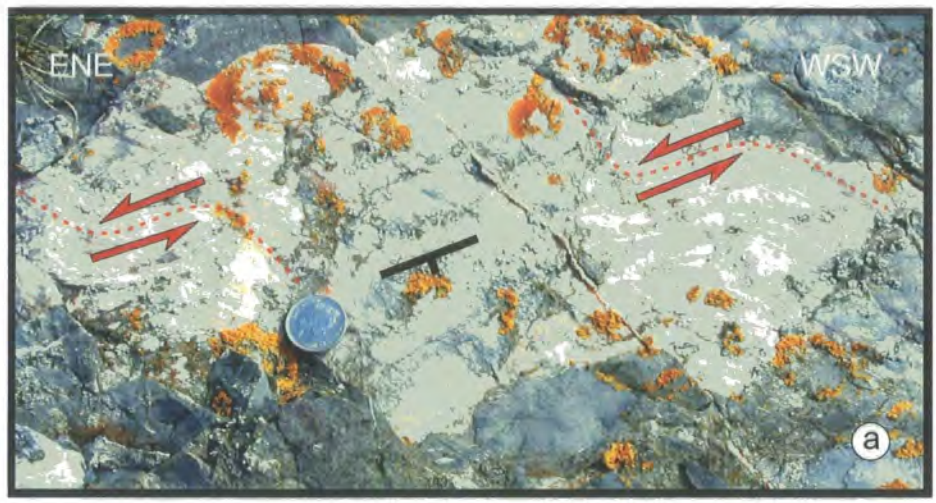

Plate 3.9. View of NW- dipping bedding- parallel detachment (see bedding symbol) surface with curved strike-parallel and dip-parallel slickenfibre lineations. Strike- and dip-parallel movements involve sinistral and NW-side-down senses of movements respectively. Dulse Craig (Figs. 3.5, 3.14, grid ref. 94916453). Coin is 2.5cm.

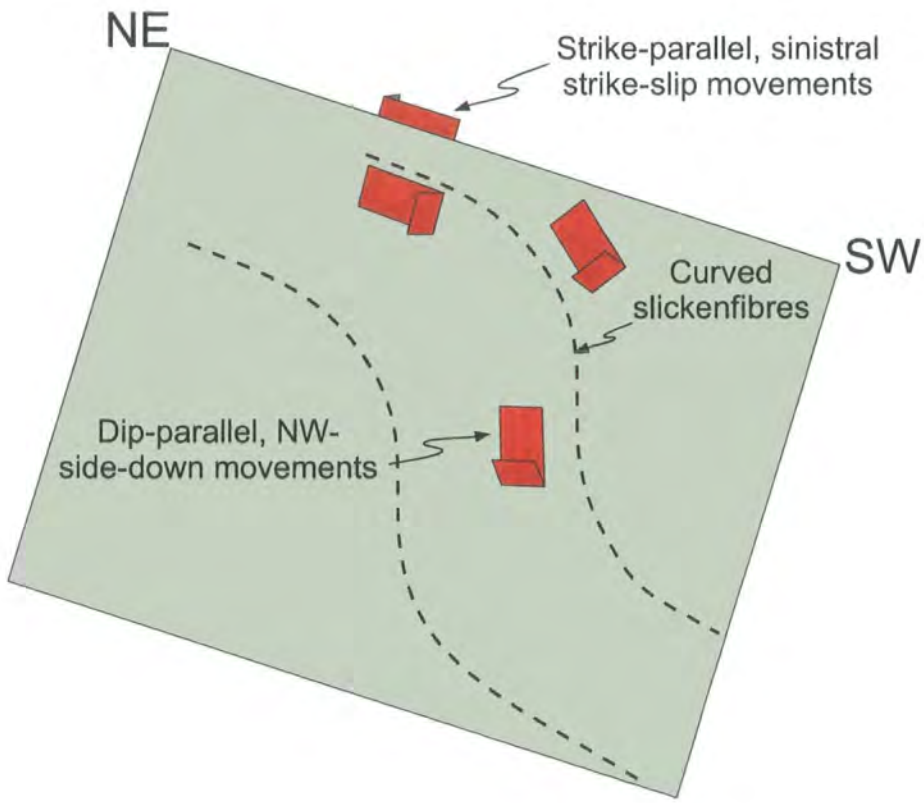

Figure 3.15. Cartoon to show kinematic compatibility of strike-parallel, sinistral strike-slip and dip-parallel, NW-side-down movements indicated by curved slickenfibres on bedding detachments at Dulse Craig

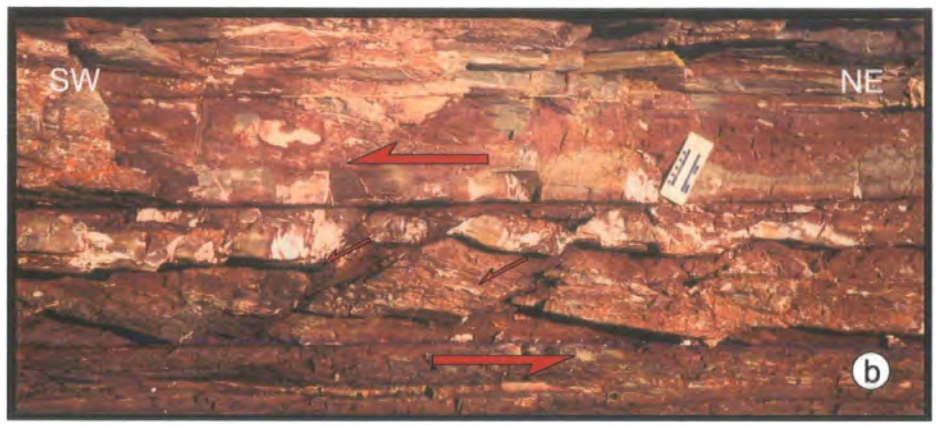

Plate 3.10. **(a)** Bedding-parallel detachment faults bounding duplex of cross-cutting R-type sinistral ramps. View down dip to NW. Dulse Craig (Figs. 3.5, 3.14 grid ref. 94826446). **(b)** Pair of carbonate mineralised R-type sinistral faults joining bedding-parallel detachment faults. View down dip to NW. Dulse Craig (Figs. 3.5, 3.14, grid ref. 94 826440).

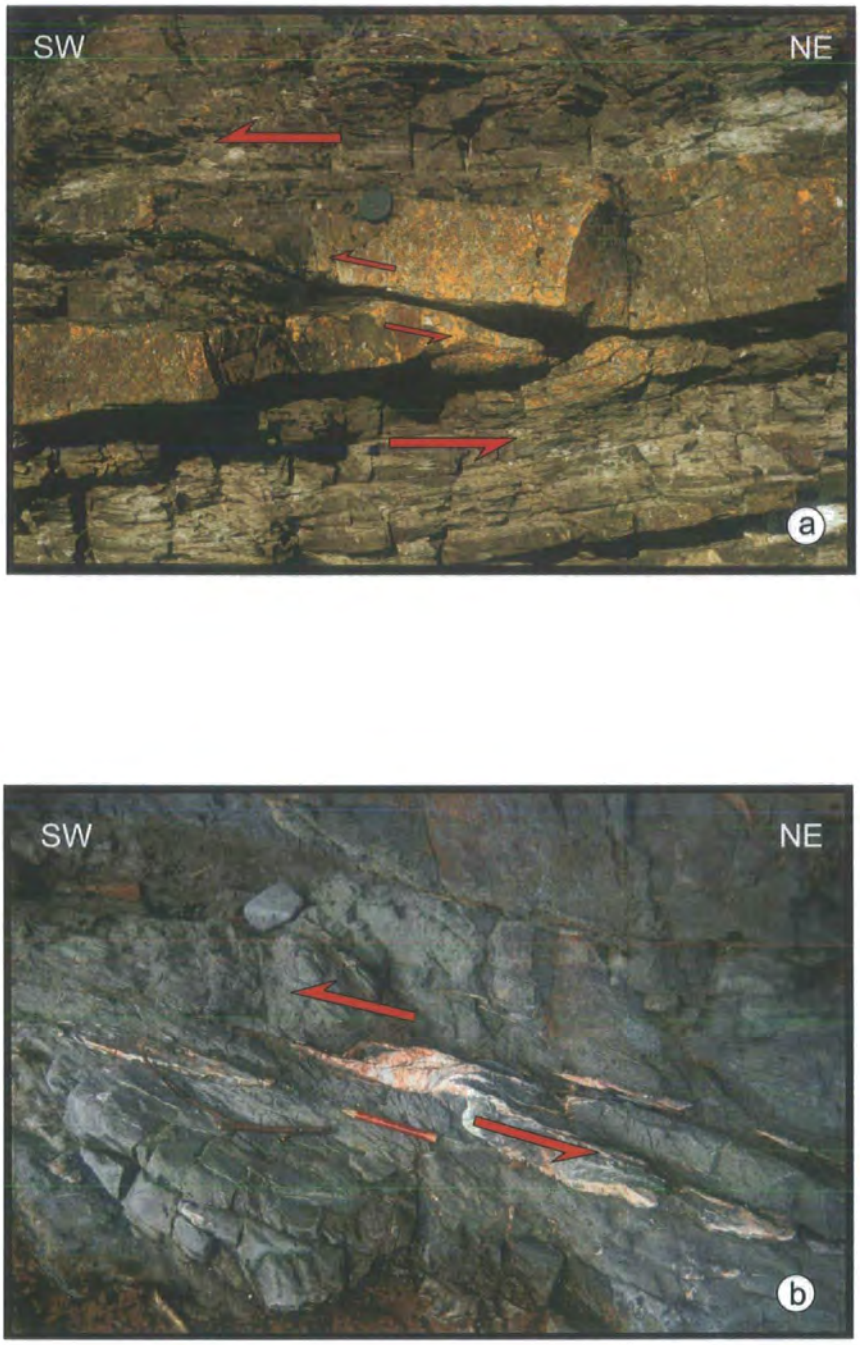

Plate 3.11. **(a)** P-type sinistral ramp within greywacke sandstone bed. The ramp becomes parallel to bedding within the thin bounding siltstone horizons. Offset is approximately 1m. View down dip to NW. Dulse Craig (Figs. 3.5, 3.14, grid ref. 94826441). **(b)** Sinistral pull-apart with carbonate infil. View down dip to NW. Dulse Craig (Figs. 3.5, 3.14, grid ref. 9481 6439).

	Domain type 1	**Domain type 2**	**Domain type 3**	**Domain type 4**
General structure	Homoclinal, dipping steeply & younging to NW	Right way-up sequence folded by NW-SE-trending folds	Homoclinal, sub-vertical, younging to NW	Homoclinal, dipping moderately & younging to NW
Fold geometry & scale	Asymmetric SE overturned folds; 10 m-scale	Slightly asymmetric, SE overturned folds 10m- to m-scale	NE-SW subvertical neutral folds Mainly m-scale	Mainly asymmetric, SE overturned folds Mainly m-scale
Fold/CBI plunge pattern	Moderately SW plunges; minor curvature (30-40°)	Mainly shallowly SW to locally NE plunges, passing through horizontal; minor curvature (<30°)	Mainly steeply plunging to SW & NE, passing through vertical; up to 110°curvature	Moderately SW to moderately NE plunging, passing through horizontal; up to 180° curvature)
Fold-cleavage relationship	No clear transection Essentially axial planar ?	Clockwise transected	Clockwise transected	Clockwise transected
Facing patterns	SW & upwards at low to moderate angles	Mainly SW & steeply upwards	Strong sideways and SW, both upwards & downwards	Mainly sideways SW or NE or upwards to SE
Bedding-// faults	ACW oblique flexural slip dominant, with subordinate sinistral & NW-side down	ACW oblique flexural slip	Complex & diffuse, with strong sinistral component.	?Absent? or cannot be separated from detachments
Detachment geometry & kinematics	Generally bedding-// Sinistral & NW-side down	Conjugate thrusts in hinge regions of some folds, with component of sinistral shear on NW-dipping thrusts Bedding-// set absent	Generally bedding-// Sinistral, with NW side down dominant	Generally bedding-// with well-defined R and P ramps Dominantly sinistral with subordinate set showing dip-slip NW-side-down movements

Table 3.1 Summary of structural elements of domains 1-4.

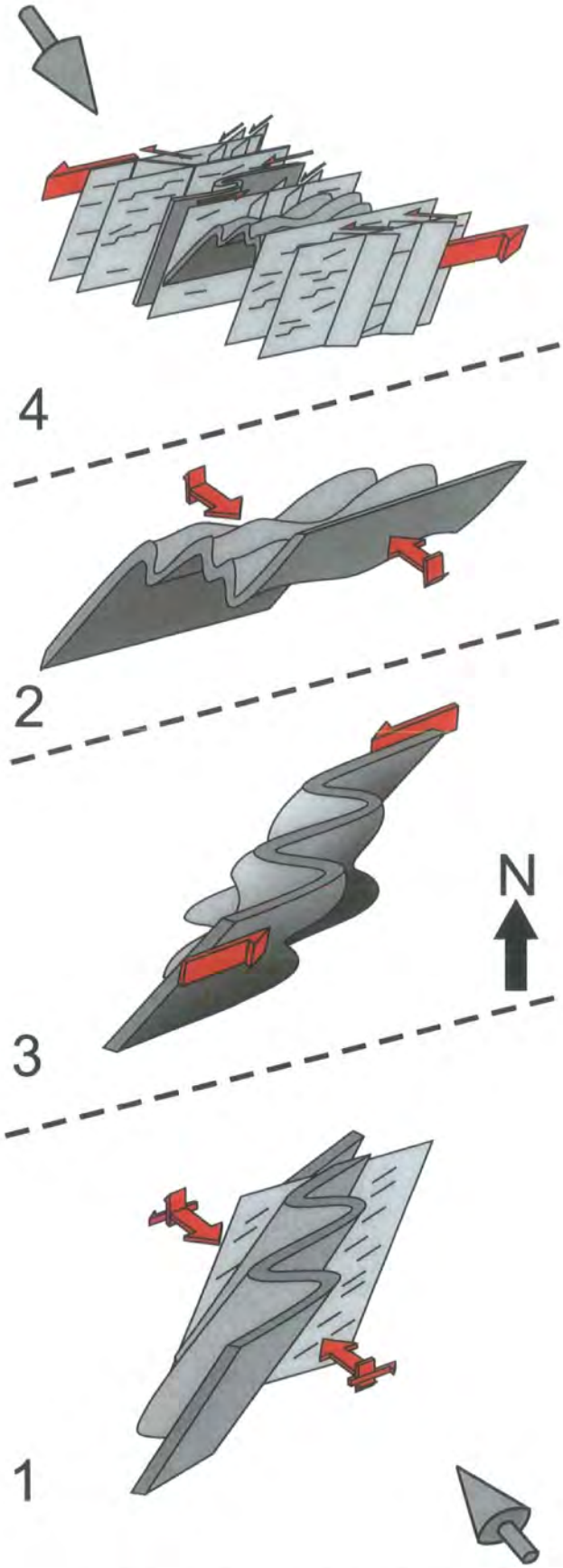

Figure 3.16. 3-D summary of the structures in Domains 1-4 of the Eyemouth-Burnmouth area. (See text for details).

hinge curvilinearity, with extreme variations in facing direction. Top-to-the-SE and subordinate top-to-the-NW conjugate thrusts are locally developed. Interlinked systems of predominantly sinistral detachment faults are developed lying parallel to or at low-angles to bedding. Slickenlines associated with other bedding-parallel shears suggest anticlockwise oblique flexural slip during folding in most, if not all of the section. Collectively, these features are interpreted to indicate components of NW-SE contraction, top-to-the-SW sinistral shear and lesser amounts of top-to-the-SE thrusting. Similar structural assemblages have been briefly described elsewhere in the Southern Uplands terrane, notably in the Hawick Group rocks of the Wigtown Peninsula and Kirkcudbright areas (e.g. see Kemp 1987; Barnes *et al.* 1987; Stone *et al.* 1996).

The relative age relationships, significance and origin of the structures described in this chapter will be discussed in relation to transpressional deformation further in chapter 6.

Chapter 4

The Structure and Kinematics Between Cahore Point and Kilmichael Point: SE Ireland

4.1 Introduction

The Caledonian Orogen in Ireland can be divided into seven potentially suspect terranes, (Fig. 4.1) that were assembled during the Palaeozoic, sinistral oblique closure of the Iapetus Ocean (Dewey & Shackelton 1984; Soper & Hutton 1984; Max *et al.* 1990; Murphy *et al.* 1991; Soper *et al.* 1992). The terrane boundaries, where exposed, are faults or complex shear zones that generally exhibit evidence of sinistral shear and/or transpression (Murphy *et al.* 1991). The present chapter is concerned with the geology of the Leinster Terrane and more specifically the Leinster Massif (Fig. 4.2)

The Leinster Massif (Max *et al. 1990)* comprises the easternmost section of the Leinster Terrane, and includes the Rosslare Terrane (Murphy *et al.* 1991). The Leinster Terrane is bounded to the north and north-west by the Lowther Lodge and Navan faults respectively (Figs. 4.1, 4.2). The Navan Fault is considered to be the continuation of the Iapetus suture in Ireland. To the south the Ballycogly Mylonite Zone (BMZ) forms the boundary between the Leinster and Rosslare terranes (Figs. 4.1, 4.2). The Massif is mostly composed of a thick sequence of Lower Palaeozoic sediments, plutonic and volcanic rocks that were deformed during the closure of the Iapetus Ocean and subsequent intrusion of the Leinster Granite. A number of major shear zones and strike parallel sinistral faults have been recognised (Fig. 4.2) (e.g. Hollywood Shear Zone (HSZ), Wicklow Fault Zone (WFZ) & East Carlow Deformation Zone (ECDZ); McArdle & Kennedy 1986; Max *et al.* 1990; McConnell *et al.* 1999; McConnell 2000). Folds are often clockwise transected by their associated cleavage (e.g. Murphy 1985) and are thought to be related to a regional, sinistral transpression broadly contemporaneous with the shear zones and/or strike-slip faulting.

This chapter presents a synthesis of part of the regional geology of the Leinster Terrane and Massif, providing a brief history of previous work and a detailed account of folds and associated structures in an area of deformed Cambrian, Ordovician and Silurian rocks exposed along the coast of counties Wicklow and Wexford in SE Ireland.

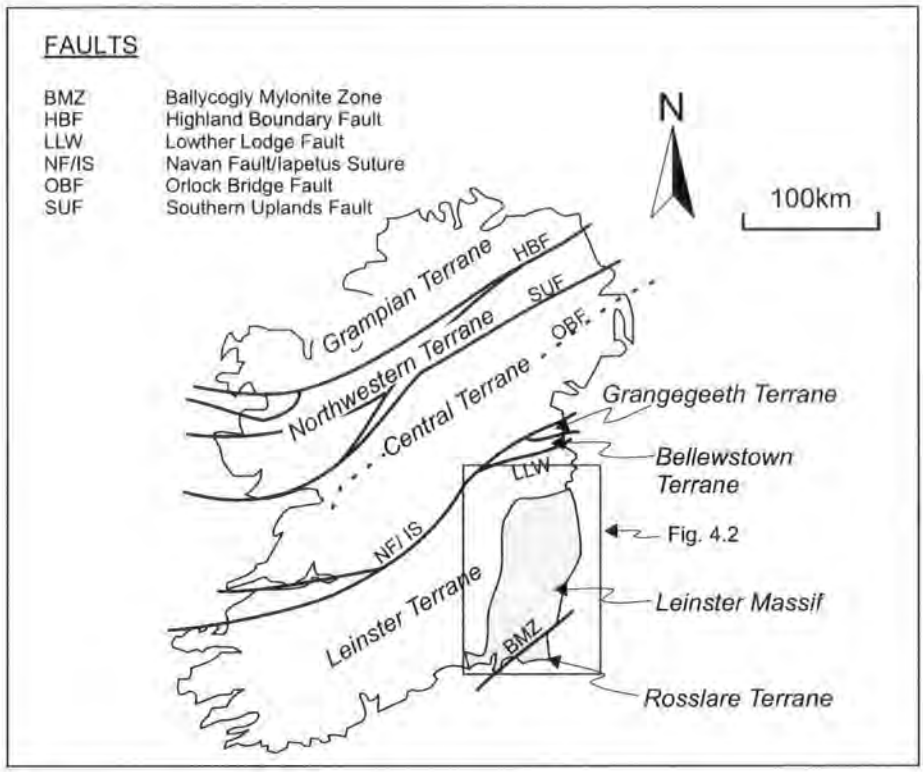

Figure 4.1. Simplified Palaeozoic terrane map of Ireland (after Holdsworth *et al.* 2000) The Leinster Massif, which is part of the Leinster and Rosslare terranes is highlighted.

Period	Events	Orogeny
Carboniferous		
Devonian △	Continued mountain building, rapid erosion & deposition under semi-arid conditions. Intrusion of Leinster Granite complex during sinistral Acadian deformation	Acadian
Silurian △	Marine & continental margin deposition. closure of Iapetus Ocean, continental collision & initiation of mountain building	Caledonian
Ordovician ▲ △ ▲	Mudstone deposition on abyssal Iapetus Ocean floor. Island arc & back-arc volcanism along SE margin of Iapetus as ocean floor is subducted beneath it.	
Ordovician ▲	Sedimentation is terminated by uplift of Cambrian basin margin to form a local landmass off SE margin of Iapetus Ocean as Rosslare Terrane is emplaced	Monian
Cambrian	Deposition in basin followed by continental rifting. Generation of new oceanic crust in newly formed Iapetus Ocean to NW	
Precambrian	Formation of Rosslare Complex gneisses to the SE, forming basement to all subsequent sedimentation in Leinster	Cadomian

▮ Sedimentary rocks of this age present in Leinster Massif

△ ▲ Period of intrusive igneous activity, volcanism

Table 4.1. Summary of the Lower Palaeozoic geological evolution of SE Ireland. Based on Tietzsch-Tyler *et al.*(1994a & b).

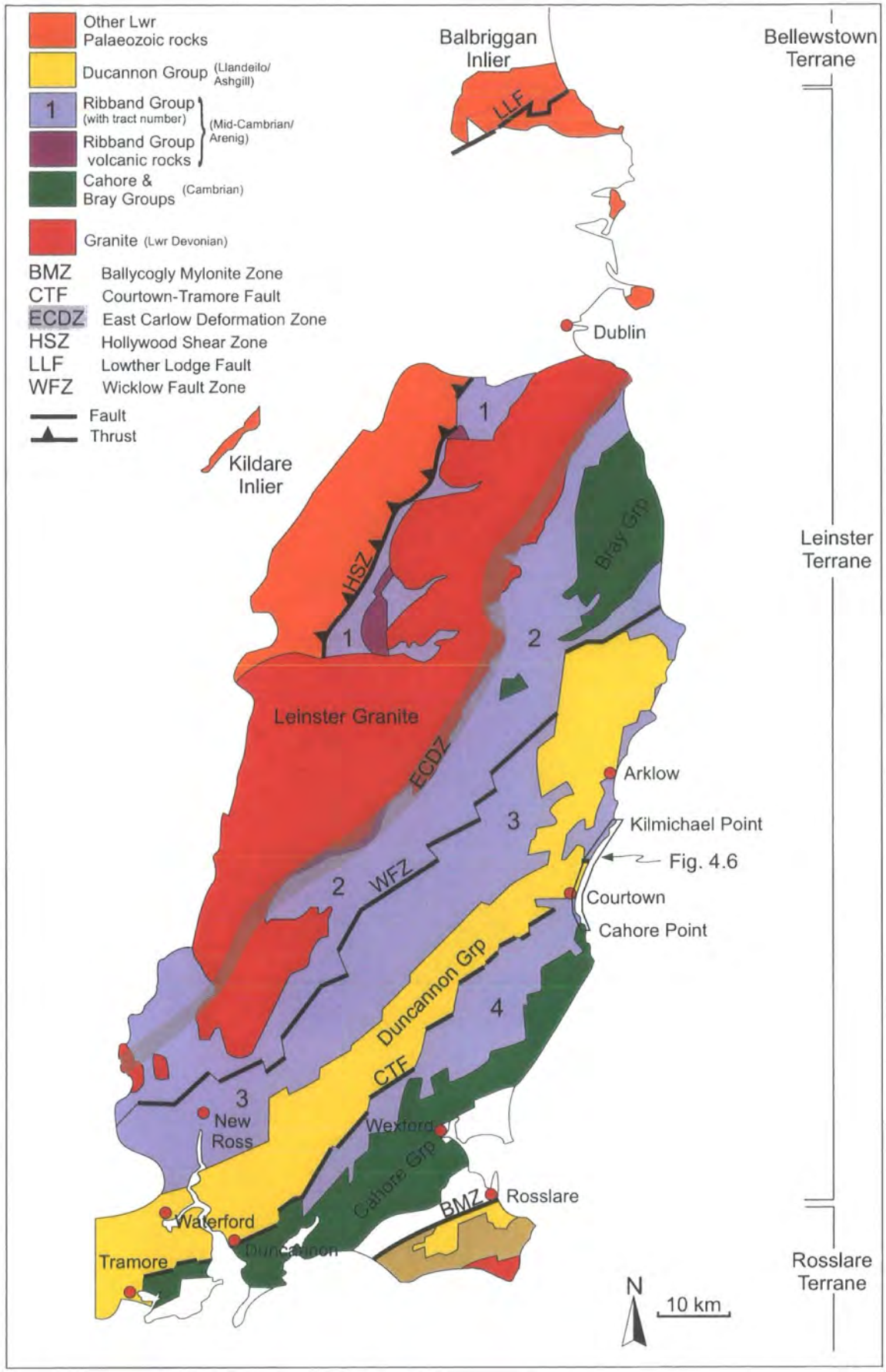

Figure 4.2. Simplified geological map of the Leinster Massif showing main stratigraphic units and major faults and shear zones (after McConnell *et al.* 1999; Tietzsch-Tyler *et al.* 1994). Box shows location of Fig. 4.6.

4.2 Regional setting and structural evolution

For the greater part of the Lower Palaeozoic SE Ireland formed part of a crustal block (Eastern Avalonia) that was located along the edge of Gondwana (Fig. 4.3). The Lower Palaeozoic rocks of the Leinster Massif record the development of volcanic arcs and marginal basins produced by oceanic plate subduction. Deformation occurred during the accretion of island arcs and the final closure of the Iapetus Ocean as the landmasses of Eastern Avalonia and Laurentia collided (Woodcock 2000a). Table 4.1 outlines the chronology of these events within SE Ireland.

Until recently, the structural geology of the Lower Palaeozoic of SE Ireland was thought to be relatively straightforward. The main belt of the mid-Ordovician Duncannon Group rocks (Fig. 4.2) was believed to occupy the centre of a syncline (the Campile Syncline), with the Ribband Group rocks to the NW forming an anticline (Gardiner 1970). The steep NE-trending penetrative cleavage present throughout the region was generally regarded as a late Silurian regional 'S1' cleavage produced during the climax of the Caledonian Orogeny, since it cuts Silurian rocks to the north-west of the Leinster Granite (Gallagher *et al.* 1994 and references therein).

Hutton & Murphy (1987), Tietzsch-Tyler (1989, 1996), Max et al (1990) and Murphy et al. (1991) challenged this rather simplistic view of the structural evolution of SE Ireland. Based in part on the correlation of the Cahore Group with the along-strike Monian Supergroup of Anglesey (Fig. 4.4, Tietzsch-Tyler & Phillips 1989; Gibbons *et al.* 1994), Tietzsch-Tyler (1989, 1996) proposed that an early Ordovician (Arenig) orogenic episode referred to as the Monian Orogeny, was preserved in the southern part of SE Ireland. This event, it was suggested, could be related to the emplacement of the Rosslare Terrane. Tietzsch-Tyler (1989, 1996) argued that an angular unconformity exposed at Tramore (Fig. 4.2) between the Duncannon Group and the cleaved Tramore shales of the Cahore Group provided direct evidence for tectonic cleavage formation prior to the mid-Ordovician (Tietzsch-Tyler 1989, 1996). Therefore, the Cahore and Ribband Groups should show evidence of an extra cleavage when compared with the Duncannon Group. These observations and the recognition of several NE-SW trending, fault bounded domains prompted a re-evaluation of the structural evolution of SE Ireland.

Several models have been proposed (e.g. Max *et al.* 1990; Murphy *et al.* 1991; Tietzsch-Tyler *et al.* 1994a) to accommodate the new evidence. The consensus seems to be that

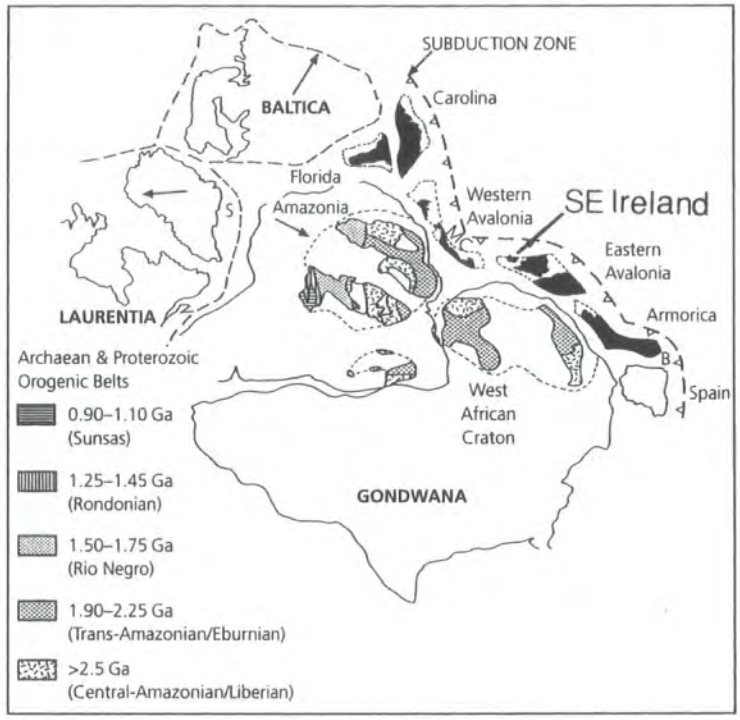

Figure 4.3. The position of Eastern Avalonia with respect to Gondwana during the late Neoproterozoic. Present day land in black (after Nance & Murphy 1996).

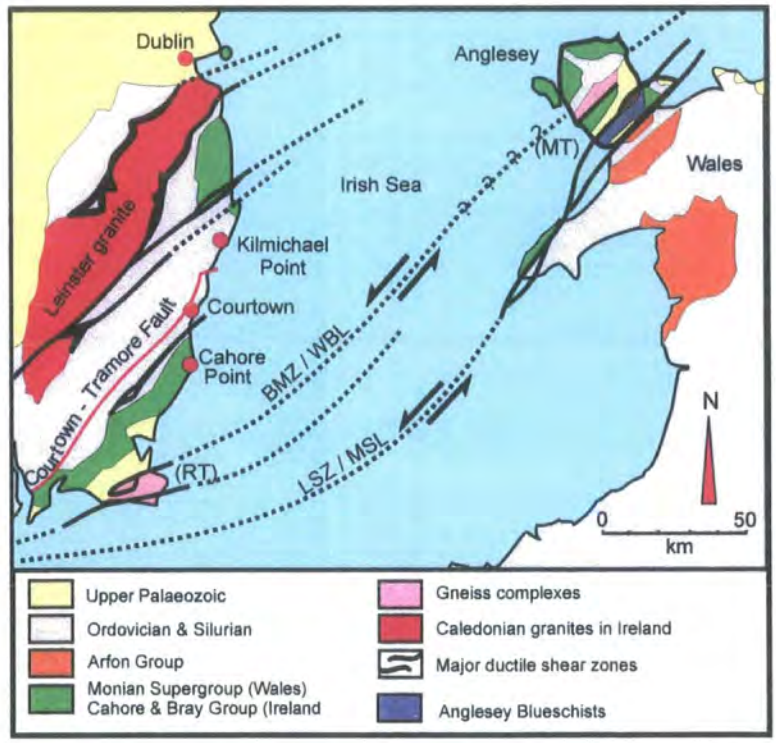

Figure 4.4. Simplified geological map of SE Ireland, Angelsey and NW Wales showing the main stratigraphic units, the relationship between the Rosslare Terrane (RT) and the Monian Terrane (MT) and major ductile shear zones (BMZ / WBL = Ballycogly Mylonite Zone / Wexford Boundary Lineament, LSZ / MSL = Llyn Shear Zone / Menai Strait Line). (Redrawn from Gibbons *et al.*1994).

the Leinster Massif can be subdivided into a series of NE-SW trending structural and stratigraphical units bounded by predominantly sinistral, NE-SW trending faults accreted during transcurrent faulting related to the Ordovician to early Devonian closure of the Iapetus Ocean (e.g. Max *et al.* 1990). However, there is some disagreement as to the status and importance of these fault-bounded units. Max *et al.* (1990) recognised seven terranes, thought to have been juxtaposed after substantial sinistral movement along transcurrent faults during the Silurian. However, Murphy *et al.* (1991) disagreed maintaining that, because there is a general stratigraphical continuity between the so-called terranes of Max *et al.* (1990) - particularly with respect to the Cambro-Ordovician sequence, - then the subdivisions do not merit terrane status. They therefore adopted the term domain rather than terrane for their subdivisions. On this basis, they have identified seven domains, five of which lie in or adjacent to the Leinster Massif. The previously separate Rosslare and Tuskar Terranes of Max *et al.* (1990) were combined to form a separate Rosslare Terrane, the northern boundary of which is the Ballycogly Mylonite Zone (BMZ) (broadly coincident with the Wexford Boundary Lineament of Gardiner (1975)) (Figs. 4.1, 4.2; Murphy *et al.* 1991). Tietzsch-Tyler *et al.* (1994a) suggested a somewhat simplified version of both models, dividing the Leinster Massif into three NE-SW trending belts, separated by major faults. The SE Belt comprises the Precambrian gneisses and amphibolites of the Rosslare Complex and part of the Cambrian Cahore Group (Fig. 4.2) (Rosslare Terrane). The Central Belt extends from the Ballycogly Mylonite Zone to the Courtown-Tramore Fault and is composed entirely of Cambrian and Ordovician sedimentary rocks. The NW Belt extends from the Courtown-Tramore Fault northwards and westwards and is composed of Ordovician sediments (Tietzsch-Tyler *et al.* 1994a). Despite these differences, all these groups of authors agree that the basic structure of the Leinster Massif is strongly heterogeneous and many of the terrane boundaries of Max *et al.* (1990) and domain boundaries of Murphy *et al.* (1991) are represented by faults and shear zones.

4.3 Lower Palaeozoic rocks and stratigraphy of SE Ireland

Situated on the northern margin of Eastern Avalonia during the Lower Palaeozoic, the main palaeogeographical feature of SE Ireland was the NE-trending Leinster Basin. In general, the basin was tectonically active during the greater part of its depositional history; the sedimentary and volcanic accumulations within it show

evidence of pulses of activity and quiescence (Brück *et al.* 1979). Deposited within this basin, four major, Lower Palaeozoic lithological assemblages have been distinguished (Figs. 4.2, 4.5). However, only the three assemblages that outcrop in the study area will be considered in this chapter. These are the Cambrian Cahore and laterally equivalent Bray Groups, the Lower Ordovician Ribband Group and the Upper Ordovician Duncannon Group (Brück *et al.* 1979; Max *et al.* 1990).

The Cahore Group (Crimes & Crossley 1968) forms a NE-SW-trending belt from the Waterford Estuary on the south coast to Cahore Point on the east coast (Fig. 4.2). Comprised predominantly of grey-green and purple feldspathic greywackes and pale quartz arenites with thin intervening shales, it has been interpreted as being characteristic of a relatively proximal marine turbidite sequence (Brück *et al.* 1979). The Bray Group, which lies on the east coast to the south of Dublin (Fig. 4.2), consists of turbiditic greywackes, shales and quartzites and is thought to be the lateral equivalent of the Cahore Group (Tietzsch-Tyler *et al.* 1994b). Both are Lower to Mid Cambrian in age, based on the presence of the trace fossil *Oldhamia* (Crimes & Crossley 1968; Brück *et al.* 1979; Tietzsch-Tyler *et al.* 1994b) and acritarchs (Gardiner & Vanguestaine 1971).

Cahore Group deposition in the deeper parts of the Leinster Basin was followed conformably by the Ordovician Ribband Group (Tietszch-Tyler *et al.* 1994b). The Ribband Group consists of a thick succession of grey, green and purple siltstones and mudstones representing a dominantly distal turbidite succession. These are intercalated with pelagic and hemipelagic sediments and locally abundant, largely intermediate to basic volcanics (Brück *et al.* 1979). The mudstones are commonly finely laminated so that they have a pin-striped appearance; consequently, early geologists referred to them as "ribband", a term that has stuck with them since (Tietzsch-Tyler *et al.* 1994b). Trace fossils from the east coast section south of Courtown (Crimes and Crossley 1968) are indicative of a deep-water environment of deposition. The many local studies and stratigraphies were summarised by Brück *et al.* (1979) and an attempt to unify these was made by Tietzsch-Tyler *et al.* (1994a, 1994b) and McConnell *et al.* (1994). Ribband Group rocks form three NE-SW trending belts across the Leinster Massif, which have subsequently been subdivided into four tracts (numbered 1 – 4, Fig. 4.2; McConnell *et al.* 1999). This more recent stratigraphy was based not only on fossil age control, but also on the stratigraphic position of a coticule package marker horizon (McConnell *et al.* 1999). The distinctive coticule package consists of coticule (spessartine-bearing

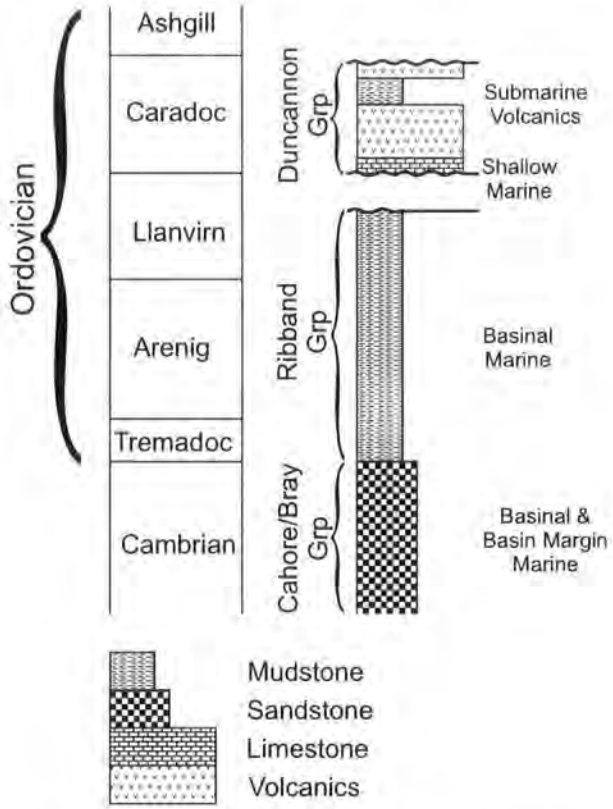

Figure 4.5. The stratigraphy of SE Ireland based on Brück *et al.*(1979); Tietzsch-Tyler *et al.* (1994a & b) and Woodcock (2000a).

quartzite) and tourmalinite, the product of an exhalative event and believed to be a stratigraphically confined package of large lateral extent within the Caledonian-Appalachian Orogen (Kennan & Kennedy 1983; McConnell *et al.* 1999). The age of the Ribband Group is poorly constrained and individual formation definitions are based mainly on the systematic change in colour through the succession. However, acritarch and graptolite faunas indicate an age range between Mid-Cambrian and early Arenig based on the basal and uppermost formations respectively (Brück *et al.* 1979; Tietzsch-Tyler *et al.* 1994b; Rushton 1996).

The Duncannon Group (Gardiner 1974) (formerly Ballymoney Group of Brenchley & Treagus (1970)) is bounded on its southern margin by the Courtown-Tramore Fault and forms a relatively narrow band extending from Waterford in the south to the east coast north of Arklow (Fig. 4.2). These rocks are characterised by early basaltic and andesitic volcanics succeeded by later rhyolites, separated by non-volcanic sedimentary sequences of variable thickness, including mudstones, siltstones, occasional quartzwackes and limestones (Brück *et al.* 1979). The thickness of the group changes considerably from SW to NE. In the New Ross area (Fig. 4.2), it has a thickness of approximately 3200m (Brück *et al.* 1979), whilst in the Courtown area (Fig. 4.2) it has a thickness of only 170-240m (Brenchley & Treagus 1970). For most part, the group rests unconformably on the Ribband Group, but the amount of overstep decreases westwards. As a result, the relationship between the Ribband and Duncannon groups appears to be conformable in the western part of the New Ross area. This relationship is attributed to westward tilting and differential erosion of the Ribband Group prior to the deposition of the Duncannon Group (Brück *et al.*1979). However, McConnell (2000) notes that no age younger than early Arenig is known for the Ribband Group and that the base of the Duncannon Group is Llandeilian to Caradoc in age. Therefore, some doubt must be cast on the suggestion that a conformable relation exists anywhere between the two groups. The identification of the trilobite *Mucronaspis* by Owen and Parkes (1996) gives an Ashgillian upper age limit to the group. In most regions, the base of the Duncannon Group is comprised of volcanics, but around Courtown (Fig. 4.2), the basal formation is limestone. This has been correlated with lithologically similar limestone around Tramore in the SW (Fig. 4.2; Brück *et al* 1979). The differences in thickness and facies variation within the Duncannon Group are broadly explained by the existence of a number of separate, fault-controlled depositional basins that were active at various times during deposition (Brück

et al. 1979).

4.4 The Cahore Point to Kilmichael Point coastal section

4.4.1 Introduction

Cahore and Kilmichael points lie on the eastern coast of counties Wicklow and Wexford and are located within the centre of the Leinster Massif (Figs. 4.1, 4.6). The rocks are exposed intermittently as a narrow band along the generally NNE - SSW trending, 20km stretch of coastline lying to the south of Kilmichael Point. The rock sequence consists of Cambrian proximal and distal turbidites of the Cahore Group that are conformably overlain by the early Ordovician distal turbidites of the Ribband Group. These in turn are unconformably overlain by upper Ordovician limestones, black mudstones and acid to intermediate extrusive volcanic tuffs of the Duncannon Group. Way up criteria, where present, have enabled a detailed analysis of fold and cleavage facing patterns to be made in addition to a standard orientation analysis using stereographic projections. Although rather scarce in some of the units, way-up indicators include graded bedding, load casts, cross-stratification and ripple marks (Plate 4.1(a), (b)). Highly weathered and altered acid intrusives occur throughout the Cahore and Ribband groups. The sequence has experienced several phases of deformation, the earliest of which appears only to be preserved in the rocks of the Cahore Group in the extreme south of the area (Tietzsch-Tyler 1996). The whole sequence has subsequently been subjected to at least two further episodes of deformation. The dominant phase of regional deformation has produced a series of NE-SW-trending folds and associated cleavage. These are post-dated by a braided network of ENE– to NE-trending, sub-vertical sinistral shear zones and fault arrays that are heterogeneously developed throughout the study area. Cross-cutting, and locally concordant basic minor intrusions of probable Caradocian age (McConnell pers. com) occur throughout the section.

Many outcrops are separated by long (up to 1km) sandy beaches making correlation of separated outcrops potentially problematic. Access to much of the section requires low water conditions as many outcrops are wholly, or partly covered at high tide. The extensive building of numerous coastal holiday complexes has limited the number of available access points along the coast. The only large-scale maps available for the area were Irish Ordnance Survey 6 in to 1 mile, produced in the late 1800's; no national grid or latitude-longitude system was provided. The national grid system

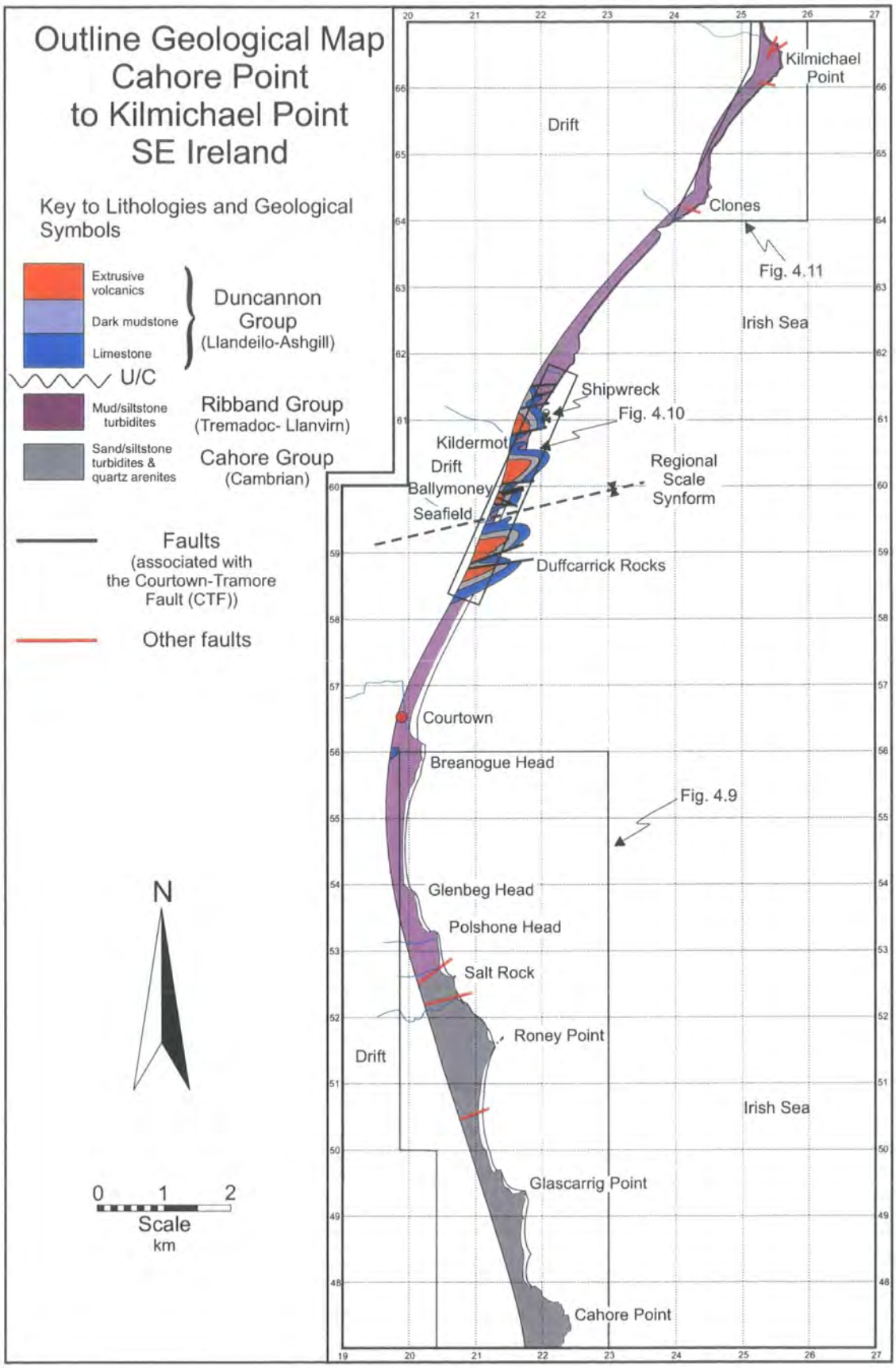

Figure 4.6. Outline geological map of the Cahore Point to Kilmichael Point coast based on mapping from this study, Crimes and Crossley (1968), Brenchley and Treagus (1970) and Tietzsch-Tyler *et al.* (1995). Boxes show locations of Figs. 4.9, 4.10 and 4.11.

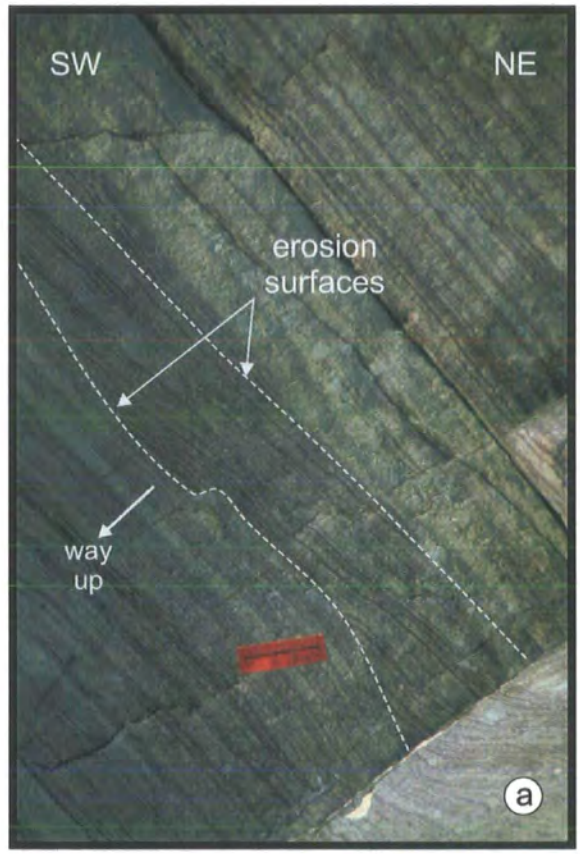

Plate 4.1. **(a)** Ripples (parallel to pencil) on bedding surface indicate younging to the NW (i.e. towards viewer). Askingarran Formation below Askingarran (Fig. 4.9 grid ref. 21255190). **(b)** Truncated cross-lamination and down-cutting erosion of underlying bedding in sediments of the Riverchapel Formation indicate that the bedding is overturned and youngs to the SW. (Fig.4.10, grid ref. 22116134).

provided on the maps accompanying the following sections was interpolated from the Irish Ordnance Survey 1:50 000 series.

4.4.2 Previous studies

Despite the excellent exposure and ease of access, the Lower Palaeozoic rocks along the Wicklow-Wexford coast around Courtown (Fig. 4.6) have received little attention from the geological community. Thus, the most recent and comprehensive studies describing the geology of this section of coast are those of Crimes & Crossley (1968) and Brenchley & Treagus (1970). The Wicklow-Wexford coast was partly re-surveyed during the production of the guide and map for Carlow and Wicklow (Tietzsch-Tyler *et al.* 1994b, 1995). However, the data and information regarding the area around Courtown was primarily based on the original mapping of Crimes & Crossley (1968) and Brenchley & Treagus (1970) (J Morris pers. com.). Previous work includes studies by Kinahan (1879) who, while undertaking a regional survey for the Geological Survey of Ireland produced an account of the stratigraphy of part of the Wexford coast. Tremlett (1959) described the structure of a large area of east Wicklow and Wexford and provided a table of the stratigraphic succession. The first detailed studies are those of Crimes and Crossley (1968) who studied the area to the south of Duffcarrick Rocks down to Cahore Point and that of Brenchley and Treagus (1970) who examined the rocks from Duffcarrick Rocks to Kilmichael Point (Fig. 4.6). Crimes and Crossley (1968) interpreted the sequence as being deposited partially by turbidity currents in a gradually shallowing sea, with an age range from Cambrian for the Cahore Group to mid-Ordovician (Caradocian) for the Courtown-Ballymoney Formations. They recognised three phases of deformation. 'F1'folds were thought to generally trend ENE-WSW and mostly plunge gently in either direction, although in the north of the area, the plunges appeared to be more variable. They also noted that although commonly isoclinal, the folds are often variable in style (Fig. 4.7a). 'F1' folds in the north of the section were shown to verge N with cleavage dipping to the S. The opposite relationship was observed in the south of the section, and in the centre of the section (e.g. around Glascarrig Point), the folds are mostly upright. Thus, the overall regional structure was interpreted as a large anticlinorium centred near to Glascarrig Point (Figs. 4.6, 4.8, Crimes & Crossley 1968). 'F1' folds were shown to be locally refolded by the 'D2' deformation producing markedly asymmetric, northerly verging, heterogeneously developed 'F2' folds with a steep southerly dipping cleavage (Fig.

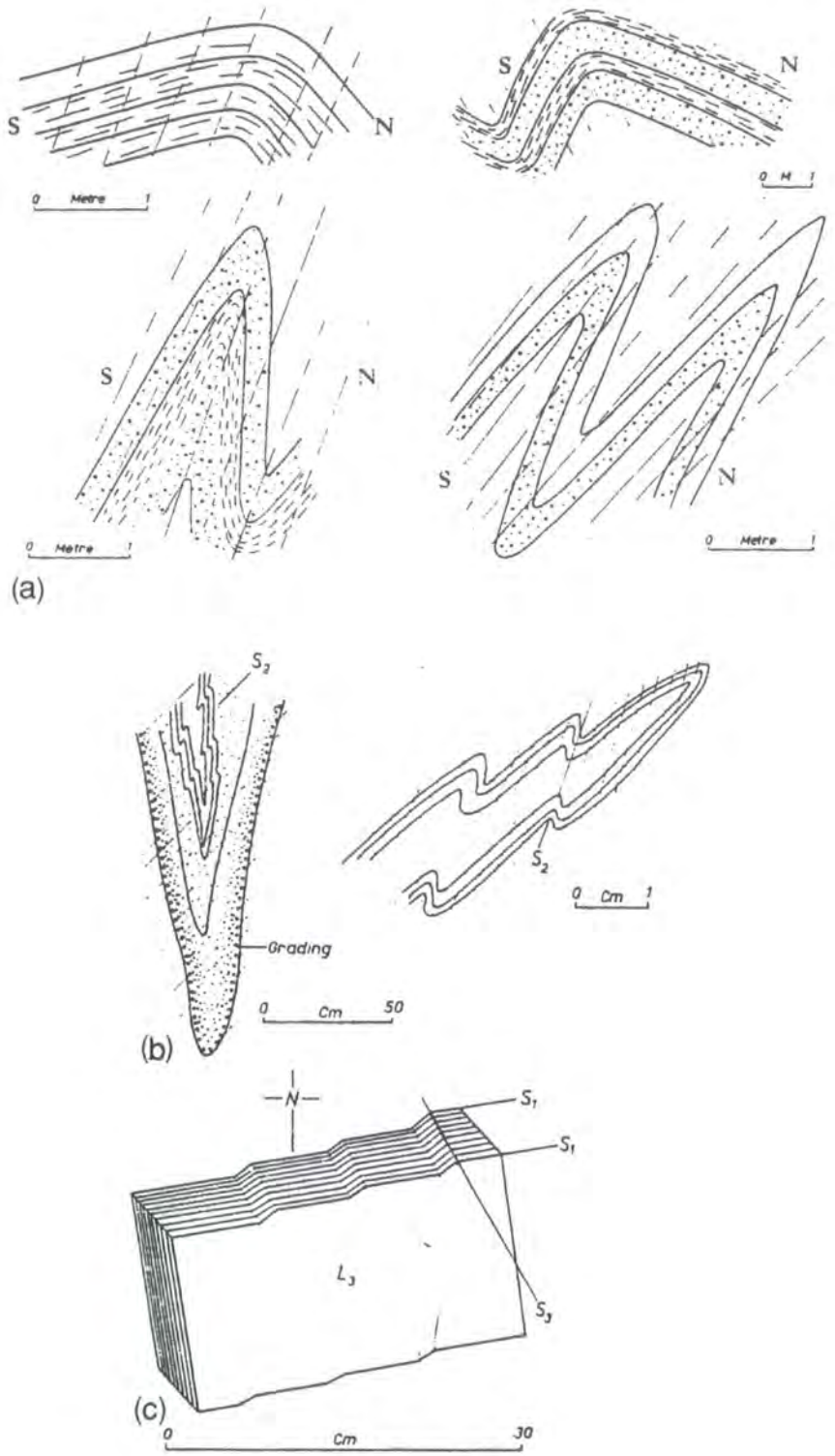

Figure 4.7. Fold styles and overprinting fold generations observed between Cahore Point and Courtown. **(a)** Variations in 'F1' fold style **(b)** Refolding of 'F1' producing asymmetric 'F2' with 'S2' cleavage. **(c)** 'F3' kink bands refolding 'S1' (from Crimes & Crossley 1968).

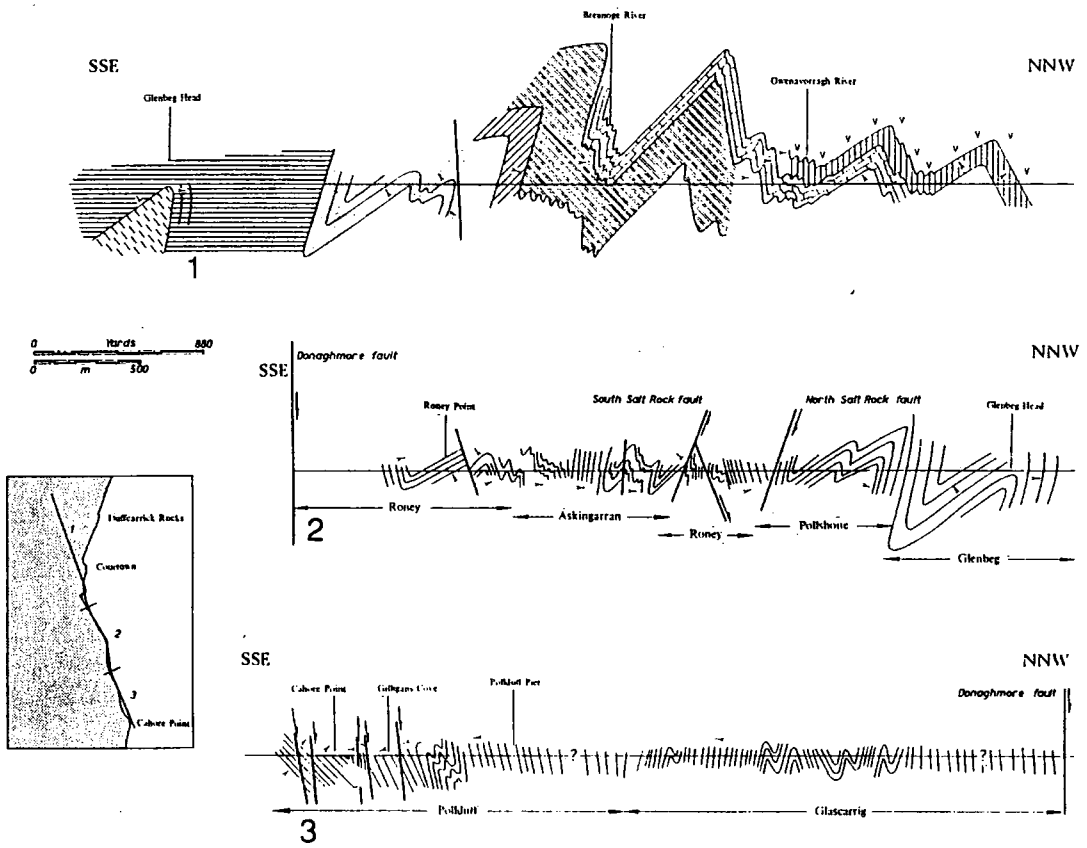

Figure 4.8. NNW-SSE sketch cross-section of Cahore Point to Courtown produced by Crimes and Crossley (1968).

4.7b). A local third set of folds, 'F3' was thought to occur trending approximately 140°-320°, showing kink bands geometries (Fig. 4.7c). Numerous faults were recorded in the section, particularly strike-slip faults (Crimes & Crossley 1968).

Brenchley and Treagus (1970) produced a number of maps for the section between Courtown and Kilmichael Point, including a large-scale map (1:2534) of the section of coast from Duffcarrick Rocks to a locality north of the shipwreck (Fig.4.6). They recognised and described two phases of deformation. 'D1', with a steep ENE-WSW trending cleavage associated with tight to isoclinal folds with variable plunges leading to both upward and downward-facing relationships. 'D2' was thought to have an ESE-WNW-trending sub-vertical cleavage with sparse, steeply plunging folds.

Tietzsch-Tyler *et al.* (1994b) suggested that Cahore and Ribband group rocks surrounding the Courtown area preserved evidence of an early Ordovician (Arenig) deformational event, (the Monian Orogeny), and that this was responsible for many of the smaller folds observed at Pollshone Head and Glenbeg Head and the folds around Askingarran. Therefore, the Cahore and Ribband groups should preserve evidence for an extra phase of deformation when compared to the Duncannon Group.

4.4.3 Lithostratigraphy

The Cahore, Ribband and Duncannon Groups described in section 4.3 are variably exposed along the 20km stretch of coastline between Cahore Point and Kilmichael Point (Fig. 4.6). They have been divided into thirteen formations by Tietzsch-Tyler *et al.* (1994b) and it is this lithostratigraphy that will be adopted here, with the revised correlation within the Ribband Group of McConnell *et al.* (1999). Table 4.2 provides a comparative correlation with the previous formation names and stratigraphy employed by Crimes & Crossley (1968) and Brenchley & Treagus (1970).

4.4.3.1 The Cahore Group

The Cahore Group comprises four formations recognised within the study area (Fig. 4.9, Table 4.2). Although the age range for the group as a whole has been suggested as Lower- to Mid-Cambrian (Crimes & Crossley 1968; Brück *et al.* 1979; Gardiner & Vanguestaine 1971; Tietzsch-Tyler *et al.* 1994a & 1994b) no separate ages are provided for the individual formations.

Glascarrig Formation. (Table 4.2, Fig. 4.9, Crimes & Crossley 1968; Tietzsch-Tyler *et al.* 1994b). Comprises green-grey and occasionally purple or buff mudstones

Crimes & Crossley 1968		Brenchley & Treagus 1970		Tietzsch-Tyler *et al.* 1994a&b; McConnell et al. 1999		
	Ballymoney Fm.	Ballymoney Grp.	Ballymoney Fm.	Duncannon Grp.	Campile Fm	
	Ballinatray Fm.		Ballinatray Fm.		Ballinatray Fm.	
	Courtown Fm.		Courtown Fm.		Courtown Fm	
Ribband Grp.	Riverchapel Fm.	Ribband Grp.	Riverchapel Fm.	Ribband Grp.	Maulin Fm.	Riverchapel Fm.
	Breanoge Fm.					
	Seamount Fm.		Clones Fm.		Ballylane Fm.	Seamount Fm.
	Glenbeg Fm.					
	Pollshone Fm.		Kilmichael Fm.			Ballyhoge Fm.
					(N of CTF)	(S of CTF)
	Askingarran Fm.			Cahore Grp.	Askingarran Fm.	
Cahore Grp.	Roney Fm				Roney Fm.	
	Pollduff Fm.				Cahore Point Fm.	
	Glascarrig Fm.				Glascarrig Fm.	

Table 4.2. Correlation of the formations between Cahore Point and Kilmichael Point. Based on Brenchley & Treagus (1970), Crimes & Crossley (1968), McConnell *et al.* (1999) and Tietzsch-Tyler *et al.* (1994b). Shading shows nomeclature adopted in present study.

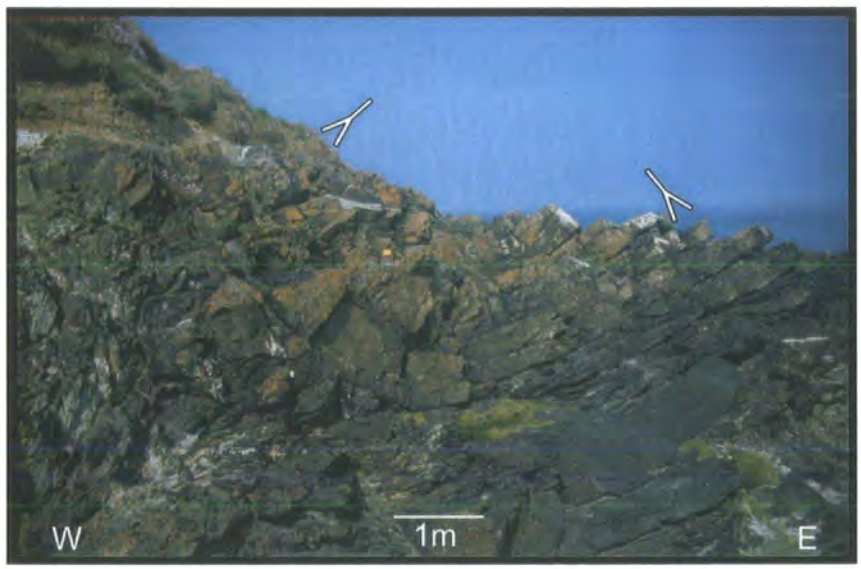

Plate 4.2. Folded quartz arenites and interbedded purple and green mudstones of the Cahore Point Formation at Cahore Point (Fig. 4.9, grid ref. 22524723).

Geological Map of Cahore Point-Breanoge Head

Key to Lithologies and Geological Symbols

- Beach
- Courtown Shear Zone

Ribband Group (Tremadoc-Llanvirn)
- Seamount Formation
- Ballyhoge Formation

Cahore Group (Cambrian)
- Askingarran Formation
- Roney Formation
- Cahore Point Formation
- Glascarrig Formation

- Intrusive rocks - Basalts

- Bedding inclined
- Bedding overturned
- Cleavage
- Foliation
- Shear bands
- Minor primary fold axis (with sense)
- Minor secondary fold axis (with sense)
- Direction of younging
- Antiformal axial trace
- Synformal axial trace
- Fault (tick on downthrow side)
- Thrust (barb on hanging wall)
- A — A' Line of Section

N

0 500 1000
m
Scale

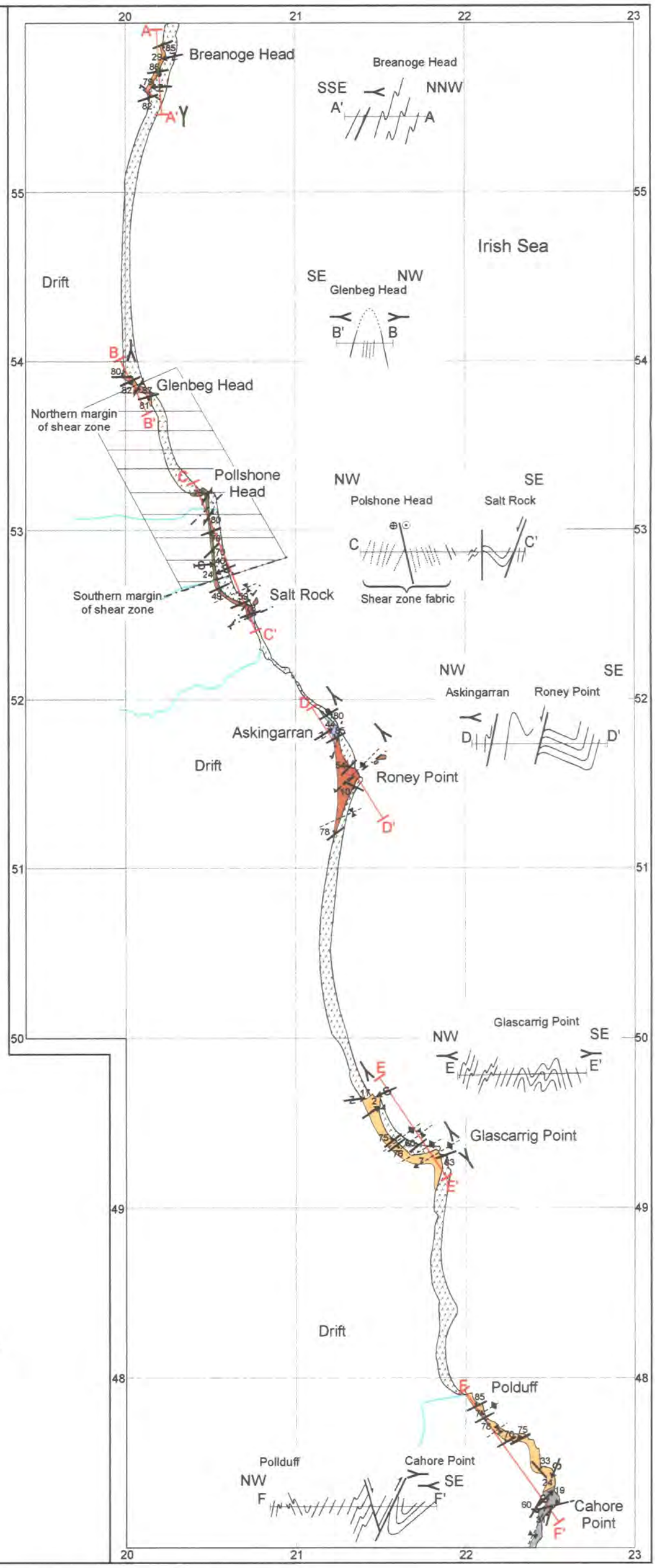

Figure 4.9. Simplified geological map and cross-sections of the coast between Cahore point and Breanoge Head

interbedded with thin-bedded subordinate greywacke sandstones or siltstones. Individual sandstone beds are usually 5 –15cm thick but occasionally may be up to 2m in thickness. It outcrops between a point just to the north of Cahore Point (grid ref. 224474) and some 600m north of Glascarrig Point (grid ref. 214497) (Fig 4.5). It forms the oldest part of the stratigraphic succession in the study area. Way-up criteria within these rocks are limited. Whilst some of the greywacke sandstones show evidence of graded bedding, most exhibit parallel lamination. The mud and siltstone units are well laminated, but, apart from rare grading and small-scale current bedding, show few sedimentary structures. The bases of some of the greywacke beds have load-casts, although few of the bases are exposed. Cleavage is not visible in the greywacke sandstones and only weakly developed within the finer grained units.

Cahore Point Formation. (Table 4.2, Fig. 4.9, Crimes & Crossley 1968; Tietzsch-Tyler *et al.* 1994b). This pale grey-green bedded quartz arenite with interbeds of pale green and purple mudstones is best seen at Cahore Point (Plate 4.2, grid ref. 22524723) although it is exposed to the south for approximately 300m and to the north for 100m. The majority of the sandstone beds are between 20-60cm thick, although occasionally they may be up to 1m. Apart from occasional graded beds, cross-lamination and sole structures, way up evidence is sparse. Cleavage is weakly developed and then only within the fine grained interbeds of purple and green mudstones.

Roney Formation. (Table 4.2, Fig. 4.9, Crimes & Crossley 1968; Tietzsch-Tyler *et al.* 1994b). Exposed at Roney Point (grid ref. 21355157) and in a fault bounded block at Salt Rock (grid ref. 20755265), this thick, massive, pale grey quartz arenite may be a lateral equivalent of the Cahore Point Formation (Crimes & Crossley 1968). The massive sandstones are interbedded with thin <20cm purple and pale green mudstones. The mudstones show parallel lamination whilst the sandstones are essentially structureless, though some show normal grading. Cleavage is only observed in the fine grained subordinate mudstones.

Askingarran Formation. (Table 4.2, Fig. 4.9, Crimes & Crossley 1968; Tietzsch-Tyler *et al.* 1994b). The Askingarran Formation consists of alternating black and grey mudstones and pale grey siltstones 2-10cm thick. In addition, there are frequent coarse siltstone or fine sandstone beds, commonly 30cm, but in places up to 1m thick. Way-up criteria within the sandstones include ripples (Plate 4.1(a)) and load casts. The formation outcrops between Roney Point and Salt Rock and again to the

north of Salt Rock and Pollshone Head (Fig. 4.9). Cleavage is penetrative and is strongly developed throughout all units (Plate 4.3(a)). The contacts with the Roney Formation and Askingarran Formation appear to be tectonic, occurring along a NNE-SSW-trending steeply, NW-dipping fault to the north of Roney Point (Fig.4.9, Plate 4.3(b)) and lying within a major sinistral shear zone between Salt Rock and Pollshone Head (Fig. 4.9).

4.4.3.2 The Ribband Group

Due to the lack of fossils within the rocks of the Ribband Group, it is not possible to erect a biostratigraphy based on relative ages of different part of the succession. There is, however, a systematic change in colour through the succession which, together with changes in subordinate rock types, allows a stratigraphy of formations to be identified (Tietzsch-Tyler *et al.* 1994b, Figs. 4.9, 4.10, 4.11, Table 4.2). The Maulin and Ballylane Formations lie to the north of the Courtown-Tramore Fault (CTF) (Figs 4.2, 4.6) while their respective laterally equivalent formations, the Ballyhoge and Seamount lie to the south of the CTF, as does the Riverchapel Formation (Figs. 4.2, 4.6, Tietzsch-Tyler *et al.* 1994b). The age range of the Ribband Group within the study area is Tremadoc for the Maulin and Ballyhoge Formations and a Lower Arenig age for the Riverchapel Formation (Crimes & Crossley 1968; Tietzsch-Tyler *et al.* 1994b). However, McConnell *et al.* (1999) suggest that the presence of the coticule package within the Maulin Formation correlates it with the Mid-Arenig, Butter Mountain Formation which lies in tract 1 of figure 4.2 rather than the stratigraphy proposed by Tietzsch-Tyler *et al.* (1994b).

Ballyhoge Formation. (Table 4.2, Fig. 4.9, Tietzsch-Tyler *et al.* 1994b). The Ballyhoge Formation comprises dark grey to black mudstones. These are commonly pin-striped with interbedded, thin, pale siltstones (Plate 4.4(a)). It is exposed along the coast around Pollshone Head (grid ref. 205533) for approximately 300m where it lies entirely within a sinistral ductile shear zone (see below).

Seamount & Ballylane Formations. (Table 4.2, Figs. 4.9, 4.11 Tietzsch-Tyler 1994b). The dark mudstones of the Ballyhoge Formation are succeeded by the thinly laminated green-grey mudstones and siltstones of the Seamount and Ballylane formations (Plate 4.4(b)). Interbedded within the laminated mudstones and siltstones are sporadic fine-grained sandstone units 10-25cm thick which often show grading and local cross-lamination. However, within the remainder of the mudstone and siltstone

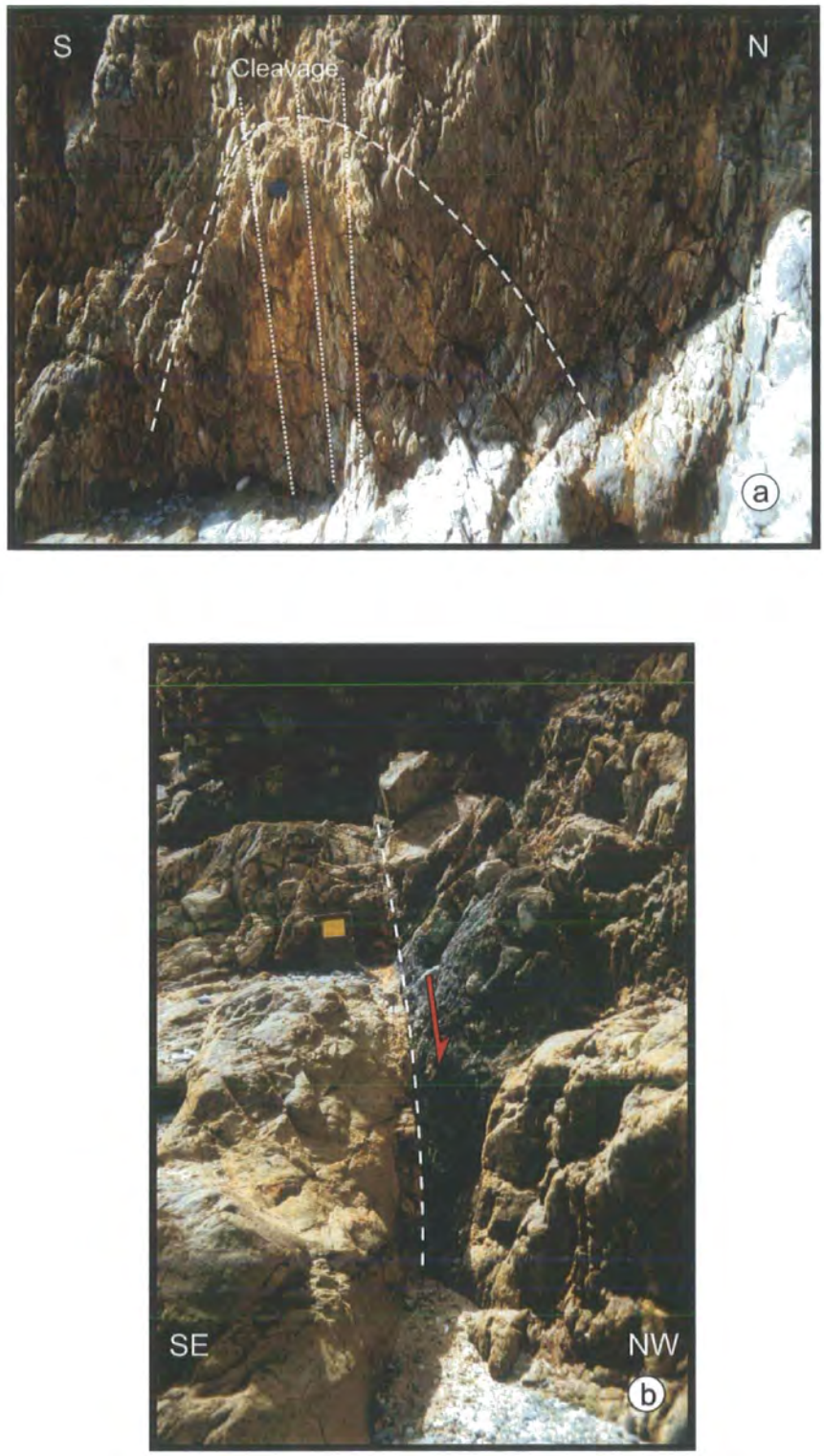

Plate 4.3. **(a)** Folded and strongly cleaved Askingarran Formation (highlighted) on the foreshore below Askingarran (Fig. 4.9, grid ref. 21305185). Lens cap is 5cm diameter. **(b)** Faulted contact (highlighted) between Roney Formation to SE and Askingarran Formation to NW (Fig. 4.9, grid ref. 21355170). Notebook for scale is 17cm high.

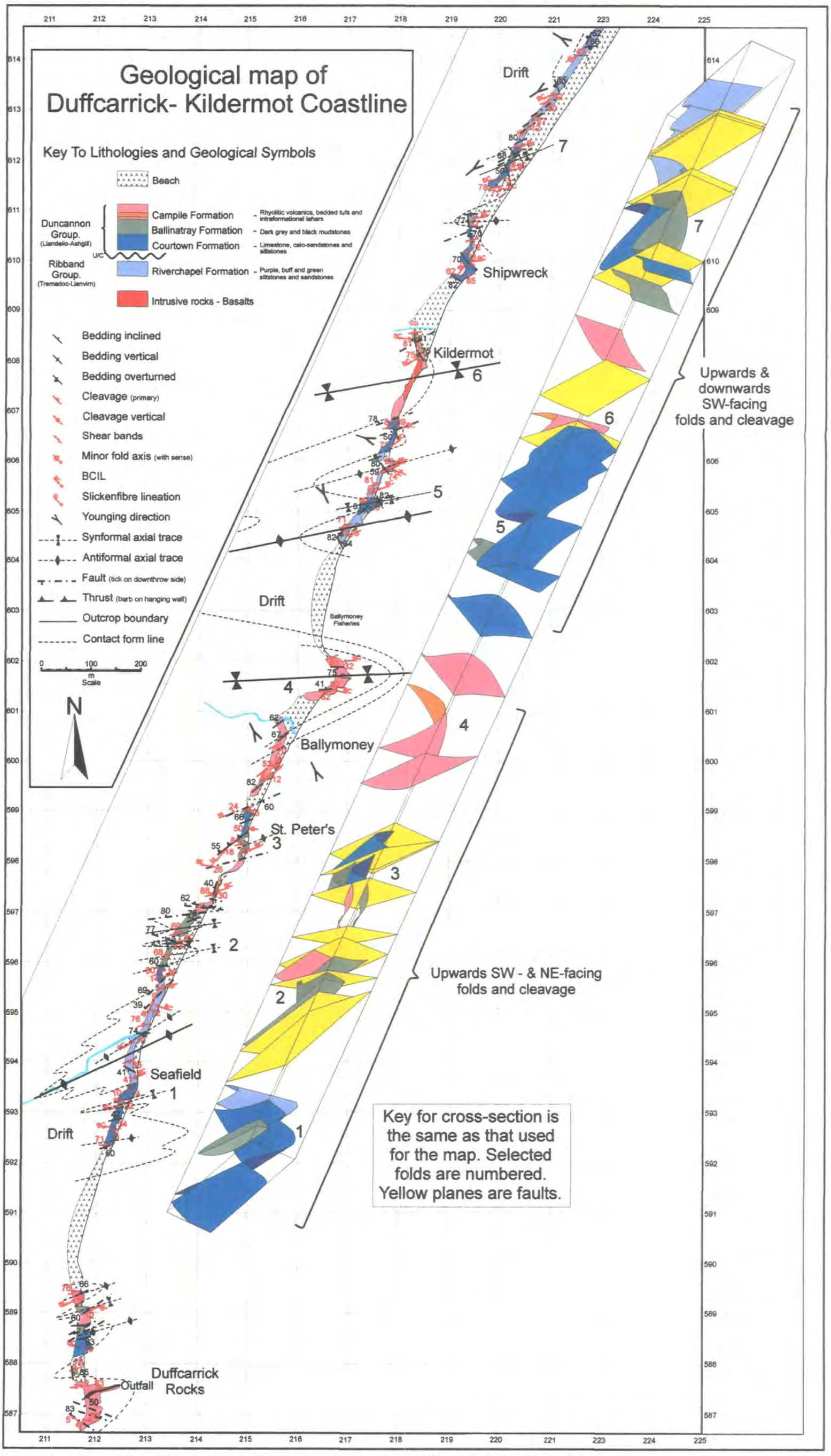

Figure 4.10. Geological map and 3-D cross-section of the Duffcarrick to Kildermot coast

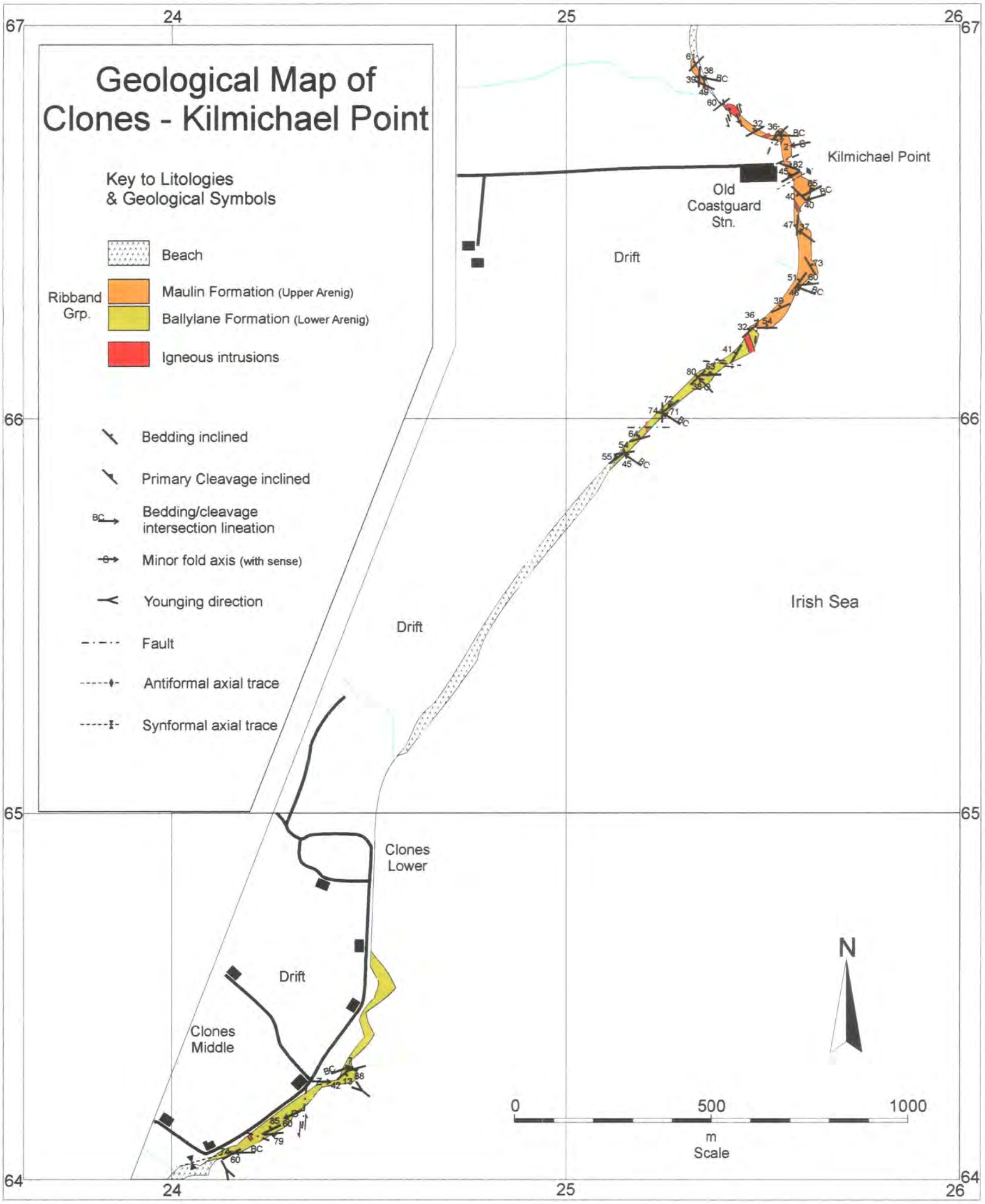

Figure 4.11. Geological map of Clones to Kilmichael Point

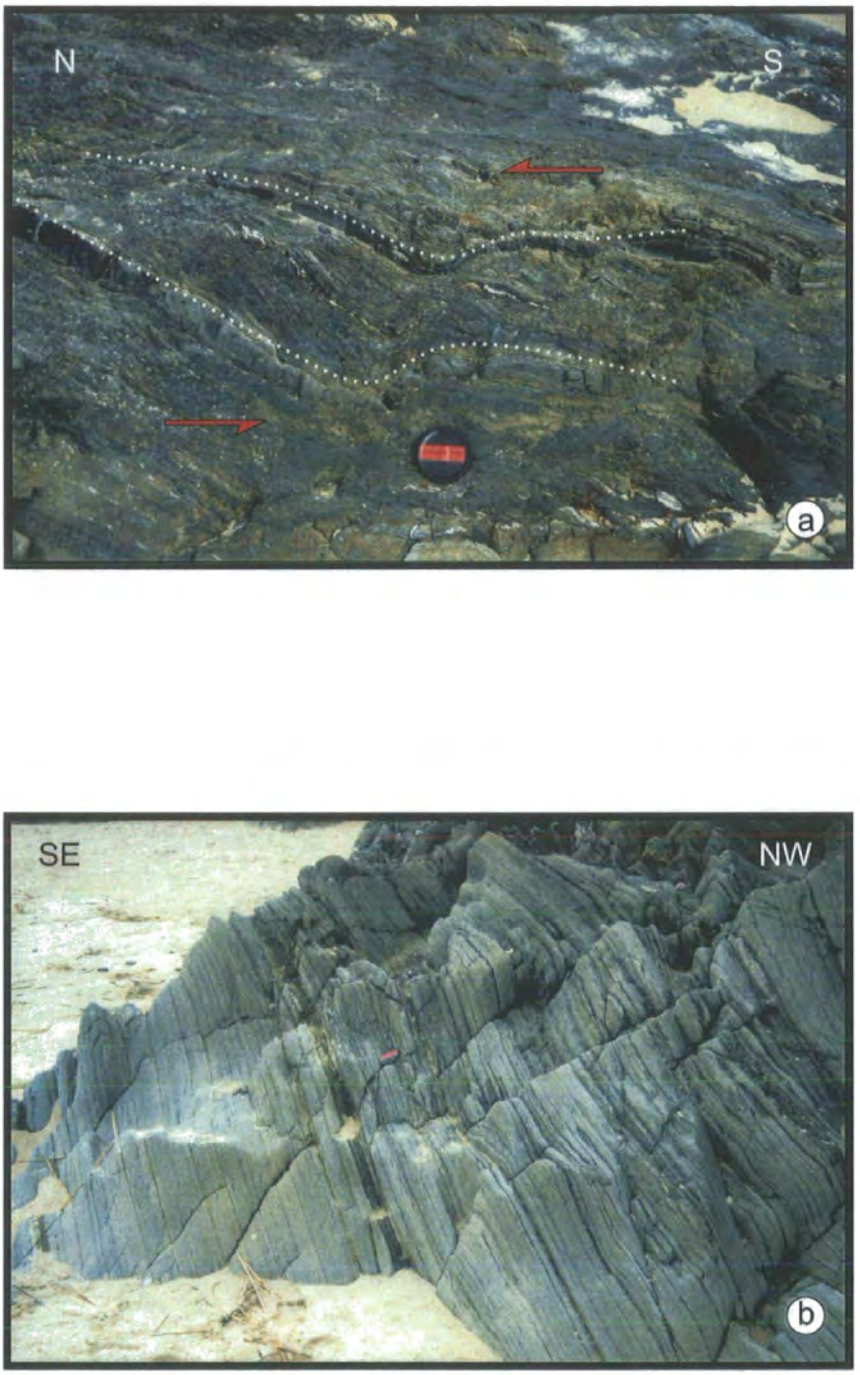

Plate 4.4. **(a)** Sinistrally folded, dark mudstones and thin sandstones (highlighted) of the Ballyhoge Formation south of Pollshone Head (Figs. 4.6, 4.9). **(b)** The Ballylane Formation at Clones. (Figs. 4.6, 4.11). (Scale on lens cap in photographs is 5cm).

units younging criteria are extremely sparse. The Seamount and Ballylane Formations outcrop to the south of Breanoge Head (grid ref. 202558) and Clones (grid ref. 241641) respectively. Despite their fine grained nature, neither of these formations shows a particularly well developed cleavage

Riverchapel Formation. (Table 4.2, Fig. 4.10, Crimes & Crossley 1968; Brenchley & Treagus 1970; Tietzsch-Tyler 1994b). The Riverchapel Formation is perhaps the most distinctive lithology within the Ribband Group. It is characterised by reddish-purple to buff coloured mudstones interbedded with grey-green mudstones and thin siltstones (Plate 4.5(a)). It is strongly cleaved with a well-developed penetrative cleavage throughout. Extensive outcrops of this rock occur all along the coast north of Duffcarrick Rocks; in particular, exposures near Seafield (grid ref. 212594, Fig.4.10) and north of the shipwreck (grid ref. 21966098, Fig. 4.10) show many of the features of this lithology. Way-up criteria include sporadic horizons of coarser siltstones/fine sandstones showing normal grading and sharp bases, whereas the mudstone/siltstone sequences show local cross-lamination and truncation of cross-laminated foresets (Plate 4.1(a)). Towards the top of the formation, sandstone units become thicker (10-20cm) and more common.

4.4.3.3 Duncannon Group.

Palaeontological evidence (Brück *et al.* 1979; Parkes 1994) suggests that the Duncannon Group (formerly Ballymoney Group of Brenchley & Treagus (1970)) rests unconformably on the Ribband Group (Plate 4.5(b)). This is supported by field observations that show the presence of:

- An angular, unconformable relationship between bedding in the Riverchapel Formation and the basal Courtown Formation of the Duncannon Group.
- An irregular, erosional surface is often exposed, with Courtown Formation sediments blanketing several cm to 10's of cm of relief within the Riverchapel Formation.

The Duncannon Group comprises three formations within the study area (Table 4.2, Fig. 4.10, Crimes & Crossley 1968; Brenchley & Treagus 1970; Tietzsch-Tyler 1994b). The basal Courtown Formation is Llandeilian to Caradoc in age (Parkes 1994) whilst the youngest unit, the Campile Formation extends into the Ashgillian (Owen & Parkes 1996).

Courtown Formation. (Table 4.2, Fig. 4.10, Crimes & Crossley 1968;

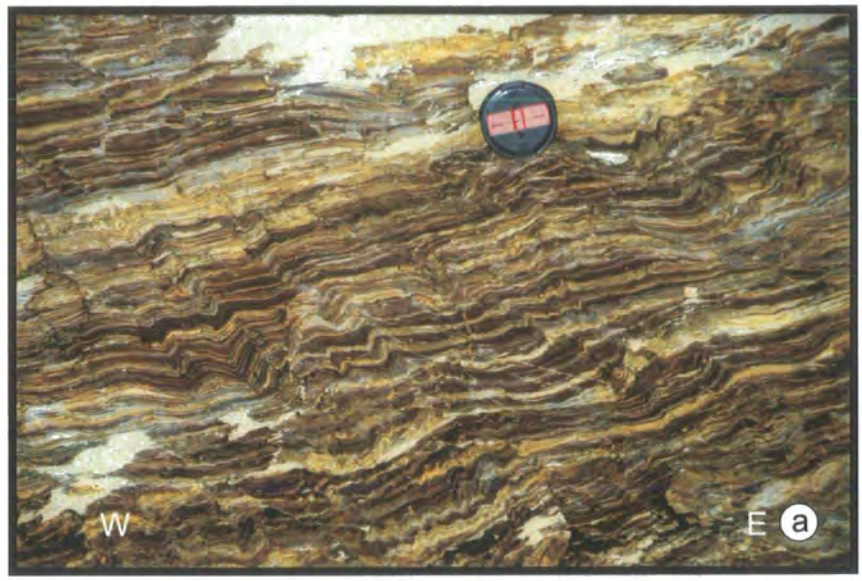

Plate 4.5. **(a)** Riverchapel Formation north of the shipwreck (Fig. 4.10, grid ref. 22056125). The bedding is folded by sinistral kink folds (scale on lens cap is 5cm) **(b)** The angular unconformity between the Courtown Fm. (Duncannon Grp.) and the underlying Riverchapel Fm. (Ribband Grp.). The unconformity is irregular with several 10's cm of relief (dashed line) in-filled by sediments of the Courtown Fm. The bedding (solid lines) in the Riverchapel Fm. dips NW and is overturned while that in the Courtown Fm. dips SE and is the right way-up. Note that the cleavage (dotted line) (& folds) post date the unconformity. North of the shipwreck (Fig. 4.10, grid ref. 21946107) (Pen for scale).

Brenchley & Treagus 1970; Tietzsch-Tyler *et al.* 1994b). This is a fossiliferous, white to blue limestone, calcareous sand and siltstone with a discontinuous basal conglomerate up to 1m thick. Clasts within the conglomerate are often composed of weathered, banded siltstones probably derived from the underlying Riverchapel Formation. Some beds within the formation appear to be mainly composed of volcaniclastic debris. Cross-bedding and grading can be seen in the coarser calcareous sandstone units (Plate 4.6(a)) and many fossils are fragmented suggesting current flow in a shallow water depositional environment. Cleavage is never penetrative, but is spaced and often anastomosing (Plate 4.6(b)). Refraction of the cleavage due to differences in lithology and grainsize are particularly marked in this formation (Plate 4.7(a)). Outcrops occur at several places to the north of Duffcarrick Rocks (Fig. 4.10), in particular around Seafield (grid ref. 212592) and the shipwreck north of Kildermot (grid ref. 219609).

Ballinatray Formation. (Table 4.2, Fig. 4.10, Brenchley & Treagus 1970; Tietzsch-Tyler *et al.* 1994b). Outcrops of this lithology are generally of small areal extent and their contacts with the Courtown Formation and overlying Campile Formation appear to be largely tectonic (Plate 4.7(b)). The rocks are black to dark-grey, laminated mudstones with occasional, pale, silty laminae. Cleavage is strongly developed, penetrative and is often the main planar fabric in these rocks (Plate 4.8(a)).

Campile Formation. (Table 4.2, Fig. 4.10, Brenchley & Treagus 1970; Tietzsch-Tyler *et al.* 1994b). Formerly the Ballymoney Formation (Brenchley & Treagus 1970), this is a succession of intermediate to acid tuffs. They are particularly well exposed at Duffcarrick Rocks, Ballymoney and Kildermot (Fig. 4.10). Bedding is generally of a massive nature. However, around Ballymoney (grid ref. 21576003) thin tuffs are interbedded with thin mudstones. The presence of slumps within some of these units suggests deposition in water (Plate 4.8(b)). Brenchley & Treagus (1970) note the presence of a number of laharic breccias up to 1m thick throughout the succession (Plate 4.9(a)). Cleavage is weak or absent in the massively bedded units and lahars, but well developed and penetrative within the bedded sequences (Plate 4.9(b)).

4.5 General structure

Three phases of deformation can be recognised within the area. The first phase which has only been identified in the Cahore Group in the southernmost part of the

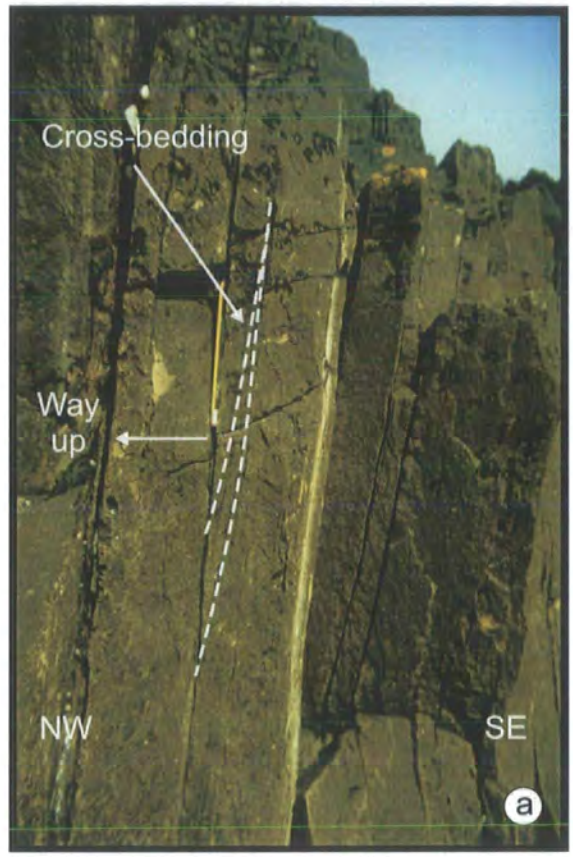

Plate 4.6. **(a)** View looking at end of steeply NW dipping bedding of the Courtown Fm. Cross-bedding (labelled) indicates younging to NW (grid ref. 21786064, Fig.4.10). **(b)** Looking down on steeply SE-dipping cleavage within the Courtown Fm. Cleavage planes have an anastomosing geometry.

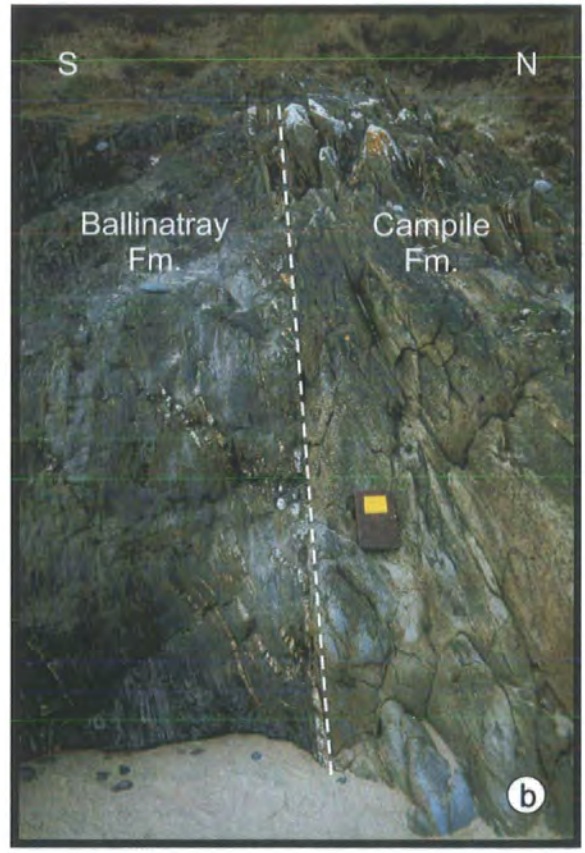

Plate 4.7. **(a)** Refracted cleavage within the Courtown Fm. on northern limb of an anticline. Bedding (highlighted) dips moderately to NW and cleavage dips steeply to NW. Southern end of Seafield (grid ref. 21245925, Fig. 4.10). **(b)** Faulted contact between the mudstones of the Ballinatray Fm. and the overlying volcanics of the Campile Fm. North end of Duffcarrick Rocks (grid ref. 21175890, Fig. 4.10)

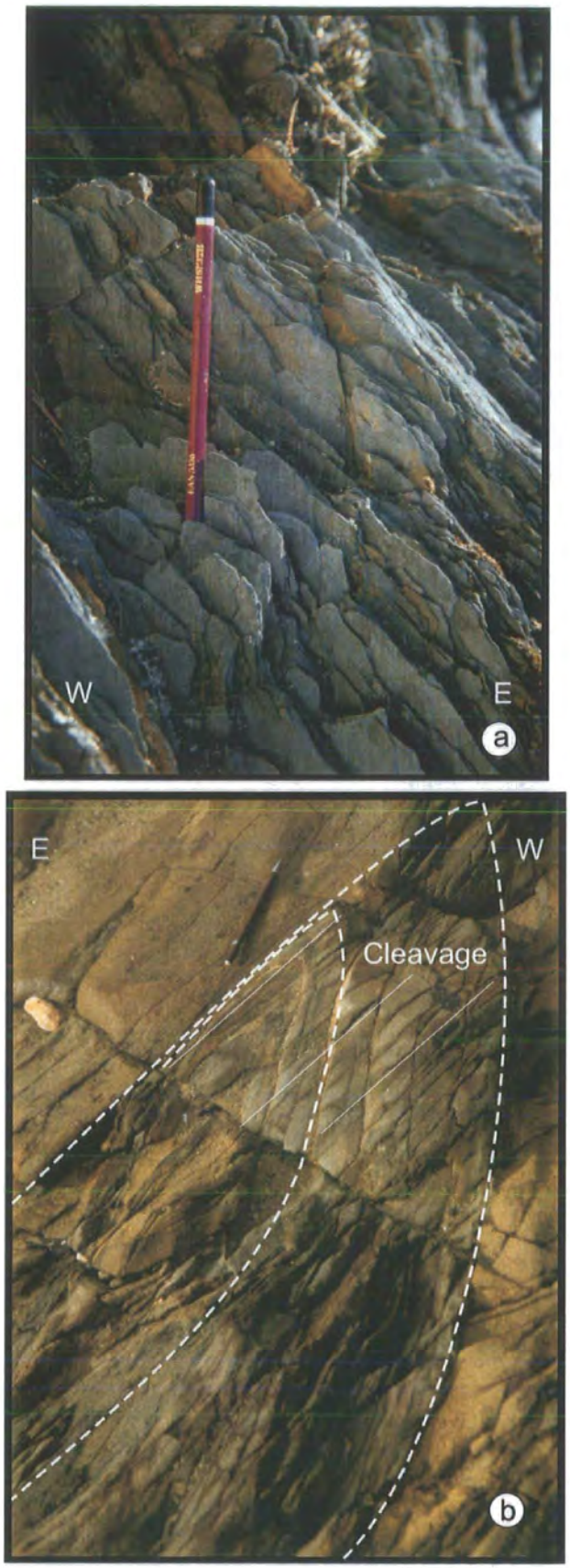

Plate 4.8. **(a)** Strong penetrative cleavage within dark mudstones of the Ballinatray Fm. Feint bedding traces can be seen within the cleavage planes. The pencil shows the plunge of the intersection lineation. (Fig 4.10, grid ref. 21255878). **(b)** Slump fold due to soft sediment deformation (outlined), indicating that the sediments were deposited in water. Tectonic cleavage is only visible within the finer grained units and not the bounding coarse grained beds. Near Ballymoney (Fig. 4.10, grid ref. 21576003).

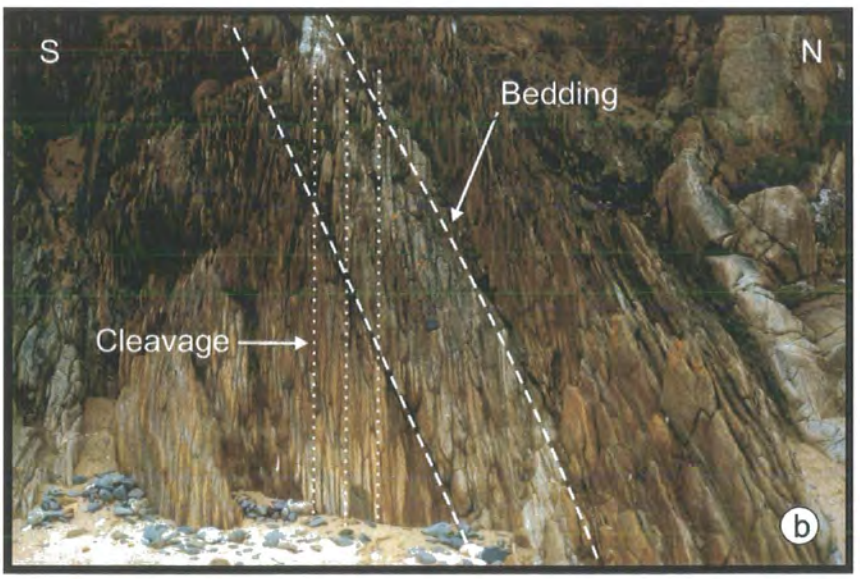

Plate 4.9. **(a)** Agglomerate within the Campile Fm. Mug is 20cm high. North of Kildermot (grid ref. 21836087, Fig. 4.10) . **(b)** Bedding and cleavage relationship in bedded tuffs of the Campile Fm. at Ballymoney (grid ref. 21556000, Fig. 4.10). Bedding dips moderately to NW. Cleavage dips steeply to SE. Intersection lineation plunges gently SW.

study area around Cahore Point (Fig. 4.9) consists of a weak SE-facing cleavage with no identified associated folds (see below). This has been refolded by a second and regionally dominant phase of deformation, producing moderately inclined to upright folds that plunge gently to steeply NE or SW. Locally, fold hinges are highly curvilinear , passing through the vertical to display upward and downward facing relationships. Cleavage, where developed, is generally axial planar. The main phase structures are post-dated by a braided network of ENE-to NE-trending, sub-vertical sinistral shear zones and fault arrays that are heterogeneously developed throughout the study area. The largest structure, the Courtown Shear Zone, forms a ca. 1km wide ENE-trending belt of sinistral shear located between Salt Rock and Glenbeg Head (Fig. 4.9). The effect of the regional unconformity separating the Cahore and Ribband Group and the Duncannon Group on the structure within the study area will be discussed later in this chapter.

Despite the extensive polyphase deformation on cm to m scales, the general impression of the main phase of deformation along the coastal exposure between Cahore Point and Kilmichael Point (Fig. 4.6) is that of a NW-dipping and SE-verging folded sequence (Fig. 4.12(i)). Poles to bedding lie along a rather diffuse NE-dipping girdle that defines a shallowly SW-plunging β axis. The reasonably well-defined broad point maximum is consistent with a steeply NW-dipping mean bedding plane (Fig. 4.12(i)). Minor primary fold axes are distributed very significantly along a girdle lying sub-parallel to the mean fold axial plane (Fig. 4.12(ii)). This suggests that the fold hinges are significantly curvilinear, something that is confirmed by field observations (see below). The main cleavage is variably developed throughout the section and appears to be lithologically controlled. Fine-grained lithologies, such as the Ballinatray and Riverchapel Formations contain a strong, penetrative fabric (Plate 4.10(a) and (b)), whilst coarser lithologies such as the Roney Point Formation show little evidence of cleavage. No mineral lineations are visible on exposed cleavage surfaces. Cleavage-bedding intersection lineations (BCIL) and poles to cleavage planes are broadly consistent with the primary minor fold plunges and axial plane data. However, the BCIL show a SW-plunging maxima, with a mean plunge that is steeper (ca. 25°) than the mean fold plunge (Figs. 4.12(ii) and 4.12(iii)). The mean cleavage plane exhibits a small amount (ca. 4°) of apparent clockwise transection (Fig. 4.12(iv)). Fold and cleavage facing directions collectively exhibit approximately 270° of variation, from sideways NE, through upwards to SW sideways and downwards (Figs. 4.13(i) and

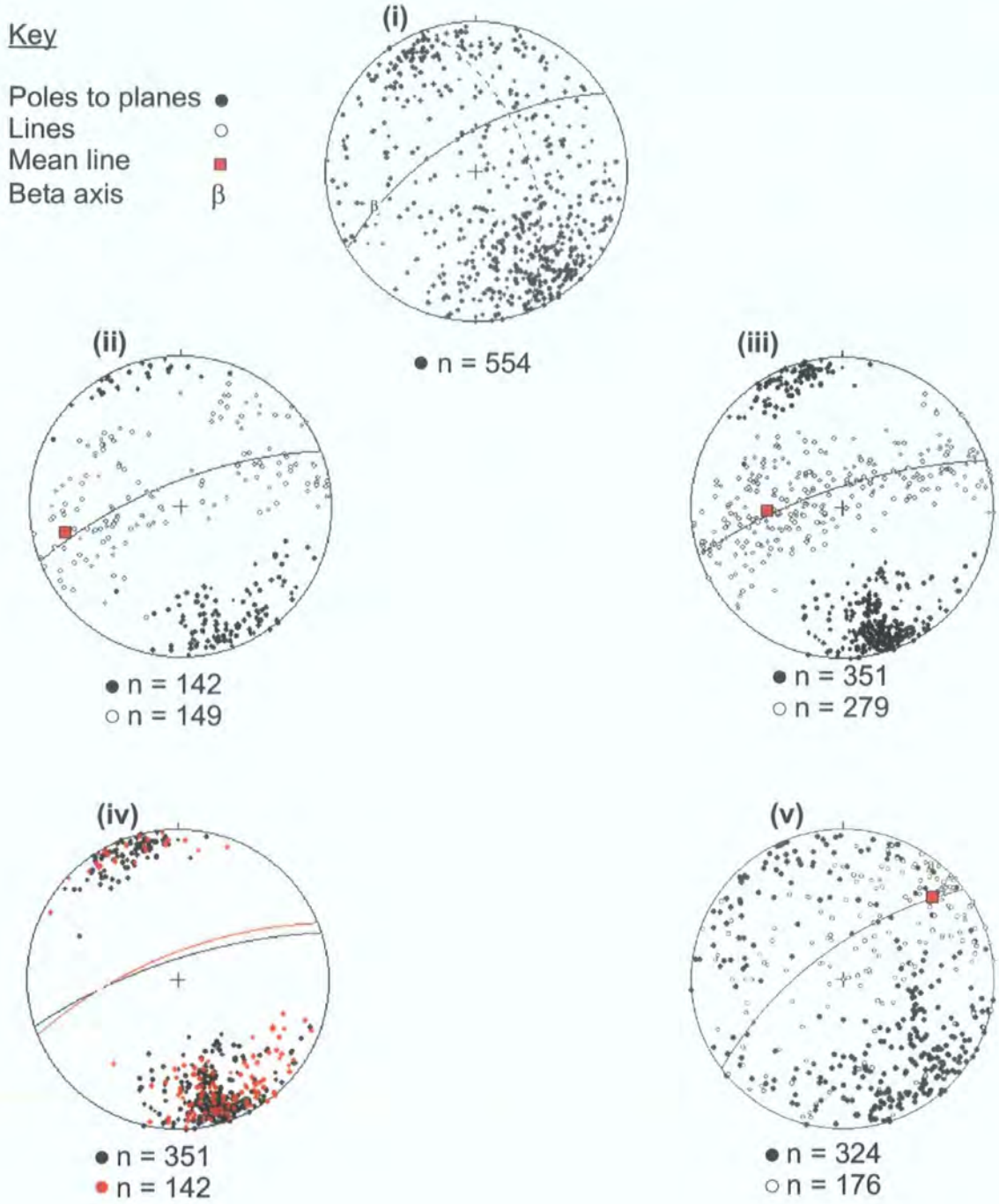

Figure 4.12. Stereoplots of structural data from the area between Cahore Point and Kilmichael Point. **(i)** Poles to bedding, with best-fit great circle (dashed, 160/61N), Mean bedding (solid, 059/70N) and regional β axis (29/250). **(ii)** Poles to fold axial planes and fold hinges, with mean fold hinge (24/257) and axial plane (solid black, 068/76N) shown. **(iii)** Poles to cleavage and bedding-cleavage intersection lineation (BCIL), with mean BCIL (49/267) and cleavage plane (solid black, 072/79N) shown. **(iv)** Poles to fold axial planes and cleavage with mean planes shown. Fold axial planes (red, 068/76N) and cleavage (black, 072/79N). ca. 4° of apparent clockwise transection. **(v)** Poles to fault planes and slickenfibre lineations with mean mean lineation (21/047) and fault plane (solid, 053/73N) shown.

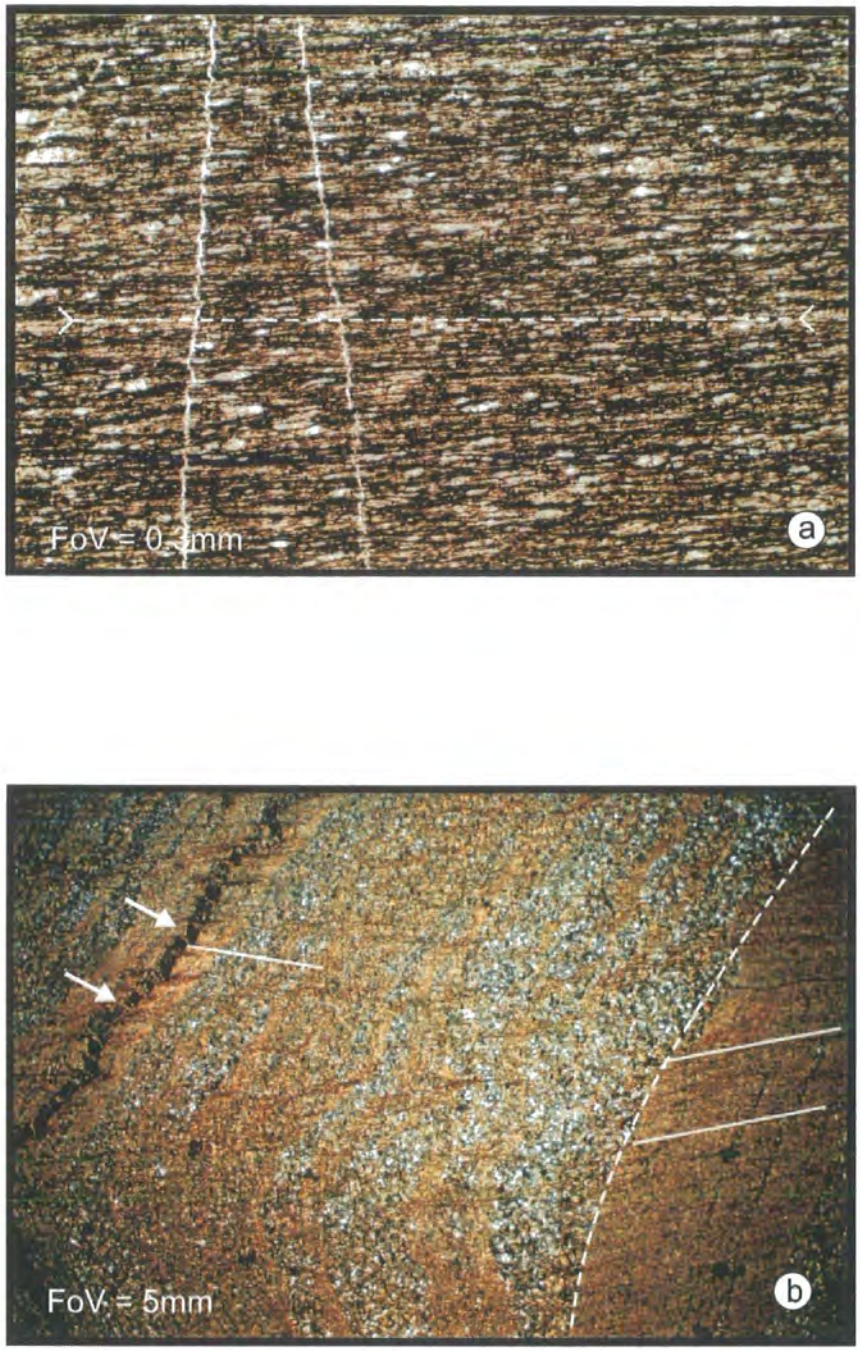

Plate 4.10. Thin section micrographs showing the main tectonic cleavage in rocks from the Cahore Point-Kilmichael Point section. **(a)** Slatey cleavage (highlighted) defined by elongated and flattened quartz grains within the mudstones of the Ballinatray Fm (taken in PPL. sample IBM 4(b), grid ref. 21485983). **(b)** Pressure solution cleavage within the siltstones of the Riverchapel Fm. Orientation of bedding and cleavage is shown by the dashed and solid lines repectively. The quartz vein (arrowed) shows small offsets due to pressure solution. (taken in XPL, sample IBM 1, grid ref. 21686045).

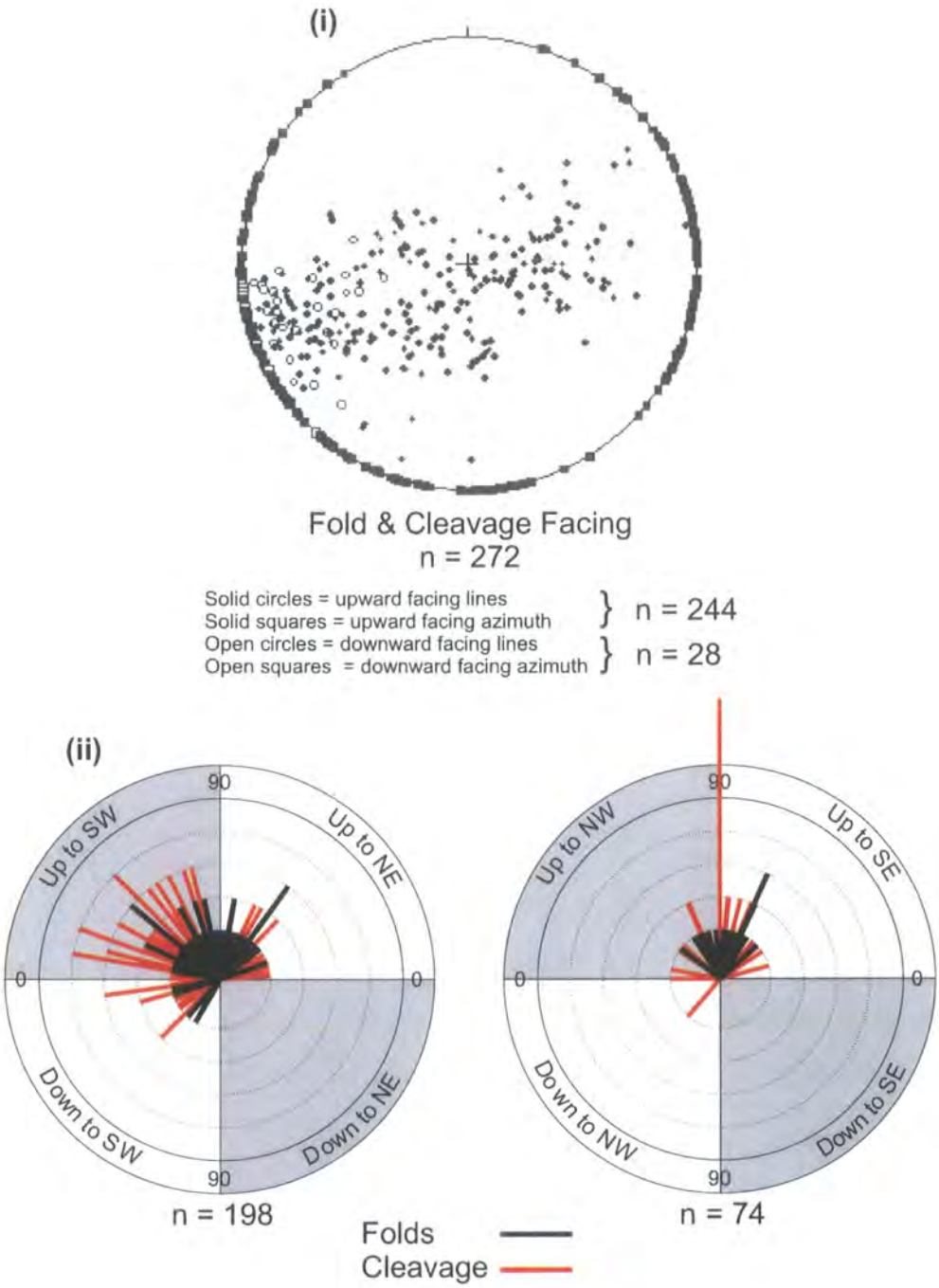

Figure 4.13. Facing data from the area between Cahore Point and Kilmichael Point **(i)** Fold and cleavage facing lines and azimuths plotted using the construction method of Holdsworth (1988) (see section 1.3). **(ii)** Plots showing the pitch of fold and cleavage facing directions in planes parallel to the fold axial and cleavage planes in which they were measured.

4.13(ii)). The area is extensively faulted, displaying oblique thrusts, steeply inclined sinistral and dextral, possibly conjugate strike-slip faults and normal dip-slip faults (e.g. Plate 4.11(a), (b), Fig. 4.12(v)). Slickenfibre lineations show a wide range of orientations. Occasionally those on NE-trending, NW-dipping faults show complex patterns with steps indicating a sinistral and down-to-the NW sense of movement (Plate 4.12(a)). Many show shallow plunges (Plate 4.12(a), (b)), with a NE shallowly plunging mean lineation (Fig. 4.12(v)). Strike-slip deformation is widespread and heterogeneously distributed throughout the area. Three styles can be recognised, all of which appear to post-date the main phase of deformation:

1) The earliest phase is most strikingly exposed between Glenbeg Head and Salt Rock (Figs. 4.6, 4.9). Here a wide (ca. 1km), ENE-trending, sub-vertical, ductile, sinistral shear zone called the Courtown Shear Zone (see below) (e.g. Plate 4.13(a)) occurs.
2) A NE-trending braided network of semi-brittle and brittle, sinistral faults and kink folds at a scale of cm to several m's (e.g. Plate 4.13(b), (c)) (see below).
3) A series of sinistral and dextral, possibly conjugate, steeply inclined strike slip faults and tension gash arrays (Plates 4.11(b), 4.14(a), (b)). These may be broadly contemporaneous with 2 above (see below).

Detailed mapping of the Cahore Point to Kilmichael Point section shows that the deformation is polyphase and markedly heterogeneous on a mesoscale. Three distinct, possibly fault bounded domains (labelled 1-3 in Fig. 4.14) have been identified, which exhibit different structural styles that can be defined on the map scale. Domains 1 and 2 run NE-SW (labelled 1 and 2 in Fig. 4.14), lying sub-parallel to the regional strike and are thought to be broadly contemporaneous. Domain 3, the Courtown Shear Zone (labelled 3 in Fig. 4.14) strikes ENE and post-dates the main phase of deformation. The early deformation observed at Cahore Point, the structures in domains 1 and 2, the Courtown Shear Zone and the 'late' semi-brittle/brittle, sinistral fault arrays are now described separately.

4.6 Early deformation

In the southernmost part of the study area, around Cahore Point (Fig. 4.9), the rocks of the Glascarrig and Cahore Point formations preserve evidence of an early (pre-main phase deformation) cleavage (see sections 4.2 and 4.4.2). This weak fabric is only preserved in thin interbedded mudstones and is refolded by metre-to tens-of-metre-

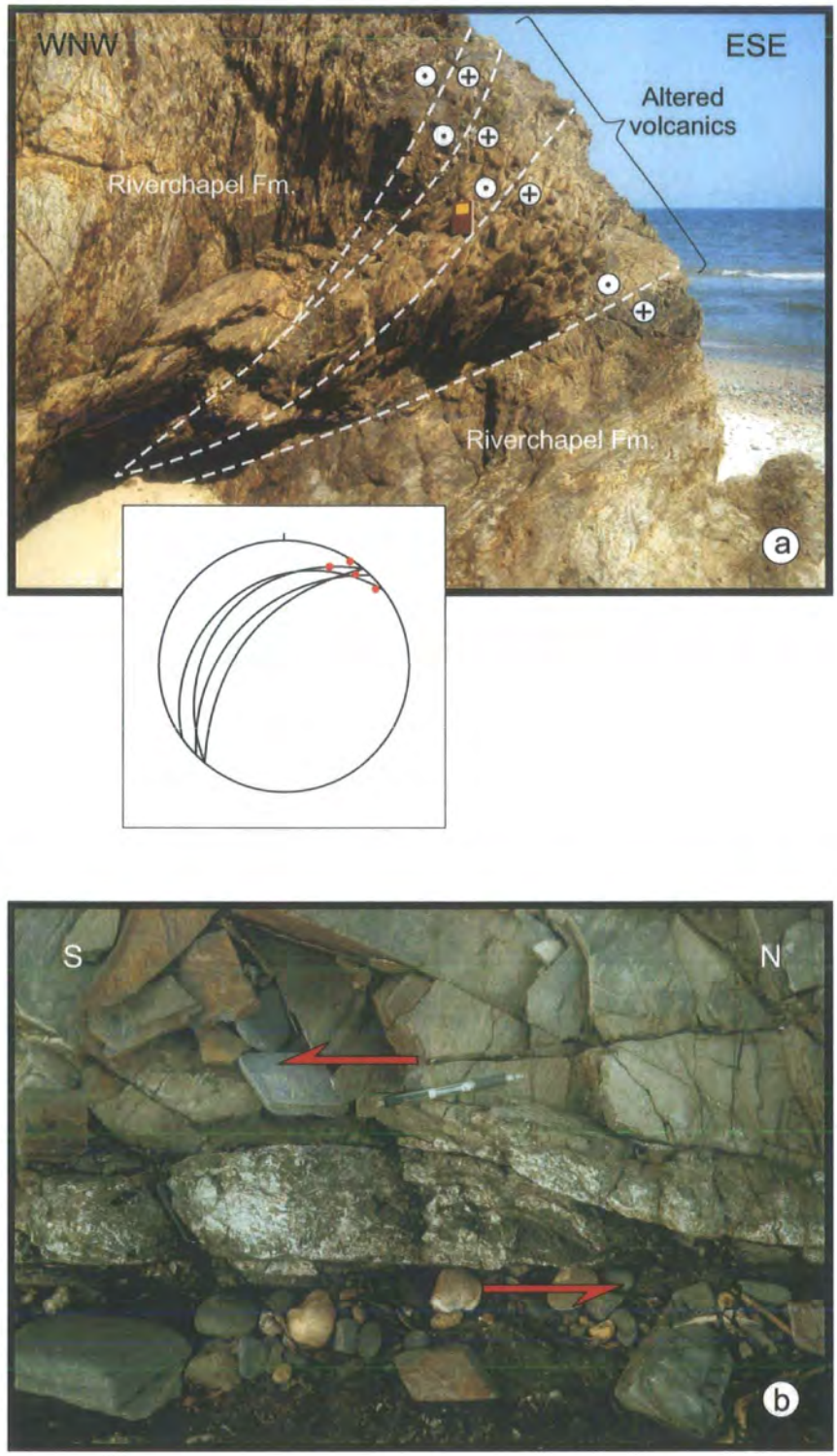

Plate 4.11. **(a)** Imbricated, NW-dipping strike-slip faults focused along and within altered volcanics north of Seafield. Inset shows stereonet of fault planes and associated slickenlines (Fig. 4.10, grid ref. 213359550). **(b)** Sinistral P-type shear with 30cm offset. Kilmichael Point (Fig. 4.11, grid ref. 25406622).

Plate 4.12. **(a)** SW-NE plunging, curved, sinistral, slickenfibres (dashed lines) overprinted by a second NE plunging set (solid lines) (Fig. 4.10, grid ref. 22026127). **(b)** Sub-horizontal slickenlines, plunge gently to NE. South of Breanoge Head (Fig. 4.9, grid ref. 20185571).

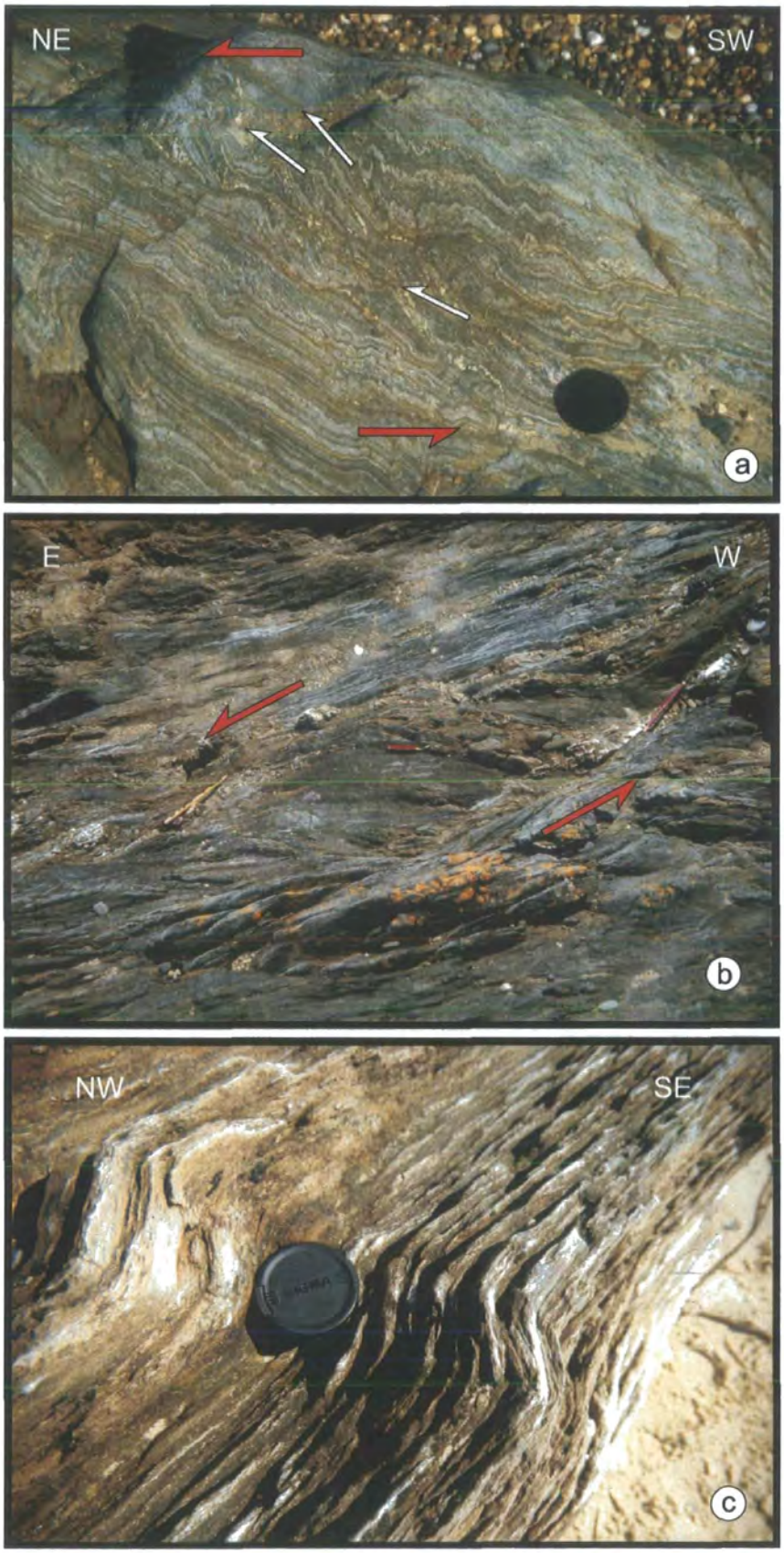

Plate 4.13. **(a)** Sinistral folds and minor faults in the Ballyhoge Fm. near Pollshone Head (Fig. 4.9, grid ref. 20495316). **(b)** Sinistral detachments bounding sigmoidal pod of mudstone. North of St. Peter's (Fig. 4.10, grid ref. 21495984). **(c)** Cleavage within calcareous sandstone of the Courtown Fm. folded by steeply plunging, sinistral kink folds. Seafield (Fig. 4.10, grid ref. 21235926).

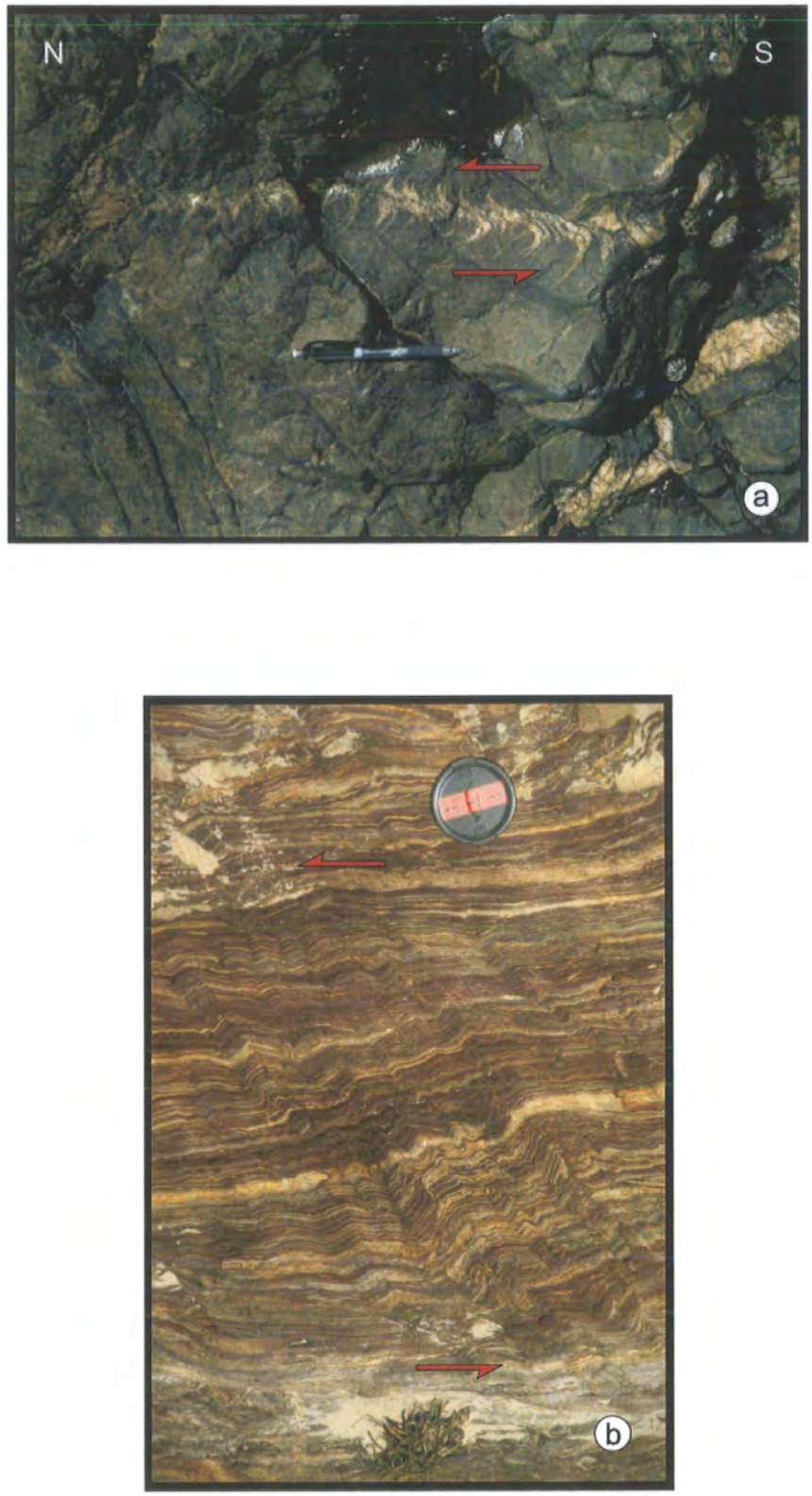

Plate 4.14b. (a) Sinistral tension gash array within a greywacke sandstone of the Glascarrig Fm. Glascarrig Point (Fig 4.9, grid ref. 21824932). **(b)** Sinistral kink folds in the Riverchaple Fm. North of the shipwreck (Fig. 4.10 grid ref. 22056125).

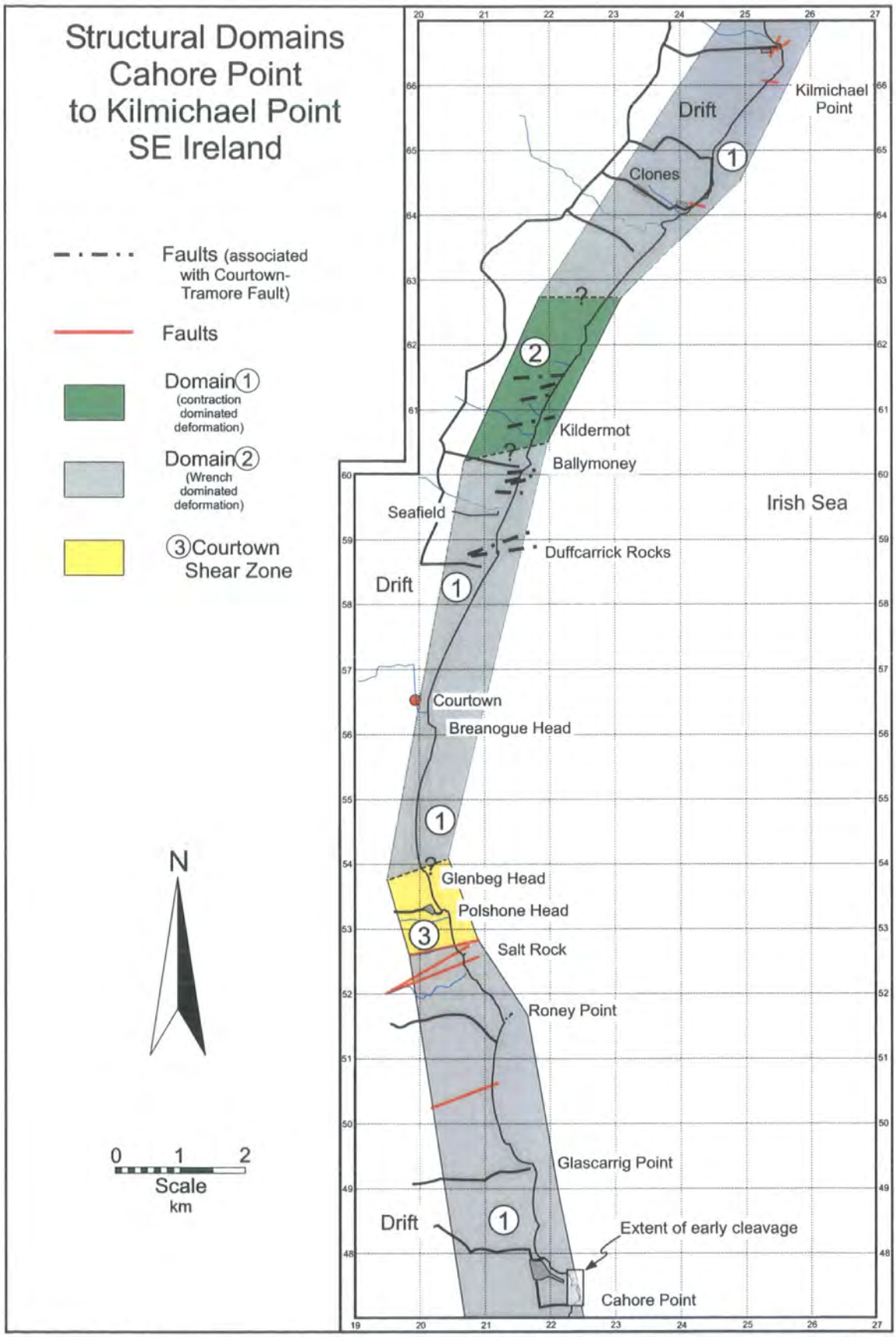

Figure 4.14. Map of structural domains identified along the coast between Cahore Point to Kilmichael Point. Underlying geological mapping based on mapping from this study, Crimes and Crossley (1968), Brenchley and Treagus (1970) and Tietzsch-Tyler *et al.* (1995).

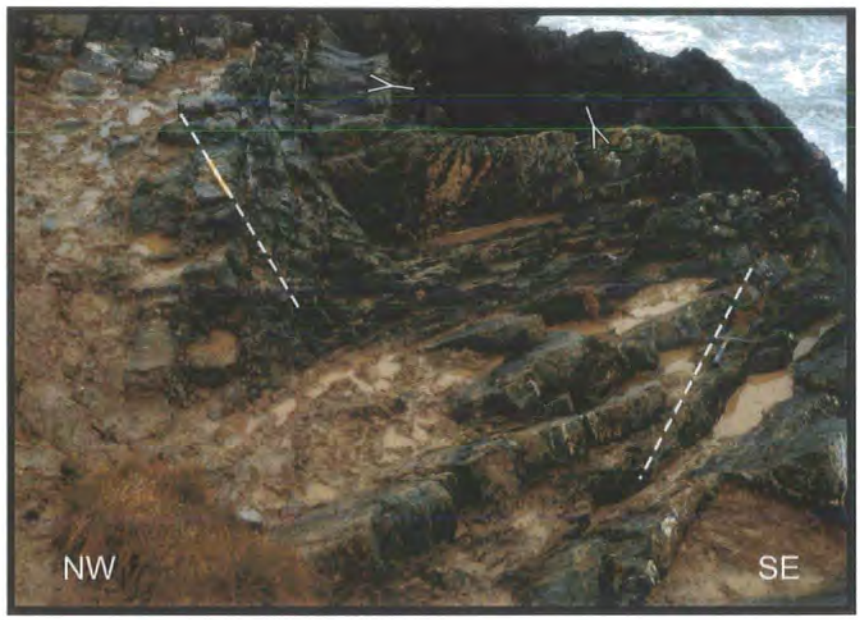

Plate 4.15. SE-verging fold near to Cahore Point (Fig 4.9, grid ref. 22502339). Early cleavage highlighted. In upper overturned limb cleavage faces down to the SE, whilst in right way-up lower limb cleavage faces up to the SE (see Fig. 4.16(a) below).

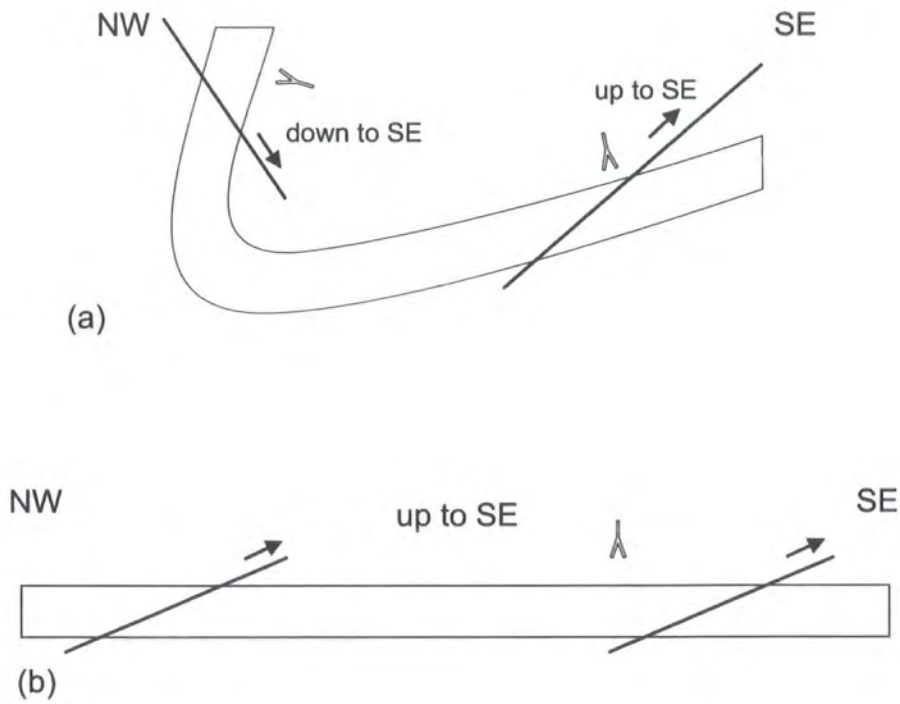

Figure 4.16. **(a)** Sketch of plate 4.15, showing orientation and facing direction of the early cleavage. **(b)** Restoring the bedding back to horizontal shows that early cleavage originally faced up to the SE.

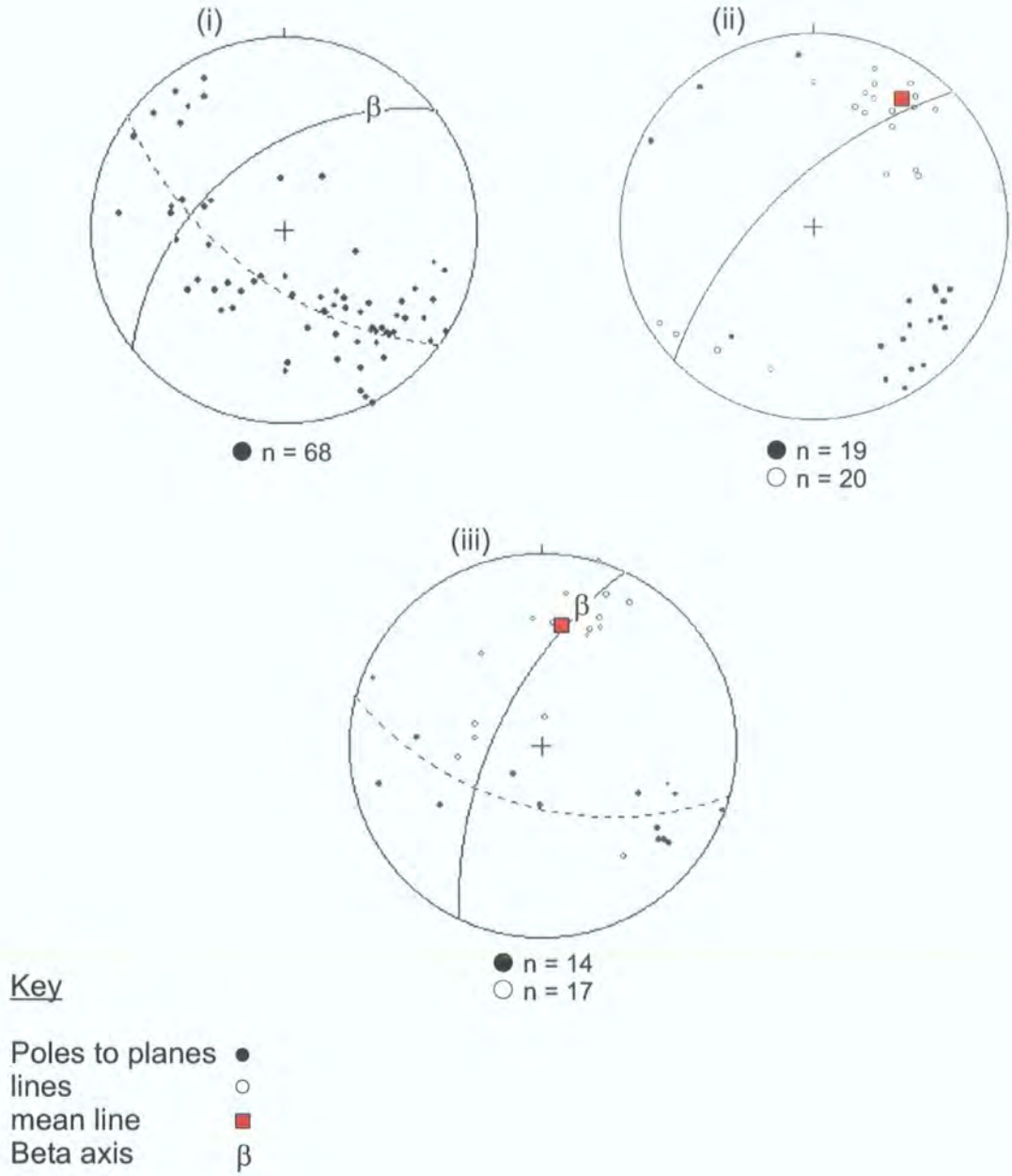

Figure 4.15. Stereoplots of structural data form Cahore Point. **(i)** Poles to bedding with, best-fit great circle girdle (dashed, 127/68S), mean plane (solid, 052/57N) and β axis (22/036) shown. **(ii)** Poles to main fold axial planes and fold hinges, with mean fold hinge (21/035) and axial plane (solid, 046/71N) shown. **(iii)** Poles to early cleavage and cleavage-bedding intersection lineation (BCIL), with mean BCIL (open square 37/009), cleavage (solid, 025/70N), best-fit great circle girdle (dashed 105/64S) and β axis (26/015) shown.

scale, SE -verging main phase folds (Plate 4.15).

At Cahore Point, poles to bedding (Fig. 4.15(i)) show a broad maxima corresponding to a steep, NW-dipping mean homoclinal plane. A subordinate number of bedding poles have been spread along a girdle to define a shallow, NE-plunging β axis. This corresponds well with the mean plunge of the main phase folds (Fig. 4.15(ii)). Poles to the early cleavage (Fig. 4.15(iii)), show a maxima corresponding to a steep, NW-dipping mean plane. Cleavage planes are significantly spread along a girdle that defines a shallow, NE-plunging β axis, that correlates closely with the maxima of their associated cleavage-bedding intersection lineation (BCIL) (Fig. 4.15(iii)) suggesting that the cleavage planes are folded. A comparison between the stereonets for the main phase fold axial plane and plunges and the early cleavage planes and their associated BCIL (Fig. 4.15(ii), (iii)) shows a close geometric relationship. This suggests that the early cleavage has been folded by the later main phase folds. The early cleavage is observed to face down to the SE in the overturned NW-dipping fold limbs and up to the SE in the NW-dipping normal limbs (Fig. 4.16(a), Plate 4.15). Restoring the folded bedding to the horizontal, shows that the early cleavage faced up to the SE prior to folding (Fig. 4.16(b)).

4.7 Description of structural domains

4.7.1 Domain 1

Comprising the greater part of the study area, Domain 1 is divided into two sections that lie either side of Domain 2 (Fig. 4.14). The southern section runs from Cahore Point through to the beach at Ballymoney Fisheries (Figs. 4.6, 4.9, 4.10). The northern boundary with Domain 2 is not exposed, but may be fault controlled. The northern section runs from north of the shipwreck to Kilmichael Point (Figs. 4.6, 4.10, 4.11). Again, the boundary with Domain 2 is not exposed and may be a fault. The structures in both sections are similar and are therefore described as a single domain.

Poles to bedding (Fig. 4.17a(i)) show a somewhat diffuse distribution. However, they define a broad maxima corresponding to a steep, NW-dipping mean homoclinal plane. The domain is folded by a series of sub-metre to 10's of metre scale folds that spread a subordinate number of bedding poles along a girdle that indicates a shallowly WSW-plunging β axis (Fig. 4.17a(i)). This corresponds well with the mean plunge of the main folds and bedding-cleavage intersection lineation (Fig. 4.17a(ii),

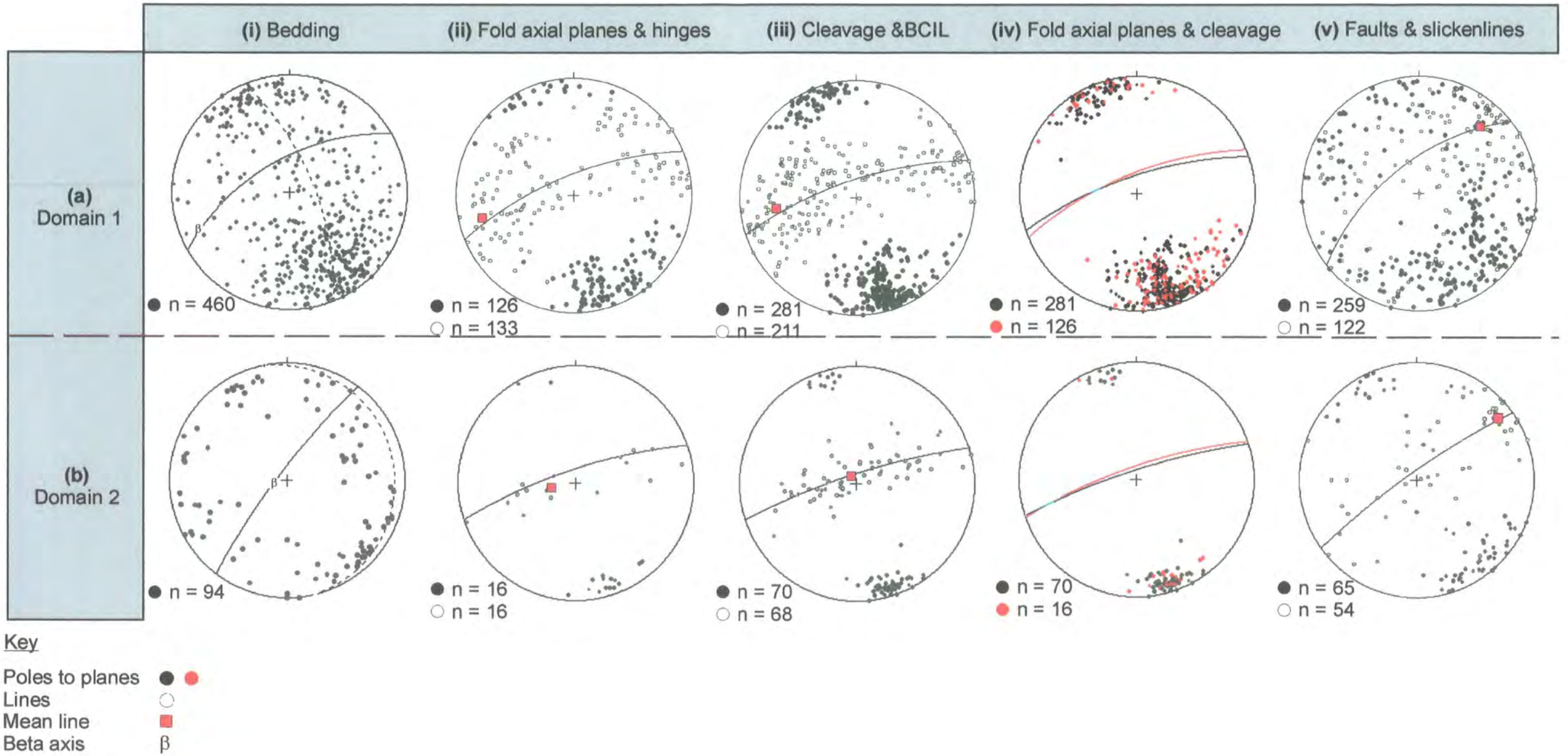

Figure 4.17. Stereoplots of structural data from **(a)** Domain 1 and **(b)** Domain 2. **(a(i))** Poles to bedding with best-fit great circle girdle (dashed, 158/73E), mean bedding (solid, 060/67N) and regional β axis (17/248). **(a(ii))** Poles to fold axial planes and fold hinges, with mean fold hinge (21/256) and axial plane (068/76N) shown. **(a(iii))** Poles to cleavage and bedding-cleavage intersection lineation (BCIL), with mean BCIL (32/262), and cleavage (072/78N) shown. **(a(iv))** Poles to fold axial planes and cleavage, with mean axial plane (solid, 068/76N) and cleavage (red, 072/78N) shown. **(a(v))** Poles to fault planes and slickenline lineations with mean lineation (24/044) and fault plane (052/68N) shown. **(b(i))** Poles to bedding with best-fit great circle girdle (dashed, 167/10E), mean bedding (solid, 037/84N) and regional β axis (80/257). **(b(ii)).** Poles to fold axial planes and fold hinges, with mean fold hinge (73/258) and axial plane (071/81N) shown. **(b(iii))** Poles to cleavage and bedding-cleavage intersection lineation (BCIL), with mean BCIL (83/331), and cleavage (072/83N) shown. **(b(iv))** Poles to fold axial planes and cleavage, with mean axial plane (solid, 071/81N) and cleavage (red, 072/83N) shown. **(b(v))** Poles to fault planes and slickenline lineations with mean lineation (15/051) and fault plane (053/83N) shown.

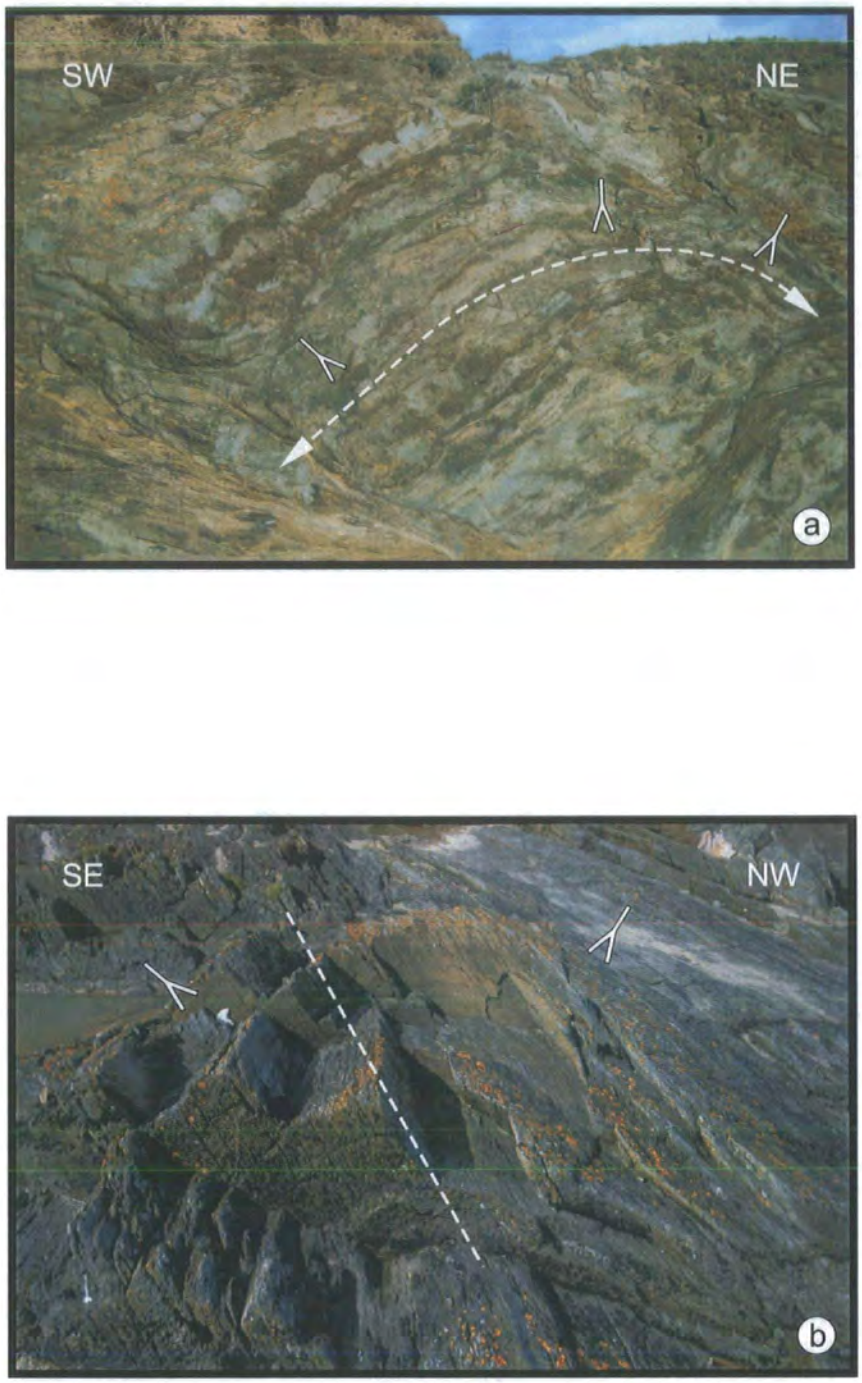

Plate 4.16. **(a)** Longitudinal hinge-parallel section through curvilinear folds in plane of cleavage. Fold hinge plunges to both SW and NE. Height of outcrop is 3m. Duffcarrick Rocks (Fig. 4.10, grid ref. 21175883) **(b)** SE-verging S-folds and axial planar cleavage (dashed line). Field of view 2m. Kilmichael Point (Fig. 4.1, grid ref. 25606661).

(iii)), which show a wide range of hinge line curvilinearity (Plate 4.16(a)).

The stereonets for cleavage and fold axial planes (Fig. 4.17a(ii), (iii)) suggest that the mean cleavage lies slightly clockwise (ca. 4°) of the mean axial plane (Fig. 4.17a(iv)). This relationship is repeated for the mean bedding-cleavage intersection lineation and the mean fold plunge (Fig. 4.17a(ii), (iii)). The relationship however, may not be statistically significant, as field observations suggest that throughout Domain 1 cleavage and axial planes are essentially parallel (Plate 4.16(b)) with only two observed occurrences of folds transected by their cleavage were recorded. The first, in folds within the volcanics of the Campile Formation on the north side of Duffcarrick rocks (Fig. 4.10, grid ref. 21175876), where the axial plane is clockwise transected by 6°. The second occurs in the Ballylane Formation at Clones (Fig. 4.11, grid ref. 24386424), where the fold is anticlockwise transected by approximately 9° (Plate 4.17(a)). Fold and cleavage vergence varies across the domain (e.g. Plates 4.16(b), 4.17(b), 4.18(a)), from SE through neutral to NW, although most verge to the SE as indicated by the steeply inclined mean planes and cross-sections (Figs. 4.17a(ii), (iii), 4.9, 4.10, 4.11). Throughout the domain, the main folds and cleavage face predominantly upwards to both the SW and NE at shallow to moderate angles (Fig. 4.18(i), (ii), Plates 4.16(a), 4.18(b)).

Poles to faults form a diffuse point maxima that define a NE-trending, moderate to steeply NW-inclined mean plane (Fig. 4.17a(v)). Though several sets of faults can be observed in the field, cross-cutting relationships are very scarce; therefore, identifying different generations of faults is problematic. A number of steeply inclined ENE-NE-trending faults with dip-slip movements define some contacts between formations (e.g. Plates 4.3(b), 4.7(b)). However, the sense of movement has largely been determined on stratigraphical grounds rather than by utilising kinematic indicators such as stepped slickenfibres or fault drag. Several NW-dipping low-angle reverse faults contain shallowly to moderately plunging slickenfibres indicating a sinistral strike-slip to top-to-the SE oblique-reverse movement sense (e.g. Plates 4.11(a), 4.19(a)). The predominant fault set, however, is the braided network of mainly sinistral, steeply inclined strike-slip faults (e.g. Plates 4.11(b), 4.13(b)). These will be discussed fully later in this chapter.

4.7.2 Domain 2

Domain 2 (Fig. 4.14) occupies an approximately 1.5km wide section of the coast

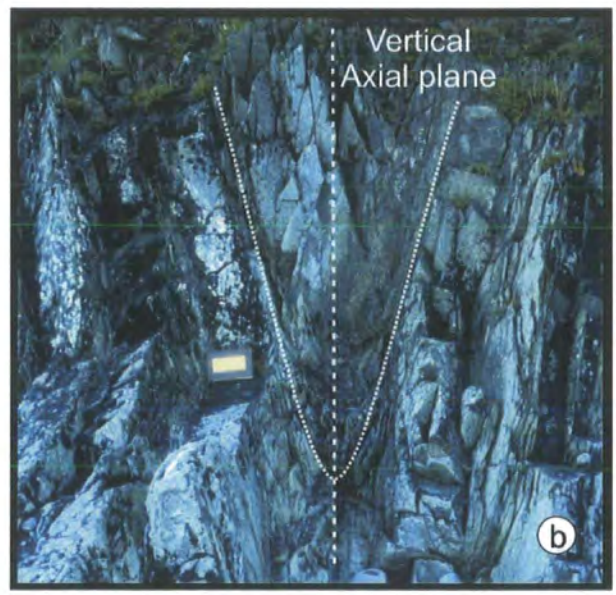

Plate 4.17. **(a)** Fold hinge anticlockwise transected by cleavage. Clones (Fig. 4.11 grid ref. 24386424). **(b)** Photograph illustrating the tight, upright fold style characteristic of the Glascarrig area. Note book for scale. North of Glascarrig Point (Fig. 4.9, grid ref. 21484963).

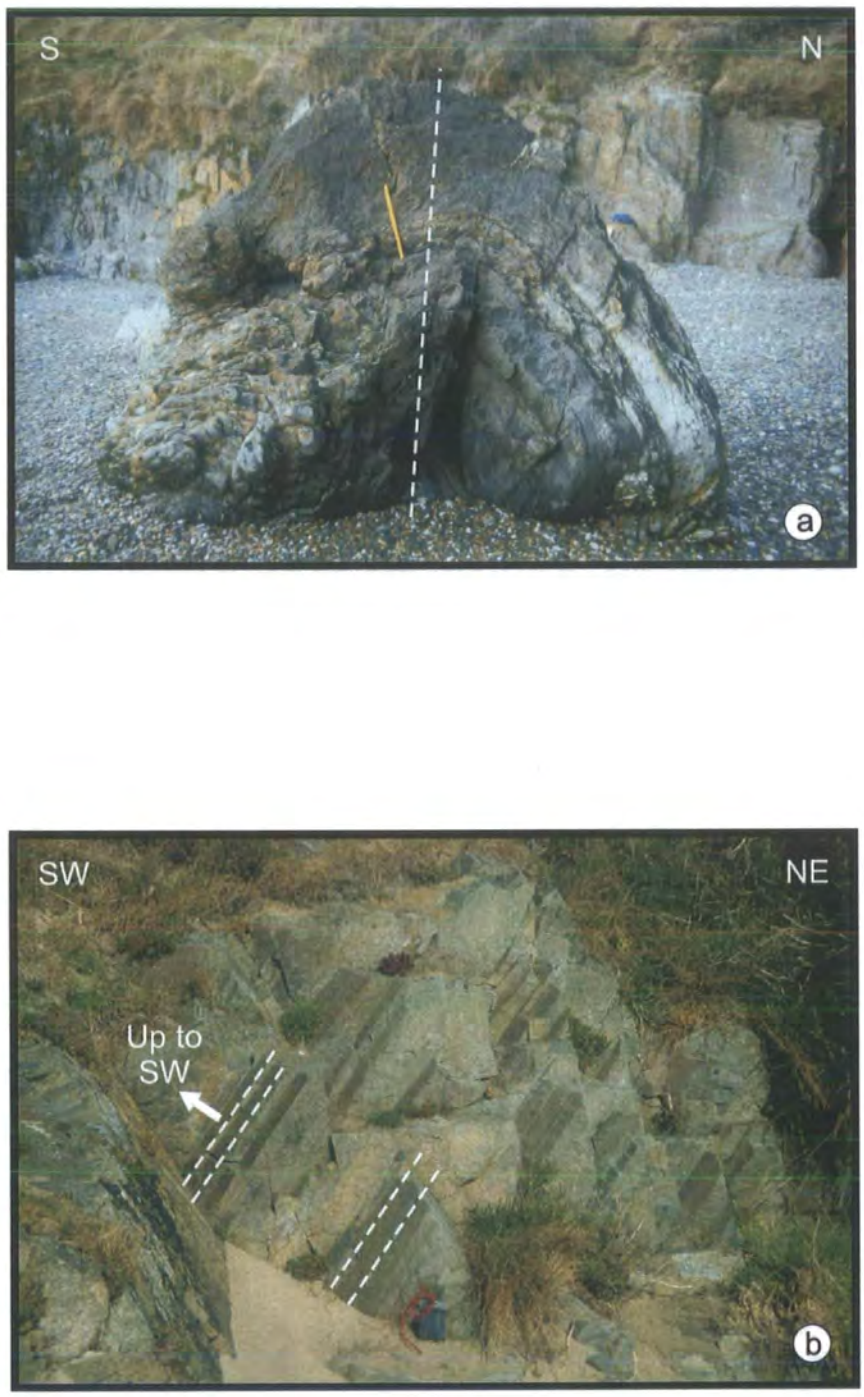

Plate 4.18. **(a)** NE-verging fold (axial plane highlighted) in calcareous sandstones of the Courtown Fm., Ballymoney (Fig. 4.10, grid ref. 21505989). **(b)** SW-plunging cleavage-bedding intersection lineation (highlighted) seen in the cleavage plane. Bedded volcanics of the Campile Fm., Ballymoney (Fig. 4.10, grid ref. 21566000).

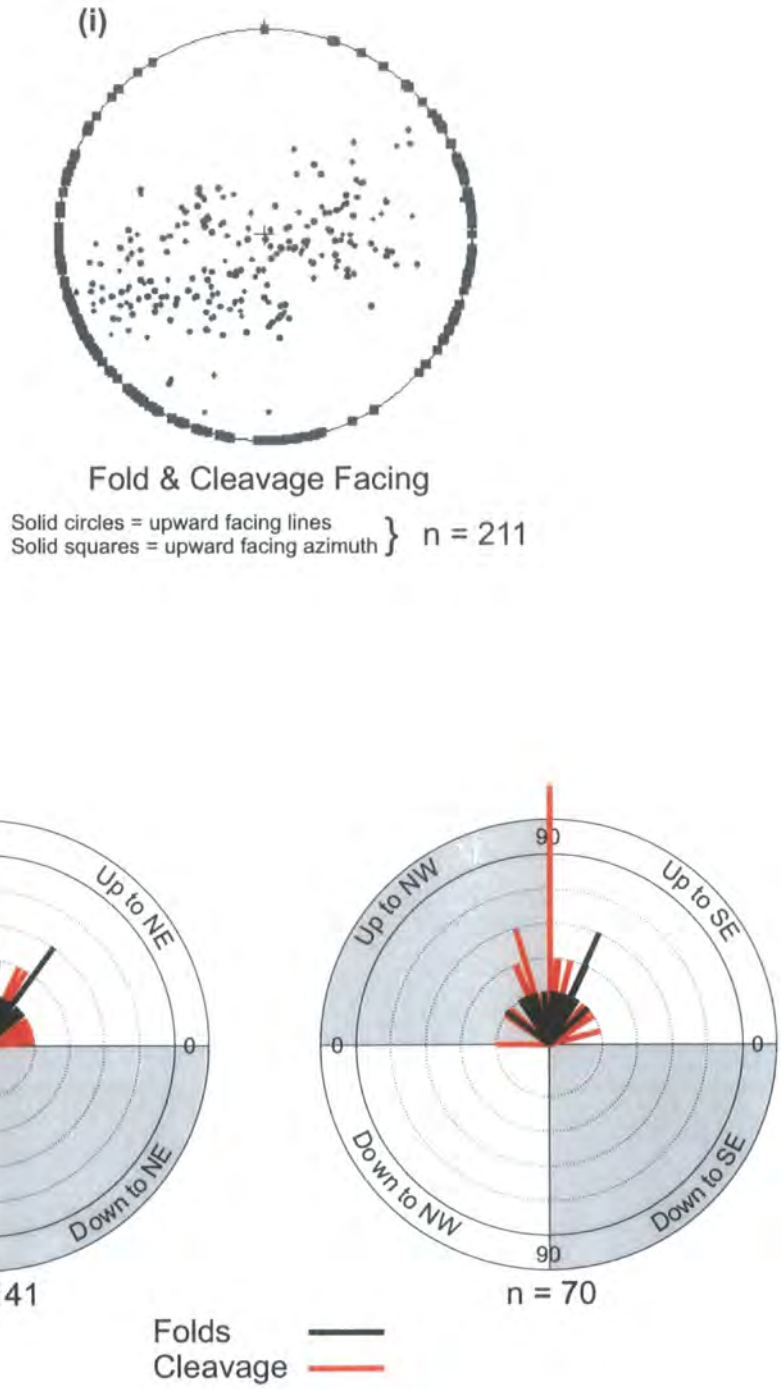

Figure 4.18. Fold facing data from domain 1 (Fig 4.14). **(i)** Fold and cleavage facing Lines and azimuths plotted using the construction method of Holdsworth (1988). **(ii)** Plots showing the pitch of fold and cleavage facing directions in planes parallel to the fold axial or cleavage planes in which they were measured.

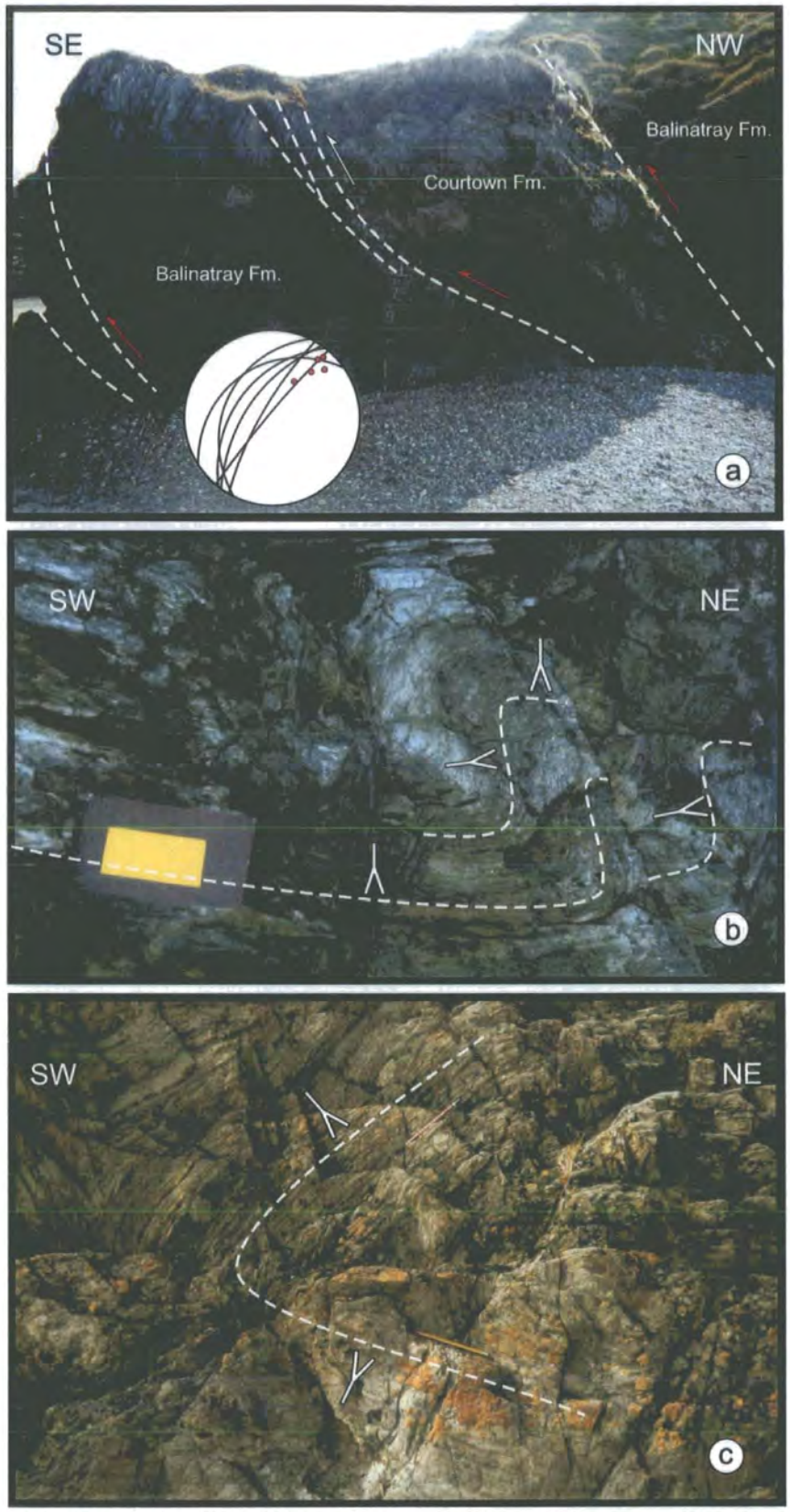

Plate 4.19. **(a)** Top-to-the-SE oblique thrusts emplace Courtown Fm. limestones on top of mudstones of the Balinatray Fm. Inset shows stereoplot of thrusts and slickenlines. Ballymoney (Fig. 4.10, grid ref. 215085989). **(b)** Highly curvilinear folds seen in the hinge-parallel, plane of cleavage. Folds that plunge steeply to NE face sideways and down to SW, whilst shallowly NE-plunging folds face up to NE. North of Ballymoney Fisheries (Fig. 4.10, grid ref. 21696044). **(c)** Upward, SW-facing and plunging folds and downward, SW-facing NE-plunging folds. Viewed in the hinge-parallel plane of cleavage, North of Ballymoney Fisheries (Fig 4.10, grid ref. 21766057). Pencil for scale.

north of Ballymoney Fisheries (Fig. 4.10). Bounded to the north and south by Domain 1, its boundaries are not exposed and its true extent cannot be calculated accurately.

Poles to bedding are broadly distributed, but a broad point maxima defines a sub-vertical NE-trending mean plane (Fig. 4.17b(i)). The area is extensively folded, spreading a subordinate number of bedding poles along a girdle that suggests a very steep SW-plunging β axis. This corresponds well with the mean fold hinge plunge and cleavage-bedding intersection lineation (Fig. 4.17b(ii), (iii)), which both show marked changes in hinge line curvilinearity often over distances of <1m (Plate 4.19(b), (c)). Most of the folds show a consistent sinistral vergence (S shapes) viewed down plunge. The stereonets for folds and cleavage are remarkably similar (Fig. 4.17(ii), (iii)). The mean cleavage plane lies only slightly (ca.1°) clockwise of the mean fold axial plane (Fig. 4.17(iv)) and is not statistically significant. Everywhere in Domain 2 field observations confirm that the fold axial planes and cleavage are parallel, although the mean cleavage-bedding intersection lineation lies significantly clockwise of the mean fold plunge. This may be an artefact of the steepness in plunge and the rather restricted fold data set due to a lack of meso-scale folds available for measurement. Fold axial planes and cleavage dip steeply NW, lying clockwise of the mean bedding orientation, as would be expected given the large number of sinistrally verging fold pairs (Fig. 4.17b (i)-(iii)). Minor folds and cleavage show predominantly SW facing directions, facing shallowly to steeply upwards where the folds plunge SW and moderately to steeply downwards where the folds plunge NE (Fig. 4.19(i), (ii), Plate 4.19(b), (c)). There are a subordinate number of NE-shallowly-plunging folds that face upwards to the NE (Fig. 4.19(i), (ii), Plate 4.19(b)). The rapid changes in the angle of plunge of fold hinges, the cleavage-bedding intersection lineation, and the facing directions of these structures were also noted by Brenchley & Treagus (1970).

Poles to fault planes display a less complex distribution than those for Domain 1, with a well-defined point maxima corresponding to a steep NW-dipping, NE-trending mean plane (Fig. 4.17b(v)). A significant number of slickenfibre lineations plunge gently to the NE and SW indicating a predominance of strike-slip movements. Occasional NE-trending faults show complex lineations patterns (e.g. Plate 4.20(a), (b)), with curved, stepped slickenfibres indicating oblique top-to-the-SE sinistral movements similar to those observed in Domain 1. Locally these contain an overprinting set of slickenfibres that plunge steeply to the NE, suggesting possible reactivation in an oblique dip-slip sense (Fig. 4.20, Plate 4.20(a), (b)).

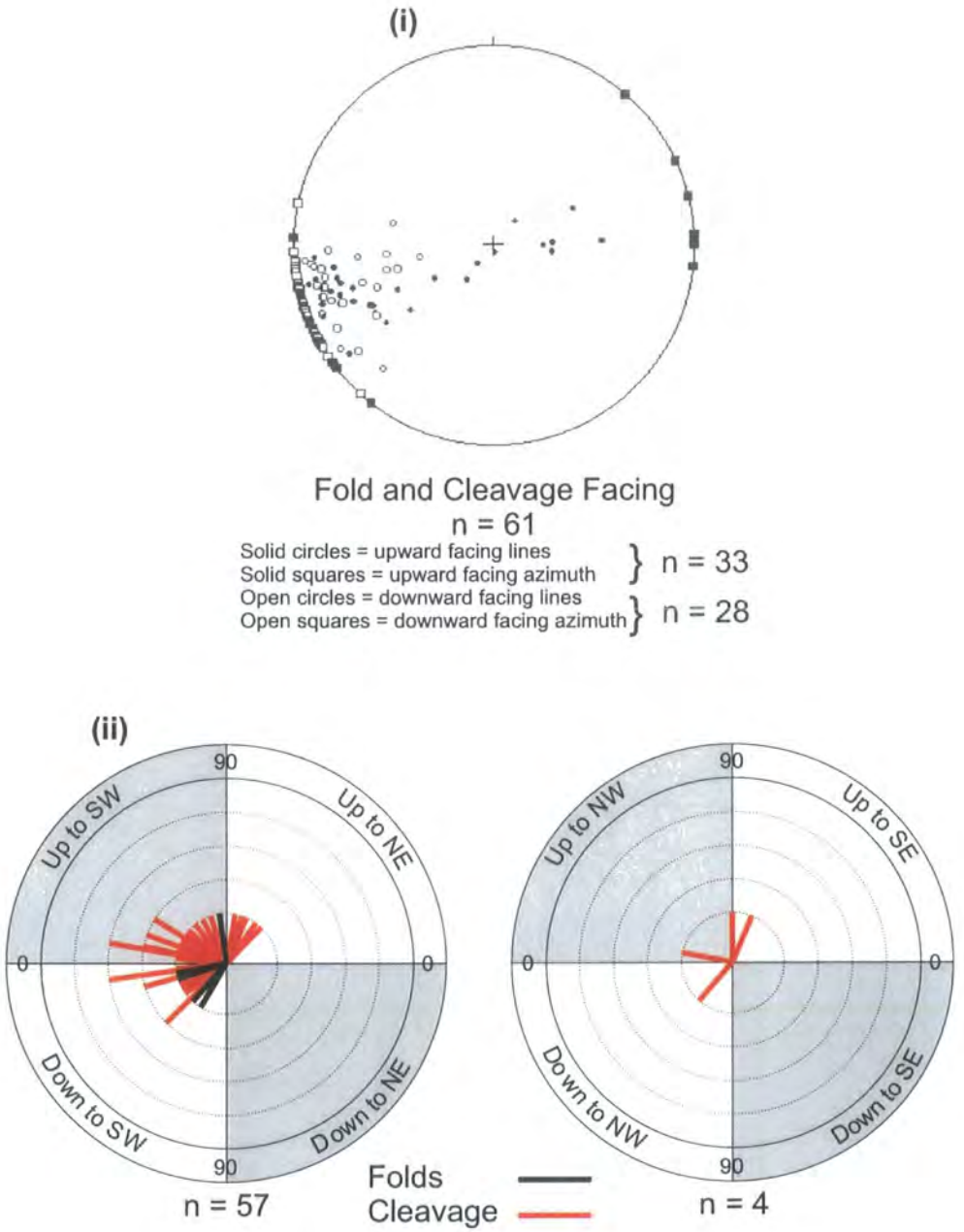

Figure 4.19. Facing data from domain 2. **(i)** Fold and cleavage facing lines and azimuths plotted using the construction method of Holdsworth (1988). **(ii)** Plots showing the pitch of fold and cleavage facing directions in planes parallel to the fold axial and cleavage planes in which they were measured.

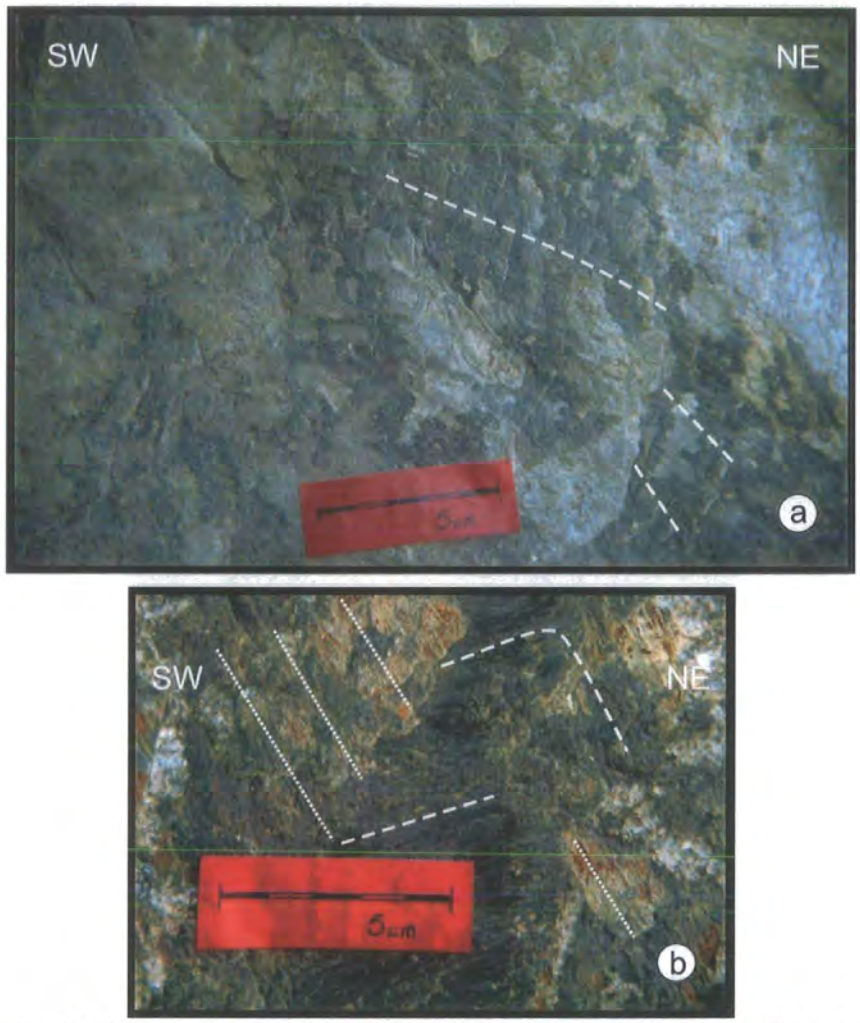

Plate 4.20. **(a)** Variable plunge of chlorite slickenfibres on NE-trending NW-dipping (i.e. away from viewer) fault plane. Steps on slickenfibres indicate top-to-SE movement. **(b)** Same fault as in **(a)** showing curved nature of chlorite slickenfibres. These are over-printed by a set of NE-plunging carbonate slickenfibres, suggesting two phases of movement along the same fault plane. Both photographs taken north of the shipwreck (Fig. 4.10, grid ref. 22026127)

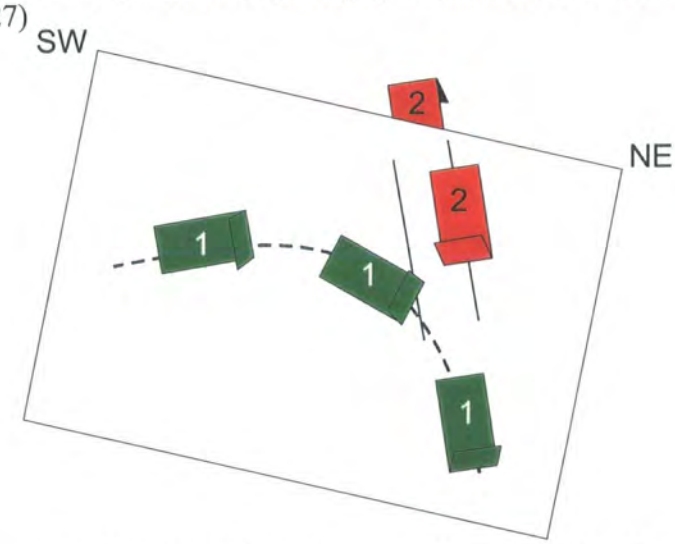

Figure 4.20. Diagram to show possible movements along the fault plane in Plates **(a)** & **(b)** above. The first movement phase (green arrows) is indicated by the chlorite slickenfibres. The second phase (red arrows) by the carbonate slickenfibres.

4.8 Courtown Shear Zone

The Courtown Shear Zone (CSZ), located between Salt Rock and Glenbeg Head (Figs. 4.6, 4.9, 4.14) is a 1.2km wide ductile, sinistral shear zone. The deformation cross-cuts and overprints the main phase of regional deformation discussed previously. The rocks within the shear zone have been assigned predominantly to the Ballyhoge Formation and consist of variably deformed dark mudstones, laminated siltstones and sporadic sandstone beds (Plates 4.4(a), 4.21(a)-(c)). The rocks are largely of a low metamorphic grade and still preserve some original bedding features such as delicate planar and cross lamination. However, some of the mudstones have been metamorphosed to phyllites (e.g. grid ref. 20515292), and within an 80m wide, high strain zone to the south of Pollshone Head (grid refs. 20495303-20395311) the rocks are chlorite schists.

The largest, exposed, section of the shear zone lies between Pollshone Head (Figs. 4.6, 4.9, 4.14, grid ref. 20485324) and a small stream north of Salt Rock (Figs. 4.6, 4.9, 4.14, grid ref. 20585269), where it is exposed for approximately 500m. Between Pollshone Head and 150m south of Glenbeg Head, the shear zone is not exposed. The northern margin of the shear zone is inferred to lie between the northern-most outcrop of Glenbeg Head, (Figs. 4.6, 4.9, 4.14, grid ref. 20115381) and the next exposure to the north (Figs. 4.6, 4.9, 4.14, grid ref. 20005390). The outcrop at Glenbeg Head preserves abundant evidence of ductile, sinistral shearing in the form of asymmetric quartz boudins and small (few cm.), steeply-plunging folds with sinistral vergence, whereas the outcrop to the north contains no evidence of ductile shearing. At Glenbeg Head the shear zone lies within the Ballylane Formation.

Poles to bedding lie along a diffuse SE-dipping great circle girdle that has a moderate ESE-plunging β axis, with a well defined point maxima that is consistent with a steeply SE-dipping homoclinal bedding plane (Fig. 4.21(i)). The main foliation is deformed by small (few cm.), generally steeply-plunging folds that have a sinistral sense of vergence, suggesting that they formed during sinistral shearing. These produce a locally well-defined crenulation fabric, which is axial planar to the folds. Minor syn-shear-fold hinges are spread along a great circle girdle that lies sub-parallel to the mean fold axial plane (Fig. 4.21(ii)) suggesting that fold hinges are moderately curvilinear. This is confirmed by field observations. Poles to shear-fold axial planes show a well defined point maxima consistent with a ENE-trending, steeply-inclined, southerly-

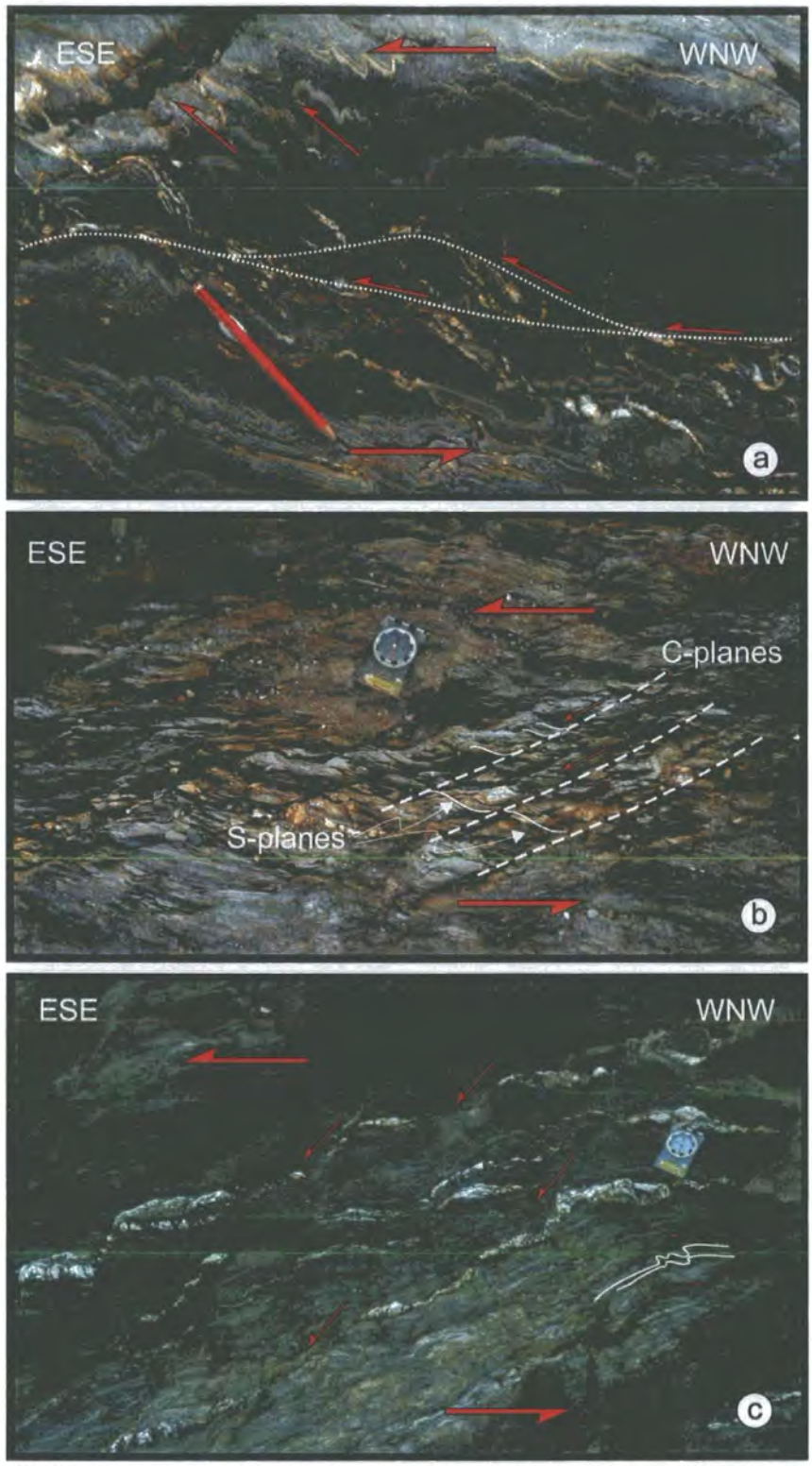

Plate 4.21. Sinistral asymmetric fabrics in rocks of the Ballyhoge Fm. in the Courtown Shear Zone. **(a)** Folds, duplex structure, detachments and P-type shears all showing a sinistral sense of shear. Looking down on sub-horizontal surface, South of Pollshone Head (Fig. 4.9, grid ref. 20495316). **(b)** Extensional shear-band fabric in mud-dominated unit. S-planes (solid lines) have a sigmoidal geometry and trend ENE. NE-trending C-planes (dashed lines) are relatively planar and off-set S-planes with a sinistral sense. This geometry is consistant with sinistral strike-slip shear. South of Pollshone Head (Fig. 4.9, grid ref. 204 95322) **(c)** Asymmetric boudins in quartz segregation veins in mudstone dominated units are coeval with sinistral folding (highlighted) in siltstone dominated units. Dominance of mudstone increases from bottom right to top left of photograph. South of Pollshone Head (Fig. 4.9, grid ref. 20485319). Note that these are all plan views.

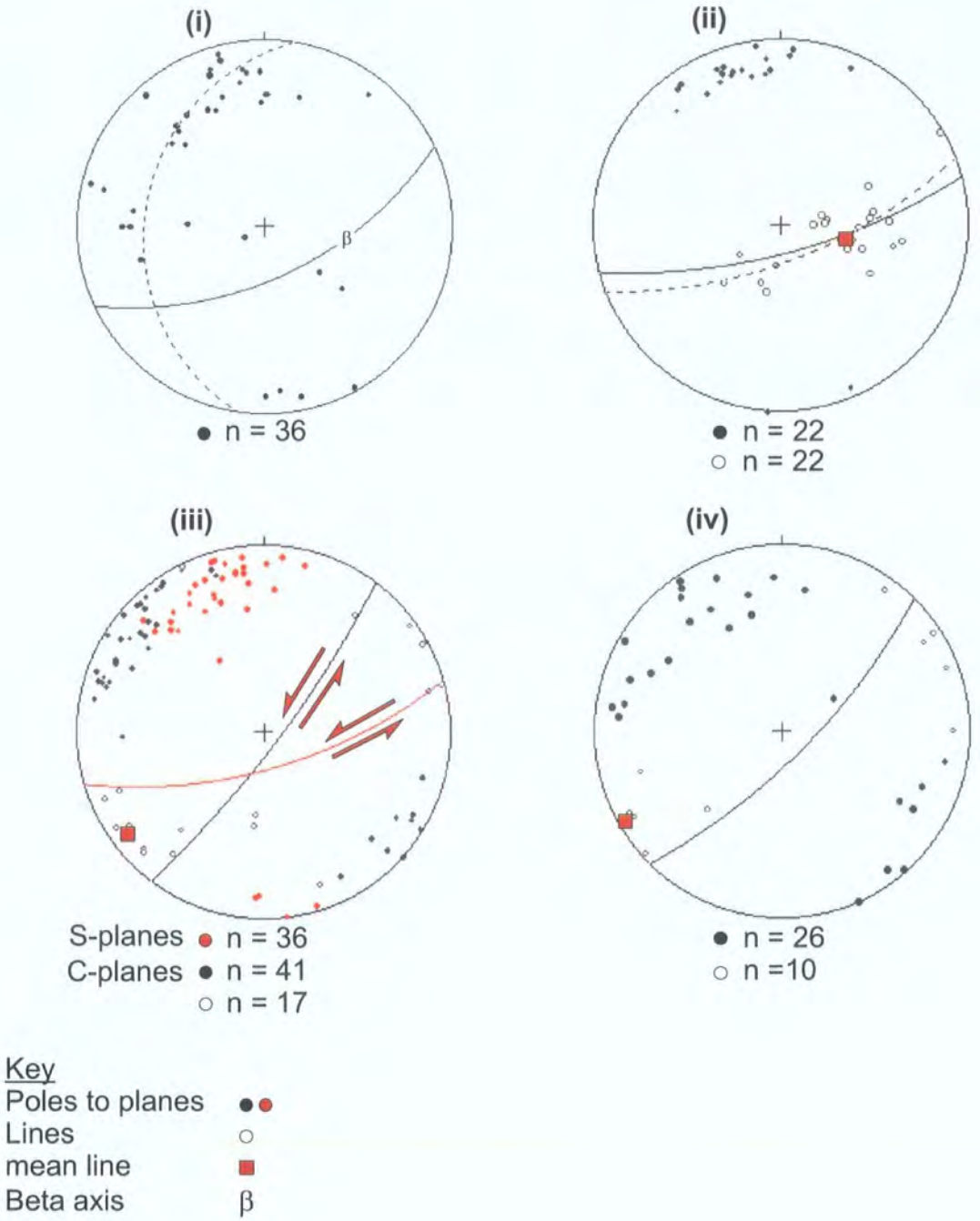

Figure 4.21. Stereoplots of structural data from the Courtown Shear Zone (CSZ). **(i)** Poles to bedding, with best-fit great circle girdle (dashed, 009/36W), mean bedding (solid, 065/68S) and regional β axis (54/099) shown. **(ii)** Poles to shear fold axial planes and fold hinges with mean fold hinge (63/103), great circle girdle (dashed, 069/74S) and mean fold axial plane (solid, 075/77S) shown. **(iii)** Poles to shear-band fabrics and mineral stretching lineation, with mean lineation (10/233), mean foliation (S-planes) (red line, 074/74S) and mean C-plane (black line, 037/83S) shown. **(iv)** Poles to fault planes and slickenline lineations, with mean lineation (4/240) and mean fault plane (solid 045/78S) shown.

dipping mean axial plane (Fig. 4.21(ii)). Poles to extensional shear band fabrics show two well-defined point maxima corresponding to a steep, ENE-trending, southerly-dipping mean S-plane (foliation) and a steep, NE-trending, southerly dipping mean C-plane (Fig. 4.21(iii)). The angular relationship between the two mean planes is consistent with a sinistral sense of shear and is confirmed by field observations. Mineral stretching lineations defined by quartz and chlorite on both S- and C-plane surfaces are mainly sub-horizontal and indicate a predominantly strike-slip movement (Fig. 4.21(iii)). Slickenline lineations are sub-horizontal, with poles to fault planes defining a steeply inclined, southerly dipping, NE-trending, mean fault plane (Fig. 4.21(iv)). The similarity in orientation between the mean fault plane and C-plane and the mean S-plane and fold axial planes (Fig. 4.21(ii)-(iv)) indicates that these structures are probably related to the same deformational event. This is also supported by the fact that faults both cut folds and crenulations and are folded locally. The same is true of S-C fabrics.

Evidence for sinistral shear is preserved on a macro- and microscopic scale (e.g. Plates 4.21(a)-(c), 4.22(a)-(c), 4.23(a), (b)). Extensional (Plates 4.21(b), (c), 4.22 (b)) and compressional (Plates 4.21(a), 4.22(a), (c), 4.23(a), (b)) structures appear to have developed contemporaneously during shearing. Extensional structures are more prevalent in mudstone dominated sequences, whereas the siltstone sequences preserve larger numbers of contractional structures (Plate 4.21(c)).

The rocks within the shear zone contain a much higher density of veining in comparison to those outside the zone. This suggests that the levels of fluid flow were elevated during shearing, with the shear zone acting as a fluid pathway. The source of the fluids and the formation of the shear zone may be related to the emplacement of the Leinster Granite to the NW (Fig. 4.2). The granite was emplaced during a phase of sinistral transtension (O'Mahoney 2000), and several ductile shear zones are thought to have been active during this time (e.g. Figs. 4.2, 4.4, East Carlow Deformation Zone, Hollywood Shear Zone; McArdle & Kennedy 1985; McConnell *et al.* 1999; Cooper & Brück 1983). These may have developed as a response to crustal softening around the relatively hot and mobile granite belt and its associated thermal aureole (Cooper & Brück 1983).

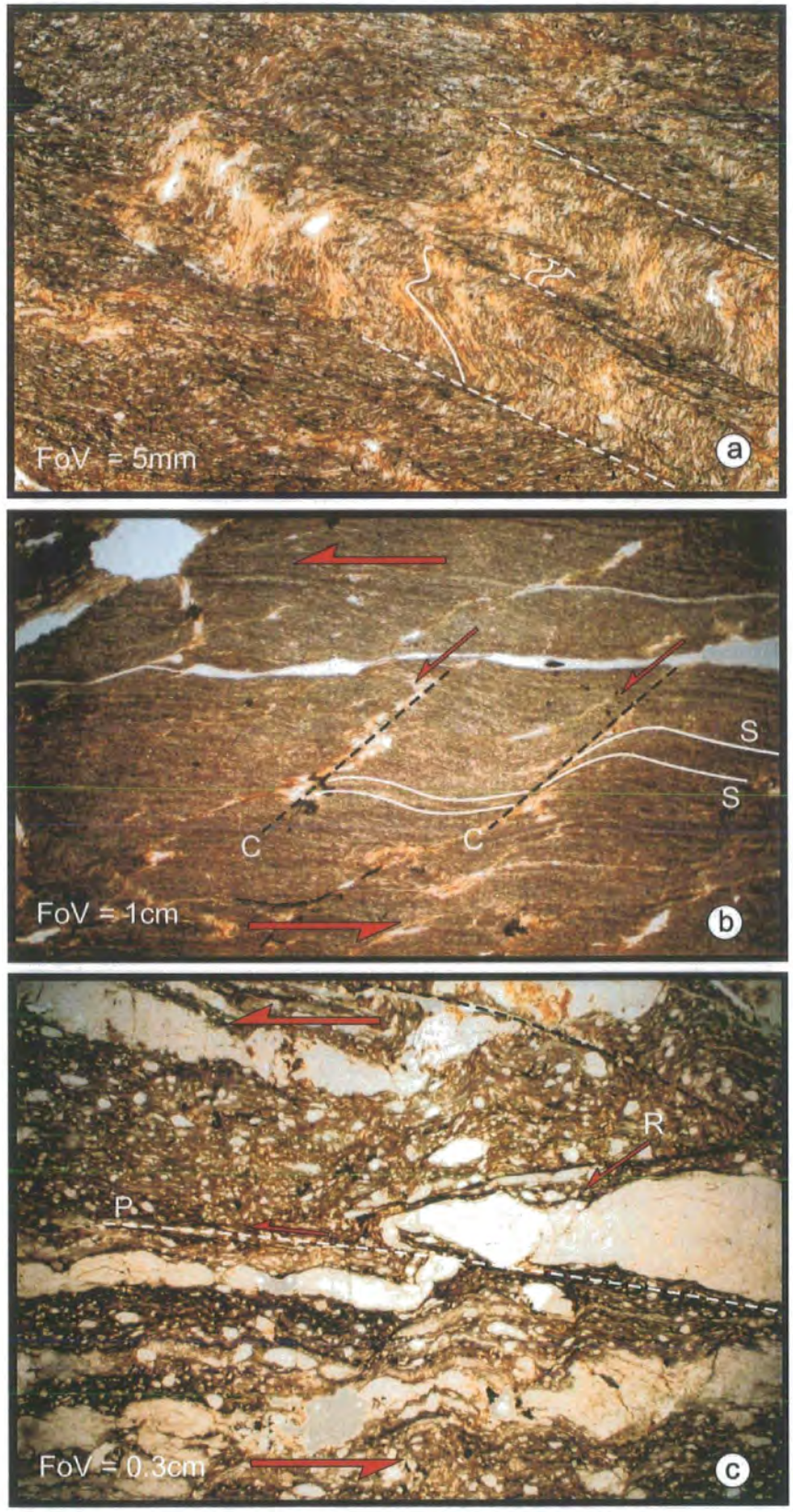

Plate 4.22. Thin section photomicrographs illustrating sinistral shear sense criteria and fabrics from the Courtown Shear Zone. **(a)** Crenulation cleavage formed by folding of main regional cleavage (solid lines) defined by pressure solution seams (dotted lines) (Sample IPS 9b. grid ref. 20495303). **(b)** Sinistral shear band fabric with S- and C-planes highlighted. (Sample IPS 9a. grid ref. 20495303). **(c)** Folded quartz vein with through-going P-type shear and R-type shear. (Sample IPS 7. grid ref. 20495297). All taken in PPL

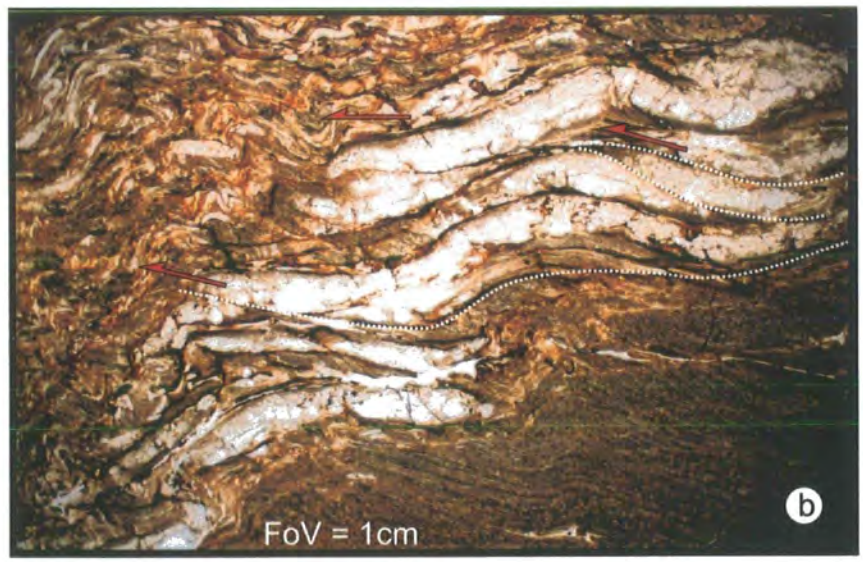

Plate 4.23. Thin section photomicrographs showing fabrics and kinematic indicators from the Courtown Shear Zone. **(a)** Sinistral folds and developing crenulation cleavage in chlorite schist. (Sample IPS10. grid ref. 20495307. Taken in XPL.). **(b)** Quartz vein showing sinistral duplex structure and pressure solution seams. (Sample IPS 8. grid ref. 20495307. Taken in PPL.).

4.9 Late stage sinistral shear

The late stage sinistral shear appears to manifest itself in two distinct, but possibly contemporaneous styles. Firstly, a NE-trending, heterogeneous braided network of predominantly sinistral, steep, strike-slip, semi-brittle shear zones and fault arrays (Plate. 4.13(b)) that appear to be confined to the area between Salt Rock and Kilmichael Point (Fig. 4.6). Secondly, a series of NNE-N-trending sinistral and ESE-trending dextral, possibly conjugate faults that are predominantly developed in the more thickly bedded turbiditic sandstones of the Cahore Group in the south of the section. However, some examples can be found at Kilmichael Point, where sinistral deformation has localised around a basic dyke (Plate. 4.24(a), (b)). The distribution of styles may be lithologically controlled, the semi-brittle deformation being more prevalent in the thinner-bedded siltstones and mudstones that are dominant north of Salt Rock, whilst the brittle faulting is restricted to the thicker sandstone units of the Cahore Group.

The most notable and representative example of the first of these structures is to be found within the bedded volcanic tuffs of the Campile Formation at Ballymoney (Figs. 4.6, 4.10, grid ref. 21576003) and has been named the Ballymoney Shear Zone (BMSZ). A detailed map of the ca. 5m shear zone (Fig. 4.22) has been drawn which shows the extent of the exposure and the variety and orientation of structures studied. Deformation consists of a series of steeply inclined, sub-parallel quartz-veined detachments that are linked by a series of sigmoidal contractional structures, formed due to sinistral rotation of the main cleavage (Plate 4.25(a), Fig. 4.23(ii), (iii))

Poles to bedding (Fig. 4.23(i)) lie along a shallow, ENE-dipping great circle girdle that corresponds with a steep SW-plunging β axis with a well-defined point maxima consistent with a steep, NW-dipping mean plane. This tallies well with the mean, cleavage-bedding intersection lineation. Poles to cleavage (Fig. 4.23(ii)) show two main point maxima that correspond with a sub-vertical mean plane. A third group of data that represent a mean plane lying anticlockwise of the main data suggest that the cleavage is folded. This is confirmed by field observations (Plate. 4.25(a)).

The second set of structures are most clearly exposed at Glascarrig Point (Fig. 4.11) where the steeply inclined bedding has been offset by a series of small sinistral and dextral faults that appear to form a conjugate set (Plates. 4.14(a), 4.25(b), (c), Fig 4.24).

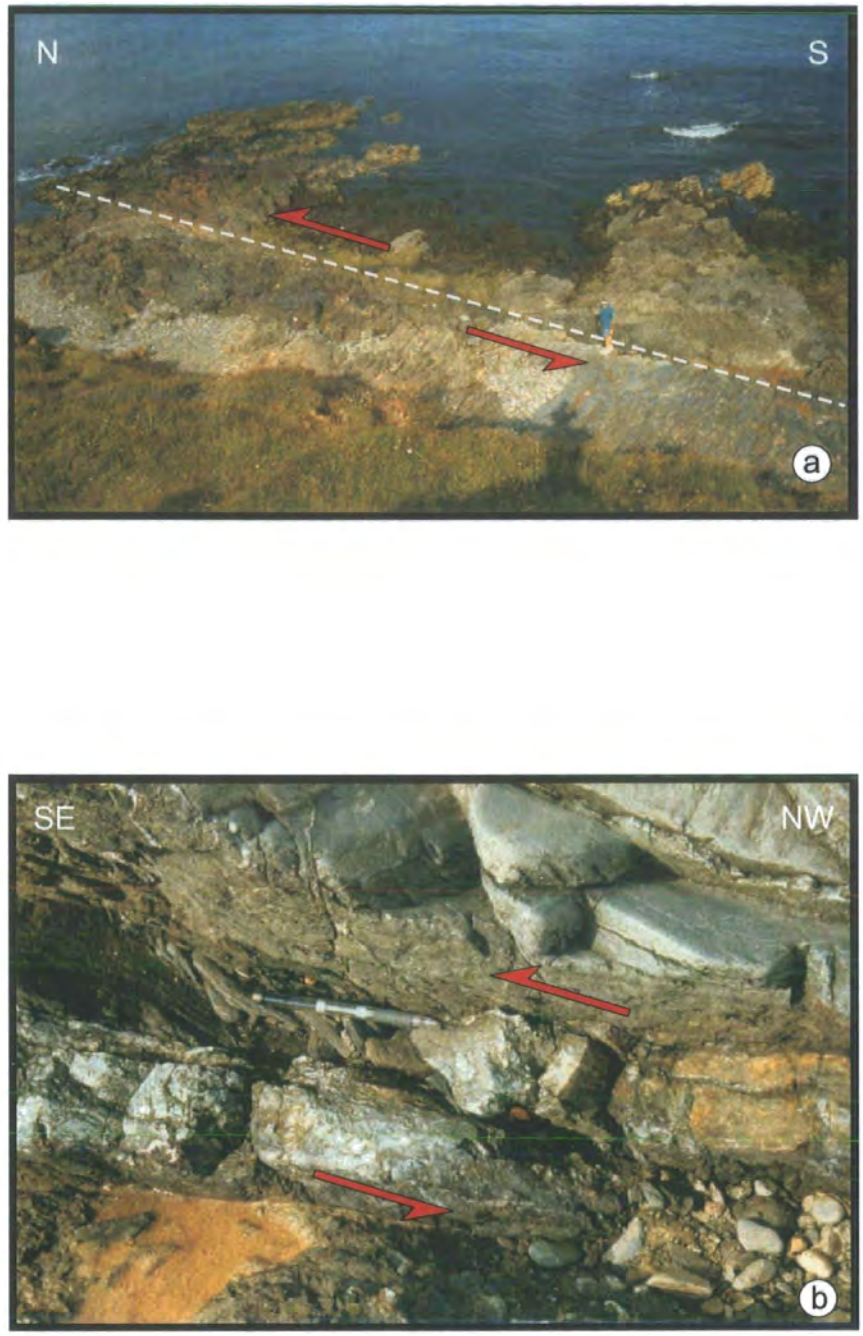

Plate 4.24. **(a)** View looking east of a late stage sinistral strike-slip fault on the foreshore at Kilmichael Point (Fig. 4.11, grid ref. 254662). **(b)** Sinistral P-type shear associated with late stage sinistral faulting at Kilmichael Point (Fig. 4.11, grid ref. 25406622)

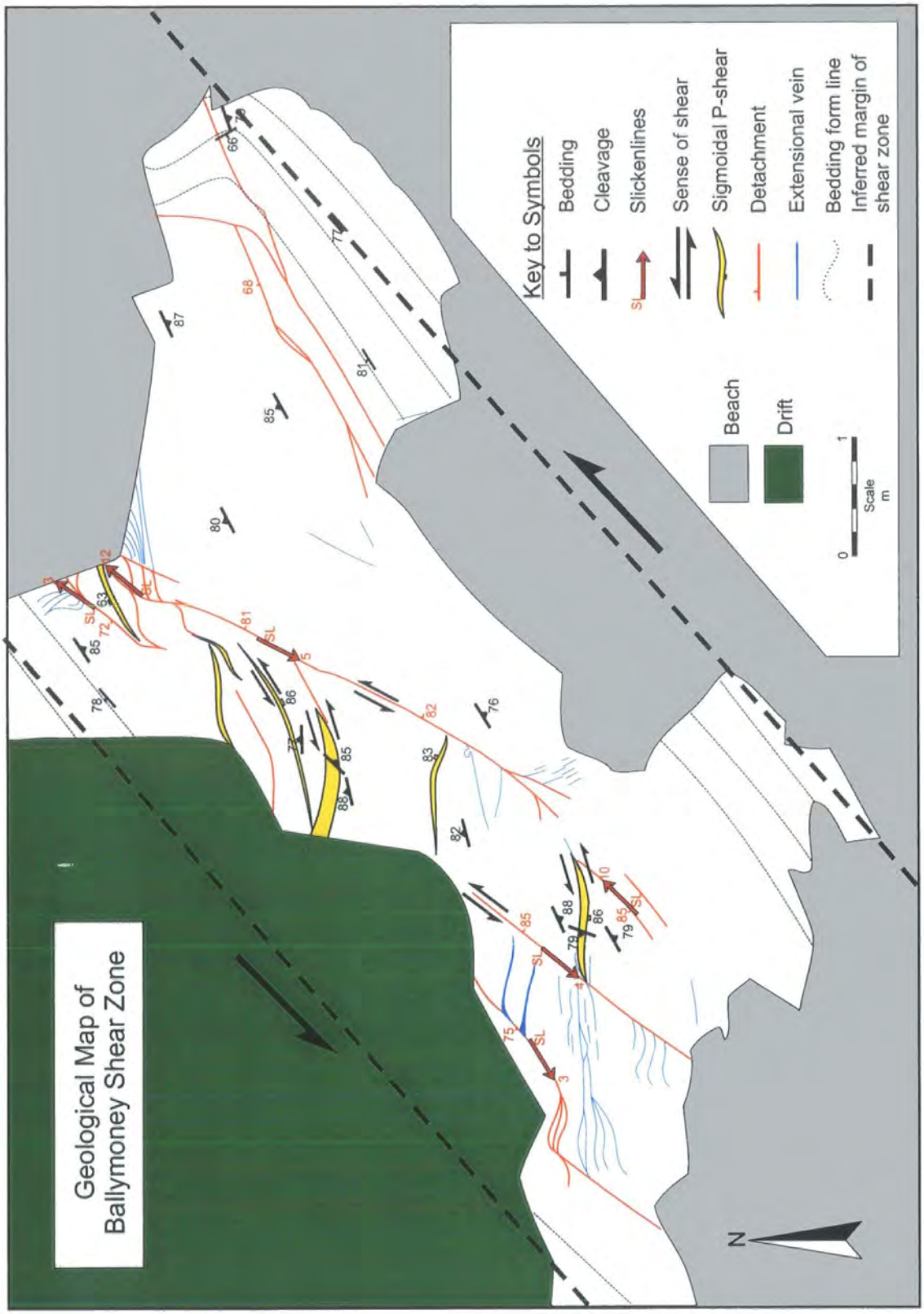

Figure 4.22. Geological Sketch map of the Ballymoney Shear Zone (grid ref. 21576003).

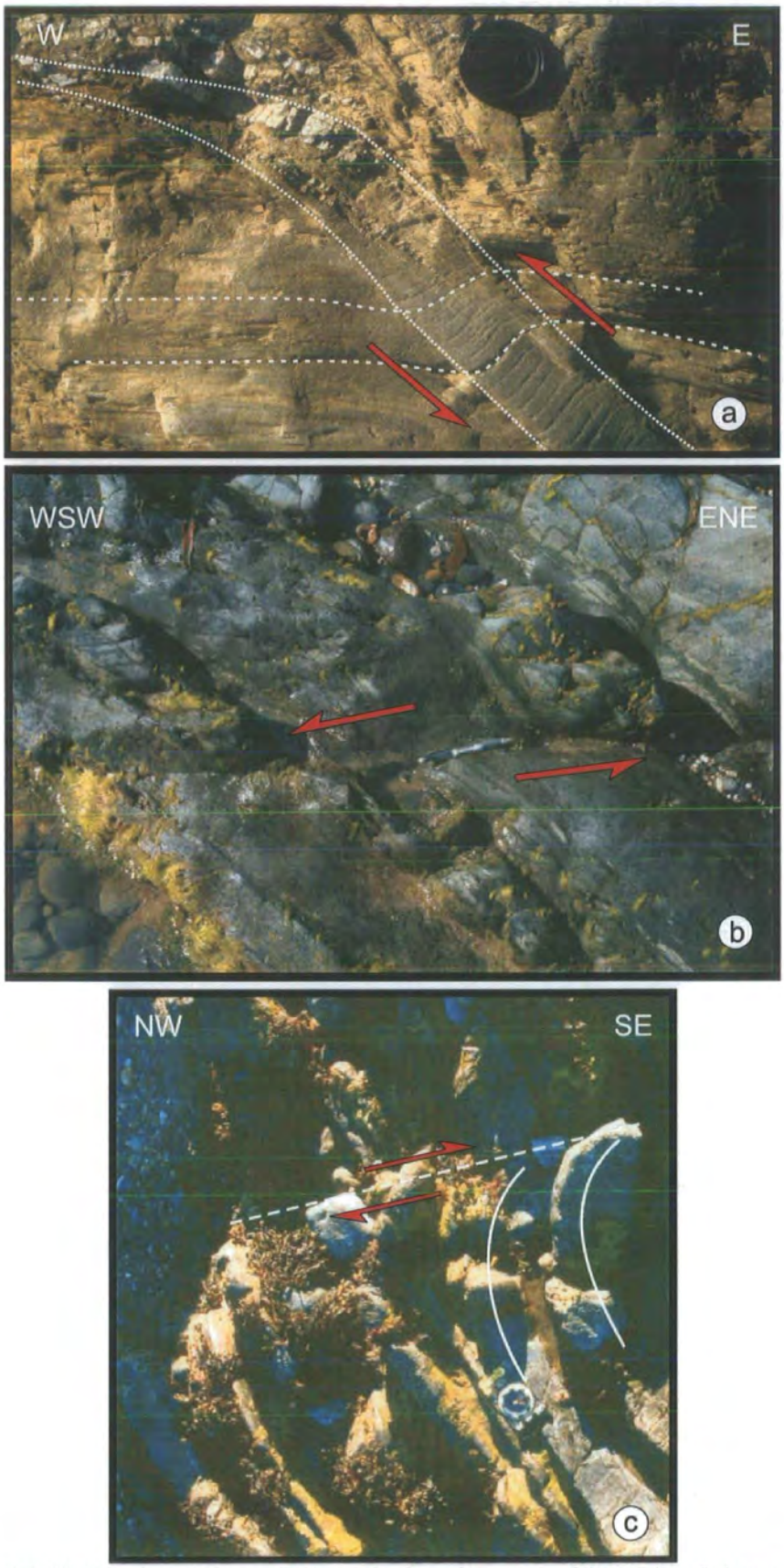

Plate 4.25. **(a)** Sinistral rotation of the primary cleavage (highlighted) has created a set of sigmoidal 'shear' band structures. These terminate in veins containing sub-horizontal slickenfibres. Ballymoney Shear Zone, Figs. 4.10, 4.22, grid ref. 21576003). **(b)** Sinistral strike-slip fault at Glascarrig Point (Fig. 4.9, grid ref. 212493). Pencil lies on fault plane. **(c)** Dextral strike-slip fault near to Glascarrig Point (Fig. 4.9, grid ref. 21854934). Note bedding deformed by fault drag.

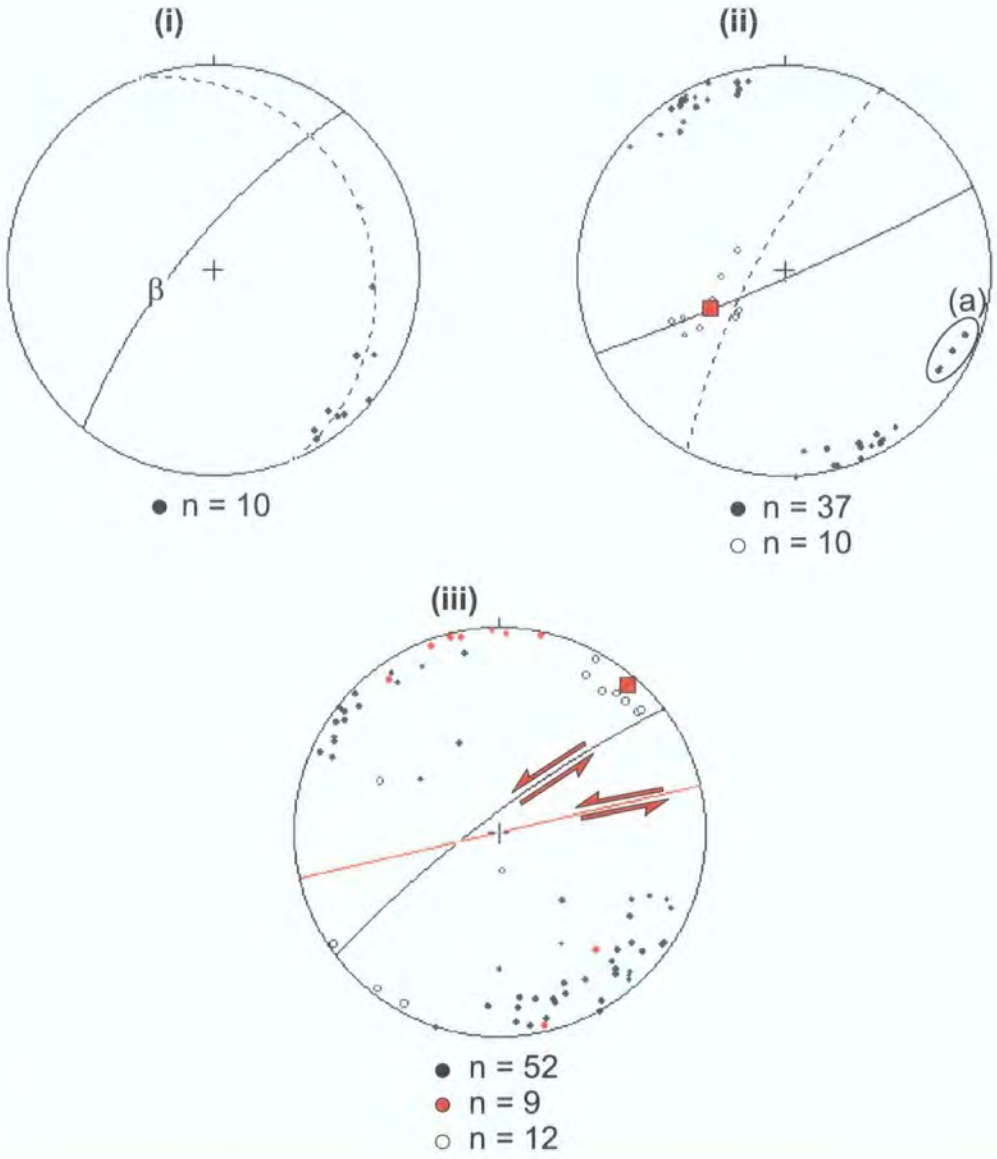

Figure 4.23. Stereoplots for structural data from the Ballymoney Shear Zone (BMSZ). **(i)** Poles to bedding, with best-fit great circle (dashed, 158/24E), Mean bedding (solid, 039/78N) and regional β axis (66/248). **(ii)** Poles to cleavage and cleavage-bedding intersection lineation (BCIL), with mean BCIL (57/243), cleavage plane (solid 062/88S), and mean plane (dashed, 028/79N) for data points (circled (a)) shown. **(iii)** Poles to detachments, P-type shears and slickenfibre lineations, with mean lineation (6/041), detachment (black line, 053/83N) and P-type shear (red line, 077/90) shown.

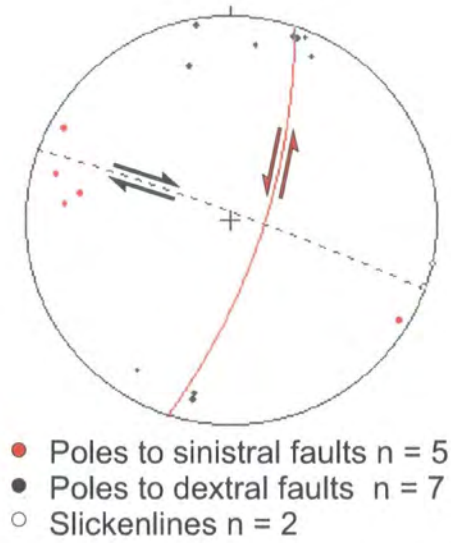

Figure 4.24. Stereoplot of faults at Glascarrig Point. Mean sinistral fault plane (red line, 018/77E). Mean dextral fault plane (black line, 110/88N)

Plate 4.26. View of the angular unconformity (dashed line) between the Riverchapel Formation of the Ribband Group and the Courtown Formation of the Duncannon Group. The unconformity is folded by the dominant phase of deformation and the cleavage (dotted line) can be traced directly across the unconformity. The Fold plunges to the SW and is upward facing. (Fig. 4.10, grid ref. 22046123). Outcrop is approximately 1.5m high. Line in sand was drawn to illustrate shape of fold.

4.10 The regional unconformity

The early Ordovician phase of deformation suggested by Tietzsch-Tyler (1989, 1996) is supposed to affect the rocks of both the Cambrian Cahore and Lower Ordovician Ribband groups. The presence of a regionally recognised unconformity that separates these two groups from the upper Ordovician Duncannon Group (see section 4.3) within the study area is therefore significant. In particular, it is important to ascertain whether or not the orientation of the structures below the unconformity been influenced by the early phase of deformation. Clear examples of structures that can be assigned to the early phase of deformation have only been observed in the Cahore Group (see section 4.6). To establish any possible differences in the dominant set of folds, cleavage and their facing patterns above and below the unconformity, these orientation data have been plotted-up separately for the 'basement' and 'cover' rocks below and above the unconformity respectively (Fig. 4.25(a), (b)(i-vi)). The stereonets and facing plots in adjacent units of basement and cover are essentially the same, although greater variations ('scatter') are found in the basement rocks. This is confirmed by field observations. It is also clear that the dominant set of structures above and below the unconformity are the same age since the main folds and cleavage can be traced directly across the unconformity (Plates 4.5(b), 4.26), and downward facing folds and cleavage occur in both the cover and rocks (Fig. 4.25(a(vi)), (b(vi))).

These findings suggest that the early Ordovician phase of deformation (Tietzsch-Tyler 1989, 1996) has not affected the rocks of the Ribband Group and appears to be restricted to a small area of rocks assigned to the Cahore Group around Cahore Point (Fig. 4.14). Thus the main phase of deformation above and below the unconformity can be attributed to the same phase of deformation.

4.11 Summary, general interpretation and regional context

The structural characteristics of the early deformation, domains 1 and 2, the Courtown Shear Zone and the late stage sinistral shear are summarised in Table 4.3 and Figure 4.26. The Cahore Point to Kilmichael Point section (Fig.4.6) contains a more complex assemblage of structures than has hitherto been described. A systematic variation in main phase strain intensity and fold geometry occurs across the region. A

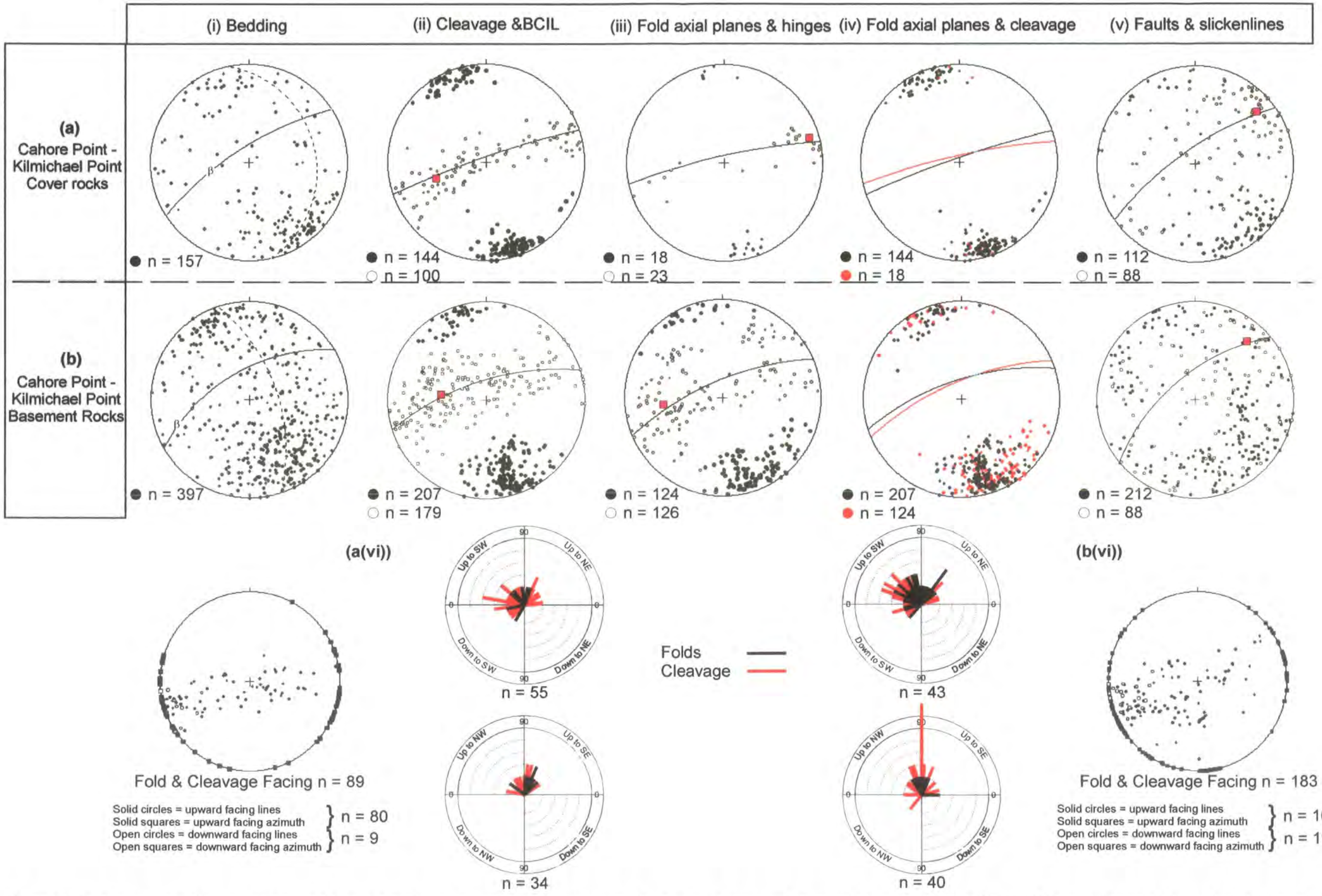

Figure 4.25. Stereoplots of structural data and facing data for the basement and cover rocks for the area between Cahore Point and Kilmichael Point. (cf. Figs. 4.12 and 4.13). **(a(i-v)** Structural data for the cover rocks. **(b(i-v))** Structural data for the basement rocks. **(a(vi))** Cover rocks fold and cleavage facing lines and azimuths (left) plotted using the construction method of Holdsworth (1988). Cover rocks plots (right) showing the pitch of fold and cleavage directions in mean planes oriented NE-SW and NW-SE. **(b(vi))** Basement rocks fold and cleavage facing lines and azimuths (right). Basement rocks plots showing pitch of fold and cleavage facing directions in planes parallel to the fold axial and cleavage planes in which they were measured.

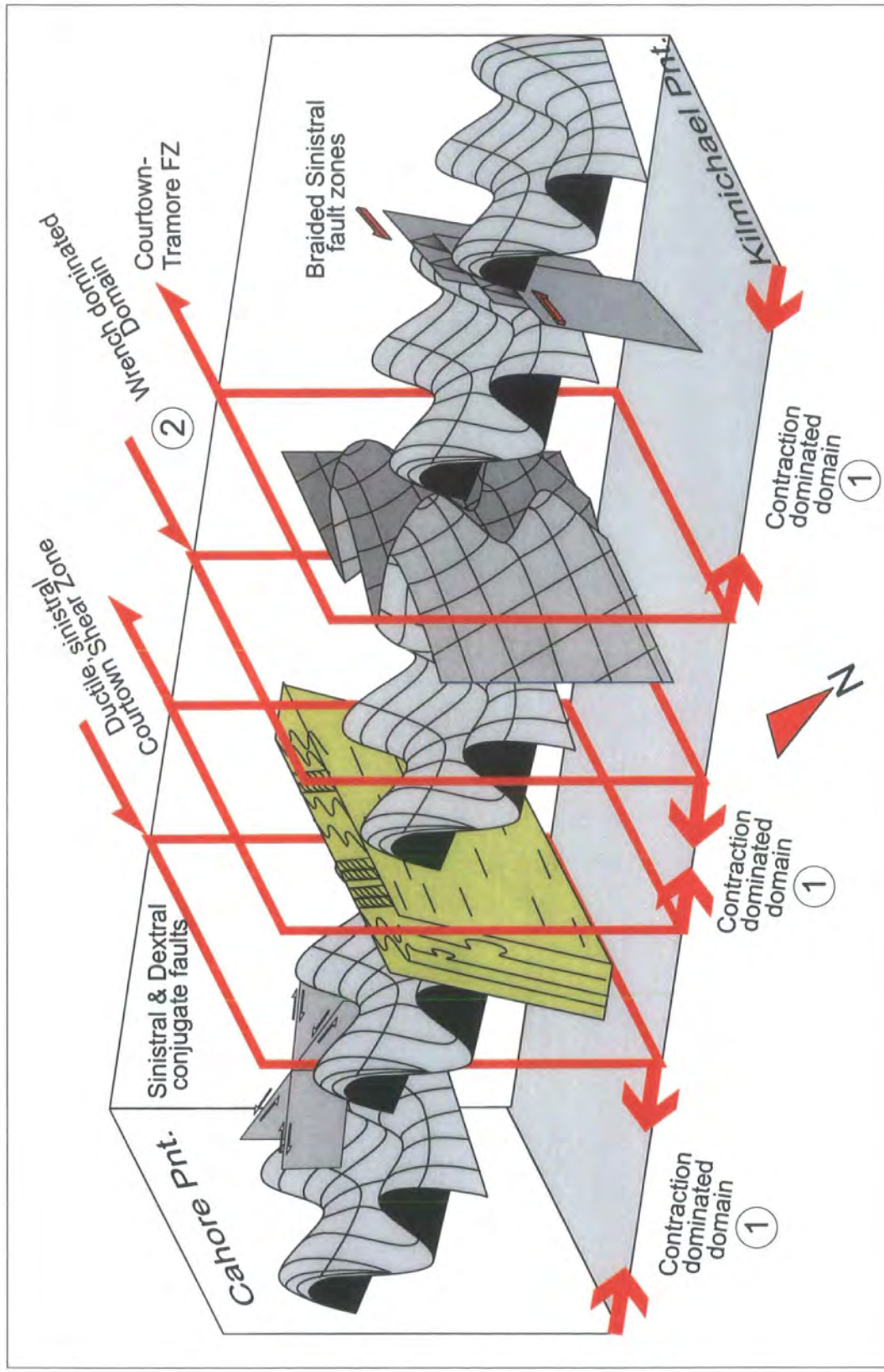

Figure 4.26. Schematic 3-D representation of the structural domains and overprinting sinistral shear and faulting between Cahore Point and Kilmichael Point.

	Domain Type 1	*Domain Type 2*	*Courtown Shear Zone*	*Late Stage Sinistral Shear*	*Early Deformation Cahore Point*
General structure	Broad fold train, younging to NW & SE	Rather diffuse, steeply dipping to NW	Homoclinal, steeply dipping to SE	Locally developed	NW moderately dipping homocline
Fold geometry & scale	Slightly asymmetric, SE verging folds; < 1m – 10m scale	ENE-WSW subvertical mainly neutral folds; < 10m scale	ENE-WSW sinistral shear folds; generally < 1m scale	Small scale 10's cm Steeply plunging S-SE-trending kink folds	No folds associated with early deformation identified
Fold/BCIL plunge pattern	Rather diffuse great circle girdle distribution. Plunging both to NE & SW, passing through horizontal; up to 180° curvature	Mainly steeply plunging to NE & SW, passing through vertical, up to 180° curvature	Moderately plunging to ENE & WSW, most folds plunge moderately to steeply to ENE	Not recorded	BCIL plunge shallowly to steeply W-NE & lie along NNE-SSW trending great circle girdle that dips steeply to WNW
Fold-cleavage relationship	Clockwise transected	No clear transection Essentially axial planar	Not applicable	Very weak axial planar cleavage	Cleavage folded about ESE-WNW trending great circle girdle dipping steeply to SSW
Detachment geometry & kinematics	Complex pattern of dip-slip and predominantly sinistral strike-slip faults	NE-SW trending dip-slip & sinistral strike-slip faults	NE-SW trending sinistral strike-slip faults	Braided network of Steep sinistral detachments. Conjugate sinistral & dextral faults in South of area	Early faults not separated from later faults
Facing patterns	NE & SW upwards at shallow to steep angles	Strong sideways and SW, both upwards & downwards	Inferred to face SW and sideways on average	Inferred to face SW and sideways on average	Cleavage originally faced SE

Table 4.3. Summary of structural elements of Domains 1 & 2, the Courtown Shear Zone, the late sinistral shear and the early deformation around Cahore Point

ca. 1.5km wide central region (Domain 2) can be defined in which the main phase of steeply inclined to upright folds display highly curvilinear hinges in both basement and cover rocks. The generally SW-facing folds are predominantly curvilinear about a moderately SW-plunging direction, so that where hinges plunge to the SW they are upward facing, whilst those plunging NE face down to the SW. To the north and south of this central zone, the main phase folds are moderately-to-steeply inclined and steeply upward facing. The shallowly-to-moderately SW- or NE-plunging whaleback folds curve about a steeply plunging line. The folds in the two domains are identical in style and both are associated with the same regional cleavage, which lies in an axial planar orientation. Therefore, all these structures appear to be broadly contemporaneous. It is suggested that the change in hinge curvilinearity reflects partitioning of a regional sinistral transpressional strain into contraction- and wrench-dominated deformational domains. The later network of sinistral faults and shear zones including the ca. 1.2km Courtown Shear Zone, appears to cross-cut and be superimposed upon the structures of the main phase of deformation, with little evidence that the earlier main phase event has significantly influenced the location of individual high strain zones or faults.

Although, evidence for sinistral transpression has been described from other areas of the Leinster Massif (e.g. Max *et al.* 1990; Murphy 1985; Murphy *et al.* 1991), there has been no previous description of the partitioning of the structural assemblages developed during transpressional deformation. As far as the author has been able to establish, this chapter also presents the first detailed description of the structures within the Courtown Shear Zone and associated later sinistral structures.

The relative age relationships, significance and origin of the structures described in this chapter will be further discussed in chapter 6 in relation to transpressional deformation.

Chapter 5

The Lower Palaeozoic Structure and Kinematics of the Isle of Man

5.1 Introduction

The Isle of Man occupies a unique geological position within the Caledonian Orogen of British Isles. Although now part of a horst block of predominantly Lower Palaeozoic rocks surrounded by Mesozoic basins, the island lies immediately SE of the projected surface trace of the Caledonian Iapetus Suture (Fig. 5.1, Woodcock *et al.* 1999a). Along most of its course, the suture is hidden beneath Upper Palaeozoic rocks, but, on the Isle of Man, Lower Palaeozoic rocks crop out close to or possibly at the suture zone (Woodcock *et al.* 1999a).

The island is composed predominantly of Lower Palaeozoic marine turbidites and debrites of the Ordovician Manx Group (Simpson 1968; Woodcock *et al.* 1999b) and Silurian Dalby Group (Fig. 5.2, Morris *et al.* 1999). These were deformed at shallow to mid-crustal levels (ca. 5-13km) within a sinistral transpression zone during the sinistral, oblique closure between Laurentia and Eastern Avalonia. Several structures thought to be related to sinistral transpression, such as folds clockwise transected by their cleavage (Fitches *et al.* 1999) and major strike-parallel sinistral faults (e.g. Niarbyl Shear Zone and Lag Ny Keeilley Shear Zone: Fitches *et al.* 1999; Quirk & Kimbell 1997) have been recognised within the Isle of Man.

This chapter presents a synthesis of the Lower Palaeozoic evolution and structure of the Isle of Man, providing a brief history of previous work and a detailed account of folds and associated structures in the Ordovician and Silurian rocks exposed at key localities around the coast.

5.2 Previous studies

Early studies on the geology of the Isle of Man include those of Lamplugh (1903) and Blake (1905). Lamplugh mapped the island for the Isle of Man Government between 1892 and 1897. His 1 inch:1 mile map was published in 1898 and his memoir followed in 1903. Lamplugh correlated the sandstone-dominated rocks of the Niarbyl and Lonan Flags, thereby indicating a synclinal structure with repetition on the NW and

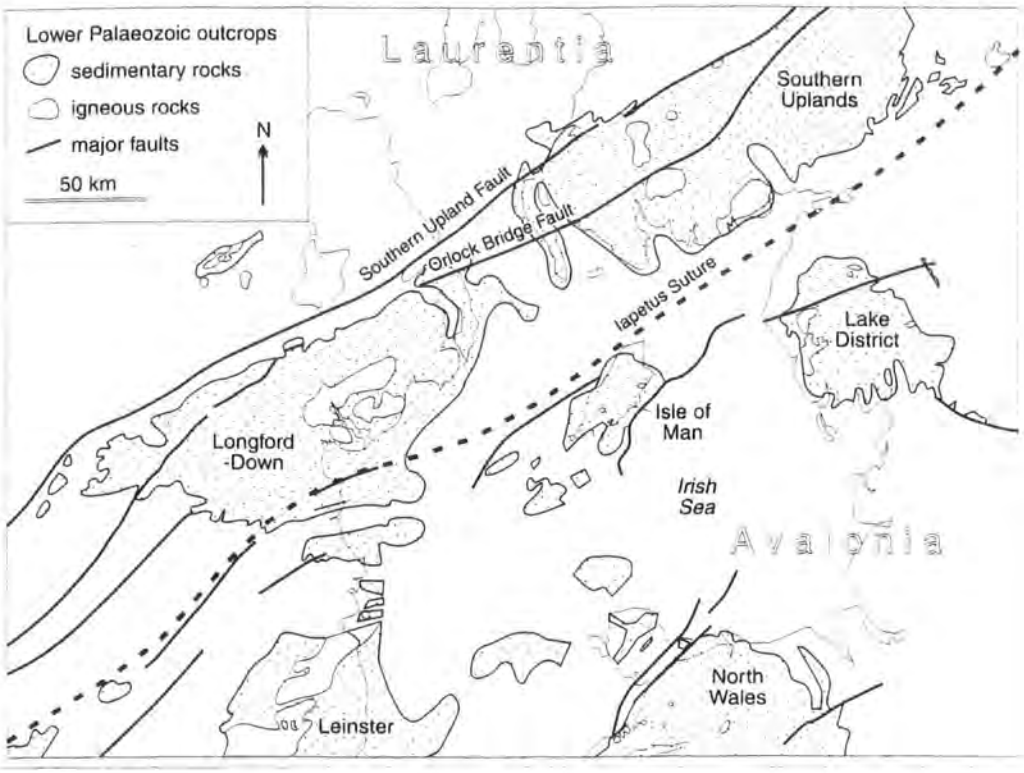

Figure 5.1. Location of the Isle of Man with respect to the Iapetus Suture and other Lower Palaeozoic regions around the Irish Sea (from Woodcock *et al.* 1999a).

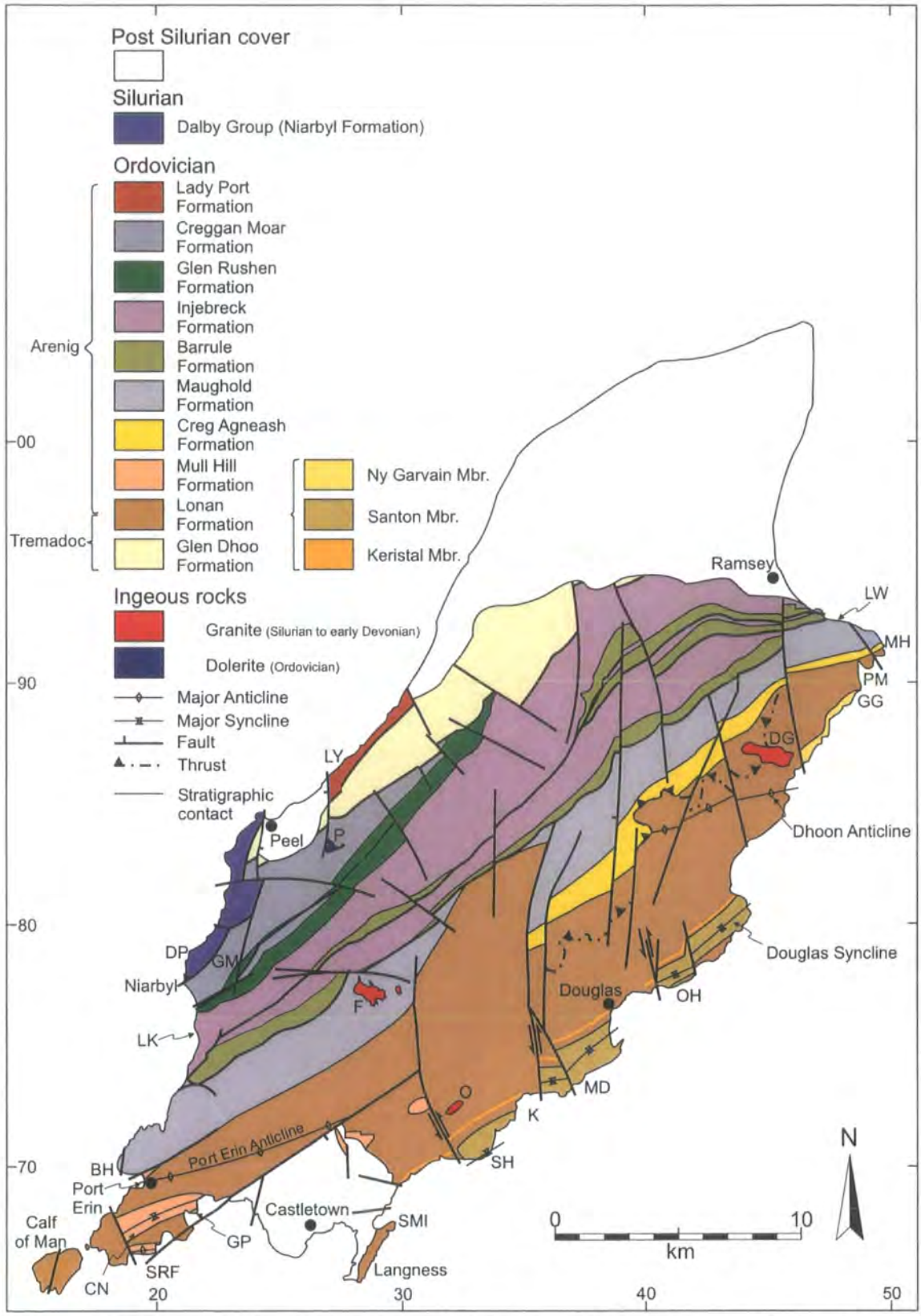

Figure 5.2. Generalised solid geology of the Isle of Man. BH - Bradda Head, CN - Cregneash, DG - Dhoon Granite, DP- Dalby Point, F - Foxdale Granite, GG - Gob ny Garvain, GM - Glen Maye, GP - Gansey Point, K - Keristal Bay, LK - Lag ny Keeilley, LW- Lewaigue, LY - Lynague, MD - Marine Drive, MH - Maughold Head, P - Poortown Complex, PM - Port Mooar, O - Oatlands Granite, OH - Onchan Head, SH - Santon Head, SMI - St. Michaels Island, SRF - Shag Rock Fault (after Woodcock *et al.* 1999; BGS 2001).

SE limbs (Fig. 5.3). In Lamplugh's stratigraphic sequence, the Lonan and Niarbyl Flags formed the lowest units and these were overlain by the Agneash and other grits. The Barrule Slates formed the highest units, and occupied the core of his NE-trending regional synclinorium (Fig. 5.3, Lamplugh 1903). He suggested that the absence of the Agneash Grits on the western side of the synclinorium was due to a thrust fault at Niarbyl. Well ahead of his time, Lamplugh deduced a fivefold succession of repeated episodes of folding and cleavage formation. Following Lamplugh's study, Blake (1905) challenged his interpretation; although he accepted Lamplugh's correlation of the Niarbyl and Lonan Flags, he suggested that the repetition of these units and the Barrule Slates was due to faulting and not folding.

Gillott (1956) suggested that the structure was anticlinal rather than synclinal, with the oldest unit, the Lonan Flags occupying the core despite its main outcrop being along the east coast. Gillott also recognised that there had been at least two episodes of folding and cleavage. The first had acute folds and axial-planar 'flow' cleavage whilst the second had more open folds and axial-planar 'fracture' cleavage (Ford *et al.* 1999).

The most comprehensive study of the island since Lamplugh (1903) was undertaken by Simpson (1963, 1964, 1965, 1968). He outlined a detailed synthesis of the Manx slate stratigraphy, structure, metamorphism and intrusions. He provided the first comprehensive descriptions of the Manx slates, which he divided into eleven units (Fig. 5.4). Simpson (1963) suggested that the Manx slates had been deposited in a geosyncline during the Cambrian, estimating a total thickness of ca. 25 000ft for the succession. His structural interpretation was similar in part to Lamplugh's, with a correlation between the Lonan Flags in the E and Niarbyl Flags on the W forming a major synclinal structure (the Isle of Man Syncline, Simpson 1963, Fig. 5.4). Within the main synclinal arrangement, Simpson (1963) recognised a series of three structural episodes (D1–D3, Fig. 5.5). The earliest phase of deformation (D1) gave rise to NE-SW-trending F1 folds with gentle to moderate SW-plunging axes, and an associated axial planar S1 cleavage, that were the products of NW-SE compression (Fig. 5.5(a)). D2 consisted of nearly vertical contraction refolding of F1, and giving rise to F2 folds with gently NW-dipping axial planes and an axial planar S2 'slippage' cleavage (Fig. 5.5(b)). D3 was the result of ENE-WSW contraction almost at right angles to previous structures, with F3 axial planes dipping ENE and axes trending NNW (Fig. 5.5(c), Simpson 1963). Simpson also noted that the highest metamorphic grades were present as a NE-trending zone, marked by the presence of cordierite, garnet and chloritoid,

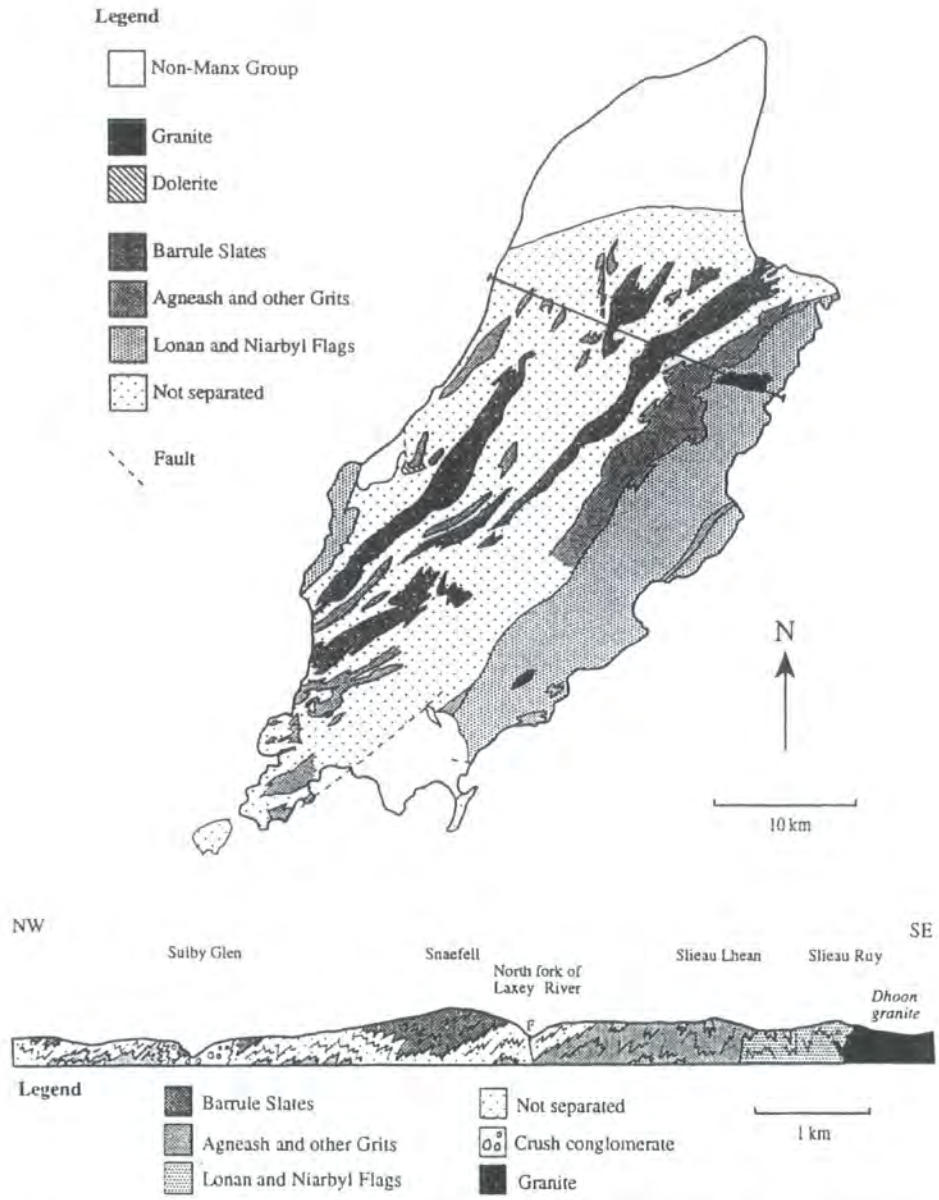

Figure 5.3. Sketch map and cross-section of the solid geology of the Isle of Man after Lamplugh's 1 inch: 1mile Geological Survey map, showing his subdivisions of the Manx Slates.

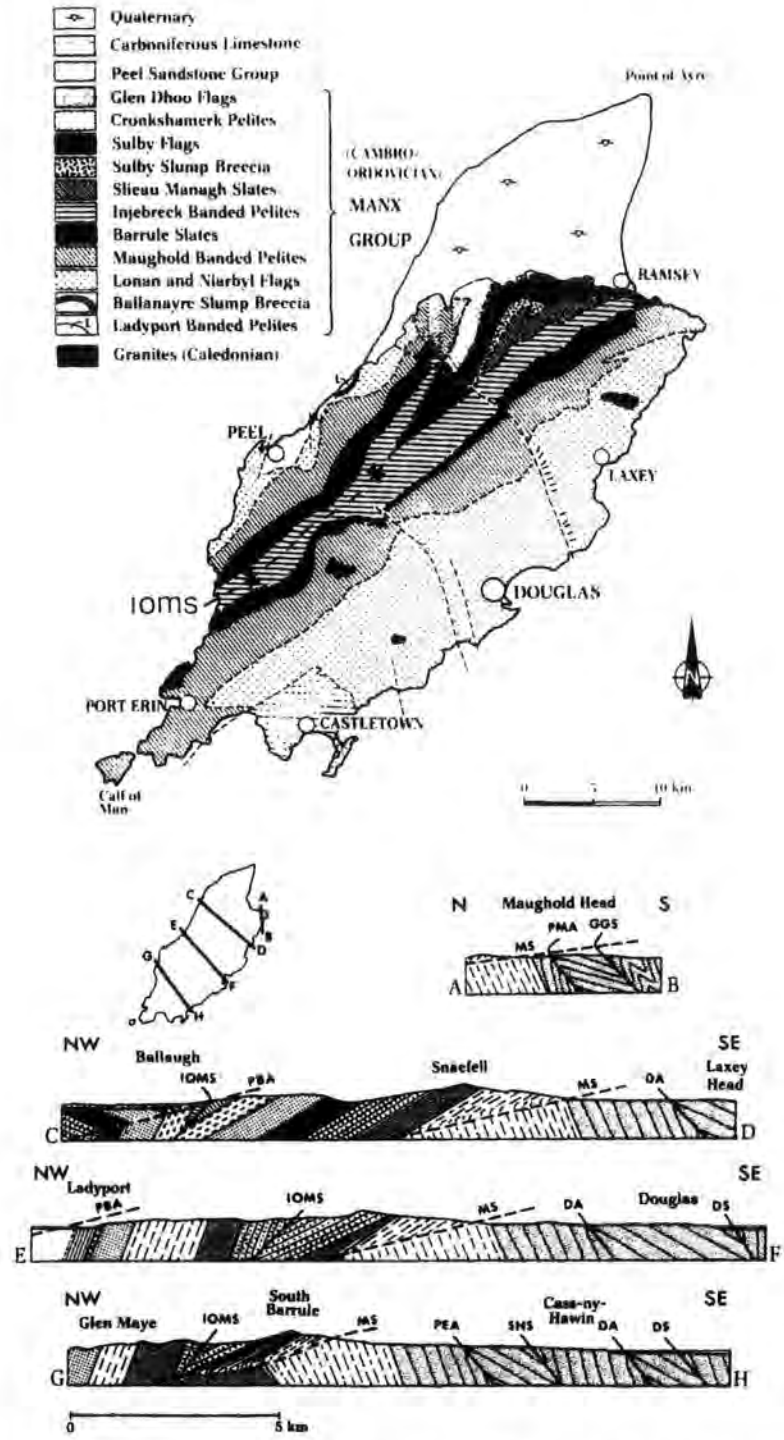

Figure 5.4. Simplified version of Simpson's 1963 map and cross-sections, showing the subdivisions of the Manx Slate Series. IOMS = Isle of Man Syncline (after Simpson 1963).

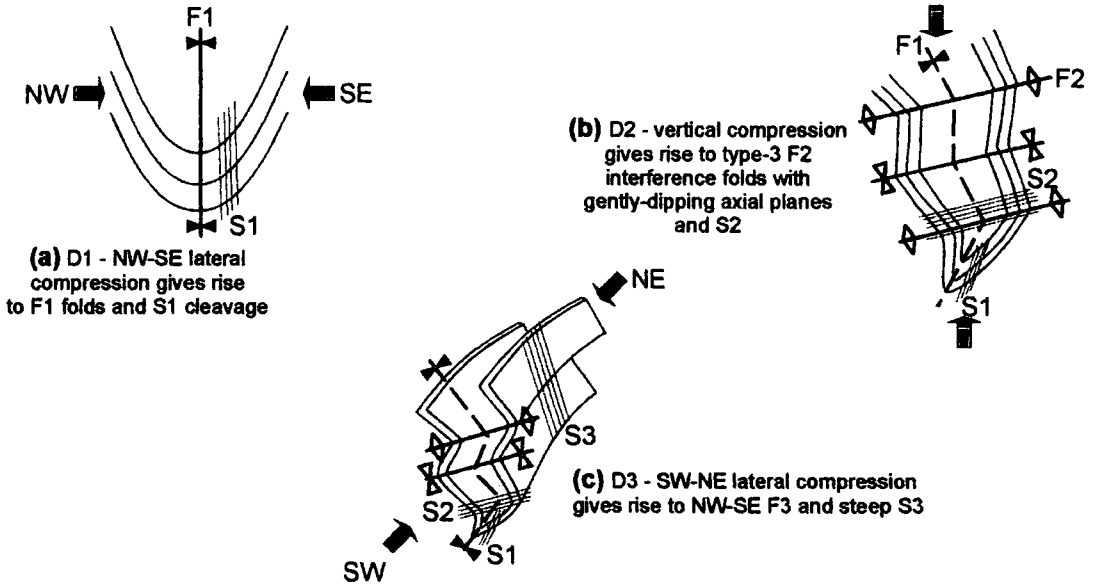

Figure 5.5. The three deformational phases recognised by Simpson (1963) **(a)** D1 **(b)** D2 **(c)** D3. (after Simpson 1963).

Figure 5.6. Interpretation of potential field lineaments from aeromagnetic, Bouguer gravity anomaly derivatives without reference to surface geology. Thick lines indicate position of strong lineaments visible on high-resolution aeromagnetic data or where lineaments coincide with more than one data set. Thin lines indicate position of other lineaments visible on separate data sets (from Quirk *et al.* 1999).

which was associated with the major F1 fold structure (the Isle of Man Syncline).

Recent interest in Manx geology was rekindled through the biostratigraphical work of Molyneux (1979) who provided the first revision of Simpson's stratigraphy. Studying samples of acritarchs from more than twenty localities he showed that there were considerable problems with Simpson's stratigraphy and hence his structural interpretation. Though still based largely on Simpson's scheme, Ford (1993) formalised the revised stratigraphy in his geological field guidebook of the island. New research (e.g. Rushton 1993; Quirk & Kimbell 1997; Stone & Evans 1997) was focused into a multidisciplinary field-based project carried out on the island between 1995 and 1998, culminating in the publication of a Geological Society Special Publication (Woodcock *et al* 1999). The research undertaken during this period provided crucial lithological, structural and biostratigraphical data that prompted Woodcock *et al.* (1999b) to propose a new stratigraphic scheme for the island with repetition of units by NE-trending strike-slip faults. The discovery of Silurian fossils in the Niarbyl Formation (Howe 1999) precluded its correlation with the Lonan Formation and made Simpson's synclinal interpretation of the Manx structure unsustainable. Quirk & Kimbell (1997) used gravity, aeromagnetic, seismic, borehole and outcrop data from the Isle of Man and the Irish Sea to study the structural framework and tectonic evolution of the Central Irish Sea. High-resolution aeromagnetic data over the island revealed a pattern of shallow lineaments which Quirk & Kimbell (1997) interpreted as a sinistral strike-slip duplex formed due to sinistral transpression (Fig. 5.6). The most recent interpretation (Chadwick *et al.* 2001) has combined recent field evidence and new palaeontological data in an attempt to resolve several of the problems raised by the interpretation of Woodcock *et al.* (1999b).

The work of Lamplugh (1903) and Simpson (1963) pre-dates the ideas of plate tectonic theory and the crucial plate tectonic setting of the island. The regional context of the Isle of Man has until recently been based on work from other related areas. In particular the Skiddaw Group of the Lake District of NW England (Cooper *et al.* 1995) and the Ribband Group of SE Ireland (Max *et al.* 1990; McConnell & Morris 1997).

5.3 Regional setting and structural evolution

Regionally the Manx Group is thought to be equivalent to the Skiddaw Group in NW England (Cooper *et al.* 1995) and the Ribband Group in SE Ireland (McConnell *et*

al. 1999). These three units are interpreted as forming part of a deep-marine, predominantly turbiditic sedimentary prism deposited on the northern continental margin of Avalonia (Fig 5.7, Woodcock & Barnes 1999; Chadwick *et al.* 2001). Although comprising broadly similar facies, there are significant differences in the detailed stratigraphy of each unit suggesting deposition in localized sedimentary systems (Chadwick *et al.* 2001).

Poorly preserved graptolites indicate that deposition of the Manx Group began during the Tremadoc or early Arenig. At this time in Leinster, a volcanic arc had already been initiated (McConnell & Morris 1997) and Iapetus oceanic crust was being subducted beneath the Avalonian margin of Gondwana (Fig. 5.8). The Manx Group sediments, mainly comprising Arenig (Lower Ordovician) deep-marine turbidites and debrites supplied from the southeast were deposited into oxygenated basins on the northwest facing active margin of Avalonia (Fig. 5.8, Woodcock *et al.* 1999a). Evidence of subduction related volcanism at this time may be preserved by the Lower Arenig Peel Volcanics (Fig. 5.2, Simpson 1963) and numerous felsic intrusions, although the precise relationship between the volcanics, felsic intrusives and arc volcanism remains uncertain (Woodcock *et al.*1999a).

Avalonia rifted away from Gondwana during the late Arenig (Fig. 5.8, Woodcock *et al.* 1999a). Debrites and manganiferous ironstones within the upper units of the Manx Group may represent episodes of down-margin mass wasting due to rift induced seismicity, and high rates of exhalation of iron and manganese rich fluids during the rifting of Avalonia from Gondwana (Fig. 5.8, Woodcock & Morris 1999; Kennan & Morris 1999).

In Leinster and the Lake District the early Ordovician sedimentary successions are overlain by later Ordovician volcanic arc successions of the Duncannon and Borrowdale groups respectively (Fig. 5.8, Max *et al.* 1990; Cooper *et al.* 1995). Any such volcanic succession is absent from the Isle of Man. However, evidence that it may have existed comes from the Poortown intrusive complex ESE of Peel (Fig. 5.2). This comprises a complex of tholeiitic basalt to basaltic andesite sills and may have formed the sub-structure to a late Ordovician volcanic succession (Piper *et al.* 1999; Power & Crowley 1999). If such an arc was constructed above the Manx Group, comparison with the Borrowdale Group suggests that it would have been predominantly subaerial and Caradoc in age (Woodcock *et al.* 1999a). Erosion of any volcanic succession and post-Caradoc sedimentary cover must have occurred prior to the overthrusting of the

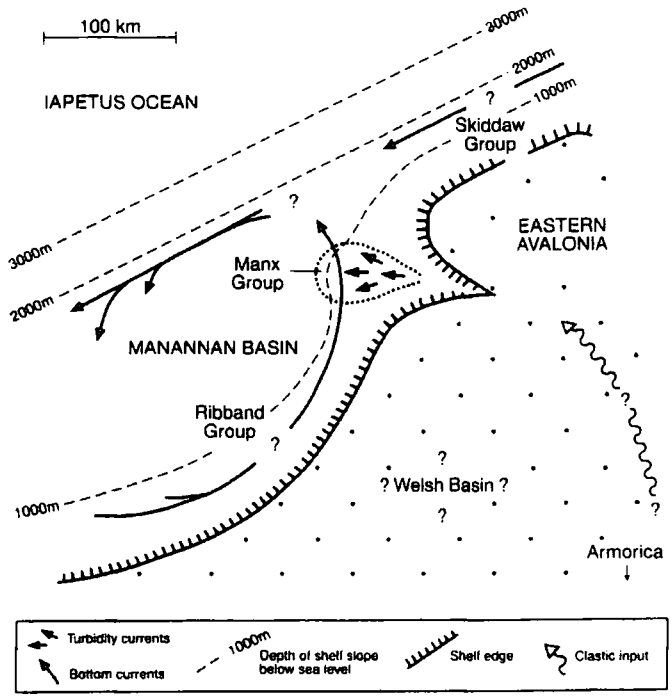

Figure 5.7. Tentative palaeogeographic reconstruction of the NW margin of Eastern Avalonia during the early Arenig showing possible current patterns and the relationship between the Ribband, Skiddaw and Manx groups (after Quirk & Burnett 1999).

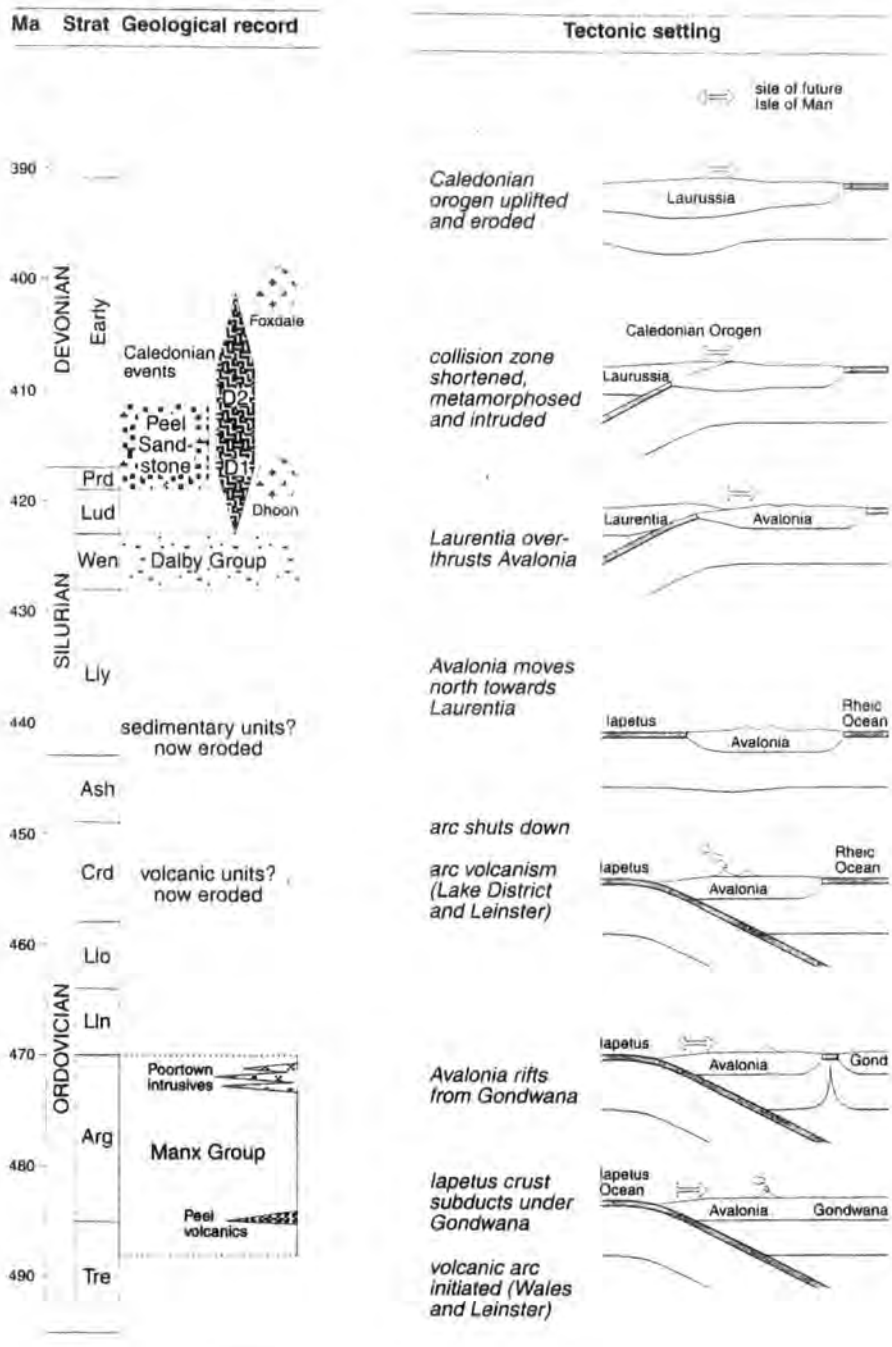

Figure 5.8. Geochronological diagram of the Lower Palaeozoic geological history of the Isle of Man (based on Woodcock *et al.* 1999a).

Dalby Group onto the Manx Group, probably in the early Devonian (Fig. 5.8, Woodcock *et al.* 1999a). During the final stages of closure of the Iapetus Ocean in the late Silurian (mid-late Wenlock), arc-derived turbidites of the Dalby Group were deposited from the northeast into an anoxic marine basin bridging both the Avalonian and Laurentian margins (Woodcock *et al.* 1999a; Chadwick *et al.* 2001). The observed contact between the Dalby and Manx groups is tectonic, and its significance remains uncertain. Barnes *et al.* (1999) favour correlation with the mid-Silurian turbidites of the Windermere Supergroup (Lake District), implying that the Dalby Group was originally deposited on the Manx Group and has been subsequently faulted into its present day relationship. In contrast, Morris *et al.* (1999) propose correlation with the Riccarton Group (Southern Uplands Terrane). This implies that the Dalby Group represents the toe end of the Southern Uplands turbidite prism, onlapping or thrust onto the Avalonian continental margin. However, if the Wenlock and Ludlow rocks of the Windermere Supergroup are regarded as the diachronous southward equivalent of the Southern Uplands deposits, the contrast between these two hypotheses is less significant (Woodcock *et al.* 1999a).

The three phases of ductile deformation (D1-D3) (Fig. 5.5) described by Simpson (1963) are essentially confirmed by Fitches *et al.* (1999). The third phase (D3) is only locally developed and could possibly be Variscan or later in age (Fitches *et al.* 1999). The precise age of the primary (D1) and secondary (D2) deformation preserved in the Manx and Dalby group rocks of the Isle of Man is not well constrained. However, as rocks of the late Wenlock Dalby Group are deformed by both events, deformation must be at earliest, late Wenlock/early Ludlow. The Foxdale Granite is thought to post-date the second phase of deformation (Fig. 5.8), and although no published dates exist for this intrusion a tentative age of 400Ma is cited by Woodcock *et al.* (1999a). These authors suggest that both the first and second phases of deformation occurred in latest Silurian or early Devonian time, between *c.*420 and 400Ma. and are considered to be equivalent to the Acadian deformation of NW England (Fig. 5.8, Soper *et al.* 1987; Fitches *et al.* 1999).

The greater part of the Manx Group outcrop falls within chlorite grade of metamorphism, i.e. low greenschist facies. Ilmenite, chloritoid, muscovite, manganese-rich garnet, tourmaline and chlorite-mica stacks are the main metamorphic minerals present, and indicate a burial depth of 10-13km and temperatures of 350-400°C (Power & Barnes 1999). Peak metamorphic conditions probably occurred between the first and

second phases of regional deformation. The highest grade of metamorphism, shown by the development of manganese-garnet, follows a NE-trending zone along the axis of the island. Although initially attributed to the elevated thermal gradient following the formation of the Isle of Man Syncline (Simpson 1963), it is now thought to be largely due to the chemical composition of the sediments (Power & Barnes 1999).

The predominantly steep dip of the sedimentary succession of the Lower Palaeozoic rocks of the Isle of Man imposes a relatively simple outcrop pattern, which, together with much of the detail of the outcrop-scale structure, was recognised by Lamplugh (1903) and Simpson (1963). However, poor biostratigraphical control, poor inland exposure, lack of demonstrable stratigraphic contacts and extensive faulting within the Manx Group have hampered successive attempts to decipher the large-scale structure of the island. Until recently, the stratigraphic sequence and associated structural model of the island was based primarily on the work of Lamplugh (1903) and Simpson (1963). However, biostratigraphic data has identified mid-Silurian (Wenlock) graptolites within the Niarbyl Flags (Howe 1999), precluding the correlation with the Lonan Flags across the Isle of Man Syncline. Following this, the Niarbyl Flags (Lamplugh 1903) have been redefined as the Niarbyl Formation, removed from the Manx Group and placed in the newly erected Dalby Group (Morris *et al.* 1999). Structural observations (Fitches *et al.* 1999; Quirk & Kimbell 1997; Quirk *et al.* 1999a & b) have also cast doubt on the simple synclinal model of Lamplugh (1903) and Simpson (1963). The reassignment of the Niarbyl Formation into the Dalby Group, and the uncertainty over the large-scale structure of the island led Woodcock *et al.* (1999a) and Fitches *et al.* (1999) to divide the Manx Group into seven NE-SW-trending, strike-parallel tectonostratigraphic tracts, with an eighth tract comprising the Dalby Group (Morris *et al.* 1999) (Labelled 1-8 in Fig. 5.9). Stratigraphic sequences may be apparent within tracts but cannot be easily correlated between tracts. The tracts are generally bounded by major NE-SW-trending sub-vertical faults or predominantly sinistral, high strain zones, (e.g. the Niarbyl Shear Zone and Lag ny Keeilley Shear Zone), but the possibility cannot be excluded that some tract boundaries are essentially stratigraphic (Woodcock *et al.* 1999). Use of such a tract system is analogous to the successful tract strategy employed in the Southern Uplands of Scotland (e.g. Barnes *et al.* 1989) and provides a useful and flexible framework on which subsequent work can be based. Implicit within the tract model was the recognition that due to the poor biostratigraphical control, formations named in one tract may be repeated, but named

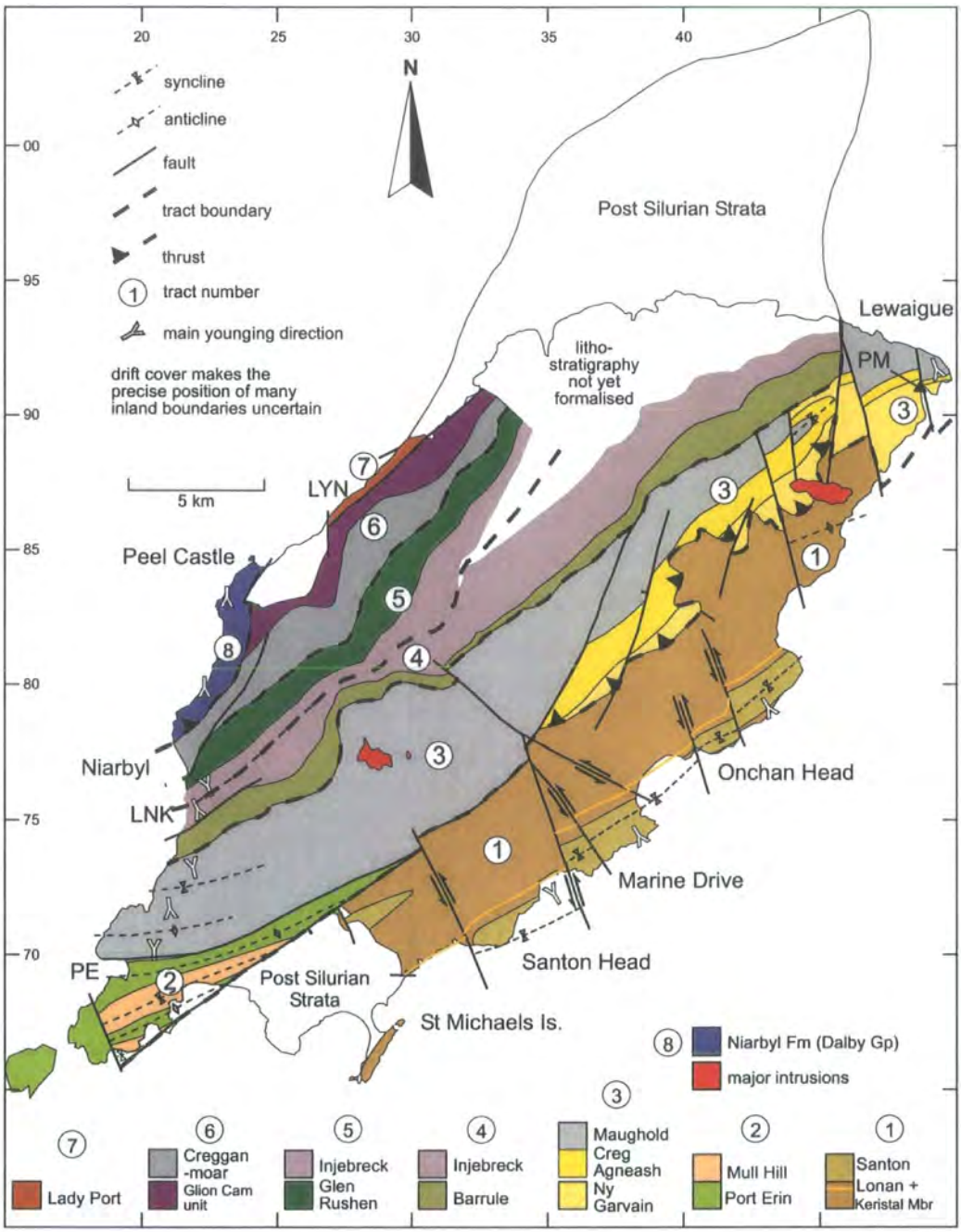

Figure 5.9. Simplified geolgical map of the Isle of Man showing the stratigraphy and tract structure (labelled 1-8) proposed by Woodcock *et al.* (1999). LNK - Lag ny Keeilley LYN - Lynague, PE - Port Erin, PM - Port Mooar.

separately in another tract. However, if correlation between separately named formations were proved, then formation names could be suppressed (Woodcock *et al.* 1999b).

5.4 Lower Palaeozoic stratigraphy and lithology of the Isle of Man

Lower Palaeozoic rocks crop out over a large part of the Isle of Man (Fig. 5.2), but are generally well-exposed only in coastal areas. Originally comprising the Manx Slate Series (Lamplugh 1903; Simpson 1963), they are now separated into two groups (Barnes & Woodcock 1999; Morris *et al.* 1999; Woodcock *et al.* 1999b).

1. The Ordovician (Tremadoc-Arenig) Manx Group (Woodcock *et al.*1999b).
2. The Silurian (Wenlock) Dalby Group (Morris *et al.* 1999).

The stratigraphy and lithology of these two groups is summarised in Table 5.1.

The Manx Group was redefined by Woodcock *et al.* (1999b), to exclude rocks of Silurian age, and twelve component formations were recognised (Table 5.1), although an area in the north of the outcrop was not mapped. Following further work, by Burnett (1999) Quirk & Burnett (1999a & b) in the north of the outcrop, recent work by the British Geological Survey (2001) and recent biostratigraphical discoveries (Molyneux 1999, 2001) the stratigraphy of Woodcock *et al* (1999) was reviewed and rationalised to ten formations and the tract system abandoned (Figs. 5.2, 5.9, Table 5.1). The stratigraphy outlined in Chadwick *et al.* (2001) will be adopted in this chapter and is described in the following sections.

The Dalby Group comprises only one formation (Niarbyl Formation, see below) which is a marine turbidite sequence with subordinate laminated hemipelagite (Fig. 5.2, Table 5.1, Morris *et al.* 1999).

5.4.1 The Manx Group

The oldest and youngest rocks of the Manx Group, the Glen Dhoo and Lady Port formations respectively, crop out in close proximity in the north of the outcrop (Fig. 5.2). Otherwise, the rocks occur in a NW-younging succession across the island, although this too is disrupted by faults which are interpreted to repeat parts of the succession (Chadwick *et al.* 2001). It should be noted that although new palaeontological evidence (Molyneux 1999, 2001) has been incorporated to revise the stratigraphy of Woodcock *et al.* (1999b), uncertainty still remains as to the precise age

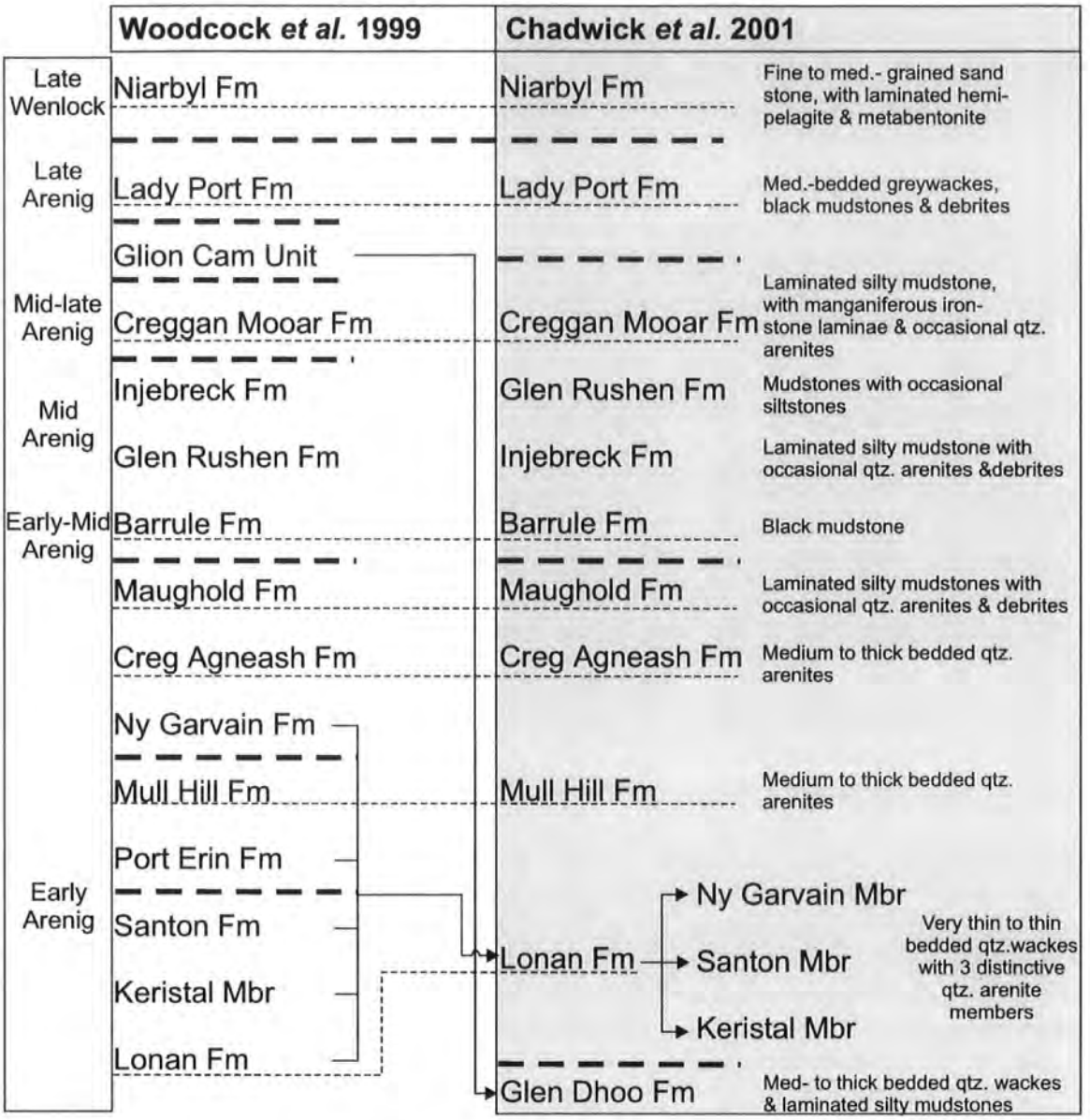

Table 5.1. The stratigraphic sub-divisions of the Lower Palaeozoic rocks of the Isle of Man, summarising the lithology and indicating the correlations between thesuccession of Woodcock *et al.* (1999b) and Chadwick *et al.* (2001). The latter succession (shaded) is adopted in this chapter. Thin dashed lines indicate agreement in correlation. Thick dashed lines show faulted contacts

of many of the component formations of the Manx Group. It is likely therefore, that further revision will be required as more biostratigraphical data become available.

5.4.1.1 Glen Dhoo Formation (Fig. 5.2, Table 5.1, Chadwick *et al.* 2001)

Rocks of the Glen Dhoo formation (Chadwick *et al.* 2001) are exposed in the NW of the Manx Group outcrop and as a fault bounded block to the west of Peel (Fig. 5.2). Formally named the Glen Dhoo flags (Simpson 1963), they now include the Glen Dhoo and Glion Cam units described by Quirk & Burnett (1999) and Woodcock *et al.* (1999b) respectively. The Glen Dhoo Formation is typically composed of mudstone with variable proportions of pale grey to white siltstone present as laminae or thin (<0.5cm) beds. Although mudstones are generally dominant, some sections appear to be composed of poorly laminated or homogeneous green-grey siltstone. Rare, thin beds of fine-grained quartzitic sandstone exhibit planar and cross-lamination. Two occurrences of volcanic rocks consisting of syn-depositional volcanic breccia are included within the Glen Dhoo Formation and are exposed in Peel Quarry (Fig. 5.2, grid ref. 23838333) and in the fault-bounded block to the west of Peel. All of the exposed contacts of the Glen Dhoo Formation are faulted, and, in part due to the poor exposure, its internal structure is largely unknown. Thus, the thickness of the Glen Dhoo Formation is difficult to determine, but it is likely to be at least several hundred metres (Chadwick 2001). Acritarch assemblages from several localities within the outcrop suggest a latest Tremadoc to earliest Arenig age (Molyneux 1979, 1999, 2001).

5.4.1.2 Lonan Formation (Fig. 5.2, Table 5.1, Woodcock *et al.* 1999b; Woodcock & Barnes 1999; Chadwick *et al.* 2001).

The Lonan Formation comprises almost a third of the Manx Group rocks and is well-exposed along the east and southwest coasts of the island (Fig. 5.2, Plate 5.1(a)). The current definition includes rocks assigned to the Port Erin, Santon and Ny Garvain formations of Woodcock *et al.* (1999b) (Table 5.1). The Santon and Ny Garvain formations have been reduced to member status joining the Keristal Member (Woodcock *et al.* 1999b), whilst, the Port Erin Formation has been correlated with the Lonan Formation and its formation name removed from the newly published 1:50 000 geological map (Chadwick *et al.* 2001). The formation consists of mainly thin- to very thin-bedded or thickly laminated, fine-grained sandstone or siltstone and mudstone couplets (Plate 5.1(b)). Each sandstone unit typically has a sharp base and grades from

Plate 5.1. **(a)** View NE along Marine Drive from The Whing (Figs. 5.2, 5.13(b), grid ref. 35907318), showing sub-vertical, NW-younging bedding of the Lonan Formation. The bedding is deformed by primary (F1) and secondary (F2) folds (highlighted) **(b)** Thinly bedded sandstone (Pale) and mudstone (dark) couplets of the Lonan Formation. Beds young to the NW and are deformed by secondary folds with sub-horizontal axial planes. Port Erin Bay, (Figs. 5.2, 5.23, grid ref. 19506943).

light grey cross-laminated fine-grained wacke, through parallel-laminated siltstone into dark grey mudstone, in some cases bioturbated. Way-up structures include flute casts, rippled bedding surfaces and channel features (Plate 5.2(a), (b)). The graded beds of the Lonan Formation are interpreted as the product of deposition from low-concentration turbidity currents in an oxygenated deep-marine environment (Woodcock & Barnes 1999). The base of the Lonan Formation is not exposed, but at least 2500m of strata are exposed between the core of the Dhoon Anticline and the highest part of the Santon Member (Fig. 5.2, Chadwick *et al.* 2001). The top of the Lonan Formation is best defined by the transition into the quartz arenite-bearing Creg Agneash and Mull Hill formations in the northeast and south of the island, respectively (Fig. 5.2). To the west of Douglas (Fig. 5.2), the boundary is more subtle and where the Creg Agneash and Mull Hill formations are absent, the Lonan Formation passes directly into the Maughold Formation (Fig. 5.2, Chadwick 2001). The age of the Lonan Formation beneath the Santon Member is constrained by acritarch assemblages from several localities. These suggest a possible late Tremadoc to early Arenig (Molyneux 2001). The Lonan Formation contains three persistent, well-exposed, distinctive fine-grained sandstone units that are described below.

1. The Keristal Member

This distinctive unit was first defined by Woodcock *et al.* (1999b) at the west side of Keristal Bay (Fig. 5.2), where a south-southeast dipping succession includes the complete thickness, (here 7m) of the Keristal member. Immediately to the north, the member is repeated over an F1 anticline-syncline fold pair (Plate 5.3(a)). The member comprises a sequence of medium- to thick-bedded quartz arenites or quartz wackes that occur in non-graded or weakly graded beds. The beds within the Keristal Member may be organized into either thinning-up or thickening-up sequences. In thinning-up sequences, the basal bed is often strongly erosional into the underlying thin-bedded turbidites and has basal flute marks (Woodcock *et al.* 1999b). Woodcock & Barnes (1999) interpreted the Keristal Member as the product of a short-lived high- to medium-concentration turbidity flows tapping a source of clean quartz sand that was distinct from the muddy sands more typical of the Lonan Formation. The Keristal Member is probably Tremadoc or earliest Arenig in age based on acritarch assemblages from the underlying Lonan Formation (Chadwick *et al.* 2001).

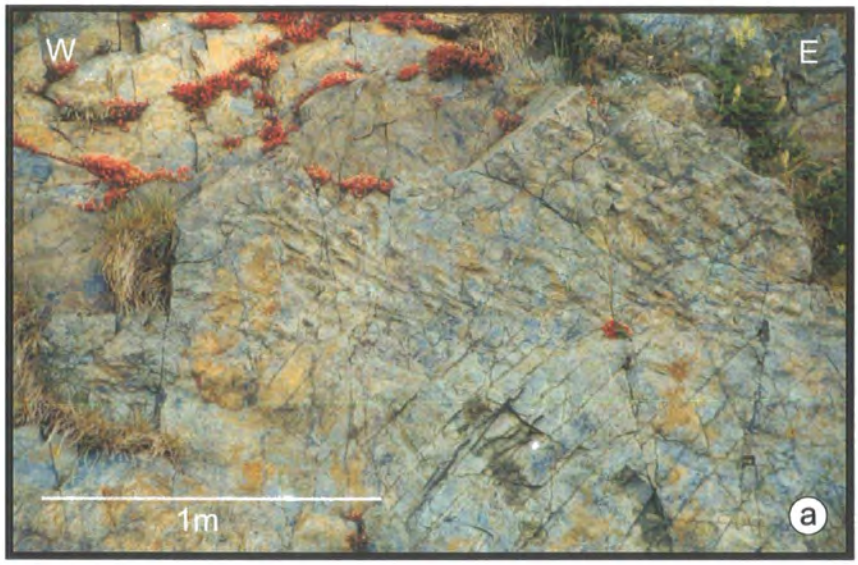

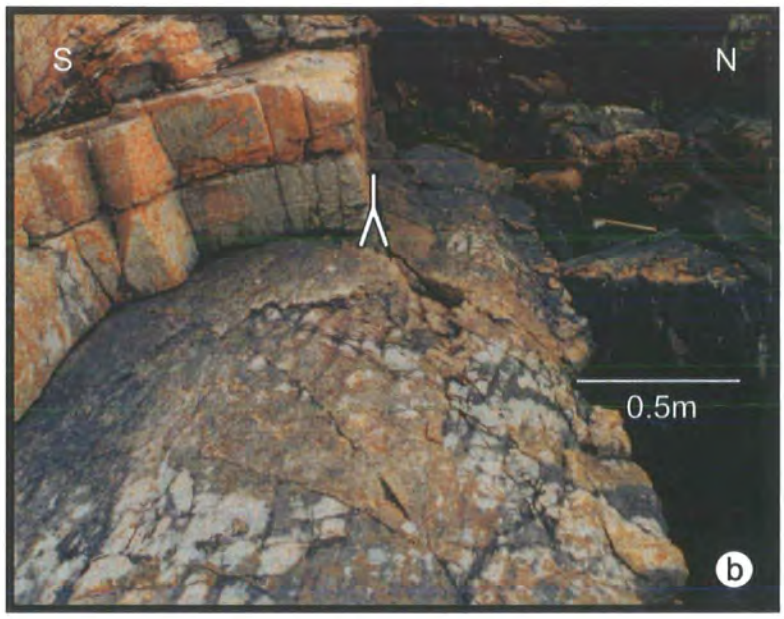

Plate 5.2. **(a)** Flute casts on the base of greywacke sandstone of the Santon Member (Lonan Formation), the bedding dips steeply and youngs to the NW (away from the viewer). The Whing, Marine Drive. (Figs. 5.2, 5.12(b), grid ref. 36057329). **(b)** Ripple marks on bedding folded by primary folds, showing that bedding is the correct way up. Baltic Rock. (Figs. 5.2, 5.12(a), grid ref. 32717023).

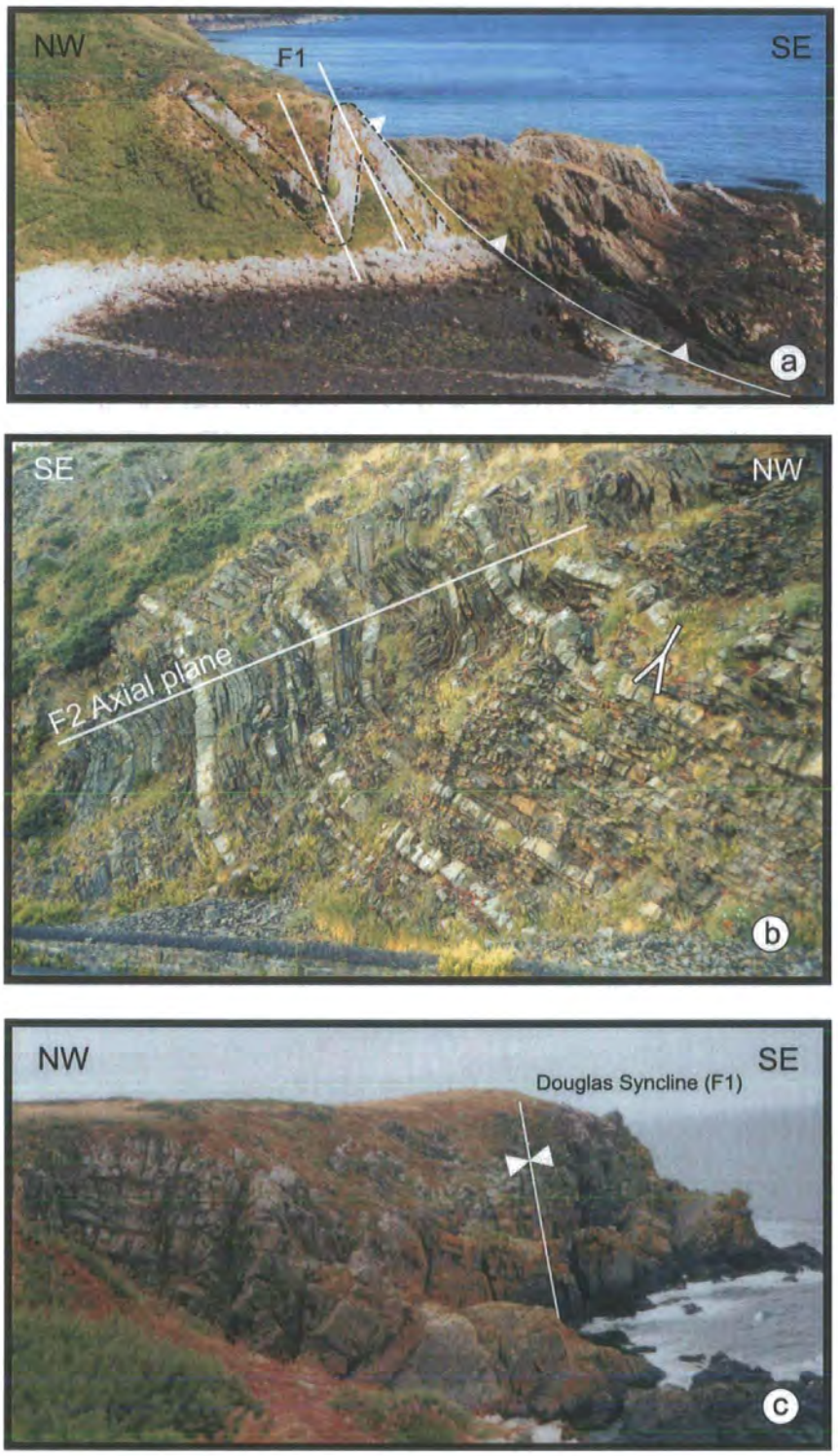

Plate 5.3. **(a)** The Keristal Member folded by a 'S'-verging, primary fold pair on the west limb of the Douglas Syncline. To the SE rocks of the Lonan Formation are thrust in a top-to-the NW sense along a NE-trending fault (highlighted). Viewed from above Keristal Bay, (Figs. 5.2, 5.12(a), grid ref. 37857399). **(b)** Medium- to thick-bedded sandstones and interbedded siltstones of the Santon Member along Marine Drive. The sequence here lies on the east limb of the Douglas Syncline and is affected by secondary folding with shallowly inclined axial planes (highlighted). (Figs. 5.2, 5.12(b), grid ref. 35617318). **(c)** Massive sandstones of the Santon Member folded by the Douglas Syncline at Santon Head. (Figs. 5.2, 5.12(a), grid ref. 333702).

2. The Santon Member

This unit is well-exposed in coastal sections from Onchan Head to Purt Veg where it outcrops in the core of the Douglas Syncline (Fig. 5.2). Originally named the Santon Formation by Woodcock *et al.* (1999b) and Woodcock & Barnes (1999) (Table 5.1) it is characterised by medium- or thick-bedded, light grey or greenish-grey wacke intercalated with a thin bedded facies more typical of the Lonan Formation. The wacke that dominates the member is particularly quartzose in places, locally becoming arenitic (e.g. Marine Drive, Fig. 5.2, Plate 5.3(b), Chadwick *et al.* 2001). An unusually thick-bedded, coarse-grained sequence is exposed near to Santon Head (Fig. 5.2, Plate 5.3(c)) and is thought to be the fill of a trunk distributary channel in the turbidite system (Woodcock & Barnes 1999). Although the top of the Santon Member is now above the present erosion level, the exposed successions are approximately 600m thick (Chadwick *et al.* 2001). Acritarch assemblages within the Santon Member indicate an early Arenig age (Molyneux 1999).

3. The Ny Garvain Member

In recognition of compositional and structural uncertainty over its correlation with the rest of the Lonan Formation the name Ny Garvain Formation was introduced by Woodcock *et al.* (1999b) (Table 5.1). During the revision of the 1:50 000 map (British Geological Survey 2001), the name has been restricted to a package of relatively thickly bedded sandstone which crops out along the coast southwards from the headland of Gob ny Garvain (Fig. 5.2). It is possible, based on lithological similarities that it is equivalent to the Santon Member farther south (Chadwick *et al.* 2001).

5.4.1.3 Creg Agneash Formation (Fig. 5.2, Table 5.1, Woodcock *et al.* 1999; Woodcock & Barnes 1999; Chadwick *et al.* 2001).

This formation was described first by Woodcock *et al.* (1999b) and outcrops as a relatively narrow, NE-trending band extending from Maughold Head to a point approximately 5km NW of Douglas where it dies out. The Mull Hill Formation, (see below) which crops out along strike to the SW, is lithologically similar and may be a lateral equivalent (Fig. 5.2, Chadwick *et al.* 2001). The Creg Agneash Formation is best exposed at Maughold Head (Fig. 5.2). The formation is characterized by white quartz arenite, typically thin or medium bedded (Plate 5.4(a)). The sandstone beds are massive or weakly graded from medium or fine sand to very fine sand or silt (Chadwick *et al.*

2001). Beds have weakly defined, often upward-thinning, parallel lamination sometimes with a thin overlying ripple cross-laminated division (Woodcock *et al.* 1999b). The Creg Agneash Formation is interpreted as the depositional product of medium-concentration turbidity currents, punctuating a persistent background of low-concentration events in a deep marine environment (Woodcock *et al.* 1999b). At Maughold Head (Fig. 5.2) the formation is about 180m thick, although the base is faulted. The outcrop width increases to the SW where the outcrop may be as much as 750m thick, although there may be some repetition due to folding or faulting. The base of the formation, which is gradational with the Lonan Formation, is exposed in the River Laxey (Fig. 5.2, grid ref. 41838670) and on the coast near to Maughold Head (Fig. 5.2, grid ref. 49839130). The top of the formation is transitional into the Maughold Formation (see below) with the sandstone beds decreasing gradually in thickness before giving way abruptly to laminated silty mudstone (Chadwick *et al.* 2001). The Creg Agneash Formation is only dated by its overlying relationship to the Tremadoc to early Arenig Lonan Formation. Although poorly preserved, the sparse, low diversity acritarch assemblages discovered thus far are characteristic of the lower Arenig in the Lake District (Molyneux 2001).

5.4.1.4 Mull Hill Formation (Fig. 5.2, Table 5.1; Woodcock *et al.* 1999b; Woodcock & Barnes 1999; Chadwick *et al* 2001).

First described by Woodcock *et al.* (1999b), the Mull Hill Formation is exposed in coastal sections on the Cregneash Peninsula (Fig 5.2). The strata exposed at the Chasms (grid ref. 19346638) is repeated by a large recumbent fold pair, to re-emerge at Gansey Point (grid ref. 215680, Fig. 5.2, Fitches *et al.* 1999). An outcrop of quartzose sandstone exposed at Spaldrick (grid ref. 19406957) on the NW margin of Port Erin Bay has also been assigned to the Mull Hill Formation (Fig. 5.2, Woodcock *et al.* 1999b). The formation is characterised by light grey to white, medium- to very thick-bedded quartz arenite, which contrasts very strongly with the thin or very thin-bedded facies of the underlying Lonan Formation. The sandstones fine upwards from medium-grained sand to very fine sand or silt. Beds are typically massive or parallel laminated at the base with an overlying cross-laminated division (Plate 5.4(b), Woodcock *et al.* 1999b). The contact between the Mull Hill Formation and the underlying Lonan Formation is gradational over about 25m. Woodcock *et al.* (1999b) estimated a thickness of between 350-400m for the formation across the Cregneash Peninsula, whilst the outcrop at Spaldrick, interpreted as a lateral margin of the Mull Hill turbidite

Plate 5.4. **(a)** Thin- to medium-bedded rocks of the Creg Agneash Formation at Maughold Head, (Figs. 5.2, 5.26, grid ref. 49859150). **(b)** Fining-up and cross-stratification within quartz arenites of the Mull Hill Formation at Gansey Point (Figs. 5.2, 5.24, grid ref. 21306811). Viewed end on to steeply NW-dipping and younging bedding. Lens cap is 55mm in diameter.

system is about 40m thick, although the top of the formation is not exposed (Chadwick *et al.* 2001). Dating of the Mull Hill Formation is based on its interpreted overlying relationship with the Tremadoc to early Arenig Lonan Formation (Chadwick *et al.* 2001).

5.4.1.5 Maughold Formation (Fig. 5.2, Table 5.1, Woodcock *et al.* 1999b; Chadwick *et al.* 2001).

The Maughold Formation (Woodcock *et al.* 1999b) is exposed in largely inaccessible cliff sections around Maughold Head in the NE and Bradda Head in the SW (Fig. 5.2). The formation is dominated by dark grey mudstone in bedded or disrupted facies, but also contains significant amounts of quartz arenite (Plate 5.5(a)). A matrix supported pebbly mudstone containing intraformational clasts of mudstone, siltstone and fine-grained sandstone becomes an important facies between Spaldrick (grid ref. 19166956) and the north flank of Lhiattee ny Beinee (grid ref. 21357300) in the SW of the outcrop (Plate 5.5(b)). Bioturbation is common as spots or as discordant silt-filled or mud-filled burrows (Chadwick *et al.* 2001). Quartz arenites occur as thin to medium beds and resemble the Creg Agneash/Mull Hill facies. The sandstone beds, which have sharp top and basal contacts, are not discernibly graded and commonly contain tabular cross-sets through the thickness of each bed (Plate 5.5(a)). Woodcock *et al.* (1999b) interpreted the mudstones of the Maughold Formation to be the product of hemipelagic deposition and low-concentration turbidity flows into a deep marine, periodically oxygenated basin. The bedded facies were redeposited as pebbly mudstones due to instability within the basin. The contact with the underlying Creg Agneash Formation is gradational and although faulted, a similar relationship is assumed with the Mull Hill Formation at Port Erin (Chadwick *et al.* 2001). Where the quartz arenite units are absent to the west of Douglas, a gradational contact with the Lonan Formation has been inferred, although the similarity of the facies precludes an accurate definition of the contact. The NW contact with the Barrule Formation, (see below) is interpreted to be faulted, although an original stratigraphical relationship between the two Formations seems likely (Chadwick *et al.* 2001). Uncertainty about the structure precludes accurate thickness estimates for the Maughold Formation, although 500 to 600m has been suggested by Woodcock *et al.* (1999b). As with many formations within the Manx Group the age of the Maughold Formation is based on its interpreted position above the Tremadoc to early Arenig Lonan Formation. However, poorly preserved acritarch assemblages suggest that it is not older than Arenig

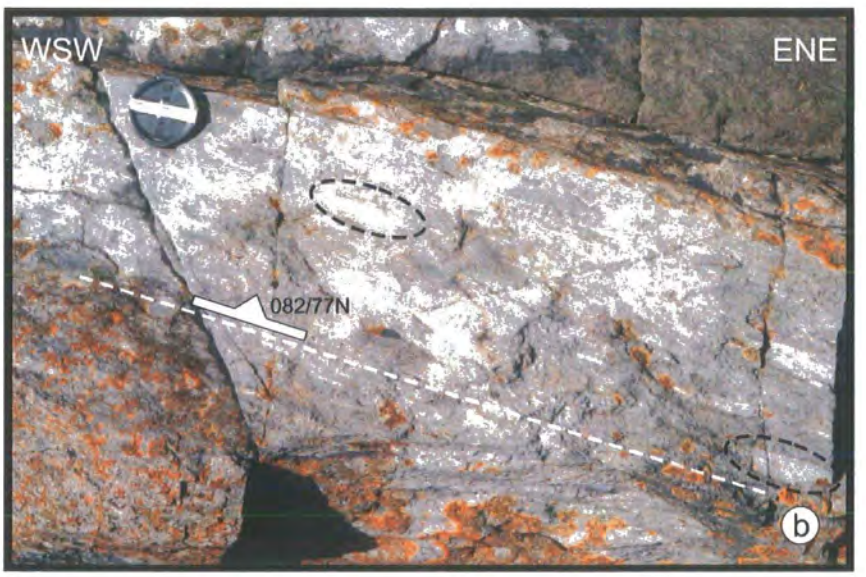

Plate 5.5. **(a)** Cross-stratified quartz arenites of the Maughold Formation. End view onto NW-dipping and younging beds, Bradda Head (Figs. 5.2, 5.23, grid ref. 18406974). **(b)** Pebbly mudstone unit of the Maughold Formation. Clasts (circled) are flattened within the plane of the primary cleavage (dashed line and orientation). On the foreshore below the Bradda Hotel (Figs. 5.2, 5.23, grid ref. 19286965). Lens cap in both pictures is 55mm.

(Molyneux 2001).

5.4.1.6 Barrule Formation (Fig. 5.2, Table 5.1, Quirk & Burnett 1999; Woodcock *et al.* 1999b; Chadwick *et al.* 2001).

Outcrops of the Barrule Formation form the NE-trending upland spine of the Isle of Man. It is exposed along the coast at Lewaigue (Fig. 5.2, grid ref. 468930) on the NE coast extending down to the NE of Burroo Mooar (grid ref. 216735) on the W coast. It consists of remarkably homogeneous medium to dark grey and black pelite with faint but persistent parallel diffuse laminae (Plate 5.6(a), Chadwick *et al.* 2001). The Barrule Formation is interpreted as hemipelagic mud deposited in anoxic bottom water (Woodcock *et al* 1999b). The thickness of the formation is conjectural in the absence of evidence of way-up and internal structure and because the base is never seen. Simpson (1963) estimated a thickness of up to 1030m whereas Woodcock *et al.* (1999b) calculated a thickness of 750m assuming a homoclinal succession. The maximum outcrop width is 900m, but the thickness may be less if it is folded and/or internally imbricated by faults (Chadwick *et al.* 2001). The boundaries of the formation are poorly exposed and frequently faulted. Contact with the Maughold Formation is interpreted as a major fault, with repetition of the Barrule Formation and the base of the Injebreck Formation occurring to the SW of Ramsey (Fig. 5.2, Chadwick *et al.* 2001). The interpreted stratigraphic position above the Lonan Formation and below the middle Arenig Creggan Moar Formation (see below) implies a mid-Arenig age for the Barrule Formation. This is supported, though not confirmed by poorly preserved acritarchs (Chadwick *et al* 2001).

5.4.1.7 Injebreck Formation (Fig. 5.2, Table 5.1, Woodcock *et al.* 1999b; Chadwick *et al.* 2001).

The Injebreck Formation was defined by Woodcock *et al* (1999b) and is well-exposed on the west coast of the island and to the south of Ramsey (Fig. 5.2). In many respects, it is similar to the Maughold Formation, being dominated by laminated dark mudstone with a variable proportion of thinly interbedded siltstone and fine-grained sandstone (Plate 5.6(b), Chadwick *et al.* 2001). However, it also contains units of quartz arenite (e.g. at Lag ny Keeilley, grid ref. 21577459), which are weakly graded and typically planar-laminated, although some ripple cross-lamination is apparent in some thinner beds (Chadwick *et al.* 2001). The lower part of the formation, along with a discontinuous sliver of the top of the Barrule Formation, is repeated by the Lag ny

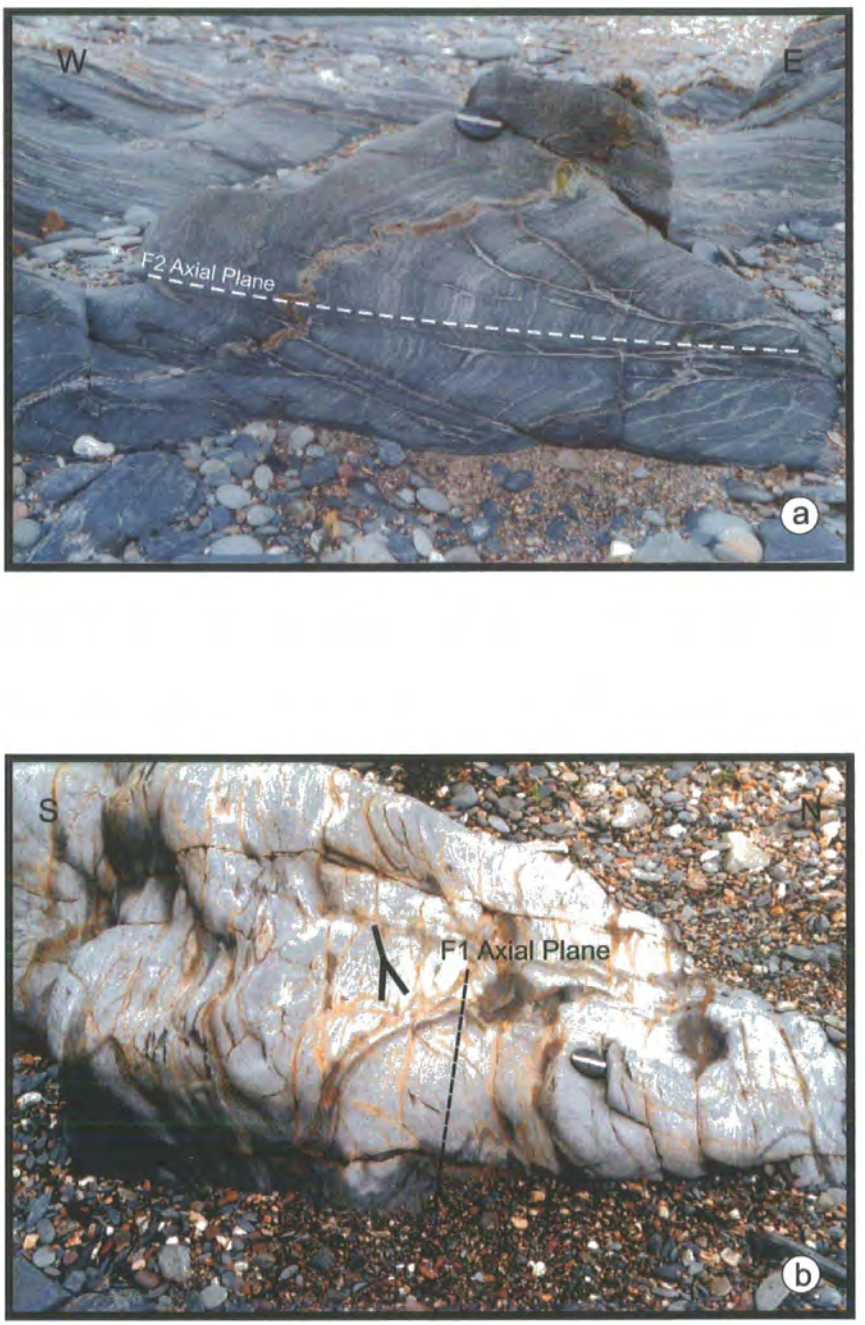

Plate 5.6. **(a)** Waterwashed mudstones of the Barrule Formation, showing fine siltstone laminae. The rocks have been deformed by secondary folds producing sub-horizontal axial planes (highlighted). Near BallureWalk, Lewaigue (Figs. 5.2, 5.27, grid ref. 463093 30). **(b)** Upward-facing primary folds in rocks of the Injebreck Formation, north of Ballure Walk, Lewaigue. (Figs. 5.2, 5.27, grid ref. 46159345). Lens cap in both photographs is 55mm diameter.

Keeilley Fault (grid ref. 21577459, Chadwick *et al.* 2001). Here it consists of a thick sequence of quartz arenites and less mature greenish-grey sandstone, with layers of conglomerate up to 30cm thick in a background of laminated siltstone and mudstone. The sequence immediately south of the Lag ny Keeilley fault is affected by a narrow (ca. 20m) zone of predominantly sinistral high strain (the Lag ny Keeilley Shear Zone, see below). The Injebreck Formation is interpreted as an anoxic hemipelagic background facies, with occasional low-concentration turbidity flows. The sandstone-dominated facies represent periods of medium- to high-concentration flows, some of which were highly quartzose (Woodcock *et al.* 1999b). A thickness of several hundred metres, allowing for repetition by folding is suggested for the formation. The SE boundary is gradational with the underlying Barrule Formation, whilst the northern boundary is gradational with the Glen Rushen Formation (see below, Chadwick *et al.* 2001). Woodcock *et al.* (1999b) interpreted this as a south-younging sequence passing stratigraphically up into the Injebreck Formation. Subsequently, the recent resurvey work (British Geological Survey 2001), has suggested that at this point the succession is in fact north-younging (Chadwick *et al.* 2001). The age of the Injebreck Formation is poorly constrained and is based in part on poorly preserved, sparse acritarch assemblages found at a variety of localities within the formation. This data combined with the inferred stratigraphical position of the formation above the Lonan Formation but below the Creggan Moar Formation (see below) suggests an early to mid-Arenig age (Chadwick *et al.* 2001).

5.4.1.8 Glen Rushen Formation (Fig. 5.2, Table 5.1, Woodcock *et al.* 1999b; Chadwick *et al.* 2001).

The Glen Rushen Formation is named after Glen Rushen (grid ref. 24457845) and is exposed intermittently from Glen Helen (grid ref. 29528432) in the north to Fheustal (grid ref. 21737654) on the west coast forming a narrow NE-trending strip (Fig. 5.2). Woodcock *et al.* (1999b) defined the Glen Rushen Formation separately from the Barrule Formation although they considered it likely that the two were equivalent. However, the recent recognition of the stratigraphical position of the Glen Rushen Formation between the Injebreck and Creggan Moar formations precludes this possibility (Chadwick *et al.* 2001). Lithologically, the Glen Rushen Formation is similar to the muddy facies within the Injebreck Formation. It is composed of laminated, medium to dark grey or bluish grey mudstone with variable proportions of sub-millimetre, pale siltstone laminae. The laminae are laterally persistent and

bioturbation is absent. Woodcock *et al.* (1999b) interpreted the formation as an anoxic hemipelagic facies, with occasional input of low-concentration turbidity flows (Woodcock *et al.* 1999b; Chadwick *et al.* 2001). A suggested thickness of no more than 250-500m was proposed by Woodcock *et al.* (1999b), although this is poorly constrained in the absence of evidence for internal structure. Sparse acritarch faunas from several localities within the Glen Rushen Formation suggest a mid-Arenig age (Chadwick *et al.* 2001).

5.4.1.9 Creggan Moar Formation (Fig. 5.2, Table 5.1; Kennan & Morris 1999; Woodcock *et al.* 1999b; Chadwick *et al.* 2001).

This formation was defined by Woodcock *et al.* (1999b) to include rocks containing distinctive, very thin (<5mm) beds of manganiferous ironstone. This is well exposed on the west coast to the south of Niarbyl (Fig. 5.2, grid ref. 21187758) for approximately 1km and was fully described by Kennan & Morris (1999), who suggested that this lithology may be the precursor to the distinctive coticule seen widely throughout the early Ordovician succession within the Appalachian-Caledonian Orogen (see section 4.3). The formation is dominated by sandstone or siltstone and dark grey mudstone, with very thin beds of manganiferous ironstone (Plate 5.7(a)). The thin or very thin sandstone/siltstone beds consist of very fine-grained pale or greenish grey or occasionally reddish brown sand. The manganiferous beds weather to a bright reddish brown or dark brown to black colour, and occur singly or are clustered (Plate 5.7(a), Chadwick *et al.* 2001). Quartz arenite is also present as sporadic pale grey, faintly laminated, thin to medium beds (Plate 5.7(b)). The Creggan Moar Formation is interpreted mostly as the product of low-concentration turbidity flows and exhalative manganese deposits into oxygenated bottom waters (Woodcock *et al.* 1999b). The top of the formation is not seen and is in fault contact with the Glen Dhoo Formation in the north and the Silurian Niarbyl Formation (see below) at Niarbyl Bay (grid ref. 21187758) in the south. This, combined with extensive internal deformation precludes an accurate estimation of thickness to be made, although, it is likely to be in the order of several hundred metres (Chadwick *et al.* 2001). Recent work by Molyneux (2001) indicates an age range of mid- to late Arenig.

5.4.1.10 Lady Port Formation (Fig. 5.2, Table 5.1, Woodcock *et al.* 1999b; Woodcock & Morris 1999; Chadwick *et al.* 2001)

Described in detail by Woodcock & Morris (1999), the Lady Port Formation

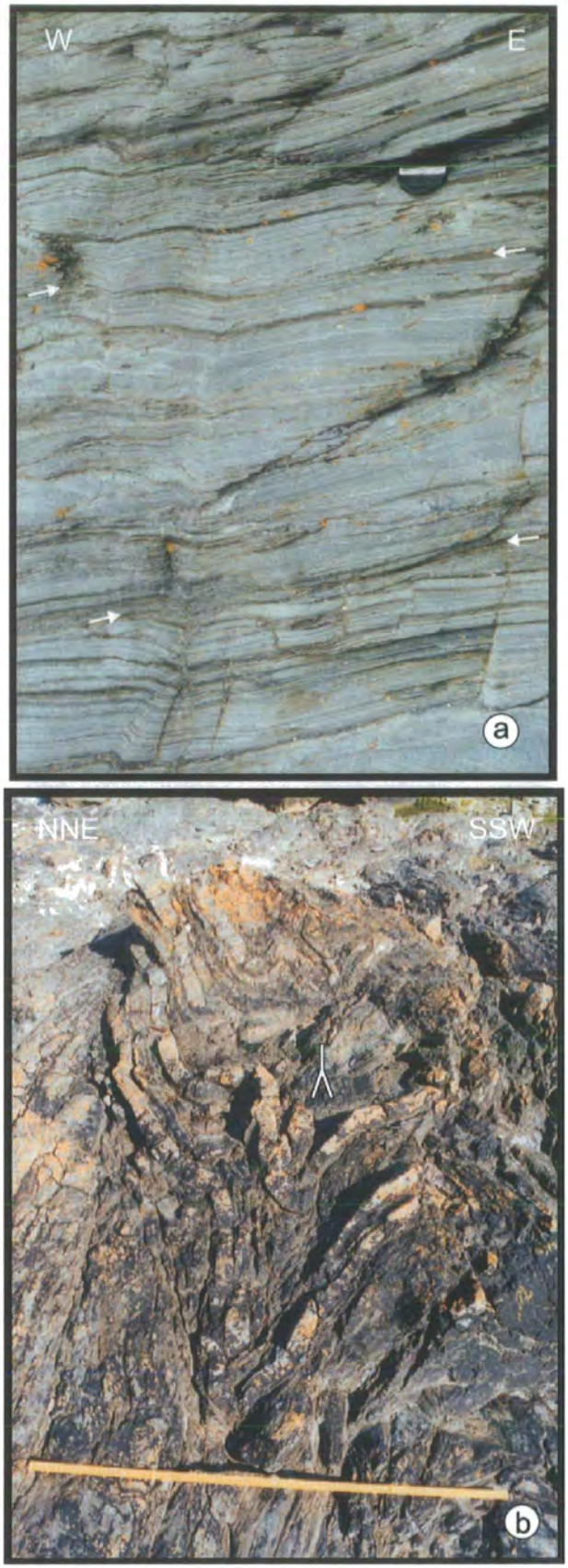

Plate 5.7. **(a)** Thin, pale, greenish-grey siltstones and darker mudstones of the Creggan Moar Fm., with thin dark brown laminae of manganiferous ironstone (highlighted). Niarbyl (Figs. 5.2, 5.29, grid ref. 21187758). Lens cap is 55mm in diameter. **(b)** Folded thin-bedded quartz arenites of the Creggan Moar Fm. Niarbyl (Figs. 5.2, 5.29, 5.30, grid ref. 21177756). Metre ruler for scale.

outcrops as a narrow fault bounded, NE-trending strip near to Lady Port on the NW coast of the island (Fig. 5.2). The formation is highly heterogeneous, but the most common lithology is medium grey to black mudstone, thinly to thickly laminated due to alternations of siltstone and clay-rich mudstone. Light grey, quartzose sandstone punctuates the mudstone succession in places, typically forming thin or very thin beds. In facies similar to that of the Creggan Moar Formation, distinctive, buff or black manganiferous beds a few millimetres thick occur north of Ballanayre (grid ref. 28108710). At Ballanayre Strand (Fig. 5.2, grid ref. 27638678) thin- to medium-bedded, light grey to greenish-grey wackes occur (Chadwick *et al.* 2001). Beds fine upwards from fine or very fine-grained sandstone to mudstone. Parallel- and ripple cross-lamination is present in some localities, although beds are often highly bioturbated and strongly disrupted by soft-sediment slumping and tectonic deformation (Plate 5.8(a), Woodcock & Morris 1999). Well exposed along the coast near to Ballanayre Strand are beds of pebbly mudstone (Plate 5.8(b)). These contain clasts typically 1 to 5cm in diameter, but which are commonly up to 25cm in size, and are thought to be cohesive debris flows (Woodcock & Morris 1999). Large blocks of bedded sediments occur within the succession, and their similarity with other formations such as the distinctive manganiferous ironstone bearing facies of the Creggan Moar Formation suggests that they may be blocks within an olistostrome (Woodcock & Morris 1999; Chadwick *et al.* 2001). The Lady Port Formation is interpreted as the product of deposition in a mudstone-prone deep marine sub-basin that was subject to repeated slumping and debris flow. Quartz arenites preserve evidence of medium-concentration turbidity flows carrying mainly quartzose sands (Woodcock *et al.* 1999b). Estimating the thickness of the Lady Port Formation is difficult since the formation is internally complex, incompletely exposed and structurally isolated. However, Woodcock *et al.* (1999b) estimate a thickness of not more than few hundreds of metres. Molyneux (1999) suggested that, based on limited palaeontological evidence, the Lady Port Formation is probably late Arenig in age, but added the caveat that due to the complex and disrupted nature of the formation this should be regarded as a maximum age (Chadwick *et al.* 2001).

5.4.2 Dalby Group

At present, the Dalby Group comprises only the Niarbyl Formation.

5.4.2.1 Niarbyl Formation (Fig. 5.2, Table 5.1, Morris et al. 1999; Chadwick et al.

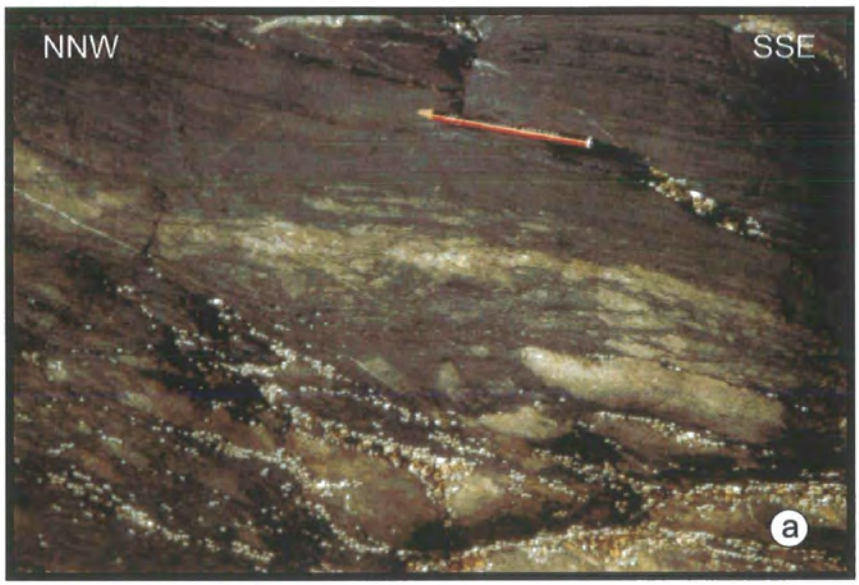

Plate 5.8. **(a)** Soft sediment deformation within the Lady Port Formation, Lynague. (Fig. 5.32, grid ref. 28408742). **(b)** Clasts of siltstone and mudstone within slump breccia of the Lady Port Formation, Lynague (Fig. 5.32, grid ref. 27888698)

2001).

The Niarbyl Formation is well exposed on the west coast between Peel and Niarbyl (Fig. 5.2). It comprises predominantly fine- to medium-grained sandstone and silty mudstone, but includes thinly laminated hemipelagite and rare metabentonite beds (Chadwick *et al.* 2001). Most of the succession consists of thin-, medium- or thick bedded, pale grey sandstone with thin mudstone partings (Plate 5.9(a)). Sole marks are common on sandstone beds (Plate 5.9(b)) indicating palaeocurrent directions that are dominantly from the NW. Bouma sequences, characteristic of turbidite deposits are well developed within the sandstone beds, which occur in thinning- and thickening-upwards successions up to 15m thick. Sporadic thicker massive sandstones are thought to be sandstone lobe deposits, and to represent channel fill deposits. Thin metabentonite beds were first recorded by Lamplugh (1903) from Contrary Head (grid ref. 224815) and three occurrences were described by Morris *et al.* (1999) from Dalby Point (grid ref. 21257875). The hemipelagite, (Plate 5.9(c)) which comprises alternate layers of organic material and siltstone, was probably deposited from suspension (Morris *et al.* 1999).

The Niarbyl Formation is incompletely exposed, and all of its contacts with the Manx Group are faulted. In the south around The Niarbyl it is juxtaposed alongside a broad, ductile, high strain zone (the Niarbyl Shear Zone, Simpson 1963; Morrison 1989; Roberts *et al.* 1990; Morris *et al.* 1999) within the Creggan Moar Formation by a low angled fault (the Niarbyl Thrust, Fitches *et al.* 1999). The contact with the Creggan Moar Formation in the SE and that with the Glen Dhoo Formation near Peel are also interpreted as being tectonic. Morris *et al* (1999) suggest that, after removing the effects of folding and faulting the exposed succession has a thickness in the order of 1250m.

5.5 Areas of study on the Isle of Man and general structure

5.5.1 Areas of study

The rocks of the Manx and Dalby groups are generally well-exposed around the coast of the Isle of Man (Fig. 5.2, 5.9). Fieldwork was focused on a number of well-exposed, easily accessible key localities (Fig. 5.10). The tract system defined by Woodcock *et al.* (1999b) and Fitches *et al.* (1999) (Fig. 5.9) provided a useful framework for the collection of structural data, and will be employed when discussing

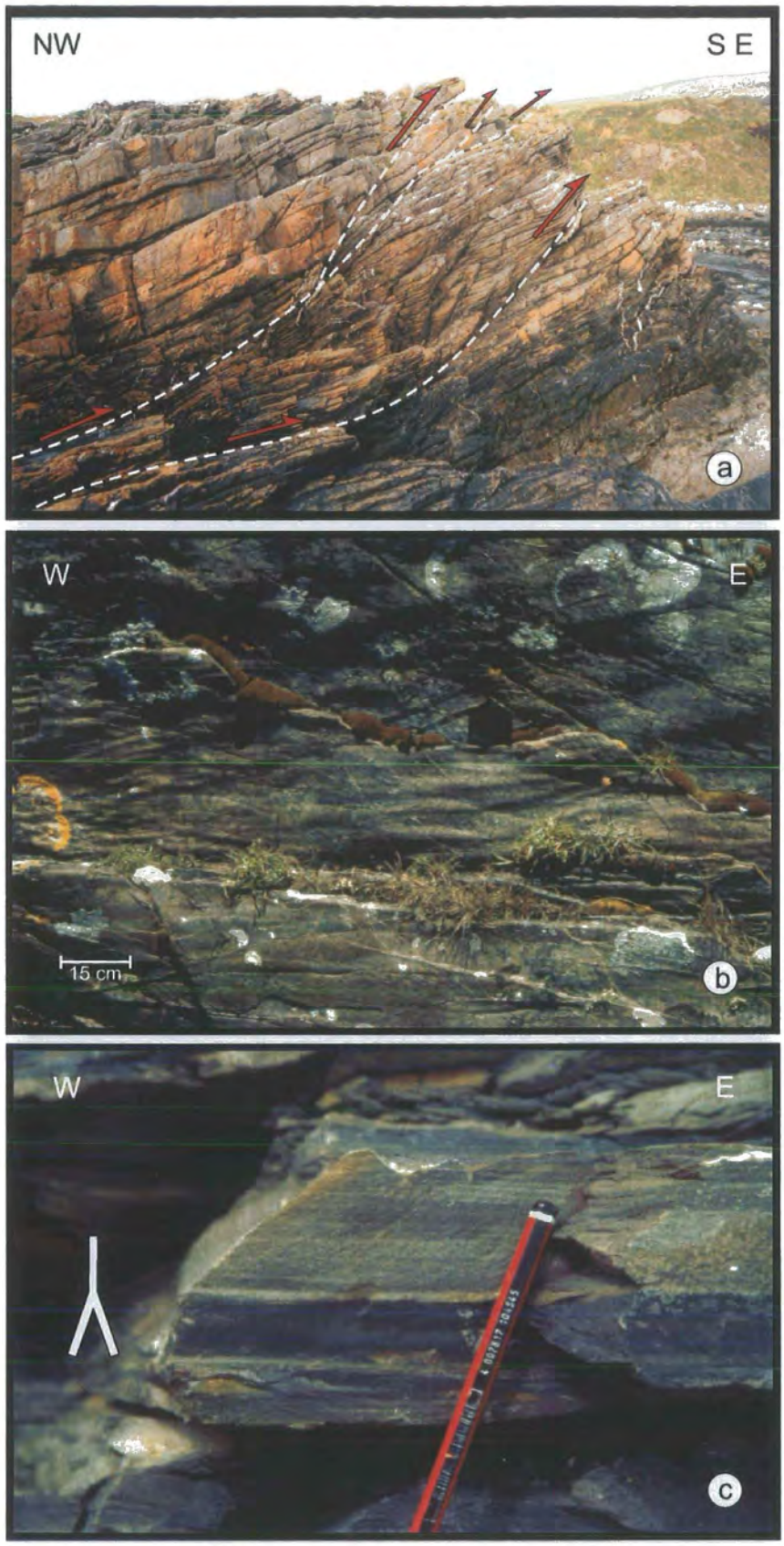

Plate 5.9. **(a)** Top-to-SE thrusting associated with the Niarbyl Thrust in rocks of the Niarbyl Formation on The Niarbyl (Fig. 5.29, grid ref. 21087756). **(b)** Flute casts on the base of overturned bedding, near to Dalby Point. (Fig. 5.35, grid ref. 21277865). **(c)** Hemipelagite unit within the Niarbyl Formation showing normal grading. Near to Lhoob Doo (Fig. 5.35, grid ref. 21157835)

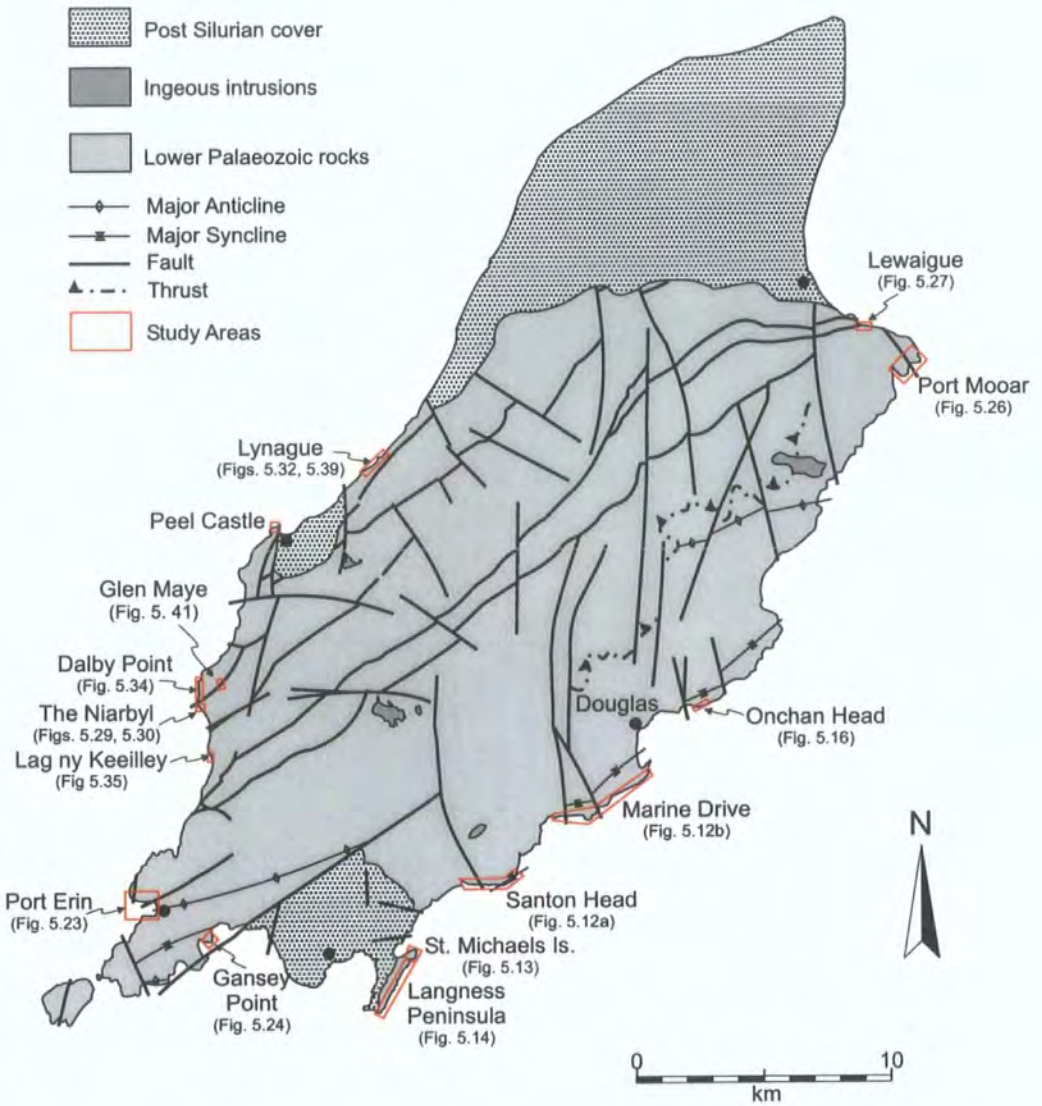

Figure 5.10. Generalised geological map of the Isle of Man showing the location of areas studied..

the structure of the island. Data were collected from seven of the eight tracts; tract 5 was omitted due to very poor access and limited exposure (Fig. 5.9). Access to many sections, e.g. Lynague, Lewaigue, Niarbyl and Port Erin (Fig. 5.10) requires low water conditions as outcrops may be partly or wholly covered at high tide. Many localities are only accessible from a small number of safe access points (e.g. Lag ny Keeilley, Maughold Head). As in Eyemouth and SE Ireland, way-up criteria have been used to provide a detailed analysis of fold and cleavage facing patterns, in addition to the standard orientation analysis using stereographic projections. However, in many of the mudstone units way-up criteria is ambiguous or absent, therefore in such areas no facing analysis was possible. Overall, the three-phase deformation of the Lower Palaeozoic rocks on the island described by Simpson (1963) and Fitches *et al.* (1999) is confirmed. As noted by Fitches *et al.* (1999), D3 is only locally developed and has a similar orientation to structures observed by these authors in Carboniferous rocks near Castletown. These structures have therefore been attributed to Variscan deformation by Fitches *et al.* (1999) and will not be considered further in this thesis.

5.5.2 General structure

The large-scale primary fold pattern (F1 of Simpson (1963) and Fitches *et al.* (1999)) that dominates the structure of the island is largely confirmed by bedding data (Fig. 5.11a(i)). Poles to bedding lie along a NNW-trending, WSW-dipping girdle that defines a shallowly ENE-plunging β axis, with a well-defined broad point maxima that is consistent with a moderately NW-dipping mean bedding plane (Fig. 5.11a(i)). Minor primary fold axes show an ENE-plunging maximum that corresponds with the regional β axis, but are distributed very significantly along a girdle lying sub-parallel to the mean fold axial plane (Fig 5.11a(ii)). This relationship suggests that the fold hinges are significantly curvilinear. This is confirmed by field observations (see below). The primary cleavage (S1 of Simpson (1963) and Fitches *et al.* (1999)) is variably developed throughout the island and appears to be lithologically controlled. Coarse-grained lithologies, such as the Santon Member show little evidence of cleavage (Plate 5.10(a)), whereas finer-grained lithologies such as the Lonan Formation, contain a strong penetrative cleavage (Plate 5.10(b)). In areas where secondary deformation (D2 of Simpson (1963) and Fitches *et al.* (1999)) is particularly intense, the primary cleavage is often preserved in the coarser-grained lithologies, whilst the secondary cleavage (S2 of Simpson (1963) and Fitches *et al.* (1999)) is preserved in the silt and mudstone horizons (see below, Plate 5.11(a)). No mineral lineations are visible on exposed cleavage

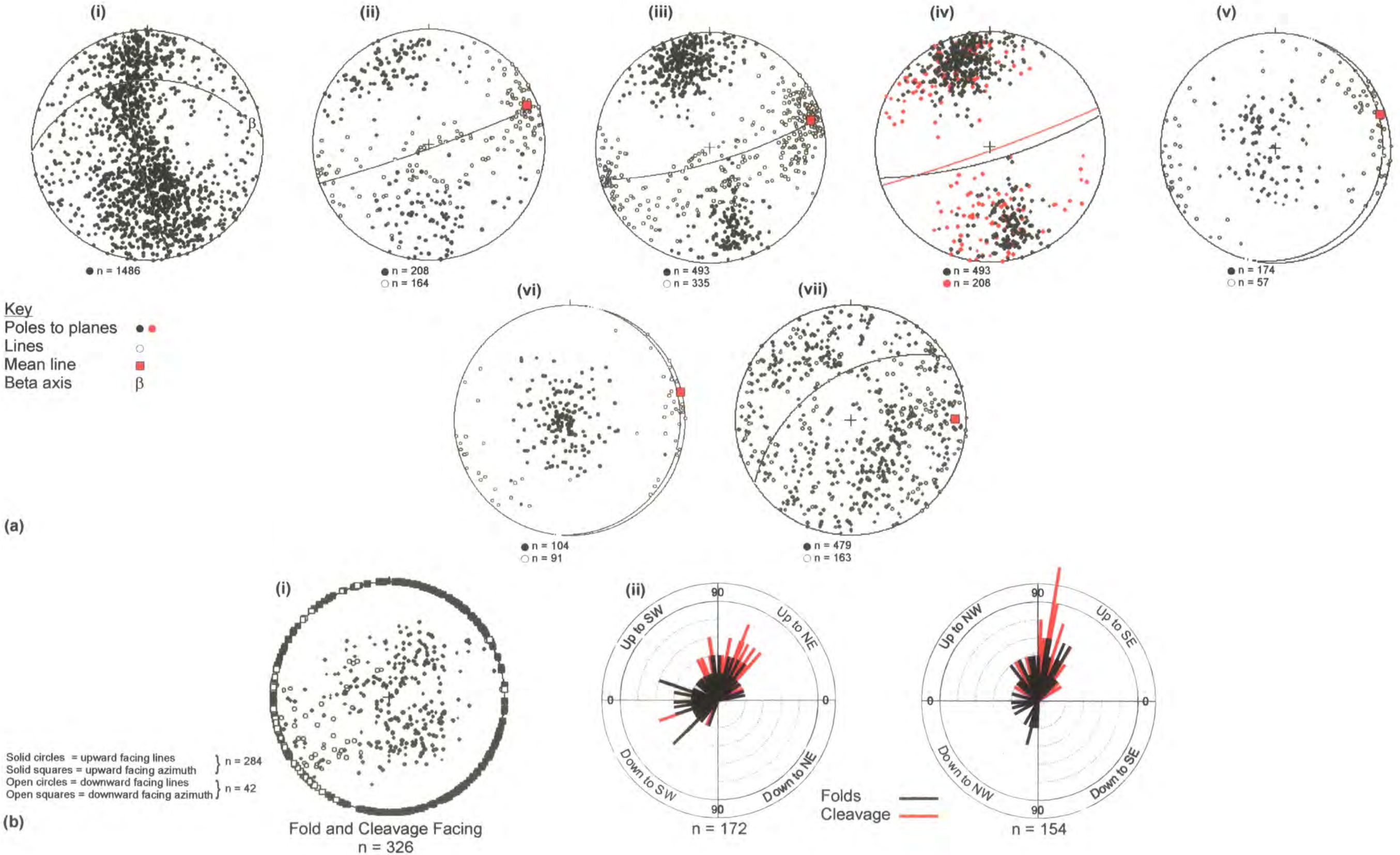

Figure 5.11. **(a)** Stereoplots of structural data for the Isle of Man. **(i)** Poles to bedding, with best fit great circle (dashed, 168/83N), mean bedding (solid, 086/43N) and regional β axis (7/078). **(ii)** Poles to primary fold axial planes and fold hinges, with mean fold hinge (10/068) and axial plane (070/88S) shown. **(iii)** Poles to primary cleavage and bedding-cleavage intersection lineation (BCIL), with mean BCIL(11/074) and cleavage plane (074/80S) shown. **(iv)** Poles to primary fold axial planes and cleavage, with mean axial plane (Red, 070/88S) and cleavage planes (black, 074/80S) shown. Apparent clockwise transection (4°). **(v)** Poles to secondary folds and fold hinges, with mean fold hinge (5/072) and axial plane (016/9N) shown. **(vi)** Poles to secondary cleavage and bedding-cleavage intersection lineation (BCIL) with, mean BCIL (0/076) and cleavage plane (008/5E) shown. **(vii)** Poles to fault planes and slickenlines with, mean slickenline (12/090) and fault plane (077/58N) shown. **(b)** Facing data for all of the Isle of Man. **(i)** Fold and cleavage facing lines and azimuths plotted using the construction method of Holdsworth (1988) (see section 1.4). **(ii)** Plots showing pitch of fold and cleavage facing directions in planes parallel to the fold axial or cleavage plane in which they were measured.

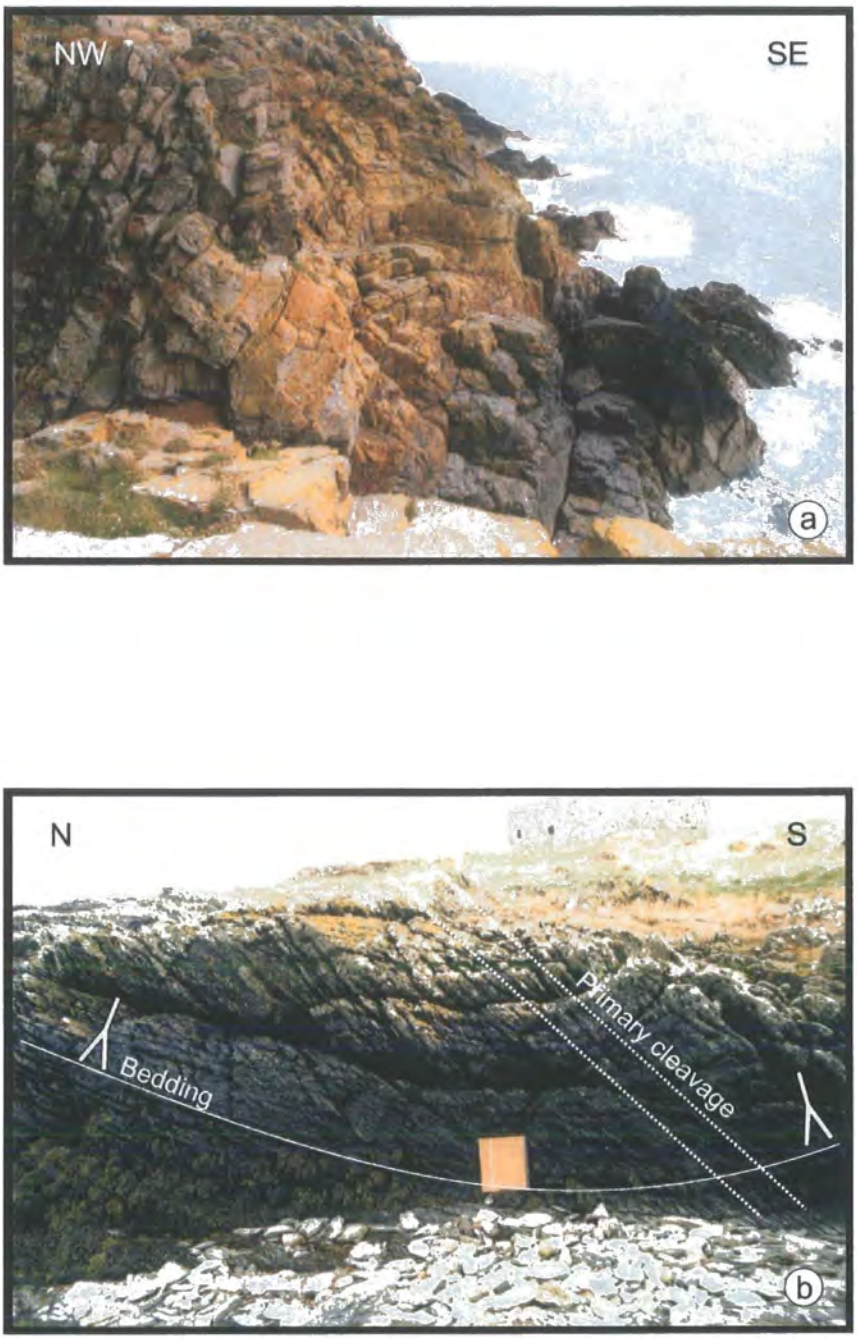

Plate 5.10. **(a)** Santon Member coarse sandstones folded by upright, upward facing primary folds. Coarse lithologies such as this preserve only a very weak primary cleavage or none at all. South of Santon Head (Fig. 5.12(a), grid ref. 33407034). **(b)** Upward facing syncline within the thinly-bedded fine sandstones and siltstones of the Lonan Formation. These contain a strongly developed penetrative primary cleavage (highlighted). NW shore of St. Michael's Island (Fig. 5.13, grid ref. 29526752). Map board is 30cm high.

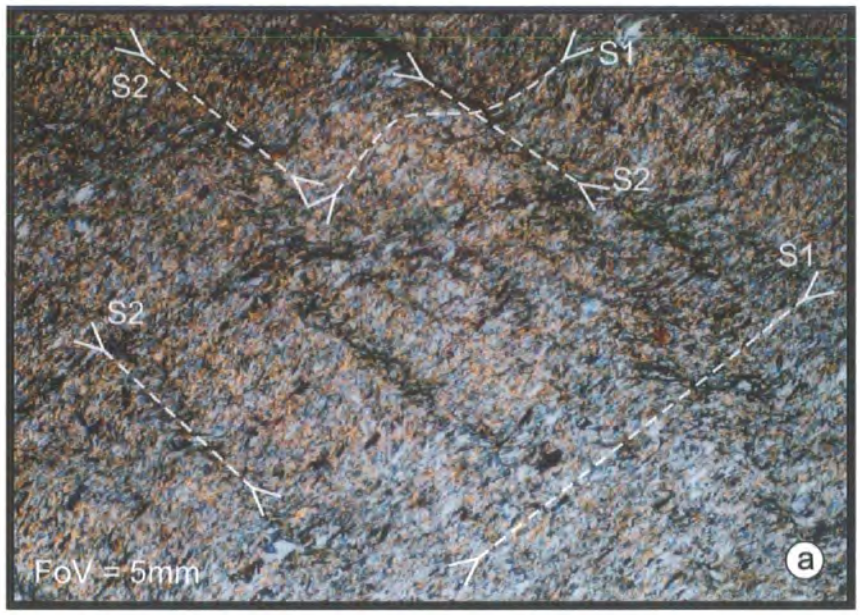

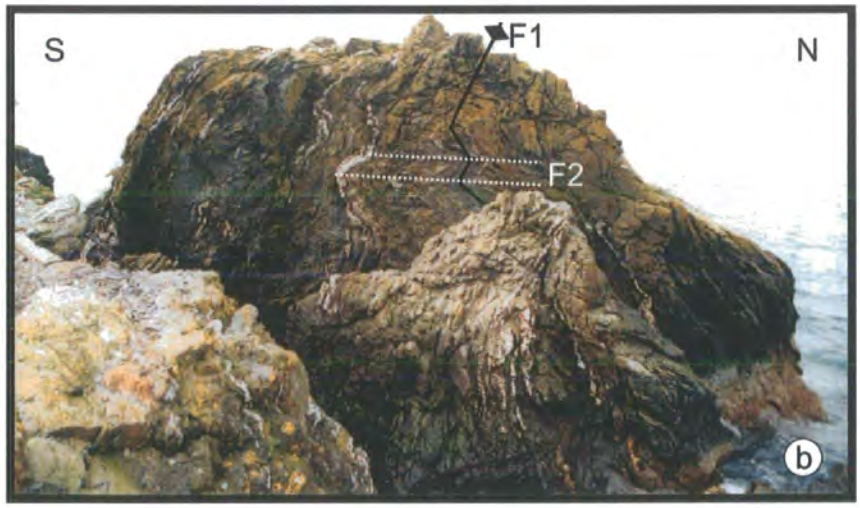

Plate 5.11. (a) Thin section micrograph showing the primary (S1) cleavage and secondary (S2) crenulation cleavage within the fine-grained sandstones of the Mull Hill Formation. The primary cleavage is defined by elongate and flattened quartz grains (grey interference colours) and aligned micas (yellow and orange interference colours). (taken in XPL. sample SP1 grid ref. 19376958). **(b)** Primary fold (F1) refolded into a type-3 interference pattern by sub-horizontal secondary folds (F2). The Castles, Port Erin Bay (Fig. 5.23, grid ref. 18806892).

surfaces. Primary bedding-cleavage intersection lineations (BCIL) and poles to cleavage planes are broadly consistent with the primary minor fold plunges and axial plane data (Fig. 5.11a(ii), (iii)). Both exhibit a small amount (ca. 4°) of apparent clockwise transection (Fig. 5.11a(iv)). Fold and cleavage facing directions collectively exhibit approximately 270° of variation, from sideways NE, through upwards to SW sideways and downwards (Fig. 5.11b(i), (ii)). Structures related to secondary deformation include type-3 refolds of primary folds (Plate 5.11(b)) and a crenulation cleavage (Plate 5.11(a)). Poles to secondary fold axial planes are broadly distributed about the horizontal, and define a shallowly ESE-dipping mean axial plane (Fig. 5.11a(v). The majority of secondary fold hinges plunge at shallow angles, with variable azimuths ranging to NNE to SE and NW to SW (Fig. 5.11a(v)). The statistical mean secondary fold hinge plunges very gently to the NE and closely correlates with both the regional β axis and the mean, primary fold plunge (Fig. 5.11a(i), (ii), (v)). Poles to secondary cleavage planes closely match those of the secondary fold axial planes (Fig. 5.11a(v), (vi)). However, there are a greater number of cleavage planes with sub-horizontal dips, these define a very gently inclined east-dipping mean cleavage plane (Fig. 5.11a(vi)). Secondary bedding-cleavage intersection lineations (BCIL) plunge gently to the SW and E, with a horizontal mean lineation (Fig. 5.11a(vi)).

The area is extensively faulted, including oblique thrusts, low-angled extensional faults, normal dip-slip faults and steeply inclined, sinistral strike-slip faults (Plates 5.12(a), (b), 5.13(a), (b), Fig. 5.11a(vii)). Poles to fault planes are broadly distributed, but a diffuse maxima defines a moderately inclined, NW-dipping mean plane (Fig. 5.11a(vii)). Slickenfibres show a full range of orientations, occasionally with multiple sets on single fault planes with steps indicating sinistral strike-slip and oblique dip-slip movements (e.g. Plate 5.14(a)). These are most commonly observed on bedding surfaces along Marine Drive (Figs. 5.10, 5.12). The majority of slickenfibres have moderate to shallow plunges suggesting that many faults possess an oblique or strike-slip component of movement. More detailed descriptions of the variety of faults observed on the island will be given in the following sections.

Detailed mapping of key sections around the coast of the island shows that the deformation is polyphase and markedly heterogeneous on a mesoscale. This confirms, and adds to the observations of Woodcock *et al.* (1999b) and Fitches *et al.* (1999). Several distinct structural domain types have been identified that appear to be broadly contemporaneous and can be defined on the map scale. Some domains correspond to

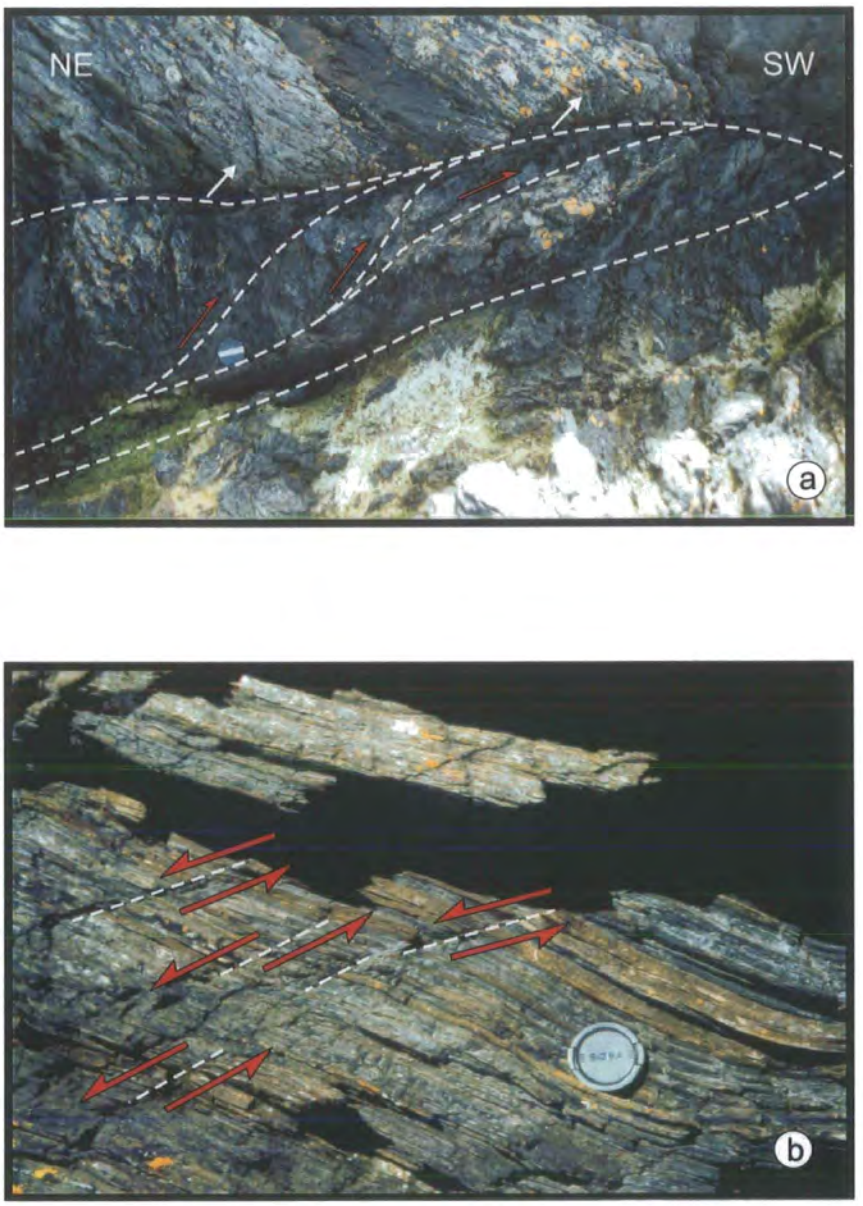

Plate 5.12. (a) Top-to-the WNW dextral oblique thrust duplex at St. Michael's Island (Fig. 5.13, grid ref. 29646746). **(b)** A series of small top-to-the-SW extensional faults, within an extensional fault duplex. Near to Dalby Point (Fig. 5.35, grid ref.21277865). Lens cap in both photographs is 55mm.

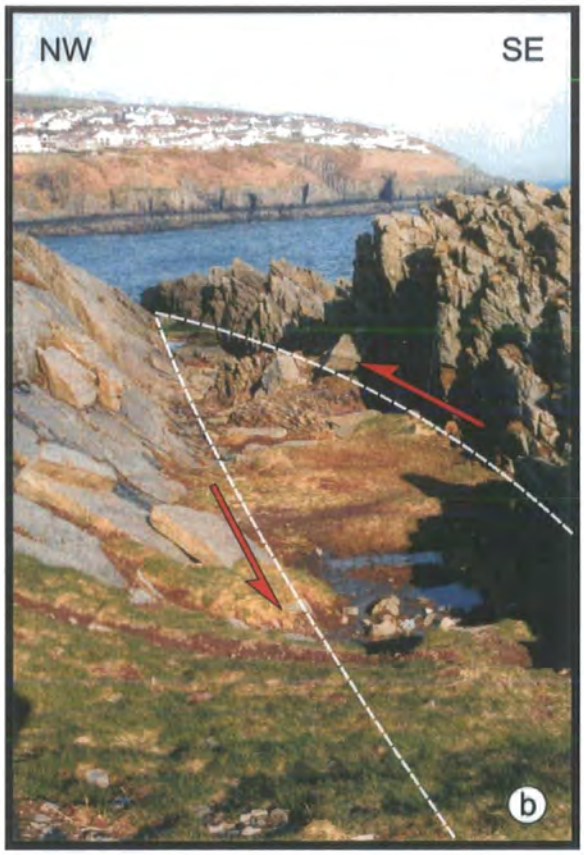

Plate 5.13. **(a)** Normal fault near to Baltic Rock (Fig. 5.12(a), grid ref. 32717023). The base of the thick sandstone bed (highlighted) is downthrown ca.1.5m to the S. **(b)** View NE along the Onchan Head Fault Zone (Figs. 5.2, 5.9, 5.16, grid ref. 402772), the margins of the fault zone are highlighted. The rocks on the SE and NW sides of the fault are relatively undeformed and belong to the Santon Mbr. and Lonan Fm. respectively.

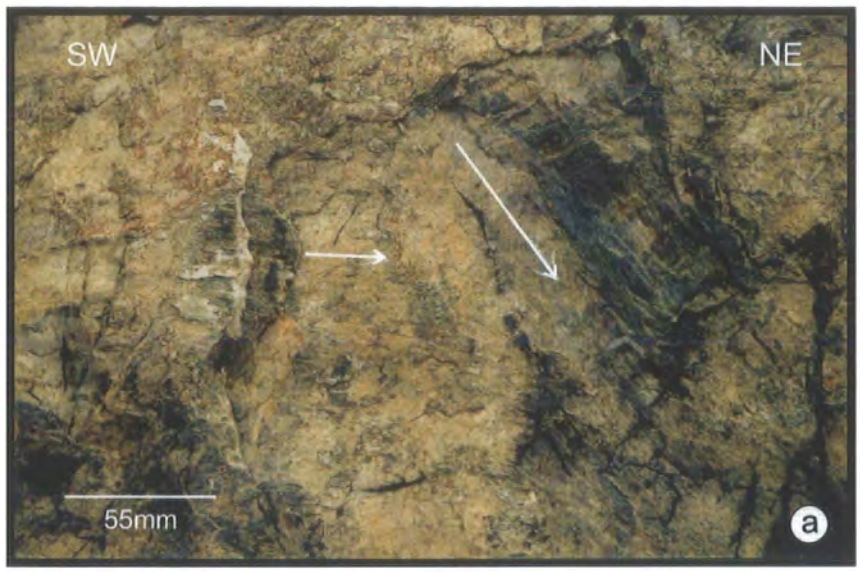

Plate 5.14. **(a)** Sinistral strike-slip and oblique dip-slip slickenfibres on steeply NW-dipping bedding. Horses Leap, Marine Drive (Fig. 5.12(b), grid ref. 569734). **(b)** small steeply plunging primary folds on the SE coast of St. Michael's Island (Fig. 5.13, grid ref. 29566726). Lens cap is 55mm across.

Outline Geological Maps of the SE Coast of the Isle of Man: Port Grenaugh to Santon Head & Keristal to Douglas Head

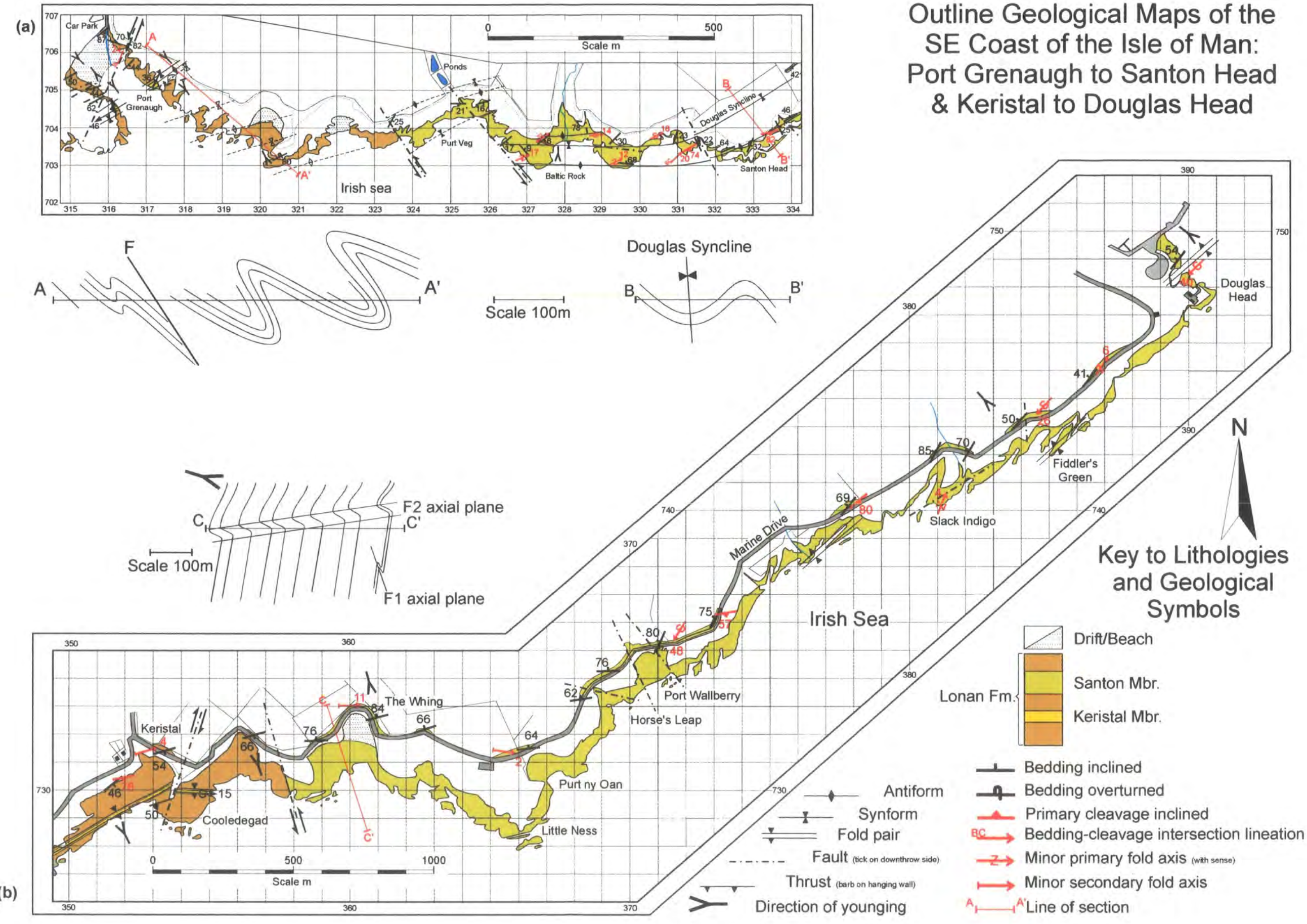

Figure 5.12. Outline Geological maps and cross-sections **(a)** Port Grenaugh to Santon Head. **(b)** Keristal to Douglas Head

the tracts of Woodcock *et al.* (1999b) and Fitches *et al.* (1999) while others either act as tract bounding structures or lie within tracts. The characteristic structures of each tract, tract bounding- or intratract-feature are now described separately.

5.6 Description of separate tracts and domains

5.6.1 Tract 1

Tract 1 (Fitches *et al.* 1999, Woodcock *et al.* 1999b, Fig. 5.9) comprises the greater part of the east coast of the island and consists entirely of rocks of the Lonan Formation (Chadwick *et al.* 2001) and its component members (Figs. 5.2, 5.9, Table 5.1). Several sections along the coast (Figs. 5.10, 5.12, 5.13, 5.14) were mapped. Exposure is generally confined to a relatively narrow coastal strip, rarely exceeding 75m in width and across-strike information of the large-scale structure is therefore limited. The southeastern boundary of Tract 1 probably lies offshore to the SE, and may correspond to the island's southern, major bounding fault (Fig. 5.1), while the northwestern boundary is inferred to be the Shag Rock Fault in the south and an unnamed thrust to the NW of Douglas (Figs. 5.2, 5.9).

Poles to bedding (Fig. 5.15a(i)) show a rather diffuse distribution, but define a broad maximum corresponding to a steep, SSE-dipping mean homoclinal plane. The tract is folded by a series of primary folds on a wide range of scales. These range from sub-metre to several tens of metres (Plates 5.14(b), 5.15(a)), and spread a subordinate number of bedding poles along a girdle that indicates a shallowly E-plunging β axis (Fig. 5.15a(i)). This appears to be contrary to the distribution shown by the plunge of the primary folds, which exhibit a wide range of hinge line curvilinearity and whose mean plunges steeply to the SE (Fig. 5.15a(ii)). This is mirrored in part by the primary bedding-cleavage intersection lineation, (Fig. 5.15a(iii)) although the mean lineation corresponds more closely to the regional β axis (Fig. 5.15a(i)). This wide variation in fold hinge and bedding-cleavage intersection lineation plunge is largely restricted to the St. Michael's Island and Langness Peninsula (Figs. 5.2, 5.10, 5.13, 5.14 see below). Although poles to primary fold axial planes and primary cleavage planes are very broadly coincident, defining steep SE- and SSE-dipping mean planes respectively (Fig. 5. 15a(ii), (iii)), the axial planes are markedly clockwise transected by the cleavage (ca. 13°) (Fig. 5.15a(v)). This relationship is confirmed by field evidence at several localities throughout tract 1 (e.g. Fig. 5.12(a), (b), grid ref. 33227024, 37807400).

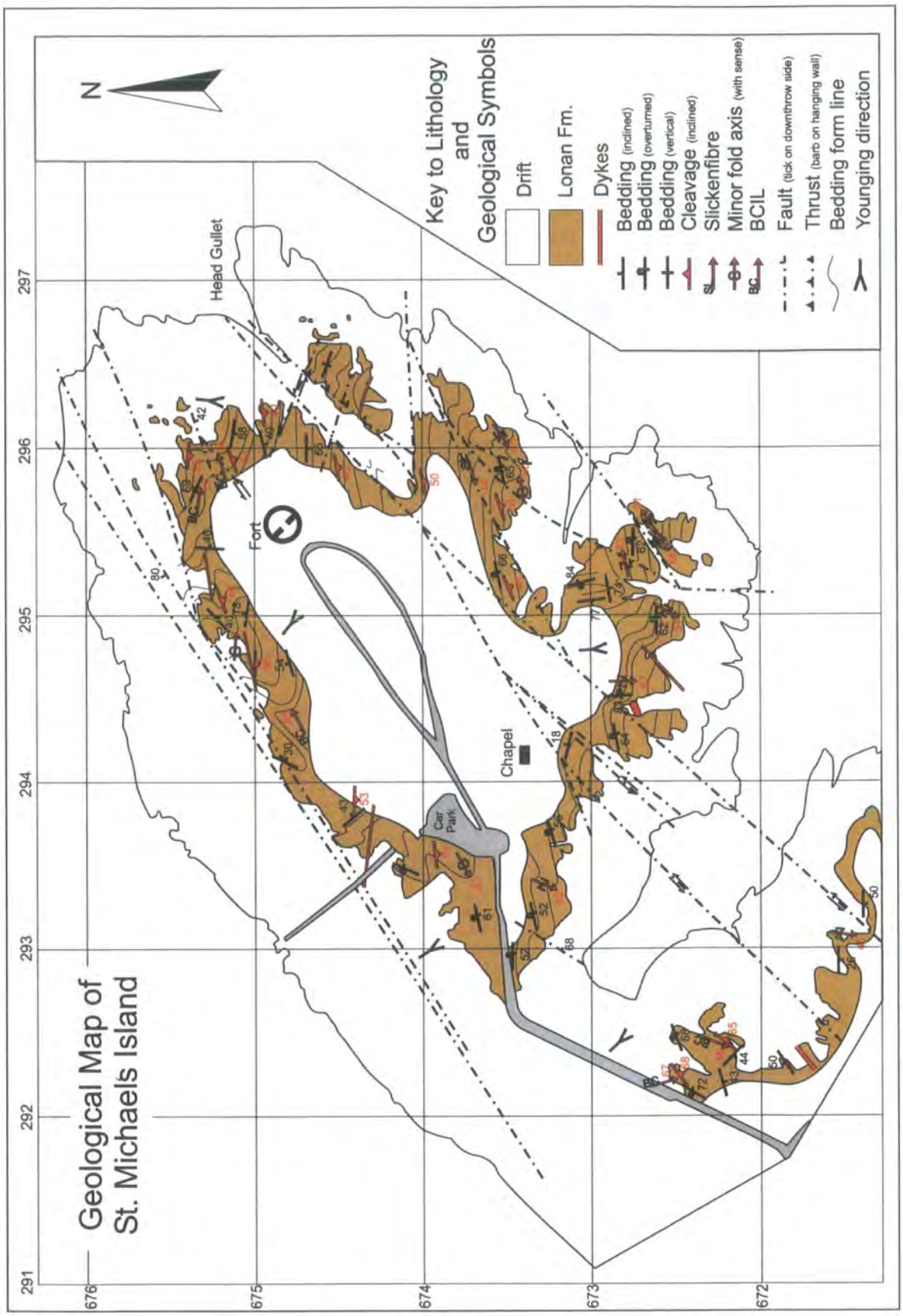

Figure 5.13. Geological Map of St. Michael's Island

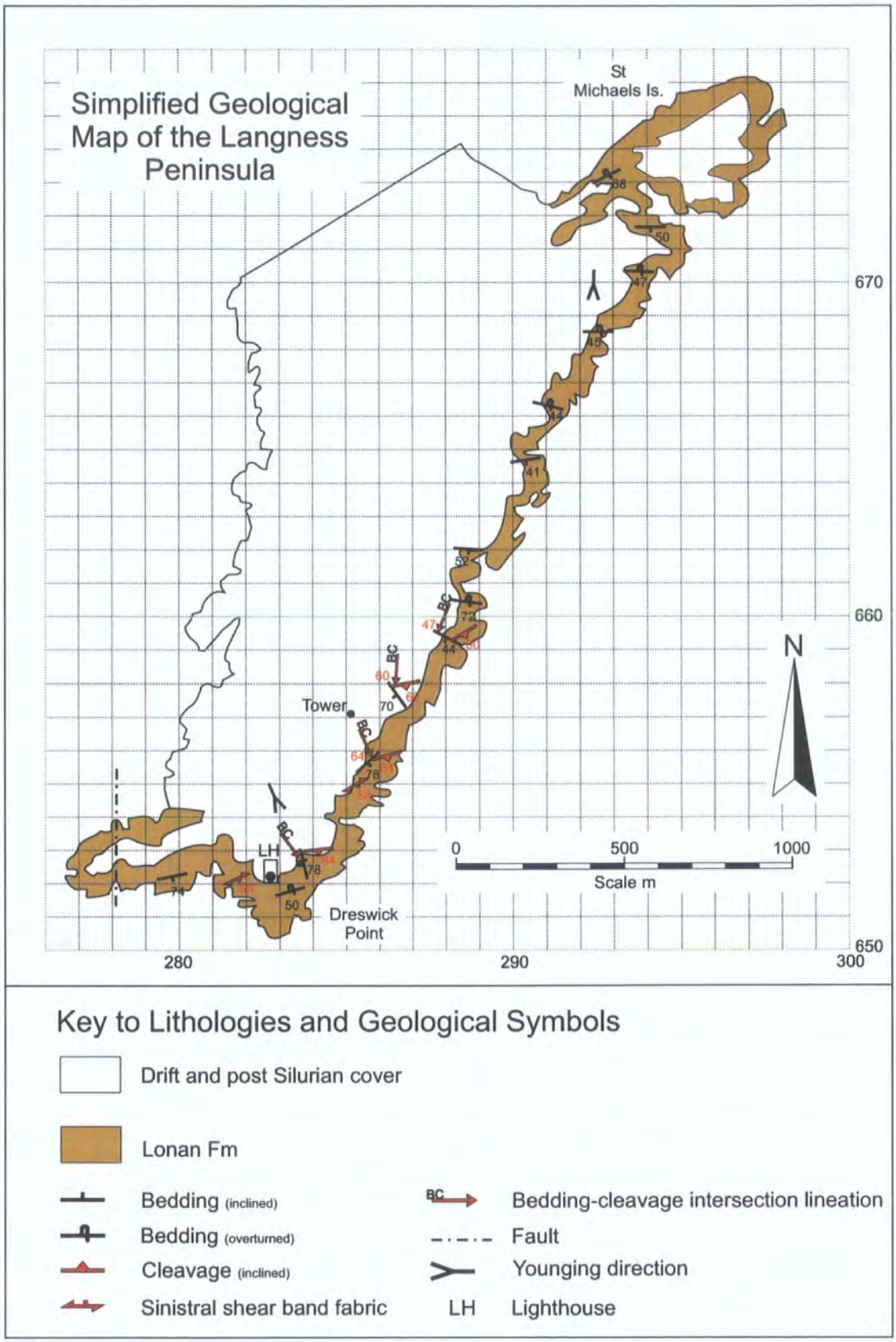

Figure 5.14. Simplified geological map of Langness Peninsula and St. Michael's Island

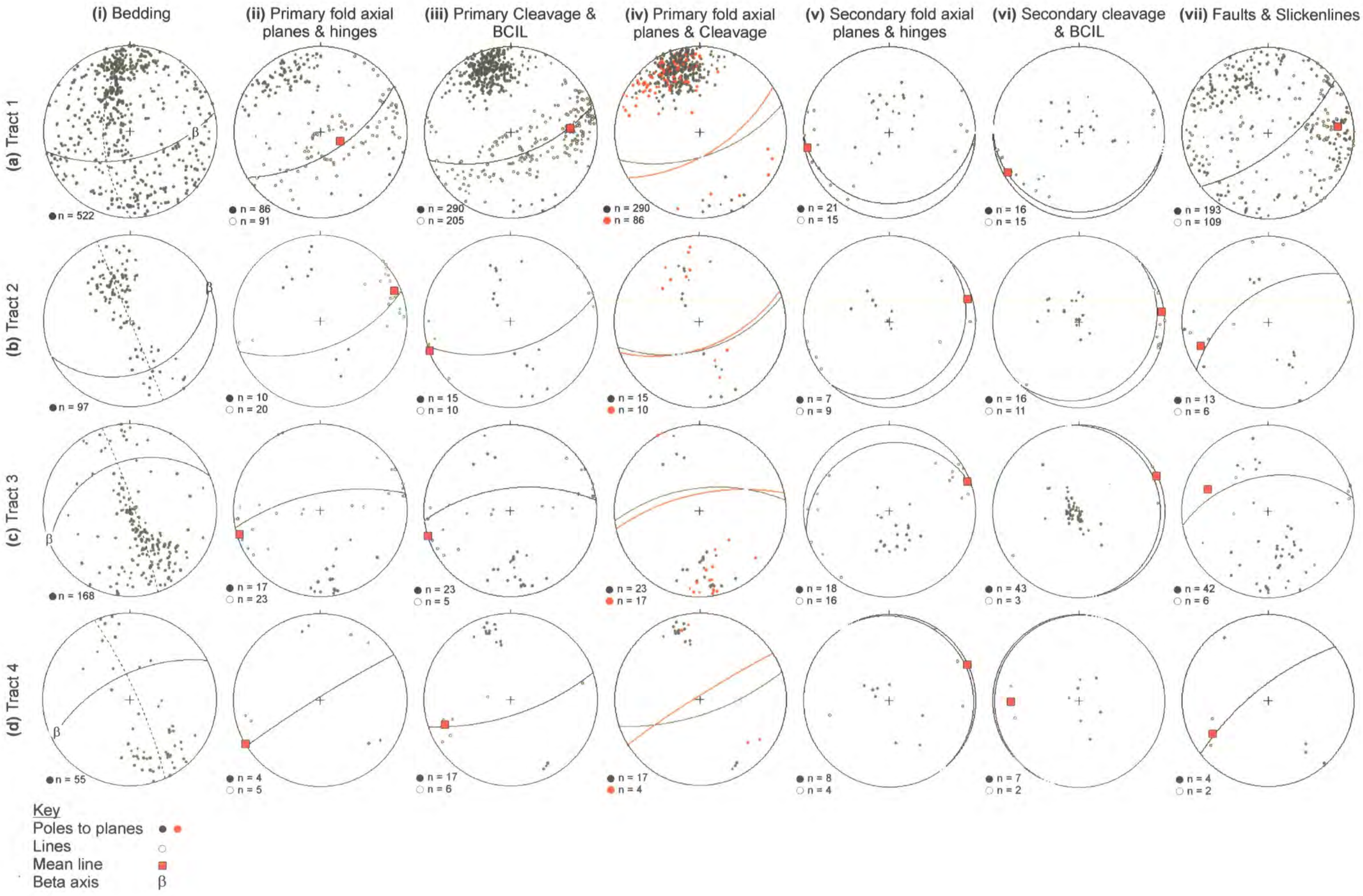

Figure 5.15. Stereoplots of structural orientation data from Tracts 1-4 (a-d respectively). In each case (i) Poles to bedding planes (ii) Poles to primary fold axial planes and hinges (iii) Poles to primary cleavage planes and BCIL (iv) Poles to primary fold axial planes (red) and primary cleavage planes (black), with mean axial (red) and cleavage (black) planes shown. (v) Poles to secondary fold axial planes and hinges (vi) Poles to secondary cleavage planes and BCIL (vii) Poles to fault planes and slickenfibre lineations.

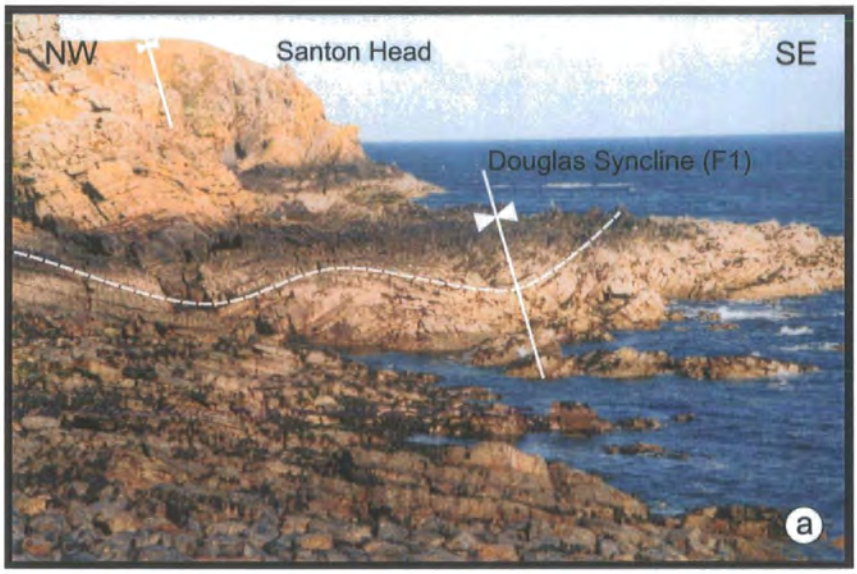

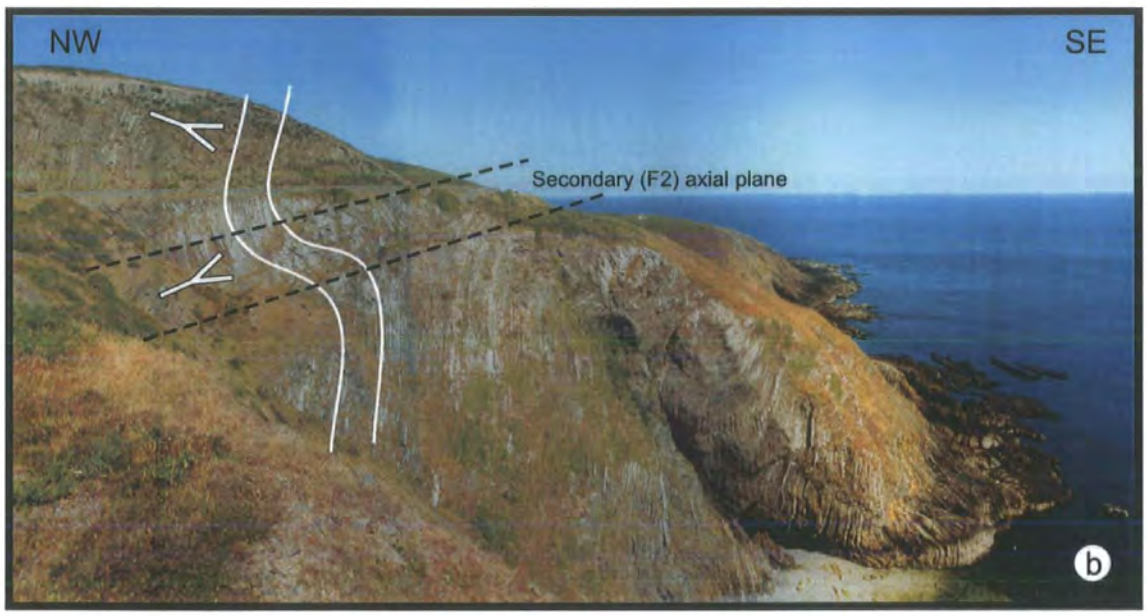

Plate 5.15. (a) View NE towards Santon Head, showing the large, upright, open primary folds of the Douglas Syncline (Figs. 5.2, 5.12(a), grid ref. 329703). Height of cliff is 30m. **(b)** Photomontage of The Whing, showing large-scale secondary folding of the east limb of the Douglas Syncline (Figs. 5.2, 5.12(b), grid ref. 35957319). Height of cliff is 100m.

Clockwise transection is particularly well developed on St. Michael's Island (Figs. 5.2, 5.13). Examples of anticlockwise transection are also observed (e.g. Fig. 5.12(a), grid ref. 32717024), although these are much less common.

Poles to secondary fold axial planes (Fig. 5.15a(v)) exhibit a broad point maximum defining a shallowly S-dipping mean plane. Secondary fold hinges plunge gently towards both the east and west, with a mean fold hinge plunging very gently WSW (Fig. 5.15a(v)). Poles to the secondary cleavage show a similar distribution to the secondary fold axial planes (Fig. 5.15a(v), (vi)). The mean cleavage plane dips very gently to the S, whilst the mean of the associated bedding-cleavage intersection lineation plunges gently to the SW. Secondary folds and cleavage were everywhere seen to be essentially axial planar. The distribution of structures due to the secondary deformation is heterogeneous. They are best observed between Port Grenaugh and Purt Veg (Fig. 5.12(a)) and along much of Marine Drive (Fig. 5.12(b)). The cliff section at The Whing (Fig. 5.12(b), grid ref. 36017302) shows large scale secondary folds on the eastern limb of the Douglas Syncline (Plate 5.15(b), Figs. 5.2, 5.12(b)). For the greater part of St. Michael's Island and Langness Peninsula (Figs. 5.2, 5.10, 5.13, 5.14) secondary folds and cleavage are not preserved (see below). Only a small area near to the lighthouse on Langness (Fig. 5.14, grid ref. 28036503) shows any evidence of secondary deformation. This is unusual, as the thinly-bedded greywacke turbidites and mudstones of the Lonan Formation exposed at these localities normally preserve strong evidence of secondary deformation. In particular the mudstone horizons normally exhibit the characteristic, subhorizontal, secondary crenulation cleavage. The reasons for the apparent absence of secondary deformation in these localities remain unclear.

Tract 1 is extensively faulted, poles to fault planes are broadly distributed with a steeply inclined, SE-dipping mean fault plane (Fig. 5.15a(vii)). Slickenfibres also show a wide variation in plunge and orientation. In the field, several sets of faults can be recognised (see (a) to (e) below).

(a) NE-trending predominantly sinistral, steeply inclined strike-slip faults (e.g. Slack Indigo, Fig. 5.12(b), St. Michael's Island, Fig. 5.13, Onchan Head, Fig. 5.16, Fig. 5.17(a), Plate 5.16(a)).

These lie sub-parallel to the general trend of the bedding, primary cleavage and fold axial planes (Fig. 5.15(a)). The NE-trending fault at Onchan Head (Figs. 5.2, 5.10, 5.16), Plate 5.16(a)) is particularly well-exposed and provides an opportunity to undertake a detailed study of its geometry and kinematics. The fault lies along the

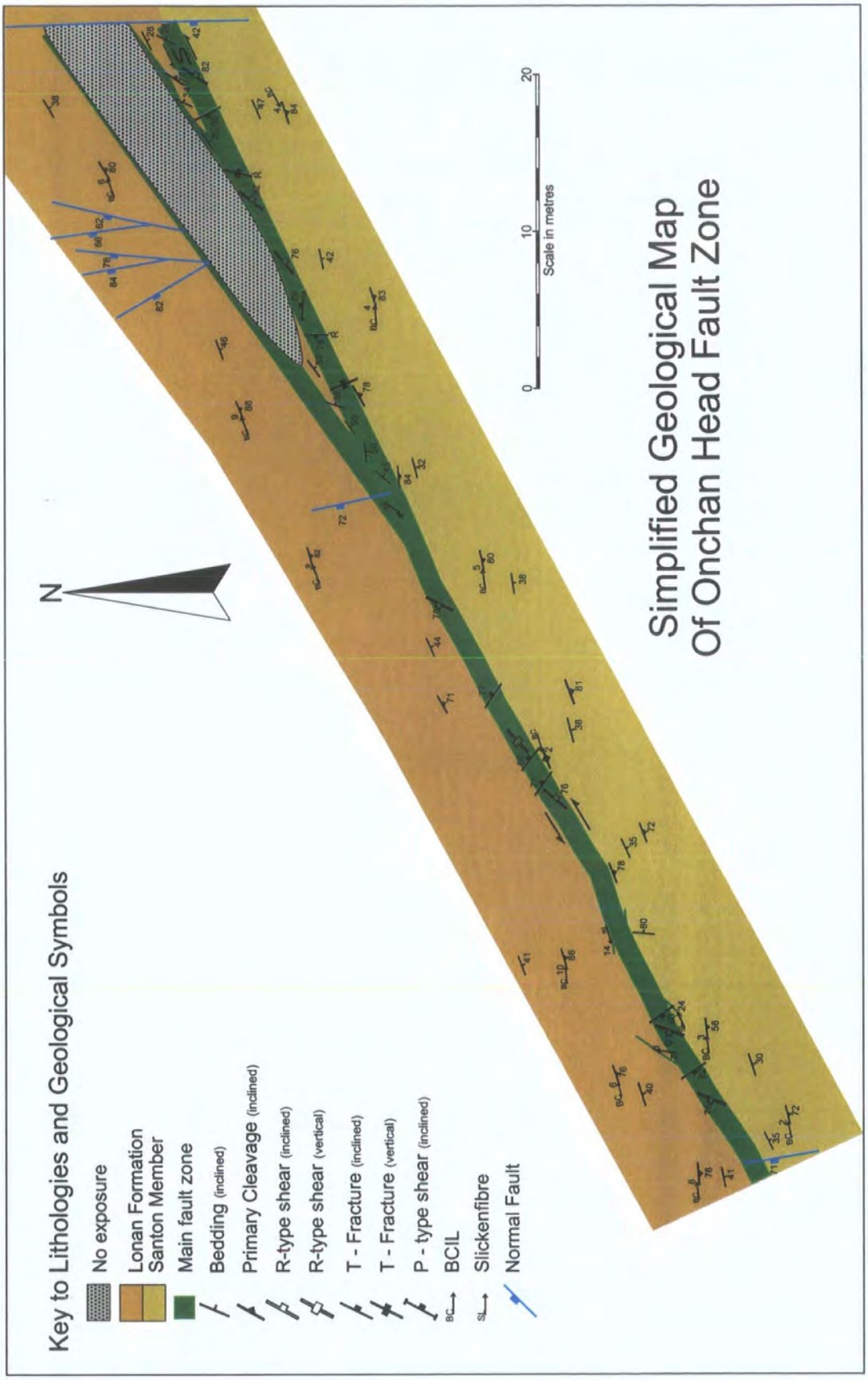

Figure 5.16. Generalised geological map of the Onchan Head Fault Zone (see Fig. 5.10 for location).

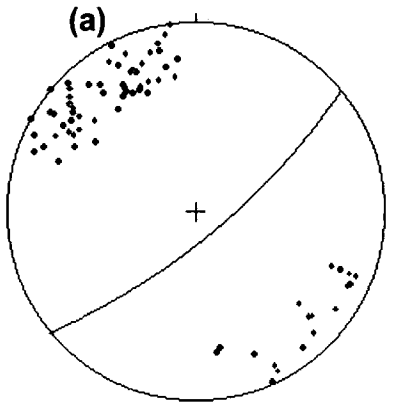

n = 74
(e.g. Slack Indigo Fig. 5.12(b), Onchan Head Fig. 5.16)

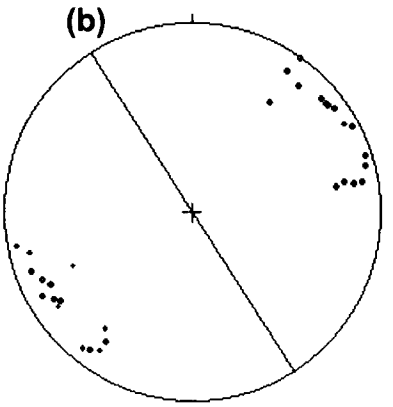

n = 32
(e.g. Purt Veg Fig. 5.12(a), Port Wallberry Fig. 5.12(b))

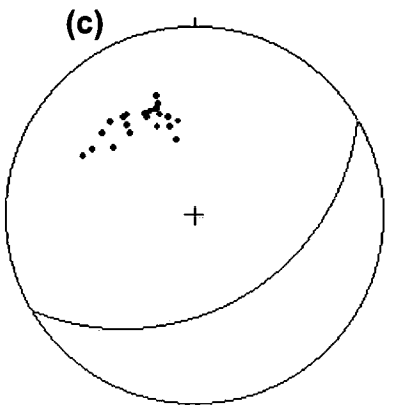

n = 24
(e.g. St. Michael's Island Fig. 5.13)

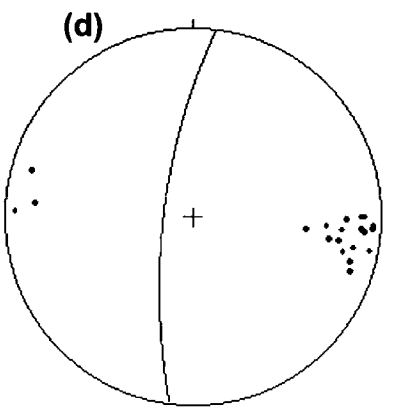

n = 20
(e.g. Cooledegad Fig. 5.12(b))

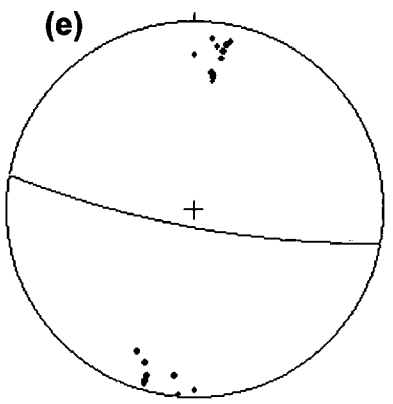

n = 22
(e.g. Baltic Rock Fig. 5.12(b))

Figure 5.17. Stereoplots for separate fault sets for Tract 1. Poles to planes and mean fault plane shown in each case (see text for details).

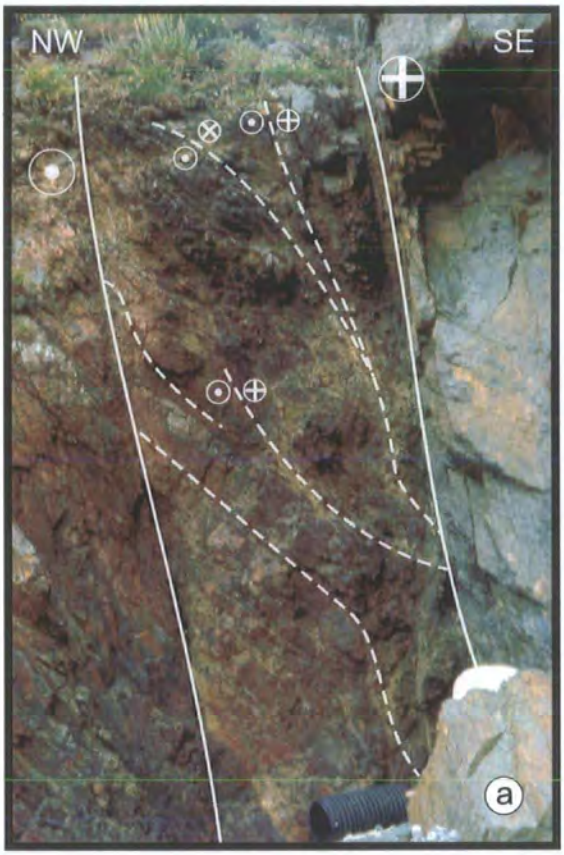

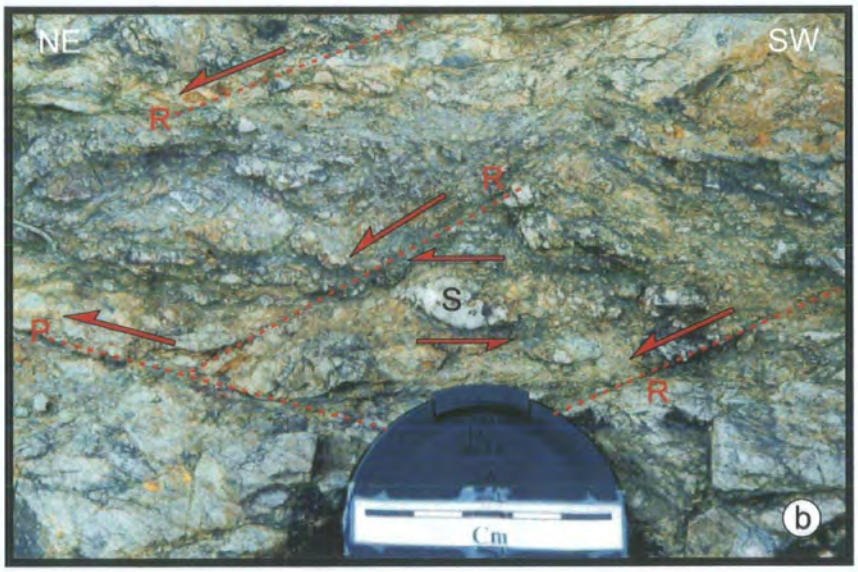

Plate 5.16. **(a)** End view of the Onchan Head Fault Zone (Figs. 5.2, 5.16, grid ref. 402772), showing the bounding faults either side of the zone and several steeply inclined fault strands (highlighted). The width of the fault zone is approximately 1m at the widest point. Bedding dips to the SE. **(b)** Fault breccia within the Onchan Head Fault Zone (Figs. 5.2, 5.16, 5.18, grid ref. 402772), with R- and P-type shears and a sigma porphyroclast (S) all with a sinistral sense of shear. View onto horizontal surface, lens cap is 55mm across.

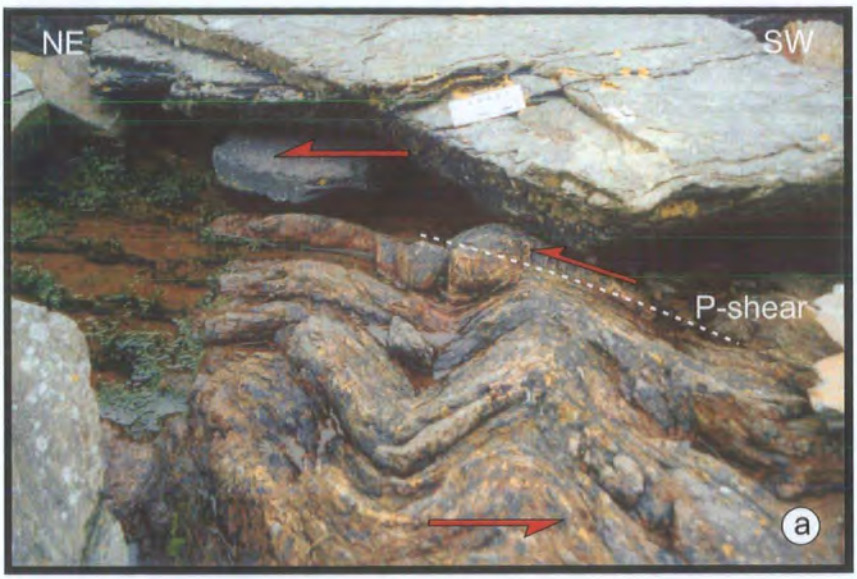

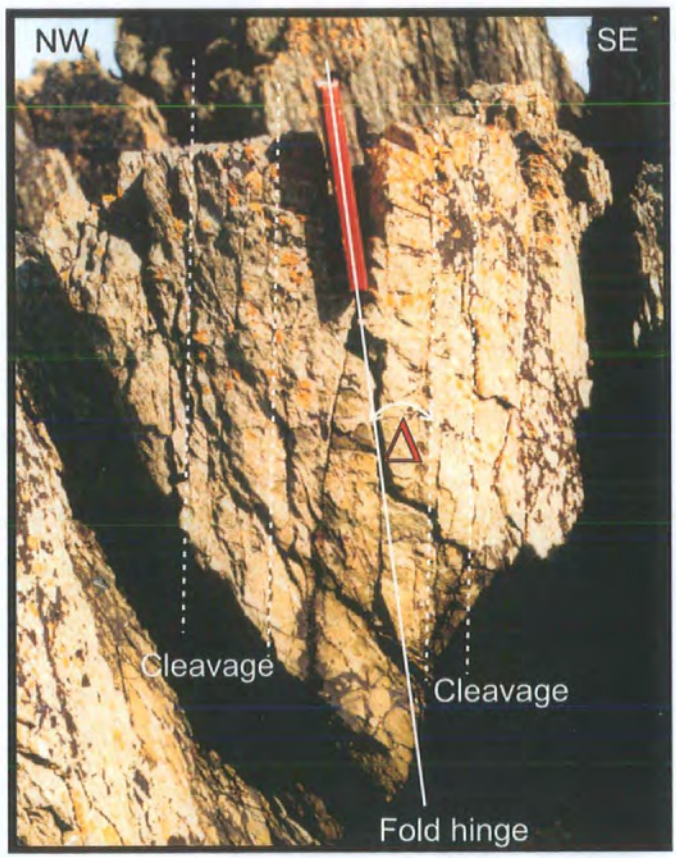

Plate 5.17. **(a)** Sinistral, NE-verging fold pair and P-shear Onchan Head Fault Zone (Figs. 5.2, 5.16, grid ref. 402772). Scale bar is 15cm. **(b)** Steeply plunging primary fold hinge, clockwise transected by the primary cleavage. The angle of transection Δ is 12°. St. Michael's Island (Figs. 5.2, 5.13, grid ref. 29556726). Note book is 15cm high.

contact between the Lonan Formation and Santon Member (Fig. 5.16). A variety of brittle (R-type and P-type Riedel shears, Plates 5.16(b), 5.17(a)) and semi-brittle (sigma porphyroclasts and minor folds, Plates 5.16(b), 5.17(a)) kinematic indicators are preserved, that indicate an overall sinistral sense of movement (Fig. 5.18(a)). A 3-D panel diagram of the fault zone illustrates the geometry and kinematics of the fault zone (Fig. 5.18(b)).

(b) NNW- to NW-trending, predominantly sinistral strike-slip faults (e.g. Purt Veg, grid ref. 325703, Fig. 5.12(a), Fig. 5.17(b)).

Field mapping during this and previous studies (e.g. Quirk & Burnett 1999) suggest that these faults may have offsets of several hundred metres to kilometres. For example, faults at Purt Veg, the fault to the east of Cooledegad and those at Horses Leap and Port Wallberry offset the axial trace of the Douglas Syncline several hundred metres to the north (Figs. 5.2, 5.12).

(c) NE-trending, SE-dipping, dextral oblique thrusts (e.g. St. Michael's Island, grid ref. 297674, Fig. 5.13, Plate 5.12(a), Fig. 5.17(c)).

(d) NNE-trending, dextral strike-slip faults (e.g. Cooledegad, grid ref. 353730, Fig. 5.12(b), Fig. 5.17(d).

(e) WNW-trending, dip-slip normal faults (e.g. near to Baltic Rock, grid ref. 32857043, Fig. 5.12(a), Plate 5.13(a), Fig 5.17(e)).

In general all the faults described are only exposed along the coast, where they often form narrow and usually inaccessible inlets (locally called gullets). This poor access, combined with a general lack of kinematic indicators and offset markers poses significant problems in determining the sense and amount of offset along faults.

Facing directions of primary folds and cleavage exhibit approximately 270° of variation, from upwards NE, through upwards to SW sideways and downwards (Fig 5.19(i), (ii)). This wide variation is most pronounced on St. Michael's Island and Langness (Figs. 5.13, 5.14, see below).

The structures described in Tract 1 above can be divided into two distinct structural domains.

1. Domains of upright to moderately inclined upward-facing primary folds with whaleback geometries and clockwise transected cleavage.
2. Domains of generally upright primary folds, clockwise transected by cleavage, with highly curvilinear, often steeply plunging fold hinges, facing both upwards and downwards.

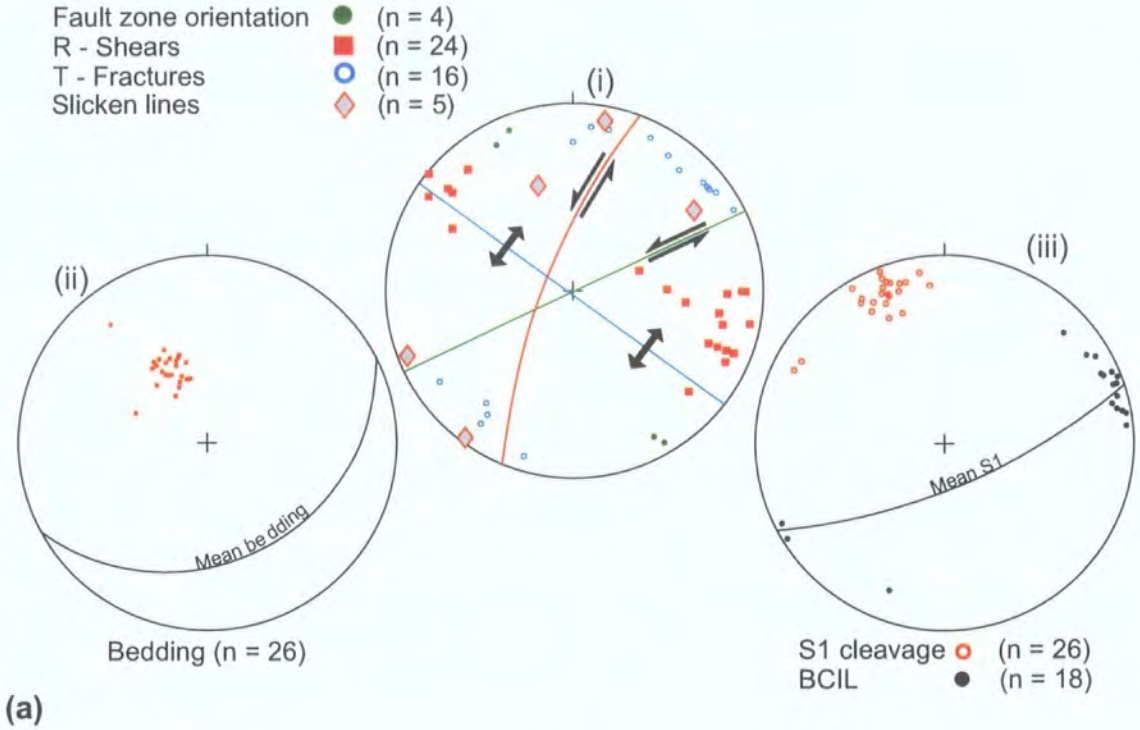

(a)

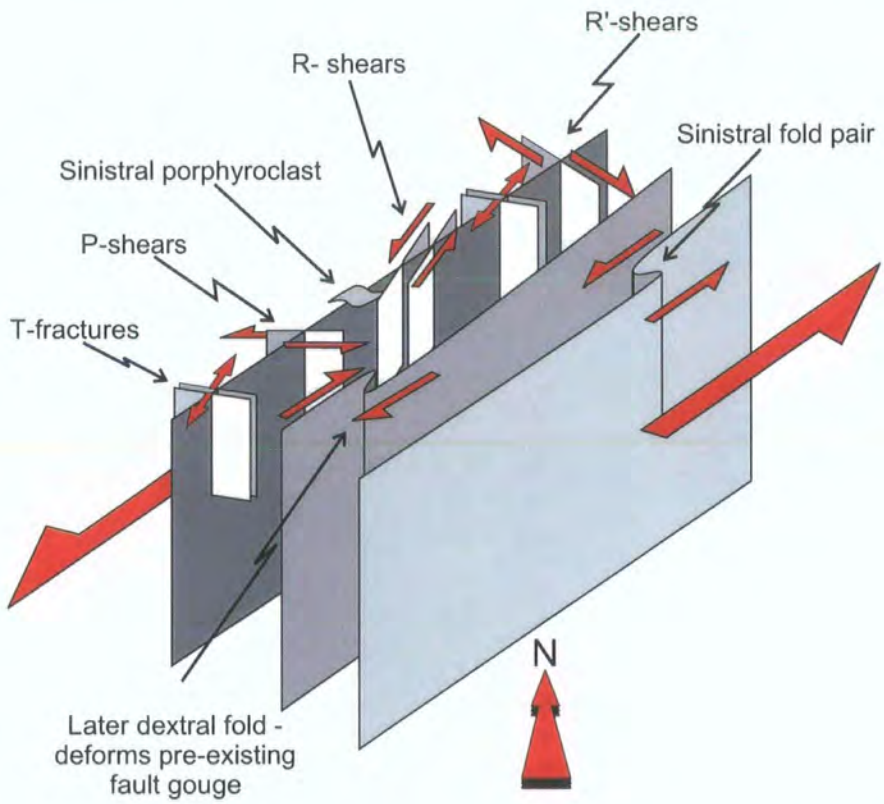

(b)

Figure 5.18. **(a)** Stereoplots of structural orientation data from Onchan Head Fault Zone (i) Poles to kinematic indicators with mean planes for R-shears (red), T-fractures (blue) and fault zone (green) shown. (ii) Poles to bedding planes with mean plane shown. (iii) Poles to primary cleavage planes with mean cleavage shown. **(b)** 3-D schematic panel diagram illustrating kinematics and geometry of the Onchan Head Fault Zone.

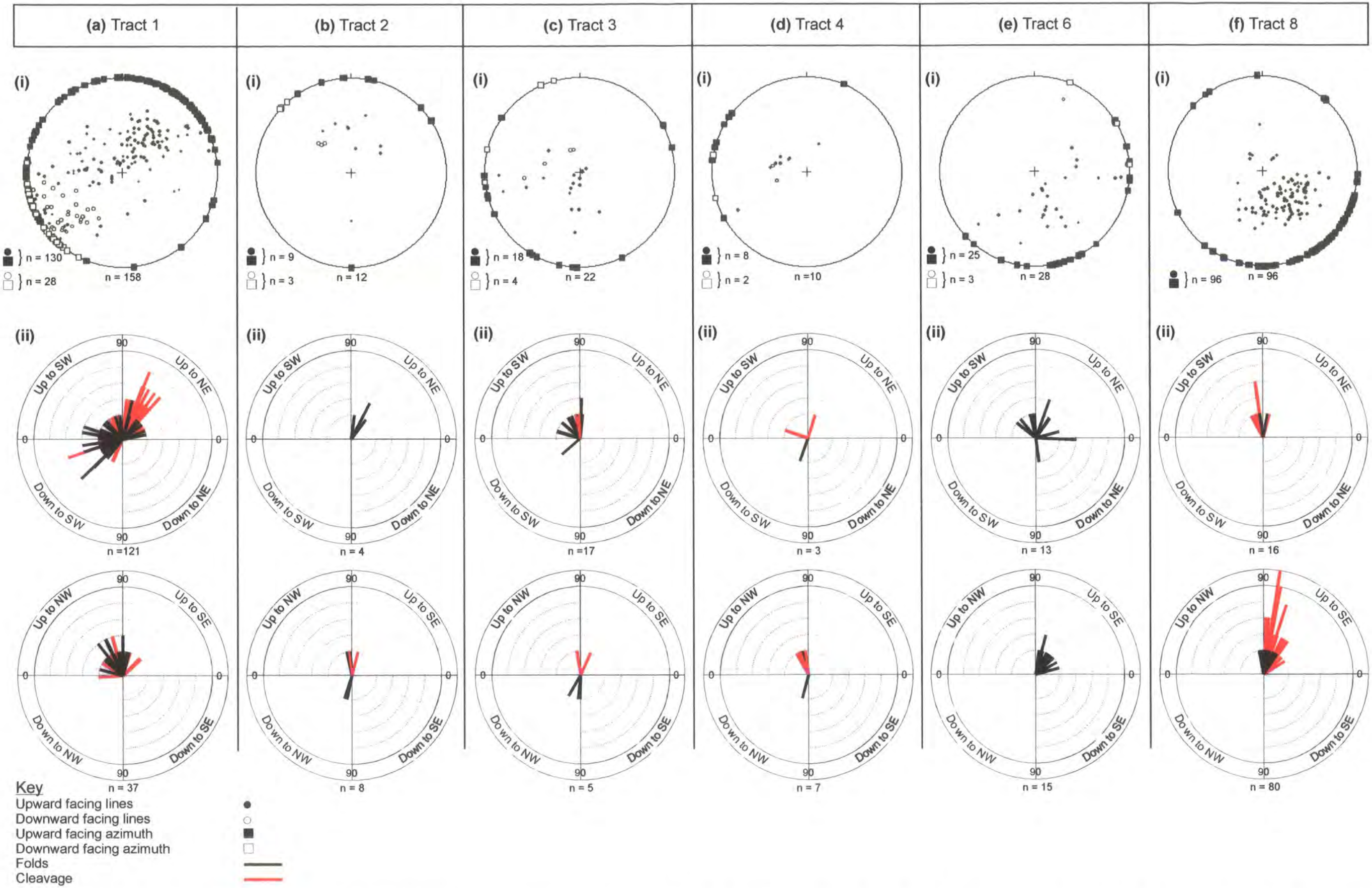

Figure 5.19. Facing data from the Isle of Man for Tracts 1, 2, 3, 4, 6 and 8 (labelled a-f respectively). **(i)** Fold and cleavage facing lines using the construction method of Holdsworth (1988). **(ii)** Plots showing the pitch of fold and cleavage facing directions in planes parallel to the fold axial and cleavage planes in which they were measured.

5.6.1.1 Domain 1 Port Grenaugh to Onchan Head

Domain 1 comprises the bulk of Tract 1 excluding St. Michael's Island and Langness Peninsula (Fig. 5.20). The NW boundary is the boundary of Tract 1 with Tract 2, whilst the SE boundary although not exposed, is interpreted to lie in a NE-trending line somewhere between St. Michael's Island and Castletown, where the Manx Group rocks are unconformably overlain by Carboniferous rocks (Fig. 5.20).

Poles to bedding (Fig. 5.21a(i)) are largely distributed along a girdle that defines a very shallowly NE-plunging β axis with a broad point maximum corresponding to a steep SE-dipping mean plane. Primary fold hinges plunge gently to both the NE and SW, whilst the calculated mean primary fold hinge (Fig. 5.21a(ii)) plunges very gently to the SW. Poles to primary fold axial planes (Fig. 5.21a(ii)) show a broad point maximum corresponding to a steeply SE-dipping mean plane, that is significantly clockwise transected (ca. 15°) by the mean primary cleavage (Fig. 5.21a(ii)-(iv)). This relationship is observed in the field, where individual folds show clockwise transection angles of up to 14° (e.g. Fig. 5.12(b), grid ref. 38407430). The mean bedding-cleavage intersection lineation (BCIL) plunges very gently to the NE and corresponds closely to the regional β axis (Fig. 5.21a(i), (iii)). This relationship is somewhat surprising given the pronounced clockwise transection indicated by the stereoplots (Fig. 5.21a(ii)-(iv)) and supporting field evidence confirming the transecting relationship. The reason for this unusual result remains unclear.

Poles to fault planes (Fig. 5.21a(v)) show a broad distribution, however, a diffuse point maximum defines a steeply inclined SE-dipping mean fault plane. Slickenfibre lineations exhibit a wide variety of orientations, with a moderately E-plunging mean lineation (Fig. 5.21a(v)). A subordinate number of slickenfibres are preserved on bedding planes, and lie at an oblique angle to minor, primary fold hinges. Sense of shear determined from slickenfibre steps observed in the field show that the sense of shear on opposite fold limbs are reversed, showing a pattern consistent with flexural slip folding, (Ramsay 1967), but with a very significantly oblique component (Fig. 5.22). Minor primary folds and cleavage face moderately to steeply upwards to the NW, SE, NE and SW (Fig. 5.21a (vi), (vii)).

5.6.1.2 Domain 2 St. Michael's Island and Langness Peninsula

St. Michael's Island and the Langness Peninsula are situated on the SE coast of the Island (Figs. 5.2, 5.10, 5.13, 5.14, 5.20). In common with Domain 1, both St.

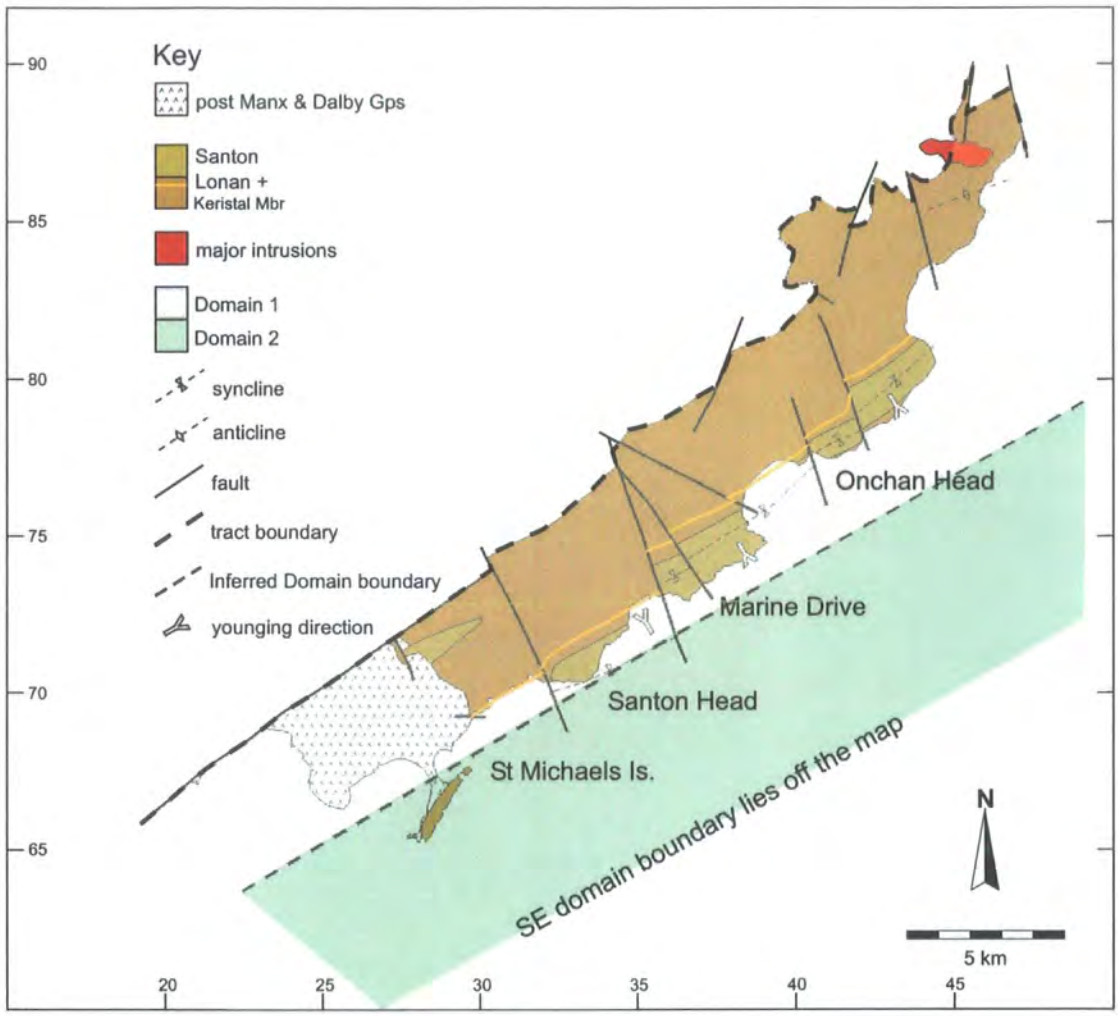

Figure 5.20. Map of Tract 1 showing the extent of Domains 1 and 2 and the interpreted position of the boundary between them (see Fig. 5.9 for location of Tract 1).

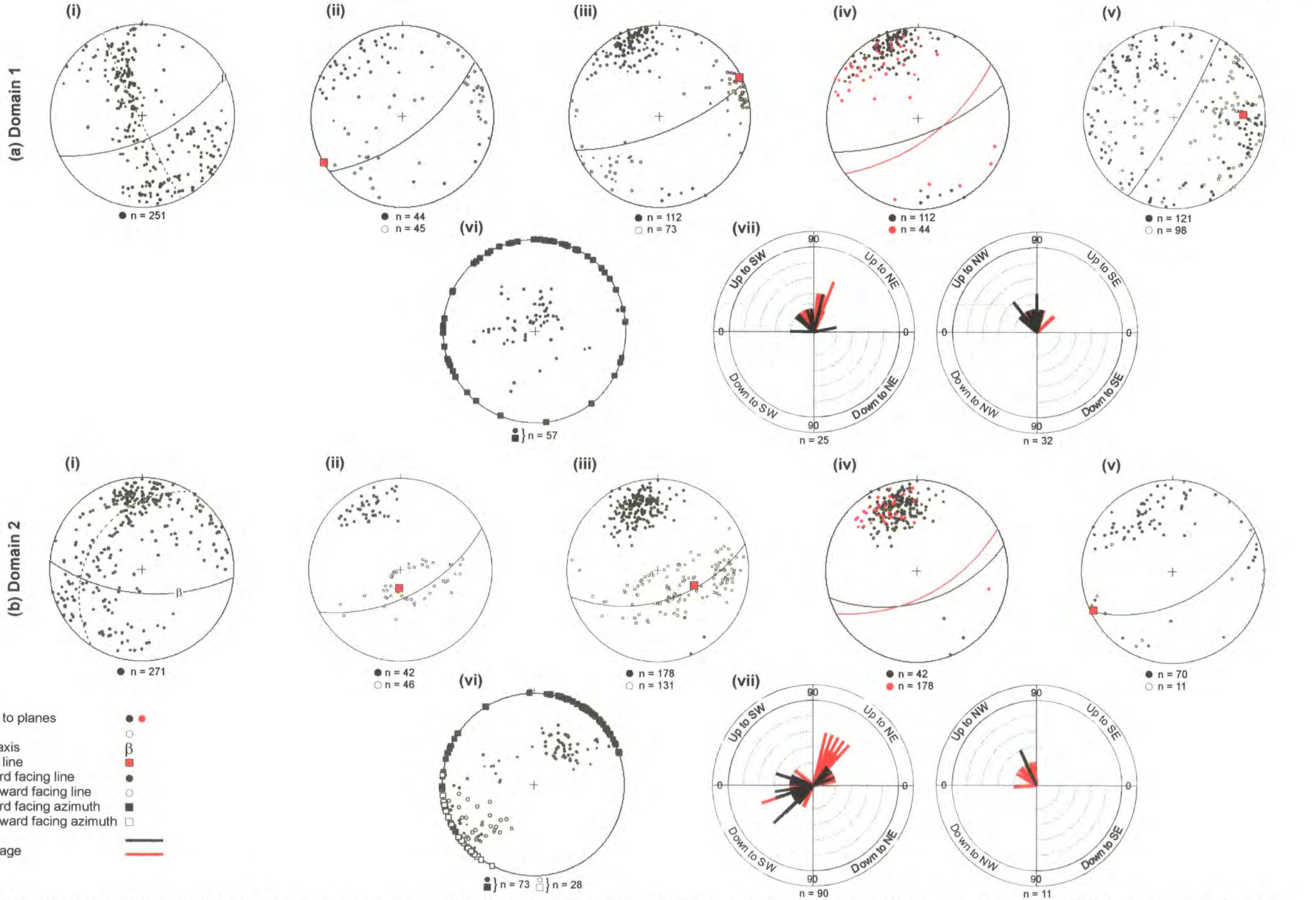

Figure 5.21. Stereoplots of structural and facing data from domains 1 and 2 of Tract 1 (labelled (a) i- vii and (b) i-vii respectively). In each case **(i)** Poles to bedding planes, **(ii)** Poles to primary fold axial planes and fold hinges, **(iii)** Poles to primary cleavage and BCIL, **(iv)** Poles to primary fold axial planes (red) and cleavage planes (black), **(v)** Poles to fault planes and slickenlines, **(vi)** Plot of fold and cleavage facing lines and azimuths using the construction method of Holdsworth (1988). **(vii)** Plots showing the pitch of fold and cleavage facing directions in mean planes parallel to the fold axial and cleavage planes in which they were measured.

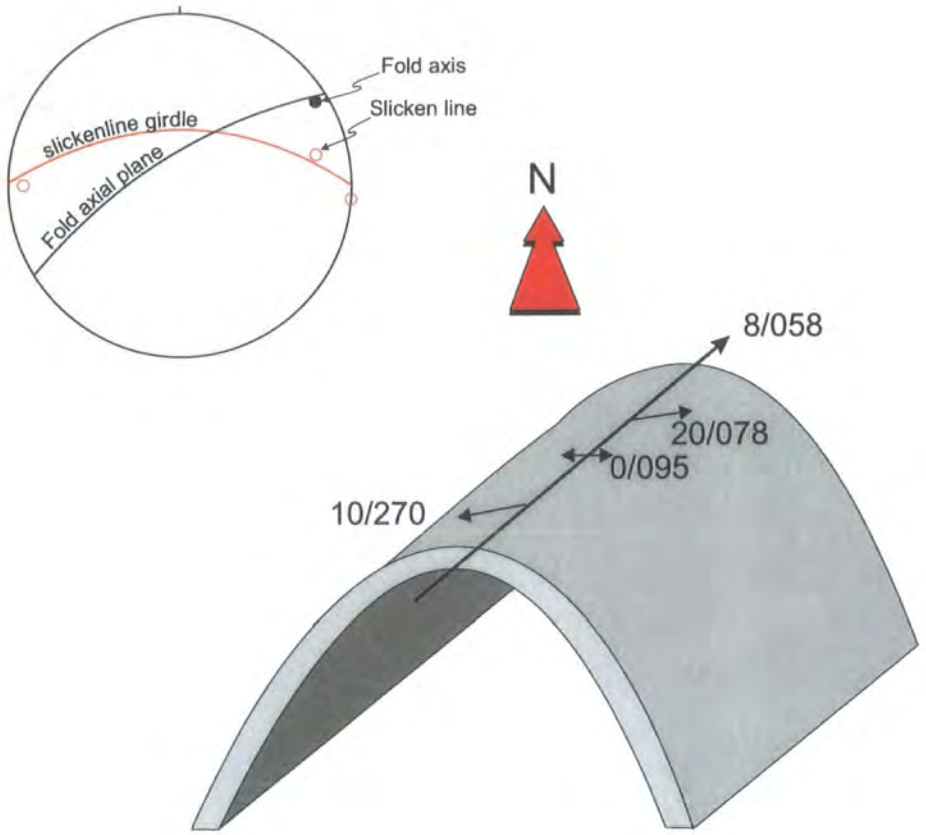

Figure 5.22. Cartoon and stereoplot illustrating the oblique relationship between bedding-parallel slickenlines and the fold axis of minor primary folds in Domain 1 of Tract 1 (Fig. 5.12(b), grid ref. 38407430).

Michael's Island and Langness comprise rocks of the Lonan Formation. As discussed previously the NW boundary with Domain 1 is not exposed, whilst the SE boundary of Domain 2 lies offshore.

Poles to bedding (Fig. 5.21b(i)) show a wider variation than those for Domain 1 (cf. Fig. 5.21a(i)). However, a broad point maximum defines a steeply S-dipping mean homoclinal-bedding plane (Fig. 5.21b(i)). Extensive primary folding spreads a significant number of poles along a great circle girdle that corresponds to a steep to moderately ESE-plunging β axis. This is contrary to the mean fold hinge plunge (Fig. 5.21b(ii)), which lies significantly clockwise (ca. 50°) of the β axis and plunges steeply to the S. This apparently large obliquity may be an artefact of the steep fold plunge (Plate 5.17(b)) and the relatively restricted fold data set, since the mean bedding-cleavage intersection lineation (Fig. 5.21b(iii)) corresponds closely to the β axis defined by bedding (Fig. 5.21b(i)). However, this relationship seems at odds with the poles to primary fold axial planes (Fig. 5.21b(ii)) which are markedly (ca. 14°) clockwise transected by cleavage (Fig. 5.21b(iv), Plate 5.17(b)). Both bedding-cleavage intersection lineations and fold hinges are spread along the mean cleavage and axial planes respectively (Fig. 5.21b(ii), (iii)), exhibiting up to 160° of curvilinearity within their respective planes over distances of several metres (Plate 5.18(a)). Folds with steep plunges in St. Michael's Island and the Langness Peninsula were noted by Simpson (1963) and Fitches *et al.* (1999). Minor primary folds and cleavage exhibit predominantly SW and NE facing directions, with a subordinate number facing to the NW (Fig 5.21b(vi), (vii)). Minor fold hinges and bedding-cleavage intersection lineations (BCIL) (Fig. 5.20b(ii), (iii)) that plunge to the NE face upwards at shallow to steep angles to the NE, whilst those that plunge to the SW face upwards, sideways and downwards to the SW (Fig. 5.21b(vi), (vii).

Poles to faults show a broad distribution defining a steeply SE-dipping mean fault plane (Fig. 5.21b(v)). Slickenfibre lineations are predominantly shallowly-plunging, or sub-horizontal, with a very gently SW-plunging mean lineation (Fig. 5.21b(v)). This suggests that many of the faults have strike-slip kinematics, a view supported by field observations (Plates 5.12(a), 5.18(b)). In addition, a significant number of these show a sinistral sense of movement (Plate 5.18(b)). St. Michael's Island in particular is traversed by a zone comprising several, strike-slip faults (Fig. 5.13, Plate 5.19). These divide the island into two, with the majority of primary folds exposed along the NW coast of St. Michael's Island (Fig. 5.13) plunging gently to the

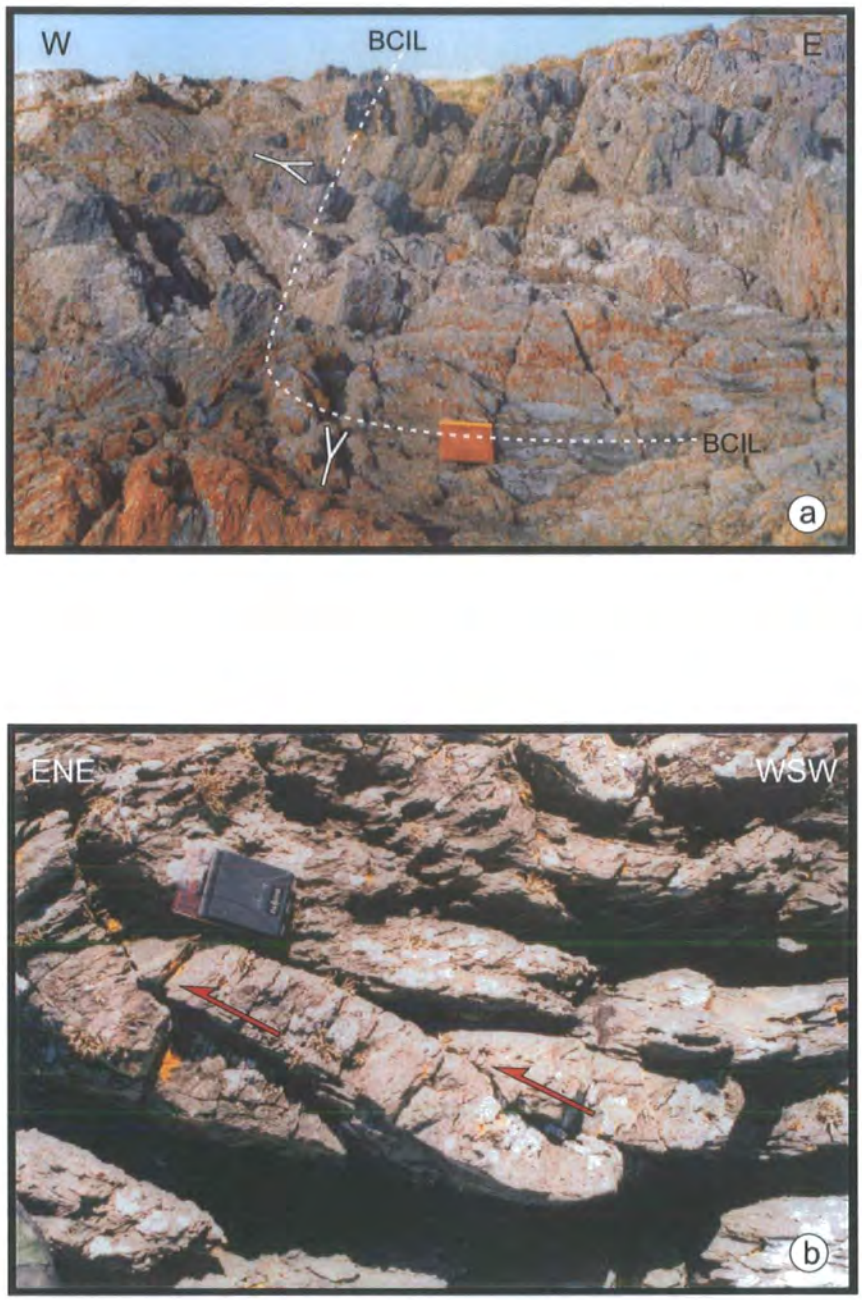

Plate 5.18. **(a)** Curvilinear bedding-cleavage intersection lineation (BCIL) (highlighted) on St. Michael's Island (Fig. 5.13, grid ref. 29466727). The facing changes from up to the SW round to down to the SW. The map board is 30cm across and lies in the plane of the primary cleavage. **(b)** Sinistral, P-type shears in steep S-dipping bedding, St. Michael's Island (Fig. 5.13, grid ref. 29546727). View looking down onto end of bedding. Lens cap is 55mm across.

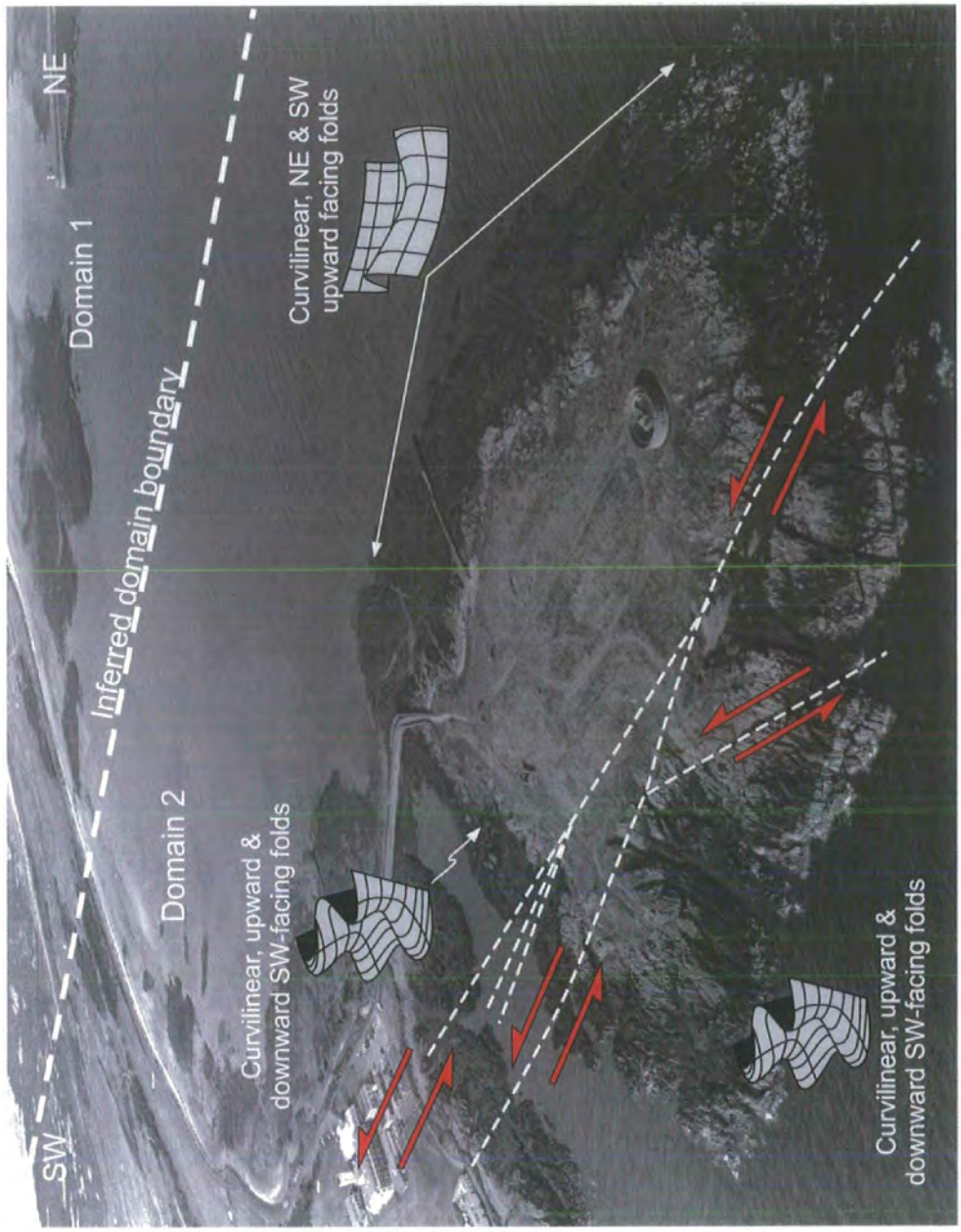

Plate 5.19. Oblique aerial view of St. Michael's Island, looking NW, showing several NE-trending, sinistral, strike-slip faults. Primary folds and cleavage on the NW side of the Island face predominantly up to the SW and NE , whilst on the SE side they face up and down to the SW (see Figs. 5.2, 5.13).

NE, and facing up to the NE, whilst those on the SE coast plunge more steeply to both the NE and SW, and face upwards and downwards to the SW. However, a subordinate number of folds exposed N of the fault zone and lying W of the chapel and car park (Fig. 5.13, grid ref. 293673, Plate 5.19) plunge steeply to the S and SW. This perhaps implies that sinistral movements along the fault zone have offset the more steeply plunging folds observed on the SE coast of the island. Along the SE coast of the Langness Peninsula (Fig. 5.14) the folds generally plunge moderately to steeply to the S and SE.

At the extreme southern end of the Langness Peninsula near to Dreswick Point (Fig. 5.14, grid ref. 282652) they is a broad zone (ca. 250m) of sinistral shear bands developed within the thinly-bedded units of the Lonan Formation (Plate 5.20(a)). These form centimetre to metre wide, steeply SE-dipping zones where bedding and the primary cleavage are offset in a consistently sinistral sense. These structures were also noted by Fitches *et al.* (1999) to be developed locally on the Calf of Man (Fig. 5.2, grid ref. 157662) and on the flanks of Snaefell (Fig. 5.2, grid ref. 401879). Some of the shear bands are clearly deformed by secondary folds (Plate 5.20(b)), indicating that they must have developed during or shortly after the main phase of deformation.

5.6.2 Tract 2

Tract 2 (Fitches *et al.* 1999, Woodcock *et al.* 1999b, Figs. 5.9, 5.10, 5.23, 5.24) forms a NE-trending, wedge shaped zone bounded to the south by the Shag Rock Fault and to the north by an inferred fault separating rocks of the Mull Hill Formation from those of the Maughold Formation on the north side of Port Erin Bay. Two areas within Tract 2 were studied, Port Erin Bay (Fig. 5.23) and Gansey Point (Figs. 5.2, 5.24). The majority of the Port Erin Bay section is composed of thinly-bedded, sandstone and mudstone couplets of the Lonan Formation (Chadwick *et al.* 2001) (Plate 5.1(b)). The remainder, are comprised of quartz arenites of the Mull Hill Formation (Chadwick *et al.* 2001) (Plate 5.4(b)), which, outcrop to the south of Spaldrick Bay (Fig. 5.23, grid ref. 193696). Gansey Point is predominantly composed of sediments of the Mull Hill Formation (Fig. 5.24).

Poles to bedding planes (Fig. 5.15b(i)) show a well-defined point maximum that corresponds to a moderately SE-dipping homoclinal mean plane. However, this pattern is in part due to bedding that is overturned on the NW limb of the Port Erin Anticline (Fig. 5.23) Minor, primary and secondary folds spread a subordinate number of poles

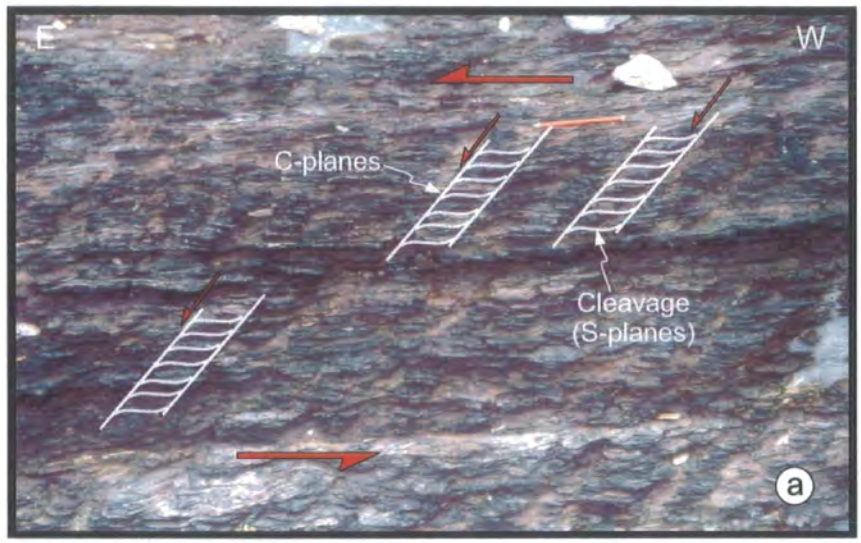

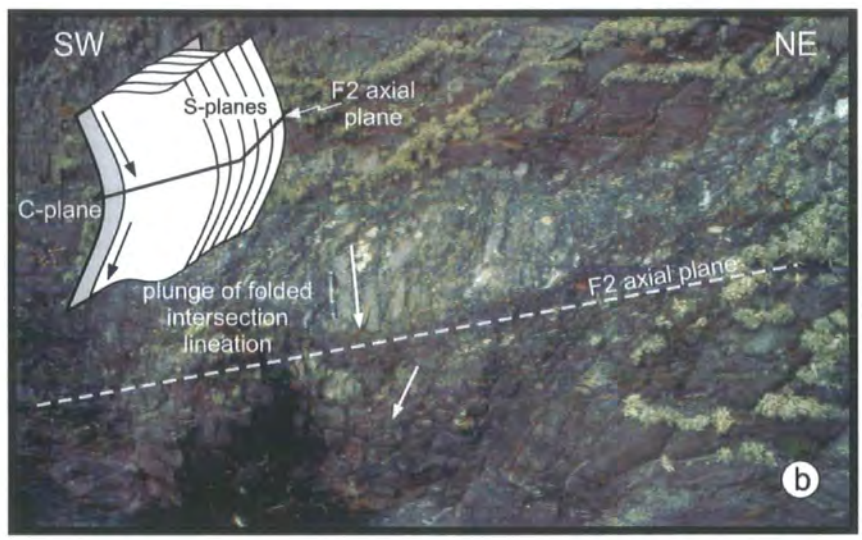

Plate 5.20. **(a)** Sinistral shear band fabric deforming the primary cleavage in rocks of the Lonan Formation near to the Lighthouse on the Langness Peninsula (Fig. 5.14, grid ref. 28176521). **(b)** Sinistral shear bands deformed by secondary folds. The intersection lineation between the S- and C-planes is folded plunging towards the SE and NW. See inset for interpretation. Langness Peninsula (Fig. 5.14, grid ref. 28176521).

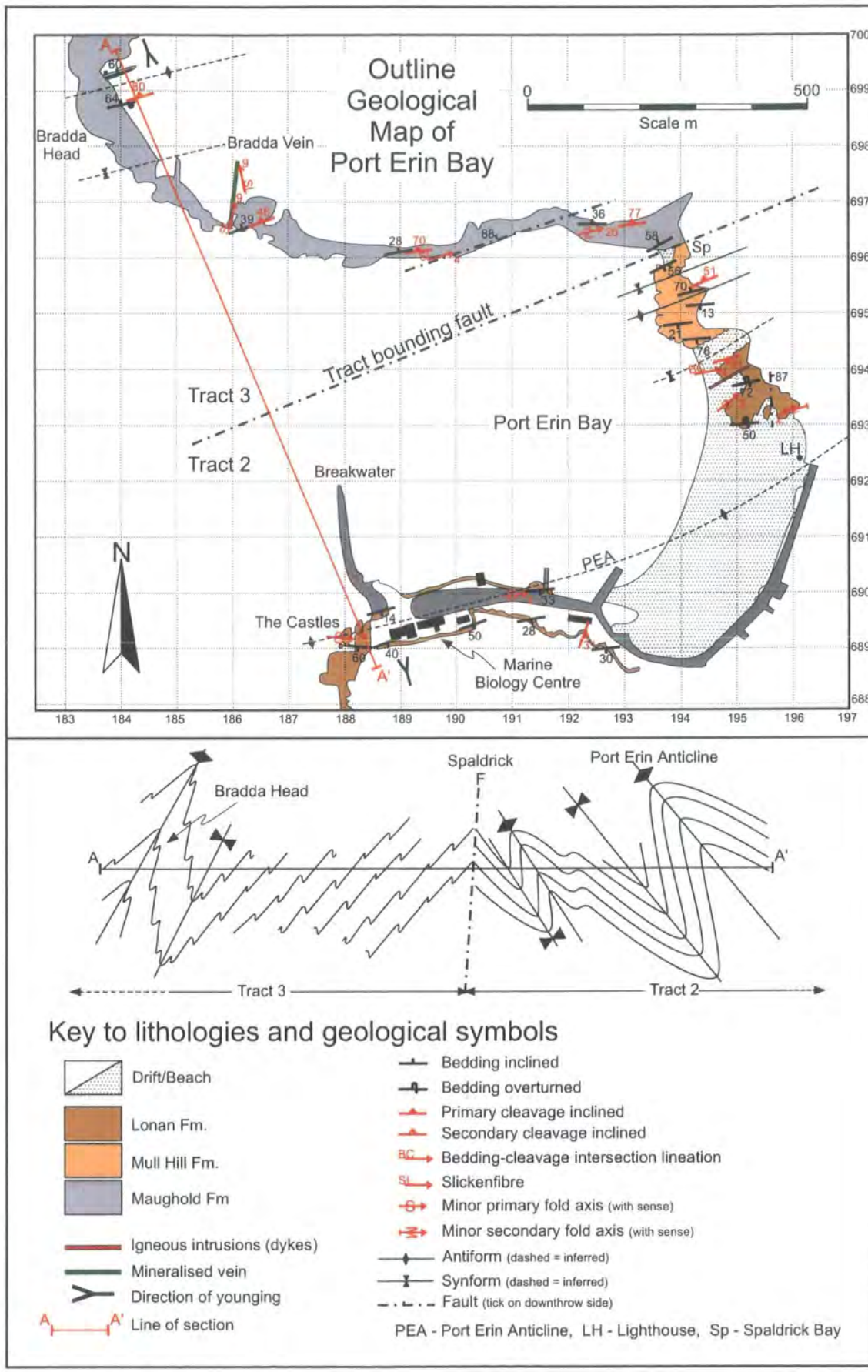

Figure 5.23. Outline geological map and cross-section of Port Erin Bay (see Fig. 5.10 for location).

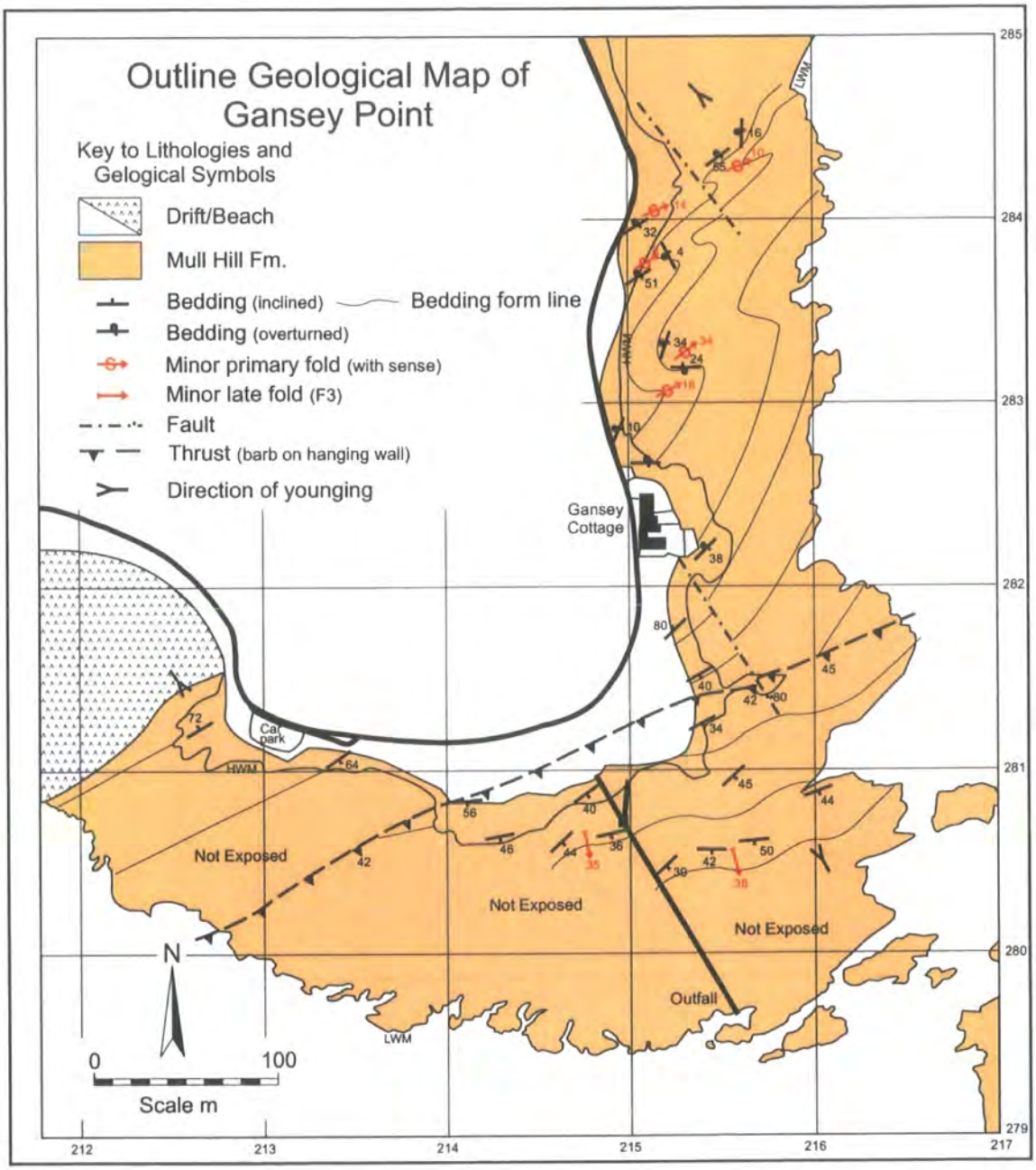

Figure 5.24. Outline geological map of Gansey Point (see Fig. 5.10 for location).

Plate 5.21. **(a)** NW-verging primary S-fold pairs Port Erin Bay (Fig. 5.22, grid ref. 1952 6936). The SE limb of the upper fold pair is boudinaged with quartz infilling the neck. The NW limbs of both folds are truncated by a late SE-dipping fault. Lens cap is 55mm across. **(b)** Type 3 fold interference pattern due to refolding of Primary (F1) syncline by secondary folds. Port Erin Bay (Fig. 5.23, grid ref. 19586931). Scale is 15cm.

along a sub-vertical great circle girdle that defines a sub-horizontal β axis. Poles to primary fold axial planes (5.15b(ii), Plate 5.21(a))) define a moderate to steep SE-dipping mean axial plane, whilst the mean primary fold hinge (Fig. 5.15b(ii)) plunges very gently to the NE, corresponding closely to the regional β axis (Fig. 5.15b(i)). The stereoplot for the primary cleavage (Fig. 5.15b(iii)) shows two broad point maxima that define a steep SE-dipping mean plane. In addition, poles to cleavage planes appear to lie on a great circle girdle with a similar orientation as that defined by the bedding (Fig 5.15b(i), (iii). This suggests that the cleavage has been folded by the secondary phase of deformation, resulting in primary cleavage planes that dip to both the NW and SE (Fig. 5.15b(iii)). This is confirmed by field observations (Plate 5.11(b)) and was noted by Fitches *et al.* (1999) (Fig. 5.25(a)). Bedding-cleavage intersection lineations (Fig. 5.15b(iii)) trend NE-SW with a sub-horizontal (1^{o}) mean lineation. The stereoplots for primary fold axial and cleavage planes (Fig. 5.15b(ii), (iii), (iv)) suggest that the mean cleavage plane lies slightly clockwise of the mean axial plane (ca. 4^{o}). However, these stereonet relationships may not be statistically significant and field observations suggest that everywhere in Tract 2 primary cleavage and fold axial planes are essentially parallel.

In Port Erin Bay (Fig. 5.23) primary folds and cleavage face steeply upwards to the NE and SW (Fig. 5.19b(i), (ii)). However, at Gansey Point (Fig. 5.24) some folds face steeply down to the SW (Fig. 5.19b(i), (ii)). This is due to the bedding being overturned on the common limb of a large primary fold pair, which occupies much of the SE coast of the Cregneash Peninsula (Fig. 5.2). This was described by Fitches *et al.* (1999) (Fig. 5.25(b)).

Secondary deformation is well preserved in the rocks of the Lonan Formation at Port Erin and clearly overprints structures related to the primary phase of deformation (Plates 5.21(b), 5.22(a)). However, the thicker bedded quartz arenites in the Gansey Point area fail to record evidence of secondary deformation, and therefore all the secondary deformation data in tract 2 is from Port Erin. Poles to secondary fold axial and cleavage planes, (Fig. 5.15b(v), (vi)) show relatively broad point maxima defining shallowly SE-dipping mean planes, whilst the mean fold hinge and bedding-cleavage intersection lineation plunge very gently ENE (Fig. 5.15b(v), (vi)).

Faulting does not appear to be extensive in Tract 2. Poles to fault planes (Fig. 5.15b(vii)) have a moderately to steeply NW-dipping mean plane, with a shallowly SW-plunging, mean slickenfibre lineation. At Gansey Point (Fig. 5.24), the headland is cut

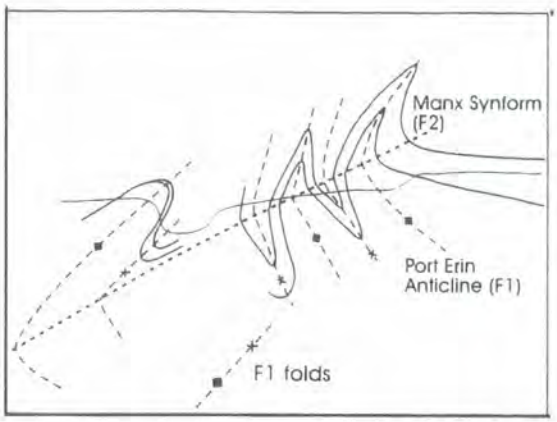

(a)

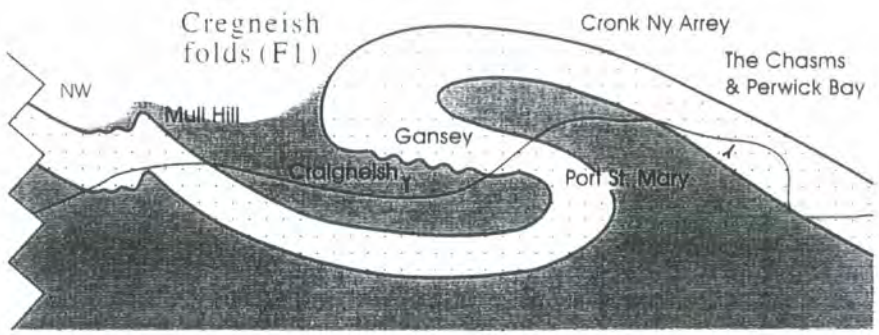

(b)

Figure 5.24. (a) Folding of primary folds and cleavage by large-scale secondary folds in Port Erin Bay (see Fig. 5.22), causes primary fold axial planes and cleavage to dip to the NW and SE. **(b)** Locally downward facing parasitic folds seen at Gansey Point, lie on the common limb of a large-scale recumbent primary fold on the Cregneish Peninsula (see Figs. 5.2, 5.23) (both figures from Fitches *et al.* 1999).

by a top-to-the-NW thrust fault within the coarse sandstones of the Mull Hill Formation. This in turn is cut by a NW-trending, steeply inclined, sinistral, strike-slip fault (Fig. 5.23, grid ref. 21576815).

5.6.3 Tract 3

Tract 3 (Fitches *et al.* 1999, Woodcock *et al.* 1999b) extends from Maughold Head in the NE to Bradda Head in the SW (Figs. 5.9, 5.10, 5.23, 5.26, 5.27) and is fault bounded to the NW and SE. It comprises rocks of the Lonan Formation around Port Mooar (Figs. 5.2, 5.26, grid ref. 487907), the Maughold Formation at Bradda Head (Figs. 5.2, 5.23, grid ref. 183698), and the Injebreck and Barrule formations at Lewaigue (Figs. 5.2, 5.27, grid ref. 460930). Tract 3 is predominantly covered by drift and much of the exposure around the coast is inaccessible. However, three areas assigned to Tract 3 by Fitches *et al.* (1999) and Woodcock *et al.* (1999b) were studied. These were Spaldrick to Bradda Head on the SW coast (Figs. 5.10, 5.23), Port Mooar to Maughold Head on the east coast (Figs. 5.10, 5.26) and a short section of the NE coast at Lewaigue south of Ramsey (Figs. 5.10, 5.27). Although all assigned to the same tract, the primary fold styles of each area are rather different, and may in part be due to the contrasting lithologies present in each of the separate study areas.

Poles to bedding planes (Fig. 5.15c(i)) are largely distributed along a NNW-trending, steeply dipping great circle girdle that corresponds to a very shallowly WSW-plunging β axis. A significant number of bedding poles form a broad point maximum that defines a moderately NNW-dipping mean plane (Fig. 5.15c(i)). Poles to primary fold axial planes (Fig. 5.15c(ii)) define a steeply inclined, NNW-dipping mean axial plane, whilst the mean primary fold hinge plunges very gently to the WSW, corresponding closely to the regional β axis (Fig. 5.15c(i), (ii)). Fold hinges in general, plunge shallowly or moderately to the ENE and WSW (Fig. 5.15c(ii)), and only around Lewaigue (Figs. 5.2, 5.10 5.26) are folds with steep plunges observed (see below). Primary folds around Bradda Head (Figs. 5.2, 5.23, Plate 5.22(a)) are close to tight and verge to the SE. Those at Port Mooar (Figs. 5.2, 5.26, Plate 5.22(b)) are open and upright, whilst primary folds at Maughold Head are close to tight and verge to the NW (Figs. 5.2, 5.26, Plate 5.23(a)). The orientation of the primary fold axial planes and hinges is closely matched by those of the primary cleavage planes and bedding-cleavage intersection lineation (BCIL) (Fig. 5.15c(ii), (iii)). Poles to primary cleavage planes define a steeply NNW-dipping mean cleavage plane, whilst the mean BCIL is sub-

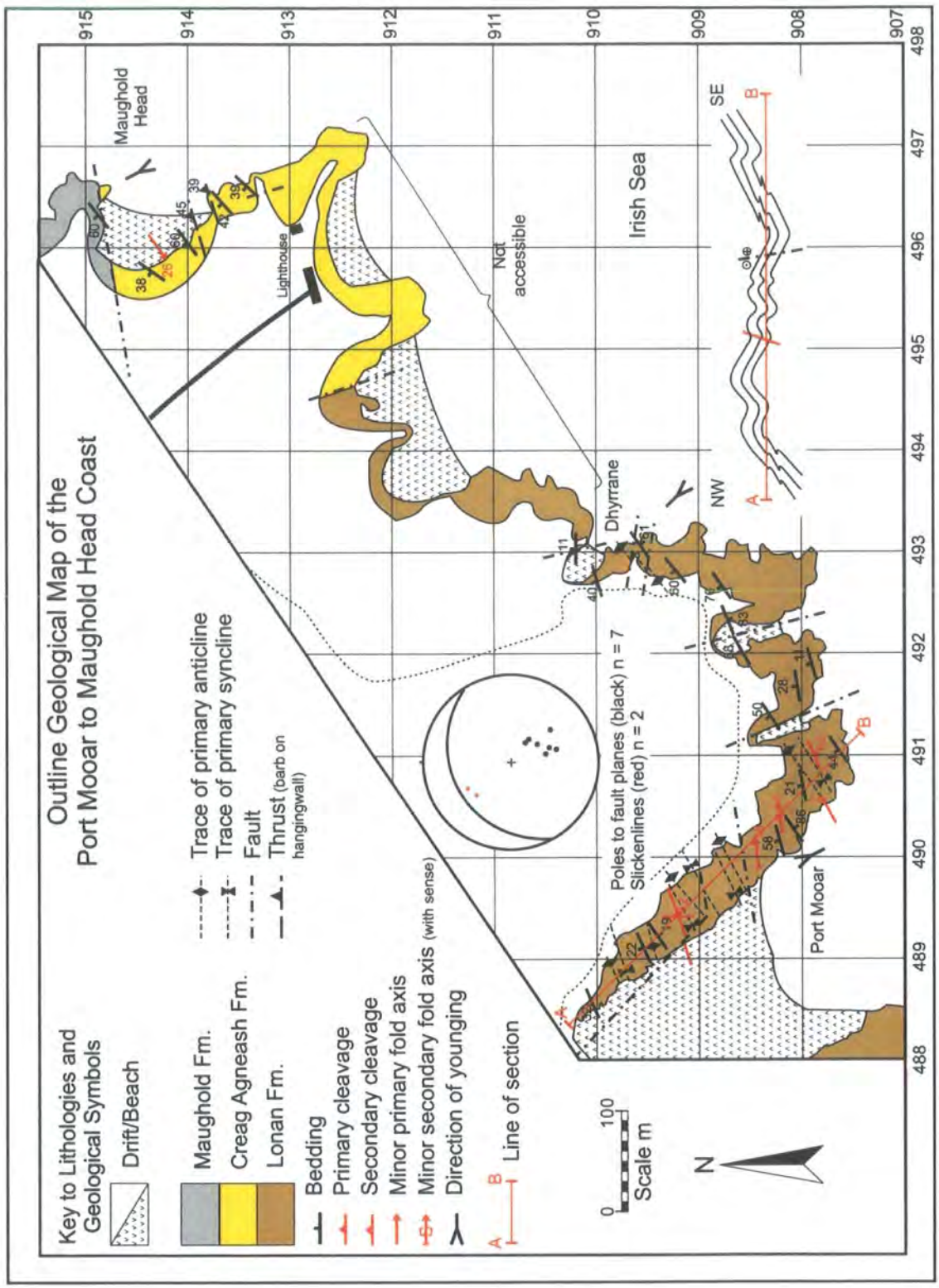

Figure 5.26. Outline geological map and sketch cross-section of the Port Mooar to Maughold Head Coast. Stereoplot shows thrust faults and slickenlines from Maughold Head.

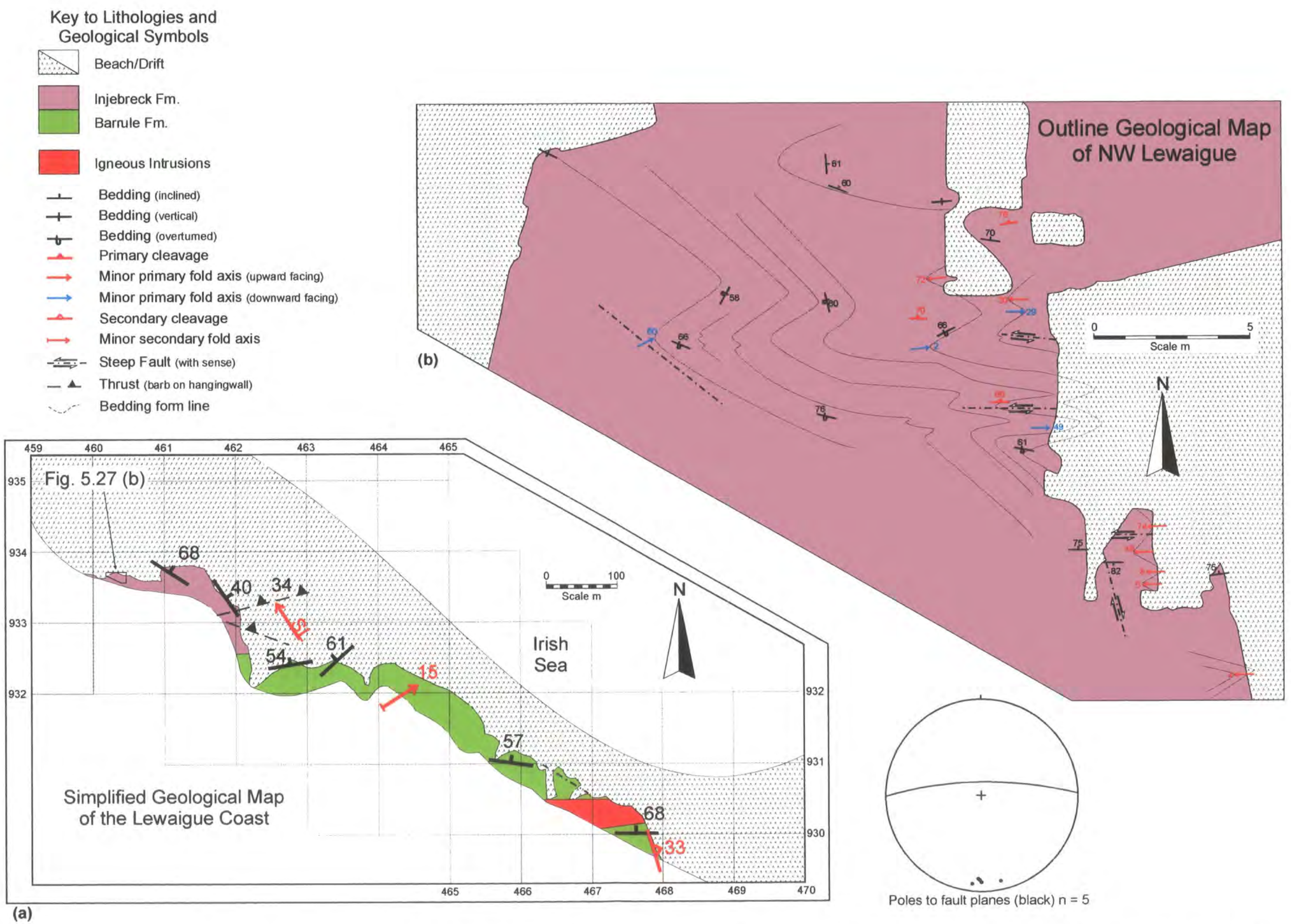

Figure 5.27. **(a)** Simplified geological map of Lewaigue (see Fig. 5.10 for location), with stereoplot for sinistral strike-slip faults (see text for details). Box shows location of Fig. 5.27(b). **(b)** Large-scale outline geological map of the extreme NW of Lewaigue.

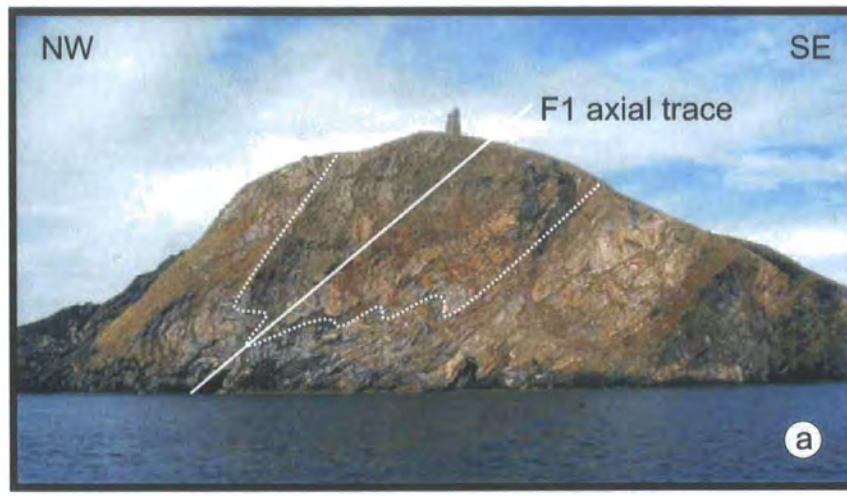

Plate 5.22. (a) Major SE-verging (F1) primary synform within the Maughold Formation of Tract 3 at Bradda Head (Fig. 5.23, grid ref.184699). Cliff is approximately 100m high. Upright, open primary folds within the Lonan formation of Tract 3 at Port Mooar (Fig. 5.26, grid ref. 48919095).

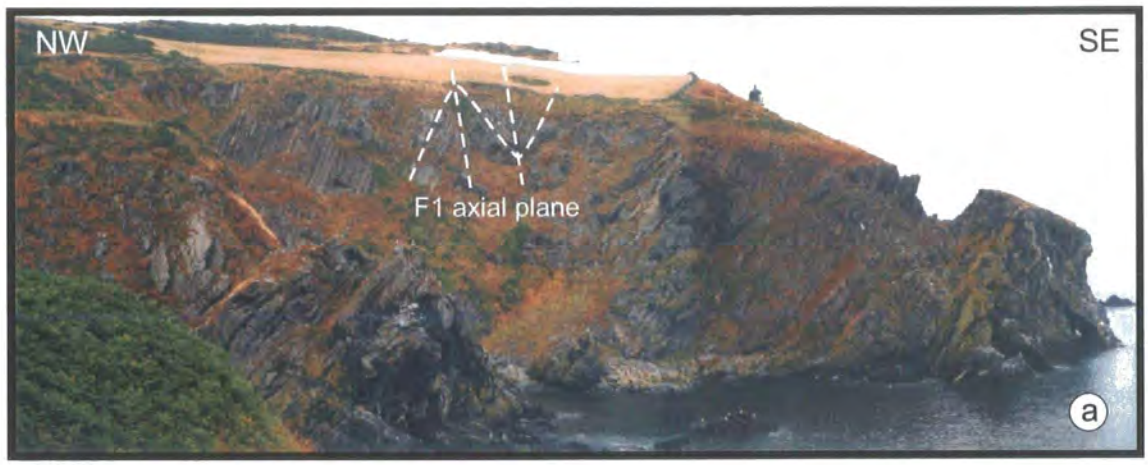

Plate 5.23. **(a)** NW-verging primary folds in rocks of the Creg Agneash Formation south of Maughold Head. (Figs. 5.2, 5.26, grid ref. 496912). **(b)** Sub-horizontal secondary folds and axial planar crenulation cleavage. Port Mooar (Figs. 5.2, 5.26, grid ref. 48869100).

horizontal with a WSW trend (Fig. 5.15c(iii)) and corresponds closely to the regional β axis (Fig. 5.15c(i)). The stereoplots for primary fold axial planes and cleavage (Fig. 5.15c(iv)) suggest that folds are slightly (ca. 5°) clockwise transected by cleavage. However, field observations where fold axial planes and cleavage were measured together indicate that they are essentially parallel.

Poles to secondary fold axial planes (Fig. 5.15c(v)) exhibit a well-defined point maximum that defines a shallowly NNW-dipping mean axial plane (Plate 5.23(b)). Secondary fold hinges (Fig. 5.15c(v)) plunge very gently towards the ENE, SW and NW, with a sub-horizontal, NNE-trending, mean fold hinge. Secondary folds dominate the structure of the Lewaigue coastline (Fig. 5.2, Plate 5.6(a)). Poles to secondary cleavage planes define a very shallowly E-dipping mean plane (Fig. 5.15c(vi)), with a sub-horizontal, ENE-trending, mean bedding-cleavage intersection lineation. At Port Mooar (Fig. 5.26) the secondary cleavage is very strongly developed, particularly in the finer-grained units (Plate 5.24(a)) where it overprints the primary cleavage producing a strong crenulation cleavage (Plate 5.24(b)).

Poles to fault planes show a broad point maximum defining a moderately inclined NNW-dipping mean fault plane (Fig. 5.15c(vii)). Slickenline lineation data is rather restricted, with a mean lineation that plunges moderately to the WNW suggesting an oblique component to the fault movement. However, three sets of faults can be distinguished in the field.

1. NE-SW-trending, NW-dipping low angled faults, with a top-to-the SE dip-slip sense of movement (Fig. 5.26, Plate 5.25(a)). These are particularly well developed around Maughold Head (Fig. 5.26,grid ref. 496915).
2. E-W-trending, steeply N-dipping, strike-slip faults with a predominantly sinistral sense of movement (Plate 5.25(b)). These have small offsets (few cm) and are most noticeable around the northern end of Lewaigue (Fig. 5.27(b)) where they are sub-parallel to the primary cleavage.
3. NNW-SSE-trending, steeply ENE-dipping, faults (Plate 5.26(a)). Fitches *et al.* (1999) suggest that these are normal faults. However, if they form part of the NNW-trending fault set observed along the coast south of Douglas (Figs. 5.2, 5.12) they may be sinistral strike-slip faults. Only one fault plane was exposed (Plate 5.26(a)) and this contained no kinematic indicators.

Primary folds and cleavage face predominantly up to the SW at moderate to steep angles (Fig. 5.19c(i), (ii)). The exception to this are several small folds exposed

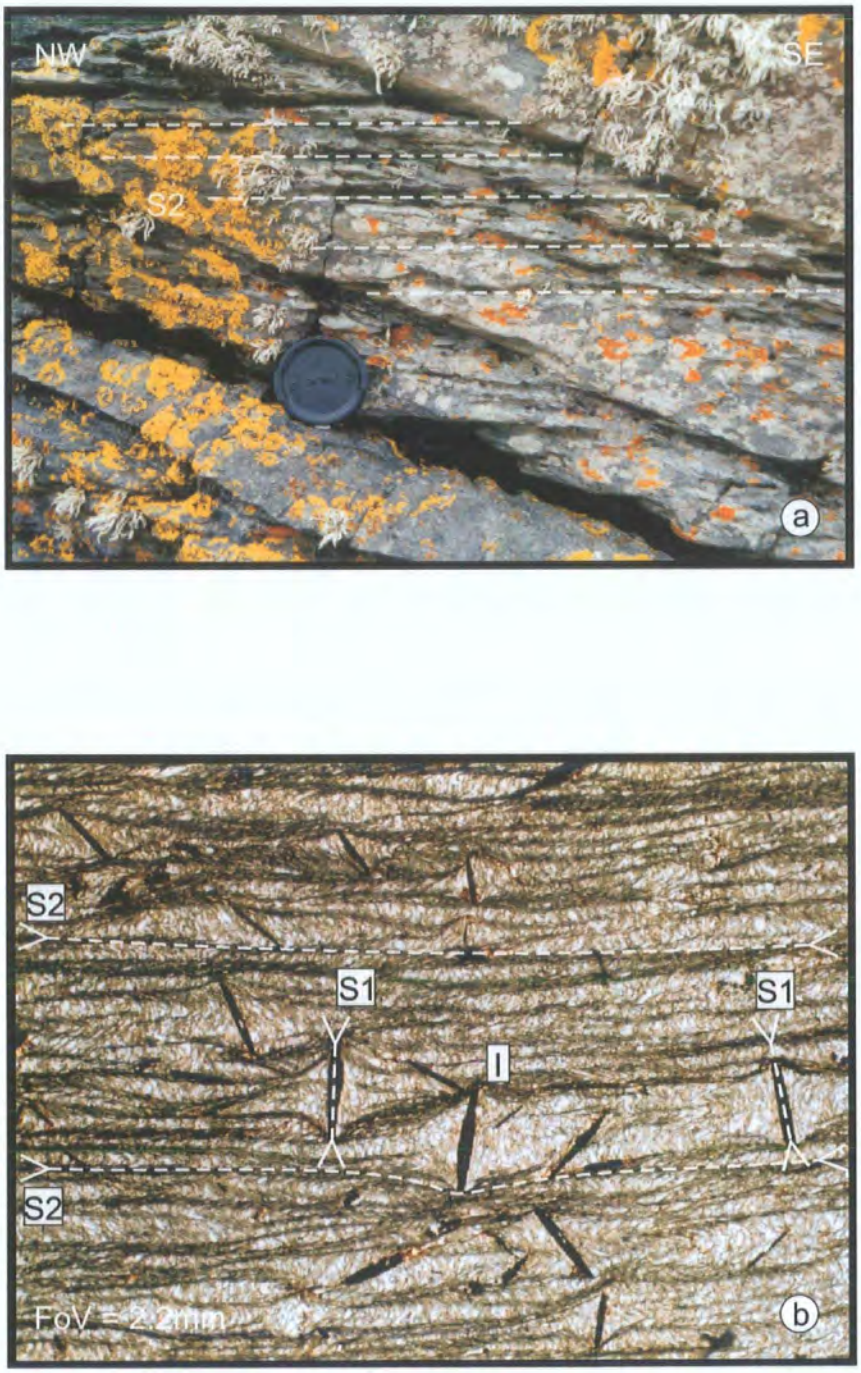

Plate 5.24. **(a)** Strong sub-horizontal secondary (S2) cleavage developed in siltstone/ mudstone horizons within the Lonan Fm. Port Mooar (Figs. 5.2, 5.26, grid ref. 48959095). Lens cap is 55mm across. **(b)** Thin section micrograph showing the strongly developed secondary (S2) crenulation cleavage within a siltstone sample from the Lonan Fm. The primary cleavage (S1) is highlighted by ilemenite platelets (I) and lies at a high angle to S2. Some platelets show deflection of S2 around the tips of the grains suggesting that the ilmenite grew prior to the development of S2. (Sample PM 2, grid ref. 49059083).

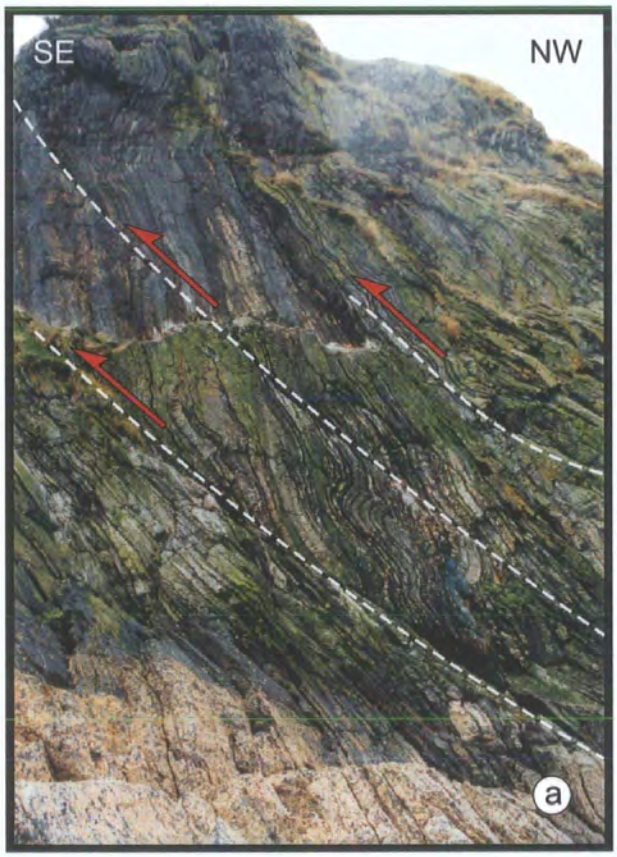

Plate 5.25. **(a)** Top-to-the-SE thrusts at Maughold Head (Figs. 5.2, 5.26, grid ref. 49629139). Cliff is approximately 30m high. **(b)** Small sinistral faults utilising primary cleavage planes within rocks of the Injebreck Formation. NW end of Lewaigue coast (Figs. 5.2, 5.27 (a) & (b), grid ref. 46039336).

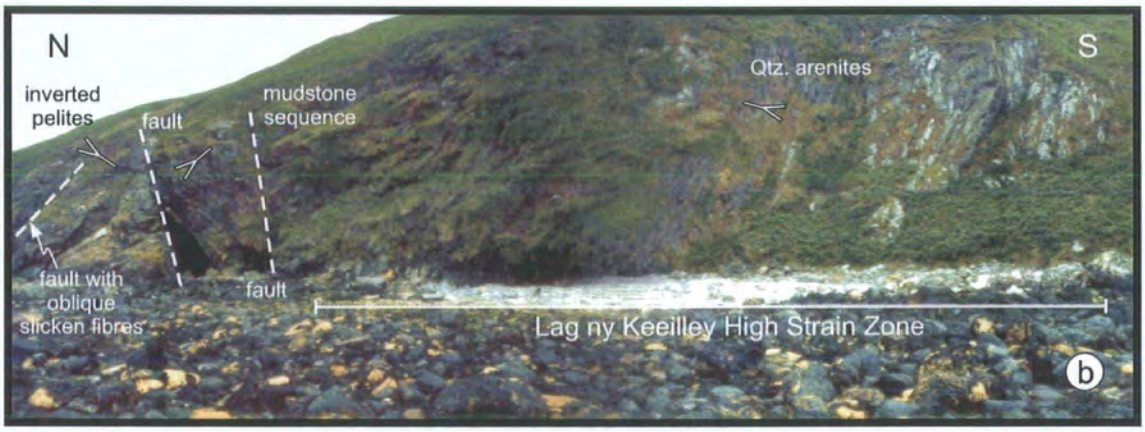

Plate 5.26. **(a)** Exposed NNW-trending fault plane at Dhyrnane Bay (Fig. 5.26, grid ref. 49309101). Two small extensional faults with top-to-the-SE displacements are highlighted. Rucksack in foreground for scale. **(b)** Photomontage of the shoreline beneath the hermits chapel at Lag ny Keeilley (Figs. 5.2, 5.28, grid ref. 216746). See Figure 5.28 for details

on a water worn outcrop to the south of Ramsey (Figs. 5.2, 5.27). Here a number of small (<2m) folds are observed to face up or down to the west. Folds that plunge to the west face up to the west, whilst those that plunge to the east, face down to the west (Fig. 5.19c(i), (ii)).

Unfortunately, the thick growth of seaweed, the dark, generally unlaminated nature of the Barrule Formation, and the pervasive secondary deformation along much of the Lewaigue coastline precluded a detailed study of the large-scale structure of the primary deformation in this area.

5.6.4 Tract 4

Tract 4 (Fitches *et al.* 1999, Woodcock *et al.* 1999b) forms the 'spine' of the Isle of Man (Fig. 5.9). The only readily accessible section is exposed on the foreshore below the old hermits chapel at Lag ny Keeilley (Figs. 5.2, 5.9, grid ref. 21627470, Plate 5.26(b)). Although comprising rocks assigned to the Barrule and Injebreck formations (Woodcock *et al.* 1999b, Chadwick *et al* 2001) only rocks of the Injebreck Formation are exposed on the foreshore at Lag ny Keeilley. Tract 4 is fault bounded to SE and NW against tracts 3 and 5 respectively (Fig. 5.9). A prominent brittle fault (Plate 5.26(b)) and ductile high-strain zone, (Fig. 5.28) (see below) separate a north-younging quartz arenite sequence to the south and an inverted sequence of pelite and quartz arenite to the north (Fitches *et al.* 1999, Kennan & Morris 1999, Woodcock *et al.* 1999b). This fault also corresponds with the axial trace of Simpson's (1963) Isle of Man Syncline (Fig. 5.4).

Poles to bedding planes (Fig. 5.15d(i)), although largely distributed along a steeply NE-dipping great circle girdle corresponding to a very shallowly SW-plunging β axis, have a broad, point maximum defining a steeply NW-inclined mean bedding plane (Fig. 5.15d(i)). Minor primary folds (Fig. 5.15d(ii)) are scarce with axial planes dipping to both the NW and SSE, whilst fold hinges plunge to the NE and WSW. Poles to primary cleavage planes and bedding-cleavage intersection lineations (BCIL) (Fig. 5.15d(iii)) define a steep SE-dipping mean plane and a gently SW-plunging mean lineation. On the stereoplot, the mean cleavage plane and BCIL show an apparent clockwise transection of the mean fold axial plane and fold hinge (Fig. 5.15d (ii)-(iv)). However, as no field evidence of transection was observed, this may be due to the limited fold data set, rather than a real transecting relationship. Poles to both secondary fold axial and cleavage planes (Fig. 5.15d(v), (vi)) define sub-horizontal mean planes,

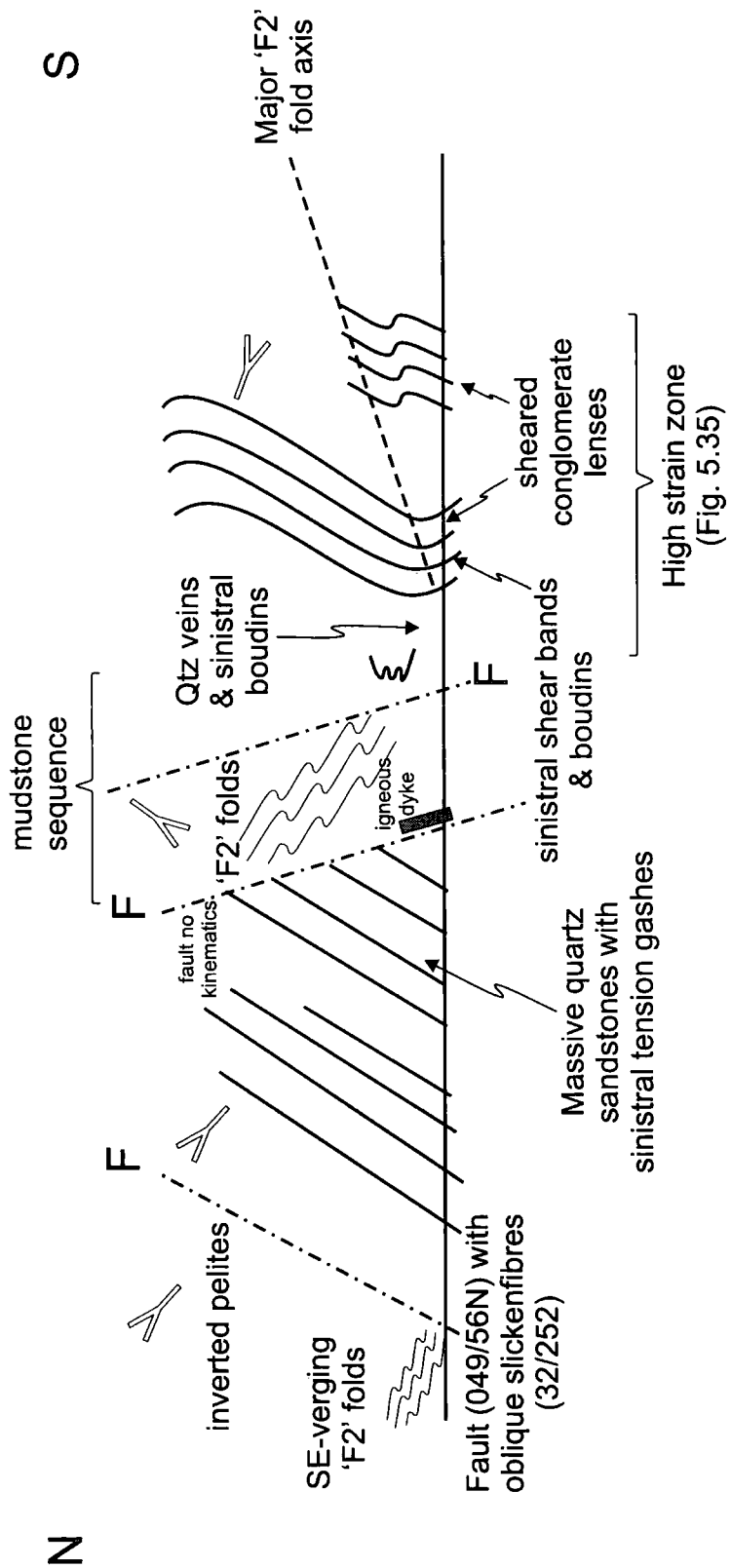

Figure 5.28. Schematic sketch cross-section of the Lag ny Keeilley foreshore (not to scale)

whilst their respective mean lineations plunge very gently and gently to the NE and W respectively. Poles to fault planes (Fig. 5.15d(vii)) define a steeply N-dipping mean fault plane, whilst the gently SW-plunging mean slickenline lineation suggest a strong oblique component to the fault movement. Throughout the Lag ny Keeilley coastal section studied there is extensive evidence for strike-slip shearing with a predominant sinistral sense (see below). Primary fold and cleavage facing directions are predominantly up to the NW (Fig. 5.19d (i), (ii)), although two folds were seen to face down to the NW and SW. This may be due to local refolding of primary folds during secondary deformation, although there was no evidence of the secondary crenulation cleavage even within the more pelitic units (Plate 5.27(a)).

5.6.5 Tract 6

The main area of study in Tract 6 was around The Niarbyl (Figs. 5. 2, 5.9, 5.10, 5.29, 5.30, grid ref. 210775) on the west coast of the island. Here the rocks of the Creggan Moar and Niarbyl formations are exposed along a short section of foreshore. The SE boundary lies approximately 2km to the south along a relatively inaccessible section of coast. However, the NW boundary is exposed along the foreshore and the base of The Niarbyl (Fig. 5.29, Plate 5.27(b)) This is a low angled fault, named the Niarbyl Thrust (Lamplugh 1903; Simpson 1963; Morrison 1989; Roberts *et al.* 1990; Fitches *et al.* 1999) that separates the Ordovician Creggan Moar Formation in the footwall from the Silurian Niarbyl Formation in the hangingwall. Lying immediately below the Niarbyl Thrust are the phyllonitic mylonites of the Niarbyl High Strain Zone (NHSZ) (Morrison 1989; Roberts *et al.* 1990; Fitches *et al.* 1999). Both the Niarbyl Thrust and NHSZ will be discussed fully in sections (5.6.7 and 5.7.3). Structural data relating to Tract 6 were collected to the SW of the NHSZ between Niarbyl Bungalow and Knockuskey Cottage (Fig. 5.29, grid refs. 21217762 and 21237755 respectively). The rocks in this area all belong to the Creggan Moar Formation, and include manganiferous ironstone (Plate 5.7(a)) and thin to medium bedded quartz arenite (Plate 5.7(b)). Although the large scale structure of the area is difficult to discern due to the generally very thinly laminated nature of the rocks, it was possible to construct a large-scale map and cross-section (Fig. 5.30) of a small area of foreshore containing a folded sequence of thin bedded quartz arenites. The general structures show by the map can be divided into two areas separated by a NE-trending inferred fault. To the SE of the fault the thinly bedded quartz arenites have been folded into a series of gently SE-plunging,

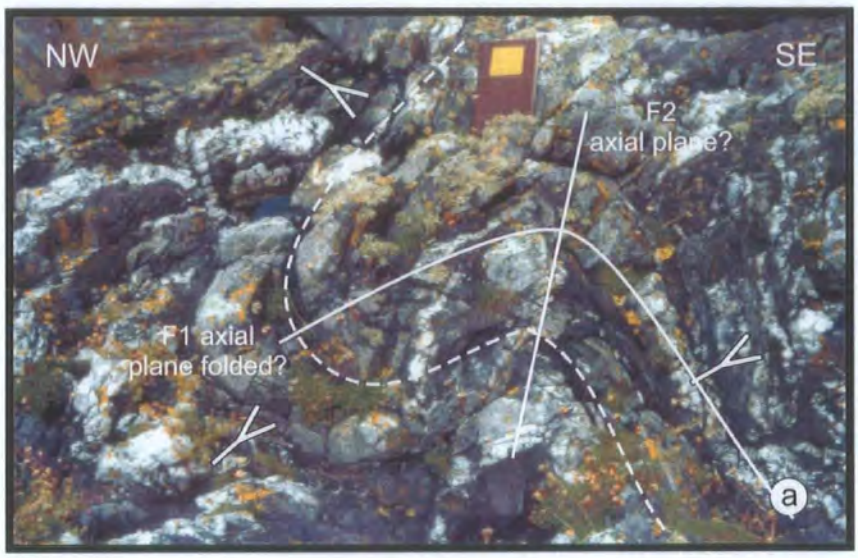

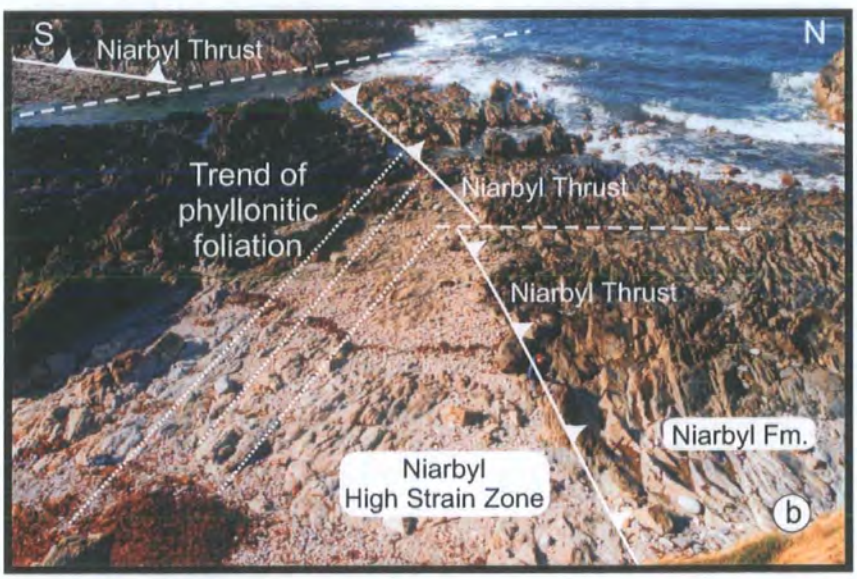

Plate 5.27. **(a)** Downward facing folds, possibly due to refolding by secondary deformation, on the foreshore below the hermits chapel at Lag ny Keeilley (Fig. 5.2, grid ref. 21577459). **(b)** The Niarbyl Thrust exposed at low tide on the foreshore at Niarbyl Bay (Figs. 5.2, 5.29, grid ref. 211776). The thrust (highlighted) is cut by a number of later faults (dashed). The phyllonitic fabric in the rocks of the Niarbyl High Strain Zone is oblique to and truncated by the thrust. Figure for scale.

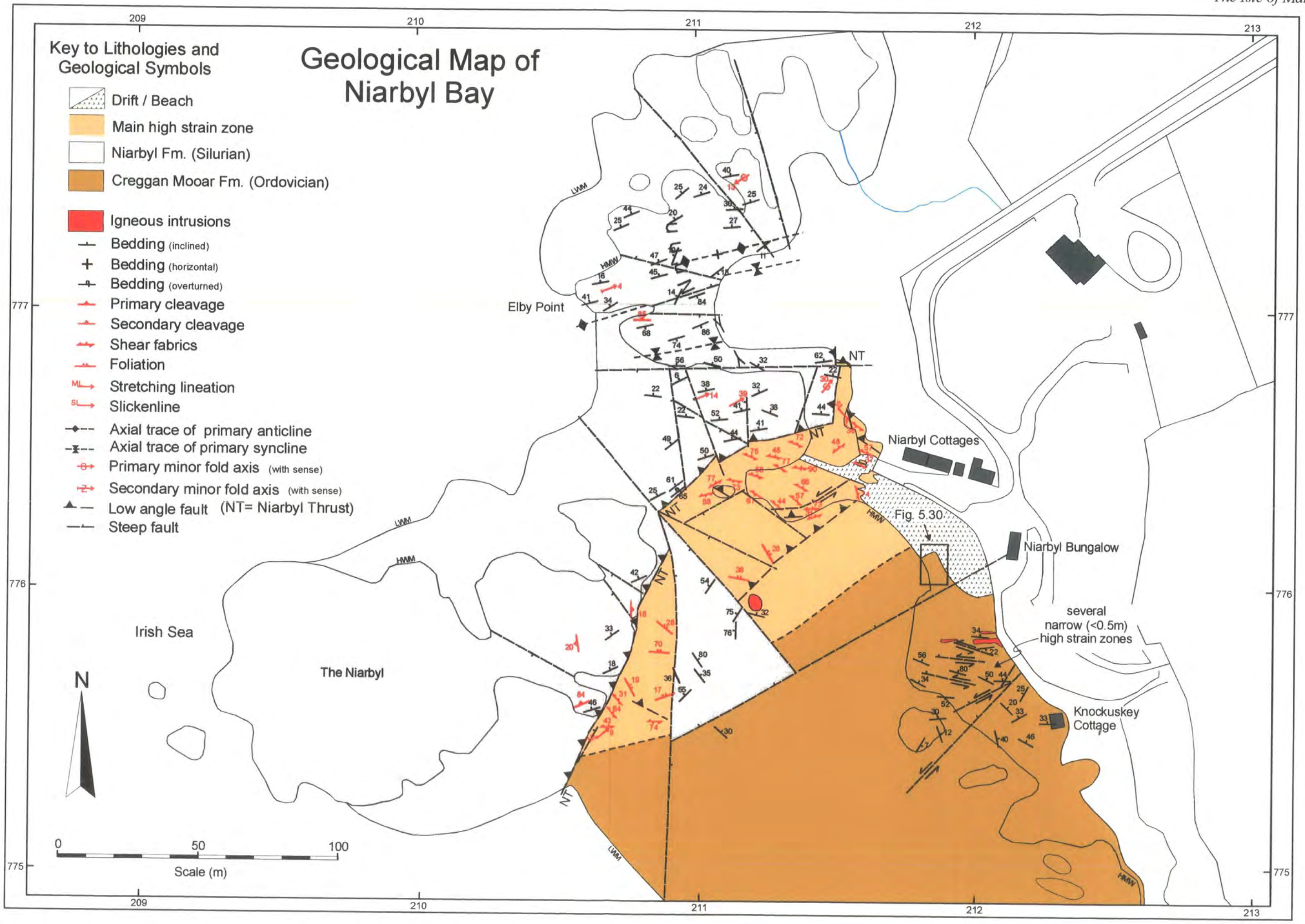

Figure 5.29. Geological map of Niarbyl Bay (see Fig. 5.10 for location).

Figure 5.30. Large-scale map and cross-section to illustrate the general structure of Tract 6

close to tight SW-verging primary folds (Plates 5.7(b), 5.28(a)). These folds are dissected by several moderate- to steeply inclined, SE-trending, sinistral strike-slip faults. In the extreme SE of the area the bedding becomes difficult to pick out due to extensive quartz veining, but appears to have been deformed by secondary folds. To the NW of the inferred fault, the bedding is much thinner, with very thin (5mm) laminae of the characteristic manganiferous ironstone (Plate 5.7(a)). This has been folded into a series of steeply-plunging tight to isoclinal folds (see section 5.7.3). At the extreme N of the outcrop a series of NE-trending, steeply-inclined faults cross-cut a thin igneous sheet and show small (<2m) sinistral offsets.

Poles to bedding (Fig. 5.31a(i)) show a well-defined point maximum corresponding to a moderately NNE-dipping mean bedding plane. The area is folded by a series of sub-metre folds (Plates 5.7(b), 5.28(a)) that spread a subordinate number of bedding poles along a girdle that indicates a shallowly ESE-plunging β axis (Fig. 5.31a(i)). This corresponds closely with the mean plunge of the primary folds (Fig. 5.31a(ii)). Many folds within the quartzites show accommodation features including steeply inclined P-type shears (Plate 5.28(b)) that indicate a sinistral sense of shear. Poles to primary cleavage (Fig. 5.31a(iii)) exhibit a well-defined point maximum corresponding to a NW-SE-trending, vertical mean plane. No bedding-cleavage intersection lineations were recorded in this tract. The stereonets for primary folds and cleavage planes (Fig. 5.31a(ii), (iii)) suggest that the mean cleavage lies significantly (ca. 31^{o}) anticlockwise of the mean axial plane (Fig. 5.31a(iv)). It is unclear as to whether the relationship may, or may not be statistically significant, as folds and their associated cleavage were not observed together. Poles to secondary fold axial planes and cleavage (Fig. 5.31a(v), (vi)) show an essentially sub-horizontal geometry, with a very shallowly ESE-plunging, mean fold axis. Bedding-cleavage intersection lineations for the secondary cleavage were not observed. Poles to fault planes, although broadly distributed define a moderately steep, NNE-dipping mean plane (Fig. 5.31a(vii)). Many faults are steeply inclined, with predominantly sinistral displacements (Plate 5.29(a)) that appear to define a system of interlinked strike-slip faults (Fig. 5.30). Minor primary folds show predominantly upwards facing patterns (Fig. 5.19e(i), (ii)). Facing is mostly steeply to moderately up to the SW, NE, SE, with a few folds facing gently to steeply downwards to the NE.

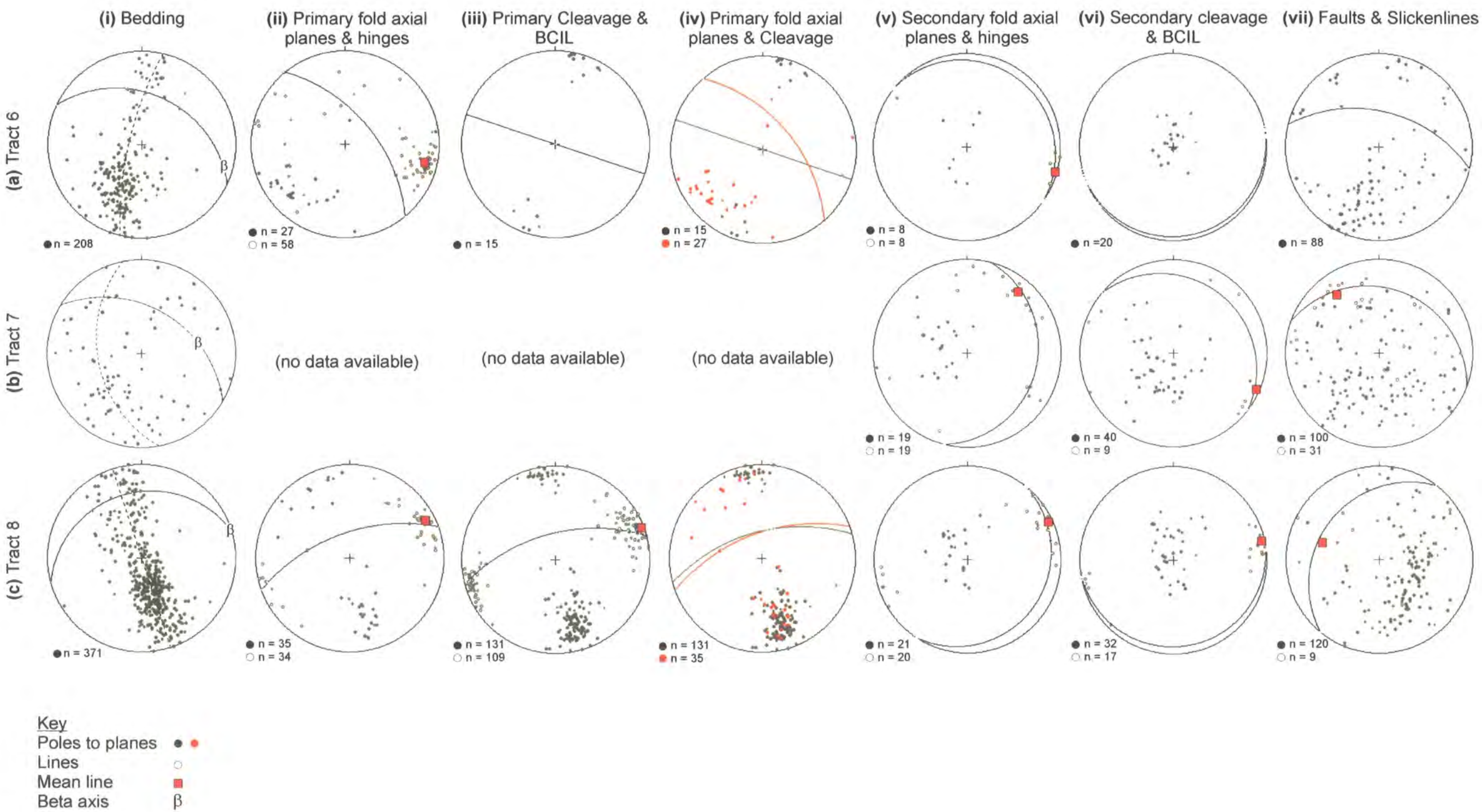

Figure 5.31. Stereoplots of structural data fromTracts 6-8 of the Isle of Man (labelled (a), (b) and (c)i-vii respectively). In each case **(i)** Poles to bedding planes, **(ii)** Poles to primary fold axial planes and fold hinges, **(iii)** Poles to primary cleavage planes and BCIL, **(iv)** Poles to primary fold axial (red) and cleavage (black) planes, with mean axial plane (red) and cleavage plane (black) shown. **(v)** Poles to secondary fold axial planes and fold hinges, **(vi)** Poles to secondary cleavage and BCIL, **(vii)** Poles to fault planes and slickenlines.

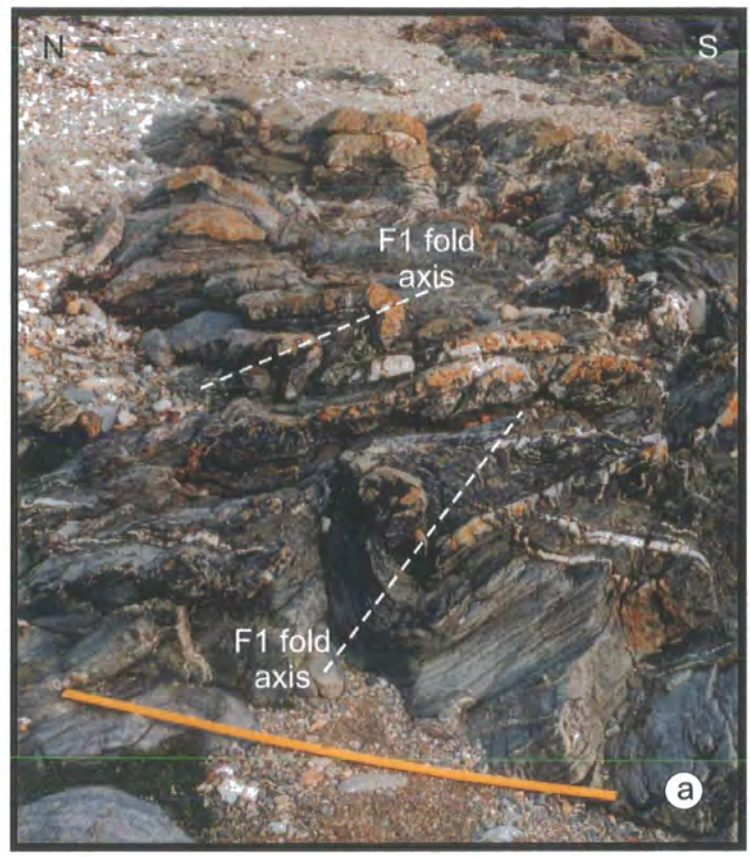

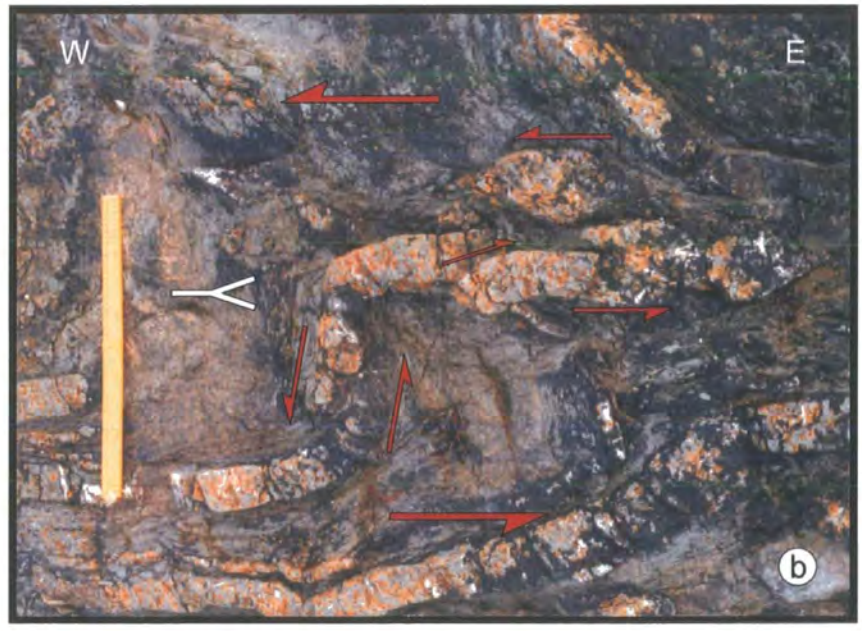

Plate 5.28. **(a)** S-verging (F1) primary folds within thin quartz arenite units of the Creggan Moar Formation at Niarbyl (Figs. 5.29, 5.30, grid ref. 21197761). Metre rule for scale. **(b)** Sinistral-verging primary fold with sinistral and dextral accommodation structures. View onto sub-horizontal surface. Folds face sideways to the W. Niarbyl Bay (Figs. 5.29, 5.30, grid ref. 21197760). Ruler is 0.5m.

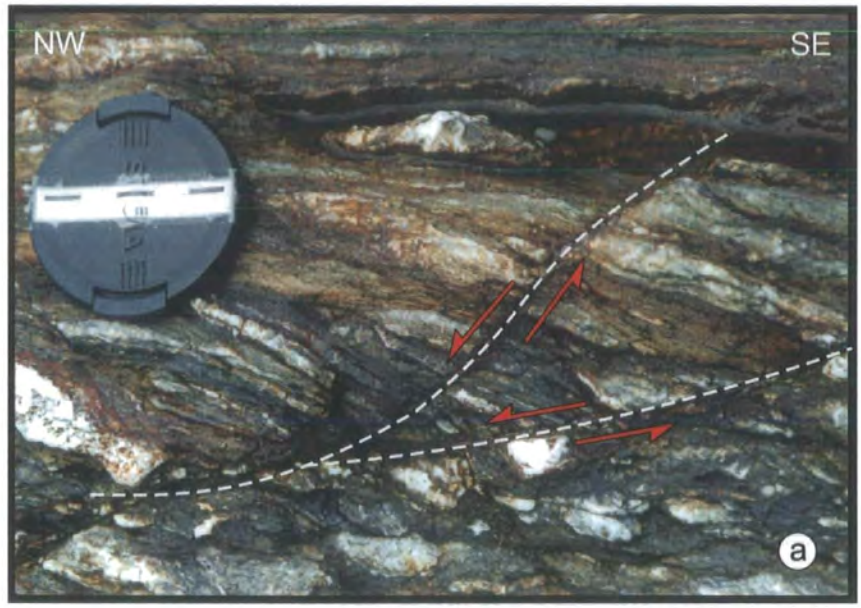

Plate 5.29. **(a)** Minor faults with small (2-3cm) sinistral offsets cross-cut sinistral quartz augen in protophyllonitic fabric within one of several narrow high strain zones to the S of the main outcrop of the Niarbyl High Strain Zone. (Fig. 5.29, grid ref.21217756). View down onto sub-horzontal surface. **(b)** Laminated siltstones and mudstones within the Lady Port Formation at Lynague. (Fig. 5.32, grid ref. 28138714)

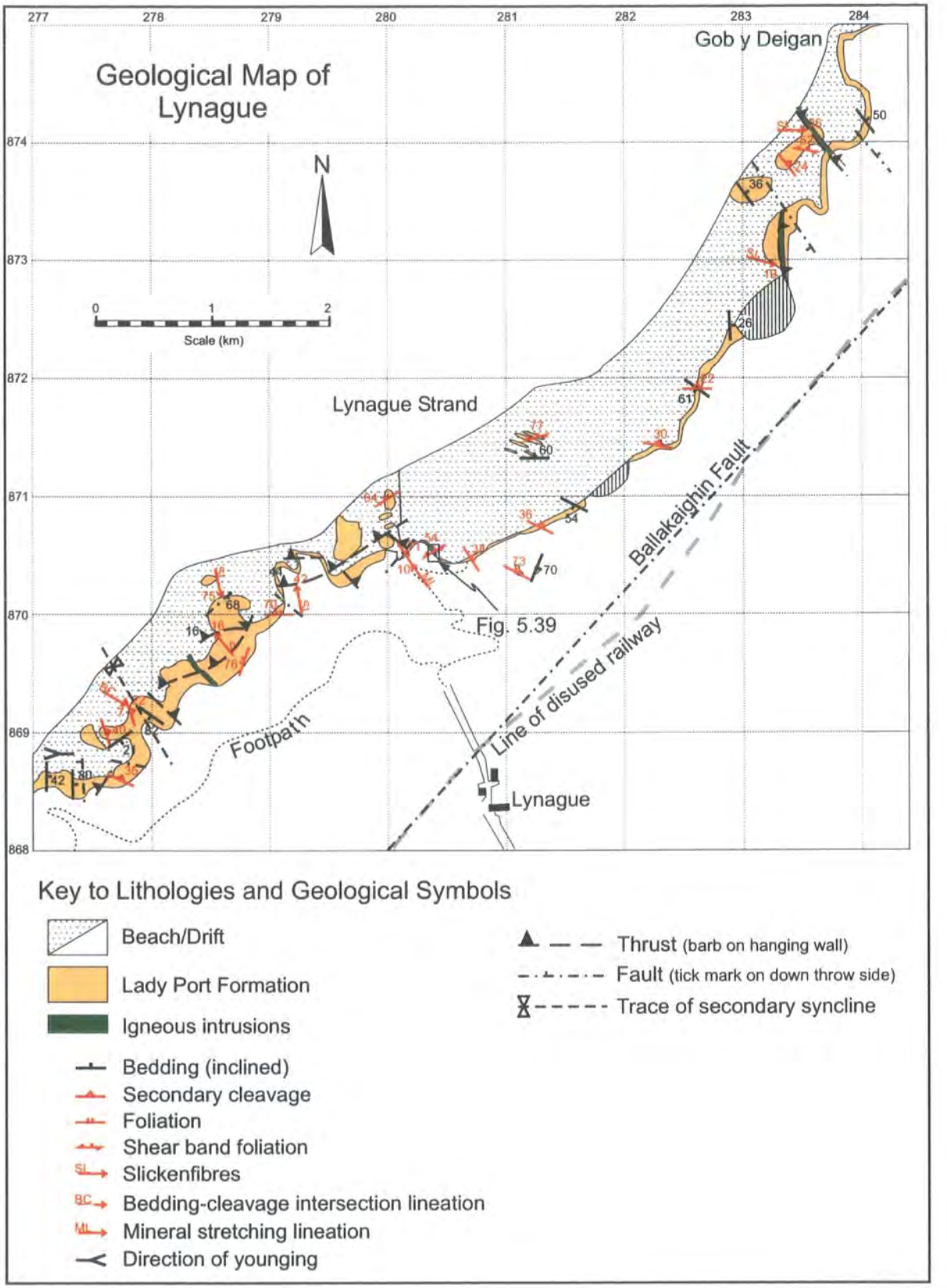

Figure 5.32. (a) Simplified map of the Lynague coastline (box shows locality of Fig. 5.36)

5.6.6 Tract 7

Tract 7 ((Fitches *et al.* 1999, Woodcock *et al.* 1999b) lies on the NW coast of the island (Figs. 5.9, 5.10, 5.32), where it forms a narrow strip approximately 4km long. The tract is bounded to the SE by the Ballakaighin Fault (Fig. 5.32, Woodcock & Morris 1999). The outcrop described here forms the middle section of the tract, lying between Gob y Deigan and Glion Broigh (Fig. 5.32, grid refs. 28388749, 27668686) and is approximately 2km long. It is comprised of laminated siltstones, (Plate 5.29(b)) mudstones, rare manganiferous ironstones and debrites (Plate 5.8(a), (b)) of the Lady Port Formation, with a number of sheet-like igneous intrusions, some of which appear to have been intruded into soft or partly lithified sediments (Woodcock *et al.* 1999b; Woodcock & Morris 1999). Between Gob y Deigan and the southern end of Lynague Strand (Fig. 5.32) bedding is often difficult to trace for more than a few metres and is frequently disrupted by soft sediment deformation (Plate 5.8(a)). The area also preserves evidence of sinistral shear (Plate 5.30(a)). This is most strongly developed at the southern end of Lynague Strand in a series, of narrow NW-trending high strain zones (see below).

The large-scale structure of this tract is difficult to determine. There appear to be no minor primary folds or cleavage, and the main tectonic fabric outside the high strain zone is a penetrative phyllitic foliation that most closely matches the secondary cleavage observed elsewhere on the island. Poles to bedding (Fig. 5.31b(i)) are broadly distributed, with a moderately NNE-dipping mean plane. There is however, some suggestion of a distribution along a moderately WSW-dipping girdle corresponding to a moderately ENE-plunging β axis. Poles to secondary fold axial planes define a shallowly E-dipping mean axial plane with a shallowly NE-plunging, mean fold hinge (Fig. 5.31b(v)). The mean secondary cleavage plane (Fig. 5.31b(vi)) dips gently to the NE, whilst the mean bedding-cleavage intersection lineation plunges very gently to the SE.

Faults form one of the dominant structural features of Tract 7. Poles to fault planes (Fig. 5.31b(vii)) although broadly distributed define a shallow NNE-dipping mean plane. Four main sets of faults can be distinguished (Fig.5.33).

a) Steep to moderately dipping faults (Plate 5.30(b)) These faults strike mostly to the N or NW and show normal displacements that displace all other structures (Fig. 5.33(a), Plate 5.30(b)).
b) NW-trending, NE-dipping, low angled faults (Fig. 5.33(b), Plates 5.30(b), 5.31(a)).

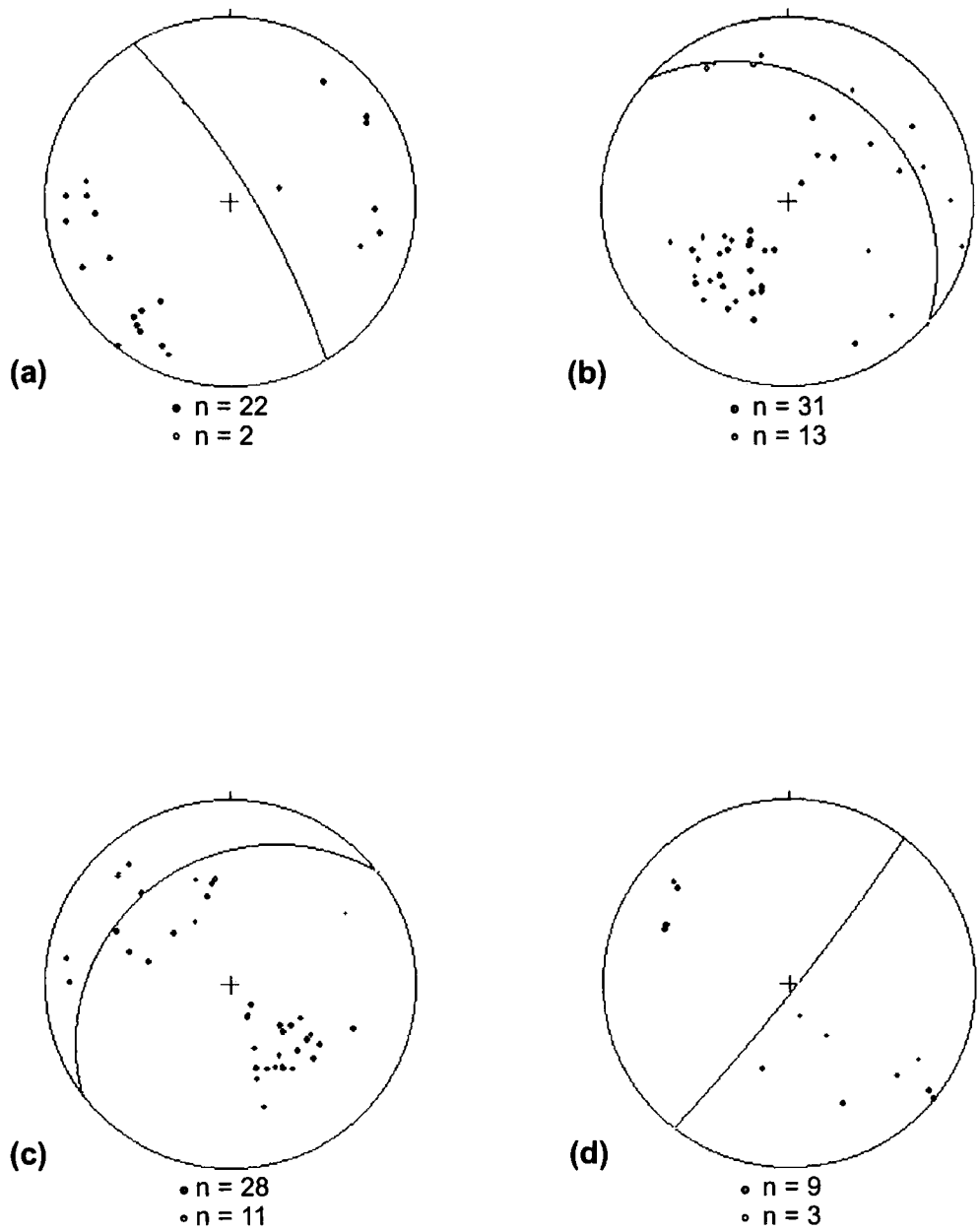

Figure 5.33. Stereoplots of faults from Tract 7 . **(a)** Poles to fault planes (black) and slickenlines (red) for NW to NE-striking, steeply inclined faults, mean plane 149/81N. **(b)** Poles to NW-trending low angled faults and slickenlines, mean plane 132/36N, mean slickenline12/124. **(c)** Poles to NE-trending low angled faults and slickenlines, mean plane 053/33N, mean slickenline 31/320. **(d)** Poles to NE-trending, steeply inclined faults and slickenlines, mean plane 038 88N.

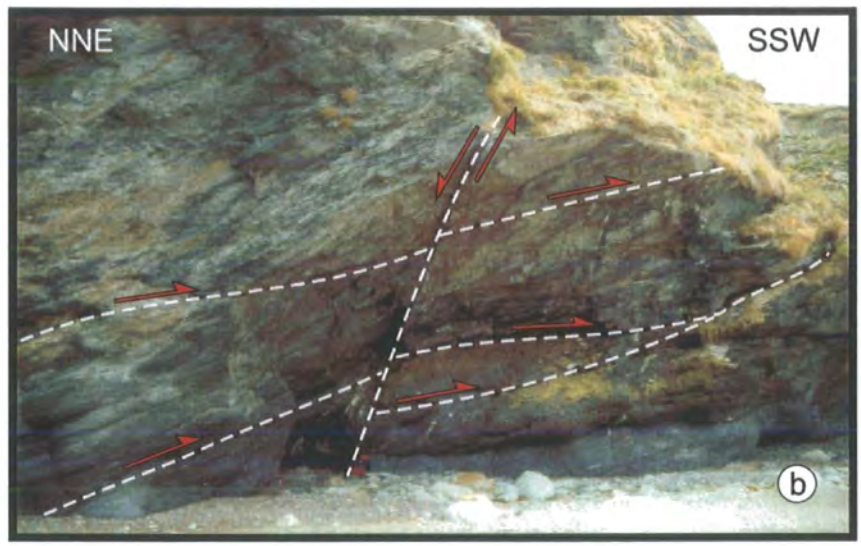

Plate 5.30. **(a)** Small sinistral R-shears /shear bands in laminated siltstone and mudstone of the Lady Port Formation. Also note extensive soft sediment deformation and slump fold. Lynague (figs. 5.2, 5.32, grid ref. 28388740). **(b)** Low-angled top-to-the SW thrusts cut by later dip-slip normal fault. Lynague (Figs. 5.2, 5.32, grid ref. 28338733). Rucksack at base of cliff for scale.

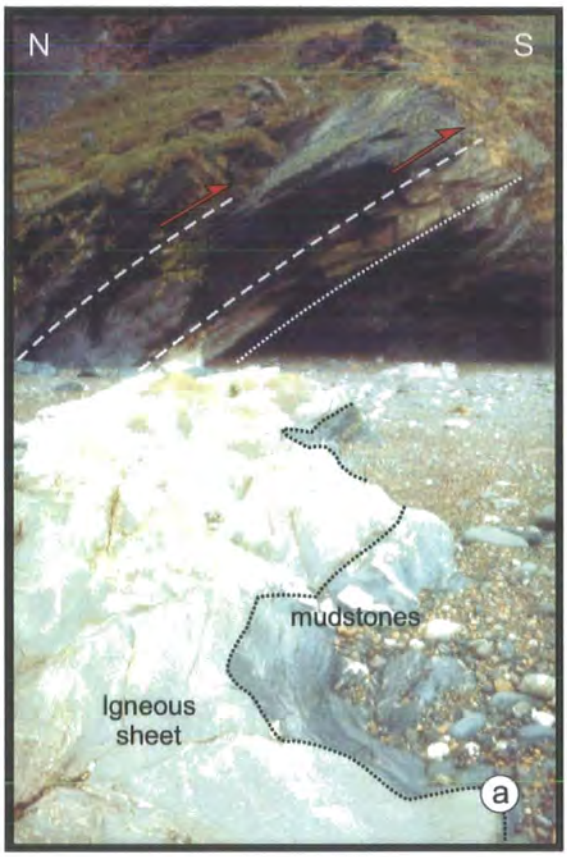

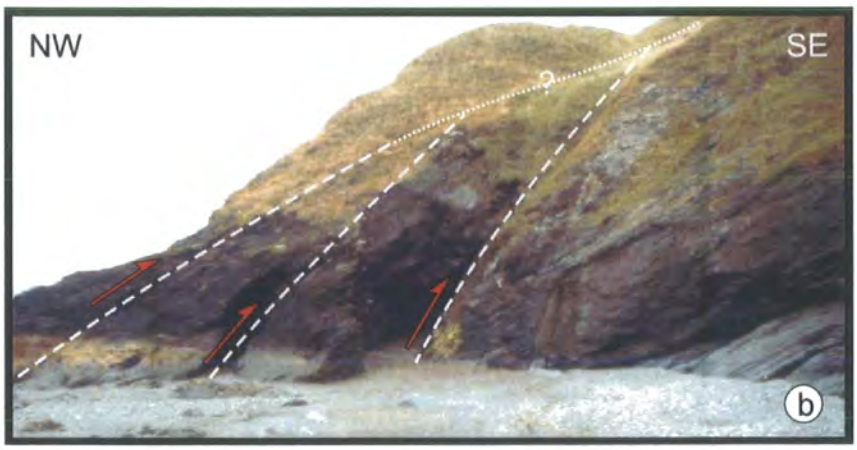

Plate 5.31. **(a)** Altered igneous sheet, with irregular lower contact (highlighted) suggests intrusion into unconsolidated sediments. Low-angled top-to-the SW thrusts appear to be closely spatially associated with the intrusions. Northern end of Lynague Strand (Figs. 5.2, 5.32, grid ref. 28388740). **(b)** NE-trending top-to-the SE thrusts. Preferential erosion along the fault planes has produced a series of arches and tunnels along the coast to the south of Lynague. (Figs. 52., 5.32, grid ref. 27918702).

Slickenlines on some of these faults suggest an oblique sense, possibly top-to-the W. Although not seen along this section of coast, Woodcock & Morris (1999) note the presence of quartz vein arrays elsewhere in Tract 7 that suggest a thrust sense of displacement.

c) NE-trending, moderate to low angled faults that mainly dip to the NW (e.g. Plate 5.31(b), Fig. 5.33(c)). Slickenlines indicate dip-slip movement, but there are no kinematic indicators to determine whether these are thrusts or low angled extensional faults. They do not appear to be cut by the faults described in 2 above, suggesting that they may be later. Due to an absence of cross-cutting relationships their age with respect to the faults in 1 above remains uncertain. However, these faults have a similar trend to the tract bounding Ballakaighin Fault (Fig. 5.32) and may be associated with this major fault.

d) NW-trending, steeply SE-dipping normal faults (Fig. 5.33(d), Plate 5.32 (a)). Again cross-cutting relationships are absent.

The absence of primary fold and cleavage data precludes the use of structural facing in this tract, while its structural isolation from the other tracts make direct comparisons difficult.

However, the orientation of the mean bedding in Tract 7 is significantly different from the general trend observed in most other tracts (Figs. 5.15(i), 5.31(i)) where a NE to ENE trend is the norm. This difference in the orientation of the mean bedding plane is also evident in Tract 6 (Figs. 5.29, 5.30, 5.31(i)), where the mean fold axial and cleavage planes (Fig. 5.31(ii), (iii)) are also rotated in a clockwise sense with respect to tracts 1, 2, 3, 4, 8 (Figs. 5.15(ii), (iii), 5.31(ii), (iii)). This suggests that tracts 6 and 7 may have been rotated following the primary phase of deformation. Woodcock and Schubert (1994) cite examples of crustal block rotation in strike-slip fault zones where clockwise rotations are the product of dextral strike-slip (Fig. 5.34). However, strike-slip deformation in tracts 6 and 7 is predominantly sinistral not dextral (see below). It is however, possible to produce clockwise block rotations during sinistral strike-slip faulting as discussed in chapter 1 section 1.4.3.2 (Fig.1.33), where the elongate blocks are separated by synthetic sinistral Riedel-type faults.

5.6.7 Tract 8

Tract 8 extends from Peel Castle to the Niarbyl and forms the western most margin of the island (Fig. 5.9). Near to Peel the tract boundary is the faulted contact

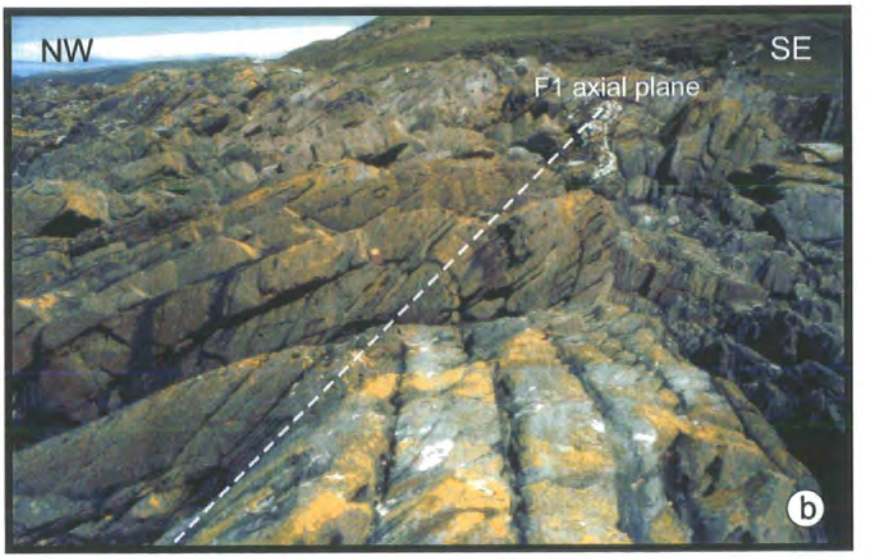

Plate 5.32. (a) NE-trending dip-slip normal fault downthrowing to SE. South of Lynague (Figs. 5.2, 5.32, grid ref. 27868702). **(b)** SE-verging primary fold within the Niarbyl Formation near to Dalby Point. (Figs, 5.2, 5.35, grid ref. 21277877). Notebook in both photographs is 15cm high.

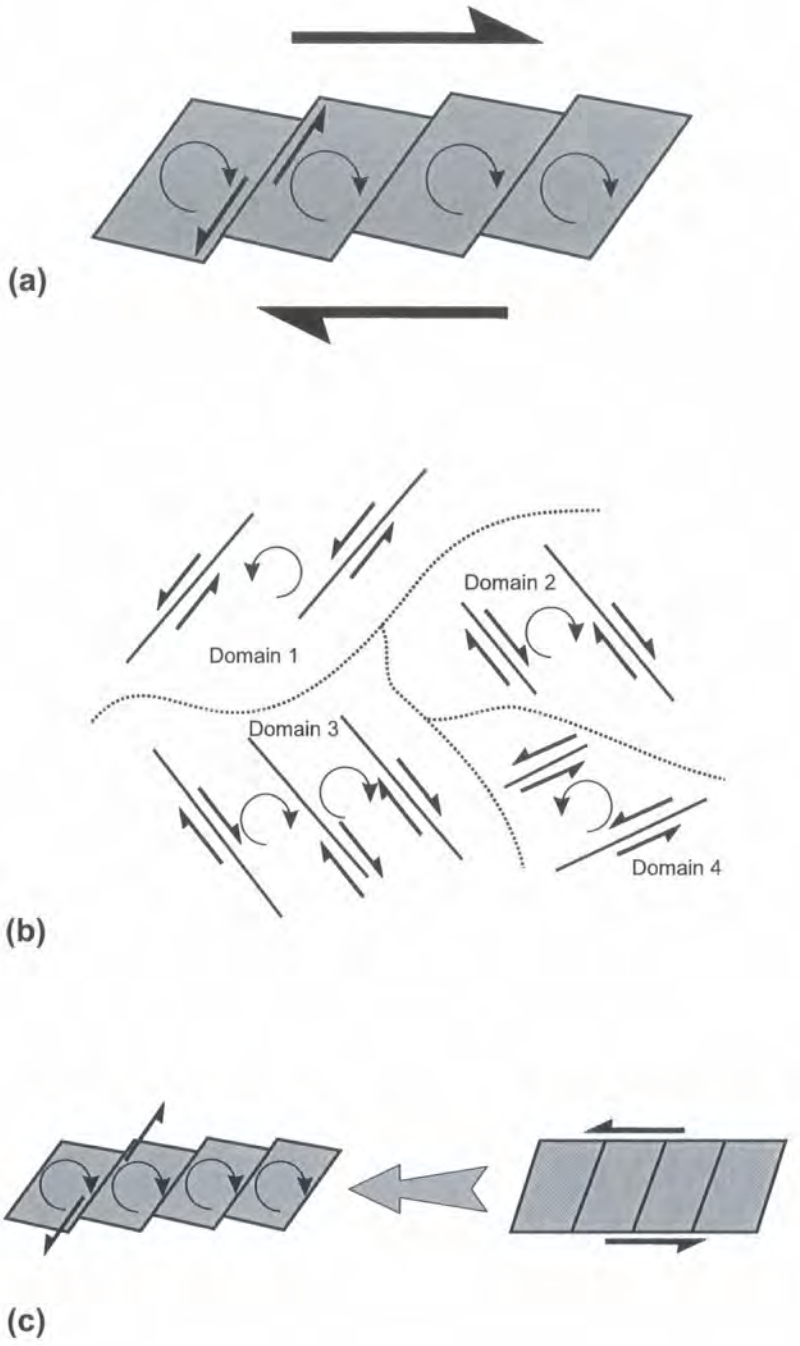

Figure 5.34. Diagram illustrating the kinematics and geometry of block rotations that may occur during strike-slip deformation **(a)** Clockwise block rotations due to dextral strike-slip faulting, with antithetic, sinistral bounding faults. **(b)** Domainal structure, with discrete areas of sinistral faults abutting areas of dextral faults and anticlockwise-rotating blocks. **(c)** Clockwise-rotating blocks due to sinistral strike-slip deformation with synthetic sinistral bounding faults. (after Woodcock & Schubert (1994) and Hanmer & Passchier (1991)).

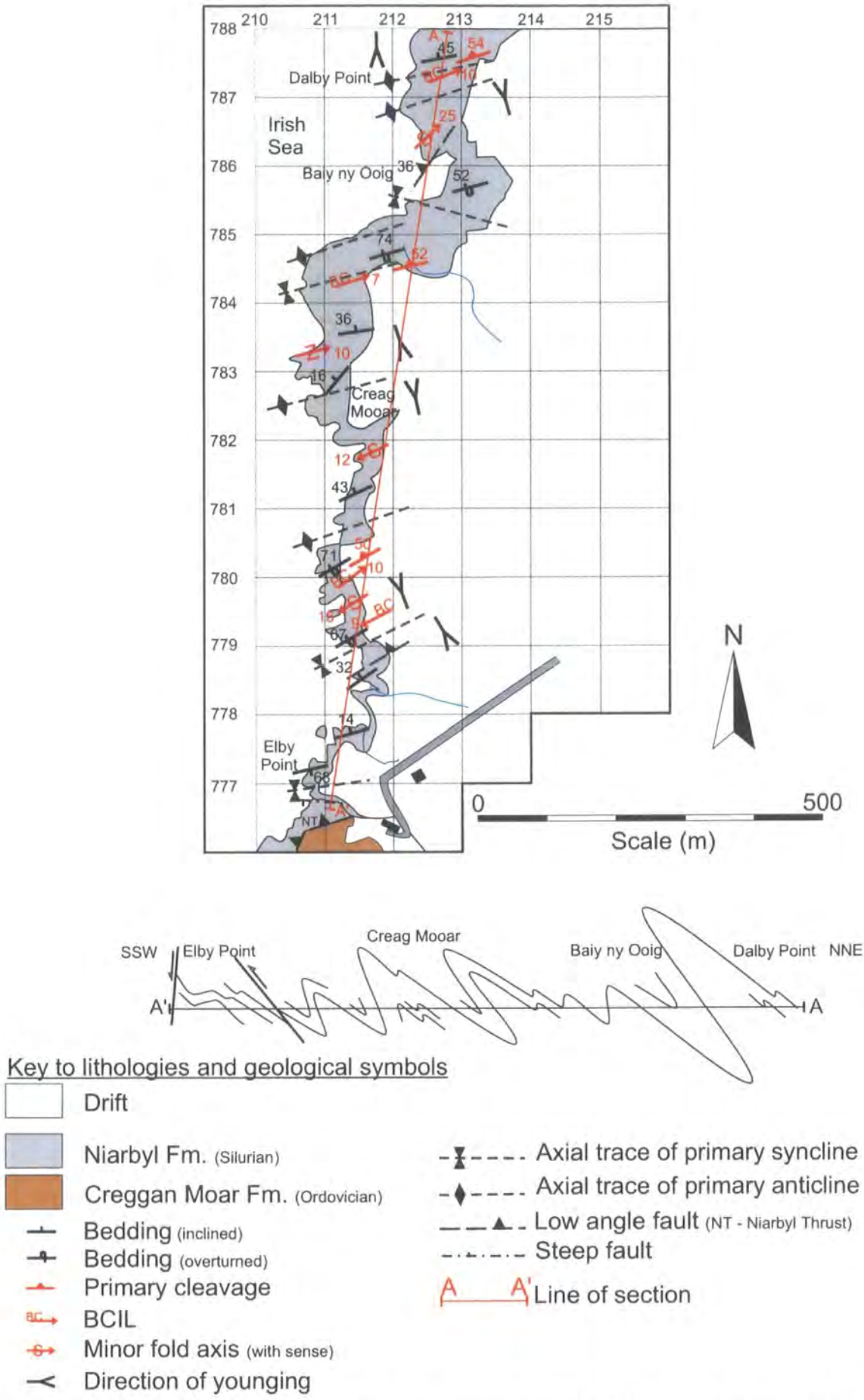

Figure 5.35. Simplified geological map and cross-section of Dalby Point to Elby Point.

with Upper Palaeozoic rocks, whilst to the south, the boundary is the Niarbyl Thrust (Fig. 5.9). Consisting entirely of rocks of the Silurian Dalby Group (Table 5.1, Figs. 5.2, 5.9) it is particularly well-exposed between The Niarbyl and Dalby Point (Figs. 5.2, 5.10, 5.29, 5.35). This was chosen as the main area of study for this tract, although some additional data was collected at Peel Castle.

Poles to bedding (Fig. 5.31c(i)) show a broad point maximum that defines a shallowly NNW-dipping mean plane. Bedding is however, often overturned to the S by a series of metre to tens-of metre scale, S-verging primary folds (Figs. 5.31c(ii), 5.35, Plate 5.32(b)). These spread a subordinate number of bedding poles along a vertical NNW-trending great circle girdle corresponding to an ENE-trending horizontal β axis. This corresponds closely to the mean plunge of minor primary folds and bedding-cleavage intersection lineations (Fig. 5.31c(i), (ii), (iii)) which mostly show only minor amounts of hinge line curvilinearity (20-30°). The stereonet for primary cleavage and fold axial planes (Fig. 5.31c(ii), (iii), (iv)) suggest that the mean cleavage plane and mean BCIL lie slightly clockwise of the mean axial plane and fold plunge (ca. 5°). This is confirmed by field observations (e.g. Fig. 5.35, grid ref. 21277877, Plate 5.33(a)). Primary folds and cleavage predominantly face steeply upwards to the SE (Fig. 5.19f(i), (ii)).

Poles to secondary fold axial and cleavage planes show similar distributions, with well-defined point maxima corresponding to very gently inclined mean planes (Fig. 5.31c(v), (vi), Plates 5.33(b), 5.34(a)). The stereonets for secondary fold axial and cleavage planes suggest that the mean cleavage plane lies significantly clockwise of the mean axial plane (Fig. 5.31c(v), (vi)). However, field observations indicate that everywhere in Tract 8 the secondary fold axial and cleavage planes are essentially parallel.

The structure of Tract 8 is dominated by the presence of low -angled, NW-dipping faults (Fig. 5.31c(vii), Plate 5.34(b)). Poles to fault planes define a moderately NW-dipping mean fault plane with a moderately NW-plunging, mean slickenline lineation (Fig. 5.31c(vii)). Offset markers indicate predominantly top-to-the SE displacements consistent with the sense of overturning on the primary folds. Although individual displacements are generally less than 0.5m (Plate 5.35(a)), the large number of faults suggests that the overall displacement could be relatively large. The most prominent of these low angled faults is the Niarbyl Thrust, which forms the boundary with Tract 6 (Figs. 5. 9, 5.29, Plates 5.27(b), 5.35(b)). Although, stratigraphically, this

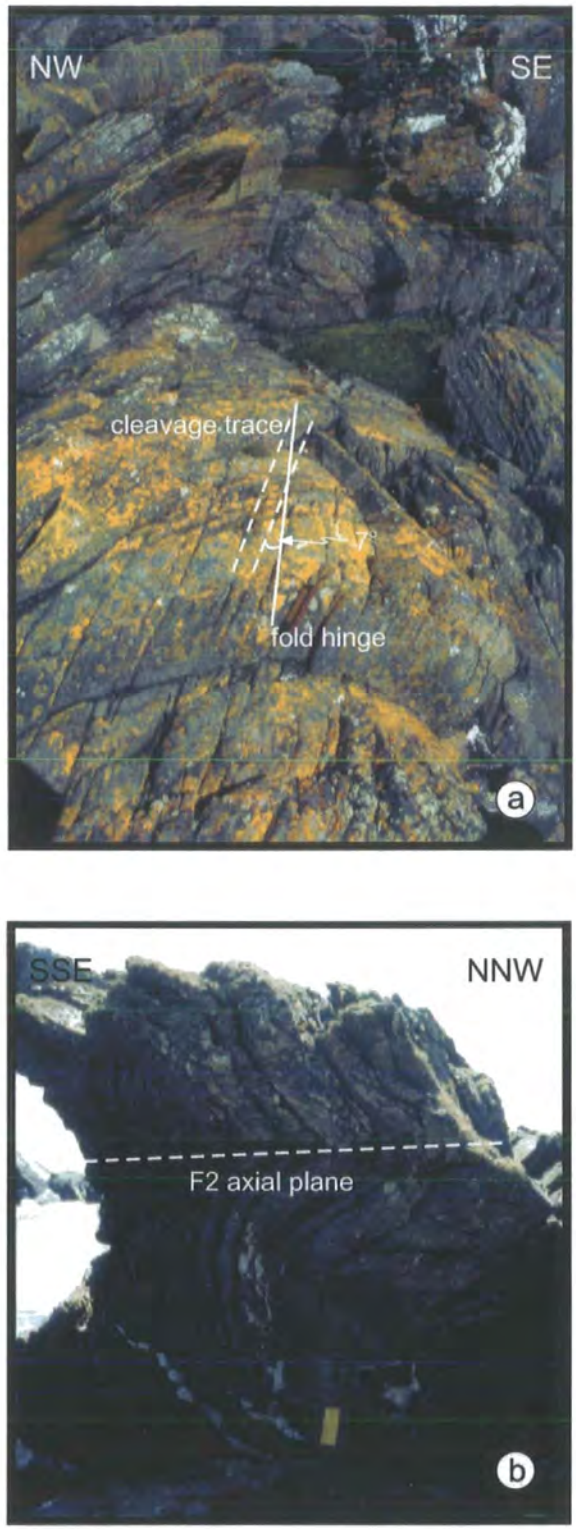

Plate 5.33. **(a)** SE-verging, clockwise transected, primary fold at Dalby Point. Cleavage (dashed line) lies 7° clockwise to the fold hinge (solid line). (Figs. 5.2, 5.35, grid ref. 21 277877). Fold is approximately 1m across. **(b)** Sub-horizontal secondary (F2) folds in bedded turbidites of the Niarbyl Formation. Baiy ny Ooig (Fig. 5.35, grid ref. 21307858). Notebook for scale.

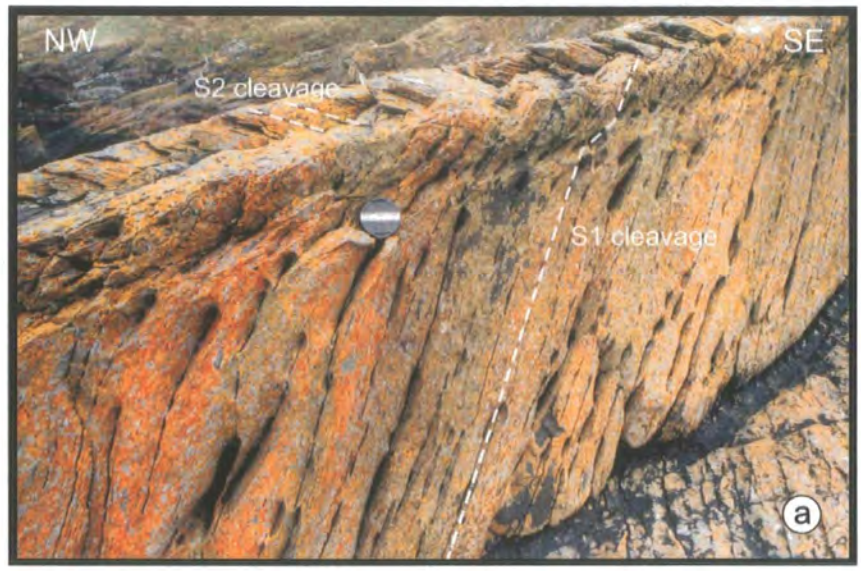

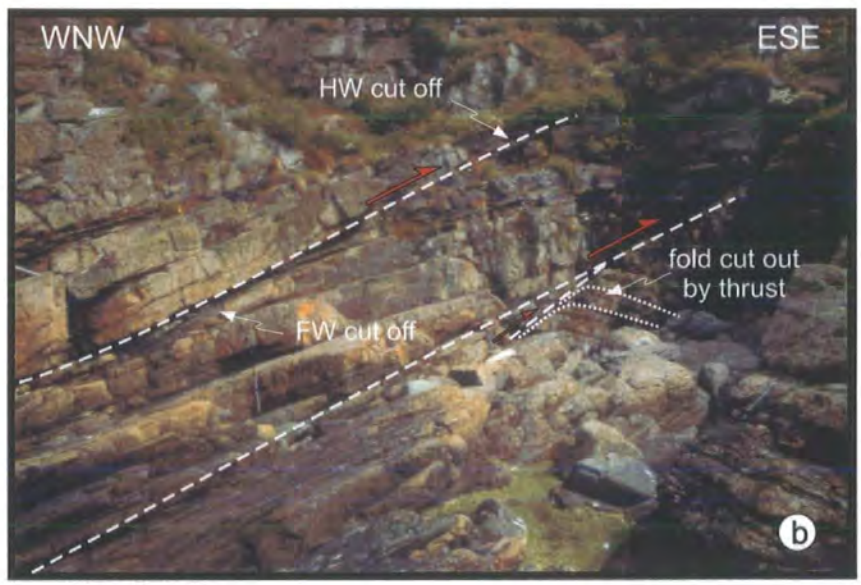

Plate 5.34. **(a)** Primary (S1) and secondary (S2) cleavages in Niarbyl Formation turbidites: S1 is preserved in the coarser sandstone units, refracting within finer layers, whilst S2 is only preserved in the finest units of siltstone and mudstone. Elby Point. (Figs. 5.29, 5.35, grid ref. 21077771). Lens cap is 55mm across. **(b)** Top-to-the SE thrusts associated with the Niarbyl Thrust. The upper thrust has an offset of approximately 7m. North of Elby Point (Fig. 5.35, grid ref. 2117889). Pole above lower thrust is 1m high.

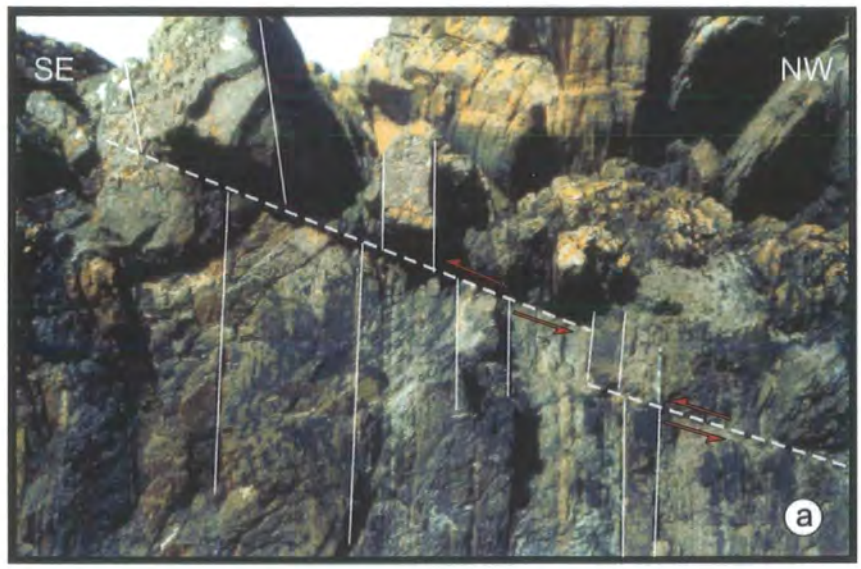

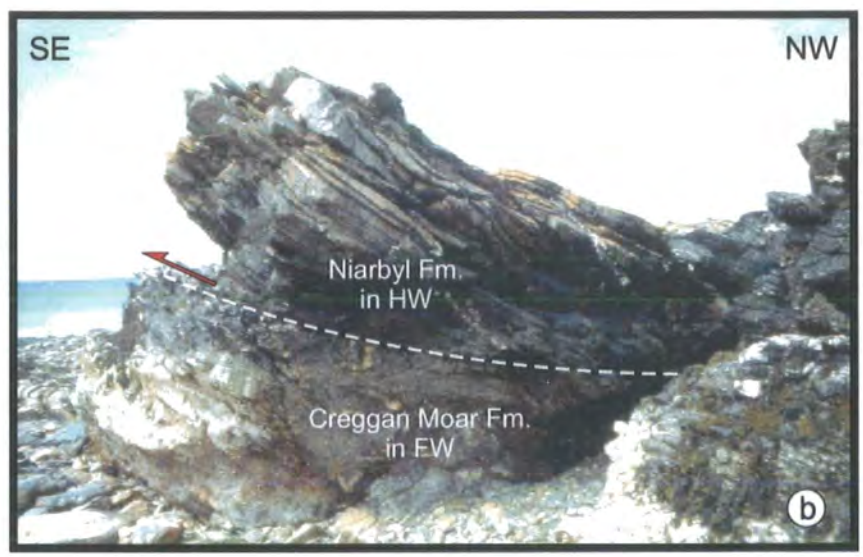

Plate 5.35. **(a)** Top-to-the-SE directed thrusts associated with the Niarbyl Thrust, with small (<0.5m) offsets in steeply inclined bedding (highlighted). Creag Mooar (Fig. 5.35, grid ref. 21117821). Pen for scale. **(b)** The Niarbyl Thrust on the Niarbyl (Fig. 5.29, grid ref. 21067756). The thrust emplaces relatively undeformed rocks of the Niarbyl Fm. on top of highly sheared and deformed rocks of the Creggan Moar Fm. Height of outcrop is about 2.5m.

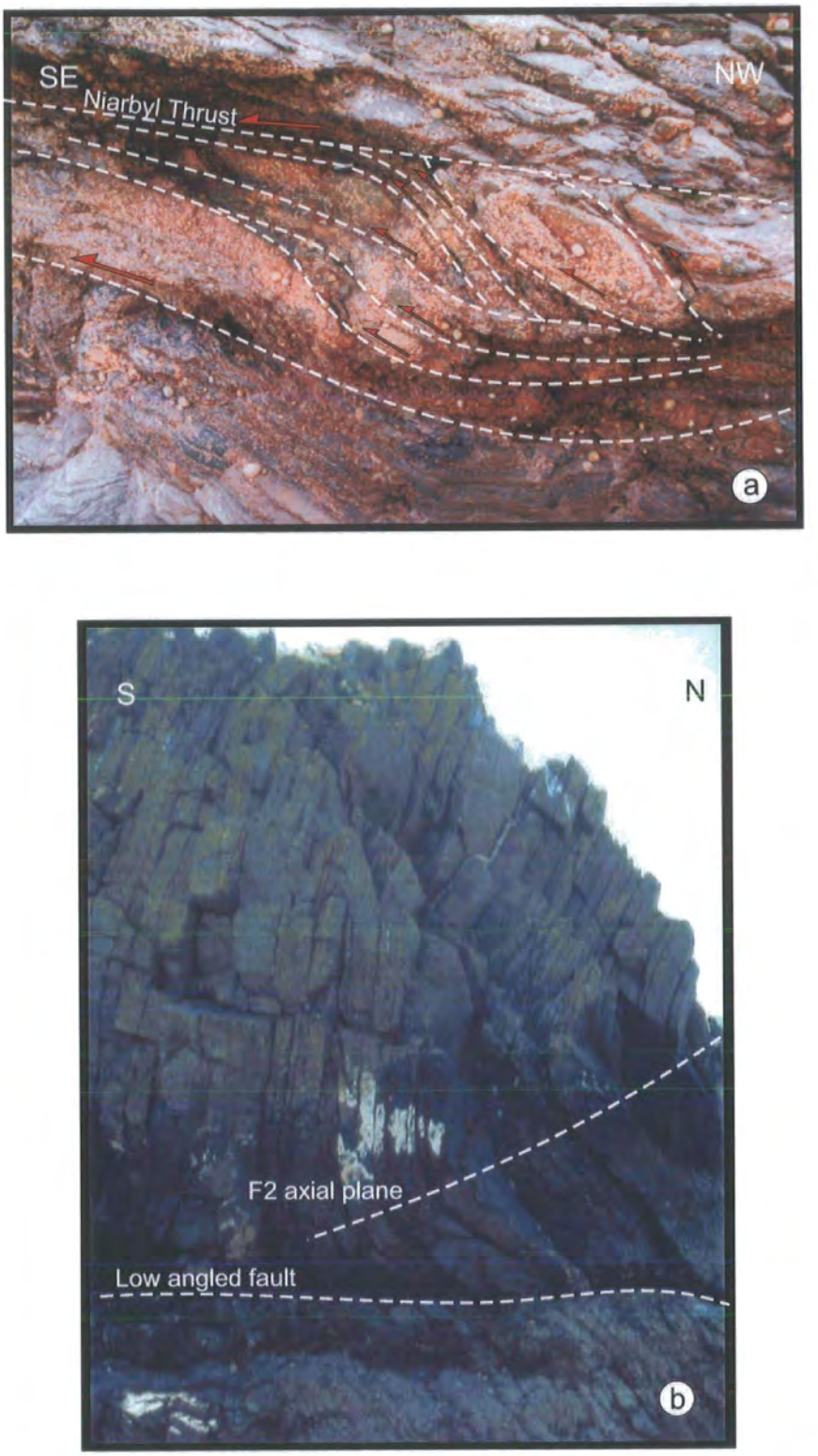

Plate 5.36. (a) Thrust duplex in the footwall of the Niarbyl Thrust. The Niarbyl (Fig. 5.29, grid ref. 21067756). **(b)** Low angled top-to-the NW fault associated with F2 folds (Fig. 5.29, grid ref. 21127805).

fault places Silurian rocks on top of Ordovician rocks, i.e. younger on top of older, the presence of a small thrust duplex at the base of the thrust at The Niarbyl (Fig. 5.29, Plate 5.36(a)) and the top-to-the SE offsets in other similarly orientated faults just to the NW, (Plate. 5.34(b)) suggests a thrust geometry and kinematics. This view is supported by Fitches *et al.* (1999), Morris *et al.* (1999) and Quirk *et al.* (1999). An additional set of faults trend NNW to NNE, have shallowly inclined fault planes and show small (a few cm) top-to-the-W or -NW extensional displacements (Plate 5.12(a)). These appear to be closely associated with secondary folds and may be broadly contemporaneous (Plate 5.36(b)).

5.7 High strain zones

Several zones of relatively intense ductile deformation have been identified within the Lower Palaeozoic rocks of the Isle of Man (Morrison 1989; Quirk & Kimbell 1997; Fitches *et al.* 1999; Morris *et al.* 1999; Quirk *et al.* 1999a). Three of the best examples of these high strain zones are described below.

5.7.1 Lag ny Keeilley High Strain Zone

The Lag ny Keeilley High Strain Zone (Fitches *et al.* 1999) is a NE-SW-trending zone of high strain exposed within the quartz sandstones and mudstones of the Injebreck Formation (Woodcock *et al.* 1999b; Chadwick *et al.* 2001) along the foreshore below the old hermits chapel at Lag ny Keeilley (Figs. 5.2, 5.9, 5.10, grid ref. 216747). Exposures of structures within the high strain zone are limited to a series of small wave-cut outcrops at the base of the steep weathered cliffs leading down to the foreshore (Fig. 5.36, Plate 5.26(b)). A cover of thick, Quaternary drift deposits precludes mapping the high strain zone inland.

While the most intensely deformed rocks occur within a 5m wide belt of mudstones in the uppermost northern part of the shear zone (Fig. 5.36), related structures are evident for approximately 100m to the north and south (Plates. 5.27(a), 5.37(a)). Within the thick-bedded quartz arenites in the southernmost part of the shear zone deformation is less intense, although a few intraformational lenses of conglomerate are locally strongly deformed (Plate 5.37(b)).

A series of E-W-trending quartz veins (Fig. 5.37(i)) preserve evidence of shear deformation, including asymmetric boudins and folding that are consistent with a

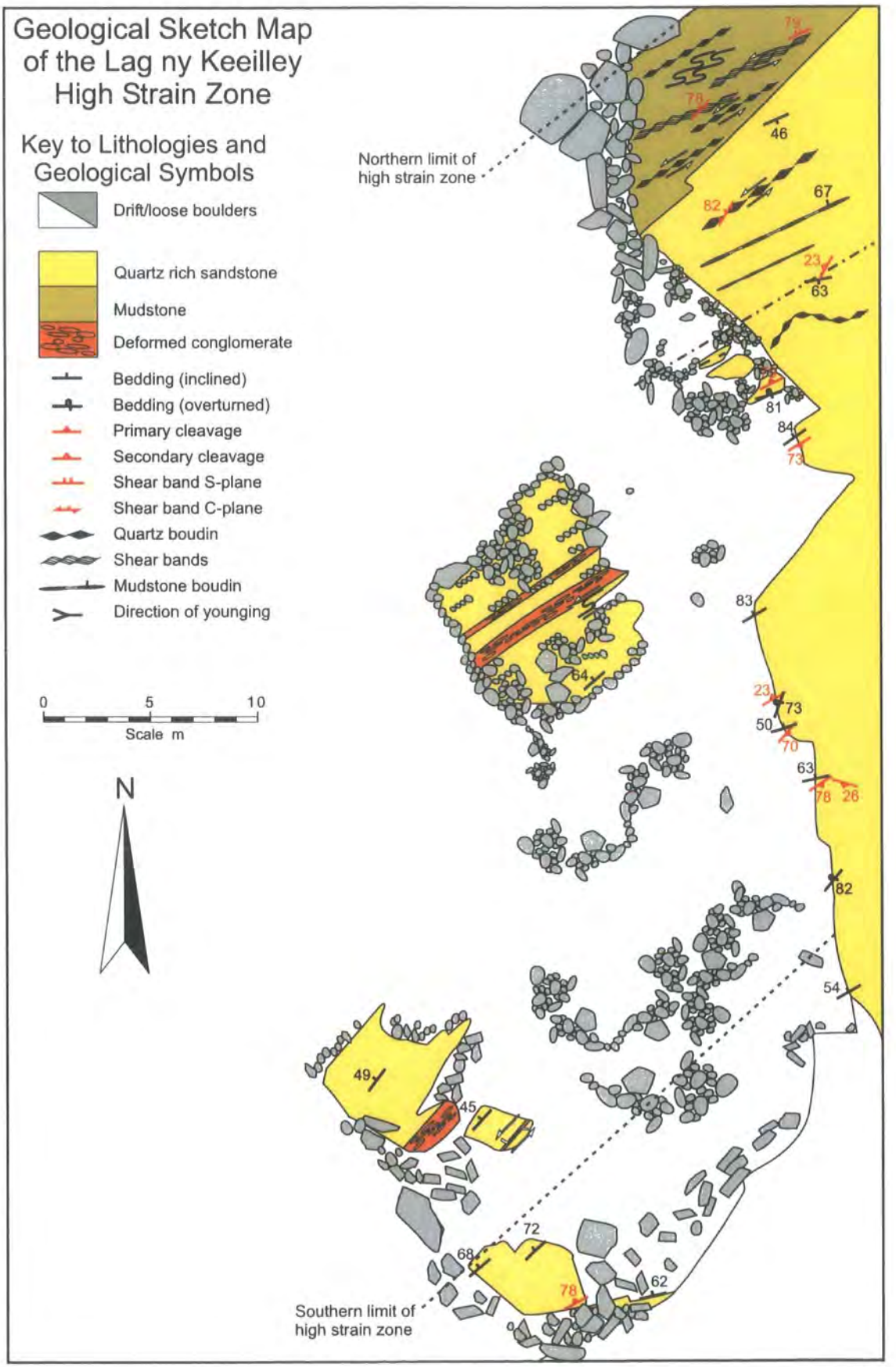

Figure 5.36. Geological sketch map of the Lag ny Keeilley High Strain Zone, showing the main structural elements.

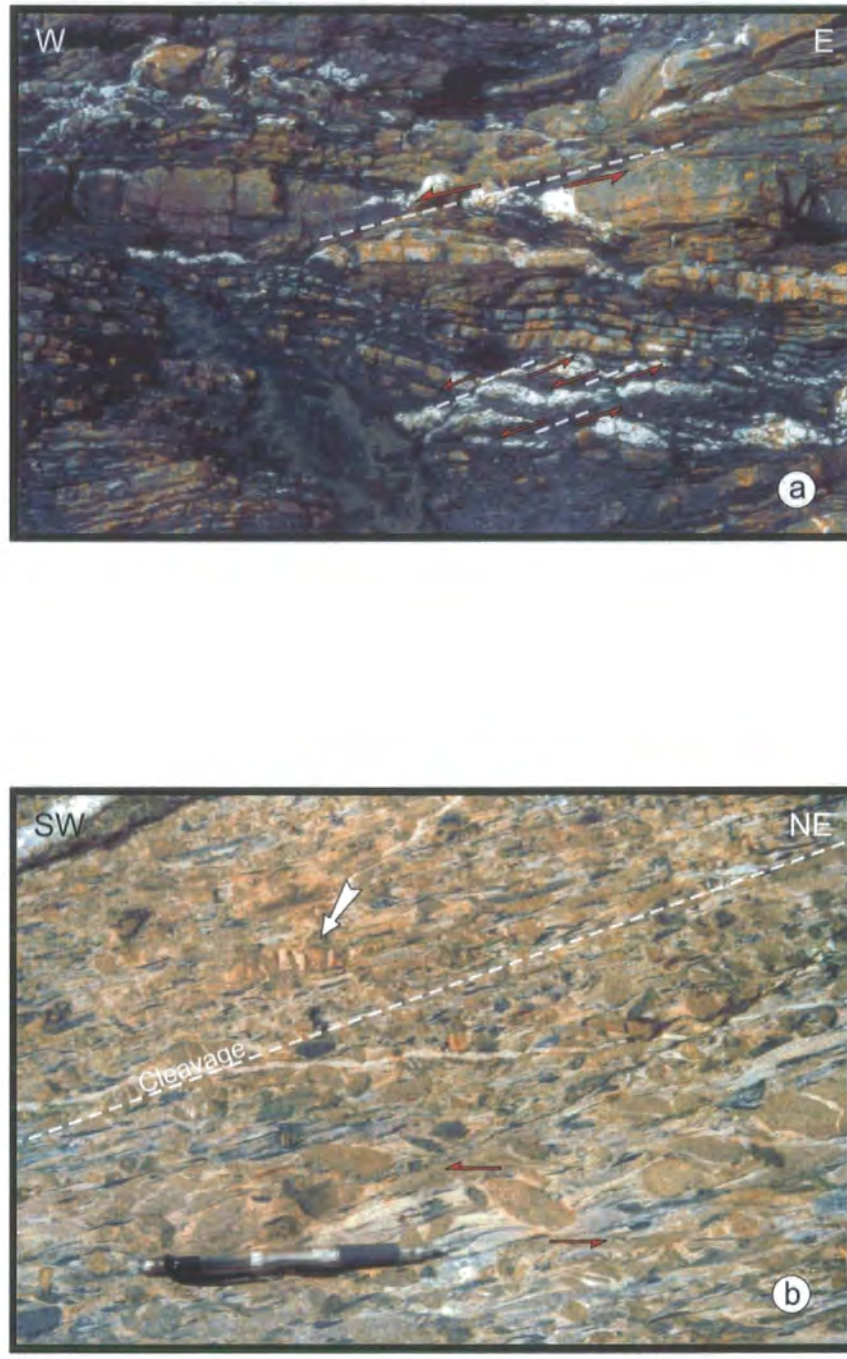

Plate 5.37. **(a)** Sinistral, asymmetric boudin within sandstone unit of the Injebreck formation. Extensive quartz veining within interbedded siltstones and mudstone are also boudinaged and exhibit a sinistral sense of shear. On the foreshore below the chapel at Lag ny Keeilley (Fig. 5.2, grid ref. 21577459). Thick sandstone unit is about 0.5m thick. **(b)** Deformed pebble conglomerate. The pebbles are flattened within the plane of the primary cleavage (highlighted). Individual pebbles show evidence of sinistral shear, e.g. near to pen, and boudinage, with quartz filled necks (arrowed). Lag ny Keeilley foreshore (Figs. 5.2, 5.36, grid ref. 21617464).

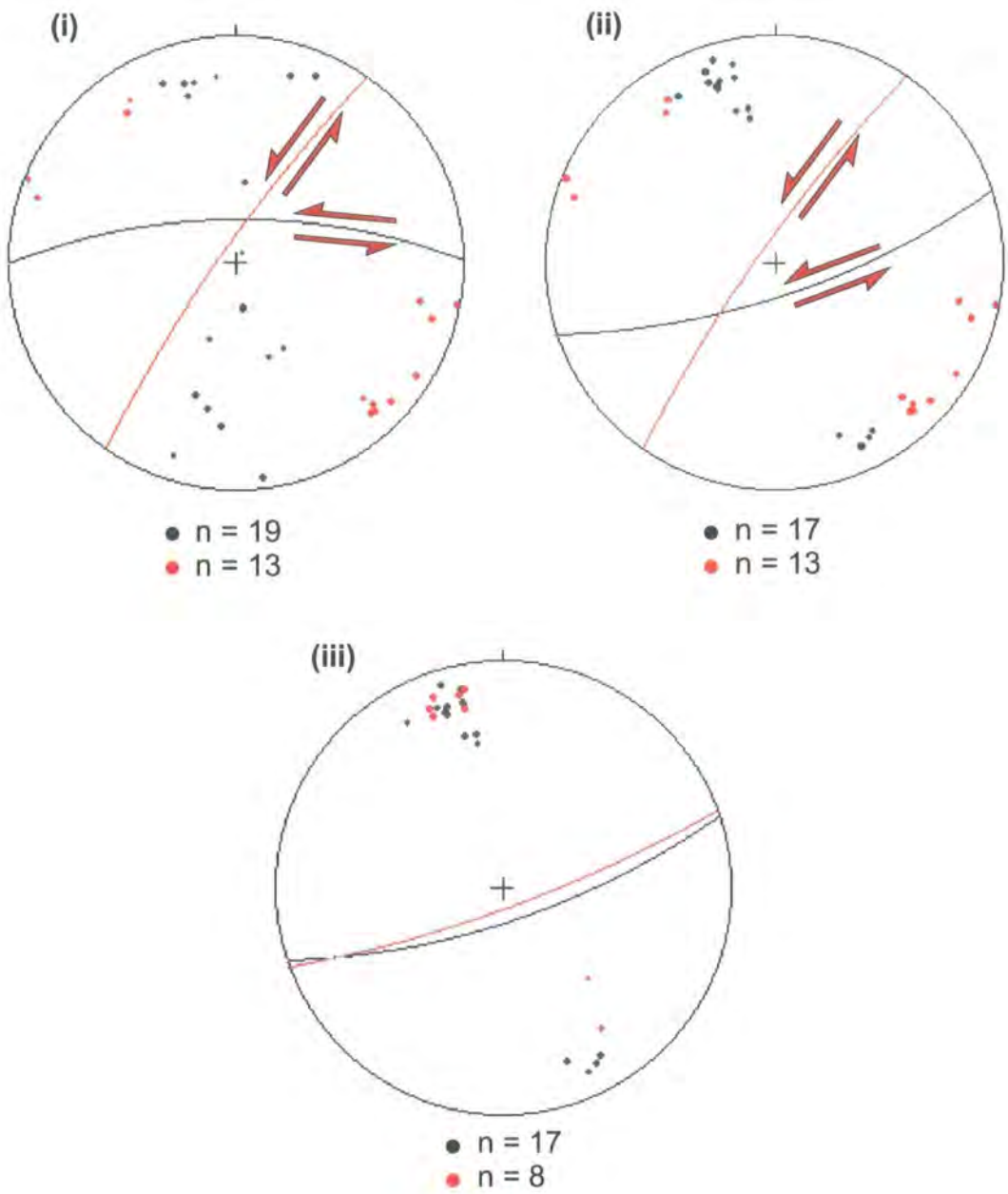

Figure 5.37. Stereoplots of structural data from the Lag ny Keeilley High Strain Zone. **(i)** Poles to quartz veins (black) and R-type shears (red) associated with asymmetric quartz boudins, with mean quartz vein (black,090/75N) and R-type shear (red, 035/84N) shown. **(ii)** Poles to S-Planes (black) and C-Planes (red), with mean S-Plane (Black, 072 /78S) and C-Plane (red, 035/84N) shown. **(iii)** Poles to primary cleavage (black) and flattened clasts (red), with mean cleavage (black, 072/78S) and mean clast (red, 070/83S) shown.

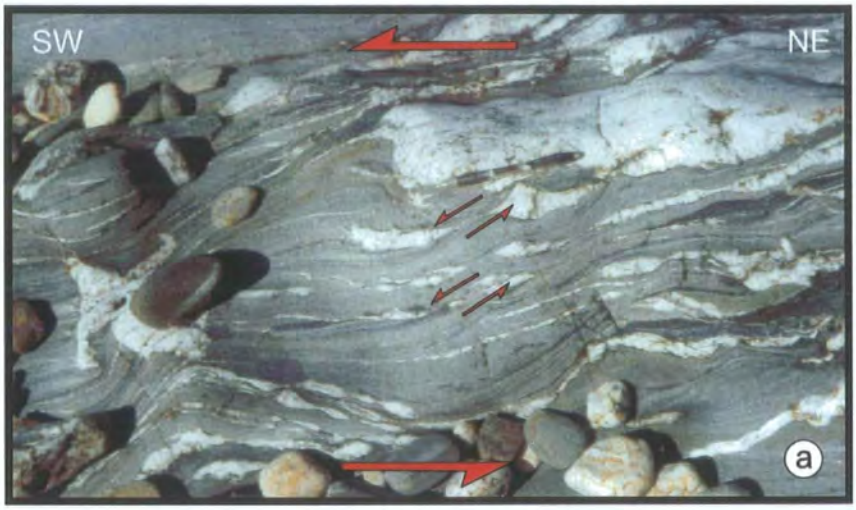

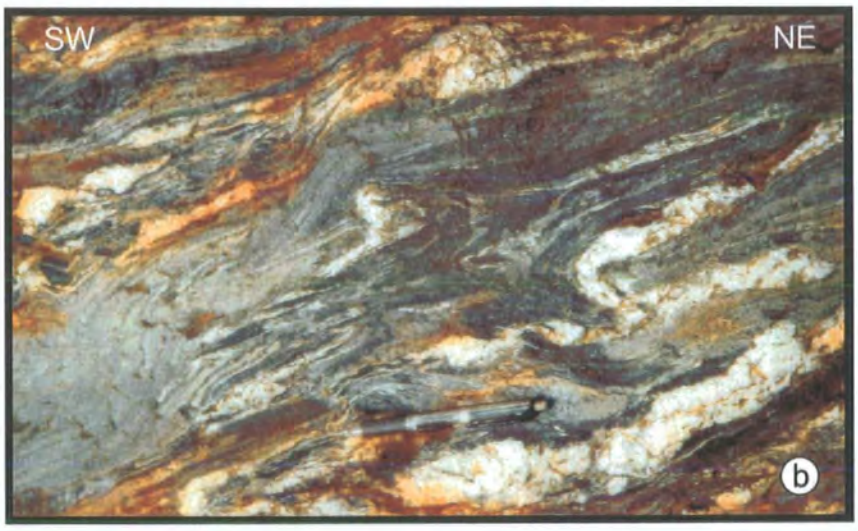

Plate 5.38. **(a)** Asymmetric quartz boudins with a sinistral sense of shear, some of which are folded. The folds also have a sinistral sense of shear. Lag ny Keeilley foreshore (Figs. 5.2, 5.36, grid ref. 21627467). **(b)** Sinistrally verging folded quartz veins on the foreshore at Lag ny Keeilley (Figs. 5.2, 5.36, grid ref. 21627467). The extensive iron staining is due to iron pyrites within the sandstones hosting the veins. Note both photographs are looking down onto sub-horizontal surfaces.

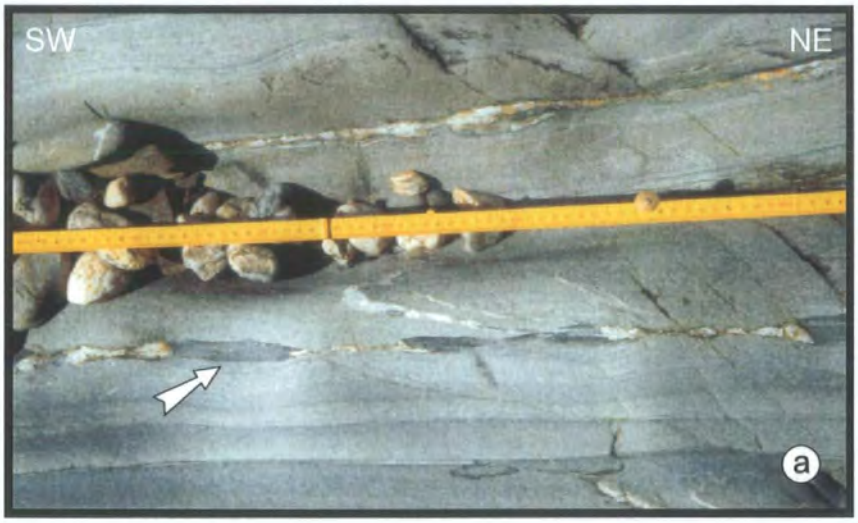

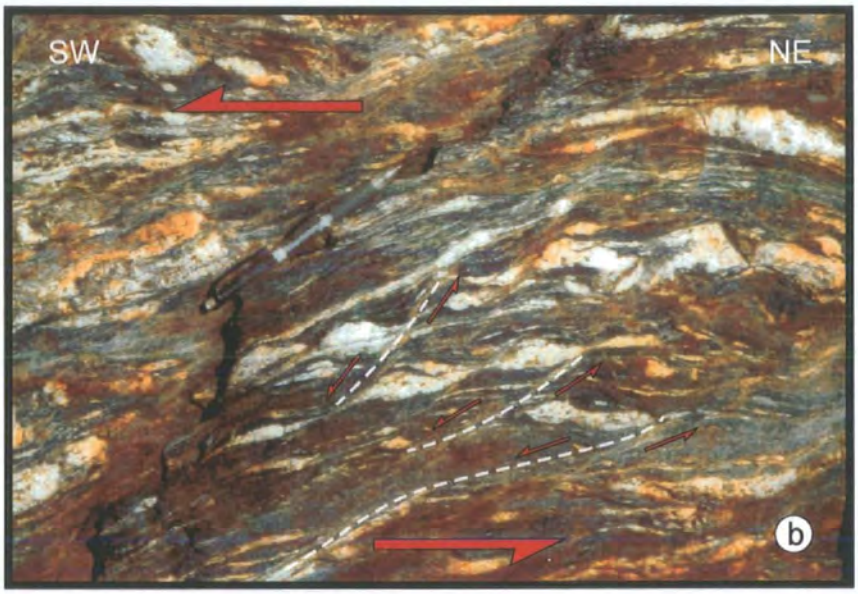

Plate 5.39. **(a)** 'Inverse' boudins of thin mudstone layer within sandstone unit. See text for possible explanation. Lag ny Keeilley (Figs. 5.2, 5.36, grid ref. 21677467). **(b)** Sinistral shear bands and asymmetric boudins within a mudstone unit of the Injebreck Formation. note extensive iron staining from iron pyrites within the mudstone. Lag ny Keeilley (Figs. 5.2, 5.36, grid ref. 21677467). Both photographs are looking down onto sub-horizontal surfaces.

sinistral sense of shear (Plate 5.38(a), (b)). These are particularly extensive within the mudstones in the upper part of the shear zone, possibly indicating that this acted as a conduit for fluid flow during deformation. Within the quartz arenites, sporadic thin mudstone layers have been stretched about vertical boudin axes (Plate 5.39(a)) producing a set of rather unusual, less competent boudins within a more competent matrix. The reason for this is unclear, although Fitches *et al.* (1999) suggest that the mudstone boudins may now occupy spaces left when early brittle boudins in the adjacent rocks underwent ductile necking as they deformed into inverse boudins. Poles to shear band fabrics (Fig. 5.37(ii)) show two sets of well-defined point maxima corresponding to a steep, ENE-trending, southerly-dipping mean S-plane (primary cleavage) and a steep NE-trending, northerly-dipping mean C-plane. The angular relationship between these two planes is consistent with a sinistral sense of shear and is confirmed by field observations (Plate 5.39(b)). Clasts within the deformed conglomerates are flattened within the plane of the primary cleavage (Fig. 5.37(iii)), with clasts preserving both sinistral and dextral asymmetric boudins with quartz filled necks, often with examples of each occurring adjacent to one another (Plate 5.40(a), (b)). Dextral kinematic indicators are sub-ordinate within the deformed conglomerates, and the presence of abundant sinistral asymmetric boudins, shear bands and the vergence of syn-shear folds indicate that the overall sense of shear is predominantly sinistral (Fig. 5.38).

The structures described above are, based on the available field evidence all thought to have developed contemporaneously during shearing, and formedat the same time as, or very shortly after the primary phase of deformation (i.e. D1 of Simpson (1963) and Fitches *et al.* (1999)).

The geological interpretation and significance of the Lag ny Keeilley Shear Zone remains uncertain, although three models have been proposed (Fitches *et al.* 1999; Chadwick *et al.* 2001).

1. A major strike-slip shear zone of regional significance (Fitches *et al.* 1999).
2. A localised belt of strain partitioning during the primary phase of deformation, between rheologically different rock packages without regional significance (Fitches *et al.* 1999).
3. A localised zone of high strain associated with top-to-the SE thrust faulting.

The third of these interpretations (Chadwick *et al.* 2001) appears unlikely as the orientation of the fabric and the kinematic indicators preserved at Lag ny Keeilley

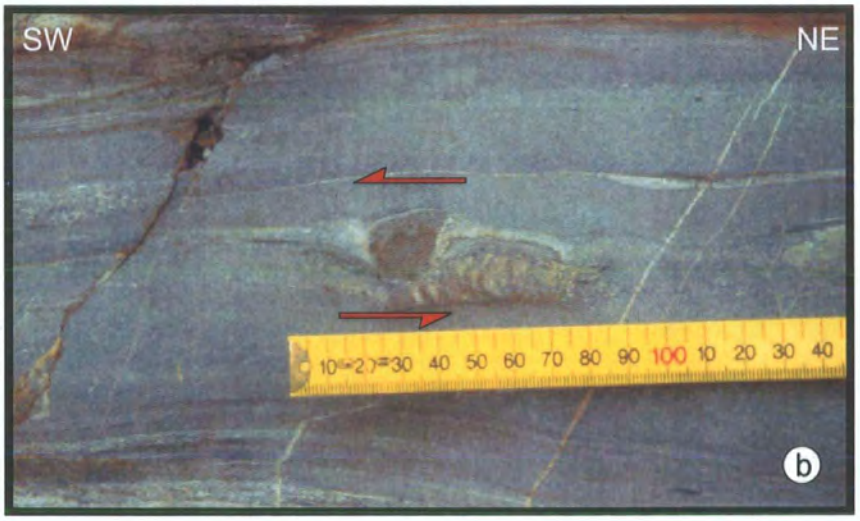

Plate 5.40. **(a)** Pebble in deformed conglomerates with asymmetric quartz-necked boudins. These show a dextral sense of shear. **(b)** δ porphyroclast within deformed conglomerate, shows sinistral sense of shear. Both photographs from Lag ny Keeilley (Figs. 5.2, 5.36, grid ref. 21637466)

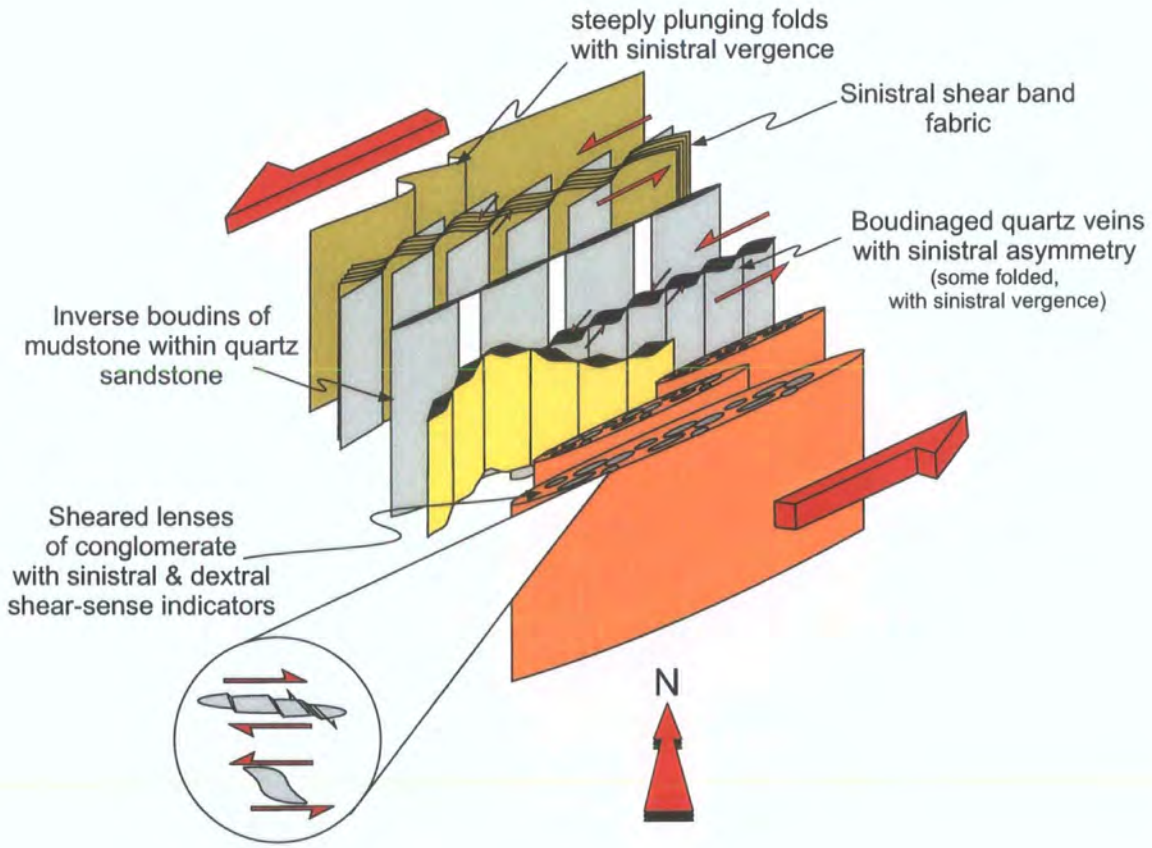

Figure 5.38. 3-D schematic panel diagram illustrating the kinematics and geometry of the Lag ny Keeilley Shear Zone.

support a steeply inclined sinistral, strike-slip sense of movement rather than a top-to the-SE sense. The shear zone lies at the junction between two thick sequences in which younging is opposed, where there is a marked competence contrast; it is also the location for Simpson's (1963) Isle of Man Syncline (see section 5.6.4, Fig. 5.4). These observations led Fitches *et al.* (1999) to suggest that the shear zone at least records localised deformation within a major F1 fold. Fitches *et al.* (1999) provide no rationale for their alternative interpretation that the Lag ny Keeilley High Strain Zone may be of regional significance. However, they suggest that because the shear zone lies within a tract rather than as a tract bounding structure its regional significance is in doubt. The view proposed here supports the interpretation of Fitches *et al.* (1999) that the Lag ny Keeilley High Strain Zone most probably represents a zone of strain partitioning that occurred during the primary phase of deformation. However, the similarity in its orientation (NE-SW) to both the tracts described by Fitches *et al.* (1999) and Woodcock *et al.* (1999b) and to several other major Palaeozoic structures in and around the Irish Sea (e.g. Wexford Boundary Lineament, Wicklow Fault Zone, Menai Straits Fault Zone, (Gardiner (1975); Max *et al.* (1990); Gibbons *et al.* (1994)) suggests a regional control on its orientation.

5.7.2 Lynague Shear Zone

The presence of zones of high strain within Tract 7 was noted by Quirk *et al* (1999) and Woodcock (pers. com.). Quirk *et al.* (1999) briefly describe a NW-trending shear zone exhibiting a planar phyllonitic fabric with dextral sense of shear, outcropping at the southern end of Lynague Strand (Fig. 5.32, grid ref. 281871). The present study has identified several, NW-trending, narrow ductile shear zones at the southern end of Lynague Strand and beneath the igneous sheet exposed to the S of Gob y Deigan (Figs. 5.2, 5.32, grid ref. 280870). Accurate mapping of the geometry and full extent of the high strain zones has proved problematic, due to a combination of poor exposure, (most of which is only exposed at low tide) and extensive marine growth (Plate 5.41(a)). Therefore, a structural log drawn through a section of one of the high strain zones (Fig 5.39(a), see Fig. 5.32 for location) and structural data for all the high strain zones mapped (Fig. 5.39(b)), have been used to illustrate the general geometry, kinematics and orientation of structures within the high strain zones.

The rocks along this section of coast have been assigned to the Lady Port Formation (Chadwick *et al.* 2001; Woodcock *et al.* 1999b; Woodcock & Morris 1999),

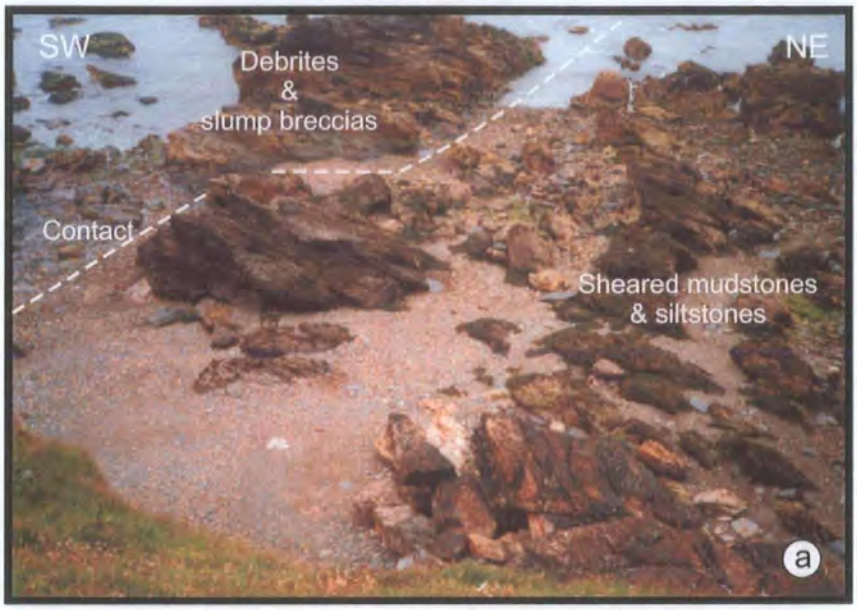

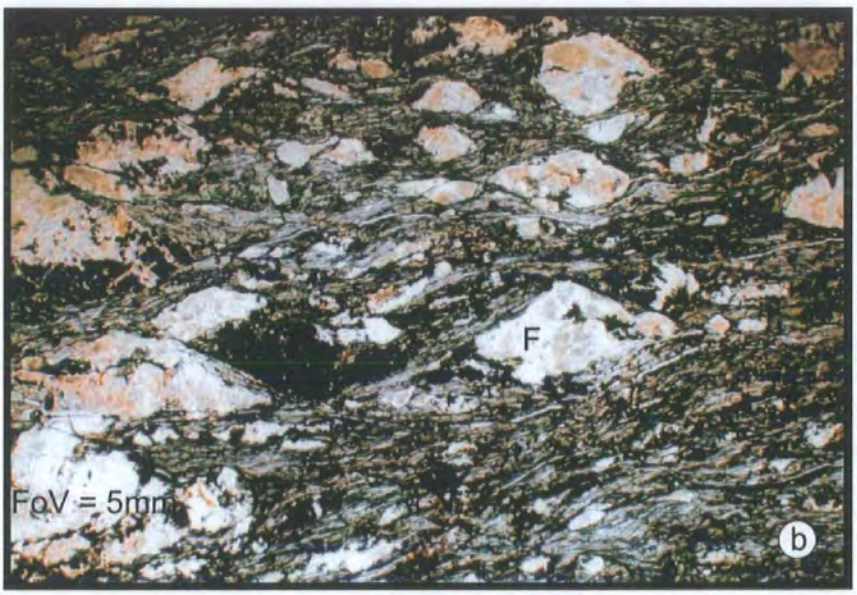

Plate 5.41. **(a)** View of part of the foreshore at Lynague (Fig. 5.32, grid ref. 280875). Tectonically relatively undeformed debrites and slump breccias of the Lady Port Fm. are overlain along a low angled NE-dipping detachment by sheared mudstones and siltstones. These appear to occur as narrow NW-trending high strain zones. **(b)** Chlorite-rich phyllonite from one of the high strain zones exposed along the Lynague coast. Note interconnected weak layer of chlorite and white mica surrounding σ porphyroclasts of re-crystallized and altered feldspar (F). shear bands in the micaceous layers and porphyroclasts define a sinistral sense of shear. (Sample LYN12a, taken in PPL, grid ref. 28048705).

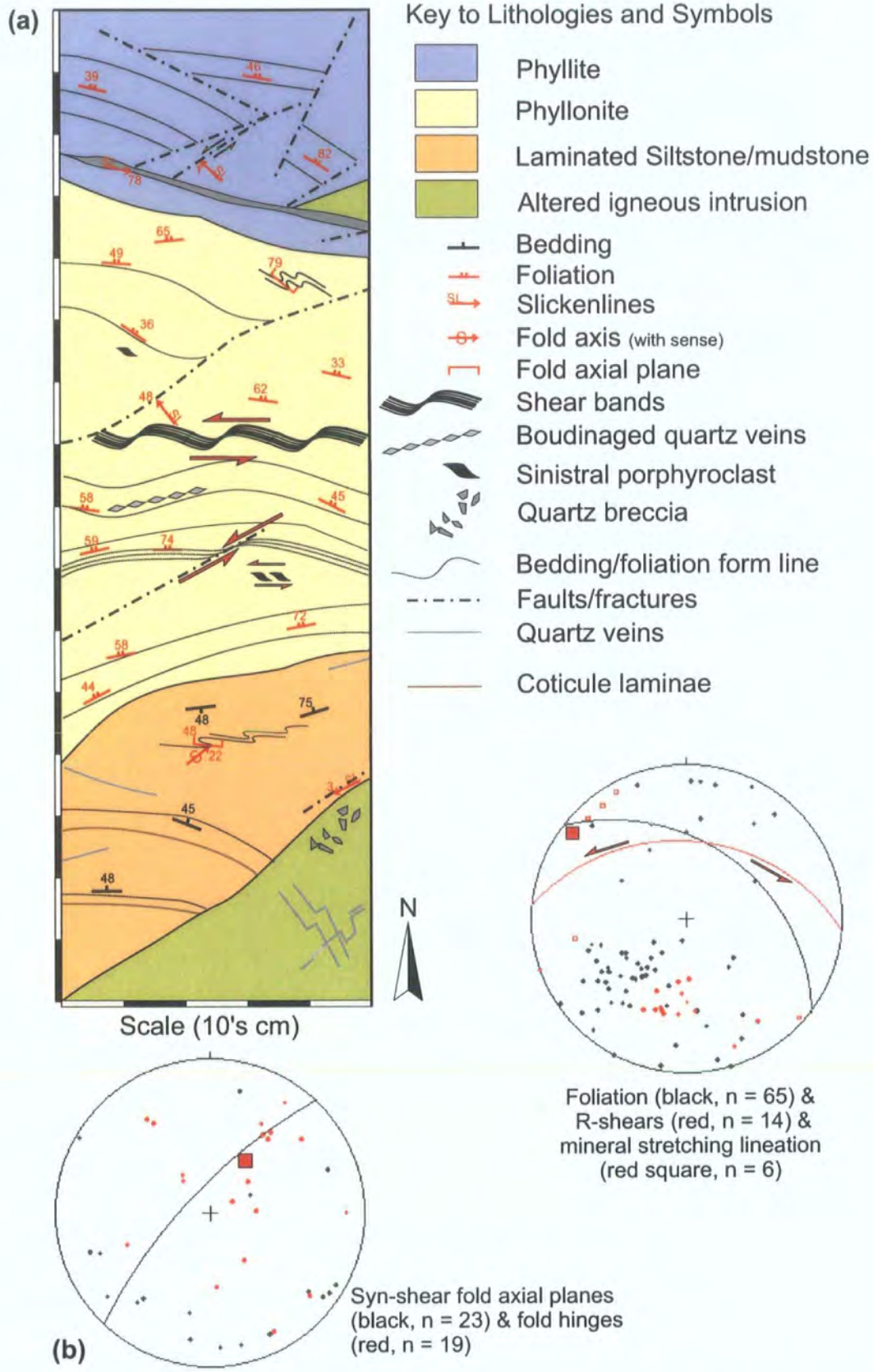

Figure 5.39. **(a)** Structural log through part of the Lynague Shear Zone. (see Fig. 5.32 for location). **(b)** Stereoplots of structural orientation data from Lynague Shear Zone. Mean foliation (black, 127/50N), R-shear (red, 095/48N) and mineral stretching lineation (red square, 9/307) shown. Mean syn-shear fold axial plane (black, 043/78N) and mean fold hinge (red square, 57/035) shown.

and consist of laminated siltstones (Plate 5.29(b)) and mudstones which have been intruded by a series of igneous sheets (Plate 5.31(a)).

The deformation within the ductile shear zones cross-cuts and overprints the main phase of regional deformation, but pre-dates the secondary phase of regional deformation both of which have been discussed previously (see 5.2, 5.3). The siltstones, mudstones and igneous sheets within the shear zones have been metamorphosed, and are now largely low greenschist facies phyllonites, (Plate 5.41(b)) although in areas of lower strain sedimentary structures are preserved (Plate 5.42(a)).

Poles to foliation planes (Fig. 5.39(b)(i)) show a broad point maximum corresponding to a moderately NE-dipping mean plane. A subordinate number of poles to foliation planes are spread along a NNE-trending, steeply WNW-dipping great circle girdle (Fig. 5.39(b)(i)) suggesting that the foliation is folded about a steeply plunging axis. This is confirmed by field observations, but some of the observed variation may also be due to fault bounded blocks rotating within the shear zones (Plate 5.42(b), see section 5.6.6, Fig. 5.34). Poles to extensional shear band fabrics (Fig. 5.39(b)(ii)) show two, well-defined point maxima corresponding to the foliation (S-planes) and C-planes. Mineral stretching lineations on foliation and C-plane surfaces are predominantly sub-horizontal with a very shallowly NW-plunging mean (Fig. 5.39(b)(ii)). This is consistent with a largely strike-slip sense of movement. The angular relationship between the two mean planes is consistent with a sinistral sense of shear and is confirmed by field observations (Plates 5.41(b), 5.43(a). Poles to syn-shear fold axial planes exhibit a rather scattered distribution (Fig. 5.39(b)(iii)) with a steeply NW-dipping mean axial plane. This is almost at right angles to the mean foliation (Fig. 5.39(b)(i)). The precise reason for the difference between the mean foliation and syn-shear fold axial planes is unclear. The poor exposure within the shear zone precludes a more detailed analysis. However, as discussed previously there is evidence of block rotations both within Tract 7 and the high strain zones (e.g. Plate 5.42(b)). This possibly suggests a domainal structure. The folds appear to be restricted to lower strain areas within the shear zone, and may therefore be part of a series of lower strain domains bounded by narrow zones of high strain, with minor block rotations causing the mismatch between the main foliation and syn-shear fold axial planes.

Evidence for sinistral shear is preserved on a macro- and microscopic scale (e.g. Plates 5.41(b), 5.42(a), 5.43(a), 5.43(b)). Both contractional and extensional structures appear to have developed contemporaneously during shearing. Contractional structures

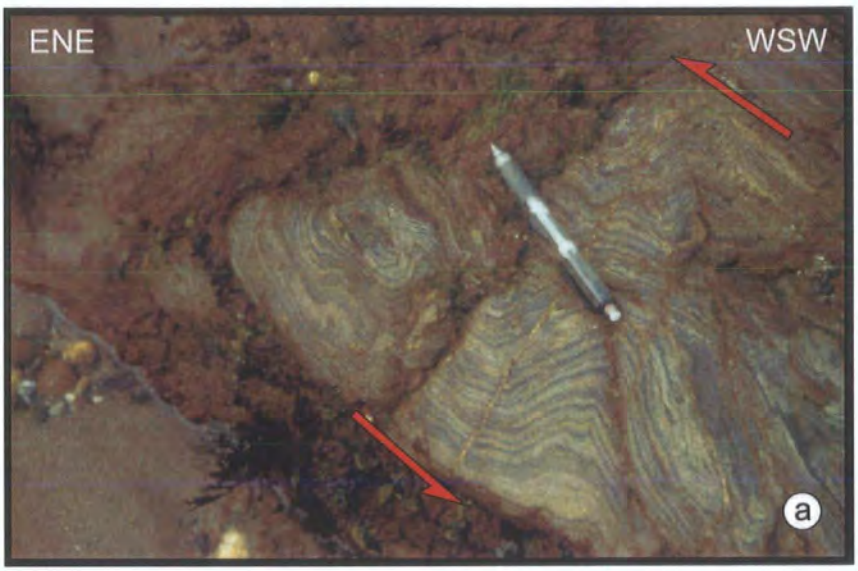

Plate 5.42. **(a)** Steeply plunging folds with sinistral vergence within laminated siltstones of the Lady Port Fm. at Lynague (Fig. 5.32, grid ref. 28138714). **(b)** Foliation within high strain zones (dotted lines) shows possible drag folds adjacent to thin detachment (dashed line). The geometry of the folds suggests a dextral sense of displacement along the detachment. No other kinematic indicators were observed. Lynague foreshore (Fig. 5.32, grid ref. 28038709).

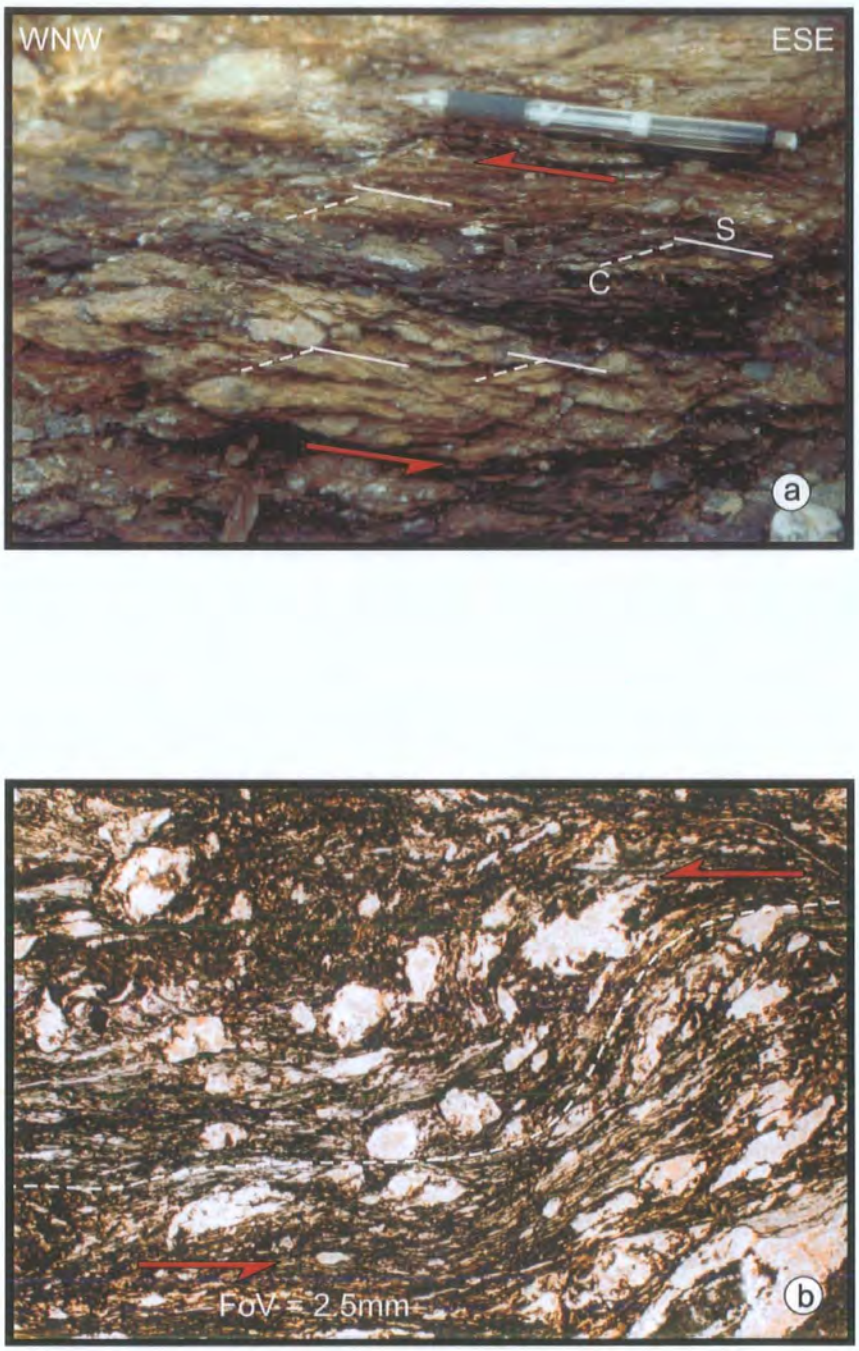

Plate 5.43. **(a)** Sinistral C/S fabric/shear bands within phyllonite. The geometric relationship between the foliation (S-planes, white solid lines) and C-planes (white dashed lines) implies a sinistral sense of shear. Lynague foreshore (Fig. 5.32, grid ref. 28 138706). **(b)** Thin section photomicrograph of chlorite-rich phyllonite, shows that the phyllonitic fabric is deformed by folds with a sinistral sense of vergence. From part of the outcrop shown in (a) above. (Sample LYN 8 taken in PPL).

are more prevalent within the slightly lower strain areas comprising the siltstones (e.g. Plate 5.42(a)), whilst within the higher strain zones comprising the phyllonites, extensional structures are more common (e.g. Plates 5.41(b), 5.43(a)).

5.7.3 Niarbyl High Strain Zone

Several authors (e.g. Lamplugh (1903), Simpson (1963), Morrison (1989), Roberts *et al.* (1990), Fitches *et al.* (1999)) have studied the Niarbyl High Strain Zone, and whilst the consensus of opinion is that it represents a zone of ductile, predominantly sinistral shear, there remains a great deal of debate and uncertainty as to the significance and exact nature of the shear zone, its extent and even the protolith in which it is developed.

Located in Niarbyl Bay (Figs. 5.2, 5.10, 5.29, Plate 5.44 grid ref. 210775) the Niarbyl High Strain Zone (Fitches *et al.* 1999) is exposed across strike for approximately 150m on the wave-cut platform (Fig. 5.29). To the N and W the shear zone is truncated by a low angled fault (Niarbyl Thrust) (Fig. 5.29, Plate 5.44). The intensity of the shear deformation decreases southwards towards Knockuskey Cottage, where the sedimentary rocks of the Creggan Moar Formation no longer show evidence of shear deformation (Plate 5.7(a)). Fitches *et al.* (1999) report, however, that several narrow zones of disrupted and transposed bedding are exposed for several hundred metres in the Creggan Moar Formation further to the S. Inland the high strain zone is covered by thick drift deposits (Fig. 5.29, Plate 5.44).

The shear zone affects a varied suite of rocks including the siltstone, mudstones and manganiferous ironstones of the Creggan Moar Formation and heavily altered igneous sheets. However, to what extent the Silurian rocks of the Niarbyl Formation are involved in the ductile deformation has been the topic of much debate. Fitches *et al.* (1999) suggest that the high strain zone is entirely restricted to the Creggan Moar Formation and intrusive sheets. However, Morris *et al.* (1999) suggest that rocks of the Niarbyl Formation make up the greater part of the shear zone exposed at Niarbyl. Although resolution of this debate will probably only be achieved using geochemical analysis, there is some field evidence supporting the suggestion that at least a small part of the shear zone involves rocks of the Niarbyl Formation. Adjacent to the narrow channel separating The Niarbyl from the rest of the bay (Fig. 5.29, grid ref. 21097763, Plate 5.45(a)) rocks of the Niarbyl Formation immediately above the Niarbyl Thrust appear to show evidence of sinistral shear (Plate 5.45(b)).

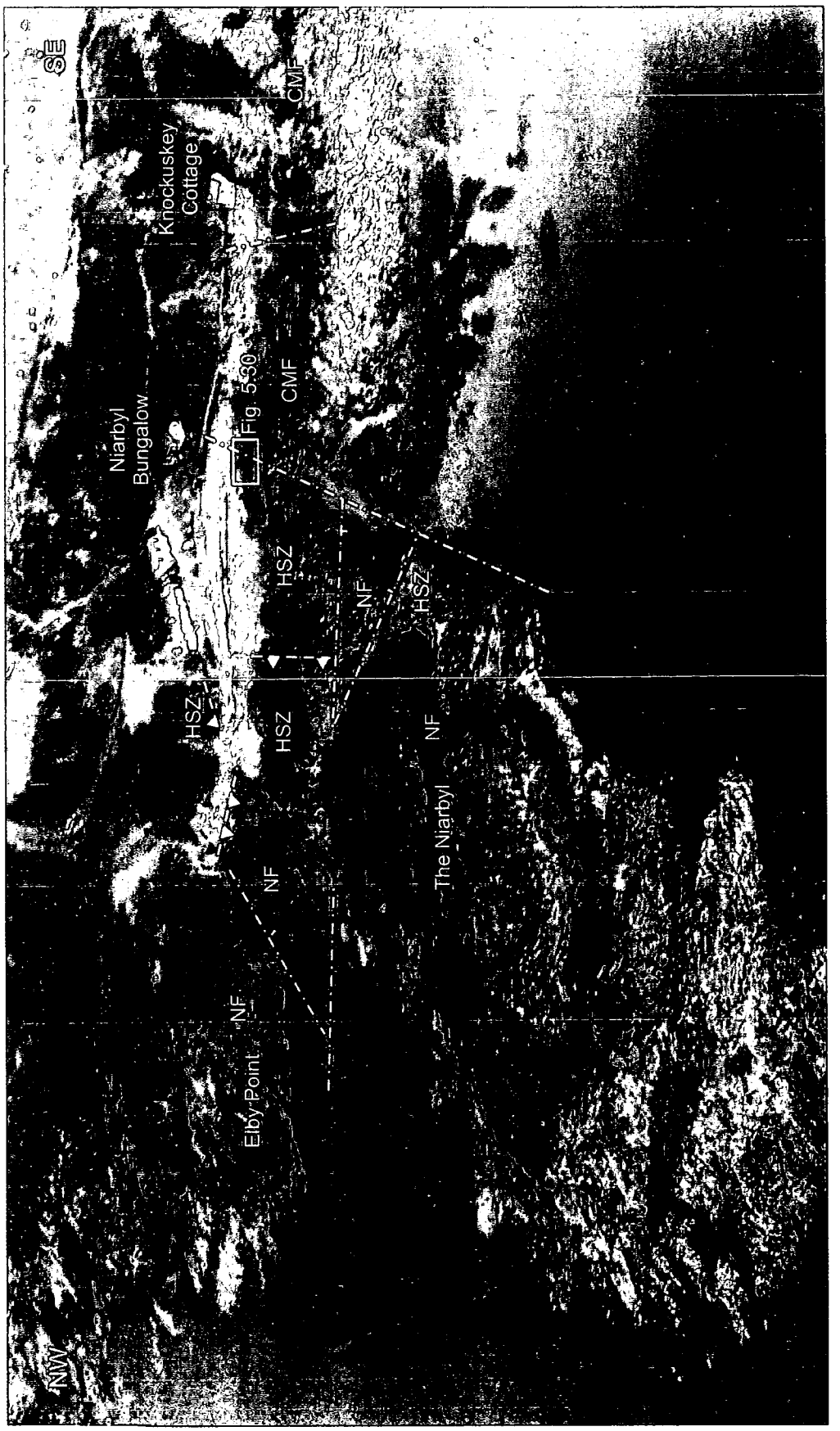

Plate 5.44. Aerial view of Niarbyl Bay (see Figs. 5.29, 5.30), with main faults marked. The Niarbyl Thrust is in red. NF-Niarbyl Fm., CMF- Creggan Moar Fm., HSZ- High strain zone

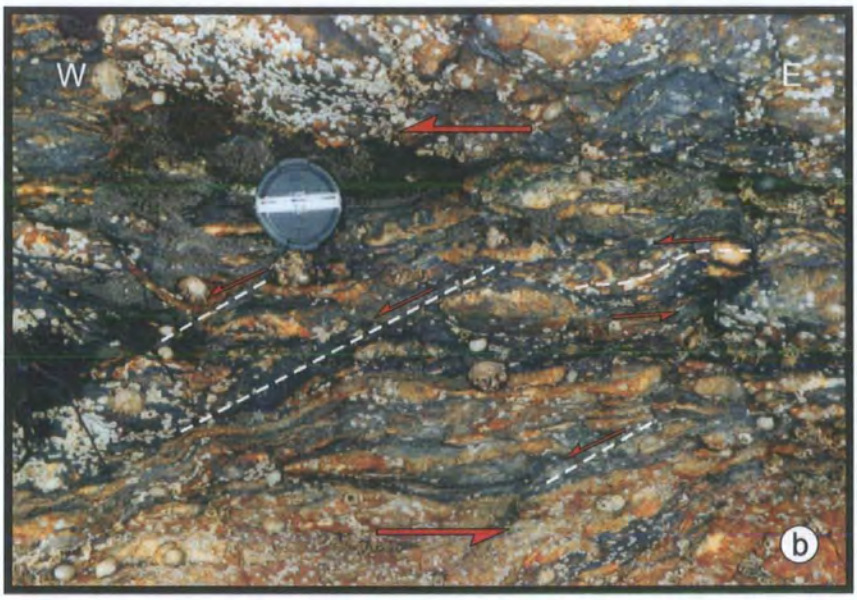

Plate 5.45. (a) The narrow inlet between The Niarbyl and Niarbyl Bay showing Niarbyl Fm. rocks in the foreground that have been deformed by sinistral shear. (Fig. 5.28, grid ref. 21097763). The outcrop in the background is approximately 2m high. **(b)** Sinistral bands and folded quartz segregation vein (highlighted) within the Niarbyl Fm.(Fig. 5.28, grid ref. 21097763). The lens cap is 55mm across.

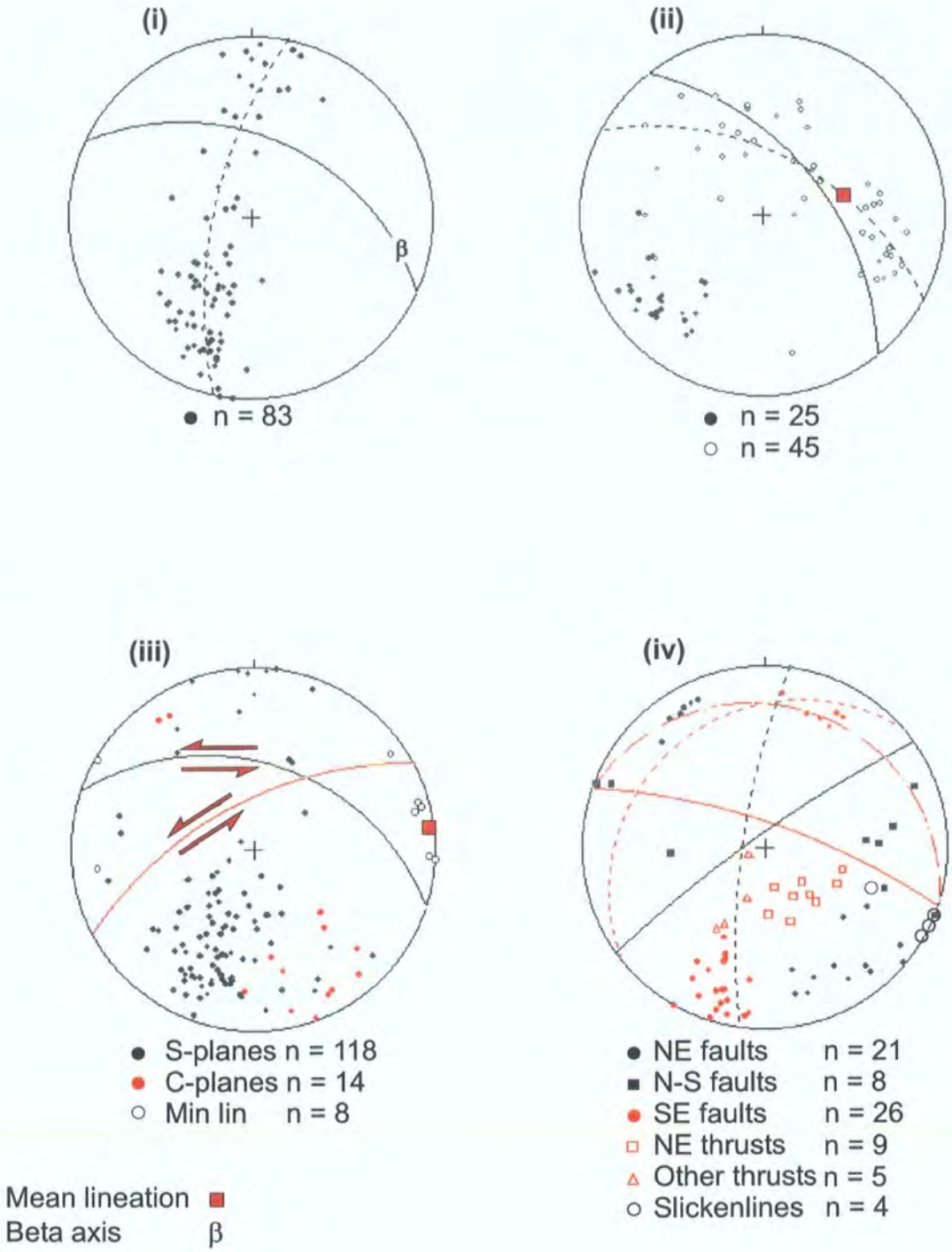

Figure 5.40. Stereoplots of structural data from the Niarbyl High Strain Zone **(i)** Poles to bedding, with best fit great circle girdle (dashed, 012/53N), mean bedding (solid, 115/73N) and regional β axis (17/102) shown. **(ii)** Poles to syn-shear fold axial planes and fold hinges, with mean fold axial plane (solid, 141/62N), mean fold plunge (52/076) and best fit girdle (dashed, 118/62N) shown. **(iii)** Poles to foliation (S-planes), C-planes and mineral stretching lineations, with mean foliation (black line, 109/51N), C-plane (red line, 062/69N) and mean lineation (3/083) shown. **(iv)** Poles to fault planes, with separate fault sets and associated mean planes shown. NE-trending (black dots, black line, 055/84N), N-trending (black squares, black dashed line, 008/80W), SE-trending, (red dots, red line, 109/79N), NE-trending thrusts (red open squares, red dashed line, 051/27N), other thrusts, (red triangles, long dashed line, 108/23N).

The Primary phase of deformation within the shear zone has a similar orientation to that outside the zone margins (c.f. Figs. 5.31a(i) & 5.40(i)). This is overprinted by ductile shearing, which is in turn overprinted by the secondary phase of regional deformation, both of which have been discussed previously (see section 5.2). During the process of ductile shearing many of the siltstone and mudstone rocks within the shear zone were converted to phyllonite.

In the southern part of the Niarbyl High Strain Zone (Figs. 5.29, 5.30, grid ref. 21187760, Plate 5.44), where shear deformation is less intense, much of the bedding is still visible, but has been tightly folded into a series of cm-scale, often steeply plunging, S-verging folds (Plate 5.46(a)). Poles to syn-shear fold axial planes (Fig. 5.40(ii)) show a well-defined point maximum corresponding to a steeply NE-dipping mean axial plane. Fold hinges are mostly moderately to steeply plunging (Fig. 5.40(ii)), exhibiting up to 110° of curvilinearity in the fold axial plane, with a moderately ENE-plunging mean fold plunge. Thin sections of the folded bedding (Plate 5.46(b)) show that the primary cleavage is deformed by the syn-shear folds forming a crenulation cleavage within the mudstone laminae. Also situated in the southern, lower intensity region of the Niarbyl High Strain Zone, are several narrow (<1m) zones, often focussed along the margins of the igneous intrusions, where bedding has been sheared into sigmoidal lenses by C-planes with a predominantly sinistral sense (Fig. 5.29, grid ref. 21207757, Plate 5.47(a)). The orientation of the S- and C-planes (Fig. 5.40 (iii)) within these areas is consistent with sinistral shear and is similar to that of shear-band fabrics observed in the higher strain parts of the shear zone (see below).

Moving northwards, disruption of bedding becomes more intense, C-planes are more common and quartz and carbonate veins are segregated to form augen, some of which have sinistral geometries (Plates 5.47(b), 5.48(a)). The most intensely sheared part of the high strain zone extends in a broad band (ca. 40m wide) from the Niarbyl Thrust to just S of the slipway (Fig. 5.29, Plate 5.44). Within this zone of intense shear, the fabric is strongly phyllonitic, with numerous sinistral porphyroclasts, extensional shear band fabrics, tightly folded quartz veins and mica fish (Plates 5.48(b), 5.49(a), (b), 5.50(a)). Poles to extensional shear band fabrics (Fig. 5.40(iii)) show two broad point maxima corresponding to a moderate, ENE-trending, N-dipping mean S-plane (foliation) and a moderate to steep, NE-trending, NW-dipping mean C-plane. The angular relationship between the two mean planes is consistent with a sinistral sense of shear and is confirmed by field observations (Plates 5.47(a), (b), 5.48(b)). Quartz

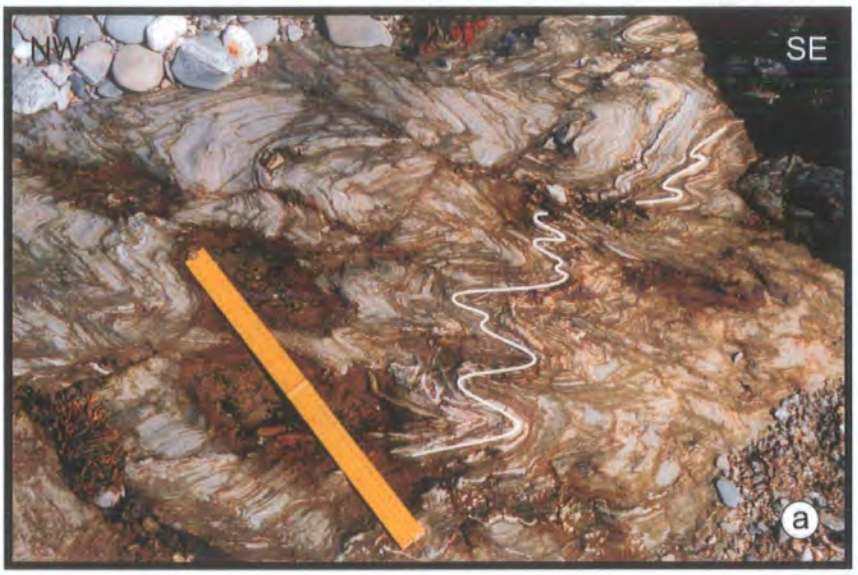

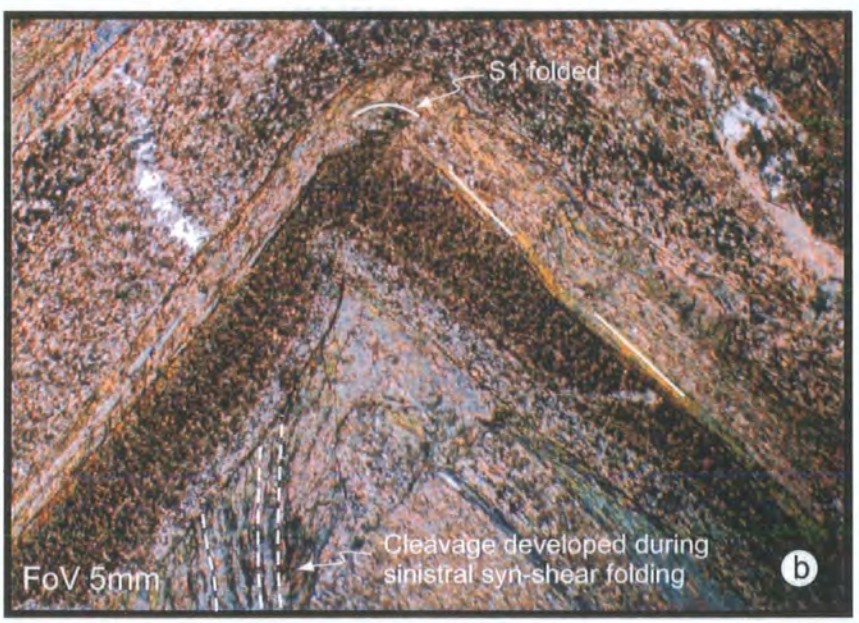

Plate 5.46. **(a)** Tight, steeply plunging folds developed during sinistral shearing. Niarbyl (Figs. 5.29, 5.30, grid ref. 21197761). Ruler is 0.5m **(b)** Thin section photomicrograph of folded siltstone of the Creggan Moar Fm. The primary cleavage (S1) defined by aligned micas is deformed by syn-shear folds. An axial planar cleavage has developed within these folds (highlighted). NB this is not equivalent to the secondary cleavage seen elsewhere on the Isle of Man (see sections 5.2 & 5.3) (sample N 15, grid ref. 21247755, taken in XPL).

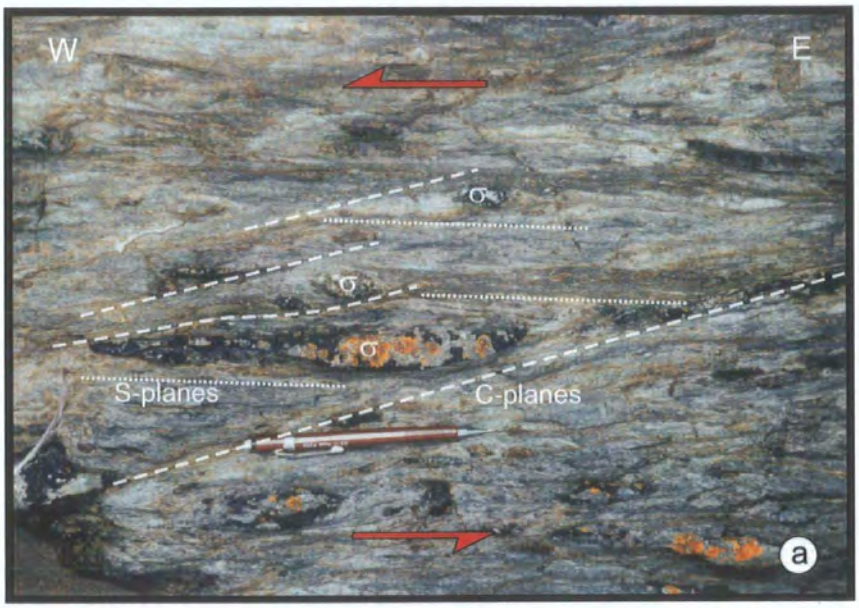

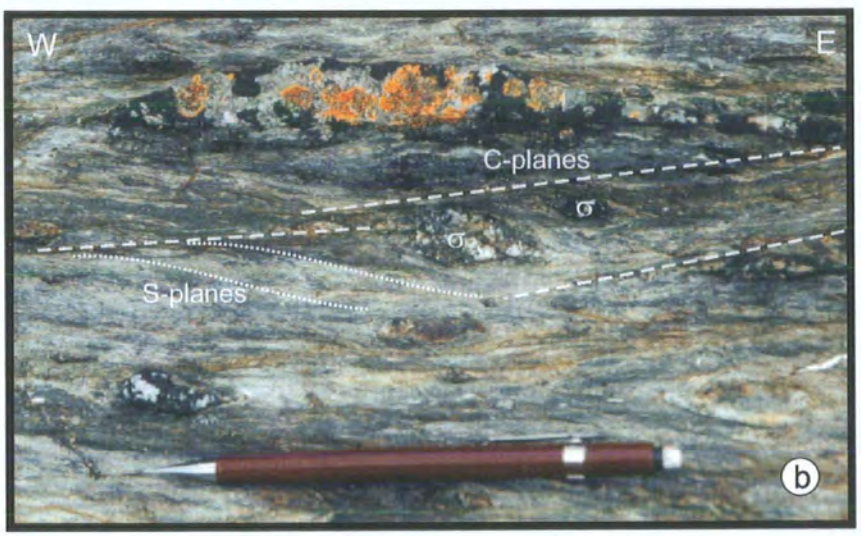

Plate 5.47. **(a)** and **(b)** Sinistral C-planes and σ porphyroclasts within the phyllonite of the Niarbyl High Strain Zone. Niarbyl (Fig. 5.29, grid ref. 21167764).

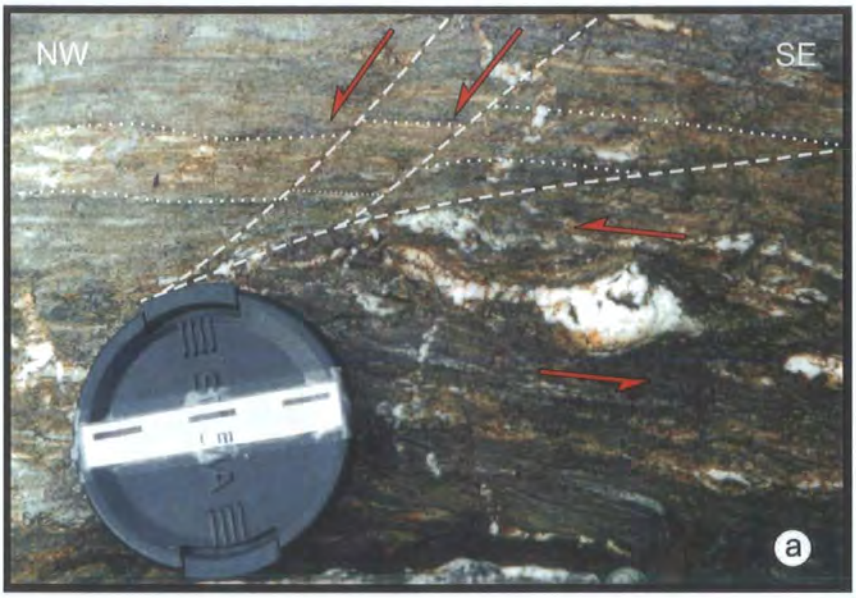

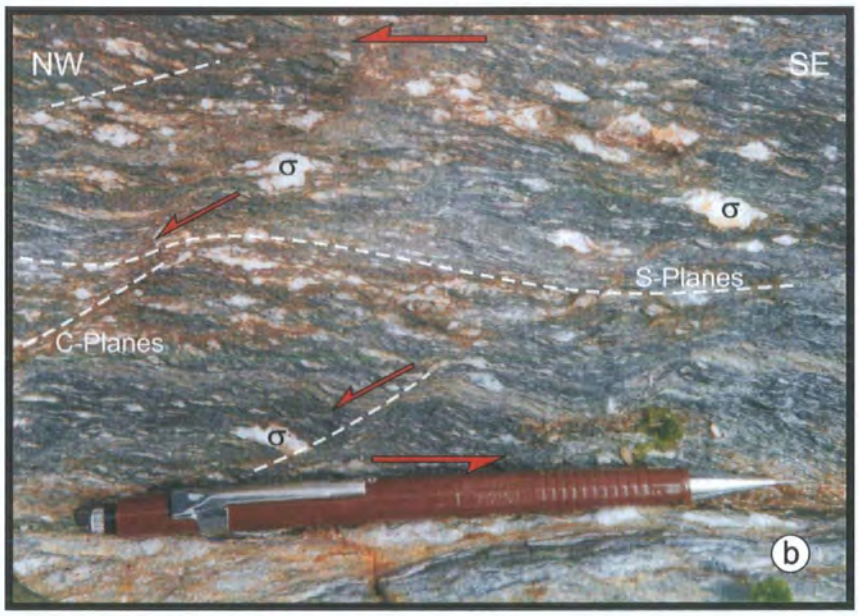

Plate 5.48. Photographs showing effects of increasing strain,moving N from Knockuskey Cottage (Fig. 5.29, Plate 5.44). Bedding (highlighted with white dotted lines) becomes more difficult to see and carbonate and quartz porphyroclasts begin to develop. The bedding is cut by small sinistral faults (Fig. 5.29, grid ref. 21217757). In the main high strain area, bedding is completely replaced by a well-developed phyllonitic foliation (S-planes) with sinistral porphyroclasts (σ) and shear bands (C-planes) (Fig. 5.29, grid ref. 21167764).

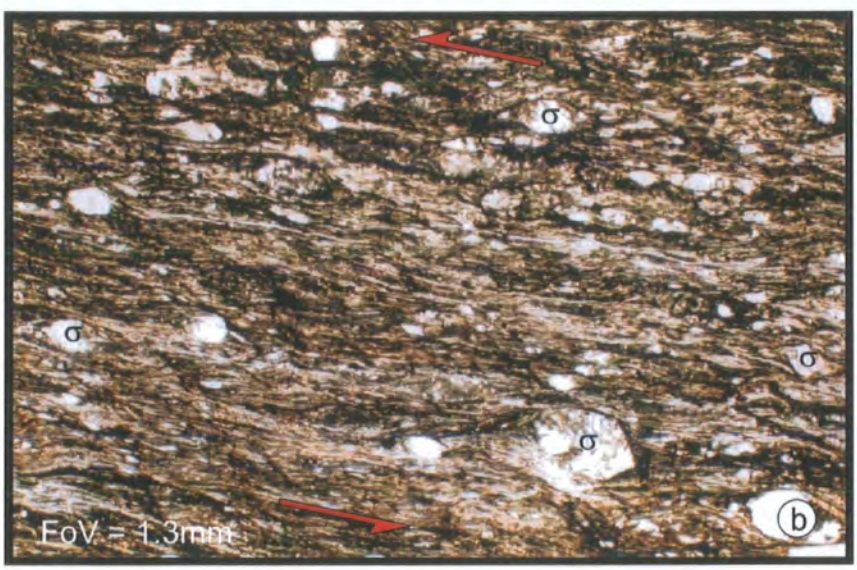

Plate 5.49. **(a)** Tightly folded quartz segregation veins (highlighted in black) with a sinistral sense of vergence. These are cut by a series of low angled detachments (highlighted in red) (Fig. 5.29, grid ref. 21147763). Lens cap is 55mm across. **(b)** Thin section photomicrograph of phyllonite with numerous quartz and carbonate σ porphyroclasts (some labelled). These all show a strong sinistral sense of shear. Sample N3, grid ref. 21157765).

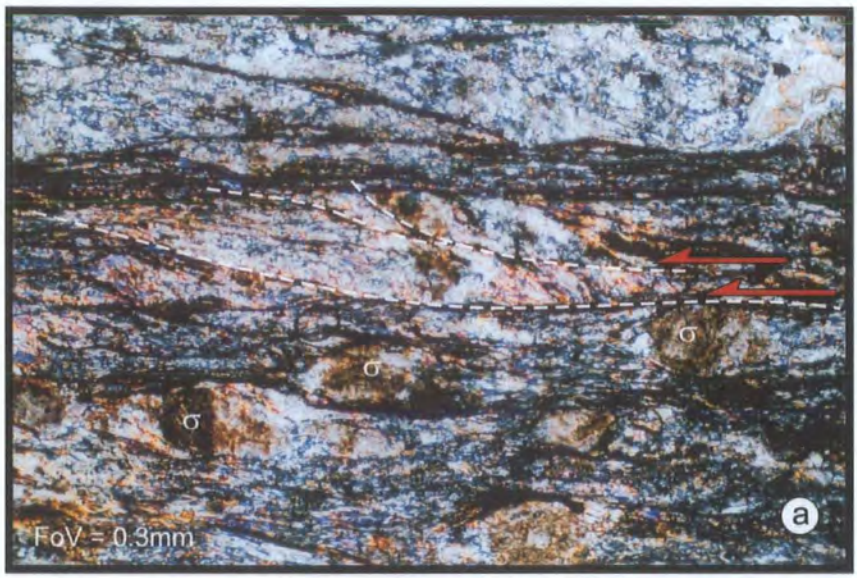

Plate 5.50. **(a)** Mica fish, composed of muscovite show a sinistral sense of shear. Also highlighted are a number of sinistral σ porphyroclasts of feldspar altered to sericite. (Sample N2, grid ref. 21157765, taken in XPL. **(b)** Large dextral porphyroclast, view down onto surface. (Fig. 5.29, grid ref. 21167765).

mineral stretching lineations on S- and C-planes are sub-horizontal and indicate a strike-slip sense of movement. Although the great majority (ca.80%) of kinematic indicators suggest a sinistral sense of shear, there are some dextral indicators (e.g. Plate 5.50(b)). The shear zone is dissected by numerous brittle faults that can be grouped into several differently orientated sets (Fig. 5.40(iv)).

1. NE-trending, steeply-inclined, strike-slip faults (Figs. 5.29, 5.30, Plate 5.29(a), (b)). The mean fault plane defined by the poles to these faults (Fig. 5.29(iv)) closely matches the mean C-plane (Fig. 5.40(iii)) and may be utilising a pre-existing weakness along the C-planes. They generally show small (few cm) sinistral offsets (Plate 5.51(a).
2. N-S-trending, moderate- to steeply-inclined, W and E-dipping faults (Fig. 5.29). These have dip-slip normal displacements (Plate 5.51(b)), and locally cross-cut the Niarbyl Thrust (e.g. Fig. 5.29, grid ref. 21137766).
3. SE-trending, steeply inclined, predominantly sinistral strike-slip faults (Figs. 5.29, 5.40(iv)). Slickenlines on fault surface indicate strike-slip kinematics, whilst displacements are predominantly sinistral and generally < 10cm.
4. NE-trending, top-to-the-SE thrusts, probably related to movement on the Niarbyl Thrust (Figs. 5.29, 5.31c(vii), 5.40(iv), grid ref. 21137763). These cut across the phyllonitic fabric, and also appear to cut across secondary folds within the high strain zone (Plate 5.52(a)). This implies that the thrusts post-date the secondary phase of deformation.
5. SE to SSE-trending low angled faults (Figs. 5.29, 5.40(iv) Plate 5.52(b)). These are well exposed in the cliff N of the slipway (grid ref. 21167767) and appear to have thrust geometries. However, slickenlines on one of the faults suggests a strike-slip sense of movement.

Neither the phyllonites of the Niarbyl High Strain Zone nor the Niarbyl Thrust can be traced inland from Niarbyl Bay, so their positions inland are open to interpretation. There is some suggestion that it may swing NE, re-emerging in Glen Maye Gorge, (Fitches *et al.* 1999; Morris *et al.* 1999, Figs. 5.2, 5.41) approximately 4km NE of Niarbyl. The rocks within the Gorge have been assigned to the Creggan Moar Formation (Fitches *et al.* 1999). However, they have a strong phyllitic fabric rather than the phyllonitic fabric observed at Niarbyl. Exposed for approximately 750m across strike the phyllites are heavily vegetated with very few fresh surfaces and, as the Glen is a Site of Special Scientific Interest (SSSI) collection of hand specimens and

Plate 5.51. **(a)** Thin section photomicrograph shows a number of shear band C-plane structures (highlighted). These have a similar geometry and orientation to the sinistral faults shown in Plate 5.29(a) that cross-cut the phyllonitic foliation and may provide a focus for these faults. (Sample N1a, grid ref.21157765, taken in PPL). **(b)** N-S-trending fault in the Niarbyl Fm. The bedding is folded by fault drag, indicating a dip-slip sense of displacement. Niarbyl Bay. (Fig. 5.29, grid ref. 21137767).

Plate 5.52. **(a)** Top-to-the SE thrusts (highlighted) cut across the phyllonitic fabric in the Niarbyl High Strain Zone. (Fig. 5.29, grid ref. 21137763) **(b)** SE to SSE-trending, low angled faults, also cut across the pyhllonitic fabric. Although these have the appearance of a thrust duplex, some detachment surfaces contain sub-horizontal slickenlines suggesting strike-slip faulting (Fig. 5.29, grid ref. 21167765).

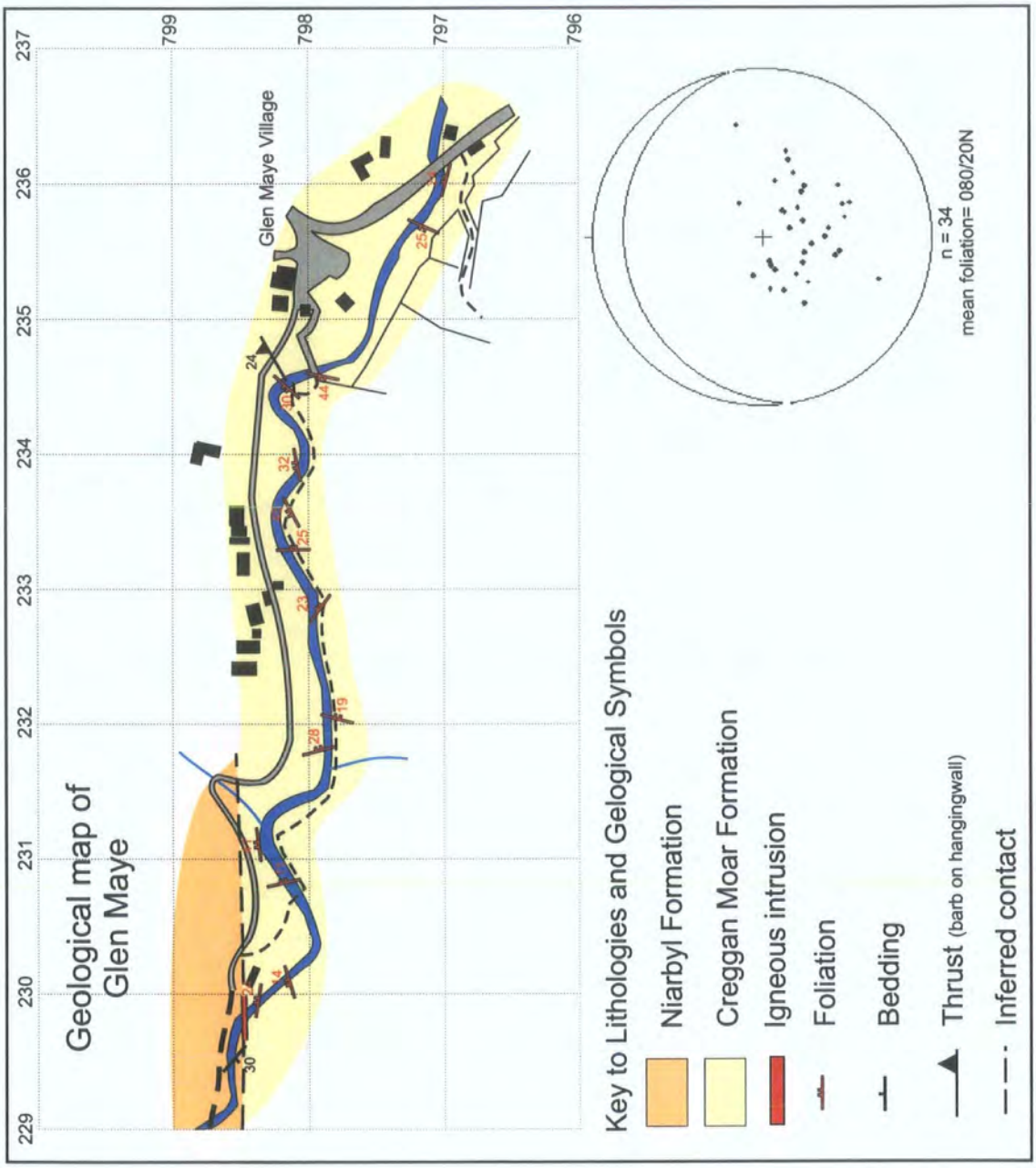

Figure 5.41. Simplified geological map of Glen Maye Gorge and stereoplot of poles to foliation. See Figure 5.10 for location.

hammering are not permitted. Despite these difficulties, it is possible to identify an ENE-trending, gently NNW-dipping phyllitic fabric (Fig. 5.41) exposed in the steep cliffs forming Glen Maye Gorge. Although the predominantly across strike exposure of the phyllites within the gorge is in the incorrect orientation to determine shear sense, a few outcrops are appropriately orientated, but provided no evidence of shear deformation. The contact between the phyllite and the Niarbyl Formation is marked by an E-W-trending igneous sheet (Fig. 5.41, grid ref. 22987985). There is no evidence of the Niarbyl Thrust that juxtaposes the Niarbyl Formation and the phyllonites of the Niarbyl High Strain Zone at Niarbyl (Fig 5.29). Based on the available field evidence, uncertainty remains as to the inland position of the Niarbyl High Strain Zone. The phyllitic fabrics observed in Glen Maye do not provide sufficient evidence to propose that they are the inland continuation of the Niarbyl High Strain Zone.

5.8 Summary, general interpretation and regional context

The structural characteristics of tracts 1-8 and of the high strain zones are summarised in Table 5.2 and Figure 5.42. The Lower Palaeozoic rocks of the Isle of Man contain a complex assemblage of primary folds, cleavage, faults and ductile shear zones that reflect variations in strain intensity during the primary phase of regional deformation. For the most part primary hinges and bedding-cleavage intersection lineations are gently curvilinear, with folds having 'whaleback' geometries. Fold and cleavage facing directions are upwards to the SW and NE. In tracts 1, 3 and 6 however, (e.g. St. Michael's Island, Langness, Lewaigue and Niarbyl) a number of the primary fold hinges and cleavage-bedding intersection lineations are highly curvilinear, and locally face downwards to the SW and NW. In all tracts, primary folds are identical in style and are associated with the same regional cleavage suggesting that all these structures appear to be broadly contemporaneous. The ductile shear deformation at Niarbyl, Lag ny Keeilley and Lynague, and the broad zone of shear band fabric observed at Langness deform the primary cleavage, and are thought to have developed very soon after or synchronously with the primary phase of deformation. It is suggested that the change in hinge line curvilinearity and ductile shearing reflect partitioning of a regional sinistral transpressional strain into contraction- and wrench-dominated deformation domains.

	Tract 1	Tract 1 Domain 1	Tract 1 Domain 2	Tract 2	Tract 3	Tract 4	Tract 6	Tract 7	Tract 8 (Niarbyl Fm.)	Post 'D1' shear zones		
										Lag ny Keeilley	Lynague	Niarbyl
General structure	Broad fold train younging to NW & SE	Broad fold train younging to NW & SE	Rather diffuse steeply dipping to S	Broad fold train younging to NW & SE	Broad fold train younging to NW & SE. SE-dipping homocline in N	NW-dipping homocline	NNE-dipping homocline	Primary structure not determined	Broad fold train younging to NW & SE	Narrow, NE-trending, steep, NW-dipping ductile sinistral shear zone	Narrow, NW-trending, moderately, NE-dipping ductile sinistral shear zone	WNW to WSE-trending, steeply dipping, ductile sinistral shear zone
Fold geometry & scale	Slightly asymmetric NW-verging folds <1m- 100m scale	Slightly asymmetric NW-verging folds <1m- 100m scale	Slightly asymmetric NW-verging folds <1m- 10m scale	Asymmetric NW-verging folds <1m- 100m scale	Asymmetric NW-verging folds in N. SE-verging asymmetric folds in S. <1m- 100m scale	Slightly asymmeric to overturned to SE <1m - 10m-scale	Slightly asymmetric to overturned SW verging folds <1m - 10m-scale	No data available	Asymmetric SE-verging, sometimes overturned folds <1m - 10m-scale	Small-scale steeply plunging sinistral folds	Small-scale steeply plunging sinistral folds	Small-scale steeply plunging sinistral folds
Fold/BCIL plunge pattern	Rather diffuse great circle girdle distribution. Plunging to both SW & NE	Folds & BCIL plunge gently SW & NE	Folds & BCIL plunge gently to steeply to NE & SW	Folds & BCIL plunge very gently SW & NE	Folds & BCIL plunge very gently SW & NE	Folds & BCIL plunge very gently SW	Folds plunge gently to steeply to both SE & SW BCIL plunges SE	No data available	Folds & BCIL plunge gently to NE & SW	No data available	No data available	No data available
Fold-cleavage relationship	Clockwise transected	Clockwise transected	Clockwise transected	Essentially axial planar	Essentially axial planar	Essentially axial planar	Uncertain. Not observed in field	No data available	Clockwise transected	No data available	No data available	Weak axial planar cleavage developed in syn-shear folds
Detachment geometry & kinematics	Complex pattern of dip-slip and sinistral strike-slip faults	Complex pattern of dip-slip and sinistral strike-slip faults	Predominately sinistral strike-slip & dextral oblique thrusts	Very few faults predominately dip-slip normal & strike-slip	Small sinistral strike-slip faults & top-to-SE thrusts	Very few recorded. Steep strike-slip	Complex pattern of sinitral strike-slip and thrust faults	Complex pattern of top-to-SE & top-to-SW thrust faults	Top-to-NW thrust faults	Sinistral R-shears & shear bands	Sinistral shear bands & R-shears	Sinistral shear bands & R-shears small sinistral faults & later top-to-SE thrusts
Facing patterns	NE & SW upward and down-ward at shallow to steep angles	NE & SW upwards-facing at shallow to moderate angles	SW upwards & downward at moderate to steep angles	NW & NE upwards at very shallow angles	Predominately SW upwards at gentle angles	Predominately NW upwards at gentle angles	SE, SW & NE upwards at steep to gentl angles	No data available	SW & NE upwards at gentle angles		Not recorded	Not recorded

Table 5.2. Summary of structural elements of tracts 1-7 (excluding tract 5) of the Isle of Man.

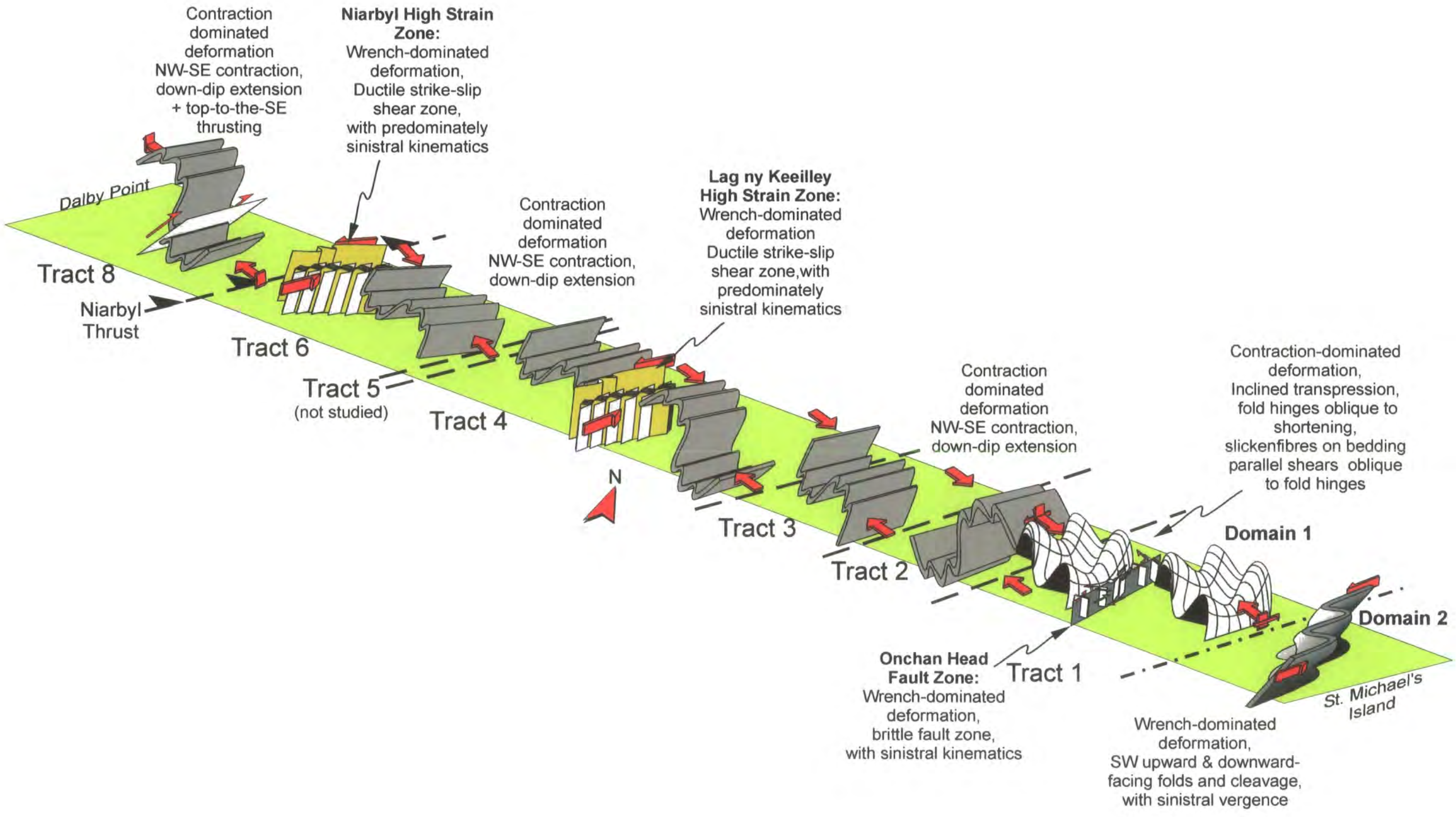

Figure 5.42. Schematic 3-D representation of the structural characteristics of tracts 1-8 (excluding tracts 5 & 7) and Domains 1 & 2 in Tract 1. Note that the NE & SW upward- facing folds on the N side of St. Michael's Island in Domain 2 are excluded for clarity (see Plate 5.19). The effects of the secondary phase of deformation have been omitted for clarity (not to scale).

Chapter 6

Deformation Patterns and Kinematic Partitioning in Eyemouth, Courtown and the Isle of Man: Discussion and Implications

6.1 Regional structure within the Iapetus Suture Zone

6.1.1 Introduction

The primary tectonic structures (folds, cleavage and faults) preserved within the Lower Palaeozoic rocks of Eyemouth (Figs. 3.5, 3.7), Cahore Point to Kilmichael Point (Courtown) (Fig. 4.6) and the Isle of Man (Fig. 5.2) were formed immediately prior to or during the Late Devonian, Acadian phase of the Caledonian Orogeny within a broad zone of sinistral transpression spatially associated with the Iapetus Suture Zone. The complex structural systems displayed in each locality are described in detail in chapters 3, 4 and 5. They include upward- and downward-facing curvilinear folds, interlinked systems of strike-slip faults, and folds clockwise transected by cleavage. The following section compares the general structure from each of the study areas in order to develop a regional picture of the structure within the Iapetus Suture Zone. Subsequent sections will examine the relative age of structures, the origins of curvilinear folds, transected folds and partitioning, a model for strain partitioning and controls of partitioning.

6.1.2 General structure

In all three areas, the primary structures have largely developed as a response to the same regional, sinistral transpression. Therefore, it is reasonable to expect that they might exhibit broadly similar geometries and orientations. The similarity in the orientation of folds, cleavage and faults across the region is well illustrated in Figure 6.1 which shows stereoplots of structural data from Eyemouth (Fig. 6.1(a)i-v), Courtown (Fig. 6.1(b)i-v) and the Isle of Man (Fig. 6.1(c)i-v). Poles to bedding (Fig. 6.1(i)a-c) show the most marked differences between the three areas, and reflect differences in the bulk structure. This is apparent not only in the girdle distribution of the bedding poles, but also in the orientation of the girdle (dashed line) and the mean bedding plane (solid line). The stereoplot for Eyemouth (Fig. 6.1(i)a) shows poles to bedding that lie along a rather diffuse NE-dipping girdle (dashed line, 149/59N) that defines a shallowly SW-

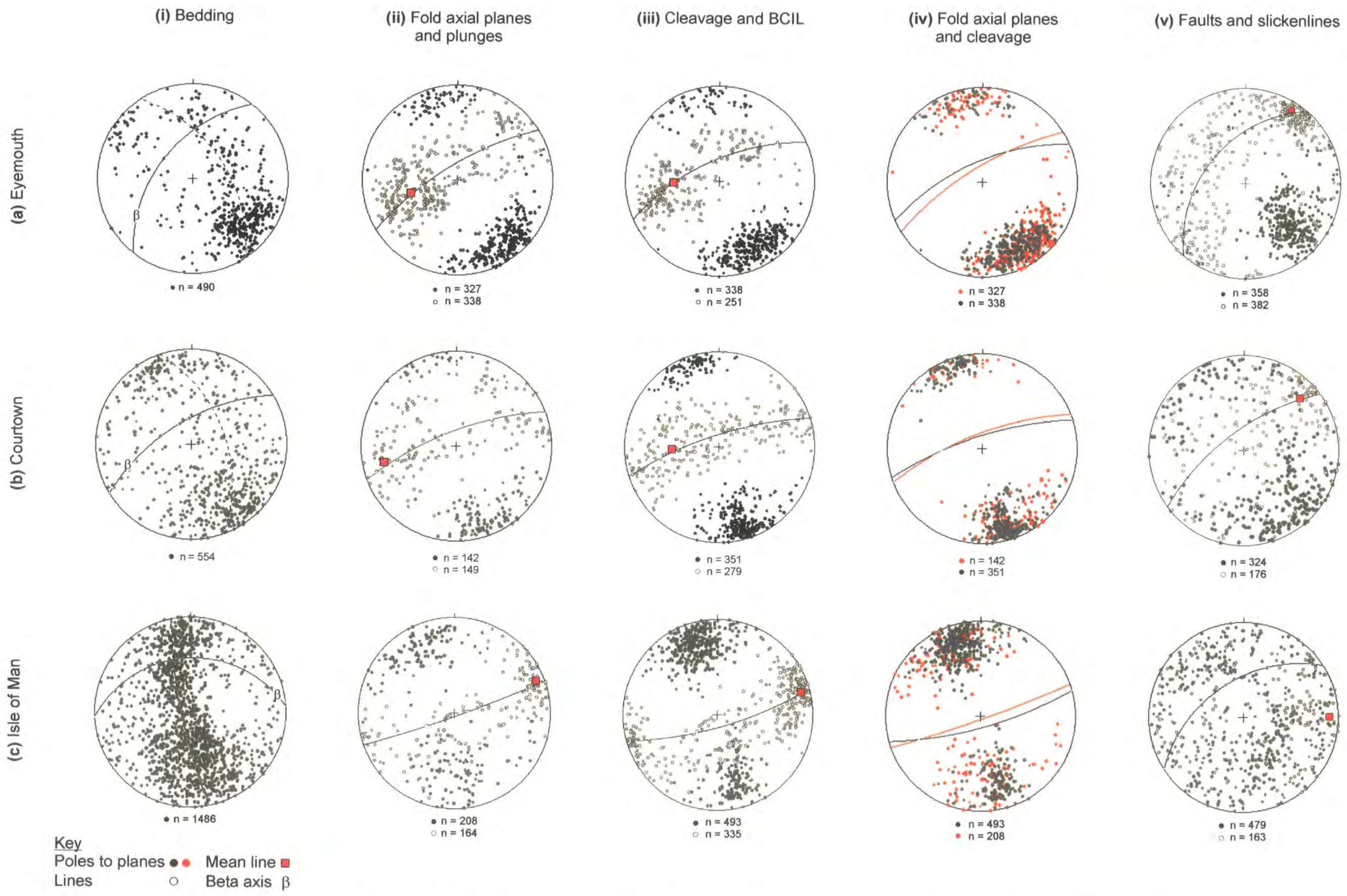

Figure 6.1. Stereoplots of structural orientation data for **(a)** Eyemouth, **(b)** Cahore Point - Kilmichael Point, **(c)** Isle of Man. In each case **(i)** Poles to bedding, **(ii)** Poles to fold axial planes and fold hinges **(iii)** Poles to cleavage and BCIL, **(iv)** Poles to fold axial and cleavage planes, **(v)** Poles to fault planes and slickenfibre lineations (see text for details).

plunging β axis (29/237) consistent with a moderately to steeply NW-dipping homoclinal mean bedding plane (030/60N). These data suggest a largely homoclinal structure for the Eyemouth section that is verified by field observations (Fig. 3.7). In Courtown, (Fig. 6.1(i)b) the distribution of bedding poles is broadly similar to that seen at Eyemouth (Fig. 6.1(i)a). However, a more diffuse distribution occurs, with a less well-defined point maximum that corresponds to a steeply NW-dipping mean bedding plane (059/70N). The β axis plunges gently to the SW (29/250), and is defined by a rather diffuse NE-dipping girdle (160/61N). This is consistent with the broadly folded structure recognised in the field across the section. In the Isle of Man, (Fig. 6.1(i)c) poles to bedding lie along a steeply WSW-dipping girdle (168/83N) that defines a gently ENE-plunging β axis (7/078), with a well-defined broad point maximum that is consistent with a moderately NW-dipping mean bedding plane (086/43N). The data presented in the stereoplot are born out by field observations, which indicate that the structure of the island is dominated by large-scale primary folds. The mean bedding plane and girdle for the Isle of Man (Fig 6.1(i)c) lie significantly clockwise of those for Eyemouth and Courtown (Fig. 6.1(i)a & b). One explanation of this may be that the Isle of Man has been rotated due to Mesozoic extensional faulting in the eastern Irish Sea between the Lake District and North Wales (e.g. Needham & Morgan 1997). However, it would be expected that the orientation of the primary folds and cleavage (Fig. 6.1(c)ii & iii) would also be rotated by a similar amount. This is clearly not the case as they both closely match the fold and cleavage data for Eyemouth and Courtown (Fig. 6.1(a) & (b)ii & iii). Significantly, the Acadian structural trend expressed by the orientation of folds and the strike of cleavage is not constant throughout the Iapetus Suture Zone (e.g. Cooper & Brück 1983; Soper & Hutton 1984; Soper *et al.* 1987). To the N of the Iapetus Suture, the trend is predominately NE-SW. To the S of the suture, the trends of folds and cleavage show more large-scale variations. For instance in SW Ireland and S Wales, the trend is E-W, swinging anticlockwise to become NE-SW through much of E Ireland, the Isle of Man and the W Lake District, finally becoming E-W in the E Lake District (Woodcock & Strachan 2000b). Soper *et al.* (1987) suggest that the pattern of Acadian deformation is strongly controlled by the triangular shape of the old rigid continental block underlying the Midland Platform (see Fig. 2.1, section 2.1). As the Midland Microcraton indented northward into the Laurentian margin, the already arcuate trend of basins around its northern corner was enhanced. This indentation was also probably responsible for wholesale rotation of crustal blocks as they wrapped

against the margin of the Midland Platform. On a more local scale, there is a close association between swings in the trend of folds and cleavage and granite intrusions (e.g. Leinster Granite, Lake District Batholith, Tan y Grisiau Granite, Fig 6.2). In Ireland, (Fig. 6.2(a), Cooper & Brück 1983) the Leinster Granite comprises five *en echelon* plutons intruded into a steep NNE-trending shear zone with a sinistral sense of displacement. The batholith was intruded during cleavage formation and both retains a fabric itself and deforms the fabric in the country rocks. The broadly NE striking cleavage is deflected towards parallelism with NNE-striking shear zones within and bordering the granite. In the Lake District, (Fig. 6.2(b), Soper *et al.* 1987) and North Wales, (Fig. 6.2(c), Woodcock *et al.* 1988) arcuate cleavage trends are also associated with granitic intrusions, with Acadian structures being moulded against the already consolidated, Ordovician plutons. Alternatively, the bedding data for the island may be skewed by data from tracts 6 and 7 (Fig 5.30(i)a, b, see section 5.6.6). The other tracts 1, 2, 3, 4 and 8 (Figs. 5.15(i)a-d, 5.30(i)c) show a pattern more consistent with that of Eyemouth and Courtown.

Stereoplots for primary folds for the three areas (Fig. 6.1(ii)a-c) are very similar, with the mean girdle planes having similar orientations (058/77N, 068/76N & 070/88S for Eyemouth, Courtown and the Isle of Man respectively). In all three areas, fold hinges show a significant degree of curvilinearity, but the distribution of the hinges and the calculated mean fold plunge are somewhat different. Fold hinges at Eyemouth (Fig. 6.1(a)ii) show a well-defined point maximum with a steeply SW-plunging mean hinge (50/252). In Courtown, the distribution of fold hinges (Fig. 6.1(b)ii) is much less well-defined than that in Eyemouth, but the calculated mean plunges shallowly to the SW (24/257). The calculated mean fold hinge corresponding to a moderately well-defined point maximum on the Isle of Man (Fig. 6.1(c)ii) plunges very shallowly to the NE (10/069).

Poles to cleavage planes and bedding-cleavage intersection lineations (BCIL) (Fig. 6.1(iii)a-c) show similar distributions to the fold axial planes and fold hinges in all three areas, (Fig. 6.1(ii)a-c) and are broadly consistent with their associated fold data. All three exhibit a small amount (ca. 4^{o}-8^{o}) of apparent clockwise transection (Fig. 6.1(iv)a-c).

Poles to fault planes and slickenfibre lineations (Fig.6.1(v)a-c) show more variation between the three areas, although the mean planes are broadly coincident (040/54N, 053/73N & 057/58N for Eyemouth, Courtown and the Isle of Man

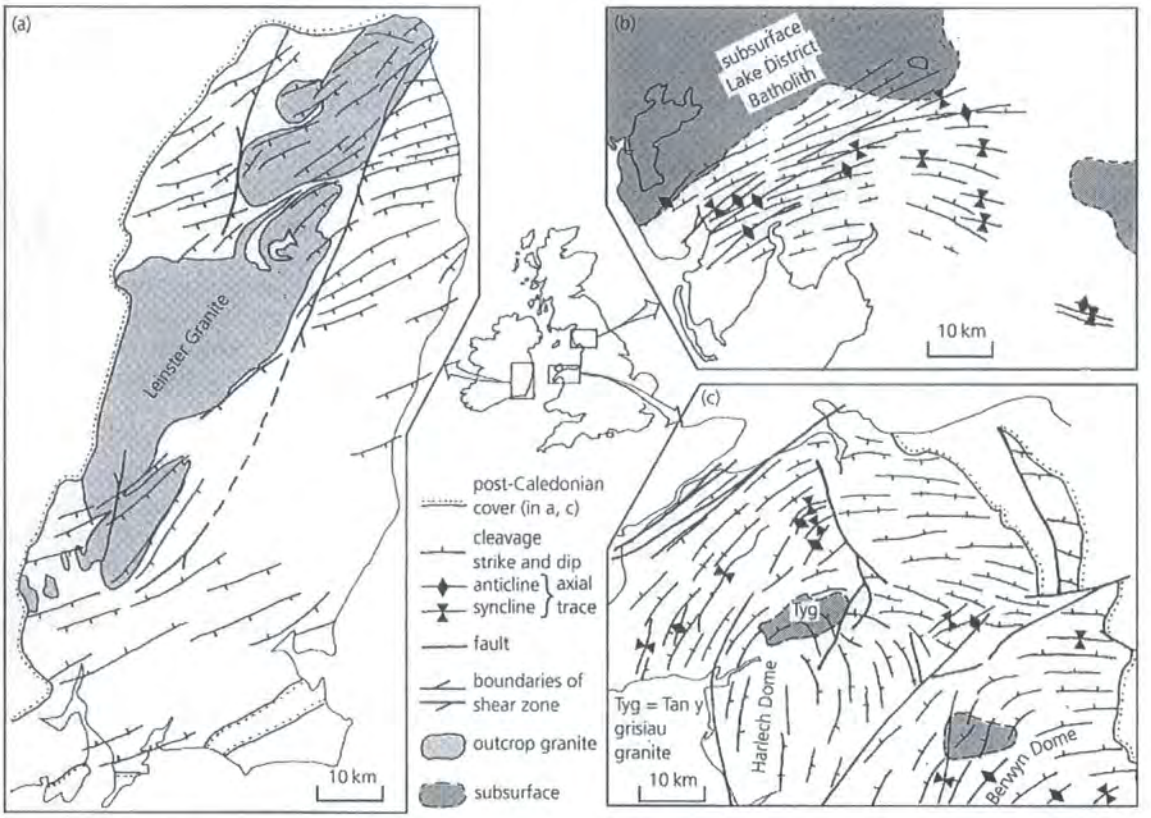

Figure 6.2. Maps showing patterns of arcuate cleavage and fold geometries in: **(a)** Leinster, **(b)** NW England, **(c)** Wales. (from Woodcock & Strachan 2000b).

respectively). There is a very close correlation between the mean fault and bedding planes of both Eyemouth and Courtown (Fig. 6.1(a)i & v & (b)i & v) suggesting that bedding may be an important controlling factor in determining the orientation of faults in these two areas. However, this does not appear to be the case in the Isle of Man (Fig. 6.1(c)i & v), but here there is a much greater spread of data most possibly due to extensive Mesozoic faulting that affected much of the Isle of Man. Slickenfibre lineations for all three areas plunge very gently to the NE or E (Fig. 6.1(v)a-c) suggesting a predominance of strike-slip movements along faults.

Eyemouth, Courtown and the Isle of Man display broadly similar patterns of fold and cleavage facing, (Fig. 6.3(a)-(c)i, ii) with a predominant number of folds and cleavage facing upwards to the NE and both upwards and downwards to the SW. Fewer data in Eyemouth and Courtown face up to the SE compared to the Isle of Man. One of the problems inherent with facing data is that the younging direction of the bedding is required to enable facing to be determined. Therefore, limited data are recorded for areas preserving folds and cleavage where there is poor younging evidence. This may mean that facing directions are not completely representative. This has not proved to be a problem for Eyemouth or Courtown (Fig. 6.3(a), (b)i & ii), but has meant that of the 326 facing data recorded for the Isle of Man, 254 are from just two tracts, tracts 1 and 8 (Fig 5.19). Despite this, facing data provide an essential tool in determining the geometry of folds with highly curvilinear folds.

6.1.3 Relative age of structures

It is important to establish whether or not the patterns of folding and marked differences in the structural patterns observed in the different domains described in each of the study areas can be attributed to overprinting of structures of different ages. Obvious overprinting structures are recognised in Eyemouth, Courtown and the Isle of Man, and are described in detail in chapters 3, 4 and 5.

6.1.3.1 Primary folds and cleavage

In all three areas the primary tectonic fabric displays a similar relationship to the primary folds, and the facing patterns, though complex, are coherent and consistent with the observed fold hinge curvatures. In the greater part of the Eyemouth and Courtown sections, and to a lesser extent in the Isle of Man, sedimentary way-up criteria are widely preserved throughout the bedded sequences as they pass around folds. These

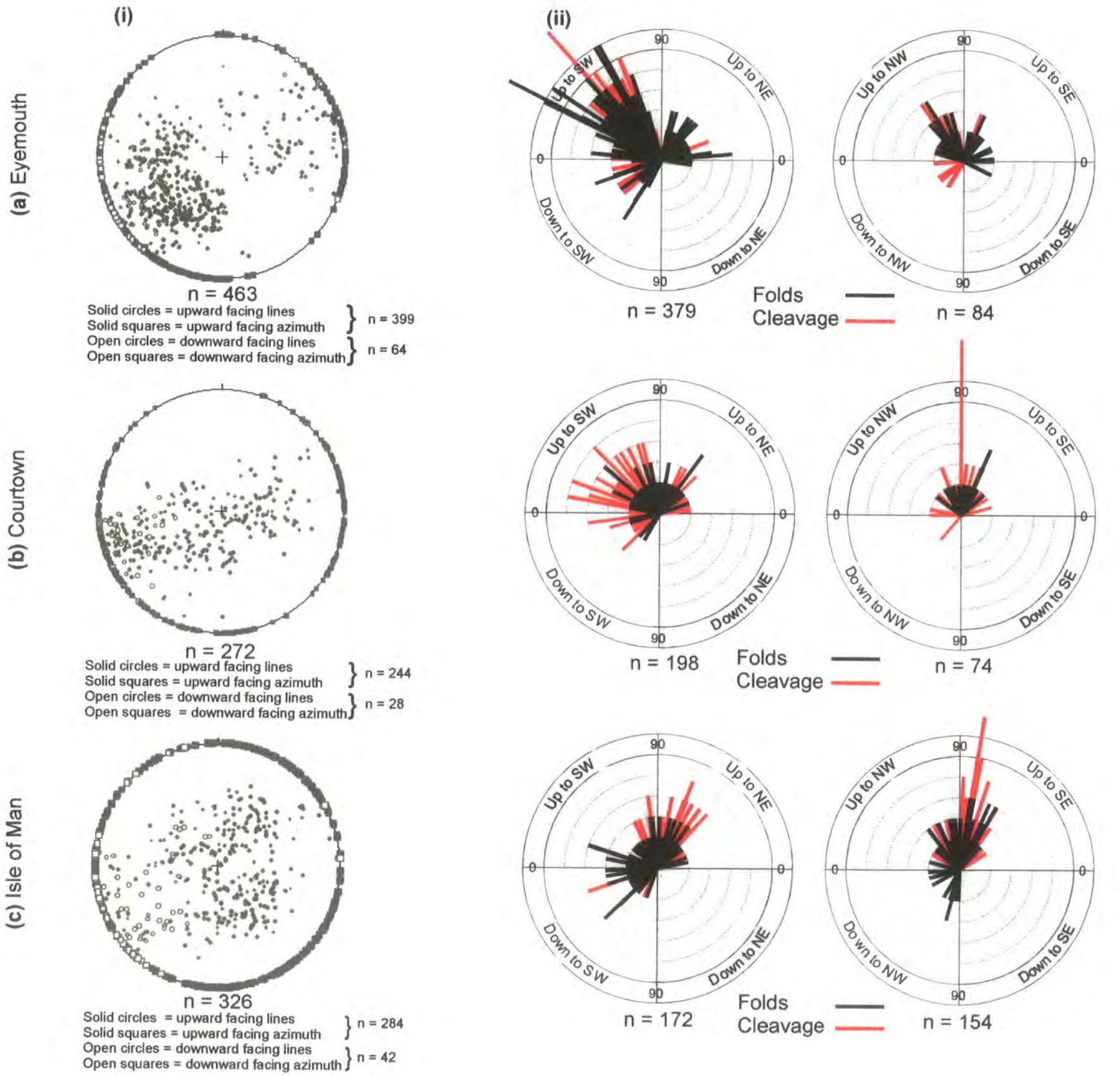

Figure 6.3. Facing data from **(a)** Eyemouth, **(b)** Cahore Point - Kilmichael Point, **(c)** Isle of Man. In each case **(i)** Fold and cleavage facing lines and azimuths plotted using the construction method of Holdsworth (1988). **(ii)** Plots showing the pitch of fold and cleavage facing directions in planes parallel to the fold axial and cleavage plane in which they were measured.

consistently indicate the presence of only one set of primary fold structures, with no clear anomalous reversals in younging that can be attributed to the presence of earlier fold structures. Thus, on this basis it is suggested that the primary folds, whether upward- or sideways- and downward-facing are the product of a single phase of deformation within each area. Synchronicity between areas is not proven.

6.1.3.2 Brittle and ductile deformation, faults, detachments and bedding parallel shears

Eyemouth-Burnmouth section

At Eyemouth, (Figs. 3.4, 3.7, 3.14) the extensive system of bedding-parallel shears related to flexural slip, detachment faults and associated veins appear to carry the same assemblage of fibrous pale grey to pink carbonate infills (e.g. Plates 3.3(b), 3.8(a), (b), 3.9(a), 3.10(b), 3.11(b)) suggesting that they formed at the same time. Therefore, by examining the relationship between these structures and the primary folds it is possible to determine whether or not they are contemporaneous sets of structures. Detachments often cross-cut folds on various scales, but they appear geometrically and kinematically linked to them. Thus in Domain 2 (see section 3.3.2, Fig. 3.10), the SE-overturned contractional folds are associated with conjugate thrust faults (e.g. Plate 3.3(a)) that appear to have formed during flexural-slip folding of local multilayer sequences in which the thickness of individual competent sandstone units is variable leading to strain compatibility problems (cf. Ramsay 1974). Significantly, some of these thrusts exhibit sinistral movement components, whilst the apparent kinematic overlap between bedding-parallel faults and detachments in domains 1 and 3 (see sections 3.3.1 & 3.3.3, Fig. 3.10) suggests that they are broadly contemporaneous features. In Domain 4 (see section 3.3.4, Fig. 3.10), many zones of folds appear to root downwards into strike-slip detachments (e.g. Plate 3.8(a)), whilst individual detachment faults are locally seen to tip-out into folds with a sense of vergence consistent with the sense of shear (e.g. Plate 3.8(a)). Detachments both cut folds and are locally folded (e.g. Plate 3.8(b)).

Cahore Point to Kilmichael Point section (Courtown)

Evidence for the synchronicity of structures in Ireland is more subtle and less extensive. The extensive carbonate veining observed in the Eyemouth-Burnmouth section is absent here, and the frequency of mineralised slickenfibres is much lower. However, a number

of faults appear to be contemporaneous with the primary folds. In Domain 1 (see section 4.7.1, Fig. 4.14), several SE-verging folds are closely associated with zones of low angle, NW-dipping faults (e.g. Plate 4.19(a)). These have the appearance of small-scale fold and thrust systems, but slickenfibres and stepped mineralisation on the fault surfaces indicate a sinistral strike-slip sense of displacement. Several thrust faults in Domain 2, (see section 4.7.2, Figs. 4.14, 4.20) exhibit oblique top-to-the SE directed movements with a significant sinistral component. The continuous and curved nature of slickenfibres on the fault surfaces suggests a progressive continuum from top-to-the SE thrusting into sinistral strike-slip (Plate 4.20)

The Isle of Man

In the Isle of Man (Fig. 5.2), determining synchronicity of structures has proved difficult. However, sinistral, ductile deformation associated with the Niarbyl (see section 5.7.3, Fig. 5.28) and Lag ny Keeilley shear zones (see section 5.7.1, Fig. 5.34) and shear band fabrics on the southern end of the Langness Peninsula (see section 5.6.1.2, Fig. 5,14) appear to be broadly contemporaneous with the primary phase of deformation. This is based on overprinting relationships between the primary folds and cleavage, sinistral shear and the regionally recognised secondary phase of deformation. Primary folds and cleavage in the three areas mentioned are deformed by ductile sinistral shear, producing a broad variety of shear-related structures including phyllonitites, syn-shear folds, C/S fabrics and shear bands (e.g. Plates 5.20(a), 5.43(a)). These in turn are deformed by the secondary phase of deformation, (e.g. Plate 5.20(b)) which is thought to have occurred shortly after the primary phase of deformation (Woodcock *et al* 1999a).

Based on these relationships, it is suggested that the primary folds, cleavage, detachments and ductile shearing in each area are all broadly related to a single phase of deformation. However, exact chronological synchronicity between the areas is not implied. Deformation across the whole of the Iapetus Suture Zone was diachronous along strike from SW to NE as the leading edge of Laurentia was thrust over Eastern Avalonia closing the wedge-shaped remnant of Iapetus ahead of it (Fig 2.18, Soper & Woodcock 1990). Nor is exact synchronicity in an absolute sense implied at Eyemouth, as there is good evidence on a regional scale for diachronous deformation across-strike in the Southern Uplands terrane (Fig 3.3, Stone 1996). Similar across-strike diachroneities may exist both in the Isle of Man and Ireland.

6.1.4 Origin of the curvilinear folds

Folds with highly curvilinear hinges occur in domains 3 and 4 of the Eyemouth section (see sections 3.3.3 & 3.3.4, Fig. 3.10), Domain 1 of the Courtown section (see section 4.7.1, Fig. 4.14) and in tracts 1, 3, 4 and 6 on the Isle of Man (see section 5.6.1, 5.6.3, 5.6.4, 5.6.5, Fig. 5.9). In their description of the folds in Domain 3 at Eyemouth, Dearman *et al.* (1962) suggest that the curved fold hinges resulted from the refolding of NE-SW folds about a later set of NW-SE trending structures (see Fig. 3.6(b)). Simpson (1965) suggests a similar mechanism for the formation of 'cross folds' on the Isle of Man. Brenchley & Treagus (1970) suggest that the rapid plunge variations in the folds along the Courtown section may be due to either inhomogeneous strain in the more incompetent lithologies, or to fold initiation by slight buckling which involved small plunge depressions oblique to the XY plane. There is however, no evidence for any NW-SE folds or associated cleavages anywhere in the areas where the curvilinear folds occur. Taken together with the lack of any evidence for earlier folds or fabrics described above, it is concluded that refolding cannot explain the geometry of the curvilinear folds.

Treagus (1992) suggests that the curvilinear folds at Eyemouth may result - at least in part - from soft-sediment deformation. Highly curvilinear slump folds are recognised elsewhere in the Southern Uplands terrane (e.g. Knipe & Needham 1986), and have geometries consistent with top-to-the-SE movements if bedding is restored to horizontal. This appears to be inconsistent with the geometry of the folds in Domain 3 at Eyemouth as they suggest top-to-the-SW movements. In addition, many SE-verging folds in domain 4 locally fold the strike-slip detachment faults (e.g. Plate. 3.8(b)) suggesting that they are not early, pre-tectonic features. There is no evidence of large-scale slump folding along the Courtown section or within the Manx and Dalby groups of the Isle of Man. Rare, small-scale slump folds are present along the Courtown section, particularly in the well-bedded volcaniclastic sediments of the Campile Formation, (e.g. Plate 4.8(b)). Although small slump folds have been recorded within the Manx Group, slump-related folding is generally only well developed in the Devonian Peel Sandstones on the Isle of Man (Ford 1972). In all three study areas, there is no compelling evidence to separate the curvilinear folds from the folds in other domains or tracts since they share the same associated cleavage, show the same styles in profile section and exhibit geometries that are wholly consistent with their less curvilinear counterparts.

A sheath fold origin for the curvilinear folds is unlikely as such structures are typically associated with highly deformed belts of pervasive ductile deformation (e.g. Carreras *et al.*, 1977; Alsop and Holdsworth, 1999). Delicate sedimentary laminations and structures are widely preserved all round the curvilinear folds observed in all of the study areas and there is no evidence of high strain in either fold limbs or hinges. On a larger scale, there is no evidence to suggest that the finite strains are significantly higher in the areas that contain curvilinear folds compared to areas where folds are less curvilinear. The cleavage is equally developed and the folds have a similar range of tightness. A further possibility is that the curvilinear folds are the products of locally constrictional strains ($1 < k \leq \infty$). This is thought to be unlikely because the axial surfaces of the folds and the cleavage are relatively planar, with no clear lineation present, i.e. there is no evidence for L or L>S strain patterns or tectonite fabrics (Flinn 1962). The absence of a linear fabric is in fact consistent with a bulk flattening strain ($1 > k \geq 0$), a characteristic feature of many transpression zones (Sanderson and Marchini 1984; Dewey *et al.* 1998).

The curved hinges could have formed due to a markedly non-parallel, 3-D oblique relationship between the bedding and the principal axes of finite strain leading to the simultaneous development of two sets of essentially orthogonal fold axes (see section 1.1.6, Treagus & Treagus, 1981). This would require that the bedding in the regions containing the highly curvilinear folds was rotated into an oblique orientation prior to fold nucleation, possibly as a result of soft-sediment disruption or growth faulting (Treagus 1992). However, there is no evidence of significant pre-tectonic disruption of the bedding in any of the areas where folds are markedly curvilinear. In addition, there is clear evidence from the oblique patterns of flexural slip folding at Eyemouth and to a lesser degree in Tract 1 on the Isle of Man, that the finite strain axes were also oblique to bedding in both domains 1 and 2 at Eyemouth and within Domain 1 on the Isle of Man where the folds do *not* exhibit highly curved hinge lines. Based on these observations it is concluded that a 3-D oblique strain model cannot account solely for the highly curved nature of the fold hinges observed in some domains.

In an area of fairly uniform strain, the presence of folds belonging to the same generation that exhibit very differing patterns of hinge line curvature may reflect contrasting histories of fold growth. Modelling studies have shown that the development of curvilinear hinges can be related to the way in which folds propagate laterally and amplify as they grow (e.g. Dubey & Cobbold 1977). If the fold hinge lines

in domains with highly curvilinear hinges were unable to propagate laterally as rapidly as those in domains where fold hinge lines are less curvilinear, it could result in more highly curved axes. Such propagation problems could reflect some variation in the mechanical properties of the multilayer sequences in each domain (cf. Ramsay & Huber 1987), but there is little compelling evidence that the sedimentary rocks are significantly different in terms of lithology, bedding thickness or spacing of competent layers. In particular, in Domain 1 on the Isle of Man, highly curvilinear and less curvilinear folds exist within identical multilayer sequences from the same stratigraphic unit. Furthermore, in Domain 2 of the Courtown section folds with highly curvilinear hinge lines are developed within the finely laminated mud and siltstones of the Ribband Group and the more massive limestones and volcanics of the Duncannon Group. Within both groups, the folds show similar variations in plunge, although in the more massive lithologies changes in plunge variation take place over several metres or tens of metres, whilst in the Ribband Group plunge variations occur over a few cm. This suggests that the nature of the multilayer sequence may influence the scale of the curvature, but not the occurrence (or not) of curvilinear fold hinges. In addition, contrasting fold growth histories alone cannot explain the profound differences in the hinge line curvature patterns between domains 3 and 4 of the Eyemouth section and domains 1 and 2 at Courtown. In Domain 3 at Eyemouth and Domain 2 at Courtown, the curved fold axes pass through the vertical, resulting in locally downward-facing fold structures, whilst the upward-facing fold hinges in Domain 4 at Eyemouth and Domain 1 at Courtown pass through the horizontal. It is proposed that this phenomenon is related to strain heterogeneity and, more specifically, to kinematic partitioning of the bulk transpressional deformation in these regions as discussed in the following section.

6.1.5 Transected folds and partitioning

There are numerous published case studies that have shown that there is a clear association between zones of transpression and the development of transecting cleavage (see section 1.1.4). Zones of sinistral and dextral transpression are associated with the development of clockwise and anticlockwise transecting relationships respectively (e.g. Murphy 1985; Treagus & Treagus 1992). The underlying cause of the relationship between the geometric sense of transection and the sense of strike-slip shear has never been adequately explained (see section 1.1.4, Soper 1986). In Courtown, cleavage and axial planes are essentially parallel and only two observed occurrences of folds

transected by their cleavage were recorded, both in the contraction dominated, Domain 1. The first, in folds within the bedded volcanics of the Campile Formation to the N of Duffcarrick Rocks, where the axial plane is clockwise transected by 6°. The second occurs in the Ballylane Formation at Clones, where the fold is anticlockwise transected by about 9°. No examples of cleavage transection were observed within the wrench-dominated Domain 2. Clockwise cleavage transection is only well-developed in tracts 1 and 8 on the Isle of Man, where folds show up to 14° of transection. In both tracts the dominant lithology is fine-grained sandstone interbedded with thin silt and mudstone units. In Tract 8 transection values up to ca 5° have been recorded, although the majority of folds show no evidence of transection. Tract 1 has been divided into two domains (Fig 5.20), in Domain 1 the strain is contraction dominated, whereas in Domain 2 strain is wrench dominated. However, both domains show similar values of clockwise transection (ca 14°). In Eyemouth, well-developed clockwise cleavage transection only occurs in those rock units where the strain is dominated by contractional strain due to the effects of strain partitioning, e.g. throughout Domain 2 and inside the m-scale rock units of Domain 4 bounded by strike-slip detachments. This association may point to a link between the development of cleavage transection and the process of kinematic partitioning. One possible explanation is that the cleavage is relatively insensitive to partitioning compared to the deformation of the layering due to folding. As a result, the folds will lie closer to being parallel with the regional shear plane in the contraction-dominated zones so that the cleavage will form clockwise and anticlockwise of their axial surfaces in regional zones of sinistral and dextral transpression respectively. However, this appears to be contrary to the occurrence of cleavage transection on the Isle of Man where both contraction- and wrench-dominated domains are affected. The apparent lack of cleavage transection at Courtown may be a sampling problem rather than an absence of transection. Apart from the examples cited above, there are very few exposed fold hinges where the relationship between the cleavage and the fold axial plane may be measured. Folds where this is possible are largely located in the N and S of the section (Fig. 4.6, e.g. Kilmichael Point and Glascarrig Point) i.e. away from the zone of greatest strain partitioning. This implies that the effects of strain partitioning are less intense in the N and S so that cleavage develops axial planar to folds.

6.1.6 Strain partitioning model

Kinematic partitioning of strain is a widely recognised feature of regional transpression zones and shear zones (e.g. Woodcock *et al.* 1988; Oldow *et al.* 1990; Holdsworth & Strachan 1991; Tikoff & Teyssier 1994; Dewey *et al.* 1998 and references therein). In all three study areas, components of NW-SE contraction, top-to-the-SW sinistral shear and top-to-the–SE thrusting occurred contemporaneously. Additionally, in the Isle of Man these were accompanied by a major phase of ductile sinistral shear along the Niarbyl and Lag ny Keeilley shear Zones. These patterns are suggestive of a bulk triclinic transpressional deformation regime (see section 1.1.2, Robin & Cruden 1994; Lin *et al.* 1998) involving components of pure shear contraction and oblique simple shear (Jones & Holdsworth 1998). This is consistent with the recognition of anticlockwise oblique flexural slip lineations in domains 1 and 2 at Eyemouth and Tract 1 (Domain 1) in the Isle of Man, which suggest that all 3 axes of the finite strain ellipsoid lie significantly oblique to bedding during folding (cf. Ramsay 1967, Treagus & Treagus 1981).

Following the method used by Jones *et al.* (1997) and Jones & Holdsworth (1998), it is possible to depict inclined transpression in terms of a 'strain triangle' (Fig. 6.4, Jones *et al.* in prep), with the interior of the triangle representing the bulk inclined and/or oblique transpressional strains. During partitioning, bulk deformation that would plot inside the strain triangle is distributed between separate domains that lie closer to the apices and edges of the triangle (Fig. 6.4). The present study has shown that a variety of structures are typically found in transpression zones, with individual sets of structures each having a particular significance in relation to bulk transpressional deformation (Fig. 6.5). Therefore it is possible to use the geometries of the folds and associated structures in all three areas to provide first-order qualitative information concerning the orientation of the bulk finite strain axes across each study area, and thus determine the patterns of strain partitioning. Because the Eyemouth-Burnmouth section provides the most complete and comprehensive set of folds and related structures, the model for strain partitioning in all three areas is strongly influenced by the model from here. In Domain 1 at Eyemouth (Figs. 6.6, 6.7(a), (b)), the steeply SW-plunging and obliquely upward-facing 'S' folds appear to be consistent with bulk homogeneous transpression involving components of NW-SE contraction and oblique sinistral, top-to-the-S simple shear. The upward-facing, gently whaleback folds of Domain 2 are consistent with a dominantly sub-horizontal NW-SE contractional strain. Using the

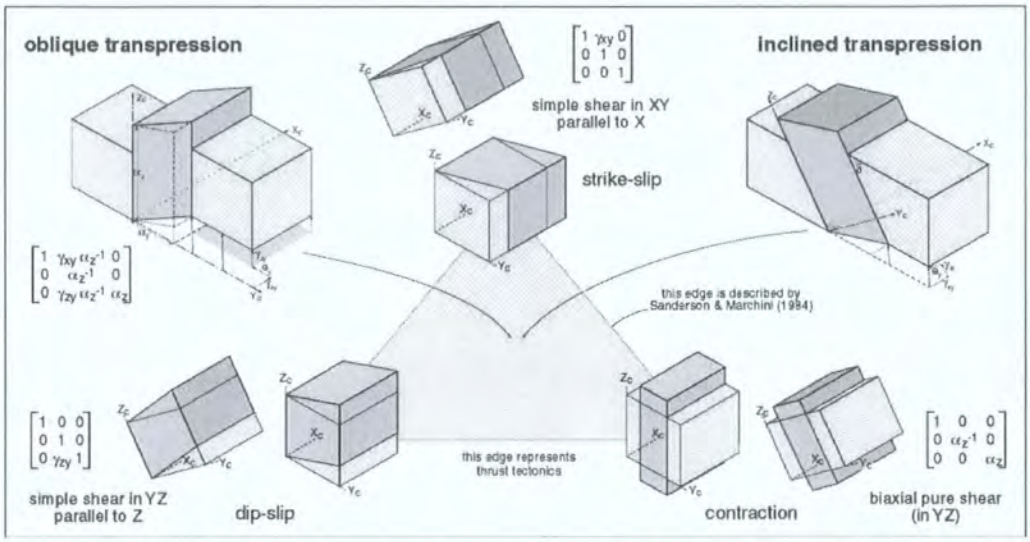

Figure 6.4. Strain triangle showing how bulk triclinic transpressional strains can be visualised in terms of three biaxial end-member strain components. In natural transpression zones there is often a marked tendency for bulk strains (which plot inside the triangle) to partition into separate deformational domains situated towards the edges or apices of the triangle. (from Jones *et al.* in prep.).

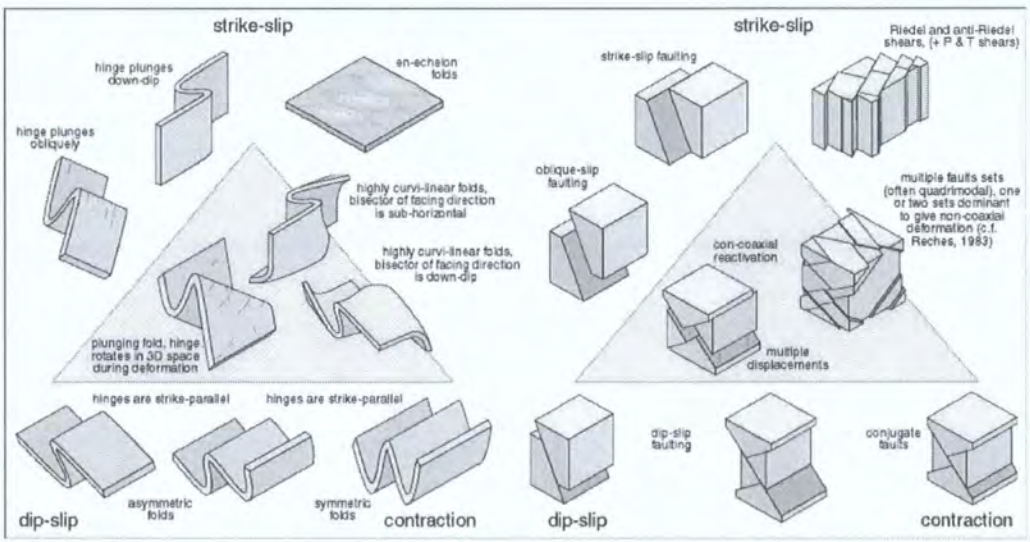

Figure 6.5. Kinematic effect of individual structures that typify triclinic transpression zones. (from Jones *et al.* in prep.).

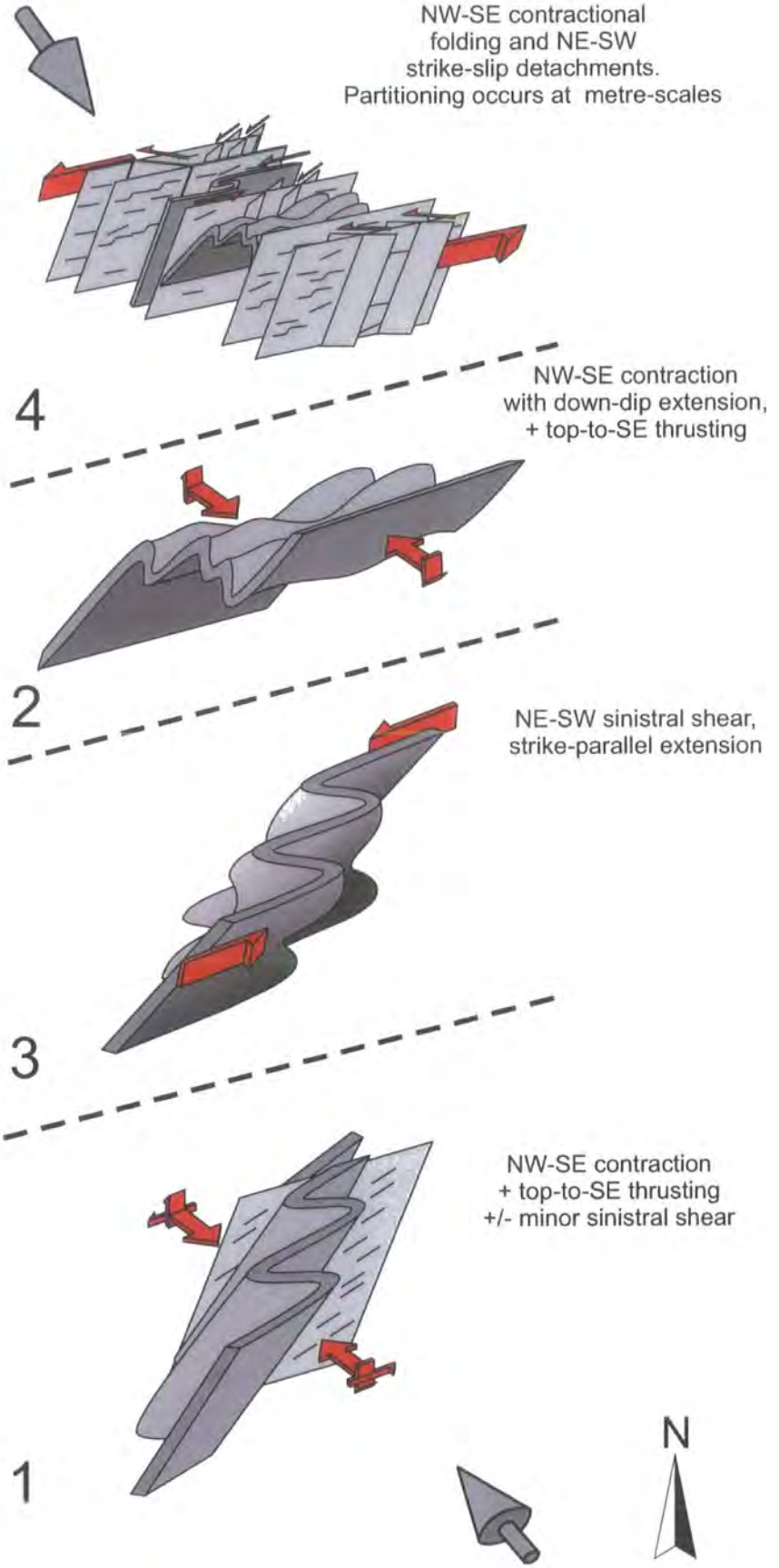

Figure 6.6. 3-D summary of the structures in Domains 1-4 of the Eyemouth-Burnmouth area. (adapted from Holdsworth *et al.* 2002b).

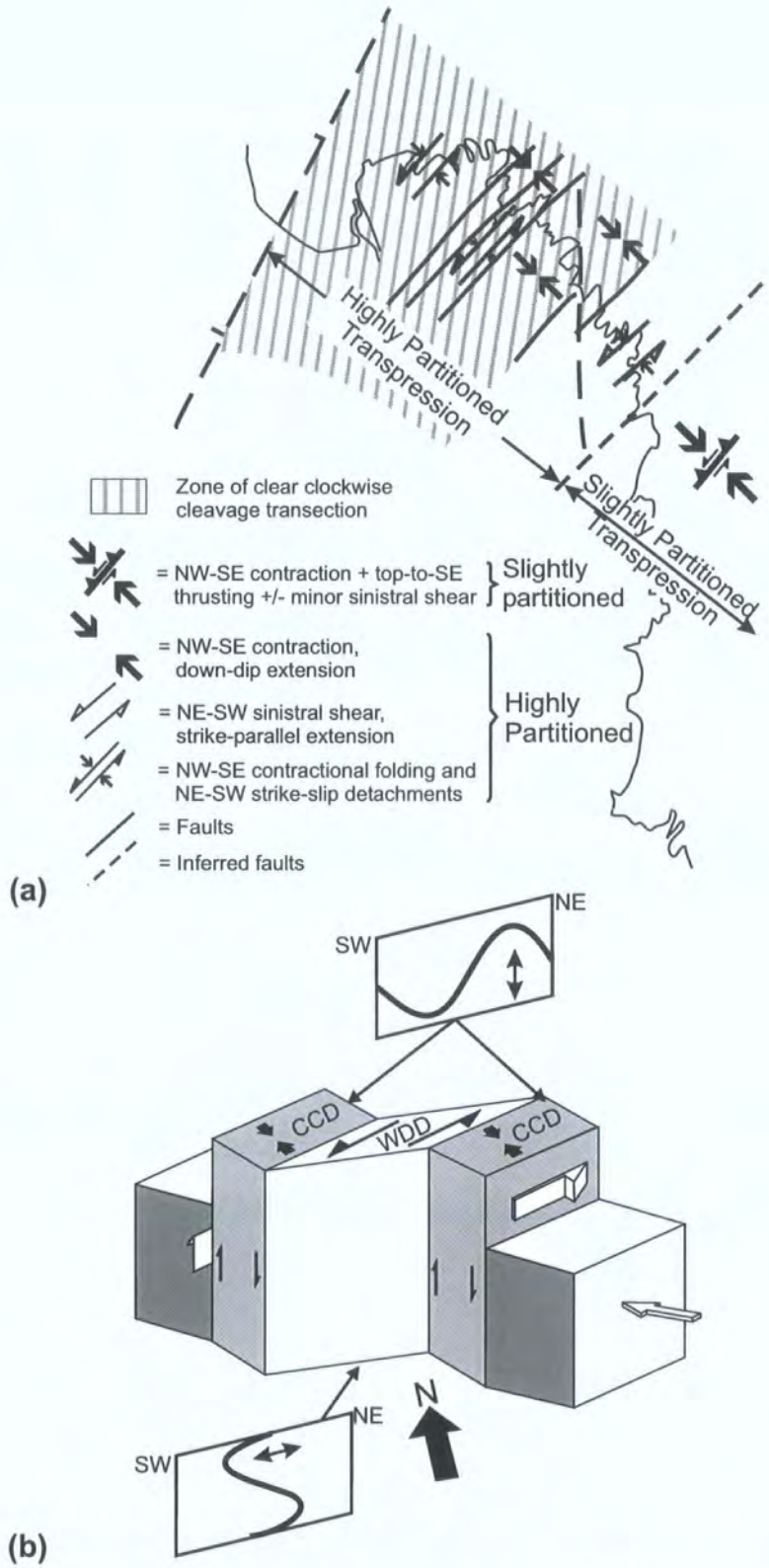

Figure 6.7. **(a)** Summary map of strain interpretation for the Eyemouth - Burnmouth area. **(b)** 3-D sketch showing a schematic transpression zone (three deformed boxes in centre) in which the bulk triclinic strain has been partitioned into contraction-dominated and wrench-dominated domains (CDD and WDD, respectively). The panels show fold axial planes and differing curvilinear fold hinge-BCIL plunge patterns (bold black lines) and inferred finite stretching axes (double headed arrows) in contraction- and wrench-dominated domains. (from Holdsworth et al. 2002b).

bisectors of the arcs of hinge-line curvature and facing (e.g. Alsop & Holdsworth 1999), it appears that the direction of finite extension in Domain 2 (Figs. 6.6, 6.7(a), (b)) plunges down the dip of the fold axial surface. The same construction used for the highly curvilinear folds in Domain 3 suggests a sub-horizontal direction of finite extension (Figs. 6.6, 6.7(a), (b)). Such rapid switches in the direction of finite extension are common in transpression zones where contractional pure shear and wrench simple shear strain components are kinematically partitioned into different domains (e.g. Sanderson & Marchini 1980; Fossen & Tikoff 1993; Tikoff & Green 1997). It is suggested that, based on the relatively minor components of sinistral shear deformation in Domain 2 and the consistent sinistral vergence of the folds in Domain 3, these are zones of contraction- and wrench-dominated strain respectively (Figs. 6.6, 6.7(a), (b)). When the estimated bulk strain for each of the four domains is plotted on the strain triangle (Fig. 6.8) they all lie within the strain triangle, with domains 2, 3,and 4 plotting nearer to the apices and edges than Domain 1. Thus, it appears that the bulk triclinic strain observed in Domain 1 is kinematically partitioned on a scale of hundreds of metres in domains 2 and 3. In addition, the widespread development of top-to-the-SE thrusts and the overall SE-vergence of the folds in Domain 2 suggests that the overall top-to-the-SE component of simple shear may also be preferentially partitioned into this zone of contraction-dominated deformation. Similarly, the sub-horizontal extension direction deduced in Domain 3 is consistent with sinistral simple shear (Figs. 6.6, 6.7(a), (b)). Therefore, it appears that the triclinic bulk strain does not partition into zones of pure shear and (oblique) simple shear as proposed by Lin *et al.* (1998), but instead into monoclinic end-member components (non-coaxial contraction and wrench simple shear). Whereas partitioning in domains 2 and 3 is on a scale of hundreds of metres, partitioning of the bulk triclinic strain in Domain 4 is into metre-scale domains of contraction-dominated monoclinic deformation bounded by an interconnected system of sinistral strike-slip faults.

The partitioning of strain, or the relative lack of partitioning in the case of Domain 1, appears to be imperfect. Thus, in Domain 1, a small degree of sinistral strike-slip deformation is apparently partitioned along detachment faults and in Domain 2 along NW-dipping thrust faults. The dominance of SW plunging folds in the latter domain may also signify the presence of a small sinistral shear strain component. Domain 4 (Figs. 6.6, 6.7(a), (b)) appears to exhibit the highest degree of partitioning, here even the sinistral and NW-side-down movements appear to have been partitioned

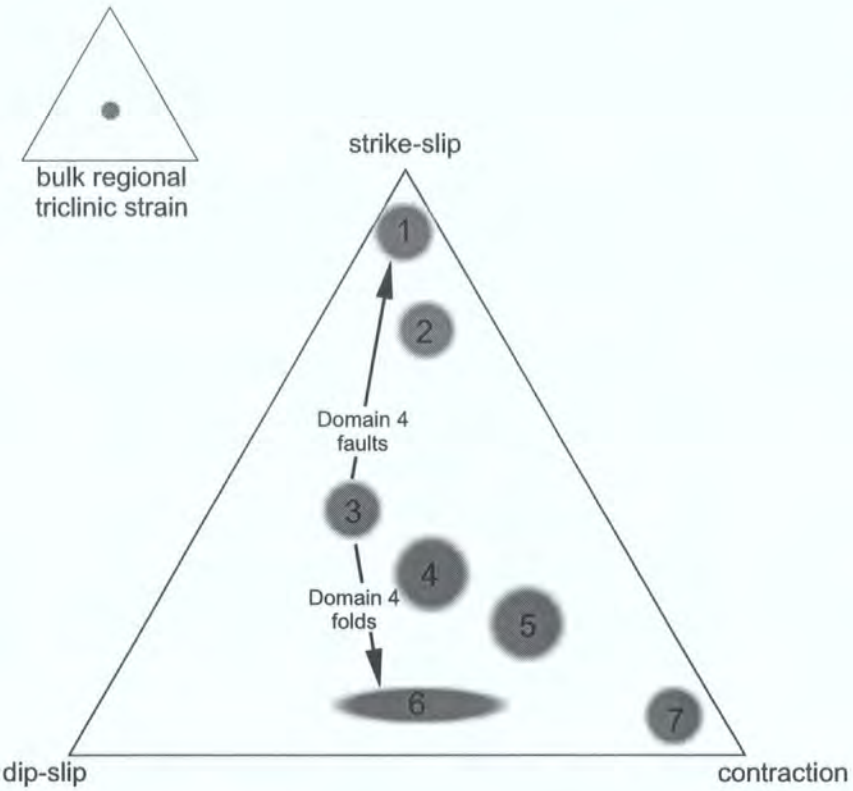

Localities and general structural characteristics represented by each zone plotted on the strain triangle:

1. Niarbyl, Lag ny Keeilley & Lynague high strain zones, & Onchan Head Fault Zone: strike-slip dominated: ductile & brittle strike-slip shear zones. Sub-horizontal mineral stretching lineation/ slickenlines, predominance of sinistral shear sense indicators.

2. Domain 2- Isle of Man, Domain 2- Courtown & Domain 3- Eyemouth: strike-slip dominated: highly curvilinear, sinistrally-verging folds. Bisector of facing is sub-horizontal & sub-parallel to strike. Folds in Domain 2- Isle of Man are strongly clockwise transected by cleavage.

3. Domain 4- Eyemouth: triclinic transpression: NW-dipping homocline, partitioned at metre-scales into sub-domains dominated by NW-SE contractional folding & NE-SW-trending sinistral strike-slip detachments. Arrows show how the bulk triclinic strain is partitioned.

4. Domain 1- Eyemouth: triclinic transpression: NW-dipping & younging homocline, folds plunge SW & verge SE. Hinges & slickenfibres on bedding parallel shears are oblique to shortening. NW-dipping sinistral detachments with gently SW-plunging slickenfibres.

5. Domain 1- Isle of Man: triclinic transpression: NW-verging folds, plunging gently to both SW and NE. Slickenfibres on bedding parallel detachments are oblique to fold hinges. Folds are clockwise transected by cleavage.

6. Domain 1- Courtown, Domain 2- Eyemouth & Tract 8- Isle of Man: dip-slip & contraction dominated: SE-verging folds, NW-dipping, top-to-the-SE thrusts. Only minor sinistral oblique component of deformation.

7. Tracts 2, 3, 4 & 6- Isle of Man: contraction dominated: SE, NW & neutral-verging folds.

Figure 6.8. Strain triangle showing the estimated bulk strain for each of the domains/ tracts from the Isle of Man, Eyemouth and Courtown (after Jones *et al.* in prep.).

locally along individual detachment surfaces. Note that this domain also exhibits metre-scale partitioning compared to scales of tens- or hundreds-of-metres seen in domains 2 and 3. This illustrates that field observations of partitioning phenomena are to some extent scale-dependent.

How do Courtown and the Isle of Man fit into the model proposed for the Eyemouth-Burnmouth section? None of the tracts or domains on the Isle of Man or at Courtown appear to be equivalent to Domain 4 at Eyemouth, and the extent of partitioning across the sections is much less well developed (see below). At Courtown, (Fig. 6.9) Domain 1 is very similar to Domain 2 at Eyemouth, although the development of top-to-the-SE thrusts is less intense. This suggests that Domain 1 at Courtown should plot in a similar position to Domain 2 at Eyemouth on the strain triangle (Fig. 6.8). Similarly, the highly curvilinear SW sideways-facing, and SW upward- or downward-facing folds in Domain 2 at Courtown would plot in the same place as the similar folds in Domain 3 at Eyemouth. Whether any parts of Domain 1 at Courtown are equivalent to Domain 1 at Eyemouth (i.e. minimally partitioned triclinic transpression) is impossible to determine as there are no bedding parallel slickenfibres to indicate any non-parallelism between the bedding planes and the axes of the finite strain ellipsoid. Therefore, at Courtown, it appears that the bulk transpressional strain has been partitioned into NW-SE directed contraction-dominated domains with a small component of top-to-the-SE sinistral strike-slip. In the Isle of Man (Fig. 6.10) the picture is again slightly different from that discussed for both Eyemouth and Courtown. Partitioning on the Isle of Man occurs on a larger scale than that seen in the other two areas and appears to be less extensive than at Eyemouth (see below). In Tract 1 (Figs. 5.9, 5.20) transpressional strain appears to have partitioned into a contraction dominated domain (Domain 1, Figs. 5.20, 6.10) and a wrench-dominated domain (Domain 2, Figs. 5.20, 6.10). However in Domain 1 there is evidence of bedding parallel shear with slickenfibres that are oblique to primary fold hinges (see section 5.6.1.1, Figs. 5.12, 5.22), implying non parallelism between the bedding and the axes of the finite strain ellipsoid. This suggests that Domain 1 on the Isle of Man may be analogous to Domain 1 at Eyemouth (i.e. minimally partitioned triclinic transpression) and should therefore plot in a similar position on the strain triangle (Fig. 6.8). Domain 2 in the Isle of Man (Figs. 5.20, 6.10) is analogous to Domain 3 at Eyemouth and Domain 2 at Courtown, and thus would plot in the same position on the strain triangle (Fig.6.8). A number of other tracts on the island exhibit very small degrees of partitioning, for instance the

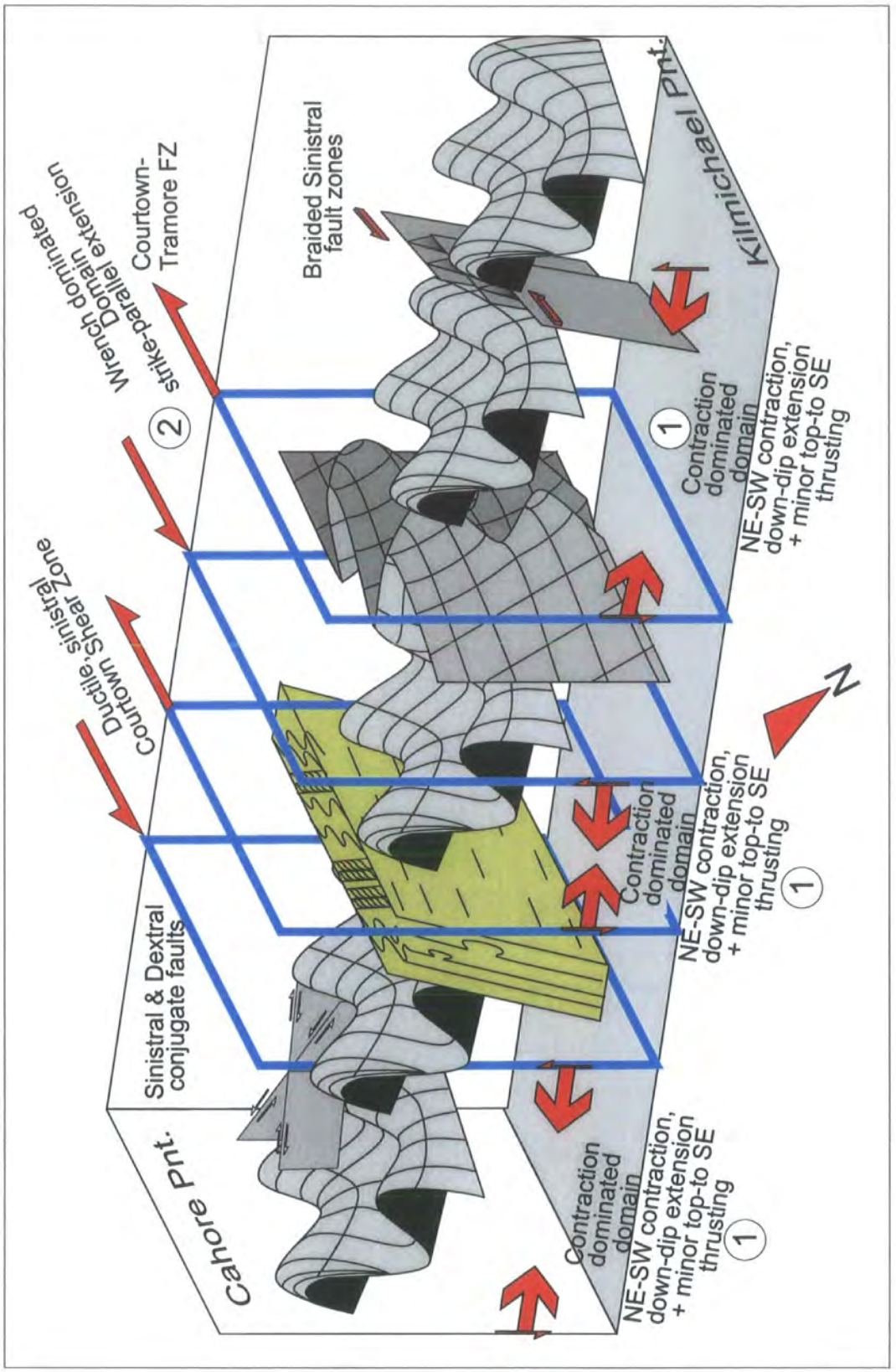

Figure 6.9. Schematic 3-D representation of the structural domains and overprinting sinistral shear and faulting between Cahore Point and Kilmichael Point.

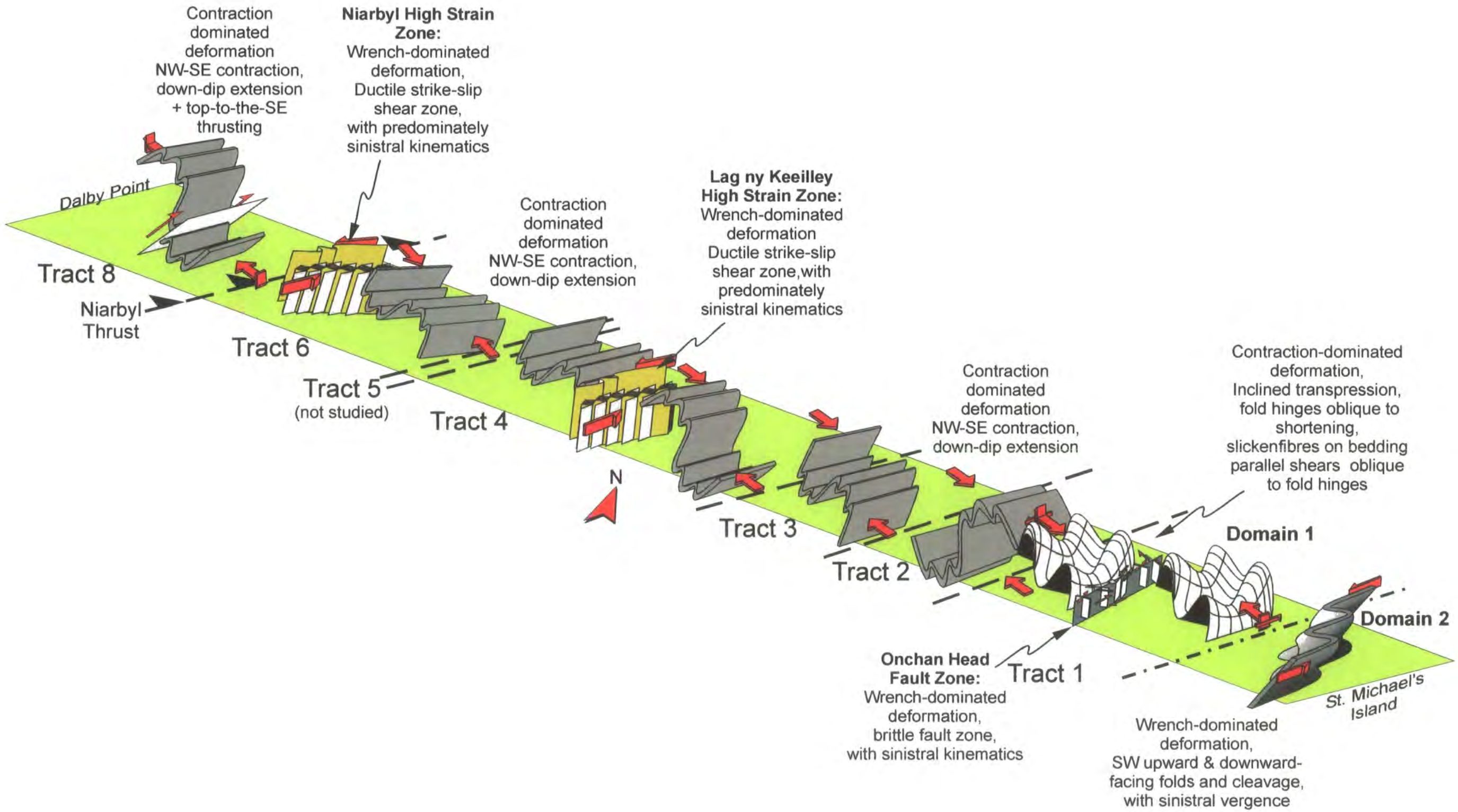

Figure 6.10. Schematic 3-D representation of the structural characteristics of tracts 1-8 (excluding tracts 5 & 7) and Domains 1 & 2 in Tract 1. Note that the NE & SW upward- facing folds on the N side of Domain 2 are excluded for clarity (see Plate 5.19)The effects of the secondary phase of deformation have been omitted for clarity (not to scale).

highly curvilinear upward and downwards facing folds in tracts 3 and 6 (see sections 5.6.3 & 5.6.5) are similar in geometry to those seen in Domain 2 on the Isle Man, Domain 3 at Eyemouth and Domain 2 at Courtown. In addition there are a number of zones of predominately strike-slip deformation, e.g. the Niarbyl and Lag ny Keeilley shear zones, a broad zone of sinistral shear band deformation on the Langness Peninsula and a zone of brittle, sinistral strike-slip faulting at Onchan Head (see sections 5.7.3, Fig. 5.29, 5.7.1, Fig. 5.36, 5.6.1.2, Fig. 5.14, 5.6.1, Fig. 5.16). In terms of the strain triangle, these areas would plot at or near to the apex (Fig. 6.8). In Tract 8 (Figs. 5.9, 6.10) the primary folds have a SE sense of vergence, are clockwise transected by cleavage, and are associated with an extensive system of top-to-the-SE thrusts, similar to folds and faults in Domain 3 at Eyemouth. None of the faults appears to have any sinistral strike-slip component, but this is based solely on bed offset and not the orientation of slickenfibres. Based on this evidence, the structures in Tract 8 should be plotted approximately mid way along the base of the strain triangle (Fig. 6.8). As with Eyemouth it appears that the bulk triclinic strain does not partition into zones of pure shear and (oblique) simple shear (e.g. Lin *et al.* 1998), but instead into monoclinic end-member components. In the Isle of Man, the bulk triclinic strain appears to be more completely partitioned into domains of contraction-dominated deformation (e.g. Tract 8) and strike-slip deformation (e.g. Domain 2, and the Niarbyl and Lag ny Keeilley shear zones) than Eyemouth or Courtown.

6.1.7 Controls on partitioning

Modelling partitioning using a homogenous plastic rheology, Tikoff & Teyssier (1994) and Teyssier *et al.* (1995) argued that it is the relative angle of convergence that controls partitioning of strain in transpression zones (see section 1.1.3), and it is the mismatch in orientation between the incremental and finite strain axes that is responsible for partitioning (section 1.1.3). However natural examples of deformation zones are rarely homogenous, and the effects of pre-existing anisotropies and rheological variations may be profound and must be taken into account. There are striking differences between the degree of partitioning observed between the Eyemouth-Burnmouth section and The Isle of Man and Courtown. In both the Isle of Man and Courtown partitioning occurs on a scale of hundreds of metres to several kilometres, whereas at Eyemouth the scale is hundreds of metres down to less than a metre. It is difficult to conceive that this variation can be due simply to a mismatch in the

incremental and finite strain axes; there must be another more local factor influencing the degree of partitioning.

In the Eyemouth - Burnmouth section, the regionally triclinic transpressional strain expressed in Domain 1 appears to become partitioned into domains of monoclinic contractional and sinistral wrenching components at smaller and smaller scales towards the N. In particular around Dulse Craig (see section 3.6.4, Fig. 3.14, 6.6(a)) strain is partitioned into sub-metre to tens of metre scale-domains. Elsewhere in the Southern Uplands terrane, sinistral strike-slip movements are often preferentially concentrated along major tract-bounding structures such as the Orlock Bridge Fault (Anderson & Oliver 1986) or the Moniaive Shear Zone (Phillips *et al.* 1995). This implies therefore, that a similar faulted boundary must lie somewhere immediately north of the Eyemouth-Burnmouth section to separate these rocks from those belonging to the Gala Group exposed further to the north (Fig. 3.1). The normal fault that currently separates the Silurian basement S of Eyemouth from Devonian and Carboniferous rocks to the N (Greig 1988) may well correspond to and reactivate this tract bounding structure. It is possible that the increased partitioning of strain observed in the north of the section reflects increased proximity to the tract-bounding fault. Stone *et al.* (1997) demonstrated that some tract boundaries have a strong geophysical expression in the deeper crust. If such crustal-scale faults are relatively weak, they could preferentially accommodate strike-slip displacements and therefore facilitate strain partitioning on a regional scale. Partitioning in Courtown and the Isle of Man may also be influenced by the close proximity of major strike-slip faults. The wrench-dominated Domain 2 at Courtown lies close to the Courtown-Tramore Fault Zone, a major NE-SW trending fault system that acts as a tract boundary within the Ribband Group. On the Isle of Man, the Niarbyl and Lag ny Keeilley shear zones are thought to represent tract bounding structures, whilst the Niarbyl Fault may be a strand of the Iapetus Suture (Woodcock *et al.* 1999a). The presence of the wrench-dominated Domain 2 and sinistral shear bands on the Langness Peninsular suggests that there may be a tract bounding fault lying offshore to the SE of the Isle of Man (see Fig. 5.1). The proximity to such a structure may influence both the degree and scale of partitioning, however other local effects may have a more profound effect on the scale of partitioning.

The presence of partitioning on a smaller scale in Domain 4 at Eyemouth, for example, may reflect an additional, more localised lithological control. The domain is significantly richer in mudstones compared to the other parts of the section. Throughout

the Eyemouth-Burnmouth section, the majority of sinistral detachments lie within mudstone horizons. All detachments and associated vein features exhibit carbonate mineralisation consistent with the presence of a syn-tectonic fluid phase (e.g. Plates 3.3(b), 3.9, 3.10(b), 3.11(b)). The localisation of detachments into mudstone horizons may be explained if they acted as fluid seals allowing significant overpressures to develop, leading to kinematic partitioning and the formation of wrench-dominated detachment faults at low angles or sub-parallel to the strong bedding anisotropy. Similar lithologically controlled overpressures may have helped facilitate bedding-parallel shearing during flexural-slip folding. The lack of significant volumes of vein material associated with the primary deformation within the rocks of the Isle of Man and Courtown may be connected to the absence of small-scale partitioning within these areas and helps to illustrate the importance of local anisotropies and rheologies in controlling partitioning.

6.1.8 Conclusions and implications

The three study areas preserve a highly heterogeneous assemblage of contemporaneous structures. These include folds, some of which are complex and highly curvilinear, interlinked strike-slip detachment faults and a regional cleavage that locally transects. Geometrically and kinematically different assemblages of these structures define a series of fault-bounded, metre to hundreds of metre-scale structural domains. In the absence of polyphase deformation or significant variations in strain intensity, these domains are interpreted to result from kinematic partitioning of a regional triclinic transpressional deformation involving components of NW-SE pure shear contraction with sub-vertical extension, top-to-the-SE dip-slip reverse simple shear, top-to-the-SW sinistral simple shear and NE-SW orientated simple shear. The structural facing patterns of the folds and associated cleavages are particularly helpful in defining the different domain types and in unravelling the structural complexities of the area. Partitioned domains of non-coaxial dip-slip contraction- and wrench-dominated deformation are likely to be typical of other regions of regional transpressional strain, especially those associated with obliquely convergent margins (cf. Fossen *et al.* 1994; Dewey *et al.* 1998; Jiang *et al.* 2001). The nature and distribution of strain appears to be controlled by the presence of mechanical heterogeneities on regional and local scales, e.g. respectively, the proximity to weak tract-bounding faults and the presence of lithologically controlled regions of high pore fluid pressures.

Features such as clockwise-transected cleavage, sinistral detachments and zones of very steeply plunging sinistrally-verging folds have often been used to infer sinistral transpressional strain. The structures in the Eyemouth-Burnmouth section, Isle of Man and Courtown support this interpretation, but further suggests that such features are most obvious in regions where significant amounts of kinematic partitioning have occurred, i.e. zones where the bulk transpressional strain has been partitioned into contraction- and wrench-dominated domains. The interpretation of the structures in the areas lends some support to the assertion that many transpression zones are triclinic in character (e.g. Robin & Cruden 1994; Lin *et al.* 1998, 1999, Jiang *et al.* 2001). However, the geometric and kinematic patterns in the different structural domains qualitatively suggest a strain model in which the transpressional deformation undergoes partitioning into monoclinic end-members (non-coaxial contraction with dip-slip simple shear and strike-slip simple shear) rather than into domains of pure shear and oblique simple shear.

This project has shown that complex systems of folds, faults and related structures can develop during a single phase of partitioned transpressional strain within a multi-layered sequence, and that it is not necessary to invoke several deformational events to account for the structural complexity observed. Partitioning appears to be strongly influenced by pre-existing weaknesses in the crust; either large-scale regionally developed faults or local rheological heterogeneities. It has also highlighted the possibility that 3-D strains are more common than originally thought, but are difficult to detect unless they are strongly partitioned into their dip-slip and strike-slip components. Although, developed during separate deformational events, the similarity in the orientation of structures at Eyemouth (Wenlock) and the Isle of Man and Courtown (Acadian) is remarkable. This perhaps indicates that the orientation of the strain axes across the region were relatively stable for some considerable time and that pre-existing basement structures may exert a strong controlling influence on the orientation of subsequent deformational events. Furthermore, the similarity in the style and variety of structures preserved within the multilayer sequences either side of the suture suggests that the deformation mechanism responsible is process driven and is not peculiar to the Iapetus Suture Zone, but may be a common feature of multi-layered sequences in regions that have been deformed during strain-partitioned transpression.

References cited in text

Alsop, G. I. & Holdsworth, R. E. 1999. Vergence and facing patterns in large-scale sheath folds. *Journal of Structural Geology*, **21**, 1335 - 1349.

Anderson, T. B. 1987. The onset and timing of Caledonian sinistral shear in County Down. *Journal of the Geological Society, London*, **144**, 817 - 825.

Anderson, T. B. & Oliver, G. J. H. 1986. The Orlock Bridge Fault: a major late Caledonian sinistral fault in the Southern Uplands Terrane, British Isles. *Transactions of the Royal Society of Edinburgh: Earth Sciences*, **77**, 203 - 222.

Armstrong, H. A. & Owen, A. W. 2001. Terrane evolution of the paratectonic Caledonides of northern Britain. *Journal of the Geological Society, London*, **158**, 475 - 486.

Armstrong, H. A., Owen, A. W., Scrutton, C. T., Clarkson, E. N. K. & Taylor, C. M. 1996. Evolution of the Northern Belt, Southern Uplands: implications for the Southern Uplands controversy. *Journal of the Geological Society, London*, **153**, 197 -205.

B. G. S. 2001. Isle of Man, solid and drift geology. 1:50 000 map series. British Geological Survey, Nottingham.

Barnes, R. P., Anderson, T. B. & McCurry, J. A. 1987. Along-strike variation in the stratigraphical and structural profile of the Southern Uplands Central Belt in Galloway and Down. *Journal of the Geological Society, London*, **144**, 807 - 816.

Barnes, R. P., Lintern, B. C. & Stone, P. 1989. Timing and regional implications of deformation in the Southern Uplands of Scotland. *Journal of the Geological Society, London*, **146**, 905 - 908.

Barnes, R. P., Power, G. M. & Cooper, D. M. 1999. The definition of sandstone-bearing formations in the Isle of Man and correlation with adjacent areas - evidence from sandstone geochemistry. *In*: Woodcock, N. H., Quirk, D. G., Fitches, W. R. & Barnes, R. P. (eds) *In Sight of the Suture: the Palaeozoic geology of the Isle of Man in its Iapetus Ocean context.* Geological Society, London, Special Publication, **160**, 139 - 154.

Barnes, R. P. & Stone, P. 1999. Trans-Iapetus contrasts in the geological development of southern Scotland (Laurentia) and the Lakesman Terrane (Avalonia). *In*: Woodcock, N. H., Quirk, D. G., Fitches, W. R. & Barnes, R. P. (eds) *In Sight of the Suture: the Palaeozoic geology of the Isle of Man in its Iapetus Ocean context.* Geological Society, London, Special Publication, **160**, 307 - 323.

Bell, A. M. 1981. Vergence: an evaluation. *Journal of Structural Geology*, **3**, 197 - 202.

Berthé, D., Choukroune, P. & Jegouzo, P. 1979. Orthogneiss, mylonite and non-coaxial deformation of granites: the example of the South Armorican Shear-zone. *Journal of Structural Geology*, **1**, 31-42.

Blake, J. F. 1905. On the order of succession of the Manx Slates. *Quarterly Journal of the Geological Society, London*, **61**, 358 - 373.

Bluck, B. J., Gibbons, W. & Ingham, J. K. 1992. Terranes. *In*: Cope, J. W. C., Ingham, J. K. & Rawson, P. F. (eds) *Atlas of Palaeogeography and Lithofacies.* Geological Society, London, Memoirs, **13**, 1 - 4.

Borradaile, G. J. 1978. Transected folds: a study illustrated with examples from Canada and Scotland. *Bulletin of the Geological Society of America*, **89**, 481 - 493.

Branney, M. J. & Soper, N. J. 1988. Ordovician volcanotectonics in the English Lake District. *Journal of the Geological Society, London*, **145**, 367 - 376.

Brenchely, P. J. & Treagus, J. E. 1970. The Stratigraphy and Structure of the Ordovician Rocks Between Courtown and Kilmichael Point, Co. Wexford. *Proceedings of the Royal Irish Academy*, **69 B**, 83-102.

Brewer, J. A., Matthews, D. H., Warner, M. R., Hall, J., Smythe, D. K. & Whittington, R. J. 1983. BIRPS deep seismic reflection studies of the British Caledonides. *Nature*, **305**, 206 - 210.

Brück, P. M., Colthurst, J. R. J., Feely, M., Gardiner, P. R. R., Penney, S. R., Reeves, T. J., Shannon, P. M., Smith, D. G. & Vanguestaine, M. 1979. South-east Ireland: Lower Palaeozoic stratigraphy and depositional history. *In*: Harris, A. L., Holland, C. H. & Leake, B. E. (eds) *The Caledonides of the British Isles - reviewed.* Geological Society, London, Special Publication, **8**, 533 - 544.

Burnett, D. J. 1999. The stratigraphy, geochemistry and provenance of the Lower Palaeozoic Manx Group, Isle of Man, Unpublished PhD thesis, Oxford Brookes University.

Carreras, J., Estrada, A. & White, S. H. 1977. The effect of folding on the *c*-axis of a quartz mylonite. *Tectonophysics*, **39**, 3-24.

Chadwick, R. A., Jackson, D. I., Barnes, R. P., Kimbell, G. S., Johnson, H., Chiverrell, R. C., Thomas, G. S. P., Jones, N. S., Riley, N. J., Pickett, E. A., Young, B., Holliday, D. W., Ball, D. F., Molyneux, S. G., Long, D., Power, G. M. & Roberts, D. H. 2001. Geology of the Isle of Man and its offshore area. Research Report RR/01/06. British Geological Survey, Keyworth. 144 pp

Cocks, L. R. M. & Fortey, R. A. 1982. Faunal evidence for oceanic separations in the Palaeozoic of Britain. *Journal of the Geological Society, London*, **139**, 467 - 480.

Cooper, A. H., Rushton, A. W. A., Molyneux, S. G., Hughes, R. A., Moore, R. M. & Webb, B. C. 1995. The stratigraphy, correlation, provenance and palaeogeography of the Skiddaw Group (Ordovician) in the English Lake District. *Geological Magazine*, **132**, 185 - 211.

Cooper, M. A. & Brück, P. M. 1983. Tectonic relationships of the Leinster Granite, Ireland. *Geological Journal*, **18**, 351-360.

Crimes, T. P. & Crossley, J. D. 1968. The Stratigraphy, Sedimentology, Ichnology and Structure of the Lower Palaeozoic Rocks of Part of North-Eastern Co. Wexford. *Proceedings of the Royal Irish Academy*, **67 B**, 185-215.

Curtis, M. L. 1993. The structural and kinematic evolution of an upper crustal transpression zone: The Lusitanian Basin, Portugal. Unpublished PhD thesis, University of Durham.

Curtis, M. L. 1998. Development of kinematic partitioning within a pure-shear dominated dextral transpression zone: the southern Ellsworth Mountains, Antarctica. *In*: Holdsworth, R. E., Strachan, R. A. & Dewey, J. F. (eds) *Continental Transpressional and Transtensional Tectonics.* Geological Society, London, Special Publication, **135**, 289 - 306.

Dearman, W. R., Shiells, K. A. G. & Larwood, G. P. 1962. Refolded folds in the Silurian rocks of Eyemouth, Berwickshire. *Proceedings of the Yorkshire Geological Society*, **33**, 273 - 286.

Dewey, J. F. 1969. Evolution of the Caledonian-Appalachian Orogen. *Nature,* **222**, 124 - 129.

Dewey, J. F. 1982. Plate tectonics and the evolution of the British Isles. *Journal of the Geological Society, London*, **139**, 371 - 412.

Dewey, J. F., Holdsworth, R. E. & Strachan, R. A. 1998. Transpression and Transtension zones. *In*: Holdsworth, R. E., Strachan, R. A. & Dewey, J. F. (eds) *Continental Transpressional and Transtensional Tectonics*. Geological Society, London, Special Publication, **135**, 1 - 14.

Dewey, J. F., Holdsworth, R. E. & Strachan, R. A. 1999. Reply to discussion on transpression and transtension zones. *Journal of the Geological Society, London*, **156**, 1048 - 1050.

Dewey, J. F. & Shackleton, R. M. 1984. A model for the evolution of the Grampian tract in the early Caledonides and Appalachians. *Nature,* **312**, 115 - 121.

Dias, R. & Ribeiro, A. 1994. Constriction in a transpressive regime: an example in the Iberian branch of the Ibero-Armorican arc. *Journal of Structural Geology*, **16**, 1543 - 1554.

Dubey, A. K. & Cobbold, P. R. 1977. Noncylindrical flexural slip folds in nature and experiment. *Tectonophysics*, **38**, 223 - 239.

Dutton, B. J. 1997. Finite strains in transpression zones with no boundary slip. *Journal of Structural Geology*, **19**, 1189 - 1200.

Fitch, T. J. 1972. Plate convergence, transcurrent faults and internal deformation adjacent to Southeast Asia and the Western Pacific. *Journal of Geophysical Research*, **77**, 4432 - 4460.

Fitches, W. R., Barnes, R. P. & Morris, J. H. 1999. Geological structure and tectonic evolution of the Lower Palaeozoic rocks of the Isle of Man. *In*: Woodcock, N. H., Quirk, D. G., Fitches, W. R. & Barnes, R. P. (eds) *In Sight of the Suture: the Geology of the Isle of Man in its Iapetus Ocean Context.* Geological Society, London, Special Publication, **160**, 259 - 287.

Flinn, D. 1962. On folding during three-dimensional progressive deformation. *Quarterly Journal of the Geological Society, London*, **118**, 385 - 433.

Ford, T. D. 1972. Slump structures in the Peel Sandstones Series, Isle of Man. *Isle of Man Natural History and Antiquarian Journal*, **VII**, 440 - 448.

Ford, T. D. 1993. The Isle of Man. Geologists' Association Guide No. 46. The Geologists' Association. 94 pp

Ford, T. D., Burnett, D. & Quirk, D. 2001. The Geology of the Isle of Man. Geologists' Association Guide No. 46. Geologists' Association, London. 92 pp

Fossen, H. & Tikoff, B. 1993. The deformation matrix for simultaneous simple shearing, pure shearing and volume change, and its application to transpression tectonics. *Journal of Structural Geology*, **15**, 413 - 422.

Fossen, H., Tikoff, B. & Teyssier, C. T. 1994. Strain modelling of transpressional and transtensional deformation. *Norsk Geologisk Tidsskrifti*, **74**, 134 - 145.

Gallagher, V., O'Connor, P. J. & Aftalion, M. 1994. Intra-Ordovician deformation in southeast Ireland: evidence from the geological setting, geochemical affinities and U-Pb zircon age of the Croghan Kinshelagh granite. *Geological Magazine*, **131**, 669 - 684.

Gardiner, P. P. R. 1975. Plate tectonics and the evolution of the southern Irish Caledonides. *Scientific Proceedings of the Royal Dublin Society*, **A5**, 385 - 396.

Gardiner, P. R. R. 1970. Regional fold structures in the Lower Palaeozoics of south-east Ireland. *Bulletin of the Geological Survey Ireland*, **1**, 47 - 51.

Gardiner, P. R. R. 1974. The Duncannon Group: An Upper Ordovician unit in south-west County Wexford. *Bulletin of the Geological Survey Ireland*, **1**, 429 - 446.

Gardiner, P. R. R. & Vanguestaine, M. 1971. Cambrian and Ordovician microfossils from south east Ireland and their implications. *Bulletin of the Geological Survey of Ireland*, **1**, 163 - 210.

Gary, M., McAfee, R. & Wolf, C. L. 1972. Glossary of Geology. American Geological Institute, Washington D.C.

Geikie, A. 1863. The Geology of eastern Berwickshire. Memoir of the Geological Survey, Scotland, London. 58 pp

Gibbons, W., Gayer, R. A. & Vogel, A. 1985. British Caledonian terranes. *In*: Gayer, R. A. (eds) *The tectonic evolution of the Caledonide-Appalachian Orogen.* Vieweg & Sohn, Braunshweig, 3 - 16.

Gibbons, W., Tietzsch-Tyler, D., Horak, J. M. & Murphy, F. C. 1994. Precambrian rocks in Anglesey, southwest Llyn and southeast Ireland. *In*: Gibbons, W. & Harris, A. L. (eds) *A revised correlation of Precambrian rocks in the British Isles.* Geological Society of London, London, Special Report, **22**, 75 - 84.

Gillott, J. E. 1956. Structural geology of the Manx Slates. *Geological Magazine*, **93**, 301 - 313.

Goodwin, L. B. & Williams, P. F. 1996. Deformation path partitioning within a transpressive shear zone, Marble Cove, Newfoundland. *Journal of Structural Geology*, **18**, 975-990.

Greig, D. C. 1988. Geology of the Eyemouth District. Memoir for 1:50 000 geology sheet 34 (Scotland). British Geological Survey, Keyworth. 78 pp

Hall, J., Brewer, J. A., Matthews, D. H. & Warner, M. R. 1984. Crustal structure across the Caledonides from the 'WINCH' seismic reflection profile: influences on the evolution of the Midland Valley of Scotland. *Transactions of the Royal Society of Edinburgh*, **75**, 97 - 109.

Hambrey, M. J. 1985. The Late Ordovician-Early Silurian glacial period. *Palaeogeography, Palaeoclimatology, Palaeoecology*, **51**, 273 - 289.

Hancock, P. L. 1985. Brittle microtectonics - principles and practice. *Journal of Structural Geology*, **7**, 437 - 457.

Hanmer, S. & Passchier, C. 1991. Shear-sense indicators: a review. Geological Survey of Canada, 72 pp.

Harding, T. P. 1973. The Newport-Inglewood trend, California - an example of wrenching style of deformation. *American Association of Petroleum Geologists Bulletin*, **58**, 97 - 116.

Harding, T. P. 1974. Petroleum traps associated with wrench faults. *American Association of Petroleum Geologists Bulletin*, **58**, 1290 - 1304.

Harland, W. B. 1971. Tectonic transpression in Caledonian Spitsbergen. *Geological Magazine*, **108**, 27 - 42.

Holdsworth, R. E. 1988. The stereographic analysis of facing. *Journal of Structural Geology*, **10**, 219-223.

Holdsworth, R. E. 1989. The geology and structural evolution of a Caledonian fold and ductile thrust zone, Kyle of Tongue region, Sutherland, N. Scotland. *Journal of the Geological Society, London*, **146**, 809 - 823.

Holdsworth, R. E. 1994. Structural evolution of the Gander-Avalon terrane boundary: a reactivated transpression zone in the NE Newfoundland Appalachians. *Journal of the Geological Society, London*, **151**, 629-646.

Holdsworth, R. E. & Pinheiro, R. V. L. 2000. The anatomy of shallow-crustal transpressional structures: insights from the Archaean Carajás fault zone , Amazon, Brazil. *Journal of Structural Geology*, **22**, 1105 - 1123.

Holdsworth, R. E. & Strachan, R. A. 1991. Interliked system of ductile strike slip and thrusting formed by Caledonian transpression in northeastern Greenland. *Geology*, **19**, 510 - 513.

Holdsworth, R. E., Tavarnelli, E., Clegg, P. 2002a. The nature and regional significance of structures in the Gala Group of the Southern Uplands terrane, Berwickshire coast, southeastern Scotland. *Geology Magazine,* **139,** (in press).

Holdsworth, R. E., Tavarnelli, E., Clegg, P., Pinheiro, R. V. L., Jones, R. R. & McCaffrey, K. J. W. 2002b. Domainal deformation patterns and strain partitioning during transpression: an example from the Southern Uplands terrane, Scotland. *Journal of the Geological Society, London*, **159**, 401 - 415.

Holdsworth, R. E., Woodcock, N. H. & Strachan, R. A. 2000. Geological framework of Britain and Ireland. *In*: Woodcock, N. H. & Strachan, R. A. (eds) *Geological History of Britain and Ireland.* Blackwell Science, London, 19 - 37.

Howe, M. P. A. 1999. The Silurian fauna (graptolite and nautiloid) of the Niarbyl Formation, Isle of Man. *In*: Woodcock, N. H., Quirk, D. G., Fitches, W. R. & Barnes, R. P. (eds) *In Sight of the Suture: the Palaeozoic geology of the Isle of Man in its Iapetus Ocean context.* Geological Society, London, Special Publication, **160**, 177 - 187.

Hutton, D. H. W. & Murphy, F. C. 1987. The Silurian of the Southern Uplands and Ireland as a successor basin to the end Ordovician closure of Iapetus. *Journal of the Geological Society, London*, **144**, 765 - 772.

Jiang, D., Lin, S. & Williams, P. F. 2001. Deformation path in high-strain zones, with reference to slip partitioning in transpressional plate boundary regions. *Journal of Structural Geology*, **23**, 991 - 1005.

Johnson, T. E. 1991. Nomenclature and geometric classification of cleavage-transected folds. *Journal of Structural Geology*, **13**, 261 - 274.

Jones, R., Clegg, P., Holdsworth, R. E., Tavarnelli, E., McCaffrey, K. J. W. & Pinheiro, R. 2001. Modelling strain partitioning in inclined transpression zones. EUG XI *Journal of Conference Abstracts* **6**.

Jones, R. R. & Holdsworth, R. E. 1998. Oblique simple shear in transpression zones. *In*: Holdsworth, R. E., Strachan, R. A. & Dewey, J. F. (eds) *Continental Transpressional and Transtensional Tectonics*. Geological Society, London, Special Publication, **135**, 35 - 40.

Jones, R. R., Holdsworth, R. E. & Bailey, W. 1997. Lateral extrusion in transpression zones: the importance of boundary conditions. *Journal of Structural Geology*, **19**, 1201 - 1217.

Jones, R. R. & Tanner, G. P. W. 1995. Strain partitioning in transpression zones. *Journal of Structural Geology*, **17**, 793 - 802.

Kelley, S. & Bluck, B. J. 1989. Detrital mica ages from the Southern Uplands using Ar-AR laser probe. *Journal of the Geological Society, London*, **146**, 401 - 403.

Kelley, S. & Bluck, B. J. 1990. Discussion on detrital mica ages from the Southern Uplands using Ar-Ar laser probe. *Journal of the Geological Society, London*, **147**, 882 - 884.

Kemp, A. E. S. 1987. Tectonic development of the Southern Belt of the Southern Uplands accretionary complex. *Journal of the Geological Society, London*, **144**, 827 - 838.

Kemp, A. E. S., Oliver, G. J. H. & Baldwin, J. R. 1985. Low-grade metamorphism and accretion tectonics; Southern Uplands Terrane, Scotland. *Mineralogical Magazine*, **49**, 335 - 344.

Kennan, P. S. & Kennedy, M. J. 1983. Coticule - a key to correlation along the Appalachian - Caledonide Orogen. *In*: Schenk, P. (ed) *Regional trends in the geology of the Appalachian - Caledonide - Hercynian - Mauritamide Orogen*. Reidel, Dordrecht, 355 - 361, .

Kennan, P. S. & Morris, J. H. 1999. Manganiferous ironstones in the early Ordovician Manx Group, Isle of Man: a protolith of coticule? *In*: Woodcock, N. H., Quirk, D. G., Fitches, W. R. & Barnes, R. P. (eds) *In Sight of the Suture: the Palaeozoic geology of the Isle of Man in its Iapetus Ocean context*. Geological Society, London, Special Publication, **160**, 109 - 119.

Kimbell, G. S. & Quirk, D. G. 1999. Crustal magnetic structure of the Irish Sea region: evidence for a major basement boundary beneath the Isle of Man. *In*: Woodcock, N. H., Quirk, D. G., Fitches, W. R. & Barnes, R. P. (eds) *In Sight of the Suture: the Palaeozoic geology of the Isle of Man in its Iapetus Ocean context*. Geological Society, London, Special Publication, **160**, 227 - 238.

Kinahan, G. H. 1879. Explanatory Memoir to accompany sheets 169, 170, 180 and 181 of the Geological Survey of Ireland. Geological Survey Ireland.

Klemperer, S. L. 1989. Seismic reflection evidence for the location of the Iapetus suture west of Ireland. *Journal of the Geological Society, London*, **146**, 409 - 412.

Klemperer, S. L. & Matthews, D. H. 1987. Iapetus suture located beneath the North Sea by BIRPS deep seismic reflection profiling. *Geology*, **15**, 195 - 198.

Kneller, B. C. 1991. A foreland basin on the southern margin of Iapetus. *Journal of the Geological Society, London*, **148**, 207 - 210.

Kneller, B. C., King, L. M. & Bell, A. M. 1993. Foreland basin development and tectonics on the northwest margin of Eastern Avalonian. *Geological Magazine*, **130**, 691 - 697.

Knipe, R. J., Chamberlain, M. I., Page, A. & Needham, D. T. 1988. Structural histories in the SW Southern Uplands, Scotland. *Journal of the Geological Society, London*, **145**, 697 - 684.

Knipe, R. J. & Needham, D. T. 1986. Deformation processes in accretionary wedges; examples from the SW margin of the Southern Uplands, Scotland. *In*: Coward, M. P. & Ries, A. C. (eds) *Collision Tectonics*. Geological Society, London, Special Publication, **19**, 51 - 56.

Kokelaar, P. 1988. Tectonic controls of Ordovician arc and marginal basin volcanism in Wales. *Journal of the Geological Society, London*, **145**, 759 - 775.

Kokelaar, P., Bevins, R. E. & Roach, R. A. 1984. Submarine silicic volcanism and associated sedimentary and tectonic processes, Ramsey Island, SW Wales. *Journal of the Geological Society, Londoni,* **142**, 591 - 613.

Lamplugh, G. W. 1903. The Geology of the Isle of Man. HMSO.

Leggett, J. K. 1987. The Southern Uplands as an accretionary prism: the importance of analogues in reconstructing palaeogeography. *Journal of the Geological Society, London*, **144**, 737 - 752.

Leggett, J. K., McKerrow, W. S. & Eales, M. H. 1979. The Southern Uplands of Scotland: a lower Palaeozoic accretionary prism. *Journal of the Geological Society, London*, **136**, 755 - 770.

Lin, S., Jiang, D. & Williams, P. F. 1998. Transpression (or transtension) zones of triclinic symmetry: natural example and theoretical modelling. *In*: Holdsworth, R. E., Strachan, R. A. & Dewey, J. F. (eds) *Continental Transpressional and Transtensional Tectonics*. Geological Society, London, Special Publication, **135**, 41-57.

Lin, S., Jiang, D. & Williams, P. F. 1999. Discussion on transpression and transtension zones. *Journal of the Geological Society, London*, **156**, 1045 - 1048.

Lintern, B. C., Barnes, R. P. & Stone, P. 1992. Discussion on Silurian and early Devonian sinistral deformation of the Ratagain Granite, Scotland: constraints on the age of Caledonian movements on the Great Glen system. *Journal of the Geological Society, London*, **149**, 858.

Lisle, R. J. 1985. The facing of faults. *Geological Magazine*, **122**, 249 - 251.

MacKenzie, D. H. 1956. A structural profile south of Eyemouth, Berwickshire. *Transactions of the Edinburgh Geological Society*, **16**, 248 - 253.

Max, M. D., Barber, A. J. & Martinez, J. 1990. Terrane Assemblage of the Leinster Massif, SE Ireland, during the Lower Palaeozoic. *Journal of the Geological Society, London*, **147**, 1035 - 1050.

McArdle, P. & Kennedy, M. J. 1985. The East Carlow Deformation Zone and its regional implications. *Bulletin of the Geological Survey of Ireland*, **3**, 237 - 255.

McConnell, B. 2000. The Ordovician volcanic arc and marginal basin of Leinster. *Irish Journal of Earth Sciences*, **18**, 41-49.

McConnell, B. & Morris, J. 1997. Initiation of Iapetus subduction under Irish Avalonia. *Geological Magazine*, **134**, 213 - 218.

McConnell, B., Philcox, M. E., Sleeman, A. G., Stanley, G., Flegg, A. M., Daly, E. P. & Warren, W. P. 1994. Geology of Kildare - Wicklow, a geological description to accompany the Bedrock Geology 1:100 000 Map Series, Sheet 16, Kildare - Wicklow. Geological Survey Ireland. 69 pp

McConnell, B. J., Morris, J. H. & Kennan, P. S. 1999. A comparison of the Ribband Group (southeastern Ireland) to the Manx Group (Isle of Man) and Skiddaw Group (northwestern England). *In*: Woodcock, N. H., Quirk, D. G., Fitches, W. R. & Barnes, R. P. (eds) *In Sight of the Suture; the Palaeozoic geology of the Isle of Man in its Iapetus Ocean context.* Geological Society, London, Special Publication, **160**, 337 - 343.

McKerrow, W. S., Leggett, J. K. & Eales, M. H. 1977. Imbricate thrust model of the Southern Uplands of Scotland. *Nature,* **267**, 237 - 9.

McKerrow, W. S. & Soper, N. J. 1989. The Iapetus suture in the British Isles. *Geological Magazine*, **126**, 1 - 94.

Means, W. D. 1987. A newly recognised type of slickenside striation. *Journal of Structural Geology*, **9**, 585 - 590.

Molnar, P. 1992. Brace-Goetze strength profiles, the partitioning of strike slip and thrust faulting at zones of oblique convergence, and the stress-heat flow paradox of the San Andreas Fault (eds) *Fault mechanics and Transport Properties of Rocks*. Academic Press, 435 - 459.

Molyneux, S. G. 1979. New evidence for the age of the Manx Group, Isle of Man. *In*: Harris, A. L., Holland, C. H. & Leake, B. E. (eds) *The Caledonides of the British Isles - Reviewed.* Geological Society, London, Special Publication, **8**, 415 - 421.

Molyneux, S. G. 1987. Probable early Wenlock acritarchs from the Linkim Beds of the Southern Upland. *Scottish Journal of Geology*, **23**, 301 - 313.

Molyneux, S. G. 1999. A reassessment of Manx Group acritarchs, Isle of Man. *In*: Woodcock, N. H., Quirk, D. G., Fitches, W. R. & Barnes, R. P. (eds) *In Sight of the Suture: the Palaeozoic geology of the Isle of Man in its Iapetus Ocean context.* Geological Society, London, Special Publication, **160**, 23 - 32.

Molyneux, S. G. 2001. Palynology of the Manx Group, Isle of Man. Report CR/01/21. British Geological Survey.

Moody, J. D. 1973. Petroleum exploration aspects of wrench-fault tectonics. *American Association of Petroleum Geologists Bulletin*, **57**, 449 - 476.

Moody, J. D. & Hill, M. J. 1956. Wrench fault tectonics. *Bulletin of the Geological Society of America*, **67**, 1207-1246.

Morris, J. H. 1987. the Northern Belt of the Longford-Down inlier, Ireland and the Southern Uplands, Scotland: an Ordovician back-arc basin. *Journal of the Geological Society, London*, **144**, 773 - 786.

Morris, J. H., Woodcock, N. H. & Howe, M. P. A. 1999. The Silurian succession of the Isle of Man: the late Wenlock Niarbyl Formation, Dalby Group. *In*: Woodcock, N. H., Quirk, D. G., Fitches, W. R. & Barnes, R. P. (eds) *In Sight of the Suture: the Palaeozoic geology of the Isle of Man in its Iapetus Ocean context*. Geological Society, London, **160**, 189 - 211.

Morrison, C. W. K. 1989. A study of the anchizone-epizone metamorphic transition. Unpublished PhD thesis, St Andrews University.

Murphy, F. C. 1985. Non-axial planar cleavage and Caledonian sinistral transpression in eastern Ireland. *Geological Journal*, **20**, 257 - 279.

Murphy, F. C., Anderson, T. B., Daly, J. S., Gallagher, V., Graham, J. R., Harper, D. A. T., Johnston, J. D., Kennan, P. S., Kennedy, M. J., Long, C. B., Morris, J. H., O'Keeffe, W. G., Parkes, M., Ryan, P. D., Sloan, R. J., Stillman, C. J., Tietzsch-Tyler, D., Todd, S. P. & Wrafter, J. P. 1991. An Appraisal of Caledonian Suspect Terranes in Ireland. *Irish Journal of Earth Sciences*, **11**, 11-41.

Nance, R. D., Murphy, J. B., Strachan, R. A., D'Lemos, R. S. & Taylor, G. K. 1991. Late Proterozoic tectonostratigraphic evolution of the Avalonian and Cadomian terranes. *Precambrian Research*, **53**, 41 -78.

Needham, D. T. 1993. The structure of the western part of the Southern Uplands of Scotland. *Journal of the Geological Society, London*, **150**, 341 - 354.

Needham, D. T. & Knipe, R. J. 1986. Accretion- and collision-related deformation in the Southern Uplands accretionary wedge, southwestern Scotland. *Geology*, **14**, 303 - 306.

Needham, T. & Morgan, R. 1997. The East Irish Sea and adjacent basins: new faults or old? *Journal of the Geological Society, Londoni,* **154**, 145 - 150.

Oldow, J. S., Bally, A. W. & Ave Lallemant, H. G. 1990. Transpression, orogenic float and lithospheric balance. *Geology*, **18**, 991-994.

Oliver, G. J. H. & Leggett, J. K. 1980. Metamorphism in an accretionary prism: prehnite-pumpellyite facies metamorphism of the Southern Uplands of Scotland. *Transactions of the Royal Society of Edinburgh: Earth Sciences*, **71**, 235 - 246.

Oliver, G. J. H., Smellie, J. L., Thomas, L. J., Casey, D. M., Kemp, A. E. S., Evans, L. J., Baldwin, J. R. & Hepworth, B. C. 1984. Early Palaeozoic metamorphic history of the Midland Valley, Southern Uplands, Longford-Down massif, and the Lake District British Isles. *Transactions of the Royal Society of Edinburgh: Earth Science*, **75**, 245 -258.

Orr, P. J. & Howe, M. P. A. 1999. Macrofauna and ichnofauna of the Manx Group (early Ordovician), Isle of Man. *In*: Woodcock, N. H., Quirk, D. G., Fitches, W. R. & Barnes, R. P. (eds) *In Sight of the Suture: the Palaeozoic geology of the Isle of Man in its Iapetus Ocean context.* Geological Society, London, Special Publication, **160**, 33 - 44.

Owen, A. W. & Parkes, M. A. 1996. The trilobite *Mucronaspis* in county Wexford: evidence for Ashgill rocks in the Leinster Massif. *Irish Journal of Earth Sciences*, **15**, 123 - 127.

Parkes, M. A. 1994. The brachiopods of the Duncannon Group (Middle - Upper Ordovician) of southeast Ireland. *Bulletin of the Natural History Museum (Geology)*, **50**, 105 - 174.

Passchier, C. W. & Trouw, R. A. J. 1996. Microtectonics. Springer-Verlag, Berlin. 289 pp

Peach, B. N. & Horne, J. 1899. The Silurian Rocks of Britain. Vol. 1, Scotland. Memoir of the Geological Survey, UK.

Petit, J. P. 1987. Criteria for the sense of movement on fault surfaces in brittle rocks. *Journal of Structural Geology*, **9**, 597 - 608.

Phillips, E. R., Barnes, R. P., Boland, M. P., Fortey, N. J. & McMillan, A. A. 1995. The Moniaive Shear Zone: a major zone of sinistral strike-slip deformation in the Southern Uplands of Scotland. *Scottish Journal of Geology*, **31**, 139 - 149.

Phillips, W. E. A., Flegg, A. M. & Anderson, T. B. 1979. Strain adjacent to the Iapetus Suture in Ireland. *In*: Harris, A. L., Holland, C. H. & Leake, B. E. (eds) *The Caledonides of the British Isles-reviewed.* Geological Society, London, Special Publication, **8**, 257 - 262.

Phillips, W. E. A., Stillman, C. J. & Murphy, T. 1976. A Caledonian plate tectonic model. *Journal of the Geological Society, London*, **132**, 579 - 609.

Pickering, K. & Smith, A. G. 1995. Arcs and backarc basins in the Early Palaeozoic Iapetus Ocean. *The Island Arc*, **4**, 1 - 67.

Piper, J. D. A. 1997. Tectonic rotation within the British paratectonic Caledonides and Early Palaeozoic location of the orogen. *Journal of the Geological Society, London*, **154**, 9 - 13.

Piper, J. D. A., Biggin, A. J. & Crowley, S. F. 1999. Magnetic survey of the Poortown Dolerite, Isle of Man. *In*: Woodcock, N. H., Quirk, D. G., Fitches, W. R. & Barnes, R. P. (eds) *In Sight of the Suture: the Palaeozoic geology of the Isle of Man in its Iapetus Ocean context.* Geological Society, London, Special Publication, **160**, 155 -163.

Platt, J. P. 1993. Mechanics of oblique convergence. *Journal of Geophysical Research*, **98**(B9), 16239 - 16256.

Powell, C. M. A. 1974. Timing of slatey cleavage during folding of Precambrian rocks, northwest Tasmania. *Bulletin of the Geological Society of America*, **85**, 1043 - 1060.

Power, G. M. & Barnes, R. P. 1999. Relationships between metamorphism and structure on the northern edge of eastern Avalonia in the Manx Group, Isle of Man. *In*: Woodcock, N. H., Quirk, D. G., Fitches, W. R. & Barnes, R. P. (eds) *In Sight of the Suture: the Palaeozoic geology of the Isle of Man in its Iapetus Ocean context*. Geological Society, London, Special Publication, **160**, 289 - 305.

Power, G. M. & Crowley, S. F. 1999. Petrological and geochemical evidence for the tectonic affinity of the (?)Ordovician Poortown Basic Intrusive Complex, Isle of Man. *In*: Woodcock, N. H., Quirk, D. G., Fitches, W. R. & Barnes, R. P. (eds) *In Sight of the Suture: the Palaeozoic geology of the Isle of Man in its Iapetus Ocean context*. Geological Society, London, Special Publication, **160**, 165 - 175.

Pratt, W. T. & Fitches, W. R. 1993. Transected folds from the western part of the Bala Lineament, Wales. *Journal of Structural GeologyI*, **15**, 55 - 68.

Quirk, D. G. & Burnett, D. J. 1999a. Lithofacies of Lower Palaeozoic deep marine sediments in the Isle of Man: a new map and stratigraphic model of the Manx Group. *In*: Woodcock, N. H., Quirk, D. G., Fitches, W. R. & Barnes, R. P. (eds) *In Sight of the Suture: the Geology of the Isle of Man in its Iapetus Ocean Context*. Geological Society, London, Special Publication, **160**, 69 - 88.

Quirk, D. G. & Burnett, D. J. 1999b. Lithofacies of Lower Palaeozoic deep marine sediments in the Isle of Man: classification scheme. *In*: Woodcock, N. H., Quirk, D. G., Fitches, W. R. & Barnes, R. P. (eds) *In Sight of the Suture: the Geology of the Isle of Man in its Iapetus Ocean Context*. Geological Society, London, Special Publication, **160**, 69 - 88.

Quirk, D. G., Burnett, D. J., Kimbell, G. S., Murphy, C. A. & Varley, J. S. 1999. Shallow geophysical and geological evidence for a regional-scale fault duplex in the Lower Palaeozoic of the Isle of Man. *In*: Woodcock, N. H., Quirk, D. G., Fitches, W. R. & Barnes, R. P. (eds) *In Sight of the Suture: the Geology of the Isle of Man in its Iapetus Ocean Context.* Geological Society, London, Special Publication, **160**, 239 - 257.

Quirk, D. G. & Kimbell, G. S. 1997. Structural evolution of the Isle of Man and central part of the Irish Sea. *In*: Meadows, N. S., Trueblood, S. P., Hardman, M. & Cowan, G. (eds) *Petroleum Geology of the Irish Sea and Adjacent Areas.* Geological Society, London, Special Publication, **124**, 135 - 159.

Quirk, D. G., Roy, S., Knott, I., Redfern, J. R. & Hill, L. 1999b. Petroleum geology and future hydrocarbon potential of the Irish Sea. *Journal of Petroleum Geology*, **22**, 243 - 260.

Ramsay, J. G. 1967. The Folding and Fracturing of Rocks. McGraw-Hill, New York.

Ramsay, J. G. 1974. Development of chevron folds. *Bulletin of the Geological Society of America*, **85**, 1741 - 1754.

Ramsay, J. G. 1980. Shear zone geometry: a review. *Journal of Structural Geology*, **2**, 83-89.

Ramsay, J. G. & Graham, R. M. 1970. Strain variation in shear belts. *Canadian Journal of Earth Sciences*, **7**, 786 - 813.

Ramsay, J. G. & Huber, M. I. 1983. The techniques of modern structural geology, Volume 1; Strain analysis. Academic Press, London. 307 pp

Ramsay, J. G. & Huber, M. I. 1987. The techniques of modern structural geology; Volume 2; Folds and fractures. Academic Press, London. 462 pp

Roberts, B., Morrison, C. W. K. & Hirons, S. 1990. Low grade metamorphism of the Manx Group, Isle of Man: a comparative study of white mica 'crystallinity' techniques. *Journal of the Geological Society, London*, **147**, 271 - 277.

Roberts, J. L. 1974. The structure of the Dalradian rocks in the SW Highlands of Scotland. *Journal of the Geological Society, London*, **130**, 93 - 124.

Robin, P.-Y. F. & Cruden, A. R. 1994. Strain and vorticity patterns in ideally ductile transpression zones. *Journal of Structural Geology*, **16**, 447-466.

Roper, H. 1997. Origins of the "Berwick Monocline"; geometrical and geophysical considerations. *Scottish Journal of Geology*, **33**, 133 - 148.

Rushton, A. W. A. 1993. Graptolites from the Manx Group. *Proceedings of the Yorkshire Geological Society*, **46**, 259 - 262.

Rushton, A. W. A. 1996. *Trichograptus* from the Lower Arenig of Kiltrea, County Wexford. *Irish Journal of Earth Sciences*, **15**, 61 - 69.

Rushton, A. W.A., Stone, P. & Hughes, R. A. 1996. Biostratigraphical control of the thrust models for the Southern Uplands of Scotland. *Transactions of the Royal Society of Edinburgh: Earth Sciences* **86,** 137 - 152.

Sample, J. C. & Moore, J. C. 1987. Structural style and kinematics of an underplated slate belt, Kodiak and adjacent islands, Alaska. *Bulletin of the Geological Society of America,* **99**, 7 - 20.

Sanderson, D. J., Andrews, J. R., Phillips, W. E. A. & Hutton, D. H. W. 1980. Deformation studies in the Irish Caledonides. *Journal of the Geological Society, London*, **137**, 289 - 302.

Sanderson, D. J. & Marchini, W. R. D. 1984. Transpression. *Journal of Structural Geology*, **6**, 449 - 458.

Shackelton, R. M. 1957. Downward-facing structures of the Highland Border. *Quarterly Journal of the Geological Society, London*, **113**, 361 - 392.

Sheills, K. A. G. & Dearman, W. R. 1966. On the possible occurrence of Dalradian rocks in the Southern Uplands of Scotland. *Scottish Journal of Geology*, **2**, 231 - 242.

Simpson, A. 1963. The stratigraphy and tectonics of the Manx Slate Series, Isle of Man. *Quarterly Journal of the Geological Society, London*, **119**, 367 - 400.

Simpson, A. 1964. The metamorphism of the Manx slate Series, Isle of Man. *Geological Magazine*, **101**, 21 - 36.

Simpson, A. 1965. F1 Cross folding in the Manx slate Series, Isle of Man. *Geological Magazine*, **102**, 440 - 444.

Simpson, A. 1968. The Caledonian history of the north eastern Irish Sea region and its relation to surrounding areas. *Scottish Journal of Geology*, **4**, 135 - 163.

Simpson, C. & Schmid, S. M. 1983. An evaluation of criteria to deduce the sense of movement in sheared rocks. *Bulletin of the Geological Society of America*, **94**, 1281-1288.

Smith, R. A., Phillips, E. R., Floyd, J. D., Barron, H. F. & Picket, E. A. 2001. The Northern Belt 100 years on: a revised model of the Ordovician tracts near Leadhills, Scotland. *Transactions of the Royal Society of Edinburgh: Earth Sciences*, **91**, 421 - 434.

Soper, N. J. 1986. Geometry of transecting, anastomosing solution cleavage in transpression zones. *Journal of Structural Geology*, **8**, 937 - 940.

Soper, N. J. 1988. Timing and geometry of collision, terrane accretion and sinistral strike-slip events in the British Caledonides. *In*: Harris, A. L. & Fettes, D. J. (eds) *The Caledonian-Appalachian Orogen*. Geological Society, London, Special Publication, **38**, 481 - 492.

Soper, N. J., England, R. W., Snyder, D. B. & Ryan, P. D. 1992a. The Iapetus suture zone in England, Scotland and eastern Ireland: a reconciliation of geological and deep seismic data. *Journal of the Geological Society, London*, **149**, 697 - 700.

Soper, N. J. & Hutton, D. H. W. 1984. Late Caledonian sinistral displacements in Britain: implications for a three-plate collision model. *Tectonics*, **3**, 781 - 794.

Soper, N. J., Strachan, R. A., Holdsworth, R. E., Gayer, R. A. & Greiling, R. O. 1992b. Sinistral transpression and the Silurian closure of Iapetus. *Journal of the Geological Society, London*, **149**, 871 - 880.

Soper, N. J., Webb, B. C. & Woodcock, N. H. 1987. Late Caledonian (Acadian) transpression in north-west England: timing, geometry and geotectonic significance. *Proceedings of the Yorkshire Geological Society*, **46**, 175 - 192.

Soper, N. J. & Woodcock, N. H. 1990. Silurian collision and sediment dispersal patterns in southern Britain. *Geology Magazine*, **127**, 527 - 542.

Stille, H. 1924. Grundfragen der Vergleichenden Tektonik. Gerbrüder Borntraeger, Berlin.

Stone, P. 1995. Geology of the Rhins of Galloway district, Memoir of the British Geological Survey, Sheets 1 & 3 (Scotland).

Stone, P. 1996. Geology in south-west Scotland: an excursion guide. British Geological Survey, Keyworth, Nottingham, 214 pp.

Stone, P., Cooper, A. H. & Evans, J. A. 1999. The Skiddaw Group (English Lake District) reviewed: early Palaeozoic sedimentation and tectonism at the northern margin of Avalonia. *In*: Woodcock, N. H., Quirk, D. G., Fitches, W. R. & Barnes, R. P. (eds) *In Sight of the Suture: the Palaeozoic geology of the Isle of Man in its Iapetus Ocean context.* Geological Society, London, Special Publication, **160**, 325 - 336.

Stone, P., Floyd, J. D. & Barnes, R. P. 1987. A sequential back-arc and foreland basin thrust duplex model for the Southern Uplands of Scotland. *Journal of the Geological Society, London*, **144**, 753 - 764.

Stone, P., Kimbell, G. S. & Henney, P. J. 1997. Basement control on the location of strike-slip shear in the Southern Uplands of Scotland. *Journal of the Geological Society, London*, **154**, 141 - 144.

Strachan, R. A. 2000. Mid-Ordovician to Silurian sedimentation and tectonics on the northern active margin of Iapetus. *In*: Woodcock, N. H. & Strachan, R. R. (eds) *Geological history of Britain and Ireland.* Blackwell Science, London, 107 - 123.

Strachan, R. A., Holdsworth, R. E., Friderichsen, J. D. & Jepsen, H. F. 1992. Regional Caledonian structure within an oblique convergence zone, Dronning Louise Land, NE Greenland. *Journal of the Geological Society, London*, **149**, 359-371.

Stringer, P. & Treagus, J. E. 1980. Non-axial planar S1 cleavage in the Hawick rocks of the Galloway area, Southern Uplands, Scotland. *Journal of Structural Geology*, **2**, 317 - 331.

Tavarnelli, E. 1998. Tectonic evolution of the Northern Salinian Block, California, USA: Paleogene to recent shortening in a transform fault-bounded continental fragment. *In*: Holdsworth, R. E., Strachan, R. A. & Dewey, J. F. (eds) *Continental Transpressional and Transtensional Tectonics.* Geological Society, London, Special Publication, **135**, 107- 118.

Tavarnelli, E. & Holdsworth, R. E. 1999. How long do structures take to form in transpression zones? A cautionary tale from California. *Geology*, **21**, 1063 - 1066.

Teyssier, C., Tikoff, B. & Markley, M. 1995. Oblique plate motion and continental tectonics. *Geology*, **23**, 447 - 450.

Tietzsch-Tyler, D. 1989. The Lower Palaeozoic geology of SE. Ireland: A revaluation. *Annual Review, Irish Association for Economic Geology*, 112-119.

Tietzsch-Tyler, D. 1996. Precambrian and Early Caledonian Orogeny in south-east Ireland. *Irish Journal of Earth Sciences*, **15**, 19-39.

Tietzsch-Tyler, D. & Phillips, E. 1989. Correlation of the Monian Supergroup in Anglesey with the Cahore Group in south east Ireland: Extended Abstract. *Journal of the Geological Society, London*, **146**, 417 - 418.

Tietzsch-Tyler, D., Sleeman, A. G., Boland, M., Daly, E., O'Connor, P. & Warren, W. P. 1994a. Geology of South Wexford, a geological description of South Wexford and adjoining parts of Waterford, Kilkenny and Carlow to accompany the Bedrock Geology 1:100 000 scale map series, Sheet 23, South Wexford. Geological Survey Ireland. 62 pp

Tietzsch-Tyler, D., Sleeman, A. G., McConnell, B. J., Daly, E. P., Flegg, A. M., O'Connor, J. J., Philcox, M. E. & Warren, W. P. 1994b. Geology of Carlow - Wexford, a geological description to accompany the Bedrock Geology 1:100 000 scale map series, sheet 19, Carlow - Wexford. Geological Survey Ireland. 56 pp

Tikoff, B. & Fossen, H. 1993. Simultaneous pure and simple shear: the unifying deformation matrix. *Tectonophysics*, **217**, 267 - 283.

Tikoff, B. & Greene, D. 1997. Stretching lineations in transpressional shear zones: an example from the Sierra Nevada batholith, California. *Journal of Structural Geology*, **19**, 29 - 39.

Tikoff, B. & Teyssier, C. 1994. Strain modelling of displacement-field partitioning in transpressional orogens. *Journal of Structural Geology*, **16**, 1575 - 1588.

Tjia, H. D. 1971. Fault movement, reoriented stress field and subsidiary structures. *Pacific Geology*, **5**, 49-70.

Todd, S. P., Murphy, F. C. & Kennan, P. S. 1991. On the trace of the Iapetus suture in Ireland and Britain. *Journal of the Geological Society, London* **148**, 869 - 880.

Torsvik, T. H., Smethurst, M. A., Meert, J. G., Van der Voo, R., McKerrow, W. S., Brasier, M. D., Sturt, B. A. & Walderhaug, H. J. 1996. Continental Break-up and collision in the Neoproterozoic and Palaeozoic: A tale of Baltica and Laurentia. *Earth-Science Reviews*, **40**, 229-258.

Torsvik, T. H., Trench, A., Svensson, I. & Walderhaug, H. J. 1993. Palaeogeographic significance of mid-Silurian palaeomagnetic results from southern Britain - major revision of the apparent polar wander path for Eastern Avalonia. *Geophysics Journal International*, **113**, 651 - 668.

Treagus, J. E. 1992. Caledonian Structures. In: Caledonian Structures in Britain: south of the Midland Valley . (ed. Treagus J. E.), Chapman & Hall, London, 177 pp.

Treagus, J. E. & Treagus, S. H. 1981. Folds and the strain ellipsoid: a general model. *Journal of Structural Geology*, **3**, 1 - 17.

Treagus, S. H. & Treagus, J. E. 1992. Transected folds and transpression : how are they related? *Journal of Structural Geology*, **14**, 371 - 367.

Tremlett, W. E. 1959. The structure of the Lower Palaeozoic rocks of the Arklow District, Ireland. *Quarterly Journal of the Geological Society, London*, **115**, 17 - 40.

Turner, J. P. 1997. Strike-slip fault reactivation in the Cardigan Bay basin. *Journal of the Geological Society, London*, **154**, 5 - 8.

Twiss, R. J. & Moores, E. M. 1992. Structural Geology. W.H. Freeman & Co., New York. 532 pp

Weijermars, R. 1991. The role of stress in ductile deformation. *Journal of Structural Geology*, **13**, 1061-1078.

White, S. H., Burrows, S. E., Carreras, J., Shaw, N. D. & Humphreys, F. J. 1980. On Mylonites in ductile shear zones. *Journal of Structural Geology*, **2**, 175 - 187.

Wilcox, R. E., Harding, T. P. & Seely, D. R. 1973. Basic wrench tectonics. *American Association of Petroleum Geologists Bulletin*, **57**, 74 - 96.

Wilson, J. T. 1966. Did the Atlantic close and the reopen? *Nature,* 676 - 681.

Woodcock, N. H. 1984. The Pontesford Lineament, Welsh Borderland. *Journal of the Geological Society, London*, **141**, 1001 - 1014.

Woodcock, N. H. 1990. Transpressive Acadian deformation across the Central Wales Lineament. *Journal of Structural Geology*, **12**, 329 - 337.

Woodcock, N. H. 2000a. Ordovician volcanism and sedimentation on Eastern Avalonia. *In*: woodcock, N. H. & Strachan, R. A. (eds) *Geological history of Britain and Ireland.* Blackwell Science, London, 153 -167.

Woodcock, N. H. 2000b. Late Ordovician to Silurian evolution of Eastern Avalonia during convergence with Laurentia. *In*: Woodcock, N. H. & Strachan, R. A. (eds) *Geological history of Britain and Ireland.* Blackwell Science, London, 168 - 184.

Woodcock, N. H. & Barnes, R. P. 1999. An early Ordovician turbidite system on the Gondwana margin: the southeastern Manx Group, Isle of Man. *In*: Woodcock, N. H., Quirk, D. G., Fitches, W. R. & Barnes, R. P. (eds) *In Sight of the Suture: the Palaeozoic geology of the Isle of Man in its Iapetus Ocean context.* Geological Society, London, **160**, 89 - 107.

Woodcock, N. H. & Morris, J. H. 1999. Debris flows on the Ordovician margin of Avalonia: Lady Port Formation, Manx Group, Isle of Man. *In*: Woodcock, N. H., Quirk, D. G., Fitches, W. R. & Barnes, R. P. (eds) *In Sight of the Suture: the Palaeozoic geology of the Isle of Man in its Iapetus Ocean context.* Geological Society, London, Special Publication, **160**, 121 - 138.

Woodcock, N. H., Morris, J. H., Quirk, D. G., Barnes, R. P., Burnett, D., Fitches, W. R., Kennan, P. S. & Power, G. M. 1999b. Revised lithostratigraphy of the Manx Group, Isle of Man. *In*: Woodcock, N. H., Quirk, D. G., Fitches, W. R. & Barnes, R. P. (eds) *In Sight of the Suture: the Geology of the Isle of Man in its Iapetus Ocean Context.* Geological Society, London, Special Publication, **160**, 45 - 68.

Woodcock, N. H., Quirk, D. G., Fitches, W. R. & Barnes, R. P. 1999a. In sight of the suture: The early Palaeozoic geological history of the Isle of Man. *In*: Woodcock, N. H., Quirk, D. G., Fitches, W. R. & Barnes, R. P. (eds) *In Sight of the Suture: the Geology of the Isle of Man in its Iapetus Ocean Context.* Geological Society, London, Special Publication, **160**, 1 - 10.

Woodcock, N. H. & Schubert, C. 1994. Continental strike-slip tectonics. *In*: Hancock, P. L. (ed) *Continental Deformation.* Pergamon Press Ltd, Oxford, 251 - 263.

Woodcock, N. H. & Strachan, R. A. 2000a. Geological History of Britain and Ireland. Blackwell Science, London. 423 pp

Woodcock, N. H. & Strachan, R. A. 2000b. The Caledonian Orogeny: a multiple plate collision. *In*: Woodcock, N. H. & Strachan, R. A. (eds) *Geological history of Britain and Ireland.* Blackwell Science, London, 187 - 206.

Zoback, M. D., Zoback, M. L., Mount, V. S., Suppe, J., Eaton, J. P., Healy, J. H., Oppenheimer, D., Reasenberg, P., Jones, L., Raleigh, C. B., Wong, I. G., Scotti, O. & Wentworth, C. M. 1987. New evidence on the state of stress on the San Andreas fault system. *Science*, **238**, 1105 - 1111.